IMPACT OF PROTEINS, PEPTIDES, AMINO ACIDS AND FOOD ADDITIVES ON GUT MICROBIOTA

EDITED BY: Fengjiao Xin, Tingtao Chen, Xi Ma, Nuria Salazar and Xin Wang

PUBLISHED IN: Frontiers in Nutrition

frontiers Research Topics

frontiers

ISSN 1664-8714
ISBN 978-2-88976-927-8
DOI 10.3389/978-2-88976-927-8

About Frontiers

Frontiers is more than just an open-access publisher of scholarly articles: it is a pioneering approach to the world of academia, radically improving the way scholarly research is managed. The grand vision of Frontiers is a world where all people have an equal opportunity to seek, share and generate knowledge. Frontiers provides immediate and permanent online open access to all its publications, but this alone is not enough to realize our grand goals.

Frontiers Journal Series

The Frontiers Journal Series is a multi-tier and interdisciplinary set of open-access, online journals, promising a paradigm shift from the current review, selection and dissemination processes in academic publishing. All Frontiers journals are driven by researchers for researchers; therefore, they constitute a service to the scholarly community. At the same time, the Frontiers Journal Series operates on a revolutionary invention, the tiered publishing system, initially addressing specific communities of scholars, and gradually climbing up to broader public understanding, thus serving the interests of the lay society, too.

Dedication to Quality

Each Frontiers article is a landmark of the highest quality, thanks to genuinely collaborative interactions between authors and review editors, who include some of the world's best academicians. Research must be certified by peers before entering a stream of knowledge that may eventually reach the public - and shape society; therefore, Frontiers only applies the most rigorous and unbiased reviews.
Frontiers revolutionizes research publishing by freely delivering the most outstanding research, evaluated with no bias from both the academic and social point of view. By applying the most advanced information technologies, Frontiers is catapulting scholarly publishing into a new generation.

What are Frontiers Research Topics?

Frontiers Research Topics are very popular trademarks of the Frontiers Journals Series: they are collections of at least ten articles, all centered on a particular subject. With their unique mix of varied contributions from Original Research to Review Articles, Frontiers Research Topics unify the most influential researchers, the latest key findings and historical advances in a hot research area! Find out more on how to host your own Frontiers Research Topic or contribute to one as an author by contacting the Frontiers Editorial Office: frontiersin.org/about/contact

IMPACT OF PROTEINS, PEPTIDES, AMINO ACIDS AND FOOD ADDITIVES ON GUT MICROBIOTA

Topic Editors:
Fengjiao Xin, Chinese Academy of Agricultural Science, China
Tingtao Chen, Nanchang University, China
Xi Ma, China Agricultural University, China
Nuria Salazar, Spanish National Research Council (CSIC), Spain
Xin Wang, Zhejiang Academy of Agricultural Sciences, China

Citation: Xin, F., Chen, T., Ma, X., Salazar, N., Wang, X., eds. (2022). Impact of Proteins, Peptides, Amino Acids and Food Additives on Gut Microbiota. Lausanne: Frontiers Media SA. doi: 10.3389/978-2-88976-927-8

Table of Contents

frontiers in Nutrition

REVIEW
published: 08 September 2021
doi: 10.3389/fnut.2021.731930

Xylo-Oligosaccharides, Preparation and Application to Human and Animal Health: A Review

Yuxia Chen[1,2], Yining Xie[3], Kolapo M. Ajuwon[4], Ruqing Zhong[1], Tao Li[5], Liang Chen[1], Hongfu Zhang[1]*, Yves Beckers[2] and Nadia Everaert[2]*

[1] State Key Laboratory of Animal Nutrition, Institute of Animal Science, Chinese Academy of Agricultural Sciences, Beijing, China, [2] Precision Livestock and Nutrition Unit, Gembloux Agro-Bio Tech, TERRA Teaching and Research Centre, Liège University, Gembloux, Belgium, [3] School of Life Science and Engineering, Southwest University of Science and Technology, Mianyang, China, [4] Departments of Animal Sciences, Purdue University, West Lafayette, IN, United States, [5] Hunan United Bio-Technology Co., Changsha, China

OPEN ACCESS

Edited by:
Tingtao Chen,
Nanchang University, China

Reviewed by:
Junjun Wang,
China Agricultural University, China
Tizhong Shan,
Zhejiang University, China
Xin Wu,
Chinese Academy of Sciences (CAS), China

***Correspondence:**
Liang Chen
chenliang01@caas.cn
Hongfu Zhang
zhanghongfu@caas.cn

Specialty section:
This article was submitted to Nutrition and Microbes, a section of the journal Frontiers in Nutrition

Received: 28 June 2021
Accepted: 16 August 2021
Published: 08 September 2021

Citation:
Chen Y, Xie Y, Ajuwon KM, Zhong R, Li T, Chen L, Zhang H, Beckers Y and Everaert N (2021) Xylo-Oligosaccharides, Preparation and Application to Human and Animal Health: A Review. Front. Nutr. 8:731930. doi: 10.3389/fnut.2021.731930

Xylo-oligosaccharides (XOS) are considered as functional oligosaccharides and have great prebiotic potential. XOS are the degraded products of xylan prepared via chemical, physical or enzymatic degradation. They are mainly composed of xylose units linked by β-1, 4 bonds. XOS not only exhibit some specific physicochemical properties such as excellent water solubility and high temperature resistance, but also have a variety of functional biological activities including anti-inflammation, antioxidative, antitumor, antimicrobial properties and so on. Numerous studies have revealed in the recent decades that XOS can be applied to many food and feed products and exert their nutritional benefits. XOS have also been demonstrated to reduce the occurrence of human health-related diseases, improve the growth and resistance to diseases of animals. These effects open a new perspective on XOS potential applications for human consumption and animal production. Herein, this review aims to provide a general overview of preparation methods for XOS, and will also discuss the current application of XOS to human and animal health field.

Keywords: xylo-oligosaccharides, preparation, application, human health, animal health

INTRODUCTION

During the few last decades, there is increasing interest in the use of nutraceuticals or functional food additives for improving human health which has led to development of new food and feed products during the last few decades (1). Many functional products, having prebiotic characteristics, such as xylo-oligosaccharides (XOS), fructo-oligosaccharides (FOS), galacto-oligosaccharides (GOS), chitooligosaccharides (COS), alginate-oligosaccharides (AOS) have been extensively used as food and feed additives (2–6). Among these prebiotics, XOS are considered to be very promising. XOS are the degraded products prepared by chemical, physical or enzymatic degradation of xylan derived from biomass materials such as sugarcane residues, corn cobs, rice straw, etc (7) (**Figure 1**). They are composed of xylose units linked by β-1, 4-xylosidic bonds, which have a branched structure by the addition of different side groups (Moreira et al.). The degrees of polymerization of XOS are usually 2–7 (**Figure 2**) and they are known as xylobiose, xylotriose, and so on (8).

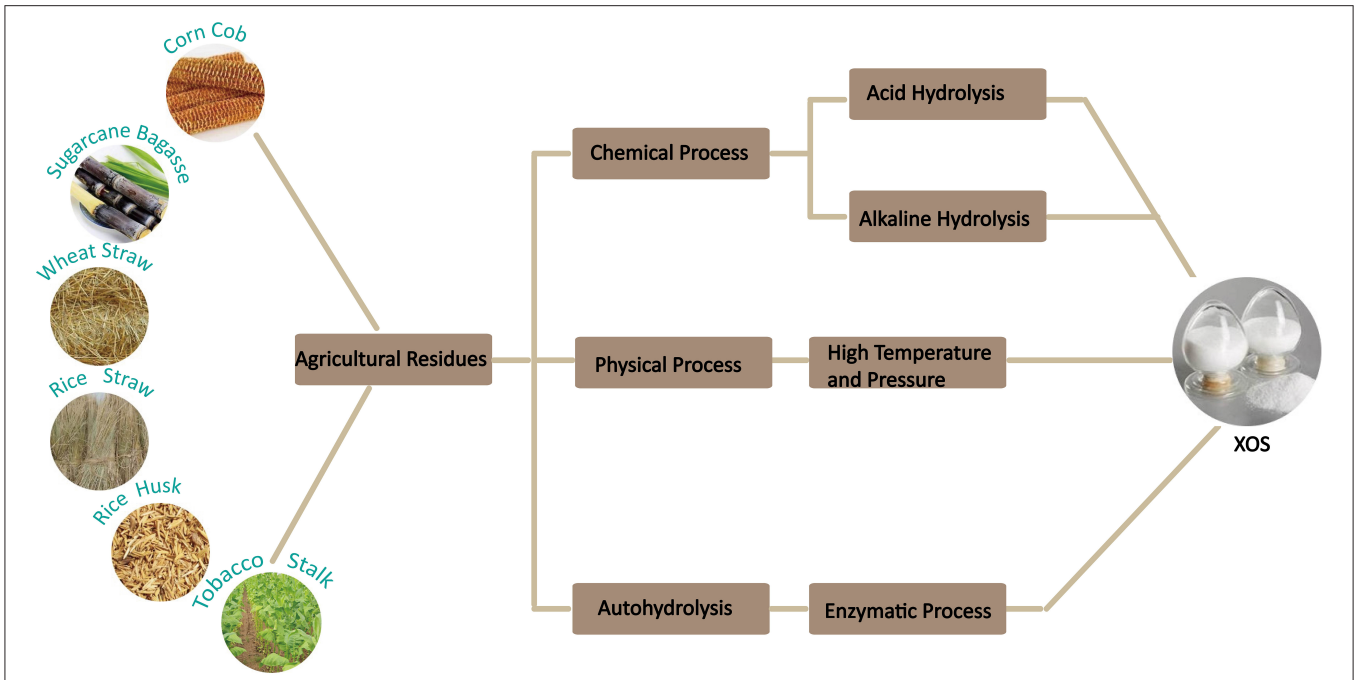

FIGURE 1 | Schematic of XOS production from agricultural residues.

XOS have a high potential to be applied for human nutrition due to its physicochemical properties such as low viscosity, high water solubility, tolerance to high temperature and acidic pH (9). Studies shown that XOS display a variety of pharmacological activities, including anti-inflammation, antioxidative, antitumor, antimicrobial properties. In addition, XOS have a potential application in the animal husbandry (10, 11). This review aims to summarize the methods of preparation of XOS and discuss the application of XOS to human and animal health.

PREPARATION AND CHARACTERIZATION OF XOS

The most widely used preparation methods of XOS are: (1) chemical degradation methods (2) physical degradation methods and (3) enzymatic degradation methods (**Figure 3**).

Chemical Process for the Production of XOS

The chemical degradation process, especially the acid and the alkaline hydrolysis methods, has been widely used for the mass production of XOS in industry due to its advantages such as simple operation and low production cost. Several studies have been conducted on producing XOS with various inorganic acids (12–16). Samanta et al. reported that the xylan from tobacco stalks was hydrolysed by tartaric acid into XOS, mainly including xylobiose and xylotriose, in addition to monomeric xylose (16). XOS production can also be obtained from corn cob xylan using weak sulphuric acid at 90°C during 30 min (12). The production of XOS depends on both acid concentration and hydrolysis time. A previous study showed that optimization of XOS production from waste xylan optimized by an orthogonal design of experiments, concluding a good extraction procedure of 20 min with 20% acetic acid at 140°C. A maximum XOS yield of more than 45.86% was obtained (14). Ying et al. studied that the increment of sulfuric acid concentration promoted the yield of xylooligosaccharides from hydrogen peroxide-acetic acid-pretreated poplar from 0.69 to 20.45% (17). In addition, Zhang et al. reported that acetic acid hydrolysis provided the highest XOS yield, up to 45.91% compared to hydrochloric acid and sulfuric acid pretreatment (15). It is widely known that the alkali solution could degrade hemicelluloses. This destruction is caused by the disruption of the hydrogen bonds with the alkaline reagent (18). In order to enhance the xylan content recovery from hemicellulose, use of appropriate alkaline concentration and pretreatment parameters are the primary conditions (19). For example, the use of higher concentration of alkali solution (15%) for extracting pineapple peels led to maximum recovery of hemicellulose. In the case of corn cobs, Samanta et al. also documented that higher concentration of alkali produced greater dissolution of hemicelluloses (12). However, these methods caused corrosion of the equipment, thus limiting their use.

Physical Process for the Production of XOS

Production XOS products by physical degradation is relatively simple and environmentally friendly compared to chemical degradation. For example, XOS can be obtained from milled aspen wood using a microwave oven, processing at 180°C for 10 min were and nextly subjected to fractionation to oligo- and polysaccharides by size-exclusion chromatography. The

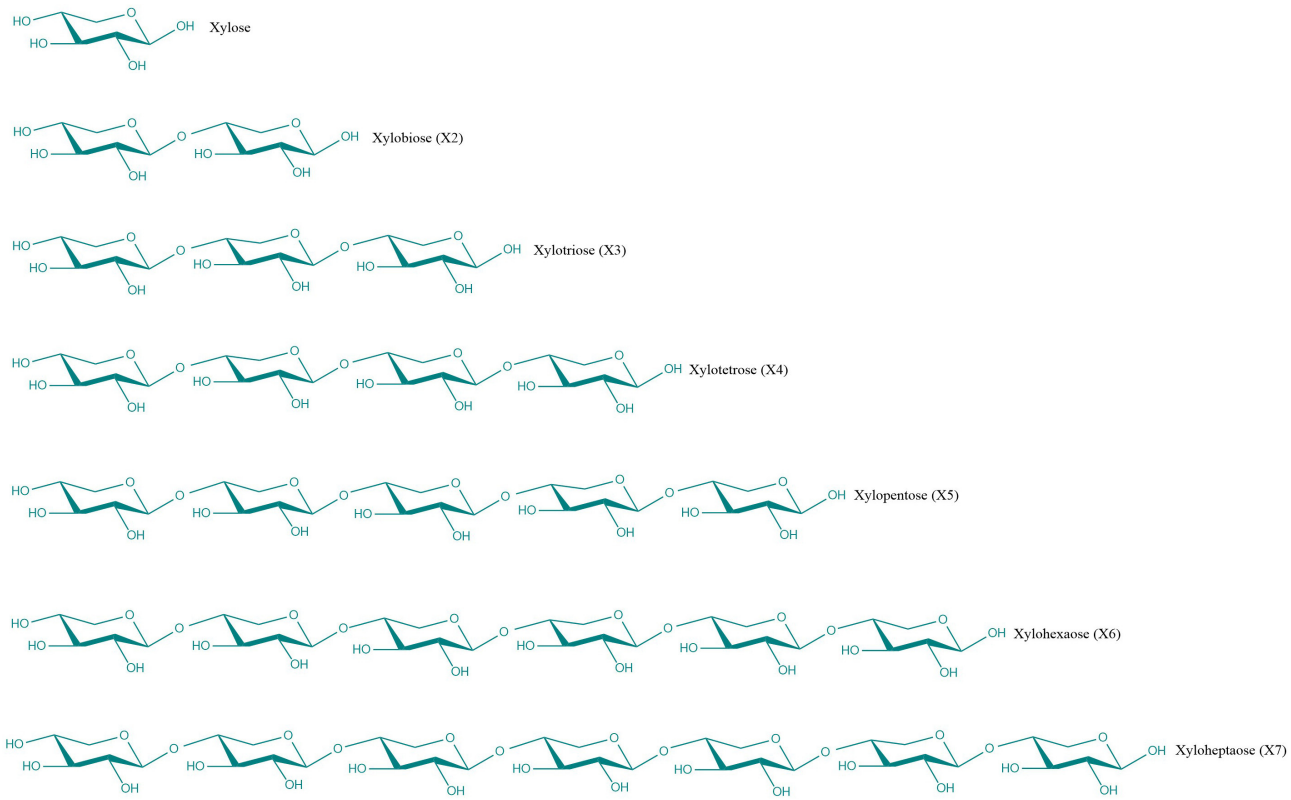

FIGURE 2 | Chemical schematic structure of XOS with low degree of polymerization.

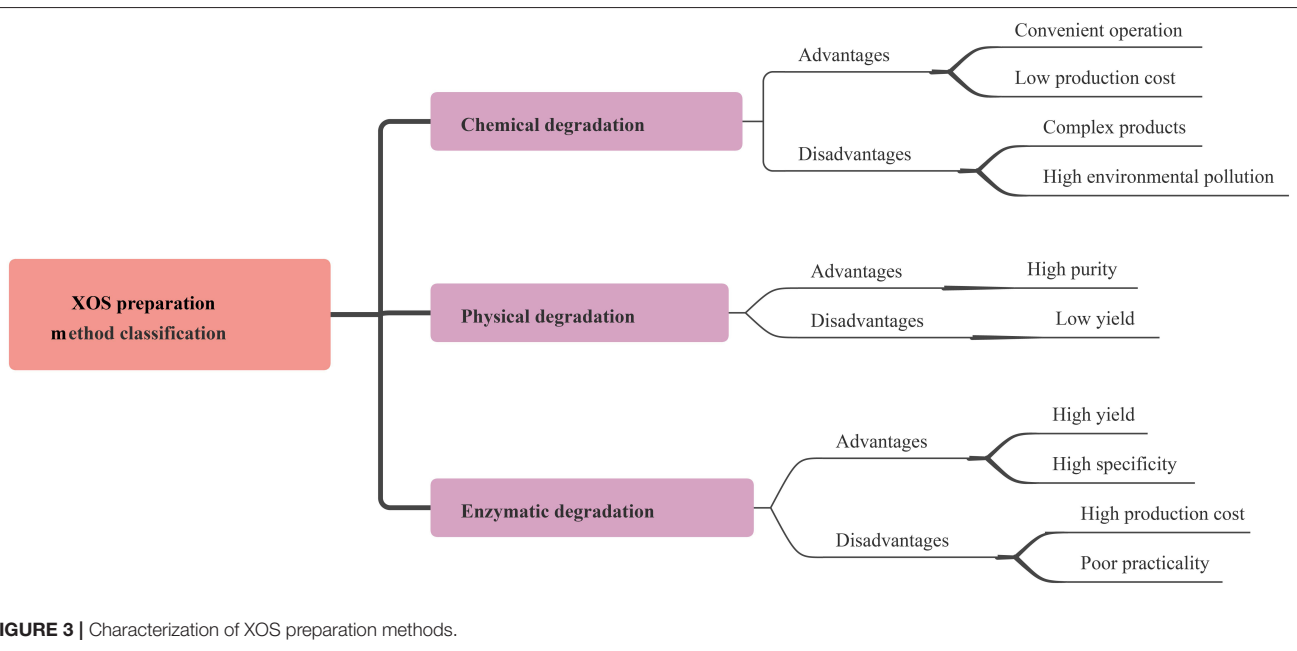

FIGURE 3 | Characterization of XOS preparation methods.

dispersion degree was smaller while the degradation effect was better (20). The hydrothermal reactor can also be used to degrade the xylan. Its fragments released from corn cob hemicellulose are partially acetylated, which improves solubility of long xylo-oligosaccharides by preventing molecular interactions between the xylan and the main chains of the xylo-oligosaccharide

TABLE 1 | Summary of XOS preparation and yields in the most recent studies.

Substrate	Pretreatment	Biocatalyst	Yxylan/ biomass (%)	Yxos/ biomass (%)	Yxos/ xylan (%)	DP	References
Corn cobs	acetic acid pH 2.7, 150°C, 30 min		30.4%	13.97%	45.9%	X2-X6	(14)
	Dilute acid followed by 135°C for 30 min	Xylanase from Penicillium corylophilum P-3-31	34.8%	23.6%	67.7%	X2-X4	(26)
	pH 6.5 and 60°C	Xylanase (PbXyn10A)	31.2%	23.4%	75%	X2-X4	(27)
	ultra-high pressure pretreatment	Streptomyces thermovulgaris TISTR1948 endoxylanase	33.4%	3.6%	10.7%	X2-X4	(28)
	190 C, 13 min	GH10 xylanase	29.9%	14.8%	49.4%		(21)
	5% (w/v) KOH, 90°C for 1 h		38.8%	11.5%	29.6%	X2-X5	(29)
Sugarcane Bagasse	Alkaline 10% (w/v) at room temperature overnight	Endo-β-1,4-xylanase rHlxyn11A	10.5%	6.0%	57.4%	X2-X3	(30)
	15% (w/v) aqueous ammonia	β-xylosidase	28.40%	19.3%	68.0%	X2-X4	(31)
	0.24M dilute H_2SO_4 90 C 31 min		33.5%	9.7%	29%	X2-X6	(13)
	5% gluconic acid hydrolysis (w/v) 60 min at 150°C	Cellulase	26.5%	14.1%	53.2%	X2-X6	(32)
	10% acetic acid at 150°C for 45 min	G. oxydans ATCC 621H	27.9%	10.9%	39.1%	X2-X6	(33)
Wheat straw	2% NaOH at 80°C for 90 min	The endoxylanase-variant K80R	8.4%	3.3%	39.8%	X2-X3	(34)
	Hydrolysis at 50°C and pH 5 for 5 h	β-1,4-endoxylanase			44%	X2-X3	(35)
	180°C 40 min	Endo-β-1-4-xylanase	73%	23%	31.5%	X2-X3	(36)
Rice straw	2% w/w sulfuric acid, 100°C, 0.5 h		65.3%	18.2%	27.8%		(37)
Rice husk	12% w/v NaOH, 110–120°C for 30 min	β-1,4-xylanase	54.5%	9.5%	17.4%	X2-X5	(38)
Pineapple peel	15% (w/v) alkali solution for 16 h at 45°C, 50°C, pH 5.0 and 15 U enzyme dose	Endo- 1, 4–Xylanase M1		23.5%	25.7%	X2-X3	(39)
Finger millet seed coat	Sodium acetate	Xylanase of Thermomyces lanuginosus	4.8%	3.4%	71.8%	X2-X3	(40)
Tobacco stalk	8% KOH or NaOH 90°C, 1M tartaric acid		17.0%	6.1%	35.7%	X1-X3	(16)

and also by preventing the binding of xylan to cellulose (21). The purity of XOS products is relatively high from physical degradation. However, there is limitation on the use of this method for large-scale production of XOS due to low yield.

Enzymatic Process for the Production of XOS

The industrial process of XOS production from natural xylan-rich agricultural residues involve enzymatic hydrolysis. As compared to the acid and alkaline hydrolysis method, production by the enzymatic degradation is relatively more economical, quick, and eco-friendly. Furthermore, enzymatic hydrolysis neither requires any special equipment nor produces undesirable byproducts. Thus, the production of XOS by enzymatic means was done from plant sources rich in xylan including corn cobs, sugarcane bagasse, wheat bran, birch wood, oat spelt, beech wood, natural grass, oil palm frond etc. These major enzymes used include β-xylosidase, glycosynthases and endo-xylanases, the latter being the key enzyme to produce XOS from xylan. They are able to reduce monomeric xylose release from the non-reducing ends of xylooligomers and xylobiose. The endo-xylanases from families GH10, GH11, and GH30 act specifically on the substituted and unsubstituted regions of xylan chain (22). Other studies focused on the use of β-xylosidases and glycosynthases for XOS production. β-xylosidases catalyze subtrate hydrolysis by inversion or retaining mechanism and are classified into six GH families: GH3, 30, 39, 43, 52, and 54. The β-xylosidases have been reported to produce longer β-XOS from β-1, 4 linkages or synthesize novel XOS (23, 24). Kim et al. documented that a glycosynthase derived from a retaining xylanase could synthesize a great variety of XOS (25). Many factors affect the yield of XOS from xylan such as the enzyme activity, the raw material, and incubation conditions including incubation pH, reaction time and temperature (19).

Table 1 summarizes the preparation process and the yields of XOS produced from xylan and xylan biomass by different approaches, often leading to high yields for several sources of substrates. Importantly, the prebiotic action of XOS requires a low degree of polymerization (DP) (9, 18). Hence, there are still some parameters in the preparation process of XOS that need to be optimized, including the production of a low DP (DP of 2–7) and the achievement of a high purity. Therefore, research

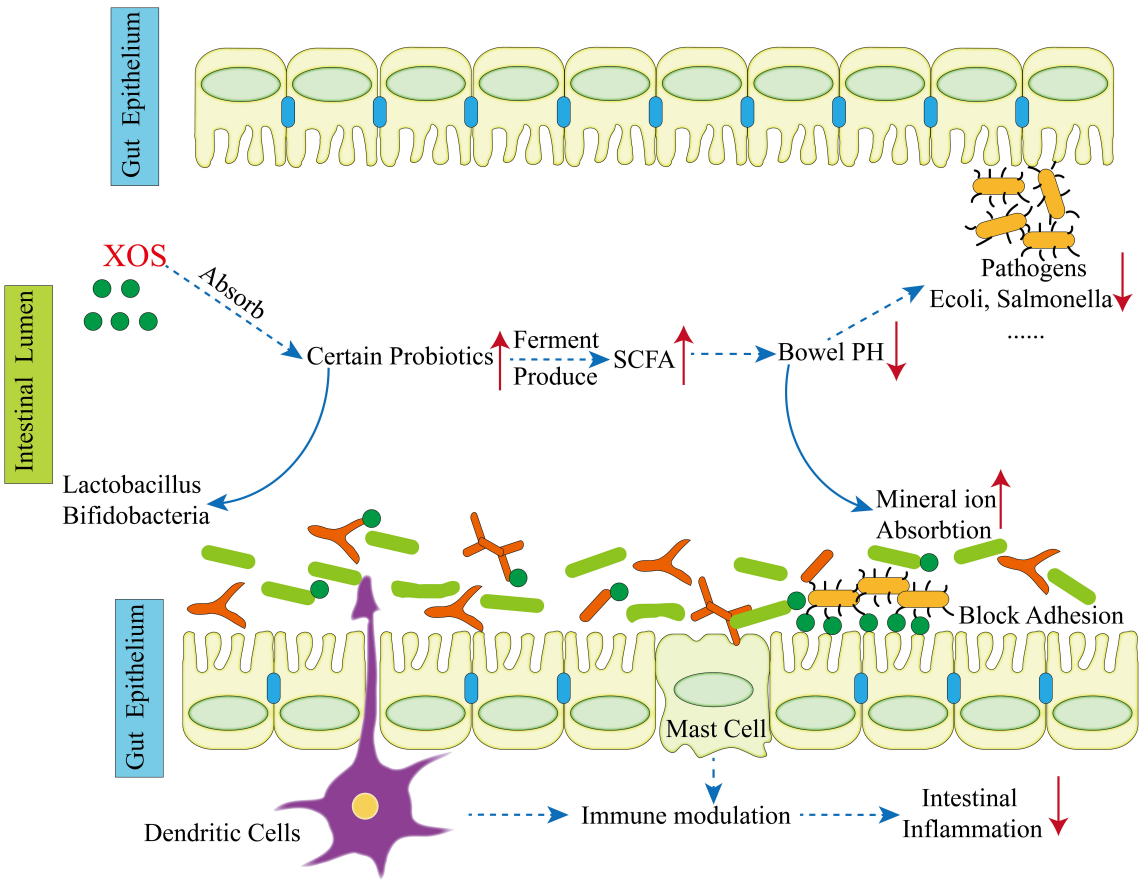

FIGURE 4 | Potential health benefits of prebiotics [quoted from (41)].

focuses on the combination and integration of the processes, testing different raw materials, extraction methods and enzymes to achieve an economically viable and health promoting product with an optimal production efficiency.

XOS APPLICATION TO HUMAN HEALTH

XOS were demonstrated to have various activities in human health such as inducing immune modulation, anti-tumor, antioxidant and anti-microbial effects (**Figure 4**).

Immune Modulation Effects of XOS

It is essential for protecting the host from diseases or repairing tissue injury to release inflammatory mediators (42, 43), and XOS is thus suggested to be an immunomodulator to prevent adverse immune-related conditions. Indeed, XOS was shown to have immunomodulatory effects by regulating expression of several proinflammatory mediators *in vitro*. XOS not only suppressed TNF-α, IL-1β, IL-6 and NO expression, but also triggered IL-10 production in lipopolysaccharide (LPS)-stimulated RAW264.7 cells (44). XOS feeding significantly decreased expression of IL-1β and IFN-γ and attenuated systemic inflammation (45). Moreover, the O-acetylated XOS derived from almond shells and their deacetylated derivatives exhibited immunomodulatory potential, based on a mitogenic rat thymocyte test (46). Finally, XOS combined with inulin attenuated the expression of IL-1β in the blood of healthy subjects fed a high-fat diet (47). Schematic presentation of XOS health benefits and their role in immune modulation are depicted in **Figure 4**.

Anti-tumor Effects of XOS

The main causes of cancer are the uncontrolled proliferation of abnormal cells which may stay at the point of mutation or metastasize into other locations. It has been shown that XOS exposure showed effect in preventing cancer (48–50). Indeed, β-1,3-Xylooligosaccharides with an average DP of 5 extracted from green alga Caulerpa lentillifera inhibited the number of viable human breast cancer MCF-7 cells in a dose-dependent manner, and induced apoptosis (50). Thus, this XOS could be a promising agent for prevention of breast cancer. Moreover, XOS supplementation reduced the level of lipid peroxidation and increased the activities of glutathione-S-transferase and catalase in colonic mucosa and liver, which may have contributed to the inhibition of colon carcinogenesis (51). *In vitro* approaches will

be useful for future mechanistic characterization of the antitumor properties of XOS. However, no systematic attempts have been carried out to study the upstream signals of caspase activation and the specific effects *in vivo*. Further research is necessary to investigate the overall anti-tumor effect of XOS.

Antioxidant Effects of XOS

During both acute and chronic diseases in humans, the abundance of free radicals usually increases. Several notable studies demonstrated that XOS had exhibited strong antioxidant and free radical scavenging activity, thus suggesting a potential use in biomedical applications (52, 53). The scavenging ability of XOS was shown to be dose-dependent (54), and this potential is likely attributable to efficient release of phenolic compounds and transfer of hydrogen atoms from the phenolic compounds to free radicals (55). Jagtap et al. revealed that the percent of antioxidant activity gradually increased reaching the maximum, 74% at a concentration of 6 mg/ml XOS using 1,1-diphenyl-2-picryl-hydrazyl (DPPH) assay, after which it did not show any further increase (56). Bouiche et al. studied that the antioxidant activity of glucuronoxylooligosaccharides (UXOS) and arabinoxylooligosaccharides (AXOS) was tested with the 2, 2′-Azino-bis (3-ethylbenzothiazoline-6-sulfonic acid) (ABTS) method (57). The results showed that the antioxidant activity of UXOS was significantly higher than the antioxidant activity of AXOS. Although both have neutral molecules, UXOS also has methylglucuronic acid (MeGlcA) decorations that confer a negative charge to the XOS. It was assumed that the MeGlcA decorations of the XOS were key elements influencing their antioxidant and radical scavenging activity of XOS (58).

Anti-microbial Effects of XOS

It has been reported that XOS have significant antimicrobial effects against several pathogenic bacterial. A host of clinically important both Gram-negative and Gram-positive bacteria have been documented to be sensitive to XOS exposure. Indeed, XOS and FOS supplementations markedly reduced the cecal pH level and increased the population of bifidobacterial compared with the control and DMH (1,2-dimethylhydrazine) treatments and the XOS treatment group had a lower abundance of *E. coli* than the DMH group. These results indicated that XOS and FOS non-digestible carbohydrates may promote the health of intestinal tract (59). In addition, some *in vitro* studies have documented that XOS supplementation produced lactic acid and acetic acid, which contributed to growth of *bifidobacteria* and *lactobacilli* strains and inhibited the growth of pathogenic strains (60–63).

XOS APPLICATION TO ANIMAL HEALTH

In this section, the recent studies on the application of XOS in animal husbandry health are provided. We have noted that most of the studies were focusing on XOS modulation of growth performance, nutrient digestibility and intestinal morphology, immune and anti-oxidant activity and gut microbiome (**Figure 5**).

Effects of XOS on Growth Performance of Animals

XOS have been used for animal nutrition and health improvement due to their potential biological functions, such as antioxidant, anti-inflammatory and antimicrobial effects. Previous studies have demonstrated the benefits of XOS on the growth performance of animals. Liu et al. reported that XOS treatment at a dose of 200 mg/kg increased average daily gain (ADG) by 17% and gain to feed (G/F) by 14% in the whole experiment, improved the apparent total tract digestibility (ATTD) of dry matter (DM), N and gross energy (GE) during 0 to 14 d in the piglets (27). Our study found that the effects of 500 mg/kg XOS (XOS500) on the growth performance during 1–28 days were very similar with that of the antibiotic chlortetracycline in the piglets. The results showed that XOS500 (500 mg/kg XOS) supplementation could significantly increase body weight (BW), ADG, average daily feed intake (ADFI) and feed to gain (F: G) of piglets (64). However, another study failed to notice significant improvement on growth performance after 0.01% XOS treatment in pigs (65). The discrepancy might be caused by the different levels of XOS used in these studies. Thus, further studies are needed to confirm the optimal dose of XOS in pigs. In addition, Yuan et.al evaluated the effects of XOS on growth performance and immune function of broiler chickens. They reported that XOS supplementation in the diet of broiler chickens significantly improved ADFI and ADG at 1–42 days when compared to the control group (66). The results of a study by Pourabedin et al. demonstrated that the feed conversion ratio (FCR) in broilers fed 2 g XOS/kg diet was lower than those fed 1 g XOS/kg diet between days 7 and 21, which is in line with other studies (67, 68). Some other researchers found that the FCR in the control group was also significantly lower for the group receiving the XOS-supplemented diet in broiler chickens for the whole trial period (67, 68). These results showed that XOS may dose-dependently improve the growth performance of animals and have potential as novel alternatives to antibiotics as growth promoters.

Effects of XOS on Nutrient Digestibility and Intestinal Morphology of Animals

The growth promoting effect of XOS has been shown to be related to improvement in nutrient digestibility. The addition of 200 mg/kg XOS with a purity of 50% supplementation has been demonstrated to improve the apparent total tract digestibility (ATTD) of dry matter (DM), nitrogen (N), and gross energy (GE) in weaning pigs on d14 (11). Similarly, the XOS supplementation significantly increased the apparent digestibility of the calcium with the increasing concentration of dietary XOS (0.1, 0.2, 0.3, 0.4 or 0.5 g/kg) in laying hens (69). The improvement of nutrient digestibility may be the result from XOS supporting normal intestinal morphology. Intestine morphology indices are often as a useful criterion to estimate the nutrient digestion and absorption capacity of the intestine. It is generally believed that the jejunum is the main segment involved in absorption of nutrients and minerals (70). Our study indicated that the XOS500 supplementation increased the villus height and villus height

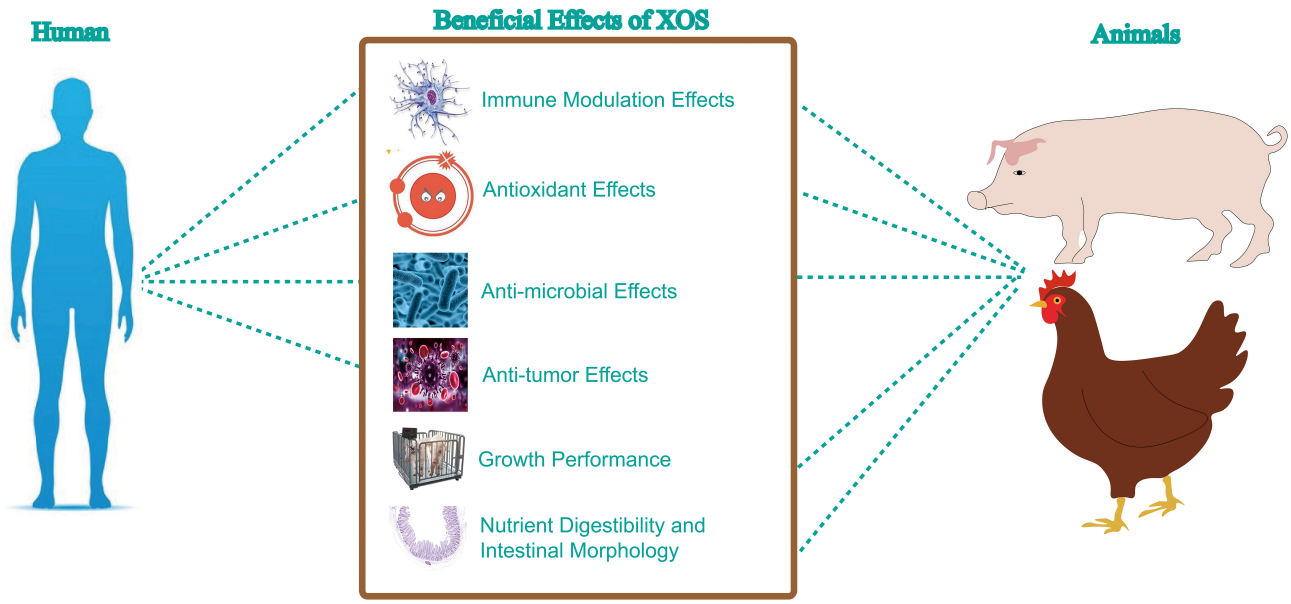

FIGURE 5 | Health beneficial effects of XOS.

to crypt depth ratio in the jejunum and ileum in comparison with the CON and XOS1000 group in the piglets, possibly improving nutrient absorption (71). Liu et al. confirmed that the XOS increased villus height to crypt depth ratio in jejunum, but did not influence villus height, crypt depth in the piglets (27). Similarly, Ding et al. reported that there was a linear improvement in villus height and villus height to crypt depth ratio of the jejunum as dietary XOS concentration increased in the laying hens (10). This is in agreement with the study of Maesschalck et al. showing that supplementation of 0.5% XOS with a purity of 35% to broiler chicken feed significantly increased the villus height in the ileum, suggesting an increase in gut health and improved nutrient absorption (68). However, 0.01% XOS with a purity of 40% in the diet of weaned piglets had little effects on the intestinal structure and villus surface area (65). In addition, the addition of 75 mg/kg XOS with a purity of 35% in the diet decreased the crypt depth of the duodenum (67). These results indicated that the use of an appropriate level of XOS may be important for increasing intestinal health and function.

Effects of XOS on Immune Modulation and Anti-oxidant Activity of Animals

XOS have been reported to display significant anti-inflammatory and anti-oxidant activities in animals in previous studies. In pigs, Yin et al. reported that dietary XOS markedly reduced serum IFN-γ concentration, indicating an anti-inflammatory effect of XOS (65), which is in line with a study in broilers showing a downregulation of the IFN-γ gene mRNA expression of jejunal mucosa. In addition, an increase in plasma IgG concentration was observed in XOS-fed 21-day-old broilers (66). Furthermore, XOS increased plasma IgA, IL-2, and TNF-α concentration compared with the control diet, and linearly improved the IgA and TNF-α concentration in plasma increasing the dietary XOS concentration in the laying hens (10). These results indicated that dietary XOS may improve cell-mediated immune response in early weaned piglets by regulating the production of cytokines and antibodies. In addition, antioxidant defense systems are regarded as important serum indices for assessing animal health. The changes in the antioxidant defense systems mainly including total antioxidant capacity (T-AOC), total superoxide dismutase (T-SOD), catalase (CAT) and glutathione peroxidase (GSH-Px) may indicate oxidative stress (72). Several studies revealed that XOS had exhibited antioxidant and radical scavenging competency (73). However, the research of Guerreiro revealed that the XOS supplementation reduced antioxidant enzyme activities in European sea bass (74).

Effects of XOS on the Modulation of Gut Microbiome of Animals

Our recent study showed that XOS500 supplementation could significantly increase the relative abundance of *Lactobacillus* genus and reduce the relative abundance of *Clostridium_sensu_stricto_1*, *Escherichia-Shigella*, and *Terrisporobacter* genus in the ileum and cecum in piglets (64). Moreover, 200 mg/kg XOS administration decreased fecal *Escherichia coli* and increased *Lactobacilli* in piglets (11). However, dietary XOS reduced the relative abundance of the *Lactobacillus* and increased the relative abundances of *Streptococcus* and *Turicibacter* (65). Furthermore, XOS and GOS both markedly decreased the numbers of intestinal *Listeria* monocytogenes in ileal samples from guinea pigs, and selectively stimulated *bifidobacteria* and *lactobacilli*, which are believed to have inhibitory effects against pathogens (75).

Similar beneficial effects of XOS have been observed in broilers. Indeed, 2 g XOS/kg diet increased the relative abundance of the *Lactobacillus* genus in the cecal microbiota of broilers (76), that can adhere to the mucosa and epithelium, promoting colonization, immunomodulation and protecting the intestinal barrier against pathogens (77). Furthermore, by the production of lactate, the lower the intestinal pH, inhibiting the growth of acid-sensitive pathogenic bacteria (78). However, the specific effect mechanism of XOS on the gut microbiome remains unclear as several studies were only done (18–20) or by microbial culture methods (21) that fail to provide accurate taxonomic composition and community structure. Thus, extensive research will be required to determine effects of XOS on the microbiome in animals.

CONCLUSION

In this review paper, we have summarized the preparation methods for XOS and its potential use as a functional food or feed additive for human and animal health. XOS seem to beneficially promoting intestinal health by selective stimulation of growth of *bifidobacteria* and *lactobacilli*. XOS also reduce the abundance of potentially pathogenic organisms. In addition, XOS exhibit a variety of biological activities including effects in suppressing inflammation, antioxidative, antitumor and antimicrobial properties. However, there are still several bottlenecks in the preparation and application of XOS. It is still difficult to obtain XOS products in large scale with high purity, and lack of consistency in quality of different batches of XOS from different polymerization degrees due to a lack of standardized preparation methods. The XOS products in the market are mainly mixtures not monomers. Technologies should be developed for producing XOS monomers with high purity at low cost. In addition, new investigations are required to further elucidate the specific molecular mechanisms of XOS. Additional information is needed on the mode of absorption of XOS in the host after oral ingestion, and the identification of related receptors or responsible for the transportation of XOS into target cells. Progress in these areas may enhance the value of XOS for applications in the prevention and treatment of human diseases and animal production.

AUTHOR CONTRIBUTIONS

YC, LC, and HZ wrote the first draft of the manuscript. NE, YB, and KA critically evaluated the manuscript. YX, RZ, and TL help check and revise the manuscript. All authors contributed to the article and approved the submitted version.

ACKNOWLEDGMENTS

The authors are grateful for the financial support from National Natural Science Foundation (31702119) and the Agricultural Science and Technology Innovation Program (CAAS-ZDRW202006-02, ASTIPIAS07) in China.

REFERENCES

1. Bitzios M, Fraser I, Haddock-Fraser J. Functional ingredients and food choice: results from a dual-mode study employing means-end-chain analysis and a choice experiment. *Food Policy*. (2011) 36:715–25. doi: 10.1016/j.foodpol.2011.06.004
2. Samanta AK, Jayapal N, Jayaram C, Roy S, Kolte AP, Senani S, et al. Xylooligosaccharides as prebiotics from agricultural by-products: production and applications. *Bioact Carbohydr Diet Fibre*. (2015) 5:62–71. doi: 10.1016/j.bcdf.2014.12.003
3. Bali V, Panesar PS, Bera MB, Panesar R. Fructo-oligosaccharides. Production, purification and potential applications. *Crit Rev Food Sci Nutr*. (2015) 55:1475–90. doi: 10.1080/10408398.2012.694084
4. Canfora EE, Van D, Hermes G, Goossens GH, Jocken J, Holst JJ, et al. Supplementation of diet with galacto-oligosaccharides increases bifidobacteria, but not insulin sensitivity, inobeseprediabetic individuals. *Gastroenterology*. (2017) 153:87–97. doi: 10.1053/j.gastro.2017.03.051
5. Yuan X, Zheng J, Jiao S, Cheng G, xFeng C, Du Y, et al. A review on the preparation of chitosan oligosaccharides and application to human health, animal husbandry and agricultural production. *Carbohydr Polym Sep*. (2019) 220:60–70. doi: 10.1016/j.carbpol.2019.05.050
6. Liu J, Yang S, Li X, Yan Q, Jiang Z. Alginate oligosaccharides: production, biological activities, potential applications. *Compr Rev Food Sci Food Saf*. (2019) 18:1859–81. doi: 10.1111/1541-4337.12494
7. Jain I, Kumar V, Satyanarayana T. Xylooligosaccharides: an economical prebiotic from agroresidues and their health benefits. *Indian J Exp Biol*. (2015) 53:131–42. Available online at: http://nopr.niscair.res.in/handle/123456789/30744
8. Aachary AA, Prapulla SG. Xylooligosaccharides (XOS) as an emerging prebiotic: microbial synthesis, utilization, structural characterization, bioactive properties, and applications. *Compr Rev Food Sci F*. (2011) 10:2–16. doi: 10.1111/j.1541-4337.2010.00135.x
9. Wei L, Yan T, Wu Y, Chen H, Zhang B. Optimization of alkaline extraction of hemicellulose from sweet sorghum bagasse and its direct application for the production of acidic xylooligosaccharides by bacillus subtilis strain MR44. *PLoS ONE*. (2018) 13:e0195616. doi: 10.1371/journal.pone.0195616
10. Ding XM, Li DD, Bai SP, Wang JP, Zeng QF, Su ZW, et al. Effect of dietary xylooligosaccharides on intestinal characteristics, gut microbiota, cecal short-chain fatty acids, and plasma immune parameters of laying hens. *Poult Sci*. (2018) 97:874–81. doi: 10.3382/ps/pex372
11. Liu J, Cao S, Liu J, Xie Y, Zhang H. Effect of probiotics and xylo-oligosaccharide supplementation on nutrient digestibility, intestinal health and noxious gas emission in weanling pigs. *Asian Austr J Anim Sci*. (2018a) 31:1660–9. doi: 10.5713/ajas.17.0908
12. Samanta A, Senani S, Kolte AP, Sridhar M, Sampath K, Jayapal N, et al. Production and *in vitro* evaluation of xylooligosaccharides generated from corn cobs. *Food Bioprod Process*. (2012) 90:466–74. doi: 10.1016/j.fbp.2011.11.001
13. Bian J, Peng P, Peng F, Xiao X, Xu F, Sun, et al. -C. Microwave-assisted acid hydrolysis to produce xylooligosaccharides from sugarcane bagasse hemicelluloses. *Food Chem*. (2014) 156:7–13. doi: 10.1016/j.foodchem.2014.01.112
14. Zhang H, Xu Y, Yu S. Co-production of functional xylooligosaccharides and fermentable sugars from corncob with effective acetic acid prehydrolysis. *Bioresour Technol*. (2017) 234:343–9. doi: 10.1016/j.biortech.2017.02.094
15. Zhang H, Zhou X, Xu Y, Yu S. Production of xylooligosaccharides from waste xylan, obtained from viscose fiber processing, by selective hydrolysis using concentrated acetic acid. *J Wood Chem Technol*. (2017) 37:1–9. doi: 10.1080/02773813.2016.1214154

16. Samanta A, Chikkerur J, Roy S, Kolte A, Sridhar M, Dhali A, et al. Xylooligosaccharides production from tobacco stalk xylan using edible acid. *Curr Sci.* (2019) 117:1521–5. doi: 10.18520/cs/v117/i9/1521-1525
17. Ying W, Xu Y, Zhang J. Effect of sulfuric acid on production of xylooligosaccharides and monosaccharides from hydrogen peroxide-acetic acid-pretreated poplar. *Bioresour Technol.* (2021) 321:124472. doi: 10.1016/j.biortech.2020.124472
18. De Freitas C, Carmona E, Brienzo M. Xylooligosaccharides production process from lignocellulosic biomass and bioactive effects. *Bioact Carbohydr Diet Fibre.* (2019) 18:100184. doi: 10.1016/j.bcdf.2019.100184
19. Jnawali P, Kumar V, Tanwar B, Hirdyani H, Gupta P. Enzymatic production of xylooligosaccharides from brown coconut husk treated with sodium hydroxide. *Waste Biomass Valori.* (2017) 9:1757–66. doi: 10.1007/s12649-017-9963-4
20. Teleman A, Lundqvist J, Tjerneld F, Stålbrand H, Dahlman O. Characterization of acetylated 4-O-methylglucuronoxylan isolated from aspen employing 1H and 13C NMR spectroscopy. *Carbohydr Res.* (2000) 329:807–15. doi: 10.1016/S0008-6215(00)00249-4
21. Arai T, Biely P, Uhliarikova I, Sato N, Makishima S, Mizuno M, et al. Structural characterization of hemicellulose released from corn cob in continuous flow type hydrothermal reactor. *J Biosci Bioeng.* (2019) 127:222–30. doi: 10.1016/j.jbiosc.2018.07.016
22. Linares-Pasten JA, Aronsson A, Karlsson EN. Structural considerations on the use of endo-xylanases for the production of prebiotic xylooligosaccharides from biomass. *Curr Protein Pept Sci.* (2018) 19:48–67. doi: 10.2174/1389203717666160923155209
23. Dilokpimol A, Nakai H, Gotfredsen CH, Appeldoorn M, Baumann MJ, Nakai N, et al. Enzymatic synthesis of beta-xylosyl-oligosaccharides by transxylosylation using two beta-xylosidases of glycoside hydrolase family 3 from Aspergillus nidulans FGSC A4. *Carbohydr Res.* (2011) 346:421–9. doi: 10.1016/j.carres.2010.12.010
24. Kurakake M, Fujii T, Yata M, Okazaki T, Komaki T. Characteristics of transxylosylation by β-xylosidase from aspergillus awamori K4. *Biochim Biophys Acta.* (2005) 1726:0–279. doi: 10.1016/j.bbagen.2005.08.009
25. Kim YW, Fox DT, Hekmat O, Kantner T, Mcintosh LP, Warren R, et al. Glycosynthase-based synthesis of xylo-oligosaccharides using an engineered retaining xylanase from cellulomonas fimi. *Org Biomol Chem.* (2006) 4:2025–20. doi: 10.1039/b601667g
26. Yang R, Xu S, Wang Z, Yang W. Aqueous extraction of corncob xylan and production of xylooligosaccharides. *LWT Food Sci Technol.* (2005) 38:677–82. doi: 10.1016/j.lwt.2004.07.023
27. Liu X, Liu Y, Jiang Z, Liu H, Yang S, Yan Q. Biochemical characterization of a novel xylanase from paenibacillus barengoltzii and its application in xylooligosaccharides production from corncobs. *Food Chem*. (2018) 264:310–8. doi: 10.1016/j.foodchem.2018.05.023
28. Seesuriyachan P, Kawee-Ai A, Chaiyaso T. Green and chemical-free process of enzymatic xylooligosaccharide production from corncob: enhancement of the yields using a strategy of lignocellulosic destructuration by ultra-high pressure pretreatment. *Bioresour Technol.* (2017) 241:537–44. doi: 10.1016/j.biortech.2017.05.193
29. Boonchuay P, Techapun C, Leksawasdi N, Seesuriyachan P, Hanmoungjai P, Watanabe M, et al. An integrated process for xylooligosaccharide and bioethanol production from corncob. *Bioresour Technol.* (2018) 256:399–407. doi: 10.1016/j.biortech.2018.02.004
30. Xue JL, Zhao S, Liang RM, Yin X, Jiang SX, Su LH, et al. A biotechnological process efficiently co-produces two high value-added products, glucose and xylooligosaccharides, from sugarcane bagasse. *Bioresour Technol.* (2016) 204:130–8. doi: 10.1016/j.biortech.2015.12.082
31. Reddy SS, Krishnan C. Production of high-pure xylooligosaccharides from sugarcane bagasse using crude β-xylosidase-free xylanase of bacillus subtilis KCX006 and their bifidogenic function. *LWT Food Sci Technol.* (2016) 65:237–45. doi: 10.1016/j.lwt.2015.08.013
32. Zhou X, Zhao J, Zhang X, Xu Y. An eco-friendly biorefinery strategy for xylooligosaccharides production from sugarcane bagasse using cellulosic derived gluconic acid as efficient catalyst. *Bioresour Technol.* (2019) 289:121755. doi: 10.1016/j.biortech.2019.121755
33. Zhou X, Xu Y. Integrative process for sugarcane bagasse biorefinery to co-produce xylooligosaccharides and gluconic acid. *Bioresour Technol.* (2019) 282:81–7. doi: 10.1016/j.biortech.2019.02.129
34. Faryar R, Linares-Pastén JA, Immerzeel P, Mamo G, Andersson M, Stålbrand H, et al. Production of prebiotic xylooligosaccharides from alkaline extracted wheat straw using the K80R-variant of a thermostable alkali-tolerant xylanase. *Food Bioprod Process.* (2015) 93:1–10. doi: 10.1016/j.fbp.2014.11.004
35. Romero-Fernandez M, Moreno-Perez S, Martins De Oliveira S, Santamaria RI, Guisan JM, Rocha-Martin J. Preparation of a robust immobilized biocatalyst of beta-1,4-endoxylanase by surface coating with polymers for production of xylooligosaccharides from different xylan sources. *N Biotechnol.* (2018) 44:50–8. doi: 10.1016/j.nbt.2018.04.007
36. Huang C, Lai C, Wu X, Huang Y, He J, Huang C, et al. An integrated process to produce bio-ethanol and xylooligosaccharides rich in xylobiose and xylotriose from high ash content waste wheat straw. *Bioresour Technol.* (2017) 241:228–35. doi: 10.1016/j.biortech.2017.05.109
37. Sophonputtanaphoca S, Pridam C, Chinnak J, Nathong M, Juntipwong P. Production of non-digestible oligosaccharides as value-added by-products from rice straw. *Agric Nat Resour.* (2018) 52:169–75. doi: 10.1016/j.anres.2018.06.013
38. Khat-Udomkiri N, Sivamaruthi BS, Sirilun S, Lailerd N, Peerajan S, Chaiyasut C. Optimization of alkaline pretreatment and enzymatic hydrolysis for the extraction of xylooligosaccharide from rice husk. *AMB Express.* (2018) 8:115. doi: 10.1186/s13568-018-0645-9
39. Banerjee S, Patti AF, Ranganathan V, Arora A. Hemicellulose based biorefinery from pineapple peel waste: xylan extraction and its conversion into xylooligosaccharides. *Food Bioprod Process.* (2019) 117:38–50. doi: 10.1016/j.fbp.2019.06.012
40. Palaniappan A, Balasubramaniam VG, Antony U. Prebiotic potential of xylooligosaccharides derived from finger millet seed coat. *Food Biotechnol.* (2017) 31:264–80. doi: 10.1080/08905436.2017.1369433
41. Aachary AA. Prebiotics: specific colonic nutrients. In: Prapulla SG, editor. *Bioactive Xylooligosaccharides From Corncob: Enzymatic Production and Applications (Thesis) submitted to Univ. Of Mysore.* Mysore: Aacharya, A. A. (2009). p. 19.
42. Durack DT, Glauser MP. The inflammatory cytokines - new developments in the pathophysiology and treatment of septic shock - discussion. *Drugs.* (1996) 52:17. doi: 10.2165/00003495-199600522-00004
43. Childs CE, Roytio H, Alhoniemi E, Fekete AA, Forssten SD, Hudjec N, et al. Xylo-oligosaccharides alone or in synbiotic combination with bifidobacterium animalis subsp. Lactis induce bifidogenesis and modulate markers of immune function in healthy adults: a double-blind, placebo-controlled, randomised, factorial cross-over study. *Br J Nutr.* (2014) 111:1945–56. doi: 10.1017/S0007114513004261
44. Chen H, Chen Y, Chang H. Immunomodulatory effects of xylooligosaccharides[J]. *Food Sci Technol Res.* (2012) 18:195–9. doi: 10.3136/fstr.18.195
45. Hansen CH, Frokiaer H, Christensen AG, Bergstrom A, Licht TR, Hansen AK, et al. Dietary xylooligosaccharide downregulates IFN-gamma the low-grade inflammatory cytokine IL-1beta systemically in mice. *J Nutr.* (2013) 143:533–40. doi: 10.3945/jn.112.172361
46. Nabarlatz D, Montane D, Kardosova A, Bekesova S, Hribalova V, Ebringerova A. Almond shell xylo-oligosaccharides exhibiting immunostimulatory activity. *Carbohydr. Res.* (2007) 342:1122–8. doi: 10.1016/j.carres.2007.02.017
47. Lecerf, J.-M., Dépeint F, Clerc E, Dugenet Y, Niamba CN, et al. Xylo-oligosaccharide (XOS) in combination with inulin modulates both the intestinal environment and immune status in healthy subjects, while XOS alone only shows prebiotic properties. *Br J Nutr.* (2012) 108:1847–58. doi: 10.1017/S0007114511007252
48. Howe GR, Benito E, Castelleto R, Cornée J, Estève J, Gallagher RP, et al. Dietary intake of fiber decreased risk of cancers of the colon rectum: evidence from the combined analysis of 13 case-control studies. *Jnci J Natl Cancer.* (1992) 84:1887–96. doi: 10.1093/jnci/84.24.1887
49. Ando H, Ohba H, Sakaki T, Takamine K, Kamino Y, Moriwaki S, et al. Hot-compressed-water decomposed products from bamboo manifest a selective cytotoxicity against acute lymphoblastic leukemia cells. *Toxicol In Vitro.* (2004) 18:765–71. doi: 10.1016/j.tiv.2004.03.011

50. Maeda R, Ida T, Ihara H, Sakamoto T. Induction of apoptosis in MCF-7 cells by beta-1,3-xylooligosaccharides prepared from caulerpa lentillifera. *Biosci Biotech Bioch.* (2012) 76:1032–4. doi: 10.1271/bbb.120016
51. Aacharya AA, Gobinatha D, Srinivasanb K, Prapulla SG. Protective effect of xylooligosaccharides from corncob on 1,2-dimethylhydrazine induced colon cancer in rats[J]. *Bioact Carbohydr Diet Fibre.* (2015) 5:146–52. doi: 10.1016/j.bcdf.2015.03.004
52. Yu X, Yin J, Li L, Luan C, Li S. Prebiotic potential of xylooligosaccharides derived from corn cobs their *In Vitro* antioxidant activity when combined with lactobacillus. *J Microbiol Biotechnol.* (2015) 25:1084–92. doi: 10.4014/jmb.1501.01022
53. Rashad MM, Mahmoud AE, Nooman MU, Mahmoud HA, Keshta AT. Production of antioxidant xylooligosaccharides from lignocellulosic materials using bacillus amyloliquifaciens NRRL B-14393 xylanase. *J App Pharm Sci.* (2016) 6:30–6. doi: 10.7324/JAPS.2016.60606
54. Gowdhaman D, Ponnusami V. Production and optimization of xylooligosaccharides from corncob by bacillus aerophilus KGJ2 xylanase and its antioxidant potential. *Int J Biol Macromol.* (2015) 79:595–600. doi: 10.1016/j.ijbiomac.2015.05.046
55. Huang D, Ou B, Prior RL. The chemistry behind antioxidant capacity assays. *J Agric Food Chem.* (2005) 53:1841–56. doi: 10.1021/jf030723c
56. Jagtap S, Deshmukh RA, Menon S, Das S. Xylooligosaccharides production by crude microbial enzymes from agricultural waste without prior treatment and their potential application as nutraceuticals. *Bioresour Technol.* (2017) 245:283–8. doi: 10.1016/j.biortech.2017.08.174
57. Bouiche C, Boucherba N, Benallaoua S, Martinez J, Diaz P, Pastor FIJ, et al. Differential antioxidant activity of glucuronoxylooligosaccharides (UXOS) and arabinoxylooligosaccharides (AXOS) produced by two novel xylanases. *Int J Biol Macromol.* (2019) 155:1075–83. doi: 10.1016/j.ijbiomac.2019.11.073
58. Valls C, Pastor FJ, Vidal T, Roncero MB, Díaz P, Martínez J, et al. Antioxidant activity of xylooligosaccharides produced from glucuronoxylan by Xyn10A and Xyn30D xylanases and eucalyptus autohydrolysates. *Carbohydr Polym.* (2018) 194:43–50. doi: 10.1016/j.carbpol.2018.04.028
59. Hsu CK, Liao JW, Chung YC, Hsieh CP, Chan YC. Xylooligosaccharides fructooligosaccharides affect the intestinal microbiota precancerous colonic lesion development in rats. *J Nutr.* (2004) 134:1523–8. doi: 10.1093/jn/134.6.1523
60. Palframan RJ, Gibson GR, Rastall RA. Carbohydrate preferences of bifidobacterium species isolated from the human gut. *Curr Issues Intest Microbiol.* (2003) 4:71–5. PMID: 14503691
61. Pan X, Wu T, Zhang L, Cai L, Song Z. Influence of oligosaccharides on the growth and tolerance capacity of lactobacilli to simulated stress environment. *Lett Appl Microbiol.* (2009) 48:362–7. doi: 10.1111/j.1472-765X.2008.02539.x
62. Ebersbach T, Andersen JB, Bergstr MA, Hutkins RW, Licht TR. Xylo-oligosaccharides inhibit pathogen adhesion to enterocytes *in vitro*. *Res Microbiol.* (2012) 163:22–7. doi: 10.1016/j.resmic.2011.10.003
63. Dotsenko G, Meyer AS, Canibe N, Thygesen A, Nielsen MK, Lange L. Enzymatic production of wheat and ryegrass derived xylooligosaccharides and evaluation of their in vitro effect on pig gut microbiota. *Biomass Convers Bior.* (2017) 8:497–507. doi: 10.1007/s13399-017-0298-y
64. Chen Y, Xie Y, Zhong R, Liu L, Lin C, Xiao L, et al. Effects of xylo-oligosaccharides on growth and gut microbiota as potential replacements for antibiotic in weaning piglets. *Front Microbiol.* (2021) 12:641172. doi: 10.3389/fmicb.2021.641172
65. Yin J, Li F, Kong X, Wen C, Guo Q, Zhang L, et al. Dietary xylo-oligosaccharide improves intestinal functions in weaned piglets. *Food Funct.* (2019) 10:2701–9. doi: 10.1039/C8FO02485E
66. Yuan L, Li W, Huo Q, Du C, Wang Z, Yi B, et al. Effects of xylo-oligosaccharide and flavomycin on the immune function of broiler chickens. *PeerJ.* (2018) 6:e4435. doi: 10.7717/peerj.4435
67. Suo HQ, Lin L, Xu GH, Xiao L, Chen XG, Xia RR, et al. Effectiveness of dietary xylo-oligosaccharides for broilers fed a conventional corn-soybean meal diet. *J Integr Agr.* (2015) 14:2050–7. doi: 10.1016/S2095-3119(15)61101-7
68. De Maesschalck C, Eeckhaut V, Maertens L, De Lange L, Marchal L, Nezer C, et al. Effects of xylo-oligosaccharides on broiler chicken performance and microbiota. *Appl Environ Microbiol.* (2015) 81:5880–8. doi: 10.1128/AEM.01616-15
69. Li DD, Ding XM, Zhang KY, Bai SP, Wang JP, Zeng QF, et al. Effects of dietary xylooligosaccharides on the performance, egg quality, nutrient digestibility and plasma parameters of laying hens. *Anim Feed Sci Tech.* (2017) 225:20–6. doi: 10.1016/j.anifeedsci.2016.12.010
70. Schokker D, Jansman AJ, Veninga G, De Bruin N, Vastenhouw SA, De Bree FM, et al. Perturbation of microbiota in one-day old broiler chickens with antibiotic for 24 hours negatively affects intestinal immune development. *BMC Genomics.* (2017) 18:241. doi: 10.1186/s12864-017-3625-6
71. Chen Y, Xie Y, Zhong R, Han H, Liu L, Chen L, et al. Effects of graded levels of xylo-oligosaccharides on growth performance, serum parameters, intestinal morphology and intestinal barrier function in weaned piglets. *J Anim Sci.* (2021) 99:skab183. doi: 10.1093/jas/skab183
72. Zhu LH, Zhao KL, Chen XL, Xu JX. Impact of weaning and an antioxidant blend on intestinal barrier function and antioxidant status in pigs. *J Anim Sci.* (2012) 90:2581–9. doi: 10.2527/jas.2011-4444
73. Wang J, Cao Y, Wang C, Sun B. Wheat bran xylooligosaccharides improve blood lipid metabolism and antioxidant status in rats fed a high-fat diet. *Carbohydr Polym.* (2011) 86:1192–7. doi: 10.1016/j.carbpol.2011.06.014
74. Guerreiro I, Couto A, Pérez-Jiménez A, Oliva-Teles A, Enes P. Gut morphology and hepatic oxidative status of European sea bass (Dicentrarchus labrax) juveniles fed plant feedstuffs or fishmeal-based diets supplemented with short-chain fructo-oligosaccharides and xylo-oligosaccharides. *Br J Nutr.* (2015) 114:1975–84. doi: 10.1017/S0007114515003773
75. Ebersbach T, Jorgensen JB, Heegaard PM, Lahtinen SJ, Ouwehand AC, Poulsen M, et al. Certain dietary carbohydrates promote Listeria infection in a guinea pig model, while others prevent it. *Int J Food Microbiol.* (2010) 140:218–24. doi: 10.1016/j.ijfoodmicro.2010.03.030
76. Pourabedin M, Guan L, Zhao X. Xylo-oligosaccharides and virginiamycin differentially modulate gut microbial composition in chickens. *Microbiome.* (2015) 3:15. doi: 10.1186/s40168-015-0079-4
77. Kravtsov E, Yermolayev A, Anokhina I, Yashina N, Chesnokova V, Dalin M. Adhesion characteristics of lactobacillus is a criterion of the probiotic choice. *B Exp Biol Med.* (2008) 145:232–4. doi: 10.1007/s10517-008-0058-x
78. Belenguer A, Duncan SH, Holtrop G, Anderson SE, Lobley GE, Flint HJ. Impact of pH on lactate formation and utilization by human fecal microbial communities. *Appl Environ Microbiol.* (2007) 73:6526–33. doi: 10.1128/AEM.00508-07

Conflict of Interest: TL is employed by Hunan United Bio-technology Co.

The remaining authors declare that the research was conducted in the absence of any commercial or financial relationships that could be construed as a potential conflict of interest.

Publisher's Note: All claims expressed in this article are solely those of the authors and do not necessarily represent those of their affiliated organizations, or those of the publisher, the editors and the reviewers. Any product that may be evaluated in this article, or claim that may be made by its manufacturer, is not guaranteed or endorsed by the publisher.

frontiers in Nutrition

ORIGINAL RESEARCH
published: 06 October 2021
doi: 10.3389/fnut.2021.739676

Effects of Different Methionine Levels in Low Protein Diets on Production Performance, Reproductive System, Metabolism, and Gut Microbiota in Laying Hens

Miaolin Ma†, Shunju Geng†, Meiling Liu, Lihong Zhao, Jianyun Zhang, Shimeng Huang and Qiugang Ma**

State Key Laboratory of Animal Nutrition, College of Animal Science and Technology, China Agricultural University, Beijing, China

OPEN ACCESS

Edited by:
Tingtao Chen, Nanchang University, China

Reviewed by:
Chunqi Gao, South China Agricultural University, China
Huan Li, Lanzhou University, China
Xinyang Dong, Zhejiang University, China

***Correspondence:**
Qiugang Ma
maqiugang@cau.edu.cn
Shimeng Huang
shimengh@hotmail.com

†These authors have contributed equally to this work

Specialty section:
This article was submitted to Nutrition and Microbes, a section of the journal Frontiers in Nutrition

Received: *11 July 2021*
Accepted: *06 September 2021*
Published: *06 October 2021*

Citation:
Ma M, Geng S, Liu M, Zhao L, Zhang J, Huang S and Ma Q (2021) Effects of Different Methionine Levels in Low Protein Diets on Production Performance, Reproductive System, Metabolism, and Gut Microbiota in Laying Hens. Front. Nutr. 8:739676. doi: 10.3389/fnut.2021.739676

This study investigated the effects of different levels of methionine (Met) in a low protein diet on the production performance, reproductive system, metabolism, and gut microbial composition of laying hens to reveal the underlying molecular mechanism of Met in a low protein diet on the host metabolism and gut microbial composition and function of hens. A total of 360 healthy 38-week-old Peking Pink laying hens with similar body conditions and egg production (EP) were randomly divided into four groups with nine replicates per treatment and 10 hens per replicate. The hens in each treatment group were fed low protein diets containing different levels of Met (0.25, 0.31, 0.38, and 0.47%, respectively) for 12 weeks. Feed and water were provided *ad libitum* throughout the trial period. The results showed that, compared with the 0.25% Met group, the final body weight (FBW), average daily gain (ADG), EP, egg weight (EW), and average daily feed intake (ADFI) in the other groups were significantly increased and feed egg ratio (FER) was decreased. Meanwhile, the EW and yield of abdominal fat (AFY) in the 0.47% Met group were higher than those in other groups. The triglyceride (TG), estradiol (E2), total protein (TP), albumin (ALB), and immunoglobulin A (IgA) in the 0.38 and 0.47% Met groups were higher than those in other groups. In addition, 16S rRNA gene sequencing revealed that there was no difference in the Sobs index, ACE index, and Shannon index among all groups. However, it is worth noting that feeding low protein diets with Met changed the gut microbial composition (e.g., the supplementation of Met increased the level of *Lactobacillus* and decreased the proportion of *Faecalibacterium*). Also, our results showed that the changes in gut microbial composition induced by the diets with different levels of Met were closely related to the changes of key parameters: ADFI, EW, FBW, TG, EM, EP, ADG, FER, and uric acid (UA). Our results highlight the role of adding an appropriate amount of Met to the low protein diet in laying hens, which could improve the gut microbial composition, production performance, reproductive system, and nutrient metabolism of laying hens. In conclusion, this study suggested that when the Met level was 0.38%, the production performance of the laying hens was pretty good.

Keywords: laying hens, methionine deficiency, low protein diets, gut microbiota, production performance, nutrient metabolism

INTRODUCTION

The poultry industry shows a trend of large-scale, intelligent, and standardized development, and the demand for protein feed resources continues to increase (1, 2). However, there are problems, such as limited protein resources, low nutrient utilization rates, and environmental pollution, caused by fecal nitrogen emission, thereby making the research on the low protein diet is becoming more and more important. In order to ensure the performance of animals, a large amount of protein is added to the diet of laying hens. However, excessive protein in the diet, which will increase the content of nitrogen and phosphorus in feces and urine, is often not put to good use (3, 4). Excessive ammonia nitrogen emission in feces will not only cause environmental pollution, but also harm the health of laying hens (5–8). Some studies have shown that reducing protein levels in the diet can effectively reduce nitrogen emissions from the feces and urine of livestock and poultry (9–11).

That refers to the low protein diet that containing less crude protein than the nutrient requirements of poultry (NRC) recommends for feeding in the diet. Following the ideal amino acid pattern is the key to feed formulation design. In essence, the need for protein in the diet is the need for amino acids, which are essential nutrients for animal growth and development that are involved in important biochemical reactions in animals (12, 13). There have also been studies on livestock and poultry that have shown that adding certain synthetic amino acids to a low protein diet can improve protein digestibility, effectively reduce nitrogen emissions (11, 14), and save feed costs (15, 16). Many studies have shown that adding a certain amount of glycine, valine, isoleucine, and methionine (Met) to a low protein diet has no negative effect on livestock and poultry and can even improve their performance in some way (17–19). In addition, it can also improve the structure and composition of the gut microbiota of livestock and poultry, increase the abundance of beneficial microbes such as *Bifidobacterium* and *Lactobacillus*, maintain the integrity of the intestinal epithelial barrier function, improve the normal functions of the intestinal epithelium, and enhance intestinal mucosal immunity in animals (20–23).

In order to avoid the negative effects of a low protein diet on livestock and poultry, we can consider adding essential amino acids to their diet to reduce harmful effects (24). Methionine, as the main limiting amino acid in the corn-soybean meal diet of laying hens, not only participates in protein synthesis, but also plays an irreplaceable role in some molecular precursors and intermediates to control oxidative stress in the body and affect cell metabolism and function (25). It was also found that dietary Met can enhance the immune response levels of poultry (26, 27). Furthermore, Met can be added into the low protein diet of broilers to meet the requirements of total sulfur-containing amino acids, but it should be added appropriately, otherwise, it will affect the growth performance of poultry (28). Zhang found that supplemented Met in the diet could change the intestinal tissue morphology and increase the body weight of Peking ducks (29). In addition, Met can provide methyl (30, 31), and use it for the methylation of toxic substances to detoxify. It can also combine with mycotoxin to weaken its toxicity. But there is still a lack of research on the effect of Met supplementation in low protein diets on laying hens, especially on the effect of gut microbiota.

Due to the current situation, low protein diets will be a trend in the future. However, the application of a low crude protein diet in laying hens is relatively rare at present, and the study on its functional effect on laying hens can better prepare balanced low protein diets, which is conducive to exerting the genetic potential of laying hens. To develop a practical understanding of Met use in low crude protein diets, a study was conducted to evaluate production performance, egg quality, reproductive system, host metabolism, and the gut microbial composition responses to different levels of Met in laying hens fed low protein diets.

Abbreviations: ADG, average daily gain; ADFI, average daily feed intake; AFY, yield of abdominal fat; ALB, albumin; BW, body weight; EP, egg production; EW, egg weight; EM, average daily egg mass; FBW, final body weight; FER, feed egg ratio; GSH, glutathione; IBW, initial body weight; IgM, immune globulin M; Met, methionine; SOD, superoxide dismutase; TG, triglyceride; TP, total protein; UA, uric acid.

MATERIALS AND METHODS

Animal Experimental Ethics

All experiments were approved by the China Agricultural University Animal Care and Use Committee (AW32301202-2-1, Beijing, China).

Animals and Experimental Design

A total of 360 commercial hens of the Peking Pink strain (Yukou Poultry Co., Ltd., Beijing, China) at the age of 38 weeks with similar egg production and healthy bodies were randomly divided into four treatment groups with nine replicates per group and 10 birds per replicate. The hens were placed in five cages (two birds in each cage) and each cage (H45 cm × W45 cm × D45 cm) was equipped with a nipple drinker and an exterior feed through to ensure feed and water were provided *ad libitum* during the entire experimental period. At the same time, to ensure that the chicken coop is closed and ventilated, the average relative humidity was routinely maintained at ∼55%, and it was ensured that the hens get 16 h of light every day. In order to meet the nutritional requirements of the laying hens (NYT33-2004), a basal corn-soybean meal diet was formulated. A pre-experiment was conducted for one week before the start of the formal experiment to ensure that the animals were acclimated to the new experimental environment and diet, meanwhile, it could empty the original intestinal contents, and estimate the approximate feed intake of the experimental animals. The four experimental groups were fed with low protein diets containing 0.25, 0.31, 0.38, and 0.47% Met (0.25% Met group, 0.31% Met group, 0.38% Met group, and 0.47% Met group), respectively. The ingredients and nutrient composition of the diets are shown in **Supplementary Table 1**.

Laying Performance and Egg Quality

The difference between the full bucket weights and the remaining feed was calculated as the weekly feed intake, and the body weights of the laying hens were recorded every week at the

same time to calculate the average daily feed intake (ADFI) and feed egg ratio (FER). The number of eggs and egg weight were accurately recorded every day to calculate the average daily egg mass (EM), egg weight (EW), and egg production (EP) rate. The hens were weighed in replicates at the beginning and end of the experiment to calculate average daily gain (ADG). After the beginning of the experiment, 30 eggs were randomly selected from each treatment group every 4 weeks to measure egg quality parameters as shown in **Table 2**.

The eggshell strength was measured by the egg force reader (ESTG-01ĄCOrka Teachnology Ltd); The eggshell thickness was measured using the eggshell thickness tester (ESTG-01, Orka Teachnology Ltd); Haugh unit, yolks color, and egg weight were measured by multifunctional egg quality tester (EA-01, Orka Technology Ltd). The eggshell color was measured by QCR color reflectometer (QCR SPA, TSS England). Weigh the eggshell, then separate the yolk with a separator, and then weigh the ratio of yolk and the ratio of albumen.

Blood Sampling and Biochemical Analysis

At the end of the experiment, blood samples were collected from the wing veins of the laying hens on the same day of sampling and centrifuged at 3,000 rpm for 15 min at room temperature to separate the serum. After that, the serum samples were collected by a pipette into 1.5-ml tubes and stored at −20°C. Triglyceride (TG), uric acid (UA), urea, total protein (TP), albumin (ALB), and immunoglobulin M (IgM) in serum were determined using an automatic biochemical analyzer (7600, Hitachi, Japan) according to the manufacturer's instructions. Superoxide dismutase (SOD) and glutathione (GSH) in the serum were determined using a commercial kit (Nanjing Jiancheng Bioengineering Institute, Nanjing, China) according to the kit instructions.

Collecting Samples

Seventy hens were euthanized and weighed by a sodium pentobarbital injection (0.4 ml/kg·BW; Sile Biological Technology Co., Ltd., Guangzhou, China). Abdominal adipose tissue was weighed to calculate the yield of abdominal fat (AFY). The liver, kidneys, fallopian tubes, and ovaries were removed, weighed, and the number of follicles was recorded to calculate the liver index, fallopian tube index, and ovary index.

DNA Extraction, Amplification, and Sequencing

The cecal contents of laying hens were collected, immediately frozen in liquid nitrogen, and stored at −80°C. Cecal microbial DNA was isolated with an Omega Bio-tek stool DNA kit (Omega, Norcross, GA, USA) and quantified by a NanoDrop 2000 spectrophotometer (Thermo Scientific, Waltham, MA, USA). Then, the V3–V4 region of the 16S rRNA gene was amplified with 338F and 806R primers with the sequence of 5′-ACTCCTACGGGAGCAGCA-3′ and 5′-GGACTACHVGGGTWTCTAAT-3′. Afterward, DNA samples were quantified, followed by the amplification of V3V4 hypervariable region of the 16S rDNA. Final amplicon pool was evaluated by the AxyPrep DNA gel extraction kit (Axygen Biosciences, Union City, CA, USA). Paired-end reads were generated with an Illumina MiSeq PE250 (Shanghai MajorBio Biopharma Technology Co., Ltd., Shanghai, China), and the reads were filtered out with default parameters.

Statistical Analysis

All results were subjected to a one-way ANOVA procedure and differences were examined using Duncan's multiple range test to evaluate the differences within treatments using SPSS version 18.0 (SPSS Institute Inc., Chicago, USA). The trends of the linear and quadratic analyses were conducted using SAS software version 8.0 (version 9.2, SAS Institute Inc., Cary, NC, USA). Differences were considered significant at $p < 0.05$. Data were expressed as the mean ± SE.

The raw paired-end reads were assembled into longer sequences, and quality was filtered by PANDAseq (version 2.9) to remove the low-quality reads. The high-quality sequences were clustered into operational taxonomic units (OTUs) with a 97% similarity using UPARSE (version 7.0) in QIIME (version 1.17) (32, 33), and the chimeric sequences were removed using UCHIME (34). Taxonomy was assigned to OTUs using the RDP classifier. The subsequent clean reads were clustered as OTUs using UPARSE (version 7.0) and annotated with the SILVA 16S rRNA gene database using the MOTHUR program (version v.1.30.1) (35). Alpha-diversity (the Chao index, Ace index, and Sob index) was calculated based on the profiles of OTU by the MOTHUR program (36). Bar plots and heat maps were generated with the "vegan" package in R (version 3.3.1). A principal coordinate analysis (PCoA) was performed based on the Bray–Curtis distance using QIIME (version 1.17). An analysis of similarities (ANOSIM) was performed to compare the similarity of bacterial communities among groups using the "vegan" package of R (version 3.3.1). A linear discriminant analysis (LDA) effect size (LEfSe) was performed to identify the bacterial taxa that are differentially enriched in different bacterial communities. In a redundancy analysis (RDA), the variance between the samples (genus-level relative bacterial abundance) is explained by the phenotype of laying hens, which were fitted to corresponding matrices in the resulting illustration (37–39). Phylogenetic Investigation of Communities by Reconstruction of Unobserved States (PICRUSt) was also used to obtain a deeper insight into different pathways based on the Kyoto Encyclopedia of Genes and Genomes (KEGG) orthology between the four groups (40). Finally, the correlations between key parameters and bacterial communities were assessed by Spearman's correlation analysis using the "pheatmap" package in R (version 3.3.1). Data were expressed as mean values.

RESULTS

Effects of Different Levels of Met Supplementation on the Laying Performance of Laying Hens With Low Protein Diets

During the experiment period (**Table 1**), dietary Met levels had significant positive effects on the performance of laying hens.

TABLE 1 | Effects of different dietary Met supplementation in low protein diets on the growth and laying performance of laying hens that are 38–50 weeks.

Indexes	0.25% Met group	0.31% Met group	0.38% Met group	0.47% Met group	SE[d]	*P*-value	Linear *P*-value	Quadratic *P*-value
IBW (g)	1,507.3	1,507.6	1,502.9	1,512	15.77	0.982	0.896	0.78
FBW (g)	1,509.9[b]	1,647.2[a]	1,629.2[a]	1,652.9[a]	17.94	<0.001	<0.001	0.003
ADG (g/d)	0.03[b]	1.70[a]	1.54[a]	1.72[a]	0.19	<0.001	<0.001	<0.001
EP (%)	68.1[b]	83.9[a]	87.4[a]	86.9[a]	1.47	<0.001	<0.001	<0.001
EW (g)	56.4[c]	60.6[a,b]	60.1[b]	61.7[a]	0.39	<0.001	<0.001	0.002
EM (g/d)	38.4[b]	50.8[a]	52.5[a]	53.5[a]	0.87	<0.001	<0.001	<0.001
ADFI (g/d)	97.4[b]	110.2[a]	109.6[a]	110.7[a]	1.3	<0.001	<0.001	<0.001
FER	2.54[a]	2.17[b]	2.09[b]	2.07[b]	0.03	<0.001	<0.001	<0.001
AFY (%)	1.32[b]	2.52[a,b]	3.29[a]	3.08[a]	0.36	0.002	0.001	0.055
Liver index (%)	2.64[a]	2.35[a,b]	2.23[b]	2.29[a,b]	0.1	0.037	0.014	0.104

[a,b,c]*Means within a column with no common superscripts differ ($p < 0.05$).*
[d]*Pooled SEM.*

TABLE 2 | The effects of different dietary met supplementation in low protein diets on the egg quality of 42-, 46-, and 50-week-old laying hens.

Indexes	Age	0.25% Met group	0.31% Met group	0.38% Met group	0.47% Met group	SE[c]	*P*-value		
							Total	Linear	Quadratic
Egg weight (g)	42	55.90[b]	59.94[a]	60.24[a]	61.90[a]	0.73	<0.001	<0.001	0.102
	46	58.47[b]	61.67[a]	61.20[a,b]	61.70[a]	0.84	0.019	0.014	0.107
	50	56.48[b]	60.23[a]	60.60[a]	61.61[a]	0.76	<0.001	<0.001	0.073
Shell (%)	42	10.94	10.81	10.8	10.63	0.15	0.523	0.154	0.922
	46	10.95[a]	10.10[b]	10.93[a,b]	10.70[a,b]	0.23	0.033	0.930	0.177
	50	10.8	10.8	10.72	10.37	0.19	0.345	0.118	0.366
Albumen (%)	42	62.36[b]	63.68[a]	63.53[a,b]	63.36[a,b]	0.32	0.025	0.056	0.026
	46	63.56	65.55	63.17	62.83	1.06	0.270	0.340	0.280
	50	61.37[b]	62.95[a,b]	62.32[a,b]	63.62[a]	0.54	0.026	0.012	0.79
Yolk (%)	42	26.69[a]	25.50[b]	25.68[a,b]	26.01[a,b]	0.28	0.018	0.138	0.008
	46	25.53	24.20	25.82	26.47	1	0.417	0.315	0.323
	50	27.82	26.27	26.96	26.01	0.52	0.071	0.045	0.560
Shell color	42	0.58	0.57	0.56	0.55	0.01	0.337	0.070	0.913
	46	55.89	56.53	54.82	56.98	0.95	0.417	0.711	0.424
	50	0.46	0.46	0.46	0.44	0.01	0.101	0.135	0.045
Shell thickness (mm)	42	0.58	0.57	0.56	0.55	0.01	0.337	0.070	0.913
	46	0.46[b]	0.46[b]	0.48[a]	0.46[b]	0.01	0.001	0.189	0.229
	50	0.46	0.46	0.46	0.44	0.01	0.101	0.135	0.045
Shell strength (N)	42	41.02	42.72	40.49	39.75	1.27	0.384	0.286	0.332
	46	40.98	40.9	41.25	40.61	1.32	0.989	0.896	0.835
	50	38.25	40.5	38.13	36.57	1.48	0.326	0.267	0.204
Haugh unit	42	84.49	83.23	82.96	83.47	1.03	0.740	0.471	0.388
	46	85.85	84.00	80.41	83.38	1.80	0.216	0.168	0.182
	50	82.23	85.58	81.61	82.53	1.89	0.466	0.717	0.523
Yolk color	42	4.86	4.77	4.83	4.60	0.10	0.240	0.100	0.500
	46	4.78	4.71	4.80	4.83	0.11	0.897	0.630	0.680
	50	4.73[a]	4.27[b]	4.43[a,b]	4.70[a,b]	0.13	0.029	0.906	0.004

[a,b]*Means within a column with no common superscripts differ ($p < 0.05$).*
[c]*Pooled SEM.*

There were no significant differences in FBW, ADG, EP, EW, EM, and ADFI between the 0.31, 0.38, and 0.47% Met groups, but they were significantly higher than those in the 0.25% Met group ($p < 0.001$). On the contrary, the FER in the 0.25% Met

TABLE 3 | The effects of different dietary Met supplementation in low protein diets on the serum parameters of laying hens that are 38–50 weeks.

Indexes	0.25% Met group	0.31% Met group	0.38% Met group	0.47% Met group	SE[c]	*P*-value	Linear *P*-value	Quadratic *P*-value
TG (mmol/L)	7.64[b]	8.51[b]	10.56[a]	11.54[a]	0.39	<0.001	<0.001	0.89
UA (μmol/L)	82.33[a]	65.00[b]	67.22[a,b]	64.56[b]	4.48	0.03	0.02	0.11
Urea (mmol/L)	0.31	0.32	0.33	0.37	0.02	0.31	0.09	0.45
TP (g/L)	37.47	35.23	39.52	39.28	1.6	0.22	0.18	0.54
ALB (g/L)	12.81[a,b]	11.41[b]	13.62[a]	13.00[a,b]	0.42	0.006	0.15	0.36
P (ng/mL)	0.84	0.84	1.05	1.13	0.19	0.61	0.21	0.85
E3 (pg/mL)	101.03[a,b]	83.91[b]	165.41[a]	172.78[a]	18.74	0.003	0.001	0.52
IgG (g/L)	5.98	6.19	6.08	6.53	0.27	0.52	0.21	0.67
IgA (g/L)	1.06[a,b]	0.99[b]	1.04[a,b]	1.12[a]	0.03	0.04	0.09	0.02
IgM (g/L)	0.8	0.83	0.79	0.89	0.03	0.15	0.11	0.32

[a,b]*Means within a column with no common superscripts differ ($p < 0.05$).*
[c]*Pooled SEM.*

group was significantly higher than the other three groups ($p < 0.001$), while there was no significant difference among the other three groups. The AFY in the 0.47 and 0.38% Met groups was significantly higher than that in the 0.25% Met group ($p < 0.01$). The EW in the 0.38% Met group was significantly lower than that in the 0.47% Met group ($p < 0.001$), the liver index was lower than that in the 0.25% Met group ($p < 0.05$), and IBW was not significantly affected by different dietary Met levels (**Table 1**).

When the diet was supplemented with 0.38% Met, the maximum EP (88.83%) was obtained. When the Met level was increased to 0.41%, the maximum EM (54.32 g/d) and minimum FER (2.04) were obtained, and the Met intake was 0.45, 0.46, and 0.46 g/d, respectively (**Supplementary Table 2**). When the dietary sulfur amino acid content was 0.62%, the maximum EP (88.28%) was obtained. When the diet contained 0.63% sulfur amino acids, the maximum EM (53.98 g/d) and the minimum FER (2.05) were obtained. At this time, the intake of sulfur amino acids was 0.69, 0.7, and 0.7 g/day, respectively (**Supplementary Table 2**).

Effects of Different Levels of Met Supplementation on the Egg Quality of Laying Hens With Low Protein Diets

As shown in **Table 2**, the EW in the 0.25% Met group at 42 and 50 weeks of age was significantly lower than that of the other three groups ($p < 0.001$). The EW at 46 weeks of age in the 0.25% Met group was lower than that in the 0.31 and 0.47% Met groups ($p < 0.05$). The eggshell proportion at 46 weeks of age in the 0.25% Met group was higher than that in the 0.31% Met group ($p < 0.05$). The albumen ratio at 42 weeks of age in the 0.25% Met group was lower than that in the 0.31% Met group ($p < 0.05$), while the albumen ratio at 50 weeks of age was lower than that in the 0.47% Met group ($p < 0.05$). On the contrary, the yolk ratio at 42 weeks of age in the 0.25% Met group was higher than that in the 0.31% Met group ($p < 0.05$). The eggshell thickness in the 0.38% Met group at 46 weeks of age was significantly higher than that in the other three groups ($p < 0.01$), and there was no significant difference among the other three groups. The yolk color value in the 0.31% Met group at 50 weeks of age was the lowest and lower than that of the 0.25% Met group ($p < 0.05$). However, other indicators such as eggshell color, eggshell strength, and Haugh unit were not significantly affected by the different levels of dietary Met (**Table 2**).

Effects of Different Levels of Met Supplementation on the Host Metabolism of Laying Hens With Low Protein Diets

The different levels of dietary Met had significant effects on a number of biochemical indices (e.g., TG, ALB, UA, E2, and IgA) in the serum of laying hens. In particular, the TG and E2 in the 0.47% Met group were significantly higher than those in the 0.31% Met group ($p < 0.01$). Furthermore, IgA was higher than that in the 0.31% Met group ($p < 0.05$), while the TG, ALB, and E2 in the 0.38% Met group were significantly higher than those in the 0.31% Met group ($p < 0.01$). The TG in the 0.25% Met group was significantly lower than that in the 0.38 and 0.47% Met groups ($p < 0.001$), and UA was higher than that in the 0.31 and 0.47% Met groups ($p < 0.05$). However, other biochemical indices were not significantly affected by different dietary Met levels (e.g., UREA, TP, P, IgG, and IgM) (**Table 3**).

Effects of Different Levels of Met Supplementation on the Reproductive System of Laying Hens With Low Protein Diets

As shown in **Table 4**, the different levels of dietary Met have extremely significant effects on tubal weight. The tubal weight of laying hens in the 0.47% Met group was significantly higher than that in the 0.25% Met group ($p < 0.01$) but it had no significant effects on oviduct length, ovary weight, and ovary weight after the removal of dominant follicles, etc., (**Table 4**).

TABLE 4 | The effects of different dietary Met supplementation in low protein diets on the reproductive system of laying hens that are 38–50 weeks.

Indexes	0.25% Met group	0.31% Met group	0.38% Met group	0.47% Met group	SE[c]	*P*-value	Linear *P*-value	Quadratic *P*-value
Oviduct weight (g)	43.8[b]	49.7[a,b]	50.7[a,b]	55.3[a]	2.19	0.009	0.001	0.774
Oviduct length (cm)	67.9	73.9	71	71.6	2.4	0.383	0.444	0.278
Ovary weight (g)	33.1	34.3	35.6	42.3	2.5	0.061	0.014	0.28
Ovarian weight except the dominant follicles (g)	5.3	5.7	5.6	5.3	0.6	0.937	0.976	0.535
The number of rhubarb follicles	3.8	3.2	3.3	3.9	0.2	0.072	0.63	0.01
The number of small yellow follicles	1	1.2	1.2	1	0.1	0.227	1	0.04
The number of white follicles	0.9	0.9	0.9	1.4	0.29	0.455	0.214	0.352

[a,b]*Means within a column with no common superscripts differ ($p < 0.05$).*
[c]*Pooled SEM.*

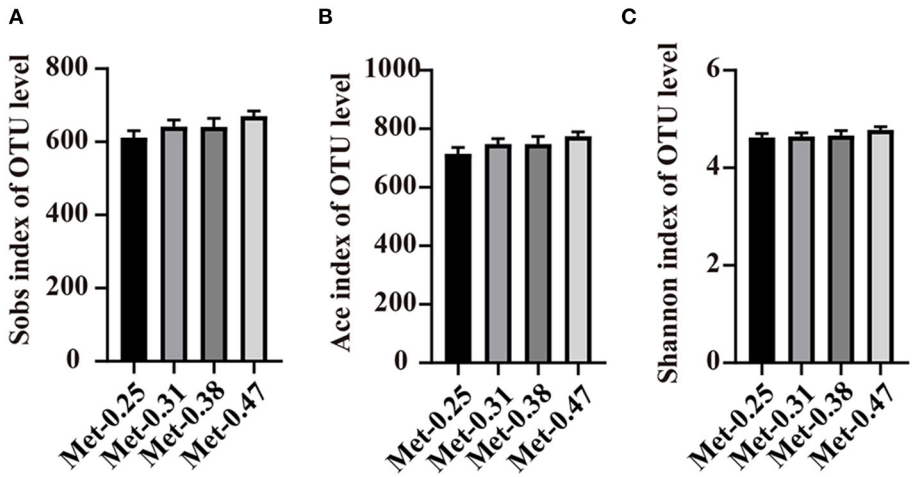

FIGURE 1 | The effects of different dietary methionine (Met) supplementation in low protein diets on the alpha diversity of the cecal microbiota in laying hens. **(A)** Sobs index of the community diversity. **(B)** Ace index of the community richness. **(C)** Shannon index of the community diversity. Data were presented as means ± SEM (n = 9 per group). Significant differences were tested by a Student's *t*-test.

Effects of Different Levels of Met Supplementation on the Gut Microbial Composition and Function of Laying Hens With Low Protein Diets

To investigate the effects of different Met levels in low protein diets on the gut microbial composition of laying hens, 16S rDNA sequencing was performed. In the end, 2,154,182 sequences were obtained. Through a clustering operation, the sequences were divided into many groups according to 97% similarity. Each group was an OTU, and a total of 1,075 OTUs were obtained, which could be divided into 19 phyla, 34 classes, and 174 genera. The results of the alpha diversity analysis showed that there was no significant difference between the Sobs index, ACE index, and Shannon index among the four treatment groups (**Figures 1A–C**).

The relative abundance at the phylum and genus levels was studied. Notably, different levels of Met in diets changed the structure and composition of the intestinal microorganism of laying hens. From the perspective of the phylum level, *Bacteroidetes* and *Firmicutes* are the two kinds of bacteria that account for the largest proportion in the cecum of laying hens, exceeding 95% of the total cecum bacteria. In addition, the proportion of *Firmicute/Bacteroidetes* in the 0.25% Met group was similar to that in the 0.47% Met group, but both were lower than that in the 0.38% Met group and higher than that in the 0.31% Met group (**Figure 2A**). At the genus level, *Bacteroides, Rikenellaceae_RC9_gut_group, Lactobacillus,* and *Unclassified_O_Bacteroidales* accounted for nearly 50% of the total cecal bacteria. *Rikenellaceae_RC9_gut_group* was the highest in the 0.31% Met group, followed by the 0.47, 0.25, and 0.38% Met groups. The relative abundance of *Lactobacillus* in the cecum of laying hens also increased with the increase of dietary Met level (**Supplementary Table 3**). The proportions of *Bacteroides* in all treatment groups was similar, with these proportions in the 0.25, 0.31, 0.38, and 0.47% Met groups being 19.62, 17.37, 18.69, and 20.31%, respectively (**Figure 2B**). The results of the PCoA showed that the gut microbiota in the 0.25, 0.31, 0.38, and 0.47% Met groups were aggregated, respectively (**Figure 2C**). These results indicated

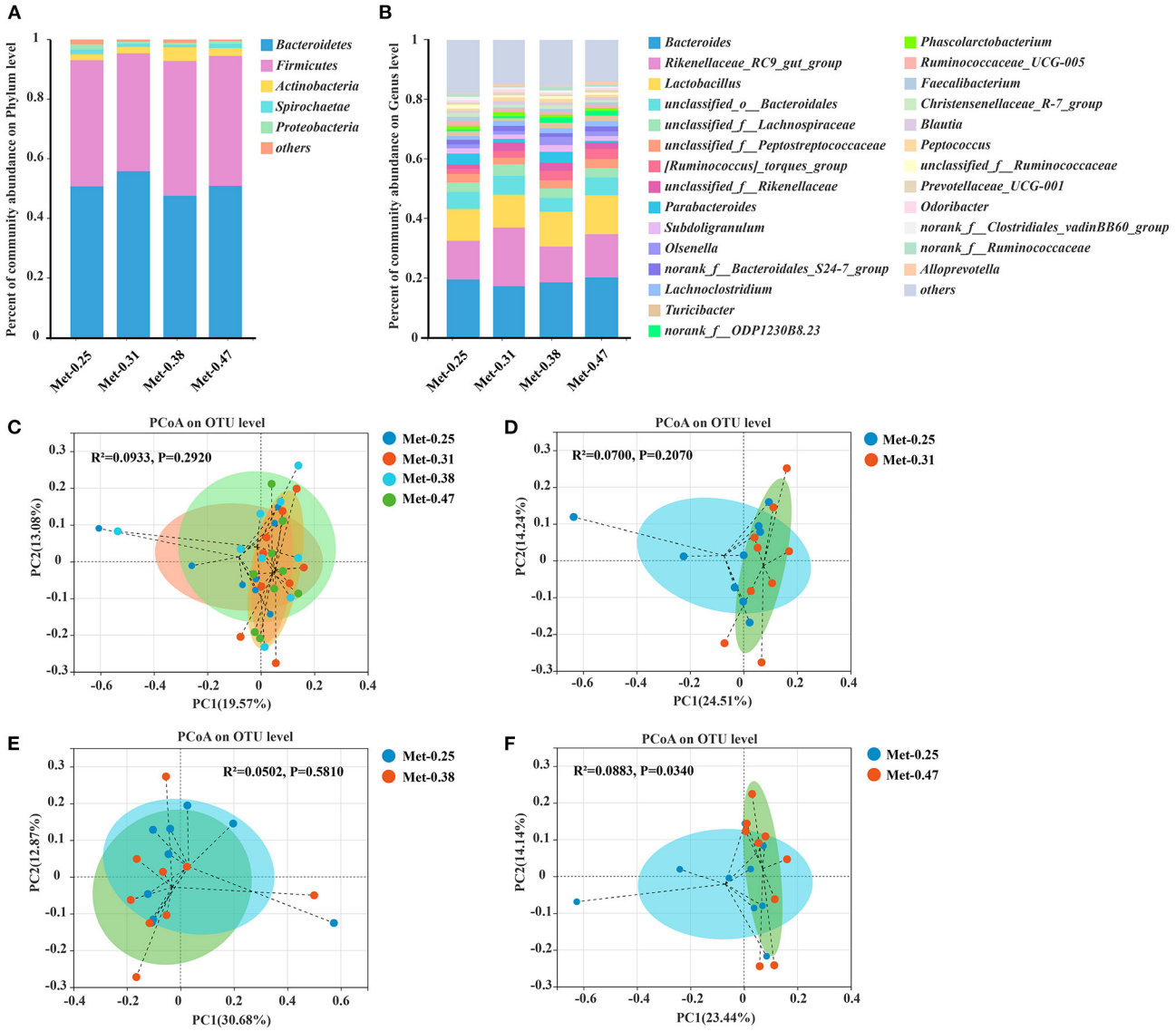

FIGURE 2 | The effects of different dietary Met supplementation in low protein diets on the relative abundance in the cecal microbiota of laying hens and the principal coordinate analysis (PCoA) (Bray–Curtis distance) plot of the gut microbial community structure between the 0.25% Met group, 0.31% Met group, 0.38% Met group, and 0.47% Met group ($n = 9$ per group). **(A)** Relative abundance of gut microbiota at the phylum level ($n = 9$ per group). **(B)** Relative abundance of gut microbiota at the genus level ($n = 9$ per group). **(C)** The PCoA in the four treatments. **(D)** The PCoA in the 0.25 and 0.31% Met groups. **(E)** The PCoA in the 0.25 and 0.38% Met groups. **(F)** The PCoA in the 0.25 and 0.47% Met groups.

that different dietary Met levels changed the gut microbiota structure of laying hens to some extent. Moreover, compared with the distribution of spots in the 0.25% Met group, the distribution of spots in the 0.31 and 0.47% Met groups was more dispersed, and the distribution pattern of spots in the 0.38% Met group was similar to that in the 0.25% Met group (**Figures 2D–F**).

The LEfSe was used to figure out which bacterial taxa were statistically and biologically responsible for these differences. As shown in **Figure 3**, compared with the 0.25% Met group, *[Eubacterium]_brachy_group*, *unclassified_p_Bacteroidetes*, *norank_c_OPB35_soil_group*, *Butyricimonas, Solobacterium*, and *Streptococcus* were enriched in the 0.31% Met group (**Figure 3A**). *Lachnoclostridium, [Eubacterium]_brachy_group, Faecalitalea, Faecalicoccus, Lachnospiraceae_UCG-002, Family_XIII_AD3011_group,* and *Enterococcus* were enriched in the 0.38% Met group (**Figure 3B**). *[Ruminococcus]_torques_group*, *Erysipelatoclostridium*, *[Eubacterium]_brachy_group*, *Brachyspira, Faecalicoccus*, *Faecalitalea*, *Coprococcus_1*, *[Clostridium]_innocuum_group*, and *Lachnospiraceae_FCS020_group* were enriched in the 0.47% Met group (**Figure 3C**).

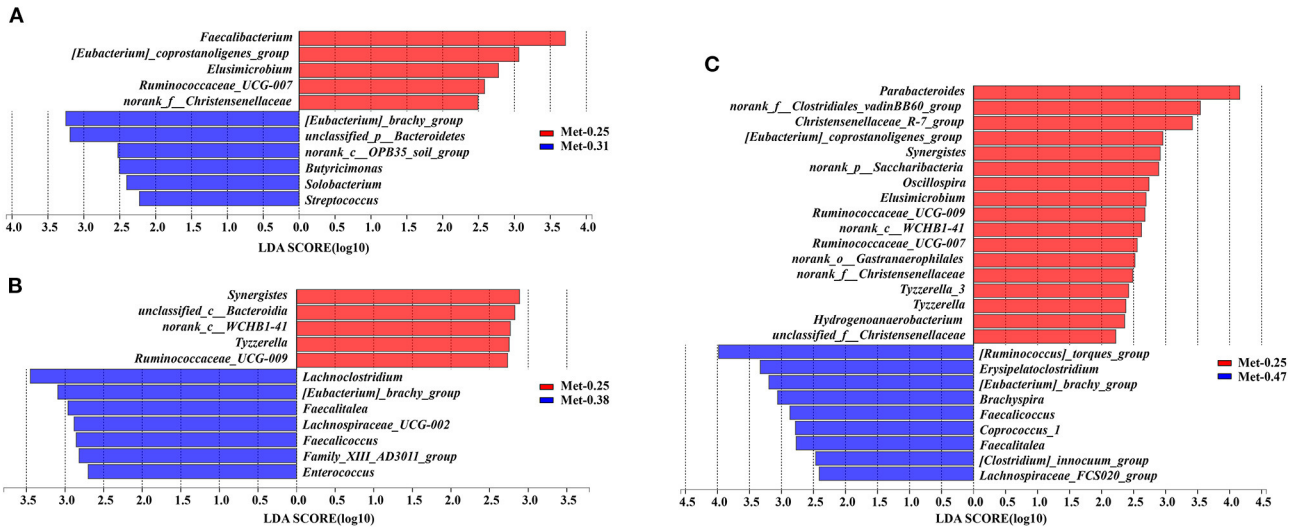

FIGURE 3 | Differentially abundant genera in the gut microbiota of laying hens between the groups supplemented with different levels of Met. Histograms of the (linear discriminate analysis) LDA score (threshold ≥ 2) are plotted. An LDA effect size (LEfSe) was performed to determine the difference in abundance ($n = 9$ per group). **(A)** The LEfSe analysis of the gut microbiota in the 0.25 and 0.31% Met groups. **(B)** The LEfSe analysis of the gut microbiota in the 0.25 and 0.38% Met groups. **(C)** The LEfSe analysis of the gut microbiota in the 0.25 and 0.47% Met groups.

As shown in **Supplementary Figures 1A,B**, the different levels of dietary Met have significant effects on the intestinal microorganisms of laying hens. For example, compared with the other three groups, the 0.25% Met group has more significant effects on *[Eubacterium]_coprostanoligenes_group*, *Ruminococcaceae_UCG-007*, *norank_f_Christensenellaceae*, *Elusimicrobium*, *Ruminococcaceae_UCG-009*, *norank_c_WCHB1-41*, and *norank_o_Gastranaerophilales*. In addition, *Ruminococcaceae_UCG-009* and *Norank_O_gastranaerophilales* were affected significantly, and the 0.31% Met group has more significant effects on [Eubacterium]_brachy_group. The 0.38% Met group has more significant effects on norank_p_Saccharibacteria, Faecalitalea, and *Family_XIII_AD3011_group*, while the 0.47% Met group has more significant effects on *Treponema_2*, *Coprococcus_1*, *Faecalicoccus, and [Clostridium]_innocuum_group* (**Supplementary Figures 1A,B**). To elucidate the underlying molecular mechanism of Met in a low protein diet on the gut microbial function of hens, a KEGG pathway analysis were performed (**Figure 4B**). Interestingly, the most enriched pathways were closely related to carbohydrate metabolism, amino acid metabolism, energy metabolism, metabolism of cofactors and vitamins, and lipid metabolism.

Correlation Between the Differential Microbes Induced by the Supplementation of Met in Low Protein Diets and Key Parameters

In order to predict the correlation between the intestinal microbial communities and key parameters, an RDA and Spearman correlation matrix were performed. As shown in **Figures 4A**, **5**, *Ruminococcaceae_UCG-007, Ruminococcaceae_UCG-00*, *norank_o_Gastranaerophilales*, and *norank_c_WCHB1-41* were positively correlated with ADFI, EW, FBW, TG, EM, EP, and ADG, among which *Ruminococcaceae_UCG-009* and *Norank_o_gastranaerophilales* were negatively correlated with FER ($p < 0.05$). On the contrary, *Faecalitalea* was negatively correlated with these traits ($p < 0.05$), while it was positively correlated with FER, but not significantly. *Elusimicrobium* was positively correlated with ADFI, EW, FBW, EM, EP, and ADG but negatively correlated with FER ($p < 0.05$). *Norank_f_Christensenellaceae* was significantly positively correlated with ADFI, EW, TG, EM, and ADG, but negatively correlated with FER and UA ($p < 0.05$). *Norank_P_Saccharibacteria* was significantly positively correlated with EW, ADFI, FBW, and TG ($p < 0.05$). *[Eubacterium]_coprostanoligenes_group* was significantly positively correlated with EW ($p < 0.05$). In contrast, *Faecalicoccus* was significantly negatively correlated with ADFI, FBW, TG, EM, EP, and ADG ($p < 0.01$), but positively correlated with FER ($p < 0.05$). *Family_xii_ad3011_group* was negatively correlated with ADFI, but positively correlated with UA ($p < 0.05$). *[Eubacterium]_Brachy_group* was negatively correlated with ADFI, FBW, EM, EP, and ADG ($p < 0.05$). *Coprococcus_1* was negatively correlated with EW and TG ($p < 0.05$). *[Clostridium]_innocuum_group* was significantly negatively correlated with FBW and TG ($p < 0.05$). There was a certain correlation between the production traits and other unmentioned intestinal microflora of laying hens, but their influence is not significant (**Figure 5**).

DISCUSSION

For a long time, Met has been used as a feed additive in livestock and poultry diets to maintain animal health and growth performance. According to previous studies, because of the

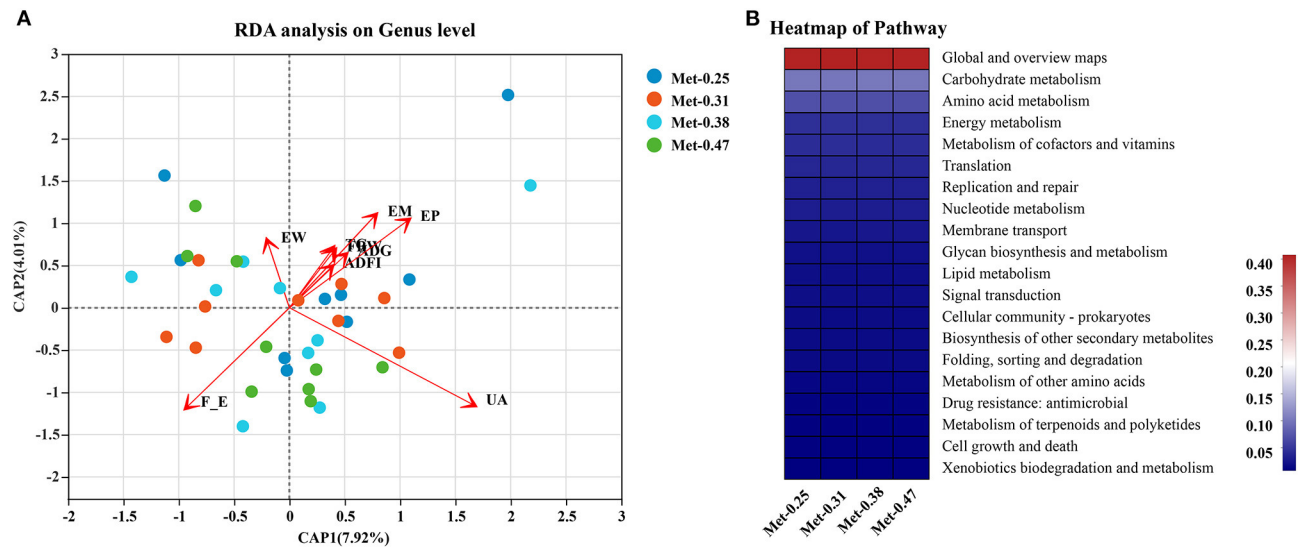

FIGURE 4 | The effects of different dietary Met supplementation in low protein diets on the composition and function of gut microbiota of laying hens. **(A)** A redundancy analysis (RDA) of the distinctive genera and the phenotype of laying hens. **(B)** The 20 most significant Kyoto Encyclopedia for Genes and Genomes (KEGG) pathways upon different dietary Met supplementation in low protein diets.

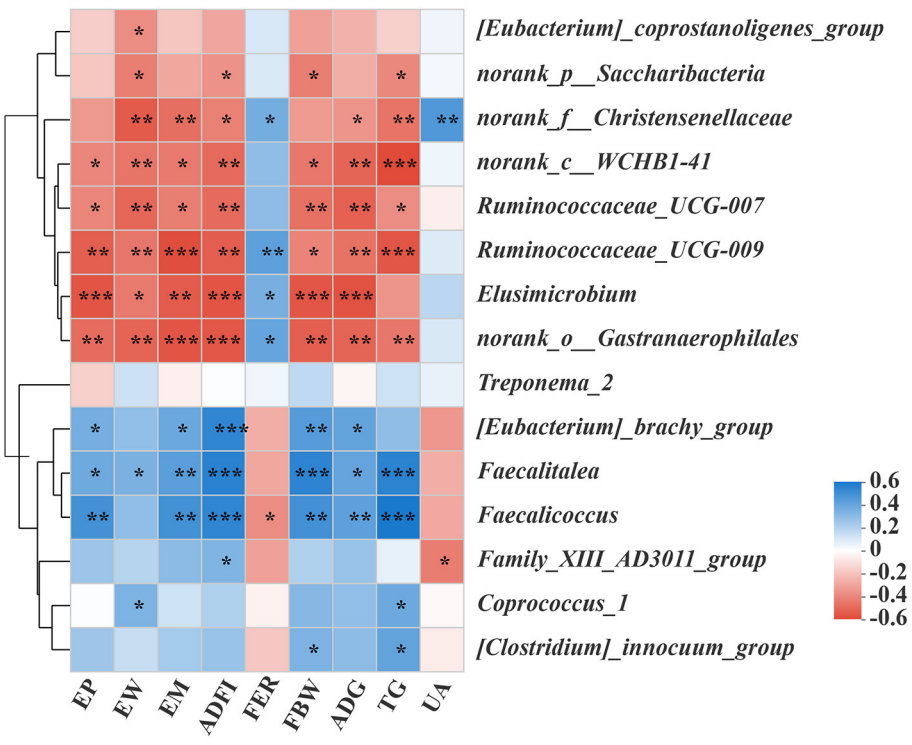

FIGURE 5 | The effects of different dietary Met supplementation in low protein diets on the difference of the gut microbiota and its correlation with the phenotype of laying hens. The correlation between the various gut microbiota and the phenotype of laying hens. Asterisks indicate significant correlations (*$p \leq 0.05$, **$p \leq 0.01$, ***$p \leq 0.001$). The blue represents a significantly positive correlation ($p \leq 0.05$), the red represents a significantly negative correlation ($p \leq 0.05$), and the white represents no significant correlation ($p > 0.05$).

lack of essential amino acids in low protein diets, production performance and egg quality are negatively affected, the intestinal morphology is damaged, and the immune response level is reduced (41–43). In this study, Peking Pink laying hens were selected as the experimental model to explore the effects of different levels of Met in the low protein diet on the performance, egg quality, serum biochemical indexes, and gut microbial composition of the laying hens. Our results showed that the supplementation of Met in the low protein diet could significantly improve various indices of laying hens.

When the dietary protein level is reduced to 13–14%, the performance of laying hens will be directly affected if the synthetic amino acids are not supplemented in time (44, 45). Keshavarz showed that the addition of synthetic amino acids to a low protein diet could effectively improve the performance of laying hens and reduce nitrogen emissions, which is also consistent with the results of others (46–48). From these, we can understand the significance of additional amino acids in the low protein diet, which is the same as the results in this experiment.

Studies have found that, if the Met intake of laying hens was increased, then EW would increase. Meanwhile, laying performance would be significantly improved, but with a decreased FER (19, 49). Similarly, we obtained the quadratic equation between Met and sulfur-containing amino acids and EP, EW, and FER. Within a certain range, the increase of Met level can increase EP and EM, while decreasing FER. These results indicated that the supplementation of Met in diets promotes the feeding and growth of laying hens and improves feed conversion ratio, which were also similar with Esteve (50). In our experiment, with the increase of Met, egg weight also increased at each stage. However, different Met levels had no significant effects on eggshell color, strength, Haugh unit, and other indices.

A number of indicators in the serum often reflect the health status of animals. When animals are in a healthy state, protein synthesis increases along with TP and ALB. In our experiment, TP and ALB in the 0.38 and 0.47% Met groups were higher than those in the other Met groups. The IgA in the 0.47% Met group was higher than that in the other three groups, which was similar to the research results of Liu et al. (51). Those indicated that the metabolism of laying hens in the 0.47% Met group was more vigorous, and the level of immune response was higher. As one of the end-products of protein metabolism in poultry, UA is usually used as an indicator to measure the requirement of amino acids. It reflects the level of protein metabolism in animals (52). Our results showed that the changes of UA were stable when the Met level was in the range of 0.31–0.47%, and UA was lower than that in the 0.25% Met group. Therefore, it could be inferred that the amino acids in laying hens in the three groups with higher Met levels were more fully utilized.

Dietary energy levels are the main nutritional factors affecting egg quality (53). Our results showed that there was a positive linear correlation between the dietary Met level and TG, which was similar to the difference in EW among all groups. We postulated that a higher TG in serum could synthesize more fat and fully meet the energy needs of laying hens, thus affecting EW. A certain amount of abdominal fat storage is beneficial to prevent insufficient energy intake from affecting laying performance (54), and, based on the results of the 0.25% Met group, we inferred that when the Met in the diet is insufficient, the liver metabolism of laying hens is disturbed and the fat transport is obstructed, leading to fatty liver disease in the end.

Normal and stable microflora is an important prerequisite to ensure the health of poultry. Intestinal microflora is involved in the metabolism and growth of the host, and also affects feed conversion and nutrient digestion and absorption by changing the intestinal tissue morphology of poultry, thus affecting their performance (55–57). Our results showed that, at the genus level, *Bacteroides*, *Rikenellaceae_RC9_gut_group*, *Lactobacillus*, and *unclassified_o_Bacteroidales* were the dominant genera accounting for nearly 50% of the total cecal bacteria of laying hens. In the meantime, the *Lactobacillus* proportion increased with the increase of Met. Yan used a metagenomic analysis technology to find that *Lactobacillus* could promote the absorption of nutrients and improve the feeding efficiency of poultry (58). Some scholars have found that *Lactobacillus* and *Bifidobacterium* can synthesize a variety of VB beneficial to animals by participating in their metabolism. It can also convert mineral elements into ions that are easily absorbed by animals to improve their utilization rate (59). In contrast to the change in the proportion of *Lactobacillus*, the proportion of *Faecalibacterium* decreases with the increase of Met in the diet. *Faecalitalea* and *Faecalicoccus* of *Clostridium* had significantly negative effects on ADFI, FBW, TG, EM, EP, ADG, and other indices, but had positive effects on FER. Other studies have shown that *Clostridia* has an adverse effect on animal performance (60), and our results are consistent with this finding. We can conclude that the supplementation of Met in diets is beneficial to laying hens. In conclusion, it can be inferred that Met in low protein diets may improve the intestinal morphology and production performance of laying hens by promoting beneficial bacteria proliferation and competitively inhibiting harmful bacteria proliferation or infection.

CONCLUSION

The use of the low protein diet could alleviate the current situation of the raw material shortage of protein feed and reduce the nitrogen emission from the feces and urine of livestock and poultry to reduce environmental pollution. Adding Met to the low protein diet could have positive effects on the production performance, reproductive system, host metabolism, and gut microbial composition of laying hens. For example, the addition of Met increased the abundance of *Lactobacillus* and decreased the proportion of *Faecalibacterium* in the gut. Meanwhile, there were also significant correlations between the gut microbiota and traits of laying hens. Specifically, the proportion of *Faecalicoccus* was significantly positively correlated with FER, but negatively correlated with ADFI, FBW, ADG, and other traits. At present, there are few studies on the effects of low protein diets on the gut microflora of laying hens. We hoped that our study will fill in some gaps in this field.

DATA AVAILABILITY STATEMENT

The datasets presented in this study can be found in online repositories. The names of the repository/repositories and accession number(s) can be found at: https://www.ncbi.nlm.nih.gov/, PRJNA745253.

ETHICS STATEMENT

The animal study was reviewed and approved by China Agricultural University Animal Care and Use Committee (AW32301202-2-1, Beijing, China).

AUTHOR CONTRIBUTIONS

MM, QM, JZ, and SG designed the study. MM, SG, and SH conducted the experiments, drafted the manuscript, polished the manuscript, and finished the submission. MM, ML, and SG guided the analysis of the experimental data. QM, LZ, and JZ helped with revisiting and reviewing the manuscript. All authors read and approved the final manuscript.

FUNDING

This study was supported by the National Science Foundation of China (Grant No. 31772621), a Special Fund for China Agricultural Research System program (CARS-40-K08), National Key Research and Development Program of China (2017YFD0500500), and the Special Fund from Chinese Universities Scientific Fund (2018TC043).

ACKNOWLEDGMENTS

We thank all the technicians in the experimental animal facility of the China Agricultural University for providing the daily care of the laying hens. We also thank Shanghai Majorbio Bio-Pharm Technology Co. for their bioinformatic analysis of the data.

SUPPLEMENTARY MATERIAL

The Supplementary Material for this article can be found online at: https://www.frontiersin.org/articles/10.3389/fnut.2021.739676/full#supplementary-material

Supplementary Figure 1 | The effects of different dietary Met supplementation in low protein diets on the difference of the gut microbiota of laying hens. **(A)** The LEfSe analysis of the gut microbiota in the four treatments. **(B)** The mean proportion of the gut microbiota in the four treatments.

Supplementary Table 1 | Ingredients and nutrient content of the diets (% DM).

Supplementary Table 2 | Regression equation between production performance and Met and sulfur-containing amino acid intake.

Supplementary Table 3 | The proportion of gut microbiota within the four Met groups on genus level.

REFERENCES

1. Ravindran V, Blair R. Feed resources for poultry production in Asia and the Pacific. III Animal protein sources. *World's Poult Sci J.* (2007) 49:219–35. doi: 10.1079/WPS19930020
2. Cao Y, Li D. Impact of increased demand for animal protein products in Asian countries: implications on global food security. *Anim Front.* (2013) 3:48–55. doi: 10.2527/af.2013-0024
3. Tomé D, Bos C. Dietary protein and nitrogen utilization. *J Nutr.* (2000) 130:1868s−73s. doi: 10.1093/jn/130.7.1868S
4. Tome D. Criteria and markers for protein quality assessment - a review. *Br J Nutr.* (2012) 108(Suppl.2):S222–9. doi: 10.1017/S0007114512002565
5. Kerr BJ, Ziemer CJ, Trabue SL, Crouse JD, Parkin TB. Manure composition of swine as affected by dietary protein and cellulose concentrations. *J Anim Sci.* (2006) 84:1584–92. doi: 10.2527/2006.8461584x
6. Aarnink AJA, Verstegen MWA. Nutrition, key factor to reduce environmental load from pig production. *Livest Sci.* (2007) 109:194–203. doi: 10.1016/j.livsci.2007.01.112
7. Hristov AN, Hanigan M, Cole A, Todd R, Mcallister TA, Ndegwa PM, et al. Review: ammonia emissions from dairy farms and beef feedlots. *Can J Anim Ence.* (2011) 91:1–35. doi: 10.4141/CJAS10034
8. Wang Y, Zhou J, Wang G, Cai S, Zeng X, Qiao S. Advances in low-protein diets for swine. *J Anim Sci Biotechnol.* (2018) 9:60. doi: 10.1186/s40104-018-0276-7
9. Nahm KH. Feed formulations to reduce N excretion and ammonia emission from poultry manure. *Bioresour Technol.* (2007) 98:2282–300. doi: 10.1016/j.biortech.2006.07.039
10. Kamran Z, Sarwar M, Nisa M, Nadeem MA, Mahmood S, Babar ME, et al. Effect of low-protein diets having constant energy-to-protein ratio on performance and carcass characteristics of broiler chickens from one to thirty-five days of age. *Poult Sci.* (2008) 87:468–74. doi: 10.3382/ps.2007-00180
11. Hernandez F, Megias M, Orengo J, Martinez S, Madrid J. Effect of dietary protein level on retention of nutrients, growth performance, litter composition and NH3 emission using a multi-phase feeding programme in broilers. *Span J Agri Res.* (2013) 11:736–46. doi: 10.5424/sjar/2013113-3597
12. Zhang S, Zeng X, Ren M, Mao X, Qiao S. Novel metabolic and physiological functions of branched chain amino acids: a review. *J Anim Sci Biotechnol.* (2017) 8:10. doi: 10.1186/s40104-016-0139-z
13. Nie C, He T, Zhang W, Zhang G, Ma X. Branched chain amino acids: beyond nutrition metabolism. *Int J Mol Sci.* (2018) 19:40954. doi: 10.3390/ijms19040954
14. Graciene CS, Edivaldo AG, Javer AVF. Performance of Japanese quails fed diets with low-protein and isoleucine. *Acta Sci Anim Sci.* (2016) 38:29533. doi: 10.4025/actascianimsci.v38i2.29533
15. Deng D, Huang RL, Li TJ, Wu GY, Xie MY, Tang ZR, et al. Nitrogen balance in barrows fed low-protein diets supplemented with essential amino acids. *Livestock Sci.* (2007) 109:220–3. doi: 10.1016/j.livsci.2007.01.122
16. Wu L, He LQ, Cui ZJ, Liu G, Yao K, Wu F, et al. Effects of reducing dietary protein on the expression of nutrition sensing genes (amino acid transporters) in weaned piglets. *J Zhejiang Univ Sci B.* (2015) 16:496–502. doi: 10.1631/jzus.B1400259
17. Ospina-Rojas IC, Murakami AE, Duarte CR, Eyng C, Oliveira CA, Janeiro V. Valine, isoleucine, arginine and glycine supplementation of low-protein diets for broiler chickens during the starter and grower phases. *Br Poult Sci.* (2014) 55:766–73. doi: 10.1080/00071668.2014.970125
18. Awad EA, Zulkifli I, Soleimani AF, Aljuobori A. Effects of feeding male and female broiler chickens on low-protein diets fortified with different dietary glycine levels under the hot and humid tropical climate. *Ital J Anim Sci.* (2017) 16:453–61. doi: 10.1080/1828051X.2017.1291288
19. Ratriyanto A, Indreswari R, Nuhriawangsa A, Purwanti E. Feed efficiency of diets with different energy and protein concentrations supplemented with methionine in laying quails. *Iop Conference.* (2018) 142. doi: 10.1088/1755-1315/142/1/012001
20. Bauchart-Thevret C, Stoll B, Burrin DG. Intestinal metabolism of sulfur amino acids. *Nutr Res Rev.* (2009) 22:175–87. doi: 10.1017/S0954422409990138

21. Chen Y, Li D, Dai Z, Piao X, Wu Z, Wang B, et al. L-methionine supplementation maintains the integrity and barrier function of the small-intestinal mucosa in post-weaning piglets. *Amino Acids.* (2014) 46:1131–42. doi: 10.1007/s00726-014-1675-5
22. Chen YP, Cheng YF, Li XH, Yang WL, Wen C, Zhuang S, et al. Effects of threonine supplementation on the growth performance, immunity, oxidative status, intestinal integrity, and barrier function of broilers at the early age. *Poult Sci.* (2017) 96:405–13. doi: 10.3382/ps/pew240
23. Zeitz JO, Kaltenböck S, Most E, Eder K. Effects of L-methionine on performance, gut morphology and antioxidant status in gut and liver of piglets in relation to DL-methionine. *J Anim Physiol Anim Nutr.* (2019) 103:242–50. doi: 10.1111/jpn.13000
24. Jariyahatthakij P, Chomtee B, Poeikhampha T, Loongyai W, Bunchasak C. Effects of adding methionine in low-protein diet and subsequently fed low-energy diet on productive performance, blood chemical profile, and lipid metabolism-related gene expression of broiler chickens. *Poult Sci.* (2018) 97:2021–33. doi: 10.3382/ps/pey034
25. Bunchasak C. Role of dietary methionine in poultry production. *J Poult Sci.* (2009) 46:169–79. doi: 10.2141/jpsa.46.169
26. Rama Rao SV, Praharaj NK, Ramasubba Reddy V, Panda AK. Interaction between genotype and dietary concentrations of methionine for immune function in commercial broilers. *Br Poult Sci.* (2003) 44:104–12. doi: 10.1080/0007166031000085283
27. Maroufyan E. The effect of methionine and threonine supplementations on immune responses of broiler chickens challenged with infectious bursal disease. *Am J Appl Sci.* (2010) 7:50. doi: 10.3844/ajassp.2010.44.50
28. Xie M, Hou SS, Huang W, Fan HP. Effect of excess methionine and methionine hydroxy analogue on growth performance and plasma homocysteine of growing Pekin ducks. *Poult Sci.* (2007) 86:1995–9. doi: 10.1093/ps/86.9.1995
29. Zhang YN, Xu RS, Min L, Ruan D, Kim HY, Hong YG, et al. Effects of L-methionine on growth performance, carcass quality, feather traits, and small intestinal morphology of Pekin ducks compared with conventional DL-methionine. *Poult Sci.* (2019) 98:6866–72. doi: 10.3382/ps/pez438
30. Schutte JB, De Jong J, Smink W, Pack M. Replacement value of betaine for DL-methionine in male broiler chicks. *Poult Sci.* (1997) 76:321–5. doi: 10.1093/ps/76.2.321
31. Ding W, Smulan LJ, Hou NS, Taubert S, Watts JL, Walker AK. s-Adenosylmethionine levels govern innate immunity through distinct methylation-dependent pathways. *Cell Metab.* (2015) 22:633–45. doi: 10.1016/j.cmet.2015.07.013
32. Edgar RC. UPARSE: highly accurate OTU sequences from microbial amplicon reads. *Nat Methods.* (2013) 10:996–8. doi: 10.1038/nmeth.2604
33. Li N, Huang S, Jiang L, Dai Z, Li T, Han D, et al. Characterization of the early life microbiota development and predominant lactobacillus species at distinct gut segments of low- and normal-birth-weight piglets. *Front Microbiol.* (2019) 10:797. doi: 10.3389/fmicb.2019.00797
34. Edgar RC, Haas BJ, Clemente JC, Quince C, Knight R. UCHIME improves sensitivity and speed of chimera detection. *Bioinformatics.* (2011) 27:2194–200. doi: 10.1093/bioinformatics/btr381
35. Schloss PD, Westcott SL, Ryabin T, Hall JR, Hartmann M, Hollister EB, et al. Introducing mothur: open-source, platform-independent, community-supported software for describing and comparing microbial communities. *Appl Environ Microbiol.* (2009) 75:7537–41. doi: 10.1128/AEM.01541-09
36. Huang SM, Wu ZH, Li TT, Liu C, Han DD, Tao SY, et al. Perturbation of the lipid metabolism and intestinal inflammation in growing pigs with low birth weight is associated with the alterations of gut microbiota. *Sci Total Environ.* (2020) 719:137382. doi: 10.1016/j.scitotenv.2020.137382
37. Koistinen VM, Kärkkäinen O, Borewicz K, Zarei I, Jokkala J, Micard V, et al. Contribution of gut microbiota to metabolism of dietary glycine betaine in mice and *in vitro* colonic fermentation. *Microbiome.* (2019) 7:103. doi: 10.1186/s40168-019-0718-2
38. Zhai Q, Cen S, Jiang J, Zhao J, Zhang H, Chen W. Disturbance of trace element and gut microbiota profiles as indicators of autism spectrum disorder: a pilot study of Chinese children. *Environ Res.* (2019) 171:501–9. doi: 10.1016/j.envres.2019.01.060
39. Phavichitr N, Wang S, Chomto S, Tantibhaedhyangkul R, Kakourou A, Intarakhao S, et al. Impact of synbiotics on gut microbiota during early life: a randomized, double-blind study. *Sci Rep.* (2021) 11:3534. doi: 10.1038/s41598-021-83009-2
40. Langille MG, Zaneveld J, Caporaso JG, Mcdonald D, Knights D, Reyes JA, et al. Predictive functional profiling of microbial communities using 16S rRNA marker gene sequences. *Nat Biotechnol.* (2013) 31:814–21. doi: 10.1038/nbt.2676
41. Torki M, Mohebbifar A, Ghasemi HA, Zardast A. Response of laying hens to feeding low-protein amino acid-supplemented diets under high ambient temperature: performance, egg quality, leukocyte profile, blood lipids, and excreta pH. *Int J Biometeorol.* (2015) 59:575–84. doi: 10.1007/s00484-014-0870-0
42. Geng S, Huang S, Ma Q, Li F, Gao Y, Zhao L, et al. Alterations and correlations of the gut microbiome, performance, egg quality, and serum biochemical indexes in laying hens with low-protein amino acid-deficient diets. *ACS Omega.* (2021) 6:13094–104. doi: 10.1021/acsomega.1c00739
43. Kidd MT, Maynard CW, Mullenix GJ. Progress of amino acid nutrition for diet protein reduction in poultry. *J Anim Sci Biotechnol.* (2021) 12:45. doi: 10.1186/s40104-021-00568-0
44. Gunawardana P, Roland DA, Bryant MM. Effect of energy and protein on performance, egg components, egg solids, egg quality, and profits in molted Hy-line W-36 hens. *J Appl Poult Res.* (2008) 17:432–9. doi: 10.3382/japr.2007-00085
45. Khajali F, Khoshouie EA, Dehkordi SK, Hematian M. Production performance and egg quality of Hy-line W36 laying hens fed reduced-protein diets at a constant total sulfur amino acid:lysine ratio. *J Appl Poult Res.* (2008) 17:390–7. doi: 10.3382/japr.2008-00002
46. Keshavarz K, Austic RE. The use of low-protein, low-phosphorus, amino acid- and phytase-supplemented diets on laying hen performance and nitrogen and phosphorus excretion. *Poult Sci.* (2004) 83:75–83. doi: 10.1093/ps/83.1.75
47. Saima KM, Jabbar MA, Mehmud A, Mahmood MMA. Effect of lysine supplementation in low protein diets on the performance of growing broilers. *Pak Vet J.* (2010) 30.
48. Arboleya S, Binetti A, Salazar N, Fernández N, Solís G, Hernández-Barranco A, et al. Establishment and development of intestinal microbiota in preterm neonates. *FEMS Microbiol Ecol.* (2012) 79:763–72. doi: 10.1111/j.1574-6941.2011.01261.x
49. Harms RH, Miles RD. Influence of fermacto on the performance of laying hens when fed diets with different levels of methionine. *Poult Sci.* (1988) 67:842–4. doi: 10.3382/ps.0670842
50. Esteve-Garcia E, Khan DR. Relative bioavailability of DL and L-methionine in broilers. *Open J Anim Sci.* (2018) 8:151–62. doi: 10.4236/ojas.2018.82011
51. Liu Y, Lin X, Zhou X, Wan D, Wang Z, Wu X, et al. Effects of dynamic feeding low and high methionine diets on egg quality traits in laying hens. *Poult Sci.* (2017) 96:1459–65. doi: 10.3382/ps/pew398
52. Featherston WR. Nitrogenous metabolites in the plasma of chicks adapted to high protein diets. *Poult Sci.* (1969) 48:646–52. doi: 10.3382/ps.0480646
53. Kang HK, Park SB, Jeon JJ, Kim HS, Park KT, Kim SH, et al. Effect of increasing levels of apparent metabolizable energy on laying hens in barn system. *Asian-Australas J Anim Sci.* (2018) 31:1766–72. doi: 10.5713/ajas.17.0846
54. Murugesan GR, Persia ME. Validation of the effects of small differences in dietary metabolizable energy and feed restriction in first-cycle laying hens. *Poult Sci.* (2013) 92:1238–43. doi: 10.3382/ps.2012-02719
55. Pan D, Yu Z. Intestinal microbiome of poultry and its interaction with host and diet. *Gut Microbes.* (2014) 5:108–19. doi: 10.4161/gmic.26945
56. Chang EB, Martinez-Guryn K. Small intestinal microbiota: the neglected stepchild needed for fat digestion and absorption. *Gut Microbes.* (2019) 10:235–40. doi: 10.1080/19490976.2018.1502539
57. Rastelli M, Cani PD, Knauf C. The gut microbiome influences host endocrine functions. *Endocr Rev.* (2019) 40:1271–84. doi: 10.1210/er.2018-00280
58. Yan W, Sun C, Yuan J, Yang N. Gut metagenomic analysis reveals prominent roles of Lactobacillus and cecal microbiota in chicken feed efficiency. *Sci Rep.* (2017) 7:45308. doi: 10.1038/srep45308
59. Leblanc JG, Milani C, De Giori GS, Sesma F, Van Sinderen D, Ventura M. Bacteria as vitamin suppliers to their host: a gut microbiota perspective. *Curr Opin Biotechnol.* (2013) 24:160–8. doi: 10.1016/j.copbio.2012.08.005
60. Shindo Y, Dobashi Y, Sakai T, Monma C, Miyatani H, Yoshida Y. Epidemiological and pathobiological profiles of Clostridium perfringens

infections: review of consecutive series of 33 cases over a 13-year period. *Int J Clin Exp Pathol.* (2015) 8:569–77.

Conflict of Interest: The authors declare that the research was conducted in the absence of any commercial or financial relationships that could be construed as a potential conflict of interest.

Publisher's Note: All claims expressed in this article are solely those of the authors and do not necessarily represent those of their affiliated organizations, or those of the publisher, the editors and the reviewers. Any product that may be evaluated in this article, or claim that may be made by its manufacturer, is not guaranteed or endorsed by the publisher.

frontiers in Nutrition

ORIGINAL RESEARCH
published: 08 October 2021
doi: 10.3389/fnut.2021.738281

Baicalin–Zinc Complex Alleviates Inflammatory Responses and Hormone Profiles by Microbiome in Deoxynivalenol Induced Piglets

Andong Zha[1,2], *Ruiqi Tu*[3], *Zhijuan Cui*[4], *Ming Qi*[1,2], *Simeng Liao*[1,2], *Jing Wang*[4], *Bie Tan*[4] *and Peng Liao*[1]*

[1] Chinese Academy of Sciences, Institute of Subtropical Agriculture, Changsha, China, [2] College of Resource and Environment, University of Chinese Academy of Sciences, Beijing, China, [3] College of Veterinary Medicine, Northwest A & F University, Yangling, China, [4] Department of Animal Science and Technology, Hunan Agricultural University, Changsha, China

This study aimed to investigate the beneficial effect of baicalin–zinc complex (BZN) on intestinal microorganisms in deoxynivalenol (DON)-challenged piglets and the association between intestinal microorganisms and host immunity and hormone secretion. Forty weaned piglets were randomly divided into four treatments with 10 piglets in each treatment: (1) control (Con) group (pigs fed basal diet); (2) DON group (pigs fed 4 mg DON/kg basal diet); (3) BZN group (pigs fed 0.5% BZN basal diet); and (4) DBZN group (pigs fed 4 mg DON/kg and 0.5% BZN basal diet). The experiment lasted for 14 days. The BZN supplementation in DON-contaminated diets changed the intestinal microbiota composition and increased intestinal microbial richness and diversity of piglets. The BZN supplementation in DON-contaminated diets also alleviated the inflammatory responses of piglets and modulated the secretion of hormones related to the growth axis. Moreover, microbiota composition was associated with inflammatory and hormone secretion. In conclusion, BZN alleviated inflammatory response and hormone secretion in piglets, which is associated with the intestinal microbiome.

Keywords: baicalin-zinc complex, deoxynivalenol, intestinal microbiome, hormone secretion, inflammatory responses, weaned piglets

OPEN ACCESS

Edited by:
Xi Ma,
China Agricultural University, China

Reviewed by:
Lvhui Sun,
Huazhong Agricultural University, China
Peixin Fan,
University of Florida, United States

***Correspondence:**
Peng Liao
liaopeng@isa.ac.cn

Specialty section:
This article was submitted to Nutrition and Microbes, a section of the journal Frontiers in Nutrition

Received: *08 July 2021*
Accepted: *06 September 2021*
Published: *08 October 2021*

Citation:
Zha A, Tu R, Cui Z, Qi M, Liao S, Wang J, Tan B and Liao P (2021) Baicalin–Zinc Complex Alleviates Inflammatory Responses and Hormone Profiles by Microbiome in Deoxynivalenol Induced Piglets. Front. Nutr. 8:738281. doi: 10.3389/fnut.2021.738281

INTRODUCTION

Deoxynivalenol (DON), originally known as vomitoxin, can cause vomiting, diarrhea, anorexia, neurological disorders, and immune dysfunction in humans and animals (1, 2). DON was reported to be the most common food-related mycotoxins all over the world (3–5). A study shows that DON was detected in 73 and 92% of wheat and corn in the USA (6). In another study in China, the detection rate of DON in corn was 93.2%, and the average concentration was 1,356.9 μg/kg (7). The DON detection rate in each region is shown as follows: East Asia (84.8%), Northern Europe (74.2%), Central America (70.0%), Central Europe (69.8%), North America (64.1%), South Africa (63.2%), Eastern Europe (59.9%), Southern Europe (52.9%), sub-Saharan Africa (49.5%), Middle East/North Africa Region (47.8%), Southeast Asia (42.5%), Oceania (34.5%), South America (26.9%), and South Asia (23.1%) (8). Pigs are very sensitive to the toxic effects of DON, and

the long-term consumption of DON in pig can delay growth and reduce immune performance (9, 10). Therefore, repairing intestinal damage induced by DON is an important subject in the livestock production.

At low DON concentrations, DON promotes the production of immune factors, thereby increasing the risk of chronic immune disease or infection susceptibility (11, 12). DON induces secretion of serum immunoglobulin M (IgM), immunoglobulin A (IgA), immunoglobulin E (IgE), and immunoglobulin G (IgG) in mice or farm animals (13–15). DON induces a significant increase in tumor necrosis factor-α (TNF-α), interleukin-8 (IL-8), interleukin-1α (IL-1α), interleukin-1β (IL-1β), and gene expression in porcine intestinal epithelial cells (IPEC-1 cell line) (16). Furthermore, some studies also showed that DON can interfere with immune response by altering intestinal microbiome balance (17, 18). Previous studies reported that the growth retardation induced by DON is associated with the secretion of satiety hormones, such as peptide YY (PYY), cholecystokinin (CCK), and 5-hydroxytryptamine (5-HT), and growth hormone (GH) (19, 20). Therefore, we intend to develop a feed additive to reduce the toxic effects of DON. Baicalin–zinc complex (BZN) is a complex of baicalin and zinc. Although there are few studies on BZN at present, it has been proved to have good anti-inflammatory and antioxidant properties, which suggest that it may relieve the toxic effects of DON in pigs (21, 22). Moreover, zinc is an essential trace element for animals. It is involved in a multitude of body functions, ranging from the metabolism of nutrients to bone development, and as an activator to mediate the immune function of pigs (23, 24). It is generally added at 2,000 mg/kg in swine production to reduce diarrhea and promote pig growth. Baicalin (5,6-dihydroxy-2-phenyl-4H-1-benzopyran-4-one-7-O-D-β-glucuronic acid) is an extract from *Scutellaria baicalensis Georgi* and *Oroxylum indicum (L.) Kurz*, and it is commonly used in the cure of gastrointestinal infections and inflammatory diseases (25, 26). The dietary baicalin supplementation is tightly correlated to the intestinal microbiota composition, and it was also reported that baicalin has good antioxidant and anti-inflammatory in some studies (26–28).

This study aimed to investigate the beneficial effect of BZN on intestinal microbiome, inflammatory responses, and hormone profiles in DON-challenged piglets and the association between intestinal microbiome and host immunity and hormone secretion.

Abbreviations: 5-HT, 5-hydroxytryptamine; HTR3A1, 5-hydroxytryptamine receptor 3A 1; HTR3A2, 5-hydroxytryptamine receptor 3A 2; HTR3B2, 5-hydroxytryptamine receptor 3B; AGRP, agouti-related protein; AKT, AKT serine/threonine kinase 1; ALB, albumin; BZN, baicalin–zinc complex; BUN, blood urea nitrogen; CCK, cholecystokinin; CCK-1R, cholecystokinin type A receptor; CCK-2R, cholecystokinin B receptor; CHOL, total cholesterol; COX-2, cyclooxygenase-2; DON, deoxynivalenol; GLP-1, glucagon-like peptide 1; GLP-2, glucagon-like peptide 2; GLU, glucose; GH, growth hormone; hs-CRP, high-sensitivity C-reactive protein; IgA, immunoglobulin A; IgE, immunoglobulin E; IgG, immunoglobulin G; IgM, immunoglobulin M; INS, insulin; INR, insulin receptor; IGF-1, insulin-like growth factor-1; IFN-γ, interferon-gamma; IL-1α, interleukin-1α; IL-1β, interleukin-1β; IL-2, interleukin-2; IL-6, interleukin-6; IL-8, interleukin-8; IL-17, interleukin-17; IL-23, interleukin-23; LEP, leptin; LDA, linear discriminant analysis; NPY, neuropeptide Y; NF-κB, nuclear factor kappa B; OTUs, operational taxonomic units; PYY, peptide YY; PCA, principal component analysis; PCoA, principal co-ordinates analysis; PMOC, proopiomelanocortin; SST, somatostatin; TLR-2, toll-like receptor 2; TNF-α, tumor necrosis factor-α.

MATERIALS AND METHODS

DON-Contaminated Diet and BZN Synthesis

Basal diet inoculate with *Fusarium graminearum* R6576 was fermented for 14 days to form DON-contaminated diet as described by Wu et al. (29). *F. graminearum* R6576 was supplied by Huazhong Agricultural University and preserved by Institute of Subtropical Sciences, Chinese Academy of Sciences (30). Baicalin was fully dissolved in 1% sodium bicarbonate solution, then equal molar ratio zinc sulfate was added to baicalin solution. After completion of the reaction, the precipitation was BZN. The dose of BZN and DON was referred to the previous literature (31).

Animals, Diets, and Experimental Design

Forty weaned piglets with an average weight of 6.13 ± 0.42 kg (Landrace × Yorkshire, 21 days of age) were individually housed in a single column at the New wellful pig farm (New Wellful Co., Ltd, Hunan, China). Piglets were randomly divided into four diets, and 10 pigs were fed to each diet. The four groups were as follows: (1) control (Con) group (basal diet); (2) DON group (4 mg DON/kg basal diet); (3) BZN group (0.5% BZN basal diet); and (4) DBZN group (4 mg DON/kg and 0.5% BZN basal diet). The composition and nutrient level of the basal diet in this experiment is shown in **Supplementary Table 1**, and it meets nutrient requirements of pigs according to National Research Committee (NRC) (32, 33). All pigs were acclimated to the room for 3 days before the experiment, and experimental diets were provided in four equal daily meals at 7:30, 11:00, 14:30, and 18:00 for 14 days. Piglets housed on a 12-h light-dark cycle with free access to water, and the barn temperature was maintained at 30°C. Randomly selected seven pigs from each group for sampling after slaughter. After blood was collected by blood vessel, it was placed at room temperature for 1 h and centrifuged at 3,000 R for 15 min. The pale yellow liquid obtained was the serum. The intestine was opened in the middle ileum, and an appropriate amount of chyme was collected in a 50-ml sterile centrifugal tube. The collected serum and ileal chyme samples were quickly stored in liquid nitrogen. Serum and ileum chymes were stored at −80°C. The experiment was carried out under the supervision of the experimental animal ethics committee of the Institute of Subtropical Agriculture (Changsha, Human Province, China) (29, 34).

16s rRNA Sequencing

The 16s rRNA analysis of ileal chyme was conducted by Novogene Co., Ltd (Beijing, China) (35). The total DNA from ileal chyme was extracted by the CTAB/SDS method, and the DNA concentration and quality met the experimental requirements. Then, diluted the DNA to 1 mg/ml with sterile water. PCR was performed with specific primers as forward primer: ACTCCTACGGGAGGCAGCAG and reverse primer: GGACTACHVGGGTWTC TAAT (amplification of 16srRNA gene V3–V4 region); the PCR amplification products were

detected and purified using a 2% agarose gel, then purified amplicons were used for the sequencing library. After the library has passed the quality assessment, it was sequenced on Ion S5TMXL (Thermo Fisher Scientific Co., Ltd., Waltham, CA, USA).

Bioinformatics Analysis

Raw reads were demultiplexed and quality-filtered as previously described (36). Operational taxonomic units (OTUs) were clustered with 97% similarity for the effective tags of all samples by using the UPARSE software (version 7.0.1001), then used the Mothur method (https://www.mothur.org/) and SILVA database to annotate the species at the level phylum, order, family, genus, and class. The R software (version 2.15.3) was used to draw principal component analysis (PCA) chart, principal co-ordinates analysis (PCoA) chart and heatmap. Alpha diversity was used to analyze the diversity of intestinal microbiome. Linear discriminant analysis effect size (LEfSe) analysis was used galaxy module [linear discriminant analysis (LDA) score >2.5].

Serum Indices (Immunoglobulins, Cytokines, Biochemical Indices, and Hormones Profiles)

Serum immunoglobulins: IgM, IgG, IgA, cytokines: TNF-α, IL-2, IFN-γ, IL-6, IL-1β, and hormones: 5-HT, GH, PYY, LEP, somatostatin (SST), insulin (INS), neuropeptide Y (NPY), insulin-like growth factor-1 (IGF-1), proopiomelanocortin (PMOC), agouti-related protein (AGRP), and glucagon-like peptide 1 (GLP-1) were determined using the commercially available ELISA kits from Nanjing Jiancheng Co., Ltd. (Jiangsu, China) (37).

The CX-4 automatic biochemical analyzer (Beckman Coulter, Brea, CA, USA) was used to measure the total cholesterol (CHOL), albumin (ALB), glucose (GLU), and blood urea nitrogen (BUN) in serum (38).

Real-Time Quantitative PCR

The total RNA was extracted from the hypothalamus and pituitary using the TRIzol Reagent (Thermo Fisher Scientific Co., Ltd, CA, USA). Real-time quantitative PCR was performed with a Roche Light Cycler 480II system (Roche Co., Ltd, Basel, Switzerland). Primers (PREMIER Biosoft International, San Francisco, CA, USA) (**Supplementary Table 1**) were designed using the Primer 5.0 software and synthesized by Sangon Biotech Co., Ltd. (Shanghai, China). The RNA extraction and real-time quantitative PCR were conducted strictly according to previous studies [RT-PCR procedure: step 1: predenaturation program (30 s at 95°C); step 2: PCR (5 s at 95°C for denaturation and 30 s at 60°C for extension); and step 3: dissociation program (5 s at 60°C)] (37, 39, 40). In addition, the relative expression of target genes was calculated by the formula $2^{-(\Delta\Delta Ct)}$ (41).

Statistical Analysis

In addition to sequencing data, serum indices and mRNA expression were analyzed by the SPSS software (version 20, IBM Corp., Armonk, NY, USA). We filled the missing values with the mean, and the data were logarithmically transformed while outliers existed. Dietary BZN, DON, and their interactions were analyzed using two-way ANOVA. If there was a significant difference, we performed the Bonferroni *t*-test. At the same time, the Duncan's test was used to analyze the significant difference, and the criterion for significance judgment was $p < 0.05$. The GraphPad Prism Software (Version 7; La Jolla, CA, USA) was used to draw the figures, and the column shows mean ± SEM (42–44).

RESULTS

Intestinal Microbiome Composition of Piglets

To characterize the composition of bacterial communities in the ileum, we collected a total of 28 piglets' ileum chymes for 16s sequencing. After quality filtering, 20,694,594 reads that were clustered into 1,096 OTU remained. At the phylum level (**Figure 1A**), *Firmicutes* was the main phylum in the intestinal microbiota of piglets among the four groups, and the relative *Firmicutes* content in the DON group is much higher (95%). The LEfSe analysis revealed that the relative *Bacteroidetes* content in the DON group was noticeably lower than that in the DBZN group (LDA > 2.5) (**Figure 1D**). At the genus level (**Figure 1B**), over 43% of reads were identified as unidentified members of *Clostridiales*. The LEfSe analysis revealed that the relative abundance of *Intestinibacter*, *Agathobacter*, and *Veillonella* in the DBZN group was noticeably higher than that in the DON group (LDA > 2.5) (**Figure 1D**). At the species level, for the Con group, intestinal microbiota was mainly enriched in genera belonging to *Bacteroides* (**Figure 1C**). The BZN group was mainly enriched by *Streptococcus*, *Clostridium bornimense*, and *Actinobacillus minor*, and the DBZN group was mainly enriched by *Lactobacillus*, *Streptococcus*, and so on (**Figure 1E**). The LEfSe analysis showed that BZN markedly increased the relative abundance of *Clostridium perfringens* in basal diet, and BZN markedly increased the relative abundance of *Streptococcus porcorum* in DON-contaminated diet (LDA > 2.5) (**Figure 1D**).

Diversity Change of Intestinal Microbiome of the Piglet

To detect the changes of intestinal microbiota composition during the experiment period, we evaluated the alpha diversity of piglet gut microbiota. The alpha diversity was first calculated using ace, chao 1, PD whole tree, and observed species. All measurements revealed that the BZN supplementation increased evenness and richness of the ileum microbiota in DON-contaminated diet ($p < 0.05$) (**Figures 2A–D**).

To further reveal the differences in intestinal microbiota composition among the four groups, we evaluated the beta diversity of piglet intestinal microbiota using the binary Jaccard indices and weighted UniFrac (**Figures 2E,F**). PCoA revealed that although there was no obvious segregation of the BZN group and Con group, the Con group, DON group, and DBZN group can be distinguished from each other. Moreover, analysis of molecular variance (AMOVA) indicated that the differences in the binary Jaccard index between the DON group and DBZN group are significant ($p < 0.05$).

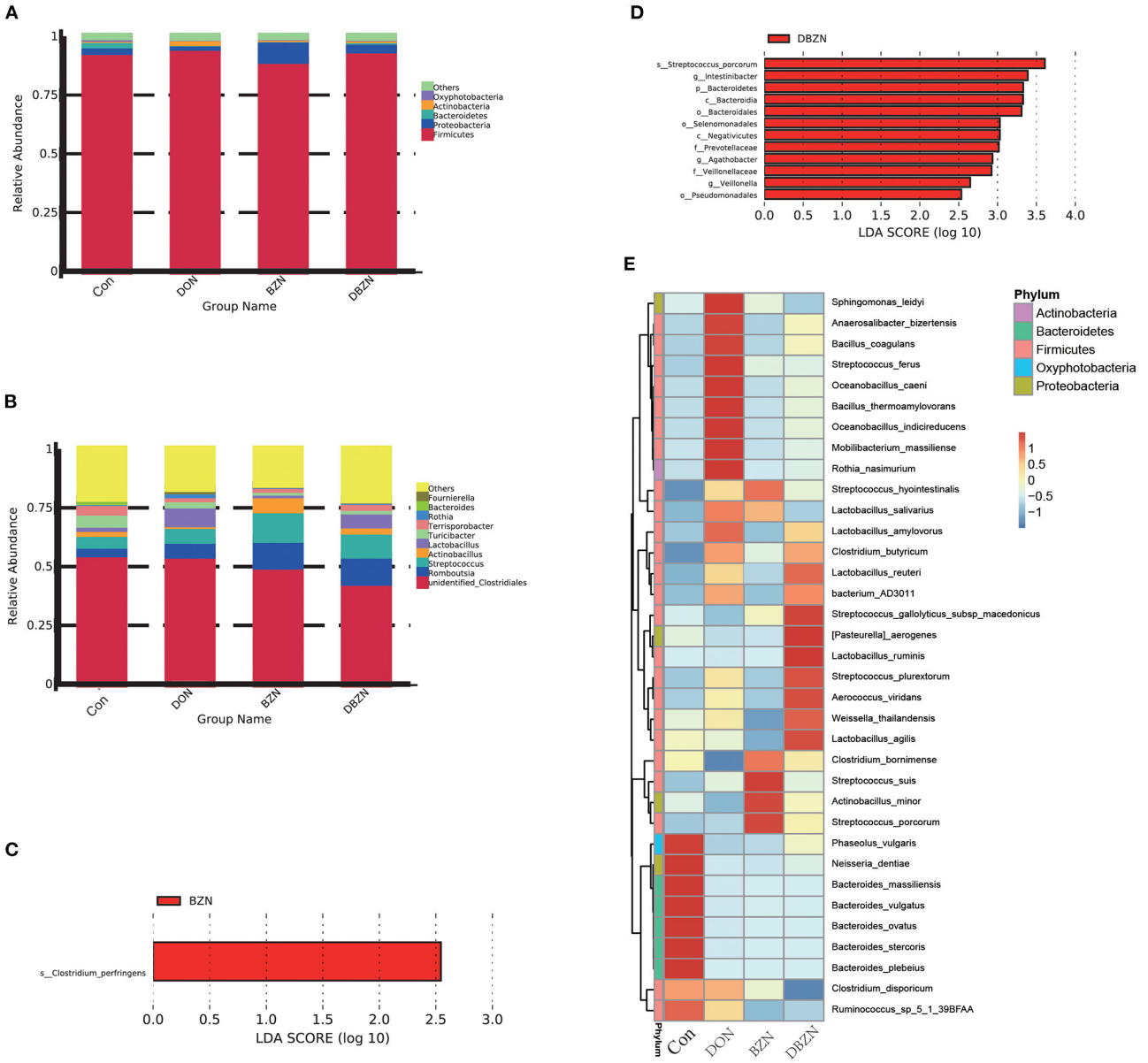

FIGURE 1 | Effects of BZN and DON on intestinal microbiome composition of piglet. **(A)** Intestinal microbiome composition at the phylum level. **(B)** Intestinal microbiome composition at the genus level. **(C)** The LEfSe analysis at different gut microbiota taxa between Con and BZN groups (LDA score >2.5). **(D)** The LEfSe analysis at different gut microbiota taxa between DON and DBZN groups (LDA score >2.5). **(E)** Heatmap showing significantly different species. Dietary treatment: Con, basal diet; DON, 4 mg/kg DON-contaminated diet; BZN, 0.5% BZN supplementation diet; DBZN, 0.5% BZN supplement in 4 mg/kg DON-contaminated diet. BZN, baicalin–zinc complex; Con, control; DON, deoxynivalenol; LDA, linear discriminant analysis.

Metabolic Functional Change of Intestinal Microbiome of the Piglet

The Phylogenetic Investigation of Communities by Reconstruction of Unobserved States (PICRUST) analysis was used to predict the function of intestinal microbiota (**Figure 3**). The results indicated that 10 pathways, including ATP-binding cassette (ABC) transporters, translation proteins, general function prediction only, ribosome Biogenesis, porphyrin and chlorophyll metabolism, sporulation, chromosome, transcription machinery, and arginine and proline metabolism were enriched in the Con group. We also identified seven pathways, such as two component system, purine metabolism, aminoacyl tRNA biosynthesis, pyrimidine metabolism, DNA repair and recombination proteins, methane metabolism, and amino acid-related enzymes were predicted to be enriched in the DON group. Seven pathways, including secretion system, transcription factors, bacterial motility proteins, transporters, fructose and mannose metabolism, cysteine and methionine metabolism

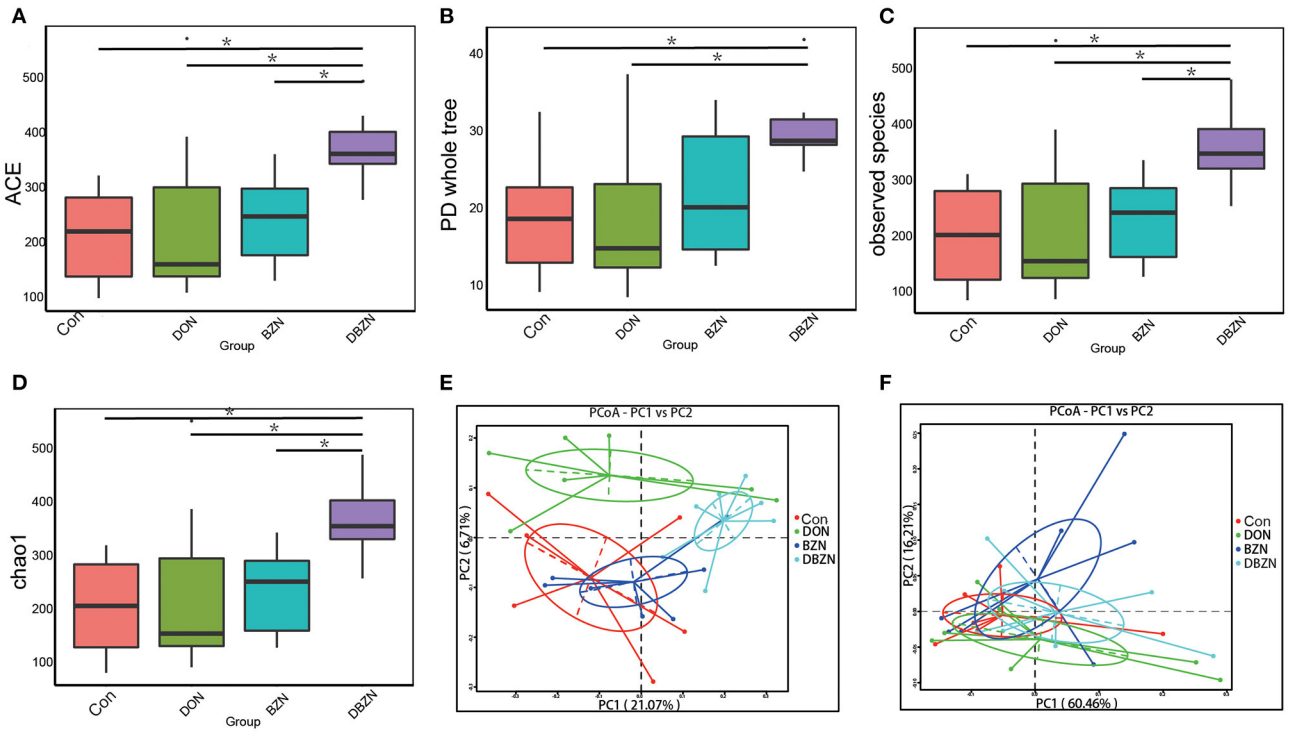

FIGURE 2 | Alpha and beta diversity change of gut microbiota. **(A)** Alpha diversity base on the ACE index. **(B)** Alpha diversity base on the Phylogenetic diversity (PD) whole-tree index. **(C)** Alpha diversity base on the observed species index. **(D)** Alpha diversity base on the chao 1 index. **(E)** Principal coordinate analysis (PCoA) based on the binary Jaccard indices. **(F)** PCoA based on the weighted UniFrac indices. Dietary treatment: Con, basal diet; DON, 4 mg/kg DON-contaminated diet; BZN, 0.5% BZN supplementation diet; DBZN, 0.5% BZN supplement in 4 mg/kg DON-contaminated diet. *$p < 0.05$. BZN, baicalin–zinc complex; Con, control; DON, deoxynivalenol.

and peptidases, were predicted to be enriched in the BZN and DBZN groups.

Serum Inflammatory Responses Correlation With the Intestinal Microbiome Abundance

Serum immunoglobulin and cytokines were significantly affected by either supplementation of BZN, DON, or interaction (**Figure 4A**). Compared with the Con group, the BZN group increased the level of IgA, IgG, IgM, IFN-γ, IL-6, IL-1β, and IL-2 in serum ($p < 0.05$). In the DON-challenged group, the dietary BZN supplementation decreased the level of IL-2 and IFN-γ in serum ($p < 0.05$). The concentration of CHOL in serum was significantly influenced by the interaction effect of DON and BZN ($p < 0.05$). Moreover, the dietary BZN supplementation significantly increased the serum concentration of BUN and GLU in serum ($p < 0.05$).

The Spearman's correlation analysis was used to calculate the relationship between inflammatory and intestinal microbiome abundance. Intestinal microbiota was significantly associated with some immunity indices (**Figure 4B**). Of these, the abundances of *Bacterium* AD3011, *Phaseolus vulgaris*, *Bacteroides vulgatus*, or *Streptococcus suis* was negatively correlated to IgG, IgM, and IL-1β, and the abundance of *Anaerosalibacter bizertensis*, *Streptococcus ferus*, *Oceanobacillus indicireducens*, *Bacillus coagulans*, *Oceanobacillus caeni*, or *Streptococcus plurextorum* was positively correlated to IL-2 and IFN-γ. Moreover, the abundance of *Lactobacillus ruminis* was negatively correlated to IL-2.

Hormone Secretion Correlation With the Intestinal Microbiome Abundance

As shown in **Figure 5A**, after 2 weeks of experimental treatments, the interaction effect of DON and BZN on GH-related hormones in serum was statistically significant ($p < 0.01$). As compared with the Con group, the concentration of INS and GH of the BZN group was increased ($p < 0.05$). However, the dietary BZN supplementation increased in the concentration of SS, and decreased the concentration of INS in DON-challenged group ($p < 0.05$). As revealed in **Figure 5**, the concentration of PYY, AGRP, LEP, GLP-1, and NPY in serum was significantly affected by either supplementation of BZN, DON, or interaction ($p < 0.05$).

The Spearman's correlation analysis was used to calculate the relationship between hormone secretion and bacterial genera abundance (**Figure 5B**). First, the abundance of *Lactobacillus agilis* were positively correlated to the AGRP concentration

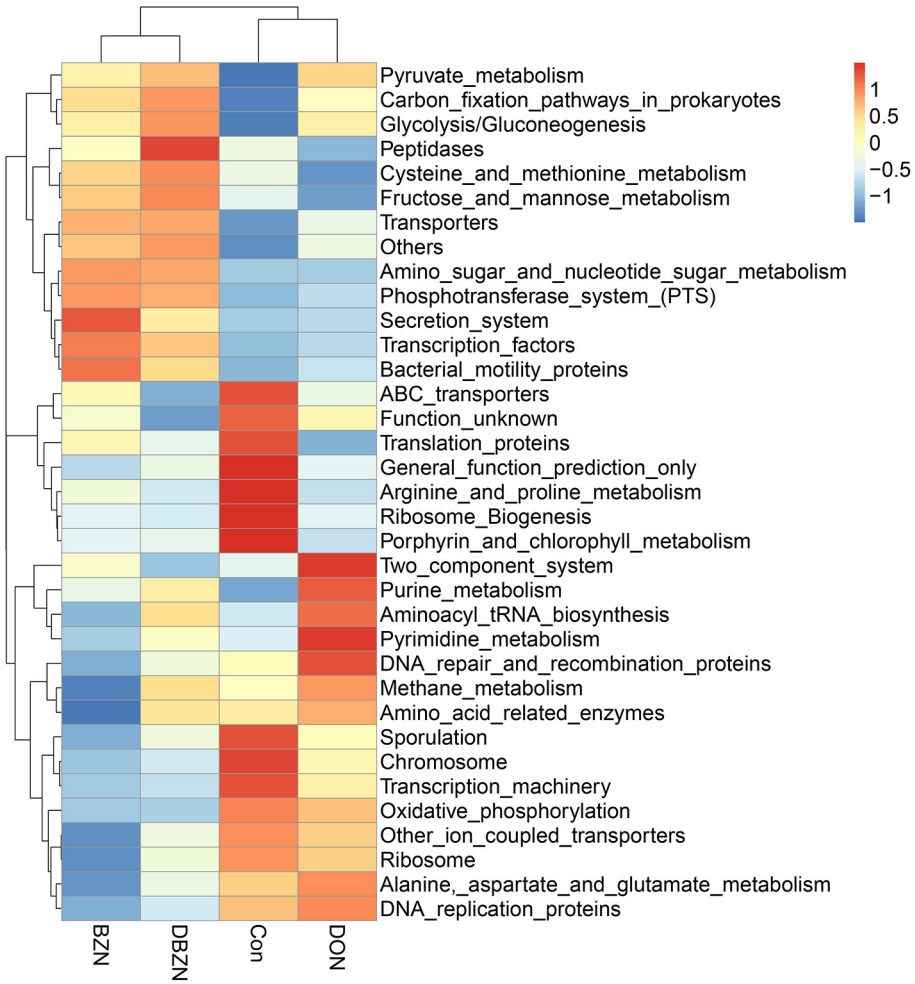

FIGURE 3 | BZN supplementation changed the metabolic functions of intestinal microbiome of piglet at KEGG level 3. Dietary treatment: Con, basal diet; DON, 4 mg/kg DON-contaminated diet; BZN, 0.5% BZN supplementation diet; DBZN, 0.5% BZN supplement in 4 mg/kg DON-contaminated diet. BZN, baicalin–zinc complex; Con, control; DON, deoxynivalenol; KEGG, Kyoto Encyclopedia of Genes and Genomes.

in serum. As the heatmap shows, the abundance of *Neisseria dentiae*, *Mobilibacterium massiliense*, *Bacteroides ovatus*, *Pasteurella aerogenes*, or *Clostridium bornimense* was negatively correlated to the INS, GH, PYY, and PMOC concentration in serum, and the abundance of *Anaerosalibacter bizertensis*, *Streptococcus ferus*, *Oceanobacillus indicireducens*, *Lactobacillus agilis*, *Bacillus coagulans*, *Bacillus thermoamylovorans*, *Weissella thailandensis*, *Oceanobacillus caeni*, *Streptococcus plurextorum*, or *Rothia nasimurium* was positively correlated to the IGF-1, INS, GH, LEP, AGRP, and NPY concentration in serum.

Relative mRNA Expression in Hypothalamus and Pituitary

As shown in **Figure 6**, among the 13 hormones or their receptor genes assayed in the hypothalamus, eight genes were affected by dietary DON, BZN, or their interaction. Specifically, dietary DON exerted a main effect on the mRNA relative levels of insulin receptor (INR), AKT, 5-hydroxytryptamine receptor (HTR)3A1, HTR3A2, HTR3B2, and cholecystokinin (CCK)-2R ($p < 0.05$). The BZN supplementation exerted the main effect on the mRNA levels of SST and HTR3B2 ($p < 0.05$), whereas there were no genes significantly influenced by an interaction between the DON supplementation and the BZN supplementation ($p > 0.05$). Among the 14 hormones or their receptor genes assayed in the pituitary, four genes were affected by dietary DON, BZN, or their interaction. Specifically, dietary DON exerted a main effect of NPY, and the mRNA expression of INR and AKT in the pituitary was affected by dietary BZN ($p < 0.05$). Notably, the mRNA levels of INR, GLP-2, and AKT in the pituitary were influenced by the interaction between the DON supplementation and the BZN supplementation ($p < 0.05$).

DISCUSSION

Deoxynivalenol is the most common mycotoxin in grains and its products, and it can cause growth retardation, anorexia,

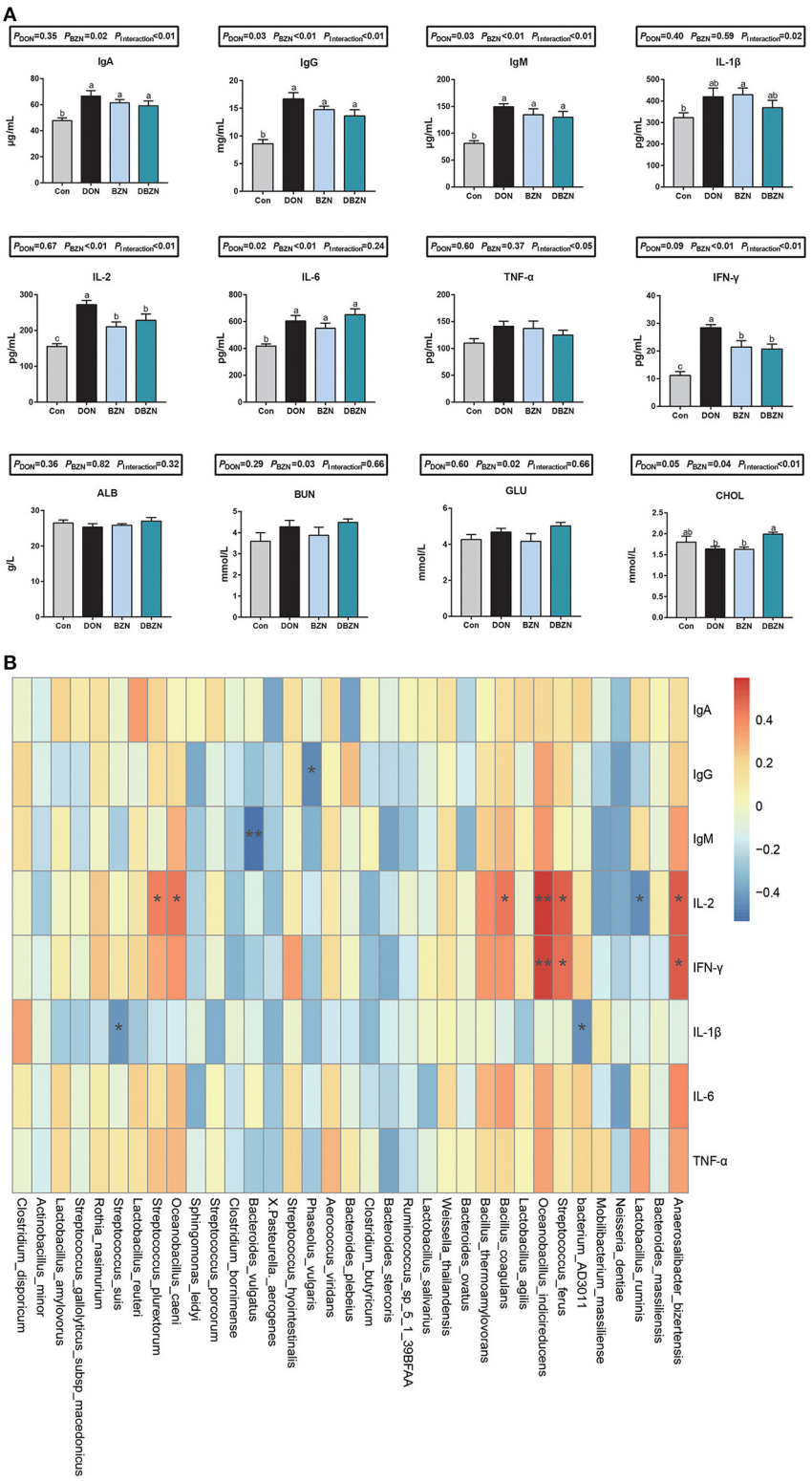

FIGURE 4 | BZN- and DON-mediated inflammatory responses and correlations with intestinal microbiome. **(A)** Serum inflammatory indices. [ab]Different letters mean significantly difference. **(B)** The Spearman correlations between the intestinal microbiome and serum inflammatory indices. $^{*}p < 0.05$, $^{**}p < 0.01$. Dietary treatment: Con, basal diet; DON, 4 mg/kg DON-contaminated diet; BZN, 0.5% BZN supplementation diet; DBZN, 0.5% BZN supplement in 4 mg/kg DON-contaminated diet. IL-1β, interleukin-1β; IgG, immunoglobulin G; IFN-γ, interferon-gamma γ; IL-6, interleukin-6; IgA, immunoglobulin A; GLU, glucose; IgM, immunoglobulin M; CHOL, total cholesterol; IL-2, interleukin-2; TNF-α, tumor necrosis factor-α; ALB, albumin; BUN, blood urea nitrogen; BZN, baicalin–zinc complex; Con, control; DON, deoxynivalenol.

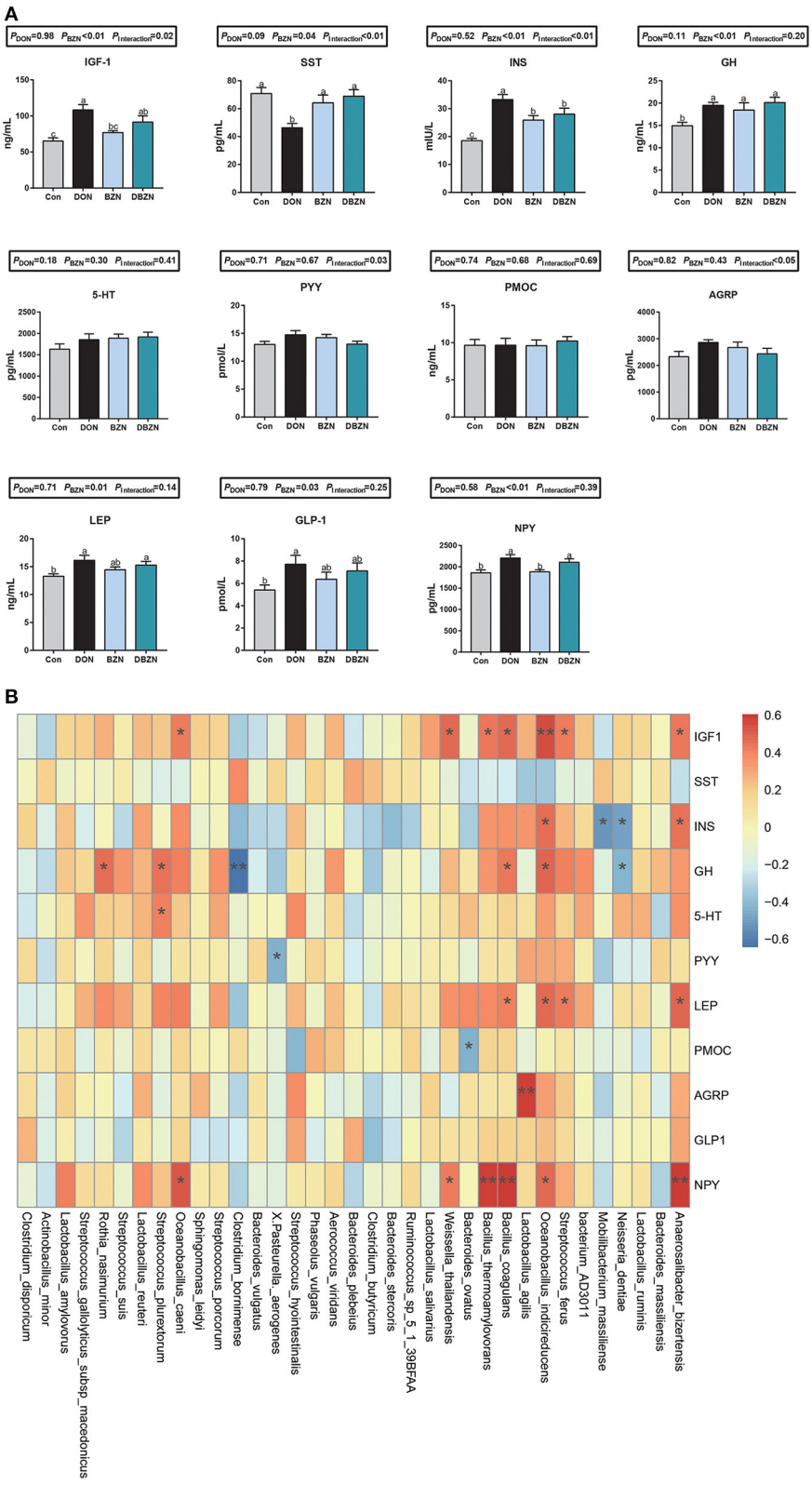

FIGURE 5 | BZN- and DON-mediated hormone secretion and correlations with gut microbiota. **(A)** The concentration of serum hormone. **(B)** The Spearman correlations between the gut microbiota and serum inflammatory makers. $^{*}p < 0.05$, $^{**}p < 0.01$. Dietary treatment: Con, basal diet; DON, 4 mg/kg DON-contaminated diet; BZN, 0.5% BZN supplementation diet; DBZN, 0.5% BZN supplement in 4 mg/kg DON-contaminated diet. IGF1, insulin-like growth factor 1; NPY, neuropeptide Y; SST, somatostatin; INS, insulin; GH, growth hormone; 5-HT, 5-hydroxytryptamine; PYY, peptide YY; PMOC, proopiomelanocortin; AGRP, agouti-related protein; LEP, leptin, GLP1, glucagon-like peptide-1; BZN, baicalin–zinc complex; Con, control; DON, deoxynivalenol. ^{a,b}different letters means significantly difference ($P < 0.05$).

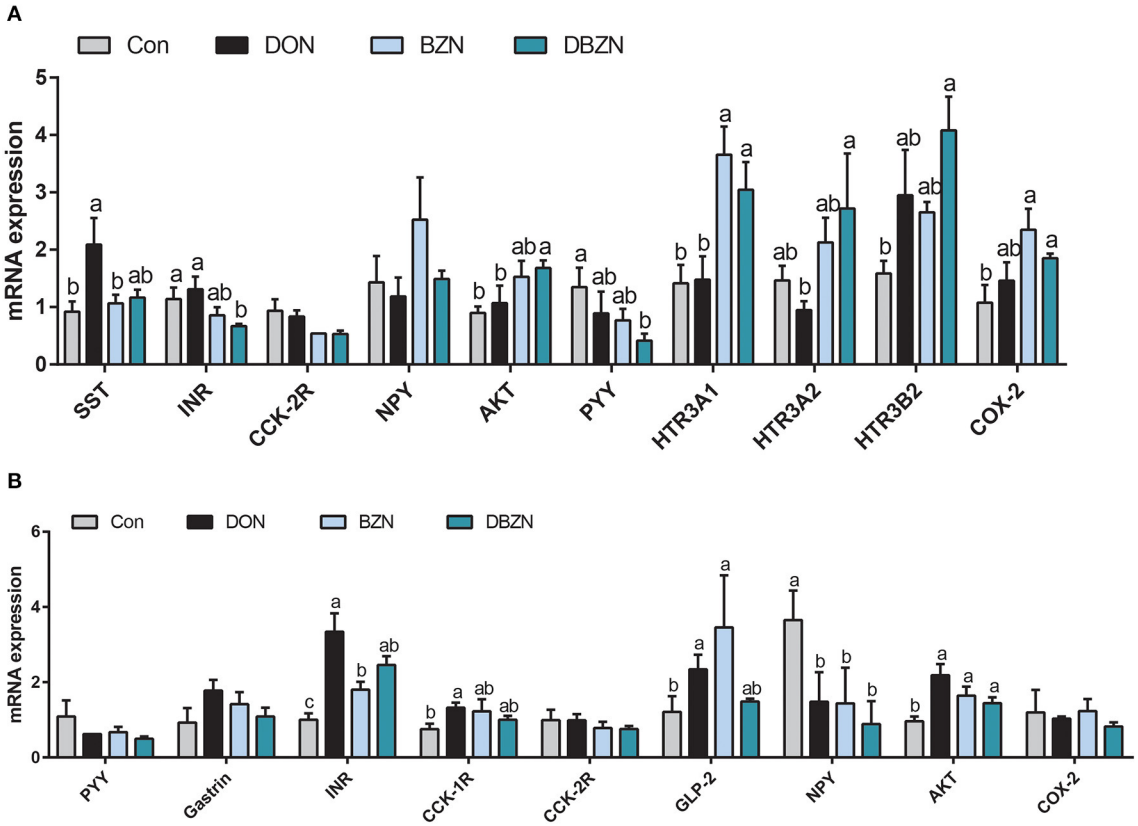

FIGURE 6 | Effect of DON and BZN in mRNA levels of hormone genes in hypothalamus **(A)** and pituitary gland **(B)**. Column was mean ± SEM ($n = 7$). Different letters mean significant differences. Dietary treatment: Con, basal diet; DON, 4 mg/kg DON-contaminated diet; BZN, 0.5% BZN supplementation diet; DBZN, 0.5% BZN supplement in 4 mg/kg DON-contaminated diet. SST, somatostatin; INR, insulin receptor; CCK-2R, cholecystokinin B receptor; NPY, neuropeptide Y; AKT, AKT serine/threonine kinase 1; HTR3A1, 5-hydroxytryptamine receptor 3A 1; HTR3A2, 5-hydroxytryptamine receptor 3A 2; HTR3B2, 5-hydroxytryptamine receptor 3B; COX-2, cyclooxygenase-2; CCK-1R, cholecystokinin type A receptor; GLP-2, glucagon-like peptide 2; BZN, baicalin–zinc complex; Con, control; DON, deoxynivalenol. ^{a,b}different letters means significantly difference ($P < 0.05$).

and immune abnormalities. In addition, DON also changes the composition of intestinal microbiota, and intestinal microbiota is closely associated with growth and immunity (17, 45). This study showed the impact of BZN supplementation on the intestinal microbiome composition, inflammatory, and hormone secretion in DON-challenged piglets.

Intestinal microbiota is the primary target of DON in animals. Dietary ingestion of DON impaired intestinal homeostasis and changed the composition of intestinal microbiome in mice, especially, DON reduced the abundance of *Streptococcus* (46, 47). Moreover, baicalin regulates intestinal microbiota homeostasis and participates in liver–gut axis interaction (48, 49). Our study showed that dietary BZN in DON-contaminated diet increased intestinal microbial richness and diversity of piglets. Increased intestinal microbial diversity indicates a better resistance to stress. This is similar to the argument that baicalin can reverse intestinal microbiota dysfunction in rats. Moreover, our results showed that there was a significant difference in beta diversity between DON and DBZN groups, which means that dietary BZN in DON-contaminated diets changed the intestinal microbiota structure of piglet. Heatmaps showed that *Lactobacillus ruminis* and *Lactobacillus agilis* were enriched in the DBZN group, and they were able to inhibit *Escherichia coli*, which means BZN may treat intestinal pathogen infection (50, 51). PICRUST showed that the dietary BZN supplementation in DON-contaminated diet enriched peptidases pathway and dietary BZN supplementation in basal diet-enriched secretion system and bacterial mobility protein pathway. In conclusion, the dietary BZN supplementation in DON-contaminated diet relieved the imbalance of the intestinal microbiome caused by DON.

Deoxynivalenol also induced the activation of nuclear factor kappa B (NF-κB) and trigger an inflammatory response, thus selectively inducing the expression of some genes, includes a series of cytokines, chemokines, and other inflammatory factors (17, 52). Studies have also shown that with a high dose of DON, the total serum IgA, IgG, and IgM levels are significantly different from those in the Con group (13, 53). Studies have shown that baicalin treatment can reduce the serum inflammatory biomarkers of spontaneously hypertensive rats, such as IL-6, IL-1β, and high-sensitivity C-reactive protein (hs-CRP). In addition, baicalin treatment can also significantly

reduce the expression of toll-like receptor 2 (TLR2), IL-1β, TNF-α, and interleukin-23 (IL-23) in the colon in Spontaneously Hypertensive Rats (SHRs) (54). Baicalin can significantly reduce the serum interleukin-17 (IL-17), IL-6, and IL-1β expression in Ulcerative Colitis (UC) rats (55). In addition, it can also reduce the expression of CD14 and IL-6 in colonic mucosa and alleviate the severity of ulcers (56). The results of these studies have shown that baicalin treatment can inhibit the inflammatory symptoms of the intestinal tract. Our research found that DON and BZN and their interaction groups can make the expression levels of IL-2, IL-6, IgG, IgA, IgM, and IFN-γ significantly different from those of the Con group. Among them, BZN reduced the expression of IL-2 and IFN-γ caused by DON, which was in accordance with the results of a previous study (52). We also observed that the dietary BZN supplementation increased the serum IL-2, IFN-γ, and INS concentration in normal piglets. These results indicate that the effects of DON in normal piglets and DON-induced piglets are different. According to the Spearman correlation analysis, the concentration of IL-2 and IFN-γ was correlated to the abundance of *Anaerosalibacter bizertensis*, *Streptococcus ferus*, *Oceanobacillus indicireducens*, *Bacillus coagulans*, *Oceanobacillus caeni*, *Lactobacillus ruminis*, *or Streptococcus plurextorum*.

Previous literature studies have shown that the growth retardation and anorexia caused by DON may be related to the regulation of hormone secretion, such as 5-HT, GH, and IGF1 (19, 57, 58). Our experiment showed that the dietary BZN supplementation in DON-contaminated diets significantly increased the SS concentration in serum and significantly decreased the INS concentration in serum. SST is a kind of tetrapeptide that can inhibit the secretion of GH and control the secretion of pituitary hormone. It is assumed that the increase of somatostatin concentration will cause growth inhibition. However, it was also noted that the addition of DON and BZN could increase the secretion of GH. Therefore, we conclude that DON unbalanced the growth axis hormone secretion, and the supplementation of BZN can rebalance growth axis hormone secretion induced by DON. Notably, the concentration of GH was positively related to the abundance of *Bacillus coagulans*, *Oceanobacillus indicireducens*, *Streptococcus plurextorum*, and *Rothia nasimurium* and was negatively related to the abundance of *Clostridium bornimense* and *Neisseria dentiae*.

CONCLUSION

Taken together, these data suggested that BZN was correlated to the change in intestinal microbiota composition and modulated inflammatory and hormone secretion in piglet after the DON exposure. Moreover, the regulation of BZN on inflammation and hormone secretion was related to the change of the abundance of intestinal microbiota.

DATA AVAILABILITY STATEMENT

The dataset can be found in NCBI (SRA data: PRJNA705396).

ETHICS STATEMENT

The animal study was reviewed and approved by The experiment was carried out under the supervision of the experimental Animal Ethics Committee of the institute of subtropical agriculture (Changsha, Human Province, China).

AUTHOR CONTRIBUTIONS

AZ involved in writing—original draft, supervision, visualization, formal analysis, and project administration. PL contributed to methodology, funding acquisition, and project administration. ZC involved in investigation, conceptualization, and formal analysis. SL and MQ contributed to methodology and software. RT analyzed data curation. BT collected resources. All authors contributed to the article and approved the submitted version.

FUNDING

This research was supported by Special Funds for Construction of Innovative Provinces in Hunan Province (2019RS3022) and the Joints Funds of the National Science Foundation of China (Grant No: U20A2054).

SUPPLEMENTARY MATERIAL

The Supplementary Material for this article can be found online at: https://www.frontiersin.org/articles/10.3389/fnut.2021.738281/full#supplementary-material

REFERENCES

1. Wang X, Chen X, Cao L, Zhu L, Zhang Y, Chu X, et al. Mechanism of deoxynivalenol-induced neurotoxicity in weaned piglets is linked to lipid peroxidation, dampened neurotransmitter levels, and interference with calcium signaling. *Ecotoxicol Environ Saf.* (2020) 194:110382. doi: 10.1016/j.ecoenv.2020.110382
2. Yang C, Song G, Lim W. Effects of mycotoxin-contaminated feed on farm animals. *J Hazard Mater.* (2020) 389:122087. doi: 10.1016/j.jhazmat.2020.122087
3. World Health Organization. Evaluation of certain contaminants in food. *World Health Organ Tech Rep Ser.* (2017) 1002:1–166.
4. Zhao L, Zhang L, Xu Z, Liu X, Chen L, Dai J, et al. Occurrence of Aflatoxin B(1), deoxynivalenol and zearalenone in feeds in China during 2018-2020. *J Anim Sci Biotechnol.* (2021) 12:74. doi: 10.1186/s40104-021-00603-0
5. Ma R, Zhang L, Liu M, Su YT, Xie WM, Zhang NY, et al. Individual and combined occurrence of mycotoxins in feed ingredients and complete feeds in China. *Toxins.* (2018) 10:113. doi: 10.3390/toxins10030113
6. Canady R, Coker R, Egan SK, Krska R, Olsen M, Resnik S, et al. T-2 and HT-2 in WHO/IPCS safety evaluation of certain mycotoxins in food. *FAO Food Nutr Paper.* (2001) 74:557–680.
7. Guan S, Gong M, Yin Y, Huang R, Ruan Z, Zhou T, et al. Occurrence of mycotoxins in feeds and feed ingredients in China. *J Food Agric Environ.* (2011) 9:163–7. doi: 10.1016/j.ifset.2011.01.006

8. Gruber-Dorninger C, Jenkins T, Schatzmayr G. Global mycotoxin occurrence in feed: a ten-year survey. *Toxins*. (2019) 11:375. doi: 10.3390/toxins11070375
9. Eriksen GS, Pettersson H. Toxicological evaluation of trichothecenes in animal feed. *Anim Feed Sci Technol.* (2004) 114:205–39. doi: 10.1016/j.anifeedsci.2003.08.008
10. Liu M, Zhang L, Chu XH, Ma R, Wang YW, Liu Q, et al. Effects of deoxynivalenol on the porcine growth performance and intestinal microbiota and potential remediation by a modified HSCAS binder. *Food Chem Toxicol.* (2020) 141:111373. doi: 10.1016/j.fct.2020.111373
11. Payros D, Alassane-Kpembi I, Pierron A, Loiseau N, Pinton P, Oswald IP. Toxicology of deoxynivalenol and its acetylated and modified forms. *Arch Toxicol.* (2016) 90:2931–57. doi: 10.1007/s00204-016-1826-4
12. Zhang L, Ma R, Zhu MX, Zhang NY, Liu XL, Wang YW, et al. Effect of deoxynivalenol on the porcine acquired immune response and potential remediation by a novel modified HSCAS adsorbent. *Food Chem Toxicol.* (2020) 138:111187. doi: 10.1016/j.fct.2020.111187
13. Pestka JJ. Deoxynivalenol-induced IgA production and IgA nephropathy-aberrant mucosal immune response with systemic repercussions. *Toxicol Lett.* (2003) 140–1:287–95. doi: 10.1016/S0378-4274(03)00024-9
14. Pestka JJ, Zhou H-R, Moon Y, Chung YJ. Cellular and molecular mechanisms for immune modulation by deoxynivalenol and other trichothecenes: unraveling a paradox. *Toxicol Lett.* (2004) 153:61–73. doi: 10.1016/j.toxlet.2004.04.023
15. Grenier B, Loureiro-Bracarense A-P, Lucioli J, Pacheco GD, Cossalter A-M, Moll W-D, et al. Individual and combined effects of subclinical doses of deoxynivalenol and fumonisins in piglets. *Mol Nutr Food Res.* (2011) 55:761–71. doi: 10.1002/mnfr.201000402
16. Cano PM, Seeboth J, Meurens F, Cognie J, Abrami R, Oswald IP, et al. Deoxynivalenol as a new factor in the persistence of intestinal inflammatory diseases: an emerging hypothesis through possible modulation of Th17-mediated response. *PLoS ONE.* (2013) 8:e53647. doi: 10.1371/journal.pone.0053647
17. Liao Y, Peng Z, Chen L, Nüssler AK, Liu L, Yang W. Deoxynivalenol, gut microbiota and immunotoxicity: a potential approach? *Food Chem Toxicol.* (2018) 112:342–54. doi: 10.1016/j.fct.2018.01.013
18. Sobrova P, Adam V, Vasatkova A, Beklova M, Zeman L, Kizek R. Deoxynivalenol and its toxicity. *Interdiscip Toxicol.* (2010) 3:94–9. doi: 10.2478/v10102-010-0019-x
19. Flannery BM, Clark ES, Pestka JJ. Anorexia induction by the trichothecene deoxynivalenol (vomitoxin) is mediated by the release of the gut satiety hormone peptide YY. *Toxicol Sci.* (2012) 130:289–97. doi: 10.1093/toxsci/kfs255
20. Amuzie CJ, Pestka JJ. Suppression of insulin-like growth factor acid-labile subunit expression–a novel mechanism for deoxynivalenol-induced growth retardation. *Toxicol Sci.* (2010) 113:412–21. doi: 10.1093/toxsci/kfp225
21. Yang H, Lu Y, Zeng XF, Li L, Zhang RP, Ren ZK, et al. Antichronic gastric ulcer effect of zinc-baicalin complex on the acetic acid-induced chronic gastric ulcer rat model. *Gastroenterol Res Pract.* (2018) 2018:1275486. doi: 10.1155/2018/1275486
22. Gao Z, Xu H, Chen X, Chen H. Antioxidant status and mineral contents in tissues of rutin and baicalin fed rats. *Life Sci.* (2003) 73:1599–607. doi: 10.1016/S0024-3205(03)00487-9
23. Hill GM, Shannon MC. Copper and zinc nutritional issues for agricultural animal production. *Biol Trace Elem Res.* (2019) 188:148–59. doi: 10.1007/s12011-018-1578-5
24. Hostetler CE, Kincaid RL, Mirando MA. The role of essential trace elements in embryonic and fetal development in livestock. *Vet J.* (2003) 166:125–39. doi: 10.1016/S1090-0233(02)00310-6
25. Li C, Lin G, Zuo Z. Pharmacological effects and pharmacokinetics properties of Radix Scutellariae and its bioactive flavones. *Biopharm Drug Disposit.* (2011) 32:427–45. doi: 10.1002/bdd.771
26. Dinda B, Dinda S, DasSharma S, Banik R, Chakraborty A, Dinda M. Therapeutic potentials of baicalin and its aglycone, baicalein against inflammatory disorders. *Eur J Med Chem.* (2017) 131:68–80. doi: 10.1016/j.ejmech.2017.03.004
27. Sowndhararajan K, Deepa P, Kim M, Park SJ, Kim S. Neuroprotective and cognitive enhancement potentials of baicalin: a review. *Brain Sci.* (2018) 8:104. doi: 10.3390/brainsci8060104
28. Fang P, Yu M, Shi M, Bo P, Gu X, Zhang Z. Baicalin and its aglycone: a novel approach for treatment of metabolic disorders. *Pharmacol Rep.* (2020) 72:13–23. doi: 10.1007/s43440-019-00024-x
29. Wu L, Liao P, He L, Feng Z, Ren W, Yin J, et al. Dietary L-arginine supplementation protects weanling pigs from deoxynivalenol-induced toxicity. *Toxins.* (2015) 7:1341–54. doi: 10.3390/toxins7041341
30. Wu L, Wang W, Yao K, Zhou T, Yin J, Li T, et al. Effects of dietary arginine and glutamine on alleviating the impairment induced by deoxynivalenol stress and immune relevant cytokines in growing pigs. *PLoS ONE.* (2013) 8:e69502. doi: 10.1371/journal.pone.0069502
31. Zha A, Cui Z, Qi M, Liao S, Chen L, Liao P, et al. Dietary baicalin zinc supplementation alleviates oxidative stress and enhances nutrition absorption in deoxynivalenol challenged pigs. *Curr Drug Metab.* (2020) 21:614–25. doi: 10.2174/1389200221666200302124102
32. Council NR. *Nutrient Requirements of Swine: Eleventh Revised Edition*. Washington, DC: The National Academies Press (2012). p. 420.
33. Zha A, Liao P, Tan B, Cui Z, Liao S, Chen L, et al. Dietary baicalin zinc supplementation alleviates oxidative stress and enhances nutrition absorption in deoxynivalenol challenged pigs. *Curr Drug Metab.* (2020) 10:614–25.
34. Chen S, Tan B, Xia YY, Liao SM, Wang MW, Yin J, et al. Effects of dietary gamma-aminobutyric acid supplementation on the intestinal functions in weaning piglets. *Food Funct.* (2019) 10:366–78. doi: 10.1039/C8FO02161A
35. Zha A, Cui Z, Qi M, Liao S, Yin J, Tan B, et al. Baicalin-copper complex modulates gut microbiota, inflammatory responses, and hormone secretion in don-challenged piglets. *Animals.* (2020) 10:1535. doi: 10.3390/ani10091535
36. Li Y, Wang X, Wang X-q, Wang J, Zhao J. Life-long dynamics of the swine gut microbiome and their implications in probiotics development and food safety. *Gut Microbes.* (2020) 11:1824–32. doi: 10.1080/19490976.2020.1773748
37. Qi M, Tan B, Wang J, Liao S, Li J, Liu Y, et al. Post-natal growth retardation associated with impaired gut hormone profiles, immune and antioxidant function in pigs. *Front Endocrinol.* (2019) 10:660. doi: 10.3389/fendo.2019.00660
38. Zhao Y, Wang J, Wang H, Huang Y, Qi M, Liao S, et al. Effects of gaba supplementation on intestinal SIgA secretion and gut microbiota in the healthy and ETEC-infected weanling piglets. *Mediators Inflamm.* (2020) 2020:7368483-. doi: 10.1155/2020/7368483
39. Wang J, Zeng L, Tan B, Li G, Huang B, Xiong X, et al. Developmental changes in intercellular junctions and Kv channels in the intestine of piglets during the suckling and post-weaning periods. *J Anim Sci Biotechnol.* (2016) 7:4. doi: 10.1186/s40104-016-0063-2
40. Duan Y, Zhong Y, Xiao H, Zheng C, Song B, Wang W, et al. Gut microbiota mediates the protective effects of dietary β-hydroxy-β-methylbutyrate (HMB) against obesity induced by high-fat diets. *FASEB J.* (2019) 33:10019–33. doi: 10.1096/fj.201900665RR
41. Yan S, Zhu C, Yu T, Huang W, Huang J, Kong Q, et al. Studying the differences of bacterial metabolome and microbiome in the colon between landrace and meihua piglets. *Front Microbiol.* (2017) 8:1812. doi: 10.3389/fmicb.2017.01812
42. Zhao L, Feng Y, Deng J, Zhang NY, Zhang WP, Liu XL, et al. Selenium deficiency aggravates aflatoxin B1-induced immunotoxicity in chick spleen by regulating 6 selenoprotein genes and redox/inflammation/apoptotic signaling. *J Nutr.* (2019) 149:894–901. doi: 10.1093/jn/nxz019
43. Andrade VS, Rojas DB, de Andrade RB, Kim TDH, Vizuete AF, Zanatta Â, et al. A possible anti-inflammatory effect of proline in the brain cortex and cerebellum of rats. *Mol Neurobiol.* (2018) 55:4068–77. doi: 10.1007/s12035-017-0626-z
44. Le T-H, Alassane-Kpembi I, Oswald IP, Pinton P. Analysis of the interactions between environmental and food contaminants, cadmium and deoxynivalenol, in different target organs. *Sci Total Environ.* (2018) 622–623:841–8. doi: 10.1016/j.scitotenv.2017.12.014
45. Qi M, Tan B, Wang J, Liao S, Deng Y, Ji P, et al. The microbiota-gut-brain axis: a novel nutritional therapeutic target for growth retardation. *Crit Rev Food Sci Nutr.* (2021) 60:1–26. doi: 10.1080/10408398.2021.1879004
46. Vignal C, Djouina M, Pichavant M, Caboche S, Waxin C, Beury D, et al. Chronic ingestion of deoxynivalenol at human dietary levels impairs intestinal homeostasis and gut microbiota in mice. *Arch Toxicol.* (2018) 92:2327–38. doi: 10.1007/s00204-018-2228-6
47. Ali-Vehmas T, Rizzo A, Westermarck T, Atroshi F. Measurement of antibacterial activities of T-2 toxin, deoxynivalenol, ochratoxin A, aflatoxin

B1 and fumonisin B1 using microtitration tray-based turbidimetric techniques. *Zentralblatt fur Veterinarmedizin Reihe A.* (1998) 45:453–8. doi: 10.1111/j.1439-0442.1998.tb00848.x
48. Zhu L, Xu LZ, Zhao S, Shen ZF, Shen H, Zhan LB. Protective effect of baicalin on the regulation of Treg/Th17 balance, gut microbiota and short-chain fatty acids in rats with ulcerative colitis. *Appl Microbiol Biotechnol.* (2020) 104:5449–60. doi: 10.1007/s00253-020-10527-w
49. Noh K, Kang Y, Nepal MR, Jeong KS, Oh DG, Kang MJ, et al. Role of intestinal microbiota in baicalin-induced drug interaction and its pharmacokinetics. *Molecules.* (2016) 21:337. doi: 10.3390/molecules21030337
50. Shi S, Cheng B, Gu B, Sheng T, Tu J, Shao Y, et al. Evaluation of the probiotic and functional potential of Lactobacillus agilis 32 isolated from pig manure. *Lett Appl Microbiol.* (2020) 73:9–19. doi: 10.1111/lam.13422
51. Yu X, Åvall-Jääskeläinen S, Koort J, Lindholm A, Rintahaka J, von Ossowski I, et al. A comparative characterization of different host-sourced lactobacillus ruminis strains and their adhesive, inhibitory, and immunomodulating functions. *Front Microbiol.* (2017) 8:657. doi: 10.3389/fmicb.2017.00657
52. He K, Pan X, Zhou HR, Pestka JJ. Modulation of inflammatory gene expression by the ribotoxin deoxynivalenol involves coordinate regulation of the transcriptome and translatome. *Toxicol Sci.* (2013) 131:153–63. doi: 10.1093/toxsci/kfs266
53. Goyarts T, Dänicke S, Tiemann U, Rothkötter HJ. Effect of the Fusarium toxin deoxynivalenol (DON) on IgA, IgM and IgG concentrations and proliferation of porcine blood lymphocytes. *Toxicol In Vitro.* (2006) 20:858–67. doi: 10.1016/j.tiv.2005.12.006
54. Wu DD, Ding LQ, Tang XT, Wang WJ, Chen Y, Zhang T. baicalin protects against hypertension-associated intestinal barrier impairment in part through enhanced microbial production of short-chain fatty acids. *Front Pharmacol.* (2019) 10:13. doi: 10.3389/fphar.2019.01271
55. Liang S, Deng X, Lei L, Zheng Y, Ai J, Chen LL, et al. The comparative study of the therapeutic effects and mechanism of baicalin, baicalein, and their combination on ulcerative colitis rat. *Front Pharmacol.* (2019) 10:15. doi: 10.3389/fphar.2019.01466
56. Fu Y-J, Xu B, Huang S-W, Luo X, Deng X-L, Luo S, et al. Baicalin prevents LPS-induced activation of TLR4/NF-kappaB p65 pathway and inflammation in mice via inhibiting the expression of CD14. *Acta Pharmacol Sin.* (2020) 42:88–96. doi: 10.1038/s41401-020-0411-9
57. Terciolo C, Maresca M, Pinton P, Oswald IP. Review article: role of satiety hormones in anorexia induction by Trichothecene mycotoxins. *Food Chem Toxicol.* (2018) 121:701–14. doi: 10.1016/j.fct.2018.09.034
58. Bonnet MS, Roux J, Mounien L, Dallaporta M, Troadec JD. Advances in deoxynivalenol toxicity mechanisms: the brain as a target. *Toxins.* (2012) 4:1120–38. doi: 10.3390/toxins4111120

Conflict of Interest: The authors declare that the research was conducted in the absence of any commercial or financial relationships that could be construed as a potential conflict of interest.

Publisher's Note: All claims expressed in this article are solely those of the authors and do not necessarily represent those of their affiliated organizations, or those of the publisher, the editors and the reviewers. Any product that may be evaluated in this article, or claim that may be made by its manufacturer, is not guaranteed or endorsed by the publisher.

frontiers in Nutrition

ORIGINAL RESEARCH
published: 13 October 2021
doi: 10.3389/fnut.2021.756565

Role of the Aryl Hydrocarbon Receptor and Gut Microbiota-Derived Metabolites Indole-3-Acetic Acid in Sulforaphane Alleviates Hepatic Steatosis in Mice

Xiuxiu Xu[1,2†], Siyuan Sun[1†], Ling Liang[1†], Chenxi Lou[1], Qijin He[1], Maojuan Ran[1], Lu Zhang[1], Jingyue Zhang[3], Chen Yan[3], Hengjie Yuan[3], Lu Zhou[1], Xin Chen[1], Xin Dai[1], Bangmao Wang[1], Jie Zhang[1*] and Jingwen Zhao[1*]*

[1] Tianjin Key Laboratory of Digestive Diseases, Department of Gastroenterology and Hepatology, Tianjin Institute of Digestive Disease, Tianjin Medical University General Hospital, Tianjin, China, [2] NHC Key Laboratory of Hormones and Development, Tianjin Key Laboratory of Metabolic Diseases, Tianjin Medical University Chu Hsien-I Memorial Hospital & Tianjin Institute of Endocrinology, Tianjin Medical University, Tianjin, China, [3] Department of Pharmacy, Tianjin Medical University General Hospital, Tianjin, China

Scope: Gut microbiome-derived metabolites are the major mediators of diet-induced host-microbial interactions. Aryl hydrocarbon receptor (AHR) plays a crucial role in glucose, lipid, and cholesterol metabolism in the liver. In this study, we aimed to investigate the role of indole-3-acetic acid (IAA) and AHR in sulforaphane (SFN) alleviates hepatic steatosis in mice fed on a high-fat diet (HFD).

Methods and Results: The HFD-fed male C57BL/6 mice were intervened with SFN for 6 weeks. HFD-mice showed classical pathophysiological characteristics of hepatic steatosis. The results showed that SFN significantly reduced body weight, liver inflammation and hepatic steatosis in HFD-fed mice. SFN reduced hepatic lipogenesis by activating AHR/SREBP-1C pathway, which was confirmed in HepG2 cell experiments. Moreover, SFN increased hepatic antioxidant activity by modulating Nrf-2/NQO1 expression. SFN increased serum and liver IAA level in HFD mice. Notably, SFN manipulated the gut microbiota, resulting in reducing *Deferribacteres* and proportions of the phylum *Firmicutes/Bacteroidetes* and increasing the abundance of specific bacteria that produce IAA. Furthermore, SFN upregulated *Ahr* expression and decreased the expression of inflammatory cytokines in Raw264.7 cells.

Conclusions: SFN ameliorated hepatic steatosis not only by modulating lipid metabolism via AHR/SREBP-1C pathway but regulating IAA and gut microbiota in HFD-induced NAFLD mice.

Keywords: NAFLD, AHR, indole-3-acetic acid, sulforaphane, gut microbiota, high-fat diet

OPEN ACCESS

Edited by:
Xi Ma,
China Agricultural University, China

Reviewed by:
Yangchun Cao,
Northwest A and F University, China
Peixin Fan,
University of Florida, United States

****Correspondence:***
Bangmao Wang
mwang02@tmu.edu.cn
Jie Zhang
zhangjie_xhk@tmu.edu.cn
Jingwen Zhao
jingwenzhao@tmu.edu.cn

† These authors have contributed equally to this work and share first authorship

Specialty section:
This article was submitted to Nutrition and Microbes, a section of the journal Frontiers in Nutrition

Received: *10 August 2021*
Accepted: *17 September 2021*
Published: *13 October 2021*

Citation:
Xu X, Sun S, Liang L, Lou C, He Q, Ran M, Zhang L, Zhang J, Yan C, Yuan H, Zhou L, Chen X, Dai X, Wang B, Zhang J and Zhao J (2021) Role of the Aryl Hydrocarbon Receptor and Gut Microbiota-Derived Metabolites Indole-3-Acetic Acid in Sulforaphane Alleviates Hepatic Steatosis in Mice. Front. Nutr. 8:756565. doi: 10.3389/fnut.2021.756565

INTRODUCTION

Approximately 25% of the global population struggles with non-alcoholic fatty liver disease (NAFLD) with a dramatically growing prevalence (1). Currently, the widely accepted pathogenesis of NAFLD is that lipid deposits accumulate in the liver, followed by the activation of immune cells and the production of proinflammatory cytokines (2, 3). Regulating metabolic nuclear receptors, such as the sterol regulatory element-binding protein-1c (Srebp-1c), carbohydrate response element-binding protein (ChREBP), and peroxisome proliferator-activated receptor γ (PPAR-γ) prevents hepatic steatosis caused by a high-fat diet (HFD), indicating that uncontrolled *de novo* lipogenesis contributes to the development of NAFLD (4–6).

Increasing numbers of studies have demonstrated that Western and high-calorie diet influences the composition of the gut microbiota (7), which in turn has gained attention with respect to metabolic diseases, such as obesity (8), metabolic syndrome (MS) (9), diabetes (10), cardiovascular disease (11), and NAFLD (12). A myriad of studies has reported the effects of gut microbial metabolites on host health and disease, which might be mediated partially through the metabolome, such as short-chain fatty acid, serotonin, bile acids, and tryptophan metabolites (13). Especially the indole-3-acetic acid (IAA) that is mainly synthesized by *Clostridium*, *Bacteroides*, and *Bifidobacterium* (14), participates in the remission of NAFLD by improving insulin resistance, oxidative stress, and lipid metabolism (3, 15). Indole and its derivatives maintain the integrity of the liver and benefit intestinal permeability and immune function, which might inhibit liver inflammation (16). Additionally, TH17/regulatory T (Treg) cells balance plays a major role in autoimmune and inflammatory diseases. Notably, previous studies reported that tryptophan catabolite promotes the differentiation of naive $CD4^+$ T helper cells into Treg cells and TH17 cells via aryl hydrocarbon receptor (AHR) (17).

AHR is a ligand-activated transcription factor widely expressed in all types of tissues and cells, especially immune cells (18). Furthermore, AHR participates in several physiological processes, including chemical and microbial defense, cell proliferation, immunity, inflammation, and energy metabolism *via* ligand binding and regulating target genes (19). Gut microbiome-derived metabolites, such as endogenous ligands of AHR alleviate gastrointestinal inflammation, atopic dermatitis, and arthritis (20–23). Accumulating evidence suggested that AHR plays a crucial role in glucose, lipid, and cholesterol metabolism in the liver (24), thereby deeming its role in the pathogenesis of NAFLD. Moreover, Kupffer cells are resident liver macrophages and the primary cells that produce various inflammatory and fibrosis mediators, play a major role in liver inflammation (25). Previous studies have also shown that the AHR agonist IAA reduces the level of proinflammatory cytokines produced by macrophages stimulated by fatty acids and LPS and inhibits the migration of macrophages to chemokines, thereby indicating that AHR and ligands regulate the macrophages (3).

Phytochemicals widely present in a variety of fruits and vegetables can prevent lipid-related diseases (26). Sulforaphane (SFN), a natural isothiocyanate compound extracted from cruciferous vegetables, exerts strong anti-inflammatory and anti-cancer effects (27). It also alleviates alcohol-induced hepatosteatosis and HFD-induced lipid accumulation in mice (28). However, whether SFN improves gut microbiota and its metabolites is yet to be elucidated.

Therefore, the objective of the present study is to test the hypothesis that SFN might regulate IAA and gut microbiota in HFD-fed mice and prevent NAFLD through activating AHR/SREBP-1C pathway.

Abbreviations: AHR, aryl hydrocarbon receptor; LPS, lipopolysaccharide; SFN, sulforaphane; IAA, indole-3-acetic acid; HFD, high-fat diet; AST, aspartate aminotransferase; ALT, alanine aminotransferase; SREBP-1c, synthase and sterol regulatory element-binding protein-1c; NRF2, NF-E2-related factor 2; FAS, fatty acid synthase; SCD1, stearoyl-CoA desaturase-1; NQO1, NAD(P)H: quinine oxidoreductase 1.

MATERIALS AND METHODS

Animals and Treatment

Male C57BL/6 mice (3–4weeks) were housed in a specific-pathogen-free (SPF) environment at the Laboratory Animal Center of Chinese Academy of Medical Sciences Institute of Radiation Medicine, with a 12 h light/dark cycle and access to food and water freely. The animal chow was purchased from Hua Fu Kang (Beijing, China). After acclimation for 1 week, the mice were randomly classified into two weight-matched groups: (1) normal chow diet (NCD) group ($n = 10$/group); (2) high-fat diet (HFD) group ($n = 20$/group) (HFD: protein 18.1%, fat 61.6%, carbohydrates 20.3%). After 22 weeks of the initial feeding period, HFD group mice were randomly assigned to two groups ($n = 10$/group): a HFD with saline, and a HFD with Sulforaphane (purity >99%, *Item NO.10496*, Cayman) 25 mg/kg intervention by gavage daily for 6 weeks. The liver tissues were harvested, weighed, and stored at −80°C for further analysis. All animal welfare and experimental procedures complied with the Laboratory Animal Management Regulations in China.

Biochemical Analysis

Following anesthetization, blood was collected from the retro-orbital plexus, and the serum was separated and stored at −80°C. The levels of alanine aminotransferase (ALT), aspartate aminotransferase (AST), cholesterol (TC), and triglyceride (TG) in serum were measured by standard procedures in the Institute of Clinical Chemistry of the Tianjin Medical University General Hospital.

Histopathology

The liver tissue specimens were immediately fixed in 4% formaldehyde, embedded in paraffin, sectioned into 4-μm-thick slices, and stained with hematoxylin-eosin (H&E) for histological examination of fat droplets. The stained tissues were assessed by a pathologist in a blinded manner, and images were captured using Leica fluorescence microscope (Leica, Germany).

Cell Culture and Treatment

Raw264.7 and HepG2 cells were obtained from the Chinese Academy of Sciences Cell Bank (Shanghai, China). Raw264.7

murine macrophages were cultured in Dulbecco's modified Eagle's medium (DMEM, Gibco) supplemented with 10% fetal bovine serum (FBS, Gibco) and 1% nonessential amino acid solution (Solarbio, Beijing, China). Then, the cells were pretreated with Sulforaphane (SFN, purity >99%) 20 μM for 6 h, followed by 300 μM palmitate (PA, Sigma Aldrich) complexed with Bovine serum albumin (BSA, #abs9156, Absin Bioscience Inc.) treatment. After 18 h, 10 ng/mL lipopolysaccharide (LPS, from Escherichia coli, O111:B4, Sigma Aldrich) was added to the culture medium, and the cells were incubated for an additional 6 h. HepG2 cells were cultured in DMEM supplemented with 10% FBS. After reaching 70% confluency, cells were stimulated with 10 μM SFN or 500 μM indole-3-acetic acid (IAA, purity: 99.1%, Sigma Aldrich) for 24 h, followed by treatment with or without 250 μM PA for another 24 h in serum-free media containing 25 mM glucose and 0.25% BSA. All cells were incubated at 37°C in a humidified atmosphere containing 5% CO_2.

RNA Isolation and RT-qPCR Analysis

Total RNA was purified from liver or cells using TRIzol (Invitrogen, Carlsbad, CA, USA.) and reverse transcribed to cDNA using TIANScript RT kit (Tiangen Inc., Beijing, China). Subsequently, quantitative PCR amplification was performed using SYBR^{TM} Select Master Mix on the ABI StepOne Plus Real-Time PCR System (Applied Biosystems). Mir-155 was detected by Bulge-Loop^{TM} miRNA qRT-PCR Starter Kit (Ribobio, Guangzhou, China). The relative mRNA or miRNA expression levels were calculated by normalizing the level of the target genes against that of the housekeeping genes, such as glyceraldehyde-3-phosphate dehydrogenase (*GAPDH*), using the $2^{-\Delta\Delta Ct}$ method. The specific primer sequences are listed in **Table 1**.

Protein Extraction and Western Blot Analysis

Total protein was extracted by RIPA buffer (Solarbio, Beijing, China) containing protease inhibitors (PMSF) (Solarbio, Beijing, China), while nuclear protein was extracted using a Nuclear Protein Extraction kit (Solarbio, Beijing, China). The protein concentrations were determined using a BCA Protein Assay kit (Solarbio, Beijing, China). The tissue lysates were separated by sodium dodecyl sulfate-polyacrylamide gel electrophoresis (SDS-PAGE) and transferred to nitrocellulose membranes (Pall Co, USA) at a voltage of 90V. Blotted membranes were blocked with 5% BSA for 1.5 h at room temperature and incubated overnight at 4°C with anti-FAS(#3180, Cell Signaling Technology), anti-SREBP-1(#NB100-2215, Novus), anti-NRF2(#12721, Cell Signaling Technology), anti-AHR (#sc-13308, Santa Cruz Biotechnology), anti-Lamin-B2(#12255, Cell Signaling Technology) and anti-β-Actin(#3700, Cell Signaling Technology), followed by incubation with horseradish peroxidase-conjugated goat anti-rabbit or anti-mouse IgG (1:5,000, Zhongshan Golden Bridge Biotechnology, Beijing, China) for 1 h at room temperature. Fluorescent bands were visualized and photographed using an SYNGENE CGQ/D2 GEL-Image System (Bio-Rad, America).

Targeted Metabolomics

Briefly, 100 μL of mouse serum samples were mixed with 10 μL indole-3-acetic-2,2-d2 acid (D2-IAA, purity: 98%, Sigma Aldrich) 100 ng/mL, and 400μL chilled methanol. The mixture was agitated for 3 min, and the supernatant was collected by centrifugation at 14,000 rpm for 10 min. The liver tissues (100 mg) were homogenized with a grinding rod and mixed with 10 μL D2-IAA (100 ng/mL) and 500 μL chilled methanol. The mixture was vortexed for 3 min, and the supernatant was collected by centrifugation at 6,800 rpm for 10 min at 4°C four times with an interval of 45 s each. Subsequently, the supernatant liquor/0.01% formic acid solution (1:9, v/v) was transferred to a new tube, vortexed for 1 min, and spun at 14,000 rpm for10 min at 4°C. Finally, 10 μL supernatant liquor was analyzed by ultra-high-performance liquid chromatography-tandem mass spectrometry (UPLC-MS/MS) system. The metabolite levels were normalized to the sample weight.

Immunofluorescence and Immunohistochemistry

Liver tissues were cut, deparaffinized, dehydrated, and incubated with specific antibodies against F4/80(#70076, Cell Signaling Technology) overnight at 4°C. Subsequently, the slides were washed with phosphate-buffered saline (PBS) three times and incubated with fluorochrome-conjugated secondary antibody for 1 h at room temperature in the dark. Subsequently, the slides were washed and incubated with Prolong Gold antifade containing DAPI and mounted for IF. IHC was carried out to determine the expression of F4/80 in the liver tissue. The slides were analyzed under a Leica fluorescence microscope (Leica, Germany).

16S rRNA Gene Sequencing

The composition of mice feces was analyzed by*16S* rRNA gene amplicon sequencing. The extracted genomic DNA was analyzed by 1% agarose gel electrophoresis, and the product was purified using Agencourt A MPure XP Nucleic Acid Purification kit (Beckman Coulter). The V3 and V4 regions of the *16S* gene were amplified by PCR and sequenced on an Illumina MiSeqPE300. Quantitative insights into microbial ecology (QIIME) software pipeline v.1.8.0 was used to analyze the raw data files. Operational Taxonomic Units (OTUs) were used clustered into represent groups and assigned to taxonomy using VSEARCH 2.7.1 at 97% similarity. Then, a representative sequence of OUT was subjected to the taxonomy analysis basing on the Sliva bacterial 16S rRNA database. Alpha-diversity (Chao1, Observed_species, PD_whole_tree, Shannon) and beta-diversity were analyzed to identify the species diversity. The relative abundance of bacteria was expressed at the percentage.

RNA *in situ* Hybridization

RNAscope Multiplex Fluorescent Reagent kit v2 (ACDbio) in combination with Opal 570 Reagent Pack (Perkin Elmer) were used for RNA *in situ* hybridization according to the manufacturer's instructions. Before mounting, the slides were counterstained with a primary antibody against F4/80 for 1 h at room temperature and processed for IF detection. Probes for murine AHR were used (ACDbio).

TABLE 1 | Primer sequences used in RT-qPCR.

Gene	Forward sequence (5′ → 3′)	Reverse sequence (5′ → 3′)
Gapdh	GGAGAAACCTGCCAAGTATG	TGGGAGTTGCTGTTGAAGTC
Mcp1	TTAAAAACCTGGATCGGAACCAA	GCATTAGCTTCAGATTTACGGGT
Il-1β	GTGTCTTTCCCGTGGACCTT	AATGGGAACGTCACACACCA
Il-6	CCAGTTGCCTTCTTGGGACT	GGTCTGTTGGGAGTGGTATCC
F4/80	CTTTGGCTATGGGCTTCCAGTC	GCAAGGAGGACAGAGTTTATCGTG
Tnf-α	GGTGCCATGTCTCAGCCTCTT	GCCATAGAACTGATGAGAGGGAG
Srebp-1c	GGAGCCATGGATTGCACATT	GGCCCGGGAAGTCACTGT
Acc1	GACAGACTGATCGCAGAGAAAG	TGGAGAGCCCCACACACA
Scd1	TTCTTGCGATACACTCTGGTGC	CGGGATTGAATGTTCTTGTCGT
Fas	GGAGGTGGTGATAGCCGGTAT	TGGGTAATCCATAGAGCCCAG
Gclm	TGACTCACAATGACCCGAAA	CTTCACGATGACCGAGTACCT
Nqo1	AGCGTTCGGTATTACGATCC	AGTACAATCAGGGCTCTTCTCG
Gclc	AGATGATAGAACACGGGAGGAG	TGATCCTAA AGCGATTGTTCTTC
Gstm1	GCAGCTCATCATGCTCTGTT	CATTTTCTCAGGGATGGTCTTC
GAPDH	CCCTTCATTGACCTCAACTACATGG	CATGGTGGTGAAGACGCCAG
SREBP-1C	CTTCCGCCCTTGAGCTG	CTGGTGTGTCCGTGTGG
NQO1	TGGTTTGGAGTCCCTGCCAT	CACTGCCTTCTTACTCCGGAAGG
ACC1	ATGTCTGGCTTGCACCTAGTA	CCCCAAAGCGAGTAACAAATTCT
FAS	CCGCGGTTTAAATAGCGTCG	CACCTCCTCCATGGCTGGT

Statistical Analysis

Data are represented as mean ± standard deviation (SD). GraphPad Prism 7 (GraphPad Software Inc., San Diego, CA, USA) was used for statistical analysis. Significant differences were analyzed using one-way ANOVA in multiple groups. $P < 0.05$ were considered as statistically significant.

RESULTS

SFN Attenuated Hepatic Steatosis in HFD-Induced NAFLD Mice

To address whether SFN curbs the progression of the disease, we used HFD-fed mice as the NAFLD model (**Figure 1A**). Representative liver photographs of mice are shown in **Figure 1B**. The liver tissues of the HFD group showed severe hepatic steatosis with marked fat droplets and balloon-like structures in the hepatocytes by H&E staining, while the administration of SFN caused a remarkable amelioration of the appearance of hepatic steatosis (**Figure 1B**). In addition, body weight, liver weight and index (liver/body weight) of the mice were increased by HFD, which were also restored by SFN treatment (**Figures 1C–E**). Similarly, the level of TC and TG in serum were largely reduced by SFN. SFN also exhibited protective effects against the HFD-induced liver damage, which was further supported by low serum AST and ALT levels (**Figures 1F–I**). Furthermore, SFN decreased mRNA expression of tumor necrosis factor-alpha (*Tnf-a*) and monocyte chemoattractant protein-1 (*Mcp-1*) in liver tissues (**Figures 1J,K**), suggesting that it significantly alleviates liver inflammation. Notably, the expression of anti-oxidative stress-related genes *Gstm1* was inhibited by HFD, but *Gstm1* ($P < 0.05$) and *Gclm* ($P < 0.01$) were upregulated by SFN treatment (**Figures 1L,M**). Thus, these data revealed that SFN drastically alleviates HFD-induced NAFLD.

SFN Administration Improved Lipid Metabolism of the Liver in HFD-Fed Mice

Herein, we assessed whether SFN displays a protective effect on hepatic lipid metabolism and observed that the expression of fatty acid metabolism genes, sterol regulatory element-binding protein-1c (*Srebp-1c*), fatty acid synthase (*Fas*), stearoyl-CoA desaturase-1 (*Scd-1*), and acetyl-CoA carboxylase 1 (*Acc1*) in the liver, was decreased by SFN administration (**Figures 2A–D**). SREBP-1C is a transcription factor involved in hepatic lipid metabolism and regulation of the expression of multiple genes in TG and fatty acid synthesis (29). Furthermore, we examined the expression of SREBP-1C and FAS in the liver by Western blot and found that the levels of both proteins were reduced by SFN (**Figures 2E,F**). Moreover, SFN had no effect on endogenous levels of total AHR protein, but markedly reduced the mRNA expression of *Ahr* in the liver tissue of HFD mice ($P < 0.01$) (**Figures 2G,H**). We also observed that SFN significantly elevated the expression of *Nqo1* ($P < 0.05$) and *Gclc* ($P < 0.01$) (**Figures 2I,J**).

SFN Alleviates Lipid Metabolism in Hepatocytes by Activating AHR

To further explore the effect of AHR on lipid metabolism, relevant experiments were conducted *in vitro* with HepG2 cells. Intriguingly, SFN also reduced the protein levels of SREBP-1C, ACC1, and FAS, and their mRNA expression in HepG2 cells (**Figures 3A–F**), which was consistent with the data in mice.

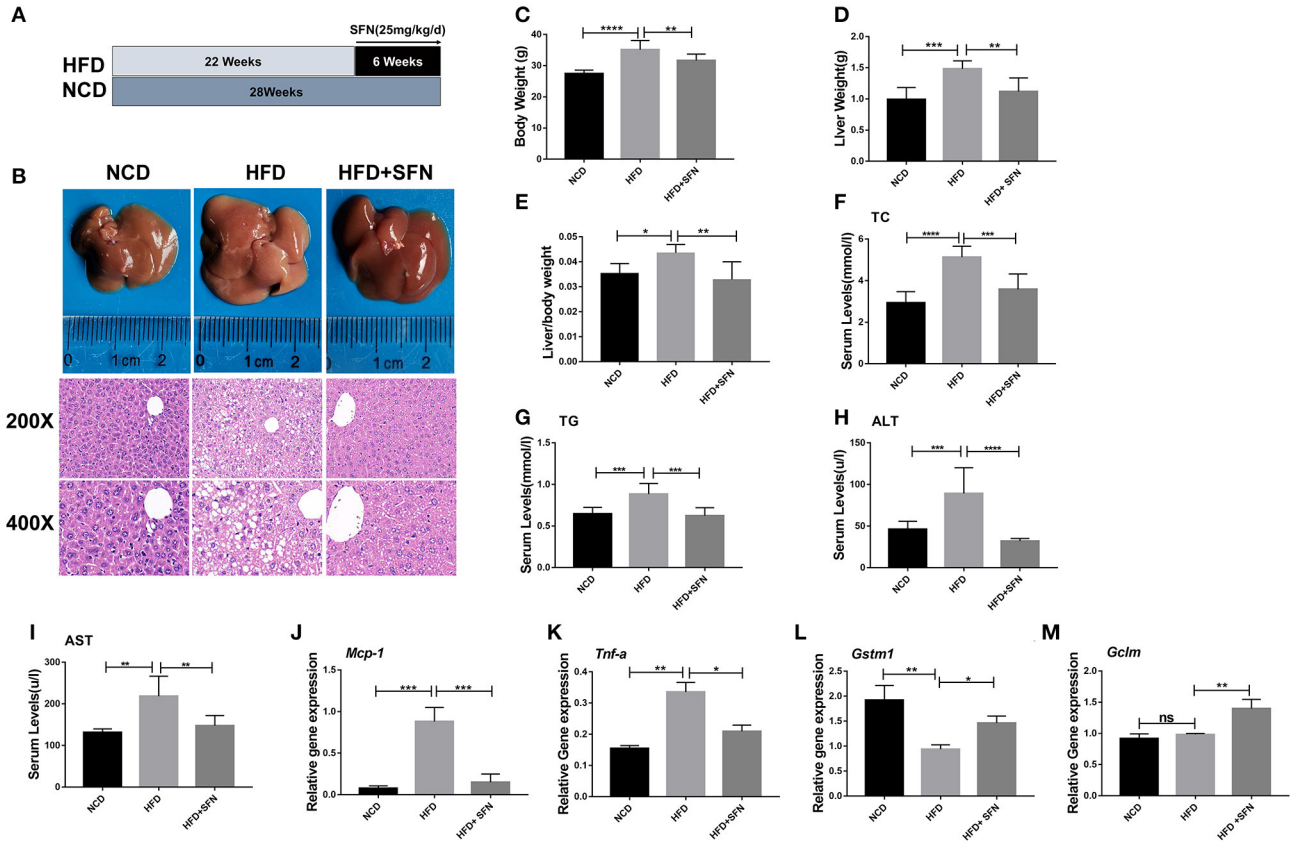

FIGURE 1 | Preventive effects of SFN on the development of HFD-induced NAFLD in mice. **(A)** Model development and treatment. **(B)** Representative liver images and H&E staining of liver sections from different groups (×400). **(C–E)** The mice body weight, liver weight and index (liver/body weight). **(F–I)** Serum levels of TC, TG, ALT and AST. **(J,K)** The expression of *Mcp-1* and *Tnf-a* in the liver. **(L,M)** SFN attenuates the expression of anti-oxidative stress mRNA. Data are presented as mean ± SD. ns, not significant, $^{*}P < 0.05$, $^{**}P < 0.01$, $^{***}P < 0.001$, $^{****}P < 0.0001$ vs. HFD group.

Especially, the protein level of ACC1 was potently reduced by SFN. Furthermore, treatment with SFN increased the nuclear protein content of AHR and NRF2 compared to the PA-treated group (**Figures 3G,H**). We also observed that SFN significantly reduces the expression of NRF2 target genes: *NQO1* ($P < 0.001$) and *GCLC* ($P < 0.01$) (**Figures 3I,J**). In addition, IAA was used as a positive control, and the results of the SFN group were like those of the IAA-positive group compared to the PA-treated cells. Taken together, SFN inhibited the progression of NAFLD by activating the AHR/SREBP-1c pathway.

Changes in Gut Microbiota Composition and Species Diversity During SFN-Treatment in HFD-Fed Mice

To evaluate the changes in the gut microbiota after SFN treatment, we conducted the *16S* rRNA sequencing analysis. Compared to the NCD group, the relative abundance of *Deferribacteres, Proteobacteria, Firmicutes*, and *Actinobacteria* from HFD mice increased at the phylum level. Interestingly, *Tenericutes* increased in the HFD+SFN group. Conversely, the abundance of *Deferribacteres* was low, which was similar to the NCD group. Moreover, the *Firmicutes*-to-*Bacteroidetes* ratio was significantly higher in HFD-fed mice (84.182) compared to the NCD-fed mice (1.028), but the ratio was decreased to 16.189 by SFN treatment. At the genus level, HFD increased the abundance of *Mucispirillum*, *Helicobacter*, *Lachnospiraceae_UCG_006*, *Lactobacillus*, and *Romboutsia* and decreased the levels of *Bifidobacterium*, *Bacteroides*, *Ruminococcaceae_UCG-014, Ruminococcaceae_UCG-010*, *Prevotellaceae_UCG-001*, and *Eubacterium_fissicatena_group*. However, SFN increased the relative abundance of *Bifidobacterium*, *Romboutsia*, and *Ruminococcaceae_UCG-014* (**Figures 4A,B**). The Venn diagrams indicated that the 184 operational taxonomic units (OTUs) were identical among the three groups (OTUs). The HFD group demonstrated the most unique genus (18 OTUs) followed by the NCD group (345 OTUs) and HFD+SFN group (29 OTUs) (**Figure 4C**). Together, these findings indicated that SFN regulates the composition of gut microbiota in HFD-fed mice.

As shown in **Figure 4D**, the rarefaction curve progressed to a plateau, which indicated that the gut microbial diversity in all the samples was captured at the current sequencing depth. The *Specaccum* species accumulation curves tended to flatten with the increase in sample size,

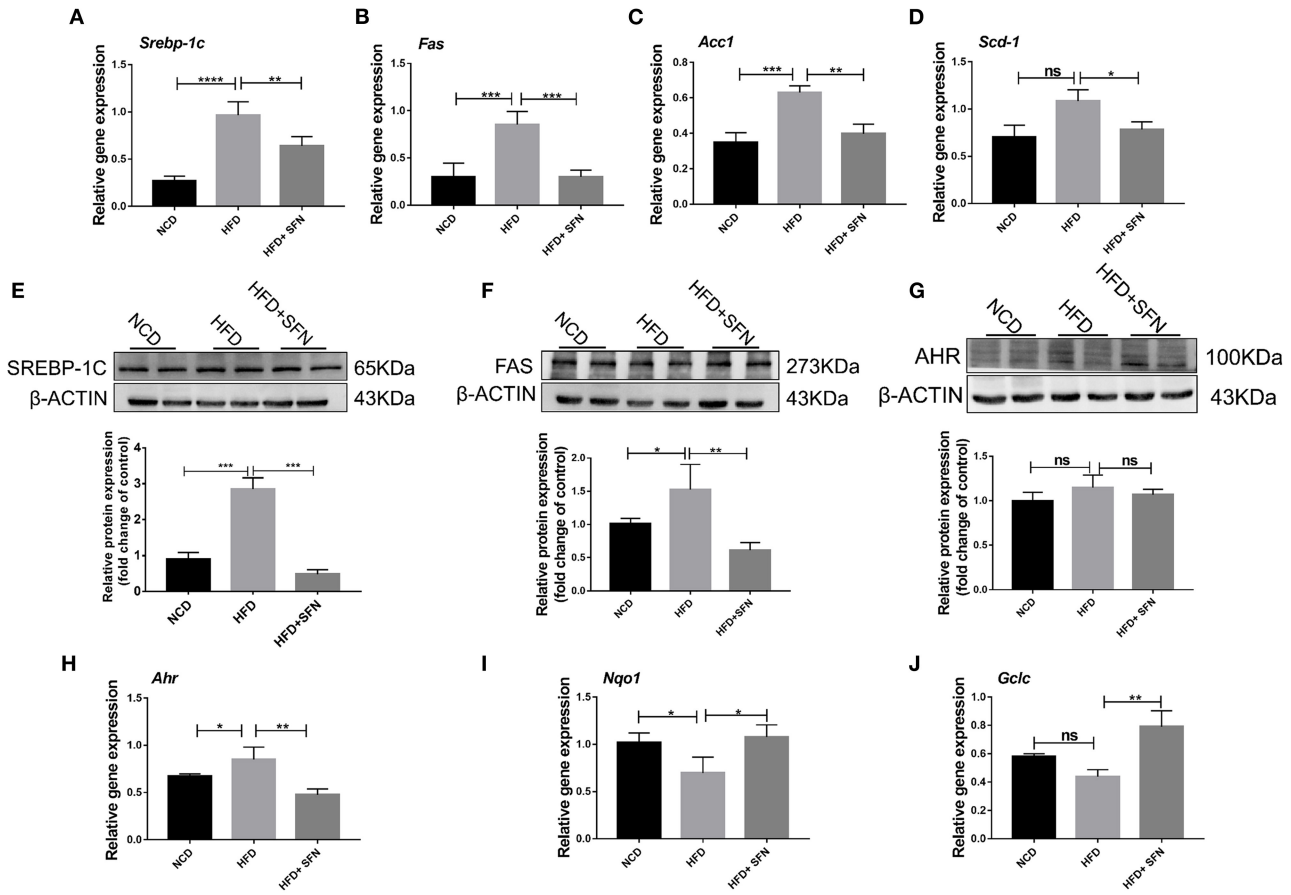

FIGURE 2 | Effects of SFN on lipid metabolism of the liver. **(A–D)** Relative mRNA levels of *Srebp-1c*, *Fas*, *Acc1* and *Scd-1* were associated with *de novo* lipogenesis in the liver. **(E,F)** Western blot showing SREBP-1C and FAS protein levels in the liver. **(G)** Levels of total AHR protein in the liver. **(H)** The expression of *Ahr* in the liver tissue. **(I,J)** Antioxidant stress relative gene expression in the liver. Data are presented as mean ± SD. ns, not significant, $^{*}P < 0.05$, $^{**}P < 0.01$, $^{***}P < 0.001$, $^{****}P < 0.0001$ vs. HFD group.

indicating that the sampling was sufficient for data analysis (**Figure 4E**). For the microbial alpha diversity, the Chao 1, observed_species, Shannon and PD_whole_tree showed that SFN intervention increased the species diversity compared with the HFD group after administration of SFN for 6 weeks (**Figure 4F**).

Principal component analysis (PCA) and principal coordinate analysis (PCoA) based on Unifrac and Bray–Curtis distance were utilized to analyze the difference in the gut microbiota of each sample. As shown in **Figures 4G,H**, there was a large gap between the HFD group and NCD group, suggesting that HFD exerts a notable effect on the composition of gut microbiota. Although there was some overlap, a certain distance was also observed between the HFD and HFD+SFN groups, indicating specific differences in the composition of gut microbiota between the two groups. Furthermore, specific bacterial taxa with varied relative abundance were identified among NCD, HFD, and HFD + SFN groups by linear discriminant analysis (LDA) effect size (LEfSe) analysis (LDA threshold is 3). As shown in **Figures 4I,J**, the major species in the NCD group were *Bacteroidetes*, at the genus level, *Bacteroidetes* and *Alloprevotella*, and at the family level, *Prevodiaceae* and *Bacteroidales_S247_group*. The species that play a significant role in the HFD group are *Deferribacteres* and *Firmicutes*. At the genus level, *Facecalibaculum*, *Romboutsia*, Lachnospiraceae_UCG_006, and Streptococcus, and at the family level, *Peptostreptococcaceae*, *Streptococcaceae*, and *Deferribacteraceae* were abundant. The key species of the HFD+SFN group were *Clostridia* class and *Clostridiales* order.

SFN Administration Altered the Level of IAA Metabolite in HFD-Fed Mice

To assess the metabolic changes in the gut microbiota remodeled by SFN, we performed targeted UPLC-MS/MS experiments to detect the content of IAA in serum and the liver of mice in the NCD group, the HFD group, and the HFD+SFN group. These analyses indicated that the levels of IAA in the liver and serum of HFD mice were notably lower than that of NCD

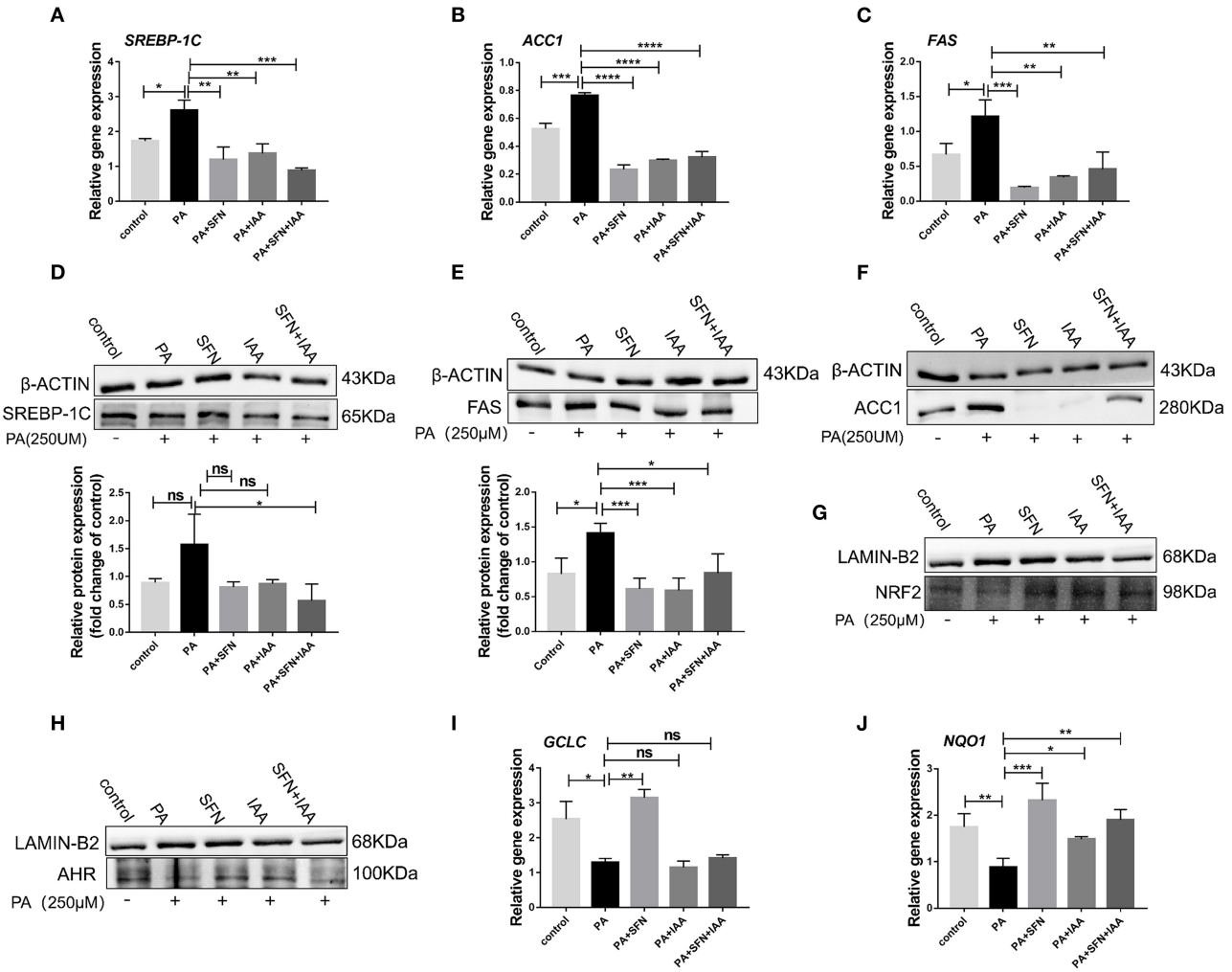

FIGURE 3 | SFN attenuates the expression of genes related to the *de novo* lipogenesis in HepG2 cells. **(A–C)** SFN decreased the mRNA expression of *SREBP-1C*, *ACC1*, and *FAS* in HepG2 cells exposed to PA. **(D–F)** SFN decreased the protein expression of SREBP-1C, FAS, and ACC1 in HepG2 cells exposed to PA. **(G,H)** Immunoblots showing NRF2 and AHR content in the nuclear fractions. **(I,J)** Antioxidant stress relative gene expression in HepG2 cells. Quantitation of results of Western blot using Image J software. Data are presented as mean ± SD. ns means not significant, $^{*}P < 0.05$, $^{**}P < 0.01$, $^{***}P < 0.001$, $^{****}P < 0.0001$ vs. HFD group.

mice but increased significantly by SFN ($P < 0.05$, $P < 0.0001$) (**Figures 5A,B**).

To further explore the relationship between metabolite IAA and gut microbiota, as shown in the Sperman heatmap (**Figure 5C**), the abscissa is the differential metabolite, and the ordinate is the different species. Red represents positive correlation, blue represents negative correlation, and the darker the color, the stronger the correlation. *Bacteroides*, *Alistipes* and *Prevotellaceae_UCG.001* were positively correlated with serum IAA and negatively correlated with serum total cholesterol (TC). However, *Romboutsia*, *Streptococcus*, *Lactococcus* and *Faecalibaculum* were positively correlated with serum TC and negatively correlated with serum IAA.

Sulforaphane Attenuates the Expression of Proinflammatory Cytokines in Macrophages

The mRNA expression of *F4/80* (macrophage surface marker) was inhibited by SFN in the liver of HFD mice (**Figure 6A**), and IHC showed similar results (**Figure 6B**). These results demonstrated that SFN reduced the number of macrophages in the liver and inhibited liver inflammation.

Furthermore, we treated Raw264.7 cells with PA and LPS to simulate the two key factors affecting the development of NAFLD to non-alcoholic steatohepatitis (NASH). Then, the expression of *Il-6*, *Il-1β*, *Mcp-1, Tnf-a,* and *Mir-155* increased significantly after PA, LPS, and PA+LPS-treatment, whereas these mRNA expression were suppressed by SFN (**Figures 6C–G**). Conversely,

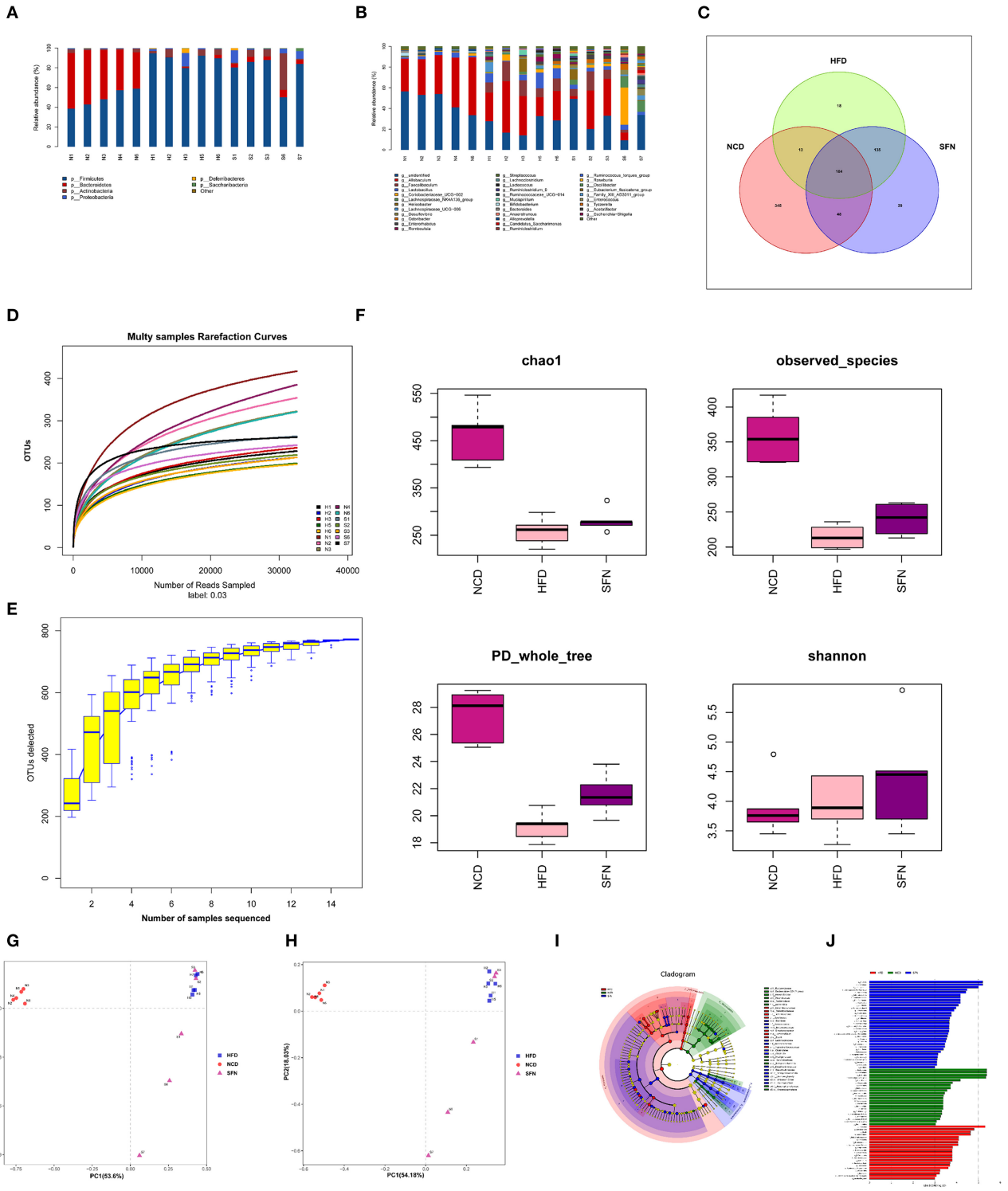

FIGURE 4 | SFN intervention manipulated the gut microbiota composition in HFD-fed mices, five animals from each group were analyzed. **(A)** At phylum level. **(B)** At genus level. **(C)** Venn diagram representation of the number of OTUs at the genus level from the NCD, HFD, and HFD+SFN group. **(D)** The rarefaction curves, **(E)** Species accumulation curves, **(F)** Chao1, Observed_species, PD_whole_tree, Shannon. **(G)** PCA based on the relative abundance of OTUs. **(H)** PCoA score plot based on Unifrac and Bray–Curtis. **(I)** Taxonomic cladogram derived from LEfSe analysis. **(J)** The species with LDA scores higher than the set value 3.

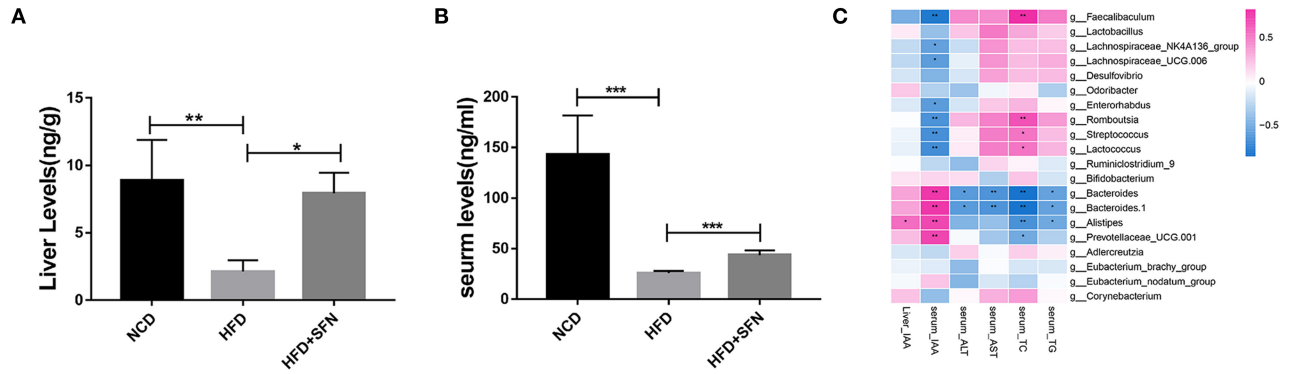

FIGURE 5 | IAA concentrations in the liver **(A)** and serum **(B)** from mice of different groups. **(C)** Heatmap of the Spearman r correlations between the gut microbial species and biomarkers. Data are presented as mean ± SD. *$P < 0.05$, **$P < 0.01$, ***$P < 0.001$ vs. HFD group.

the mRNA expression of *Ahr* was clearly increased by SFN treatment (**Figure 6H**), while the results of AHR in RNA-ISH showed that the AHR expression in the macrophages of the liver was also upregulated under SFN administration. Similarly, RNA-ISH combined with F4/80 IF staining for macrophages of mouse liver sections showed that the expression of F4/80 decreased in the HFD+SFN group, which was consistent with the results of IHC (**Figure 6I**).

DISCUSSION

Gut microbiota plays pivotal roles in the onset and progression of NAFLD and exert a marked impact on host metabolism (30, 31). Gut microbial tryptophan metabolites have been confirmed as ligands of AHR and influence the progression of obesity, type 2 diabetes (T2D), hypertension, inflammatory bowel disease (IBD), multiple sclerosis (MS), and Huntington's disease (HD) (16). However, HFD alters the structure and metabolic ability of intestinal microflora in mice, which further decreases the level of gut microbiome-derived tryptophan metabolites (3, 32, 33). In addition, AHR contributes to the establishment of intestinal microbiota in mice, and the cecal microbiota of $Ahr^{-/+}$ and $Ahr^{-/-}$ mice show different macrogenomic metabolic pathways (34). In summary, the interaction among gut microbiota, tryptophan catabolites, and AHR may plays an essential role in the development of NAFLD. However, whether metabolite IAA levels are correlated with the efficacy of drug interventions is yet to be elucidated. Herein, we investigated the diet-related AHR agonists that improved NAFLD by regulating gut microbiome-derived metabolites.

In the present study, we find the therapeutic capacity and improvement activity of sulforaphane against NAFLD can be mediated by metabolic and immune pathways (**Figure 7**).

Previous studies reported that SFN regulates lipid metabolism (35). The current data demonstrated that SFN significantly decreased the levels of serum TC and TG. In addition, SFN inhibited the *de novo* lipogenesis in both mouse and HepG2 cell experiments. These results further confirmed that SFN improves lipid metabolism.

Reportedly, AHR is distributed in various tissues and cell types, such as macrophages, Treg cells, dendritic cells (DCs), and innate lymphoid cells (ILC). However, AHR exerts different effects when activated by various ligands in different cell types, which leads to differences in the data (18). In addition, the activation of AHR/CD36 pathway promotes hepatic steatosis in mice (36), while inhibiting the activity of AHR and altering the expression levels of CYP1B1, PPARα, and SCD-1 that attenuate the diet-induced obesity and hepatic steatosis in mice (37). On the contrary, the activation of AHR by IAA negatively regulates SREBP-1C and FAS, which in turn, improves NAFLD (3). These findings implied that AHR might have a dual role in regulating liver lipid metabolism. However, we demonstrated that SFN negatively modulates the expression of lipogenesis genes, *SREBP-1C*, *FAS*, and *ACC1* via AHR activation, which was consistent with the results of the IAA treatment group. As shown in previous studies, SFN activated NRF2, indicating tight bidirectional crosstalk between AHR and NRF2 (38, 39). These results suggested that SFN improves NAFLD by activating AHR to regulate lipid metabolism.

Targeted metabolomics profiles uncovered a prominent decrease in the levels of IAA in HFD mouse serum and liver tissues, which was consistent with previous results (3). Importantly, IAA not only delays NAFLD progression by activating AHR as an endogenous ligand but also alleviates it by reducing liver lipid production, oxidative stress, and inflammation (15). Nevertheless, SFN increased the level of IAA in this study. Accumulating evidence clarified that IAA is one of the foremost tryptophan metabolites produced by intestinal bacteria, such as *Clostridium, Bacteroides, Bifidobacterium, Eubacterium hallii, Peptostreptococcus, Asscharolyticus, Lactobacillus reuteri*, and *E. coli* (14, 40). Our data demonstrated that HFD decreased the abundance of *Bifidobacterium*, *Bacteroides*, *Eubacterium_fissicatena_group*, and *Erysipelatoclostridium.* However, the relative abundance of *Bifidobacterium* and *Bacteroides* was increased by SFN treatment. Additional studies have shown that *Gammaproteobacteria* and *Prevotella* are related to endogenous ethanol production (41). The intrahepatic *Proteobacteria* was associated with NASH, ballooning degeneration, lobular and portal inflammation,

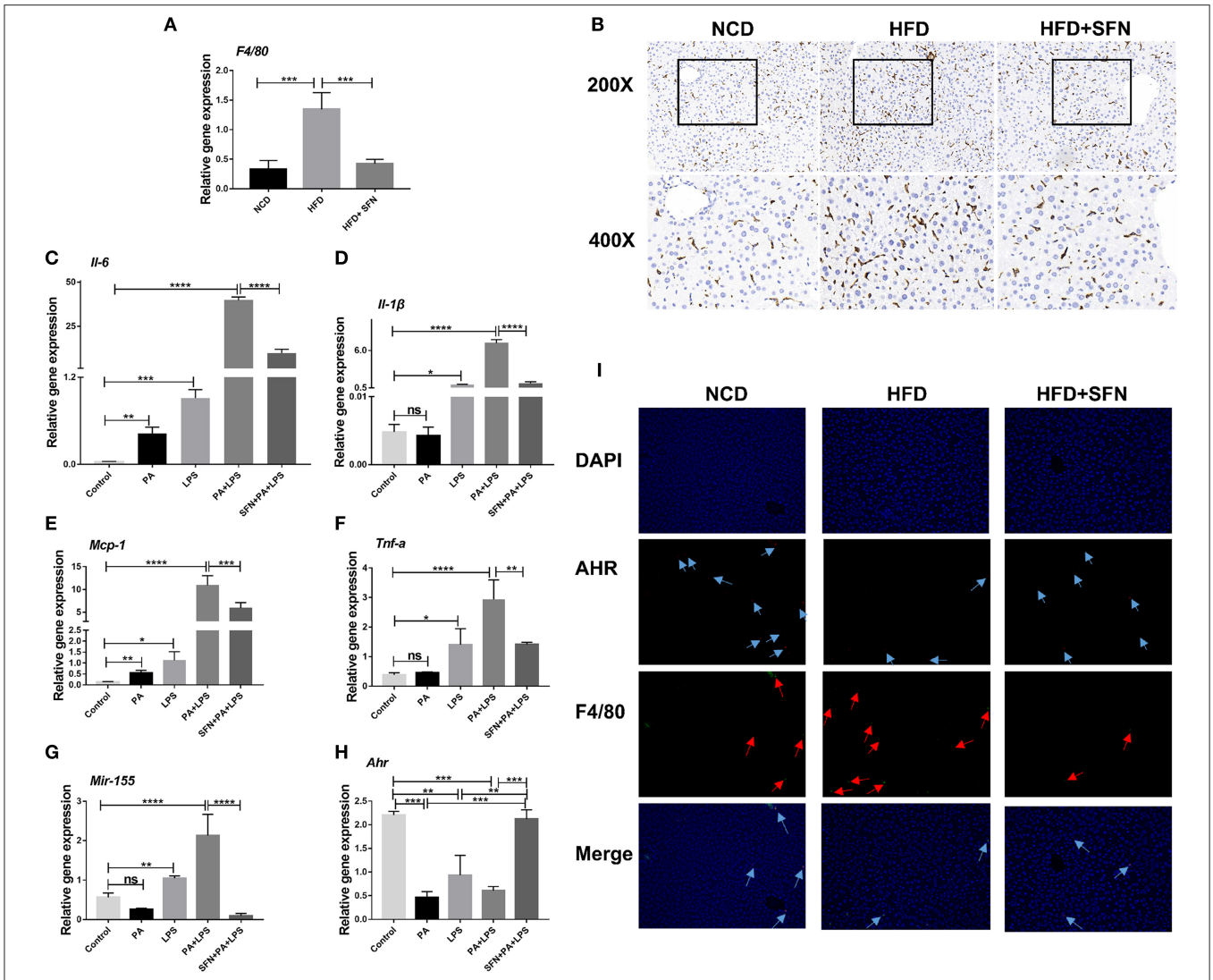

FIGURE 6 | SFN inhibited the liver inflammation effects and attenuated the expression of proinflammatory cytokines in macrophages. **(A)** The mRNA expression of *F4/80* in the liver tissue. **(B)** IHC staining displayed the expression of F4/80 (brown particles), in the livers of different groups. **(C–F)** Changes in the expression of *Il-6*, *Il-1β*, *Mcp-1*and *Tnf-a*. **(G)** *Mir-155* expression in Raw264.7 cells. **(H)** mRNA expression of *Ahr.* **(I)** AHR RNA-ISH combined with F4/80 IF staining for macrophages of mouse liver sections. Arrows indicate AHR RNA and F4/80, respectively. Original magnification, 200×. Data are presented as mean ± SD. ns, not significant, $^{*}P < 0.05$, $^{**}P < 0.01$, $^{***}P < 0.001$, $^{****}P < 0.0001$ vs. the Control group or PA+LPS group or HFD group.

and liver fibrosis (42). Correlation analysis revealed that *Cyanobacteria* and *Bacteroides* were positively correlated with IL-10 and *Ferribacteres*, *Tenericutes*, *Mucispirillum*, and *Ruminiclostridi_6* were correlated with proinflammatory reactions (43). The present study showed that SFN adjusted the comparative abundance of the related microbiota described above. Accumulating evidence showed that the abundance of gut microbiota is elevated as a result of hepatic TG production (44). Therefore, SFN could not only adjust the structure and diversity of gut microbiota but also indirectly improve NAFLD by modulating the content of gut microbiome-derived metabolite IAA.

IL-1β produced by macrophages recruit the inflammatory factors to the liver and activate hepatic stellate cells, thereby developing liver fibrosis. IL-1β also promotes adipogenesis and TG accumulation in hepatocytes by regulating the expression of Srebp-1c, which together with TNF-α triggers hepatocyte necrosis (45–47). In this study, SFN treatment reduced the mRNA expression of proinflammatory cytokines as well as upregulated the mRNA expression of *Ahr* in Raw264.7 cells. Another recent study identified that AHR negatively regulates the expression of LPS-induced inflammatory cytokines (48). In addition, the mRNA expression level of *Ahr* in peritoneal macrophages increased at 1h post-LPS treatment, reached a peak at 2 h, and then declined gradually (49). Therefore, the mRNA expression of *Ahr* in macrophages decreased after PA+LPS stimulation for 24 h, and increased in the liver tissue of HFD mice, which might be related to time.

In conclusion, the current findings demonstrated that SFN altered the gut microbiota and microbiome-derived metabolite

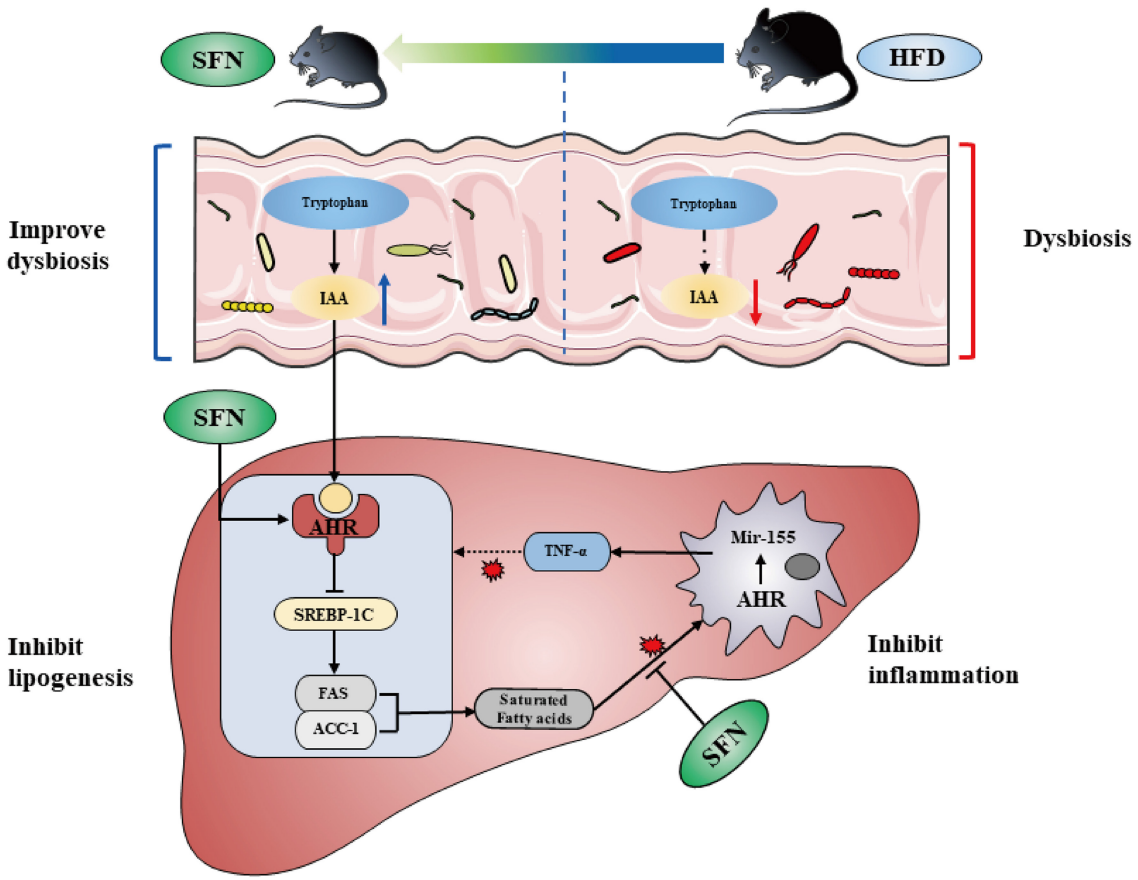

FIGURE 7 | SFN altered the gut microbiota of mice and microbiome-derived metabolite IAA. Additionally, SFN regulated liver lipid metabolism by activating AHR and inhibited chronic low-grade inflammation.

IAA of mice and regulated the liver lipid metabolism by activating AHR. These results may have important implications for unraveling the metabolic basis of the disease and provides evidence that modification of the intestinal microbiota could be therapeutic for the amelioration of hepatic steatosis in obese individuals.

DATA AVAILABILITY STATEMENT

The datasets presented in this study can be found in online repositories. The names of the repository/repositories and accession number(s) can be found at: https://www.ncbi.nlm.nih.gov/search/all/?term=PRJNA763001; Sequence Read Archive (SRA) database (SAMN21419598-SAMN21419612).

ETHICS STATEMENT

The animal study was reviewed and approved by the Institutional Review Board (or Ethics Committee) of Radiation Medicine Chinese Academy of Medical Sciences.

AUTHOR CONTRIBUTIONS

XX, SS, and LL carried out the studies and drafted the manuscript. CL, QH, MR, LZha, and JingyueZ participated in collecting data. CY, HY, LZho, XC, and XD performed the statistical analysis and participated in its design. JieZ, JingwenZ, and BW helped to draft the manuscript. All authors read and approved the final manuscript.

FUNDING

This work was supported by National Key R&D Program of China [Grant No. 2019YFC0119505]; National Natural Science Foundation of China [Grant No. 81970477]; Natural Science Foundation of Tianjin [Grant No. 18JCQNJC80700]; Tianjin Science and Technology Innovation Cooperation Project [Grant No. 19PTZWHZ00090]; and Tianjin Research Innovation Project for Postgraduate Students [Grant No. 2019YJSS188].

REFERENCES

1. Cai J, Zhang XJ, Li H. Progress and challenges in the prevention and control of nonalcoholic fatty liver disease. *Med Res Rev.* (2019) 39:328–48. doi: 10.1002/med.21515
2. Li L, Chen L, Hu L. Nuclear factor high-mobility group box1 mediating the activation of toll-like receptor 4 signaling in hepatocytes in the early stage of non-alcoholic fatty liver disease in mice. *J Clin Exp Hepatol.* (2011) 1:123–4. doi: 10.1016/S0973-6883(11)60136-9
3. Krishnan S, Ding Y, Saedi N, Choi M, Sridharan GV, Sherr DH, et al. Gut microbiota-derived tryptophan metabolites modulate inflammatory response in hepatocytes and macrophages. *Cell Rep.* (2018) 23:1099–111. doi: 10.1016/j.celrep.2018.03.109
4. Moon YA, Liang G, Xie X, Frank-Kamenetsky M, Fitzgerald K, Koteliansky V, et al. The Scap/SREBP pathway is essential for developing diabetic fatty liver and carbohydrate-induced hypertriglyceridemia in animals. *Cell Metab.* (2012) 15:240–6. doi: 10.1016/j.cmet.2011.12.017
5. Tang JJ Li JG, Qi W, Qiu WW Li PS, Li BL, et al. Inhibition of SREBP by a small molecule, betulin, improves hyperlipidemia and insulin resistance and reduces atherosclerotic plaques. *Cell Metab.* (2011) 13:44–56. doi: 10.1016/j.cmet.2010.12.004
6. Fuchs CD, Claudel T, Trauner M. Role of metabolic lipases and lipolytic metabolites in the pathogenesis of NAFLD. *Trends Endocrinol Metab.* (2014) 25:576–85. doi: 10.1016/j.tem.2014.08.001
7. Barrera F, George J. The role of diet and nutritional intervention for the management of patients with NAFLD. *Clin Liver Dis.* (2014) 18:91–112. doi: 10.1016/j.cld.2013.09.009
8. Vezza T, Rodríguez-Nogales A, Algieri F, Garrido-Mesa J, Romero M, Sánchez M. et al. The metabolic and vascular protective effects of olive (*Olea europaea L*) leaf extract in diet-induced obesity in mice are related to the amelioration of gut microbiota dysbiosis and to its immunomodulatory properties. *Pharmacol Res.* (2019) 150:104487. doi: 10.1016/j.phrs.2019.104487
9. Zeng SL, Li SZ, Xiao PT, Cai YY, Chu C, Chen BZ, et al. Citrus polymethoxyflavones attenuate metabolic syndrome by regulating gut microbiome and amino acid metabolism. *Sci Adv.* (2020) 6:eaax6208. doi: 10.1126/sciadv.aax6208
10. Zhao L, Lou H, Peng Y, Chen S, Zhang Y, Li X. Comprehensive relationships between gut microbiome and faecal metabolome in individuals with type 2 diabetes and its complications. *Endocrine.* (2019) 66:526–37. doi: 10.1007/s12020-019-02103-8
11. Wang Z, Klipfell E, Bennett BJ, Koeth R, Levison BS, Dugar B, et al. Gut flora metabolism of phosphatidylcholine promotes cardiovascular disease. *Nature.* (2011) 472:57–63. doi: 10.1038/nature09922
12. Astbury S, Atallah E, Vijay A, Aithal GP, Grove JI, Valdes AM. Lower gut microbiome diversity and higher abundance of proinflammatory genus Collinsella are associated with biopsy-proven nonalcoholic steatohepatitis. *Gut Microbes.* (2020) 11:569–80. doi: 10.1080/19490976.2019.1681861
13. Krautkramer KA, Fan J, Bäckhed F. Gut microbial metabolites as multi-kingdom intermediates. *Nat Rev Microbiol.* (2021) 19:77–94. doi: 10.1038/s41579-020-0438-4
14. Jin UH, Lee SO, Sridharan G, Lee K, Davidson LA, Jayaraman A, et al. Microbiome-derived tryptophan metabolites and their aryl hydrocarbon receptor-dependent agonist and antagonist activities. *Mol Pharmacol.* (2014) 85:777–88. doi: 10.1124/mol.113.091165
15. Ji Y, Gao Y, Chen H, Yin Y, Zhang W. Indole-3-acetic acid alleviates nonalcoholic fatty liver disease in mice via attenuation of hepatic lipogenesis, and oxidative and inflammatory stress. *Nutrients.* (2019) 11:2062. doi: 10.3390/nu11092062
16. Roager HM, Licht TR. Microbial tryptophan catabolites in health and disease. *Nat Commun.* (2018) 9:3294. doi: 10.1038/s41467-018-05470-4
17. Noack M, Miossec P. Th17 and regulatory T cell balance in autoimmune and inflammatory diseases. *Autoimmun Rev.* (2014) 13:668–77. doi: 10.1016/j.autrev.2013.12.004
18. Shinde R, McGaha TL. The aryl hydrocarbon receptor: connecting immunity to the microenvironment. *Trends Immunol.* (2018) 39:1005–20. doi: 10.1016/j.it.2018.10.010
19. Bock KW. Functions of aryl hydrocarbon receptor (AHR) and CD38 in NAD metabolism and nonalcoholic steatohepatitis (NASH). *Biochem Pharmacol.* (2019) 169:113620. doi: 10.1016/j.bcp.2019.08.022
20. Lamas B, Richard ML, Leducq V, Pham HP, Michel ML, Da Costa G, et al. CARD9 impacts colitis by altering gut microbiota metabolism of tryptophan into aryl hydrocarbon receptor ligands. *Nat Med.* (2016) 22:598–605. doi: 10.1038/nm.4102
21. Monteleone I, Rizzo A, Sarra M, Sica G, Sileri P, Biancone L, et al. Aryl hydrocarbon receptor-induced signals up-regulate IL-22 production and inhibit inflammation in the gastrointestinal tract. *Gastroenterology.* (2011) 141:237–48.e1. doi: 10.1053/j.gastro.2011.04.007
22. Yu J, Luo Y, Zhu Z, Zhou Y, Sun L, Gao J, et al. A tryptophan metabolite of the skin microbiota attenuates inflammation in patients with atopic dermatitis through the aryl hydrocarbon receptor. *J Allergy Clin Immunol.* (2019) 143:2108–19.e12. doi: 10.1016/j.jaci.2018.11.036
23. Rosser EC, Piper CJM, Matei DE, Blair PA, Rendeiro AF, Orford M, et al. Microbiota-derived metabolites suppress arthritis by amplifying aryl-hydrocarbon receptor activation in regulatory B cells. *Cell Metab.* (2020) 31:837–51.e10. doi: 10.1016/j.cmet.2020.03.003
24. Lu P, Yan J, Liu K, Garbacz WG, Wang P, Xu M, et al. Activation of aryl hydrocarbon receptor dissociates fatty liver from insulin resistance by inducing fibroblast growth factor 21. *Hepatology (Baltimore, Md).* (2015) 61:1908–19. doi: 10.1002/hep.27719
25. Rivera CA, Adegboyega P, van Rooijen N, Tagalicud A, Allman M, Wallace M. Toll-like receptor-4 signaling and Kupffer cells play pivotal roles in the pathogenesis of non-alcoholic steatohepatitis. *J Hepatol.* (2007) 47:571–9. doi: 10.1016/j.jhep.2007.04.019
26. Choi KM, Lee YS, Kim W, Kim SJ, Shin KO Yu JY, et al. Sulforaphane attenuates obesity by inhibiting adipogenesis and activating the AMPK pathway in obese mice. *J Nutr Biochem.* (2014) 25:201–7. doi: 10.1016/j.jnutbio.2013.10.007
27. Youn HS, Kim YS, Park ZY, Kim SY, Choi NY, Joung SM, et al. Sulforaphane suppresses oligomerization of TLR4 in a thiol-dependent manner. *J Immunol.* (2010) 184:411–9. doi: 10.4049/jimmunol.0803988
28. Yang G, Lee HE, Lee JY. pharmacological inhibitor of NLRP3 inflammasome prevents non-alcoholic fatty liver disease in a mouse model induced by high fat diet. *Sci Rep.* (2016) 6:24399. doi: 10.1038/srep24399
29. Soyal SM, Nofziger C, Dossena S, Paulmichl M, Patsch W. Targeting SREBPs for treatment of the metabolic syndrome. *Trends Pharmacol Sci.* (2015) 36:406–16. doi: 10.1016/j.tips.2015.04.010
30. Sonnenburg JL, Bäckhed F. Diet-microbiota interactions as moderators of human metabolism. *Nature.* (2016) 535:56–64. doi: 10.1038/nature18846
31. Wikoff WR, Anfora AT, Liu J, Schultz PG, Lesley SA, Peters EC, et al. Metabolomics analysis reveals large effects of gut microflora on mammalian blood metabolites. *Proc Natl Acad Sci USA.* (2009) 106:3698–703. doi: 10.1073/pnas.0812874106
32. Porras D, Nistal E, Martínez-Flórez S, Pisonero-Vaquero S, Olcoz JL, Jover R, et al. Protective effect of quercetin on high-fat diet-induced non-alcoholic fatty liver disease in mice is mediated by modulating intestinal microbiota imbalance and related gut-liver axis activation. *Free Radic Biol Med.* (2017) 102:188–202. doi: 10.1016/j.freeradbiomed.2016.11.037
33. Hubbard TD, Murray IA, Bisson WH, Lahoti TS, Gowda K, Amin SG, et al. Adaptation of the human aryl hydrocarbon receptor to sense microbiota-derived indoles. *Sci Rep.* (2015) 5:12689. doi: 10.1038/srep12689
34. Murray IA, Nichols RG, Zhang L, Patterson AD, Perdew GH. Expression of the aryl hydrocarbon receptor contributes to the establishment of intestinal microbial community structure in mice. *Sci Rep.* (2016) 6:33969. doi: 10.1038/srep33969
35. Lei P, Tian S, Teng C, Huang L, Liu X, Wang J, et al. Sulforaphane improves lipid metabolism by enhancing mitochondrial function and biogenesis *in vivo* and *in vitro*. *Mol Nutr Food Res.* (2019) 63:e1800795. doi: 10.1002/mnfr.201800795
36. Yao L, Wang C, Zhang X, Peng L, Liu W, Zhang X, et al. Hyperhomocysteinemia activates the aryl hydrocarbon receptor/CD36 pathway to promote hepatic steatosis in mice. *Hepatology.* (2016) 64:92–105. doi: 10.1002/hep.28518
37. Rojas IY, Moyer BJ, Ringelberg CS, Tomlinson CR. Reversal of obesity and liver steatosis in mice via inhibition of aryl hydrocarbon receptor and altered

gene expression of CYP1B1, PPARα, SCD1, and osteopontin. *Int J Obes.* (2020) 44:948–63. doi: 10.1038/s41366-019-0512-z
38. Dinkova-Kostova AT, Fahey JW, Kostov RV, Kensler TW. KEAP1 and done? Targeting the NRF2 pathway with sulforaphane. *Trends Food Sci Technol.* (2017) 69:257–69. doi: 10.1016/j.tifs.2017.02.002
39. Silva-Palacios A, Ostolga-Chavarría M, Sánchez-Garibay C, Rojas-Morales P, Galván-Arzate S, Buelna-Chontal M, et al. Sulforaphane protects from myocardial ischemia-reperfusion damage through the balanced activation of Nrf2/AhR. *Free Radic Biol Med.* (2019) 143:331–40. doi: 10.1016/j.freeradbiomed.2019.08.012
40. Russell WR, Duncan SH, Scobbie L, Duncan G, Cantlay L, Calder AG, et al. Major phenylpropanoid-derived metabolites in the human gut can arise from microbial fermentation of protein. *Mol Nutr Food Res.* (2013) 57:523–35. doi: 10.1002/mnfr.201200594
41. Ren N, Xing D, Rittmann BE, Zhao L, Xie T, Zhao X. Microbial community structure of ethanol type fermentation in bio-hydrogen production. *Environ Microbiol.* (2007) 9:1112–25. doi: 10.1111/j.1462-2920.2006.01234.x
42. Sookoian S, Salatino A, Castaño GO, Landa MS, Fijalkowky C, Garaycoechea M, et al. Intrahepatic bacterial metataxonomic signature in non-alcoholic fatty liver disease. *Gut.* (2020) 69:1483–91. doi: 10.1136/gutjnl-2019-318811
43. Li K, Zhang L, Xue J, Yang X, Dong X, Sha L, et al. Dietary inulin alleviates diverse stages of type 2 diabetes mellitus via anti-inflammation and modulating gut microbiota in db/db mice. *Food Funct.* (2019) 10:1915–27. doi: 10.1039/C8FO02265H
44. Bäckhed F, Ding H, Wang T, Hooper LV, Koh GY, Nagy A, et al. The gut microbiota as an environmental factor that regulates fat storage. *Proc Natl Acad Sci USA.* (2004) 101:15718–23. doi: 10.1073/pnas.0407076101
45. Miura K, Kodama Y, Inokuchi S, Schnabl B, Aoyama T, Ohnishi H, et al. Toll-like receptor 9 promotes steatohepatitis by induction of interleukin-1beta in mice. *Gastroenterology.* (2010) 139:323–34.e7. doi: 10.1053/j.gastro.2010.03.052
46. Petrasek J, Bala S, Csak T, Lippai D, Kodys K, Menashy V, et al. IL-1 receptor antagonist ameliorates inflammasome-dependent alcoholic steatohepatitis in mice. *J Clin Invest.* (2012) 122:3476–89. doi: 10.1172/JCI60777
47. Petrasek J, Dolganiuc A, Csak T, Kurt-Jones EA, Szabo G. Type I interferons protect from Toll-like receptor 9-associated liver injury and regulate IL-1 receptor antagonist in mice. *Gastroenterology.* (2011) 140:697–708.e4. doi: 10.1053/j.gastro.2010.08.020
48. Masuda K, Kimura A, Hanieh H, Nguyen NT, Nakahama T, Chinen I, et al. Aryl hydrocarbon receptor negatively regulates LPS-induced IL-6 production through suppression of histamine production in macrophages. *Int Immunol.* (2011) 23:637–45. doi: 10.1093/intimm/dxr072
49. Zhu J, Luo L, Tian L, Yin S, Ma X, Cheng S, et al. Aryl hydrocarbon receptor promotes IL-10 expression in inflammatory macrophages through Src-STAT3 signaling pathway. *Front Immunol.* (2018) 9:2033. doi: 10.3389/fimmu.2018.02033

Conflict of Interest: The authors declare that the research was conducted in the absence of any commercial or financial relationships that could be construed as a potential conflict of interest.

Publisher's Note: All claims expressed in this article are solely those of the authors and do not necessarily represent those of their affiliated organizations, or those of the publisher, the editors and the reviewers. Any product that may be evaluated in this article, or claim that may be made by its manufacturer, is not guaranteed or endorsed by the publisher.

frontiers in Nutrition

ORIGINAL RESEARCH
published: 13 October 2021
doi: 10.3389/fnut.2021.726108

Surface-Displayed Amuc_1100 From *Akkermansia muciniphila* on *Lactococcus lactis* ZHY1 Improves Hepatic Steatosis and Intestinal Health in High-Fat-Fed Zebrafish

Feng-Li Zhang[1], *Ya-Lin Yang*[2]*, *Zhen Zhang*[2], *Yuan-Yuan Yao*[1], *Rui Xia*[1], *Chen-Chen Gao*[1], *Dong-Dong Du*[1], *Juan Hu*[1], *Chao Ran*[2], *Zhen Liu*[3] and *Zhi-Gang Zhou*[1]*

[1] Sino-Norway Fish Gastrointestinal Microbiota Joint Lab, Institute of Feed Research of Chinese Academy of Agricultural Sciences, Beijing, China, [2] Key Laboratory for Feed Biotechnology of the Ministry of Agriculture, Institute of Feed Research of Chinese Academy of Agricultural Sciences, Beijing, China, [3] Hunan Provincial Key Laboratory of Nutrition and Quality Control of Aquatic Animals, Department of Biological and Environmental Engineering, Changsha University, Changsha, China

OPEN ACCESS

Edited by:
Xi Ma,
China Agricultural University, China

Reviewed by:
Jianmin Wu,
China Agricultural University, China
Yangchun Cao,
Northwest A and F University, China

***Correspondence:**
Ya-Lin Yang
yangyalin@caas.cn
Zhi-Gang Zhou
zhouzhigang03@caas.cn

Specialty section:
This article was submitted to Nutrition and Microbes, a section of the journal Frontiers in Nutrition

Received: *16 June 2021*
Accepted: *07 September 2021*
Published: *13 October 2021*

Citation:
Zhang F-L, Yang Y-L, Zhang Z, Yao Y-Y, Xia R, Gao C-C, Du D-D, Hu J, Ran C, Liu Z and Zhou Z-G (2021) Surface-Displayed Amuc_1100 From Akkermansia muciniphila on Lactococcus lactis ZHY1 Improves Hepatic Steatosis and Intestinal Health in High-Fat-Fed Zebrafish. Front. Nutr. 8:726108. doi: 10.3389/fnut.2021.726108

Fatty liver and intestinal barrier damage were widespread in most farmed fish, which severely restrict the development of aquaculture. Therefore, there was an urgent need to develop green feed additives to maintain host liver and intestinal health. In this study, a probiotic pili-like protein, Amuc_1100 (AM protein), was anchored to the surface of *Lactococcus lactis* ZHY1, and the effects of the recombinant bacteria AM-ZHY1 on liver fat accumulation and intestinal health were evaluated. Zebrafish were fed a basal diet, high-fat diet, and high-fat diet with AM-ZHY1 (10^8 cfu/g) or control bacteria ZHY1 for 4 weeks. Treatment with AM-ZHY1 significantly reduced hepatic steatosis in zebrafish. Quantitative PCR (*q*PCR) detection showed that the expression of the lipogenesis [peroxisome-proliferator-activated receptors (*PPAR*γ), sterol regulatory element-binding proteins-1c (*SREBP-1c*), fatty acid synthase *(FAS),* and acetyl-CoA carboxylase 1 (*ACC1*)] and lipid transport genes (*CD36* and *FABP6*) in the liver were significantly downregulated ($p < 0.05$), indicating that AM-ZHY1 could reduce liver fat accumulation by inhibiting lipid synthesis and absorption. Moreover, supplementing AM-ZHY1 to a high-fat diet could significantly reduce serum aspartate aminotransferase (AST) and alanine aminotransferase (ALT) levels, indicating that liver injury caused by high-fat diets was improved. The expression of tumor necrosis factor (*TNF*)-*a* and interleukin (*IL*)-*6* in the liver decreased significantly ($p < 0.05$), while *IL-1*β and *IL-10* did not change significantly in the AM-ZHY1 group. Compared to the high-fat diet-fed group, the AM-ZHY1 group, but not the ZHY1 group, significantly increased the expression of intestinal tight junction (TJ) proteins (*TJP1a*, *claudina*, *claudin7*, *claudin7b*, *claudin11a*, *claudin12*, and *claudin15a*; $p < 0.05$). Compared to the high-fat diet group, the *Proteobacteria* and *Fusobacteria* were significantly reduced and increased in the AM-ZHY1 group, respectively. In conclusion, the recombinant bacteria AM-ZHY1 has the capacity to

maintain intestinal health by protecting intestinal integrity and improving intestinal flora structure and improving fatty liver disease by inhibiting lipid synthesis and absorption. This study will lay a foundation for the application of AM protein in improving abnormal fat deposition and restoring the intestinal barrier in fish.

Keywords: Amuc_1100, *Lactococcus lactis*, fatty liver, intestinal health, microbiota, inflammation, zebrafish

INTRODUCTION

Fatty liver and intestinal barrier damage are widespread in most farmed fish, which severely restrict the development of aquaculture (1, 2). Therefore, there is an urgent need to develop green feed additives to maintain host liver and intestinal health. *Akkermansia muciniphila* is a human intestinal gram-negative anaerobic bacteria, with promising probiotic activities against many metabolic-related diseases such as obesity, diabetes, inflammatory bowel disease, etc. (3–7). Amuc_1100 (AM protein), a highly abundant pili-like membrane protein of *A. muciniphila,* partly recapitulates the beneficial effects of *A. muciniphila* (8, 9). Furthermore, AM protein can modulate host immune responses and specifically induce high cytokine production in peripheral blood mononuclear cells (PBMCs) likely *via* Toll-like receptor 2 (TLR2) signaling (10). Oral AM protein can activate the immune response of mice potentially *via* TLR2 (8). Other than that, AM protein can restore gut barriers and enhance the transepithelial resistance of Caco-2 cells (10). Specifically, oral AM protein enhanced the mouse intestinal barrier likely by acting on TLR2 and restoring the appropriate expression of tight junction proteins (8). AM protein can also alleviate metabolic endotoxemia, improve glucose and lipid metabolism, and reduce fat mass in high-fat diet-fed mice (8). These results indicate that *A. muciniphila* and AM protein have potential as a green feed additive in aquaculture.

As a strictly anaerobic bacteria, *A. muciniphila* is difficult to produce at an industrial scale, which limits its application in aquaculture. Compared with the bacteria, its probiotic element, AM protein, is easy to express heterologously and can be produced on a large scale, with great application potential. The applications of protein as a feed additive will face a series of problems such as a complex expression and purification process, poor stability, poor resistance, and high cost. A microbial [especially generally recognized as safe (GRAS) *lactic acid bacteria*] surface display can well circumvent the above problems, becoming attractive platforms for the surface display of heterologous proteins in various fields.

In this study, AM protein was anchored to the cell wall of fish-derived *Lactococcus lactis* ZHY1 using surface display technology. The lipid-lowering effect of recombinant bacteria on hepatic steatosis caused by a high-fat diet was tested, and the effects of the recombinant bacteria on intestinal barrier function and the inflammatory response of zebrafish were evaluated. This study will lay a foundation for the application of AM protein in improving abnormal fat deposition and restoring the intestinal barrier in fish.

MATERIALS AND METHODS

Bacterial Strains and Growth Conditions

In this experiment, *L. lactis* was isolated from the intestine of *Acipenser sinensis*. After the intestinal contents were suspended in 0.1 mM of phosphate-buffered saline (PBS), and then spread on a De Man, Rogosa and Sharpe (MRS) agar medium supplemented with calcium carbonate. Due to its high yield, we chose it as the carrier for the surface display, and it was identified as *L. lactis* by 16s rRNA sequencing, named ZHY1 (preservation number: CGMCC No. 22024). This strain was grown in a medium in M17 broth containing 0.5% glucose (HB0391, Qingdao Hope Bio-Technology Co., Ltd., Qingdao, China) and was cultured statically at 30°C.

Construction and Expression of Recombinant Bacteria AM-ZHY1

The 900-bp nucleotide coding sequence of AM was synthesized and cloned into the pET28a plasmid (Generay Biotech, Shanghai, China) and digested with XhoI (R0146S, NEB, Beijing, China) and XbaI (R0145V, NEB). The gene fragment of usp45 and AcmA was amplified by fusion PCR from the signal peptide genomic major lactococcal autolysin N-acetylmuramidase DNA of *L. lactis* MG1363 using a set of primers, usp45F (5′-CGAGCTCATATGAAAAAAAAGATTA-3′) and AcmAR (5′-GTCAGTATCTGCGAATAAAACTCGAG-3′). The amplification reaction was performed using the Q5 High-Fidelity DNA Polymerase following the recommendations of the manufacturer, and the amplicon was digested by SacI (R0156S, NEB) and XhoI. The two M0515, NEB digested products mentioned above were inserted into the shuttle vector pMG36e, and the ligation mixture was transformed into *Escherichia coli* MC1061 (TIANGEN, Beijing, China). The correct recombinant plasmid, pMG36e-usp45-AcmA-AM, was identified by DNA sequencing (Sangon Biotech, Shanghai, China) (**Figure 1**).

Lactococcus lactis ZHY1 competent cells were prepared and transformed as described previously with slight modifications (11). The overnight culture of *L. lactis* was inoculated at a 5% ratio into a fresh GM17 medium with 2.5% glycine, and then cultivated until $OD_{600} = 0.5$. The bacteria were washed two times with a pre-cooled washing buffer (17.1% sucrose, 1% glycerol), and then resuspended in a pre-chilled washing buffer and mixed with the recombinant plasmid pMG36e-usp45-AcmA-AM. The electroporator was pulsed, and the cells were plated on a GM17 agar medium containing 10 ug/ml of erythromycin. The recombinant bacteria AM-ZHY1 were selected after 48 h of culture by PCR (MG36eF: 5′-ACTCTCTGGGGACTTTCG-3′; MG36eR: 5′-TCGCCTTTACCAACTGTC-3′).

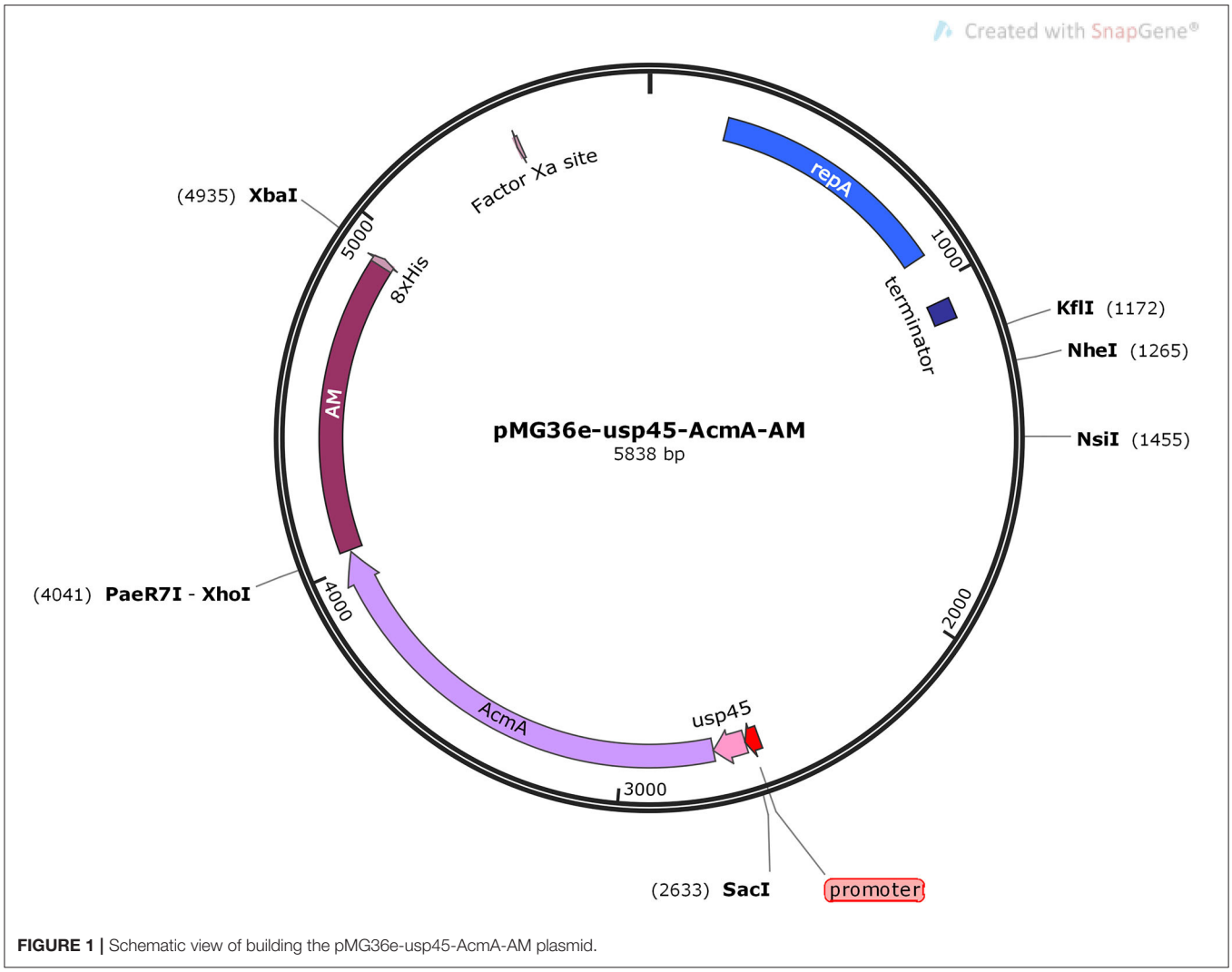

FIGURE 1 | Schematic view of building the pMG36e-usp45-AcmA-AM plasmid.

Sodium Dodecyl Sulfate-Polyacrylamide Gel Electrophoresis (SDS-PAGE) and Western Blot

The inoculation of AM-ZHY1 was performed into a GM17 medium containing 10 μg/ml erythromycin and cultured at 30°C for 48 h. The culture cells were then collected and resuspended in 1 ml of Tris-HCl (50 mM, pH 7), which contained 10 mM of magnesium chloride ($MgCl_2$) and 4% SDS buffer, at 37°C for 2 h. The mixture was denatured by heating at 100°C before loading, and the supernatant was the lysed cell wall components. The samples were analyzed by 12% SDS-PAGE (BioRad, Hercules, CA, USA) and electrophoresis at a 120-V constant voltage for 2 h.

After electrophoresis, the protein bands were transferred to a polyvinylidene fluoride (PVDF) membrane (0.45 uM, IPVH00010, Millipore, Beijing, China). After the electrotransfer was completed, the membrane was blocked in 5% skim milk and incubated overnight at 4°C with an anti-His tag monoclonal antibody (1:1,000 dilution, AB102, TIANGEN). Then, Goat Anti-mouse IgG, HRP Conjugated (1:200 dilution, CW0102, cwbiotech, Beijing, China) was added at room temperature for 2 h after washing with 0.05% TBST (50 mM Tris-HCl, 150 mM NaCl, 0.05% Tween 20). Chemiluminescent HRP Substrate (WBKLS0100, Millipore) was used to visualize protein bands.

Diets Preparation and Fish Husbandry

The experiment used zebrafish (1-month-old), AB strain. The zebrafish (n = 480, mean initial weight: 50 mg) were randomly allocated to 20 3-L tanks in the recirculation system. The zebrafish were fed for 4 weeks at 26°C, 12/12 light/dark cycle, dissolved oxygen ≥6 mg/L, total ammonia content ≤0.02 mg nitrogen/L, pH 7. All experimental and animal care procedures were approved by the Feed Research Institute of the Chinese Academy of Agricultural Sciences Animal Care Committee, under the auspices of the China Council for Animal Care (Assurance No. 2018-AF- FRI-CAAS-001).

The feed ingredients and formulas of the basal diet and high-fat diet are shown in **Table 1**. The recombinant bacteria, AM-ZHY1, and the control bacteria, ZHY1, were added to the high-fat

TABLE 1 | Ingredient and nutrient composition of the basal diet and high-fat diet.

Ingredients (g/kg diet)	basal diet	High-fat diet
Casein	400	400
gelatin	100	100
dextrin	280	160
Lard oil	0	80
Bean oil	60	80
Lysine	3.3	3.3
VC lecithin	1	1
Vitamin premix[a]	2	2
Mineral premix[b]	2	2
Calcium dihydrogen phosphate	20	20
Choline chloride	2	2
Sodium alginate	20	20
Microcrystalline cellulose	40	40
Zeolite powder	69.7	89.7
Total	1,000	1,000
Proximate composition (g/kg dry diet)		
Crude protein	449.4	448.9
Crude lipid	53.9	157.0

Vitamin premix[a] and mineral premix[b] were obtained from Beijing Xinlu United Aquatic Products Co., Ltd. The nutrition provided by the feed meets NRC standards.

diet at the amount of 10^8 cfu/g before being named the AM-ZHY1 group and ZHY1 group, respectively. Before preparation and after the feed was crushed (stored at −20°C), the viable cell numbers of *L. lactis* were determined by the plate counting method. The zebrafish were fed with the experimental diets two times a day (9:00, 17:00) at a ratio of 6% of body weight.

Growth Performance

After 4 weeks of feeding, each fish in the tanks was weighed to assess body weight gain (WG), feed conversion ratio (FCR), and survival rate (SR) (12), which showed the following: WG: $[100 \times (W_t - W_0)/W_0]$, FCR: $(W_f/W_d) \times 100$; SR $= (N_0/N_t) \times 100$; where W_0 (g), W_t (g), W_f, W_d, N_0, and N_t are the initial weight, final weight, total food intake, total weight gain, initial quantity, and final quantity of the zebrafish, respectively.

Liver TAG Content and HE Staining

The determination of the triacylglycerol (TAG) content of the zebrafish livers mainly referred to the method of Zhang et al. (13). The liver tissues (5–10 mg) from five zebrafish were homogenized in a PBS buffer. About 5 ml of methanol/chloroform (1:2) solution was added to the homogenate, and it was centrifuged (3,000 rpm, 5 min) to avoid protein sticking to the wall of the centrifuge tube. The organic components were carefully dried at 70°C with nitrogen steam. Then, the dried lipids were emulsified in chloroform with 1% Triton X-100. Each of the dried emulsified lipids was dissolved in deionized water, and we then detected the amount of TAG contained in the unit weight of the sample using a triglyceride reagent (T2449, Sigma-Aldrich, Saint Louis, MO, USA) and a free glycerol reagent (F6428, Sigma-Aldrich).

TABLE 2 | The primer sequences for quantitative (*q*PCR) analysis of lipid metabolism and inflammation-related genes.

Gene name	Forward primer (5′-3′)	Reverse primer (5′-3′)
Rps11 (Reference gene)	ACAGAAATGCCCCTTCACTG	GCCTCTTCTCAAAACGGTTG
CD36	TGAACAAAATCAAGGAGC ACACAA	ATCCGGGAAATCAGCTCATTCTT
FABP6	ACCCACAACCATCATCTC	TCTTTACCGTCCCATTTC
SREBP-1c	CAGAGGGTGGGCATGCTGGG	ATGTGACGGTGGTGCCGCTG
ATGL	GCGTGACGGATGGAGAAA	AGGCCACAGTAAACAGGAATAT
FAS	GGAGCAGGCTGCCTCTGTGC	TTGCGGCCTGTCCCACTCCT
PPARγ	CCTGTCCGGGAAGACCAGCG	GTGCTCGTGGAGCGGCATGT
ACC1	GCGTGGCCGAACAATGGCAG	GCAGGTCCAGCTTCCCTGCG
UCP2	TGCCACCGTGAAGTTTATTG	CCTCGATATTTCACCGGACC
TNFα	AAGGAGAGTTGCCTTTACCG	ATTGCCCTGGGTCTTATGG
IL-6	TCAACTTCTCCAGCGTGATG	TCTTTCCCTCTTTTCCTCCTG
IL-10	TCACGTCATGAACGAGATCC	CCTCTTGCATTTCACCATATCC
IL-1β	GGCTGTGTGTTTGGGAATCT	TGATAAACCAACCGGGACA

The zebrafish liver was carefully removed and immediately fixed in 4% paraformaldehyde. After embedding in paraffin, the sections were cut and stained with hematoxylin-eosin (HE). The cellular lipid vacuoles of the liver were observed under a microscope (Leica DMIL-LED, Wetzlar, Germany).

Serum Biochemical Measurements

Blood samples were collected from the zebrafish as previously described (14). The activities of zebrafish serum alanine aminotransferase (ALT) and aspartate aminotransferase (AST) were detected using commercial diagnostic kits (Nanjing Jiancheng Bioengineering Institute, China) according to the instructions of the manufacturer. Serum ALT and AST activities were expressed as enzyme activity units per liter (U/L).

Quantitative Real-Time PCR Analysis

The total RNA of the zebrafish liver and intestine samples were isolated using a Trizol reagent (Invitrogen, Waltham, MA, USA) and reversed transcribed to cDNA using a FastKing-RT Supermix (KR118, TIANGEN). The expression of *CD36*, *FABP6*, sterol regulatory element-binding proteins-1c (*SREBP-1c*), peroxisome-proliferator-activated receptors *(PPARγ)*, acetyl-CoA carboxylase 1 (*ACC1)*, adipose triglyceride lipase (*ATGL*), and uncoupling protein 2 (*UCP2*) of the liver; tumor necrosis factor (*TNF*)-*α*, interleukin (*IL*)-*6*, *IL-10*, and *IL-1β* of the liver; and the intestinal tight junction (TJ) proteins (*TJP1a*, *claudina*, *claudin7*, *claudin7b*, *claudin11a*, *claudin12*, and *claudin15a*) were determined by quantitative real-time PCR (*q*RT-PCR) using the SYBR Green Supermix (FP204, TIANGEN) on a Light Cycler 480 system (Roche, Basel, Switzerland). The results were analyzed by the $2^{-\Delta\Delta}$Ct method (15). The primers of all detected genes are listed in **Tables 2**, **3**, and the reference gene was Rps11.

TABLE 3 | Primers sequences for *q*PCR analysis of tight junction proteins.

Gene name	Forward primer (5′-3′)	Reverse primer (5′-3′)
Rps11 (Reference gene)	ACAGAAATGCCCCTTCACTG	GCCTCTTCTCAAAACGGTTG
Claudin7	GGAGCCCTCTGTAGCATTGTT	ATTAGGAGATGACTGACCCTTTGA
Claudin11a	ACCAGAAAGTGCCAAGAACA	AAAGCCAAAGGACATCAGACC
Claudin12	CCTCCGTCTGGTTCCTCT	GCTTTGGGTCATTGTGGG
Claudin7b	GGAGCCCTCTGTAGCATTGTTG TGTTG	ATTAGGAGATGACTGACCCTTTGA
Claudin15a	CTCTGCTCGCTCTATCTGGTTA	TTTCACGGGTGGGATGGTAT
TJP1a	CAAAGACCAACAGCACTGCC	GTGGTTTAGCGGTGATGGGA
Claudina	TCAGTGAGTTTCCTCCTATTGT	TATTCGCCGCTCCTCTTTT
TJP1b	CCCACAGATCTCCCCAAACC	CTGGAGCTCTGTAGGAGGGT

The Influence of Gut Microbes

After 4 weeks of feeding, the intestinal contents of the zebrafish from the four diet groups were obtained 4 h after the last feeding. The intestinal sample of each group contained six replicates, and six fish were pooled as a replicate. Afterward, DNA was extracted with a Fast DNA spin kit (MP, Biomedicals, Solon, OH, USA), according to the instructions of the manufacturer. The V3–V4 region of 16S rRNA was amplified with U341F (5′-CGGCAACGAGCGCAACCC-3′) and U806R (5′-CCATTGTAGCACGTGTGTAGCC-3′). The high-throughput sequencing of the gut microbes was performed at the MajorBio (Shanghai), using the Illumina HiSeq platform. Microbiota sequencing data of zebrafish intestinal flora are available from NCBI Sequence Read Archive with accession number PRJNA739824. The UPARSE-operational taxonomic unit (OTU) algorithm was used to control the quality of raw pair-end readings (16). The RDP classifier Bayesian algorithm was used to perform a taxonomic analysis at the 97% similar level (17). According to the results of the taxonomic analysis, a principal component analysis of different groups was performed using R 3.3.1 at (18).

Statistical Analysis

The statistical data were analyzed by the GraphPad Prism 5 software (GraphPad Software Inc., San Diego, CA, USA). All statistics were from six repetitions. Differences among groups were assessed using Student's *t*-test. $p < 0.05$, $p < 0.01$ and $p < 0.001$ were considered significant differences.

RESULT

Oral Administration of AM-ZHY1 Reduces Weight Gain and Liver Lipid Deposition

As shown in **Figure 2**, the fusion protein AcmA-AM was successfully expressed in the surface of the recombinant bacteria AM-ZHY1. After 4 weeks of the feeding experiment, the WG, FCR, and SR of the four groups of zebrafish were calculated.

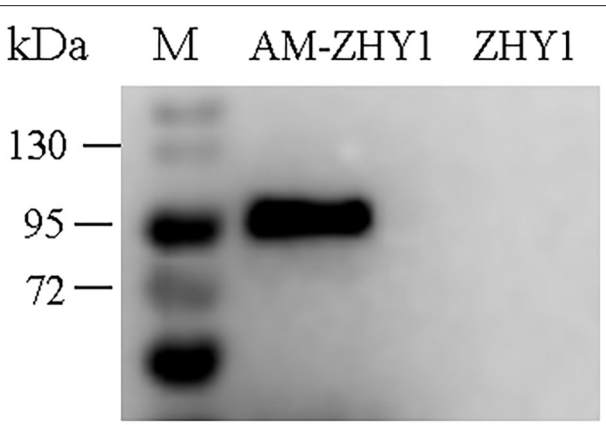

FIGURE 2 | Western blotting detects the expression of Amuc_1100 (AM) on ZHY1. Line 1: protein marker (26630, Thermo Scientific), line 2: the whole cell wall protein of recombinant strain AM-ZHY1, line 3: the whole cell wall protein of control strain ZHY1.

As shown in **Figure 3**, both the WG of the AM-ZHY1 and ZHY1 groups showed 17.7 and 43.5% lower than high-fat diet group. The FCR of the AM-ZHY1 group was 25% higher than the high-fat diet group. The SRs was unaffected by the dietary treatments.

The improvement of AM-ZHY1 on hepatic steatosis induced by the high-fat diet is shown in **Figures 4A,B**. The high-fat diet significantly increased liver fat accumulation compared with the basal diet (29.5% higher; $p < 0.05$). The supplementation of AM-ZHY1, but not ZHY1, significantly reduced TAG content in the liver compared with the high-fat diet group (by 31.6 and 7.6%, respectively; $p < 0.05$; $p = 0.28$). Moreover, the TAG content in zebrafish fed the high-fat diet with AM-ZHY1 was 26% lower than in the fish fed the high-fat diet with ZHY1 ($p < 0.05$). Accordingly, histopathologic analysis of the HE-stained liver sections showed hepatic steatosis in zebrafish fed high-fat diets, which was obviously reversed by the addition of AM-ZHY1. The effect of AM-ZHY1 on the lipid metabolism of the high-fat diet-fed zebrafish was investigated (**Figure 5**). The process of lipid metabolism mainly includes fat synthesis genes, lipolysis genes, and fat absorption-related genes at the genetic level. The expression of key enzymes involved in the *de novo* fatty acid synthesis pathway, including *ACC1* and fatty acid synthase (*FAS*), was obviously lower in the AM-ZHY1 group than the high-fat diet group (by 71.9 and 71.9%, respectively; $p < 0.05$; $p < 0.05$). The mRNA expression of the transcription factors that regulate fatty acid and triglyceride synthesis, including *PPARγ* and *SREBP-1c,* was significantly downregulated in the AM-ZHY1 group ($p < 0.05$; $p < 0.05$). However, the expression of *PPARγ* and *SREBP-1c* was not significantly reduced in zebrafish fed with ZHY1 compared with those fed the high-fat diet ($p = 0.12$; $p = 0.42$). The AM-ZHY1 significantly inhibited the expression of the lipid absorption genes *CD36* and *FABP6* ($p < 0.05$; $p < 0.05$). However, the expression of these two genes in zebrafish fed with the high-fat diet supplemented with control bacteria ZHY1 did not decrease significantly ($p = 0.58$; $p = 0.74$).

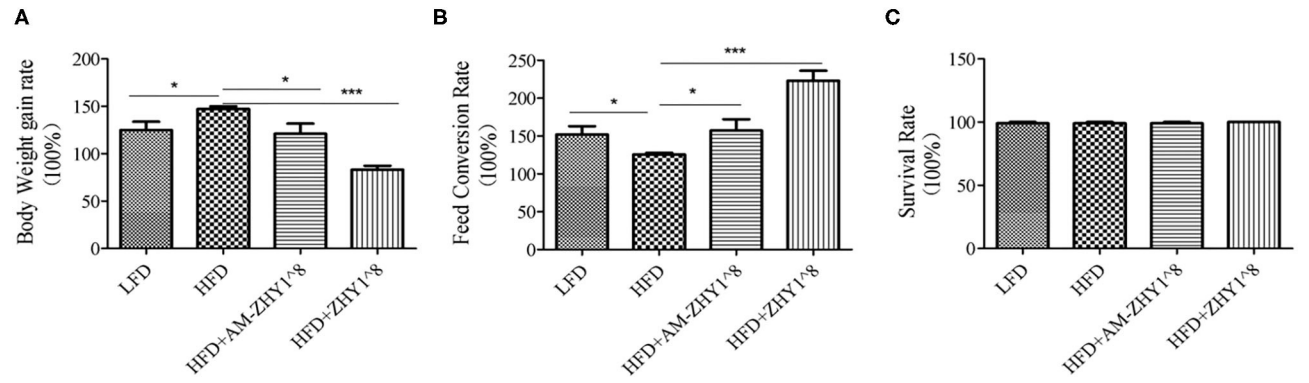

FIGURE 3 | Effects of different diets on the **(A)** body weight gain, **(B)** feed conversion rate, and **(C)** survival rate of zebrafish. Data represent as the means ± SEM. The asterisks on the horizontal line represent significant differences between the two groups. $^{*}p < 0.05$, $^{***}p < 0.001$.

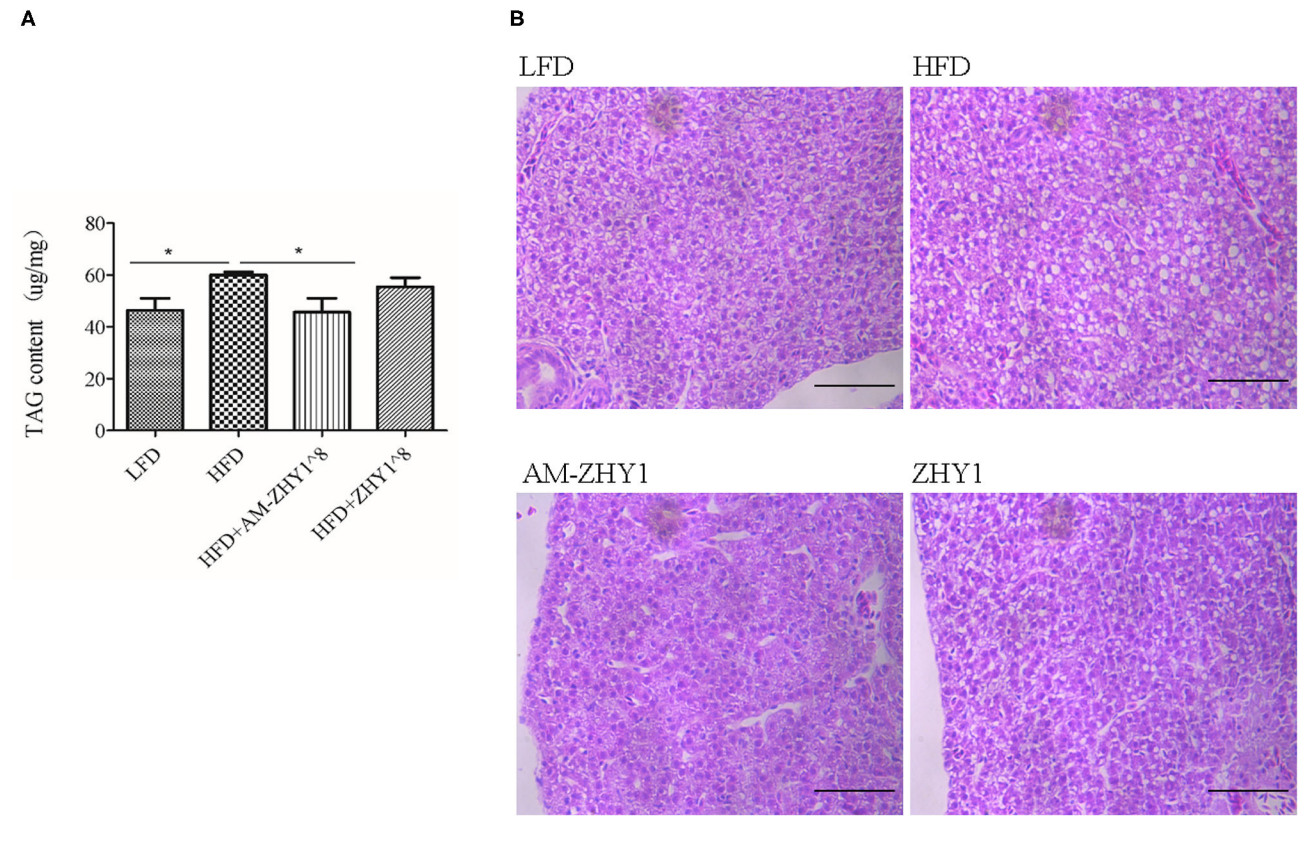

FIGURE 4 | Triacylglycerol (TAG) content of the livers of zebrafish in different groups. **(A)** TAG content of the liver, the significance level was determined by a Student's *t*-test ($^{*}p < 0.05$). **(B)** Histological changes of liver sections measured by HE staining (scale bar is 50 μm).

The addition of AM-ZHY1 and ZHY1 to the high-fat diet both inhibited the expression of the *ATGL* of zebrafish ($p < 0.05$; $p = 0.07$). Taken together, these results demonstrated that the supplement AM-ZHY1 with the high-fat diet led to the improvement of hepatic steatosis. Furthermore, this regulatory effect of AM-ZHY1 on liver lipid accumulation was through inhibiting lipid synthesis and absorption, rather than promoting lipolysis.

AM-ZHY1 Relieves High-Fat Diet-Induced Liver Injury by Regulating Lipid Metabolism and Inflammatory Responses

After the feeding experiment, the zebrafish serum ALT, AST, and liver inflammatory factor expression levels were tested to examine the effect of AM-ZHY1 on liver health. Compared with the high-fat diet group, the levels of ALT and AST were significantly reduced in the AM-ZHY1 group ($p <$

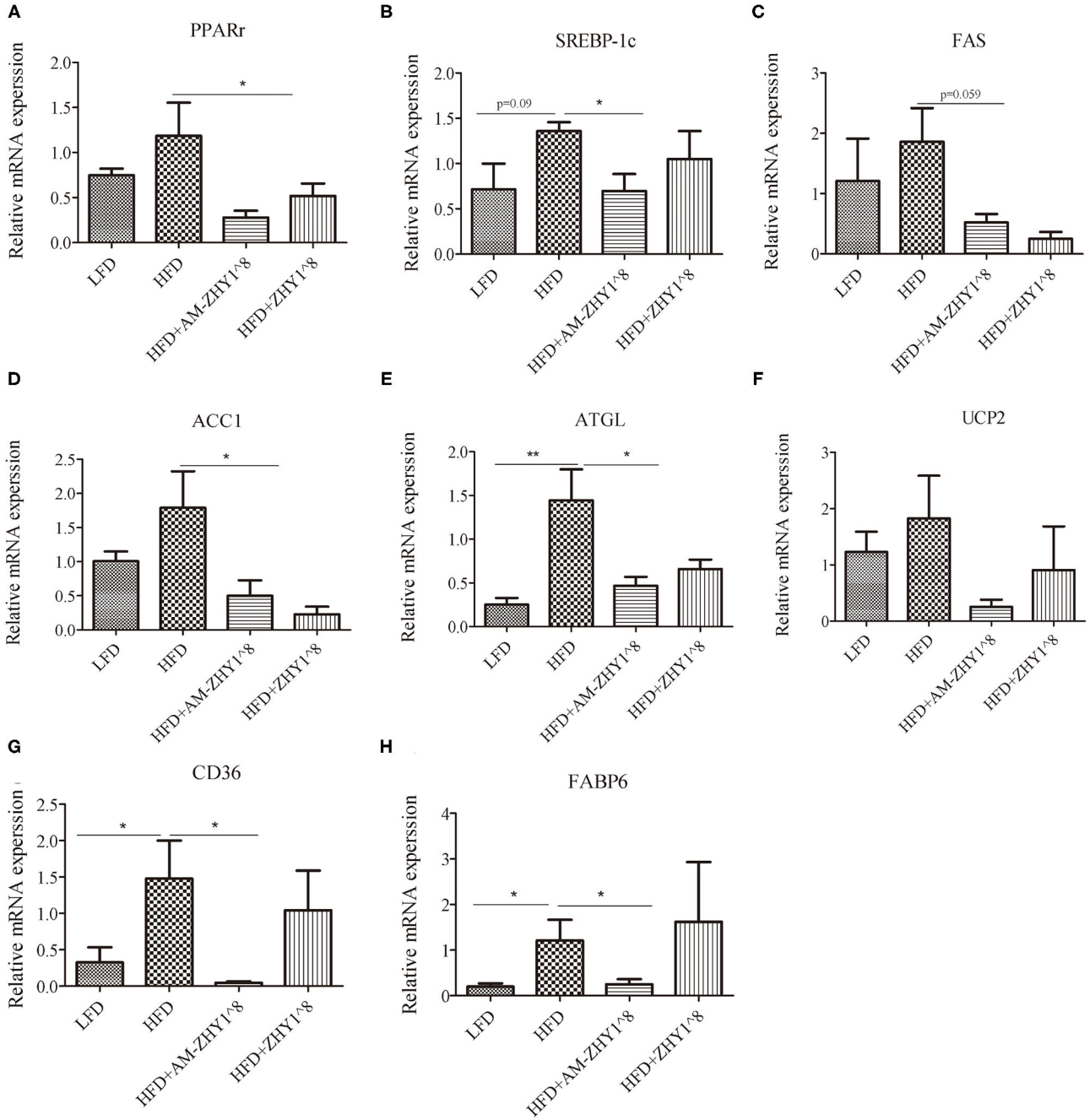

FIGURE 5 | Relative mRNA expression of lipid metabolic-related genes PPARγ **(A)**, SREBP-1c **(B)**, FAS **(C)**, ACC1 **(D)**, ATGL **(E)**, UCP2 **(F)**, CD36 **(G)**, FABP6 **(H)** of the livers of zebrafish in different groups. Data are presented as mean ± SEM ($n = 6$). The asterisks on the horizontal line represent significant differences between the two groups. *$p < 0.05$, **$p < 0.01$.

0.05, $p < 0.05$; **Figure 6**), and the expression level of *TNF-a* and *IL-6* of the liver were significantly decreased in the AM-ZHY1 group ($p < 0.05$, $p < 0.05$; **Figures 7A,B**). The expression level of *IL-1β* and *IL-10* had no significant changes in the AM-ZHY1 group ($p = 0.24$, $p = 0.18$; **Figures 7C,D**). These results indicated that an AM-ZHY1 treatment could alleviate liver injury and the inflammation caused by a high-fat diet.

AM-ZHY1 Improves High-Fat Diet-Induced Intestinal Injury by Altering Gut Microbiota Dysbiosis and Protecting Intestinal Integrity

A total of 1,519,923 high-quality 16S rRNA sequences were generated from 30 samples. After subsampling each sample to an equal sequencing depth of 33,004 reads per sample,

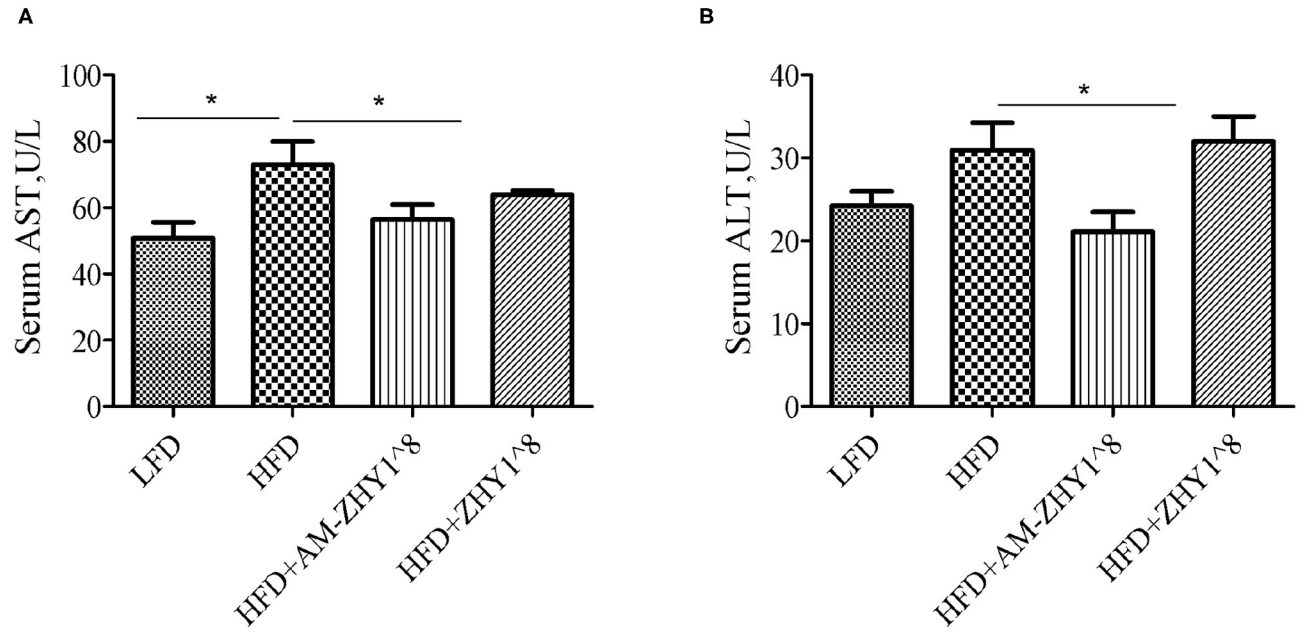

FIGURE 6 | Serum alanine aspartate aminotransferase [AST, **(A)**] and alanine aminotransferase [ALT, **(B)**] levels of zebrafish fed with a basal diet and high-fat diet, with AM-ZHY1(10^8cfu/g) and ZHY1(10^8cfu/g) supplemented with the high-fat diet. Data are presented as mean ± SEM ($n = 6$). The asterisks on the horizontal line represent significant differences between the two groups. *$p < 0.05$.

sequences were clustered into 1,706 OTUs. Treating with AM-ZHY1 could significantly change the structure of zebrafish intestinal microbiota at both the genus and phylum level (**Figure 8**). Compared to the high-fat diet group, Proteobacteria were significantly reduced, and Fusobacteria were significantly increased in the AM-ZHY1 group ($p < 0.05$; $p < 0.05$; **Table 4**). At the genus level, the relative content of *Aeromonas* was significantly reduced in the AM-ZHY1 group compared with the high-fat diet group ($p < 0.05$). The relative abundance of *Cetobacterium* was significantly increased in the AM-ZHY1 group ($p < 0.05$), which is higher than any other group. The relative content of *Plesiomonas* in the AM-ZHY1 group was consistent with that in the basal diet group. The relative contents of *Acinetobacter* and *Bacillus* did not change significantly among these groups (**Table 5**).

The effect of AM-ZHY1 supplementation on intestinal health was elucidated by detecting the gene expression of *TJP1a*, *claudina*, *claudin7*, *claudin7b*, *claudin11a*, *claudin12*, and *claudin15a*. The AM-ZHY1 group, but not the ZHY1 group, significantly increased the expression of the above-mentioned intestinal TJ proteins vs. the high-fat diet group ($p < 0.05$; **Figure 9**). The above results indicated that AM-ZHY1 could improve zebrafish intestinal barrier structure.

DISCUSSION

In this experiment, the AM protein was displayed on the surface of *L. lactis* ZHY1, and its probiotic effects, including relieving high-fat diet-induced liver steatosis and improving the barrier function of the intestinal tract, were confirmed in zebrafish. For the first time, AM protein was used to treat fish fatty liver in aquaculture, and this research, combined with surface display technology, advanced its practical application.

Studies have shown that AM protein could decrease the body weight and fat content of high-fat diet-fed mice (8). In this experiment, AM-ZHY1 reduced the high-fat diet-induced weight gain to the basal diet level, similar to the same function in mammals. However, the ZHY1 group could also significantly reduce weight gain. This may be due to the fact that *lactic acid bacteria* themselves could play an anti-obesity effect by regulating the lipid metabolism of the body and changing the composition of intestinal microbes (9, 19–22). Next, we tested the content of liver TAG and found that the content of liver TAG in the ZHY1 group did not decrease compared with the high-fat diet group, but the AM-ZHY1 group significantly reduced the accumulation of liver fat. This further confirmed that AM protein-induced weight loss by reducing liver fat accumulation, while ZHY1-induced weight loss may be due to the reduction of fat content at mesenteric, perirenal white adipose tissues, or other body mass, similar to other *Lactobacillus* species (22–24).

Furthermore, AM-ZHY1 significantly reduced the expression of lipogenic genes (*PPARγ*, *SREBP-1c*, *ACC1*, and *FAS*) and fatty acid transport-related proteins (*CD36*, *FABP6*) in high-fat diet-fed zebrafish. However, compared with high-fat diet-fed zebrafish treated with ZHY1, AM-ZHY1 had no significant effect on the expression of *ATGL* and *UCP2* in high-fat diet-fed zebrafish. These results indicated that AM-ZHY1 mainly reduces high-fat diet-induced fat accumulation by reducing fat synthesis and inhibiting fat absorption.

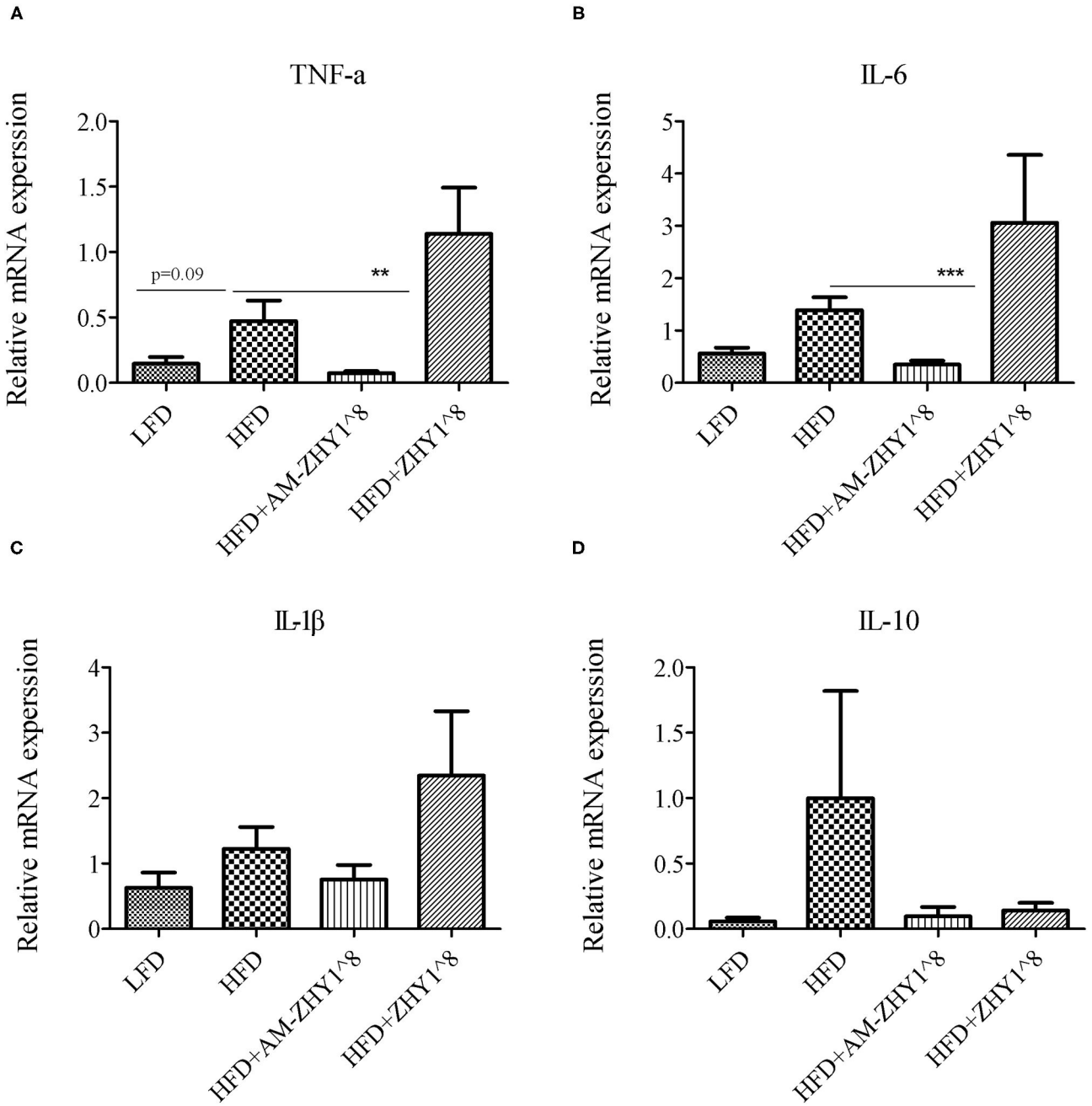

FIGURE 7 | Relative mRNA expression of inflammation related genes: TNFα **(A)**, IL-6 **(B)**, IL-1β **(C)**, IL-10 **(D)** of liver of zebrafish of different groups. Data are presented as mean ± SEM ($n = 6$). The asterisks on the horizontal line represent significant differences between the two groups. $^{**}p < 0.01$, $^{***}p < 0.001$.

The intestinal barrier function was important as a defense against foreign infections. The permeability and stability of the epithelial barrier maybe dependent on the TJs and adherens junctions between epithelial cells (25). The TJs of the intestinal epithelium were a specialized structure, mainly composed of transmembrane proteins, including *occludin*, *trillulin* and *claudin* families, and *zonula occludens* (*ZO-1*) (26, 27). These TJ proteins maintained dynamic balance through continuous remodeling and renewal under the strict regulation of extracellular and intracellular factors. The destruction of this dynamic balance would lead to intestinal epithelial barrier dysfunction which would increase intestinal epicellular paracellular permeability, and cause the translocation of luminal toxic substances and bacteria to the interior organization (28). It was reported that,

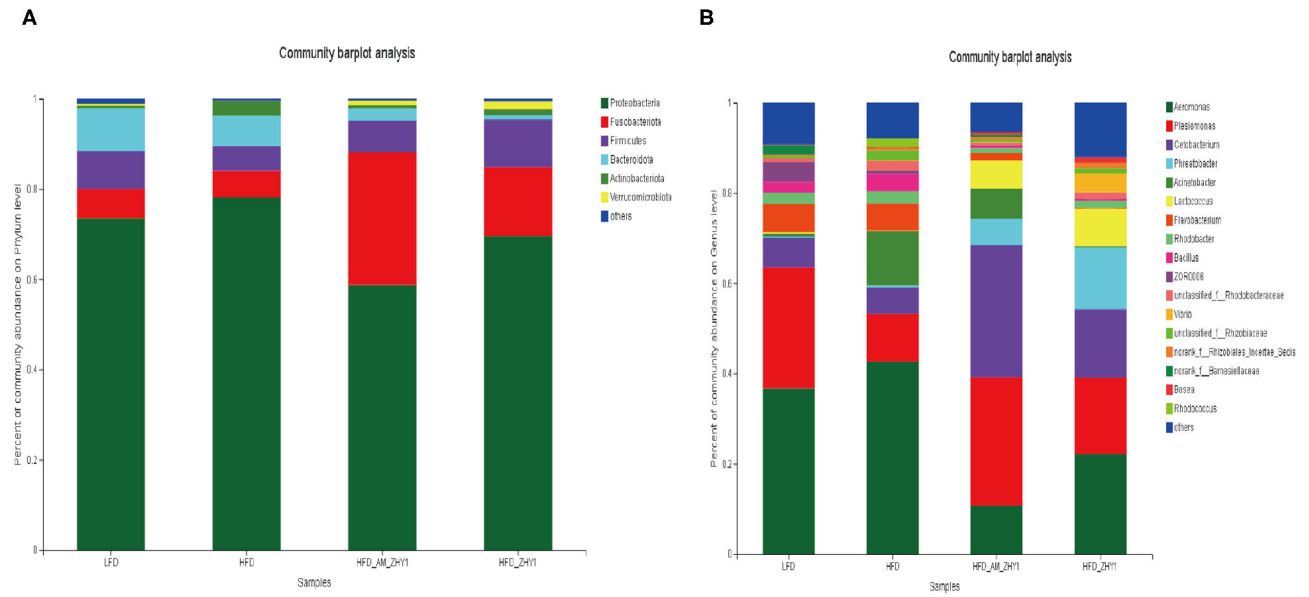

FIGURE 8 | The effect of different diets on the relative abundance of intestinal flora at the phylum in zebrafish **(A)** and the genus **(B)** level. LFD, basal diet; HFD, high-fat diet; HFD_AM_ZHY1, supplement 10^8cfu/g AM-ZHY1 based on a high-fat diet; HFD_ZHY1, supplement 10^8cfu/g ZHY1 based on a high-fat diet.

TABLE 4 | The relative abundance of each group of intestinal flora at the phylum level.

	LFD	HFD	HFD_AM-ZHY1	HFD_ZHY1
Proteobacteria	73.51 ± 11.90^{ab}	78.12 ± 6.56^{b}	58.74 ± 16.23^{a}	69.55 ± 9.57^{ab}
Fusobacteriota	6.57 ± 4.16^{a}	5.89 ± 1.78^{a}	29.33 ± 16.03^{b}	15.25 ± 11.33^{ab}
Firmicutes	8.35 ± 2.57^{a}	5.48 ± 3.13^{a}	7.11 ± 2.82^{a}	10.60 ± 7.82^{a}
Bacteroidota	9.46 ± 6.15^{a}	6.78 ± 4.65^{ab}	2.70 ± 2.22^{bc}	1.01 ± 0.86^{c}
Actinobacteriota	0.61 ± 0.26^{a}	3.13 ± 2.32^{b}	0.719 ± 0.37^{a}	1.20 ± 0.84^{a}
Verrucomicrobiota	0.30 ± 0.19^{a}	0.096 ± 0.034^{a}	0.97 ± 0.66^{a}	1.77 ± 2.26^{a}

Values are means ± SEMs; n = 6 (pool of 3 zebrafish per sample). In the same line, different letters represent significant differences, $p < 0.05$.
LFD, basal diet; HFD, high-fat diet; HFD_AM-ZHY1, supplement 10^8cfu/g AM-ZHY1 based on a high-fat diet; HFD_ZHY1, supplement 10^8cfu/g ZHY1 based on a high-fat diet.

TABLE 5 | The relative abundance of each group of intestinal flora at the genus level.

	LFD	HFD	HFD_AM-ZHY1	HFD_ZHY1
Aeromonas	36.69 ± 21.23^{bc}	42.58 ± 23.57^{c}	10.76 ± 5.29^{ab}	22.05 ± 21.15^{abc}
Plesiomonas	24.25 ± 10.79^{a}	10.63 ± 9.07^{a}	29.42 ± 10.36^{a}	17.09 ± 16.95^{a}
Cetobacterium	6.56 ± 4.16^{a}	5.88 ± 1.78^{a}	29.33 ± 16.03^{b}	15.24 ± 11.32^{ab}
Acinetobacter	0.66 ± 0.32^{a}	12.04 ± 5.49^{a}	6.63 ± 6.15^{a}	0.35 ± 0.33^{a}
Lactococcus	0.25 ± 0.09^{a}	0.09 ± 0.05^{a}	6.27 ± 2.66^{b}	8.33 ± 5.94^{b}
Bacillus	2.38 ± 1.54^{ab}	3.81 ± 2.67^{a}	0.54 ± 0.28^{a}	0.33 ± 0.24^{a}

Values are means ± SEMs; n = 6 (pool of 3 zebrafish per sample). In the same line, different letters represent significant differences, $p < 0.05$.
LFD, basal diet; HFD, high-fat diet; HFD_AM-ZHY1, supplement 10^8cfu/g AM-ZHY1 based on a high-fat diet; HFD_ZHY1, supplement 10^8cfu/g ZHY1 based on a high-fat diet.

as the TJ expression levels in the intestines of mice with high-fat diet-induced obesity decreased, the permeability of the intestine increased and even caused endotoxemia (29–31). We explored whether AM-ZHY1 had a protective effect on the destruction of intestinal barrier function caused by the high-fat diet. This study had shown that AM-ZHY1 could maintain intestinal health by increasing the expression of a series of TJ proteins (*TJP1a*, *claudina*, *claudin7*, *claudin7b*, *claudin11a*, *claudin12*, and *claudin15a*).

The homeostasis of the intestinal microbial community was vital to the gut histologic structure, metabolism, and gut immunity of fish (32, 33). A high-fat diet could cause

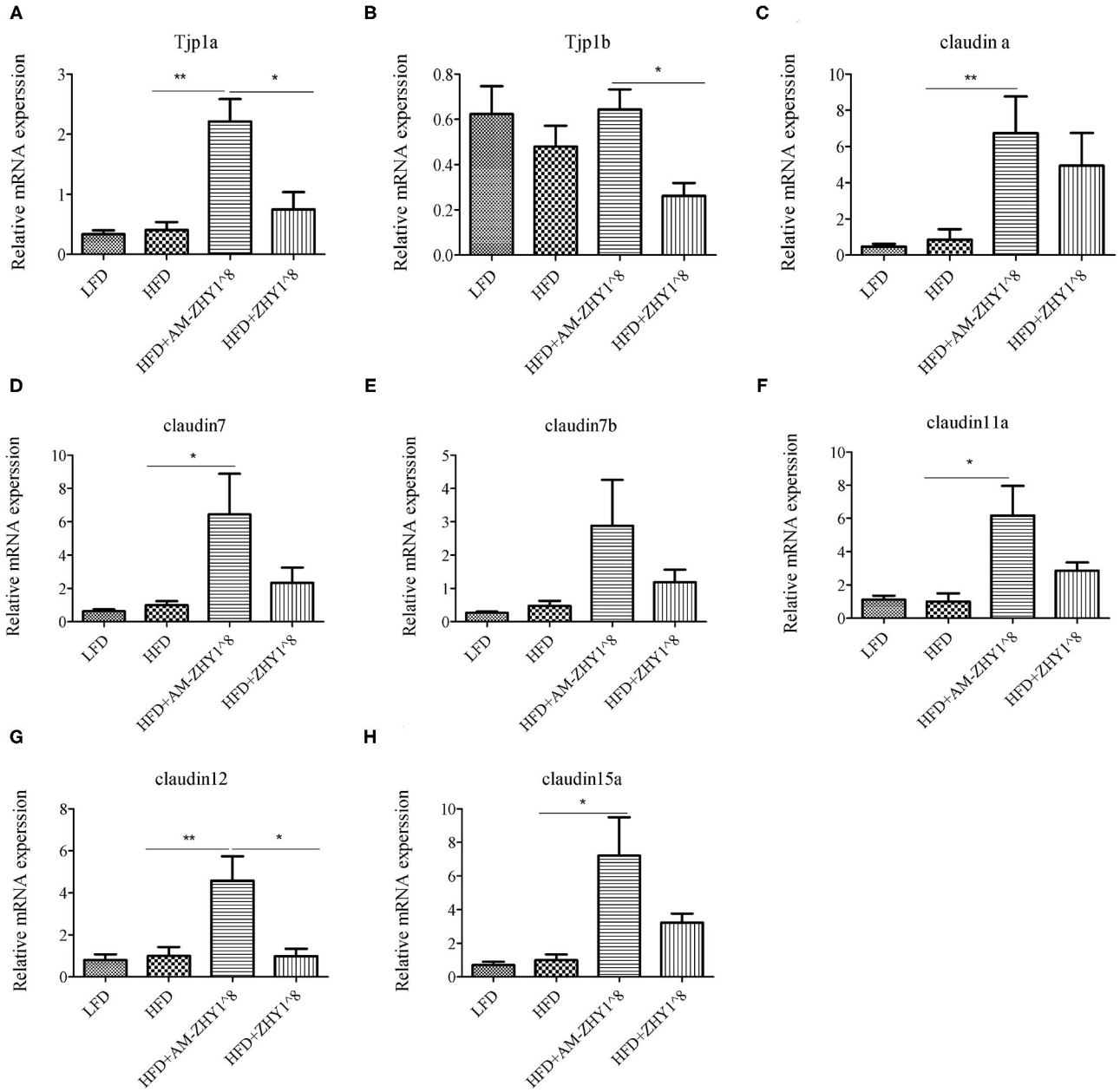

FIGURE 9 | Relative mRNA expression of the tight junction protein genes TJP1a **(A)**, TJP1b **(B)**, Claudina **(C)**, Claudin7 **(D)**, Claudin7b **(E)**, Claudin11a **(F)**, Claudin12 **(G)**, Claudin15a **(H)** of the intestines of zebrafish in different groups. Data are presented as mean ± SEM ($n = 6$). The asterisks on the horizontal line represent significant differences between the two groups. (*$p < 0.05$,**$p < 0.01$).

a bad tilt of intestinal flora and reduce the abundance and diversity of microorganisms (34, 35). In our previous studies, the increase in the abundance of *Fusobacteria* and the decrease in the abundance of *Proteobacteria* indicated that the intestinal health of the zebrafish had improved (36). In this study, the addition of the recombinant bacteria AM-ZH1 could significantly increase the abundance of *Fusobacteria* (*Cetobacterium*) in the guts of high-fat diet zebrafish.

CONCLUSION

In conclusion, AM protein was successfully anchored to the cell surface of *L. lactis* ZHY1. This recombinant *L. lactis* AM-ZHY1 could reduce hepatic fat accumulation, relieve liver injury, and inhibit liver inflammation in high-fat diet-fed zebrafish. Furthermore, AM-ZHY1 could maintain the barrier function of the intestinal tract by increasing the expression of intestinal TJ

proteins. Moreover, the relative abundance of beneficial commensal bacterium (*Cetobacterium*) was increased in the AM-ZHY1 group.

DATA AVAILABILITY STATEMENT

The datasets presented in this study can be found in online repositories. The names of the repository/repositories and accession number(s) can be found below: PRJNA739824.

ETHICS STATEMENT

The animal study was reviewed and approved by Feed Research Institute of the Chinese Academy of Agricultural Sciences Animal Care Committee. Written informed consent was obtained from the owners for the participation of their animals in this study.

AUTHOR CONTRIBUTIONS

F-LZ, Z-GZ, Y-LY, and ZZ participated in the research design. F-LZ, Z-GZ, and ZZ conducted the experiments and performed the data analysis. F-LZ, Y-YY, RX, C-CG, D-DD, JH, and CR, ZL wrote the manuscript or contributed to the manuscript. All authors contributed to the article and approved the submitted version.

FUNDING

This work was supported by grants from the National Natural Science Foundation of China (Grant Nos. 32172958, 3180131599, and 31925038), the earmarked fund for the Modern Agro-industry Technology Research System (SCGWZJ20211104-4), and the Innovation Capability Support Program of Shaanxi (2018TD-021).

REFERENCES

1. Zhao H, Luo Y, Zhang Y, Chen X, Wu Z. Effects of Bacillus subtilis on hepatic lipid metabolism and oxidative stress response in grass carp (*Ctenopharyngodon idellus*) fed a high-fat diet. *Mar Life Sci Technol.* (2020) 2:50–9. doi: 10.1007/s42995-019-00005-2
2. Liu L, Zhou R, Li ZZ, Xiao RX, Li PF, Sun XG, et al. Luteolin alleviates non-alcoholic fatty liver disease in rats via restoration of intestinal mucosal barrier damage and microbiota imbalance involving in gut-liver axis. *Arch Biochem Biophys.* (2021) 711:109019. doi: 10.1016/j.abb.2021.109019
3. Everard A, Belzer C, Geurts L, Ouwerkerk JP, Cani PD. Cross-talk between *Akkermansia muciniphila* and intestinal epithelium controls diet-induced obesity. *Proc Natl Acad Sci USA.* (2013) 110: 9066–71. doi: 10.1073/pnas.1219451110
4. Shen J, Tong X, Sud N, Khound R, Song YY, Maldonado-Gomez MX, et al. Low-density lipoprotein receptor signaling mediates the triglyceride-lowering action of *Akkermansia muciniphila* in genetic-induced hyperlipidemia. *Arteriosclerosis.* (2016) 36:1448–56. doi: 10.1161/ATVBAHA.116.307597
5. Rao Y, Kuang ZQ, Li C, Guo SY, Xu YY, Zhao DD, et al. Gut *Akkermansia muciniphila* ameliorates metabolic dysfunction-associated fatty liver disease by regulating the metabolism of L-aspartate via gut-liver axis. *Gut Microbes.* (2021) 13:1–19. doi: 10.1080/19490976.2021.1927633
6. Yoon HS, Cho CH, Yun MS, Sung JJ, You HJ, Jun-hyeong K, et al. *Akkermansia muciniphila* secretes a glucagon-like peptide-1-inducing protein that improves glucose homeostasis and ameliorates metabolic disease in mice. *Nat Microbiol.* (2021) 6:563–73. doi: 10.1038/s41564-021-00880-5
7. Wang L, Tang L, Feng Y, Zhao S, Han M, Zhang C, et al. A purified membrane protein from *Akkermansia muciniphila* or the pasteurised bacterium blunts colitis associated tumourigenesis by modulation of $CD8^{+}$T. *Gut.* (2020) 69:1988–97. doi: 10.1136/gutjnl-2019-320105
8. Plovier H, Everard A, Druart C, Depommier C, Van HM, Geurts L, et al. A purified membrane protein from *Akkermansia muciniphila* or the pasteurized bacterium improves metabolism in obese and diabetic mice. *Nat Med.* (2016) 23:107–13. doi: 10.1038/nm.4236
9. Wang H, Ni X, Xiaodan Q, Zeng D, Min L, Lei L, et al. Live probiotic Lactobacillus johnsonii BS15 promotes growth performance and lowers fat deposition by improving lipid metabolism, intestinal development, and gut microflora in broilers. *Front Microbiol.* (2017) 8:e1073. doi: 10.3389/fmicb.2017.01073
10. Ottman N, Reunanen J, Meijerink M, Pietilä TE, Kainulainen V, Klievink J, et al. Pili-like proteins of *Akkermansia muciniphila* modulate host immune responses and gut barrier function. *PLoS ONE.* (2017) 12:e0173004. doi: 10.1371/journal.pone.0173004
11. Mathiesen G, Verland L, Kuczkowska K, Eijsink V. Anchoring of heterologous proteins in multiple Lactobacillus species using anchors derived from Lactobacillus plantarum. *Sci Rep.* (2020) 10:9640. doi: 10.1038/s41598-020-66531-7
12. Guo X, Ran C, Zhang Z, He S, Jin M, Zhou Z. The Growth-promoting effect of dietary nucleotides in fish is associated with an intestinal microbiota-mediated reduction in energy expenditure. *Journal of Nutrition.* (2017) 147:781–8. doi: 10.3945/jn.116.245506
13. Zhang Z, Zhou Z, Li Y, Zhou LK, Ding QW, Xu L. Isolated exopolysaccharides from Lactobacillus rhamnosus GG alleviated adipogenesis mediated by TLR2 in mice. *Sci Rep.* (2016) 2016:e36083. doi: 10.1038/srep36083
14. Pedroso GL, Hammes TO, Escobar T, Fracasso LB, Forgiarini LF, Silveira T. Blood collection for biochemical analysis in adult zebrafish. *J Vis Exp.* (2012) 63:e3865. doi: 10.3791/3865
15. Zhang YL, Duan XD, Feng L, Jiang WD, Wu P, Liu Y, et al. Soybean glycinin impaired immune function and caused inflammation associated with PKC-ζ/NF-κb and mTORC1 signaling in the intestine of juvenile grass carp (*Ctenopharyngodon idella*). *Fish Shellfish Immunol.* (2020) 106:393–403. doi: 10.1016/j.fsi.2020.08.008
16. Edgar RC. UPARSE: highly accurate OTU sequences from microbial amplicon reads. *Nat Methods.* (2013) 10:996. doi: 10.1038/nmeth.2604
17. Maidak BL, Olsen GJ, Niels L, Ross OB, McCaughey MJ, Woese CR. The RDP (Ribosomal Database Project). *Nucleic Acids Res.* (1997) 25:109–10. doi: 10.1093/nar/25.1.109
18. Team CR. *A Language and Environment for Statistical Computing*. Vienna: Computing. (2015).
19. Yadav H, Lee JH, Lloyd J, Walter P, Rane SG. Beneficial metabolic effects of a probiotic via butyrate-induced GLP-1 hormone secretion. *J Biol Chem.* (2013) 288:25088–97. doi: 10.1074/jbc.M113.452516
20. Kondo S, Xiao JZ, Satoh T, Odamaki T, Takahashi S, Sugahara H, et al. Antiobesity effects of Bifidobacterium breve strain B-3 supplementation in a mouse model with high-fat diet-induced obesity. *Biosci Biotechnol Biochem.* (2010) 74:1656–61. doi: 10.1271/bbb.100267
21. Kang JH, Yun SI, Park MH, Park JH, Jeong SY, Park H. Anti-obesity effect of Lactobacillus gasseri BNR17 in high-Sucrose diet-induced obese Mice. *PLoS ONE.* (2013) 8:e54617. doi: 10.1371/journal.pone.0054617
22. Xie N, Yi C, Yin YN, Xin Z, Lu FG. Effects of two Lactobacillus strains on lipid metabolism and intestinal microflora in rats fed a high-cholesterol diet. *BMC Complement Altern Med.* (2011) 11:1–11. doi: 10.1186/1472-6882-11-53
23. Grompone G, Vidal DR, Guerola PM, Martinez SG, Soriano PO, Pla SL, et al. *Lactobacillus Rhamnosus Strain for Reducing Body fat Accumulation.* US9855304 (2018).

24. Jang HR, Park HJ, Kang D, Chung H, Lee HY. A protective mechanism of probiotic Lactobacillus against hepatic steatosis via reducing host intestinal fatty acid absorption. *Exp Mol Med.* (2019) 51:1–14. doi: 10.1038/s12276-019-0293-4
25. Yang H, Rao JN, Wang JY. Posttranscriptional regulation of intestinal epithelial tight junction barrier by RNA-binding proteins and microRNAs. *Tissue Barriers.* (2014) 2:e28320. doi: 10.4161/tisb.28320
26. Furuse M, Izumi Y, Oda Y, Higashi T, Iwamoto N. Molecular organization of tricellular tight junctions. *Tissue Barriers.* (2014) 2:615–21. doi: 10.4161/tisb.28960
27. Chen J, Xiao L, Rao JN, Zou T, Liu L, Bellavance E, et al. JunD represses transcription and translation of the tight junction protein zona occludens−1 modulating intestinal epithelial barrier function. *Mol Biol Cell.* (2008) 19:3701–12. doi: 10.1091/mbc.e08-02-0175
28. Cao S, Xiao L, Rao JN, Zou T, Liu L, Zhang D, et al. Inhibition of Smurf2 translation by miR-322/503 modulates TGF-β/Smad2 signaling and intestinal epithelial homeostasis. *Mol Biol Cell.* (2014) 25:1234–43. doi: 10.1091/mbc.e13-09-0560
29. Cani PD, Bibiloni R, Knauf C, Waget A, Neyrinck AM, Delzenne NM, et al. Changes in gut microbiota control metabolic endotoxemia-induced diet-induced obesity and diabetes in mice. *Diabetes.* (2008) 57:1470–81. doi: 10.2337/db07-1403
30. Serre C, Ellis CL, Lee J, Hartman AL, Rutledge JC, Raybould HE, et al. Propensity to high-fat diet-induced obesity in rats is associated with changes in the gut microbiota and gut inflammation. *Am J Physiol Gastrointest Liver Physiol.* (2010) 299:G440–8. doi: 10.1152/ajpgi.00098.2010
31. Oliveira RB, Canuto LP, Collares-Buzato CB. Intestinal luminal content from high-fat-fed prediabetic mice changes epithelial barrier function *in vitro*. *Life Sci.* (2018) 216:10–21. doi: 10.1016/j.lfs.2018.11.012
32. Guerreiro I, Enes P, Rodiles A, Merrifield D, Oliva T. Effects of rearing temperature and dietary short-chain fructooligosaccharides supplementation on allochthonous gut microbiota, digestive enzymes activities and intestine health of turbot (*Scophthalmus maximus L*) juveniles. *Aquacult Nutr.* (2016) 22:631–42. doi: 10.1111/anu.12277
33. Stagaman K, Burns AR, Guillemin K, Bohannan BJ. The role of adaptive immunity as an ecological filter on the gut microbiota in zebrafish. *ISME J.* (2017) 11:1630–9. doi: 10.1038/ismej.2017.28
34. Wong S, Stephens WZ, Burns AR, Stagaman K, David LA, Bohannan B, et al. Ontogenetic differences in dietary fat influence microbiota assembly in the zebrafish gut. *MBio.* (2015) 6:e00687. doi: 10.1128/mBio.00687-15
35. Arias-Jayo N, Abecia L, Alonso-Sáez Ramirez-Garcia A, Rodriguez A, Pardo MA. High-Fat diet consumption induces microbiota dysbiosis and intestinal inflammation in zebrafish. *Microb Ecol.* (2018) 76:1089–101. doi: 10.1007/s00248-018-1198-9
36. Zhang Z, Ran C, Ding QW, Liu HL, Xie MX, Yang YL, et al. Ability of prebiotic polysaccharides to activate a HIF1α-antimicrobial peptide axis determines liver injury risk in zebrafish. *Commun Biol.* (2019) 2:274–91. doi: 10.1038/s42003-019-0526-z

Conflict of Interest: The authors declare that the research was conducted in the absence of any commercial or financial relationships that could be construed as a potential conflict of interest.

Publisher's Note: All claims expressed in this article are solely those of the authors and do not necessarily represent those of their affiliated organizations, or those of the publisher, the editors and the reviewers. Any product that may be evaluated in this article, or claim that may be made by its manufacturer, is not guaranteed or endorsed by the publisher.

frontiers in Nutrition

ORIGINAL RESEARCH
published: 21 October 2021
doi: 10.3389/fnut.2021.729437

Effects of Nisin, Cecropin, and *Penthorum chinense* Pursh on the Intestinal Microbiome of Common Carp (*Cyprinus carpio*)

Famin Ke[1†], *Peijuan Xie*[1†], *Yanrong Yang*[1], *Liu Yan*[1], *Ailing Guo*[1], *Jian Yang*[1], *Jing Zhang*[1], *Li Liu*[1], *Qin Wang*[1] *and Xiaowei Gao*[1,2,3*]

[1] School of Pharmacy, Southwest Medical University, Luzhou, China, [2] Department of Pharmacy, The Affiliated Hospital of Southwest Medical University, Luzhou, China, [3] Department of Chemistry, Zhejiang University, Hangzhou, China

Following a ban on antibiotic use in the feed industry, trials on the effects of various immunostimulants (prebiotics, probiotics, antimicrobial peptides [AMPs], and herbs) on the survival, growth, immunity, and disease control of farmed fish in aquaculture are being rapidly conducted. The wide variety of microbes with roles in nutrition, metabolism, and immunity in the fish intestine is the primary factor affecting the fermentability and functionality of dietary immunostimulants. For this reason, the dynamic interactions between immunostimulants and the intestinal microbiome may influence fish health. In this study, the effects of two agriculturally important AMPs (nisin and cecropin) and one herb (*Penthorum chinense*) on the gut microbiome of common carp were investigated, using 16S rDNA high-throughput sequencing. The results suggest that all three substances can alter the richness, diversity, and composition of the intestinal microbiota of common carp. *P. chinense* had a similar effect on the gut microbiota of common carp to that of nisin, and both promoted more striking changes in the gut microbiota community than did cecropin. The relative abundance of Proteobacteria was lower in the nisin and *P. chinense* groups than in the control and cecropin groups. The relative abundance of Bacteroidetes in the nisin, cecropin, and *P. chinense* groups was markedly increased, compared with that of the control group. Additionally, nisin, cecropin, and *P. chinense* showed obvious anti-inflammatory effects on the fish intestine, which was reflected by significantly increasing the expression levels of two anti-inflammatory cytokines IL-10 and TGF-β. Some digestive enzyme activities in the fish intestine were also significantly enhanced by supplementing these three substances in feeds.

Keywords: nisin, cecropin, *Penthorum chinense* pursh, common carp, intestinal microbiome, feed additives

OPEN ACCESS

Edited by:
Xi Ma,
China Agricultural University, China

Reviewed by:
Seyyed Morteza Hoseini,
Iranian Fisheries Science Research Institute (IFSRI), Iran
Jixing Zou,
South China Agricultural University, China

***Correspondence:**
Xiaowei Gao
xiaoweigao@swmu.edu.cn

*These authors have contributed equally to this work

Specialty section:
This article was submitted to Nutrition and Microbes, a section of the journal Frontiers in Nutrition

Received: *23 June 2021*
Accepted: *24 September 2021*
Published: *21 October 2021*

Citation:
Ke F, Xie P, Yang Y, Yan L, Guo A, Yang J, Zhang J, Liu L, Wang Q and Gao X (2021) Effects of Nisin, Cecropin, and Penthorum chinense Pursh on the Intestinal Microbiome of Common Carp (Cyprinus carpio). Front. Nutr. 8:729437. doi: 10.3389/fnut.2021.729437

INTRODUCTION

Fishes are one of the main sources of consumable proteins for humans. Aquaculture has been growing rapidly in recent years and has now overtaken capture fisheries as the main way for humans to obtain food fish. With the increased use of intensive and high stocking-density breeding in fish farming, the risk of disease outbreaks has increased significantly (1). To avoid economic

losses caused by bacterial infections, antibiotics and chemotherapeutics have been widely used as feed additives to prevent and treat diseases in fish (2). However, studies have demonstrated that supplementing antibiotics in feeds may have negative effects on fish health, including oxidative stress, immunosuppression, and histopathological damage (3–5). In addition, overuse of antibiotics results in many side effects that threaten human health, including presence of undesired drug residues in the food chain, development, and enrichment of drug-resistant genes, and emergence of drug-resistant bacteria (6). Studies have projected that antibiotic resistance will cause 10 million deaths and $100 trillion loss in the US by 2050 if this problem remains unsolved (7). Owing to their negative effects, antibiotics used as feed additives and growth promoters in the feed industry have been banned by the European Union (EU) since 1997 (8).

To achieve sustainable development in aquaculture and provide fish products for safe and nutritious human consumption, developing alternatives to antibiotic feed additives is urgent and economically significant. Antimicrobial peptides (AMPs) are small peptide fragments with broad-spectrum antimicrobial activity, including antibacterial, antifungal, antiviral, and anti-carcinogenic properties (9). AMPs are a key component of the innate immune system of almost all organisms, and more than 2,600 AMPs have been identified to date (10). Owing to their lack of drug resistance potential, AMPs have been considered excellent alternatives to antibiotics in both the medical and feed industries. When used as feed additives, some AMPs have been shown to expedite the growth of fishes and increase the resistance of fishes to pathogens (11). However, several studies suggest that different types or concentrations of AMPs have different effects on fish health and performance when used as feed additives for specific fish species (12). Thus, expanding our knowledge regarding the effects of AMPs on different fish will help us to develop suitable AMP-based feed additives for particular fish species. Additionally, some immunostimulants, including probiotics, prebiotics, and herbs, have also shown positive effects on fish performance, disease prevention, and disease control when supplemented as feed additives (2). Several studies have investigated the effects of these reagents on growth, antioxidant and immune responses, and disease resistance in fishes, but effects on the intestinal microbiome have rarely been examined. The intestinal microbiome—a large, diverse, complex, and dynamic community of microbes that colonize the fish gut—is receiving increased attention owing to its important roles in host nutrient digestion, energy metabolism and absorption, immunity, pathogen resistance, and health maintenance (13). The composition of the fish gut microbiota is influenced by many endogenous and exogenous factors, including genetics, phylogeny, sex, body weight, age, immunity, diet, and habitat. Maintaining a normal healthy gut microbiota is essential for fish health.

Nisin is a ribosome-synthesized AMP that is naturally produced by the probiotic bacterium *Lactococcus lactis*. Post-translational modifications are needed to generate mature nisin, which consists of 34 amino acid residues containing dehydrobutyrine, dehydroalanine, one lanthionine, and four methyl-lanthionine rings (9). Nisin shows good inhibitory activity against gram-positive bacteria, including the foodborne pathogen *Listeria monocytogenes*. Owing to its "generally regarded as safe" (GRAS) status, nisin has been widely approved in the food industry by many official organizations, including the World Health Organization (WHO), the European Food Safety Authority (EFSA), and the United States Food and Drug Administration (FDA) (9). It has been reported that dietary nisin can modulate the gut microbial community and enhance the growth performance of broiler chickens (14). Cecropin, naturally generated by the moth *Hyalophora cecropia*, is a strongly cationic, amphipathic AMP with broad-spectrum antimicrobial activities (15). When used as feed additives, members of the cecropin family have shown the capacity to increase animal performance and resistance to lethal pathogen infection. Dietary cecropin increases nitrogen retention and crude fat digestibility; it also enhances apparent metabolizable energy content in broilers (16). Feeding cecropin improved the villus-height-to-crypt-depth ratio in the jejunum and ileum in piglets challenged with *Escherichia coli*, compared with that of controls (17).

Many Chinese medicinal herbs have been investigated as alternatives to antibiotics in the feed industry. When used in fish aquaculture, herbs have shown immunomodulatory, antiviral, antibacterial, and antiparasitic activities and can stimulate appetite and promote weight gain (18, 19). *Penthorum chinense* Pursh is a traditional Chinese medicine that alleviates heat and diuresis, causes detoxification, and promotes blood circulation (20). It is now widely used to treat several liver diseases, such as non-alcoholic and alcoholic fatty liver disease, as well as infectious hepatitis. The extract of *P. chinense* has strong antioxidant and anticomplement activities and can inhibit the growth of many pathogens, including *Staphylococcus aureus*, *Staphylococcus epidermidis*, and *Pseudomonas aeruginosa* (21). Additionally, a recent study demonstrated that *P. chinense* can alter the structure of the gut microbial community in mice and increase the abundance of some probiotics (22). At present, the application of *P. chinense* in aquaculture has not been documented. We assumed that the properties of *P. chinense* mentioned above may have positive effects when used as feed additives in aquaculture.

The common carp (*Cyprinus carpio* L., family *Cyprinidae*) is an omnivorous and stomachless fish. It represents the fourth most-produced fish species in aquaculture worldwide and is produced mainly in Asia and Europe (23). The effects of AMPs and certain herbs as feed additives on common carp have been reported previously; however, these studies mainly assessed and compared the changes in fish performance, blood biochemical parameters, antioxidant activity, and immunity between experimental and control groups (2, 24–30). Considering that feed additives in the fish diet are administered orally, they inevitably enter the gut and directly interact with fish intestinal microflora. Understanding the composition of the fish intestinal microbiota and the changes caused by feed additives in diets will guide the development of novel additives to improve the health and performance of fishes. Here, we report the effects of nisin, cecropin, and *P. chinense*

on the gut microbiome of common carp, and we evaluate their effects on gut health and digestive enzyme activities in this species.

MATERIALS AND METHODS

Experimental Fish and Diet Preparation

Common carp used in this study were obtained from a fish farm in Luzhou City, Sichuan Province, China. Initially, 120 healthy sub-adult fish of similar size (296.75 ± 7.22 g) were randomly distributed into four groups. Each group was housed in six plastic 200 L tanks (80 × 50 × 50 cm) with five individuals per tank. Before the feeding trial, fish were acclimatized for 2 weeks with the control diet. Commercially available nisin (amino acid sequence: ITSISLCTPGCKTGALMGCNMKTATCHCSIHVSK) was purchased from Hengkang Food Additive Co., Ltd. (Tianjin, China). Cecropin (amino acid sequence: KWKLFKKIEKV GQNIRDGIIKAGPAVAVVGQATQIAK) was obtained from Shandong Ruitai Biotechnology Co., Ltd. (Shandong, China). The stem of *P. chinense* was purchased from Sichuan Jiyuntang Traditional Chinese Medicine Co., Ltd., and crushed into powder using a high-speed universal grinder after freezing in liquid nitrogen. A commercial basal diet for common carp was used as the control diet (CON), and experimental diets were prepared by mixing nisin (0.05%, NIS), cecropin (0.01%, CEC), or *P. chinense* (4%, PCH) powder into the control diet, according to the manufacturers' instructions. The control diet used in this experiment contained 16.0% fish meal (FM), 34.0% soybean meal, 4.0% corn oil, 9.0% wheat bran, 11.0% wheat flour, 7.0% dextrin, 14.0% corn gluten, 3.0% $Ca(H_2PO_4)_2$, 0.1% vitamin mixture, and 1.0% mineral mixture. For the feed preparation, basal diets were completely ground, mixed with the corresponding additive powder, made into sinking pellets at room temperature, and stored at −20°C until use.

Experimental Design and Feeding

Experiments in this study were reviewed and approved by the Southwest Medical University Ethics Committee and performed at Southwest Medical University (Luzhou, China). During the experiment, the four groups of fish were fed twice daily with their corresponding diets at 08:00 a.m. and 18:00 p.m. Half of the water in the tanks was changed daily with tap water to maintain water quality. The water parameters were recorded and were as follows: temperature ranged from 20 to 28°C; dissolved oxygen concentration ranged from 5.2 to 6.1 mg/L; pH ranged from 7.1 to 7.9. The feeding experiment lasted for four consecutive weeks under a 12 h light/12 h dark photoperiod. The fish in each group were weighed at the beginning of the feeding experiment and at the end. Weight gain was calculated by subtracting the starting weight from the final weight.

Isolation of Intestinal Bacterial DNA and Sequencing

After the feeding experiment, we randomly selected one fish per tank, and a total of six fish from each group were used for gut microbiome analysis. After euthanasia with tricaine methanesulfonate (MS-222, Sigma, USA), the sampled fish were washed with 70% ethanol and sterile water and then dissected, and the intestinal tissues were aseptically removed from the abdominal cavity. Then, the gut contents were gently squeezed out and harvested separately into sterile tubes. After freezing in liquid nitrogen, the gut content samples were stored at −80°C until use.

Bacterial DNA was extracted from the fish gut content samples directly using the E.Z.N.A. Stool DNA kit (OMEGA, Bio-tek, USA). The purity and concentration of the resulting DNA in each sample were determined using 1% agarose gel electrophoresis and a NanoDrop™ instrument (Thermo Fisher Scientific, Wilmington, DE, USA), respectively. The V4/V5 hypervariable regions of the bacterial 16S rRNA gene were amplified using polymerase chain reaction (PCR) with the extracted genomic DNA as a template. The primer pairs used in the PCR were 338f and 806r (**Table 1**). The PCR mixture and reaction conditions were set as previously described (13). In brief, the PCR mixture consisted of 9.0 μl ddH_2O, 2.5 μl PCR buffer (10×), 1.0 μl KOD-Plus-Neo DNA polymerase, 2.5 μl dNTPs, 1 μl 338f/806r primers, and 2 μl genomic DNA template. PCR conditions were set as: 95°C for 5 min; 30 cycles of 95°C for 30 s, 55°C for 30 s, and 68°C for 30 s; and a final extension at 68°C for 5 min. After electrophoresis on a 1% agarose gel, the PCR products were purified, and the sequencing libraries were constructed and sequenced as described previously (13).

Sequence Processing and Bioinformatic Analysis

The sequencing raw reads obtained in this study were deposited into the National Centre for Biotechnology Information short read archive database under the accession number PRJNA738662. After sequencing, the resulting sequences were processed and quality-filtered to remove low-quality reads using the TrimGalore software and merged using FLASH 2, as previously described (13). Sequences with a quality score <20, ambiguous bases, mismatches in barcodes, or primers with more than 2 bases were removed. To clarify the bacterial community compositions of each group, operational taxonomic unit (OTU) analysis was performed using the Quantitative Insights Into Microbial Ecology (QIIME) toolkit (version 1.17). According to currently accepted standards for prokaryotic species, OTUs were clustered with a threshold of 97% similarity, and chimeric sequences were identified and removed as described previously (9). With a confidence threshold of 70%, the representative OTUs were annotated with taxonomic information using the SILVA ribosomal RNA gene database.

Bioinformatic analysis was performed using the i-Sanger Cloud Platform (www.i-sanger.com). Rarefaction curves were generated by plotting the number of OTUs against the number of identified sequences. The Sobs, Chao, Good's coverage, Ace, Shannon, and Simpson indices that reflected the α-diversity of each group were determined using the Mothur software. The Sobs, ACE, and Chao indices were used to reflect the richness of bacterial species in a community regardless of the abundance of each species, whereas the Shannon and Simpson indices were used to reflect species richness and species evenness.

TABLE 1 | Primers sequences, amplification temperature, and amplicon information for qRT-PCR.

Primer	Sequence (5′-3′)	Annealing temperature (°C)	Amplicon size (bp)	Accession no.
338-f	ACTCCTACGGGAGGCAGCAG			
806-r	GGACTACHVGGGTWTCTAAT			
IL1β-f	AAGGAGGCCAGTGGCTCTGT	58	69	AB010701
IL1β-r	CCTGAAGAAGAGGAGGCTGTCA			
TNFα-f	GCTGTCTGCTTCACGCTCAA	58	106	AJ311800
TNFα-r	CCTTGGAAGTGACATTTGCTTTT			
IL10-f	GCTGTCACGTCATGAACGAGAT	58	132	AB110780
IL10-r	CCCGCTTGAGATCCTGAAATAT			
TGFβ-f	ACGCTTTATTCCCAACCAAA	58	95	AF136947
TGFβ-r	GAAATCCTTGCTCTGCCTCA			
β-actin-f	GAAGTGTGGTGTGGACATCCGTAA	58	247	JQ619774.1
β-actin-r	AGACTCATCGTACTCCTGCTTGCT			

β-diversity analysis, which reflects community diversity and species differences among the four groups, was assessed by weighted UniFrac-based principal coordinate analysis (PCoA) and hierarchical clustering trees using the R software package. The Wilcoxon rank-sum test were used to determine statistically significant differences in microbial composition at the genus level between the control and the other three experimental groups. The main differences in the species level among the four groups were revealed using hierarchical clustering heatmap analysis.

Quantitative Reverse Transcription-PCR (qRT-PCR) Analysis

qRT-PCR was used to assess the transcriptional levels of target genes. Total RNA was extracted from the intestinal tissues of the sampled fish using the TRIzol method with an RNA Isolation Plus kit (Takara, Dalian, China) according to the manufacturer's instructions. After verification of the integrity and purity of the total RNA using 1.5% agarose gel electrophoresis, cDNA was obtained by reverse-transcribing RNA with a HiScript® Reverse Transcriptase Kit (Vazyme, Jiangsu, China). The primers used in this study are listed in **Table 1.** qRT-PCR was performed using a Real-Time PCR Detection System (Bio-Rad, USA) with the AceQ™ qPCR SYBR® Green Master Mix kit. The PCR program was set up as follows: 95°C for 10 min, followed by 45 cycles of 95°C for 15 s, 58°C for 30 s, and 72°C for 30 s. The relative mRNA levels of target genes were normalized using β-actin as an internal standard with the $2^{-\Delta\Delta Ct}$ method (31).

Enzyme Activity Analysis

Six fish in each group were randomly selected for digestive enzyme activity analysis. The digestive enzyme activities in the intestines of the sampled fish were determined using commercial assay kits (Jiancheng Bioengineering Company, Nanjing, China). After freezing in liquid nitrogen, intestinal samples were ground into a powder and homogenized in phosphate buffer (pH 7.4) on ice. Thereafter, the resulting samples were centrifuged at 4,000 × *g* for 10 min, and the supernatant fraction was collected. After quantification of the soluble protein concentrations using the Bradford method, the activities of amylase, lipase, and protease in each sample were analyzed. One unit of amylase activity was defined as the amount of the enzyme required to hydrolyze 10 mg starch in 30 min. One unit of lipase activity was defined as the amount of the enzyme required to hydrolyze triglyceride substrate to form 1 μmol glycerol. One unit of protease activity was defined as the amount of the enzyme required to release 1 mg tyrosine from the substrate per min.

Statistical Analysis

Unless otherwise indicated, statistical analysis was performed in GraphPad Prism 8.0 software (USA) by one-way ANOVA with Dunnett's test (for comparison between two groups) or *post hoc* Tukey-kramer test (for comparison among three or more groups). All data were considered statistically significant at $p < 0.05$.

RESULTS

Growth Performance

The results of growth performance of common carp at the end of the experimental trials are shown in **Figure 1**. There were no significant differences in survival rate or body weight gain values among the four groups, indicating that the three additives used in this study displayed negligible effects on the growth performance of common carp.

Characteristics of the High-Throughput Sequencing Data

A total of 1,182,758 valid sequences were obtained after removing low-quality reads according to the criteria mentioned in subsection Sequence processing and bioinformatic analysis of "Materials and methods." In each sample, the sequence Good's coverage index was ≥99%, and the rarefaction curve reached a saturation plateau (**Supplementary Table 1** and **Supplementary Figure 1**). These results suggest that the sequencing depth was adequate, and most bacterial phylotypes could be identified. With a 97% sequence similarity cut-off threshold, the obtained valid sequences were delineated into 688 OTUs. The total OTU numbers of the CON, NIS, CEC, and PCH

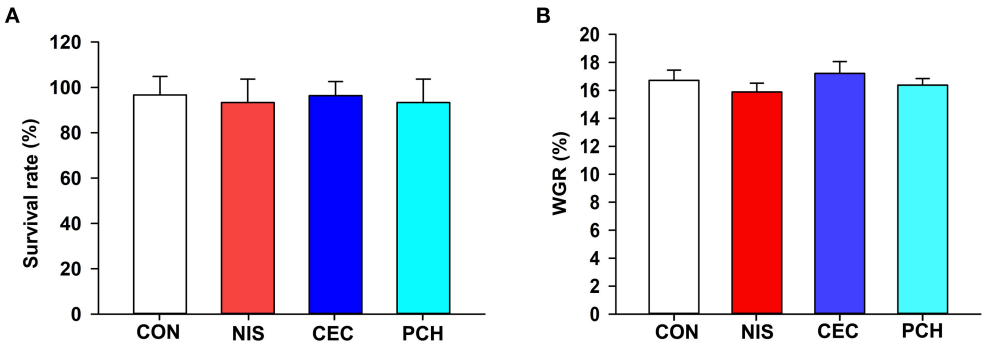

FIGURE 1 | Effects of the three additives on the growth performance of common carp. **(A)** Survival rate of the common carp in the four groups. **(B)** Weight gain rate (WGR) of the common carp in the four groups. WGR is calculated as: WGR= (final weight–initial weight) × 100/(initial weight). No significant differences were observed among the four groups.

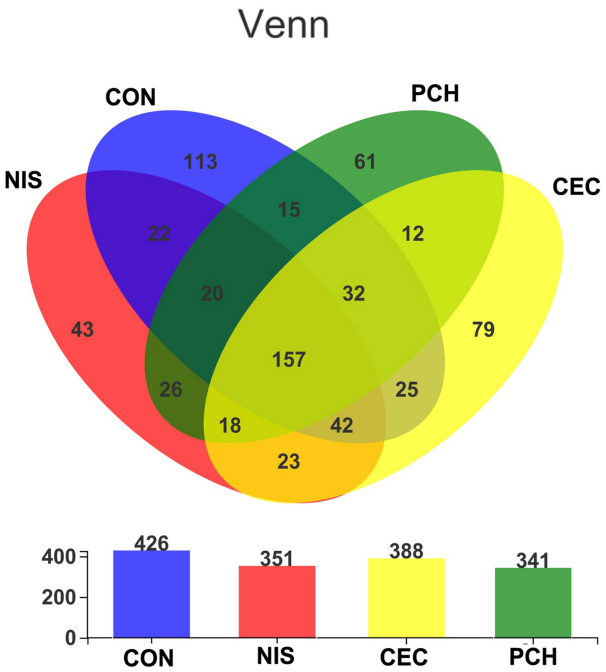

FIGURE 2 | The number of shared and unique operational taxonomic units (OTUs) in different samples. Venn diagrams showing the numbers of unique and shared OTUs among the four groups. Overlaps in the upper panel represent the shared OTUs of corresponding sample groups. The total number of OTUs in each group ($n = 6$) is shown in the lower panel.

groups were 426, 351, 341, and 388, respectively. The number of shared OTUs in the four groups was 157, whereas the number of unique OTUs was 113 in the CON group, 43 in the NIS group, 79 in the CEC group, and 61 in the PCH group (**Figure 2**).

Diversity Analysis of the Microbial Community

The α- and β-diversity of the microbial communities of the four groups were analyzed separately to determine the effects of nisin, cecropin, and *P. chinense*, when used as feed additives, on the diversity of intestinal microbial communities of common carp. The richness and community diversity indices of each group were calculated and compared. As shown in **Figure 3A**, the Sobs, ACE, and Chao indices were significantly lower in the three experimental groups than in the control group, indicating that nisin, cecropin, and *P. chinense* as feed additives reduced the species richness of the intestinal microbiota in common carp. The Shannon index was higher in the control group than in the three experimental groups, whereas the Simpson index showed the opposite trend.

According to the hierarchical clustering tree shown in **Figure 3B**, the cecropin group was clustered together with the control group, whereas the nisin group and the *P. chinense* group, clustered together, were located on different branches of the tree. PCoA analysis was performed to compare the bacterial communities among the four groups (**Figure 3C**). The weighted UniFrac distance was used to determine the PCoA score plot, and each symbol in the plot represents one sample. The discrete degree of PC1 is also shown. The two principal coordinates accounted for 58.75% of the total variation between the groups. The nisin and *P. chinense* groups were clustered together to the right of the plot and located far away from the control group, whereas the cecropin group was located near, and showed only slight dissimilarity with the control group. A structural rearrangement of the gut microbiota of common carp in the three experimental groups was also detected by partial least squares discriminant analysis, as shown in **Figure 3D**.

Composition Analysis of the Microbial Community

A total of 688 OTUs obtained in this study could be assigned to 23 bacterial phyla based on phylogenetic information. The distribution of bacterial phyla among the four groups is presented by both pie and column diagrams in **Figures 4A,B**, and the relative abundance of the bacterial phyla in each group is also shown. Proteobacteria was the most abundant phylum in all four groups, and the relative abundance of this phylum in the CON, CEC, NIS, and PCH groups was 86.12, 89.74, 64.57, and

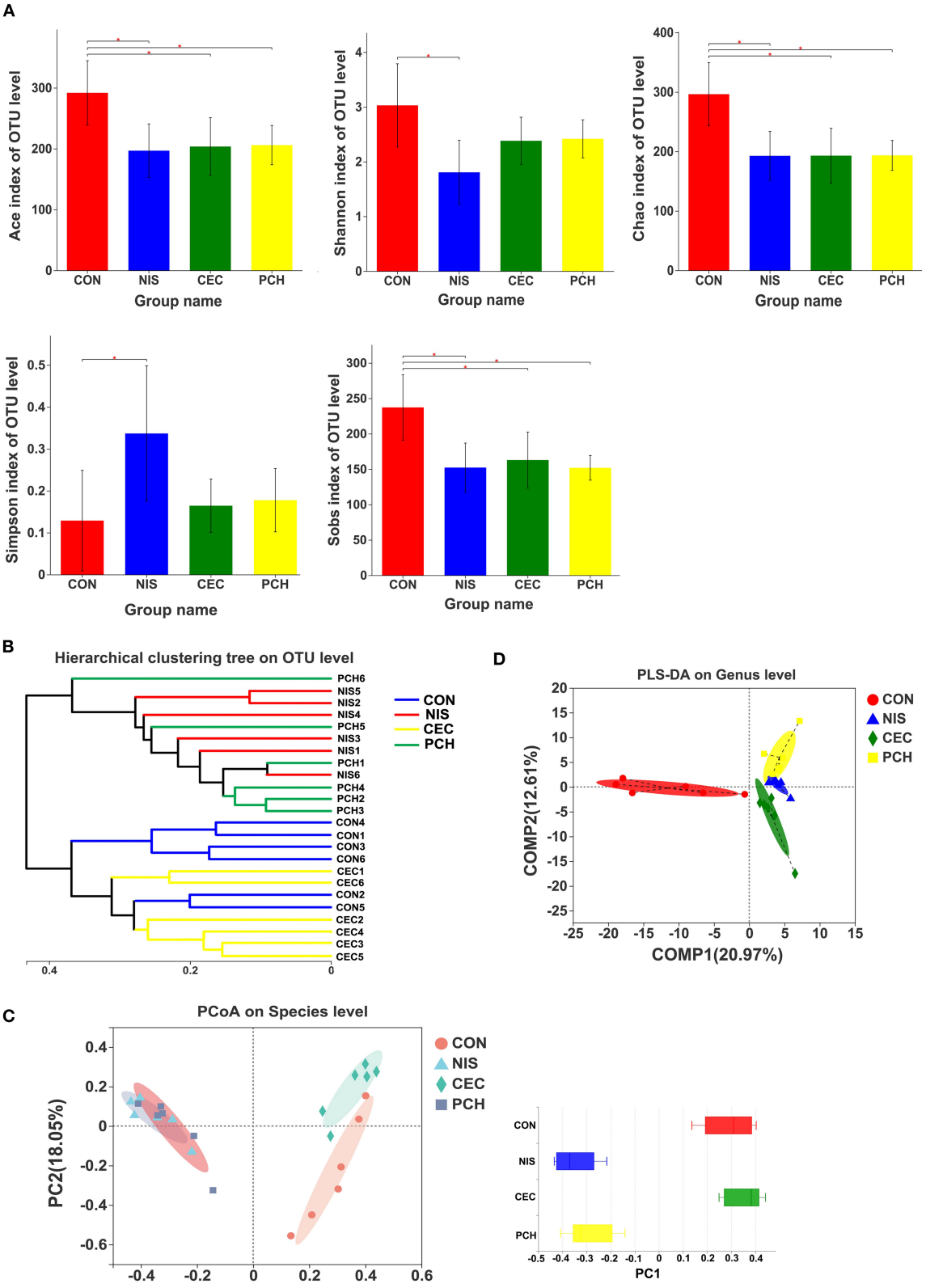

FIGURE 3 | Diversity analysis of the gut microbial communities among the four groups. **(A)** The α-diversity of gut microbial communities is significantly different between the control and the three experimental groups. Bacterial community diversity and richness were presented as the Shannon, Simpson, ACE, Chao, and Sobs

(Continued)

FIGURE 3 | indices. One-way ANOVA with Dunnett's test was used for statistical analysis to determine significant differences between the control and the three experimental groups. $p < 0.05$ was considered statistically significant (*$p < 0.05$). **(B)** Hierarchical clustering tree of Bray-Curtis distances. Each branch represents one fish gut bacterial community. **(C)** Principal coordinate analysis (PCoA) of the four groups. Principal component 1 (PC1) and 2 (PC2) explained 40.7 and 18.05% of the variance, respectively. Distances between each symbol in the plot reflect relative dissimilarities of relative bacterial communities. Discrete degree of PC1 is shown in the right panel. **(D)** Partial least squares discriminant analysis (PLS-DA) of the four groups.

63.89%, respectively, indicating that the relative abundance of Proteobacteria was lower in the NIS and PCH groups than in the control group. The relative abundance of Bacteroidetes in the NIS, PCH, and CEC groups was significantly increased: 1.84% (CON), 6.62% (CEC), 34.68% (NIS), and 30.89% (PCH), when compared with that of the control group, leading to an increase in the Bacteroidota/Firmicutes (B/F) ratio in the three experimental groups (**Figure 4C**). The phylum Desulfobacterota, which was absent in the CON group, was present in the CEC and PCH groups.

The number of bacterial genera identified from the four groups was 399, and the relative abundance of each bacterial genus is shown in **Figure 4D**. The five most abundant genera in the control group were *Aeromonas* (25.35%), *Enterobacteriaceae* (9.38%), *Pseudomonas* (8.56%), *Bosea* (6.25%), and *Shewanella* (4.49%), whereas the top five genera in the nisin group were *Comamonadaceae* (35.73%), *Flavobacterium* (32.11%), *Kaistia* (7.79%), *Pseudorhodobacter* (4.37%), and *Shewanella* (3.79%) (**Supplementary Figure 2**). The five most abundant genera in the cecropin group were *Shewanella* (29.53%), *Pseudomonas* (24.69%), *Aeromonas* (13.03%), *Enterobacteriaceae* (4.79%), and *Bosea* (3.94%), and the top five genera in the *P. chinense* group were *Flavobacterium* (30.2%), *Comamonadaceae* (18.62%), *Pseudomonas* (10.79%), *Pseudorhodobacter* (9.4%), and *Rhizobium* (4.70%). The relative abundance of each bacterial genus in the individual fish is shown in **Supplementary Figure 3**.

Analysis of Overall Changes in Microbial Community

Significant differences in the gut microbiome composition among the four groups at the phylum level were shown in **Figure 5A**. Significant variations in the relative abundance of Proteobacteria ($p = 0.03701$), Bacteroidetes ($p = 0.01154$), Actinobacteria ($p = 0.01002$), and Firmicutes ($p = 0.03049$) were observed. The CEC, NIS, and PCH groups increased in the relative abundance of Bacteroides and decreased in the relative abundance of Actinobacteriota and Fusobacteriota, compared with those in the control group. The relative abundance of Proteobacteria significantly decreased in the NIS and PCH groups, and the relative abundance of Firmicutes significantly decreased in the NIS and CEC groups.

Using the Wilcoxon rank-sum test, significant variations in the gut microbiome composition between the control group and the other three experimental groups at the genus level were determined (**Figure 5B**). The abundance of three genera, including *unclassified_f_Comamonadaceae*, *Flavobacterium*, and *Legionella*, significantly increased, while that of five genera, including *Aeromonas*, *Bosea*, *Devosia*, *unclassified_f_Rhizobiaceae*, and *Mycobacterium*, significantly decreased in the NIS group compared with those in the CON group. Furthermore, the genus *Thermomonas*, which was detected in the CON group, disappeared in the NIS group. The CEC group significantly increased in the abundance of *Shewanella*, *Chryseobacterium*, and *Psychrobacter* and decreased in the abundance of *Bosea*, *Devosia*, *Mycobacterium*, *unclassified_f_Rhizobiaceae, Thermomonas*, and *norank_f_Rhizobiales_Incertae_Sedis*, compared with those in the control group. The abundance of the genera *Flavobacterium*, *unclassified_f_Comamonadaceae*, *Pseudorhodobacter*, and *Allorhizobium-Neorhizobium-Pararhizobium-Rhizobium* increased, whereas that of the genera *Bosea*, *unclassified_f_Rhizobiaceae*, *Mycobacterium*, and *Thermomonas* significantly decreased in the PCH group, compared with those in the control group. A ternary plot was used to visually represent the composition and proportional distribution of the dominant genera in the CON, NIS, and CEC groups (**Figure 5C**). These results suggest that different AMPs (nisin and cecropin) have different effects on the composition of the gut microbial community in common carp. LEfSe analysis was performed to determine significantly different bacteria among the four groups (**Figures 6A,B**). We also performed hierarchical clustering heatmap analysis at the species level to reveal the changes in the entire gut microbial community structure of common carp caused by nisin, cecropin, and *P. chinense* (**Figure 6C**).

Effects of nisin, cecropin, and *P. chinense* on Immune-Related Gene Expression

The expression levels of immune-related genes (TNF-α, IL-1β, IL10, and TGF-β) in the four groups were determined using qRT-PCR. As shown in **Figure 7**, the expression levels of IL10 significantly increased in the NIS and CEC groups compared with that of the control group. By contrast, the PCH group did not show any significant differences. The NIS and PCH groups showed significantly higher TGF-β expression levels than the CON and CEC groups. There were no significant differences detected between the CON group and the three experimental groups in terms of IL-1β or TNF-α gene expression levels.

Effects of nisin, cecropin, and *P. chinense* on Gut Digestive Enzyme Activity

Digestive enzyme activities in the intestines of common carp were determined and compared between the control and the three experimental groups (**Table 2**). Intestinal amylase activities in all groups were not significantly different. The NIS and CEC groups showed significantly higher protease activity than the CON group. The lipase activities in the CEC and PCH groups

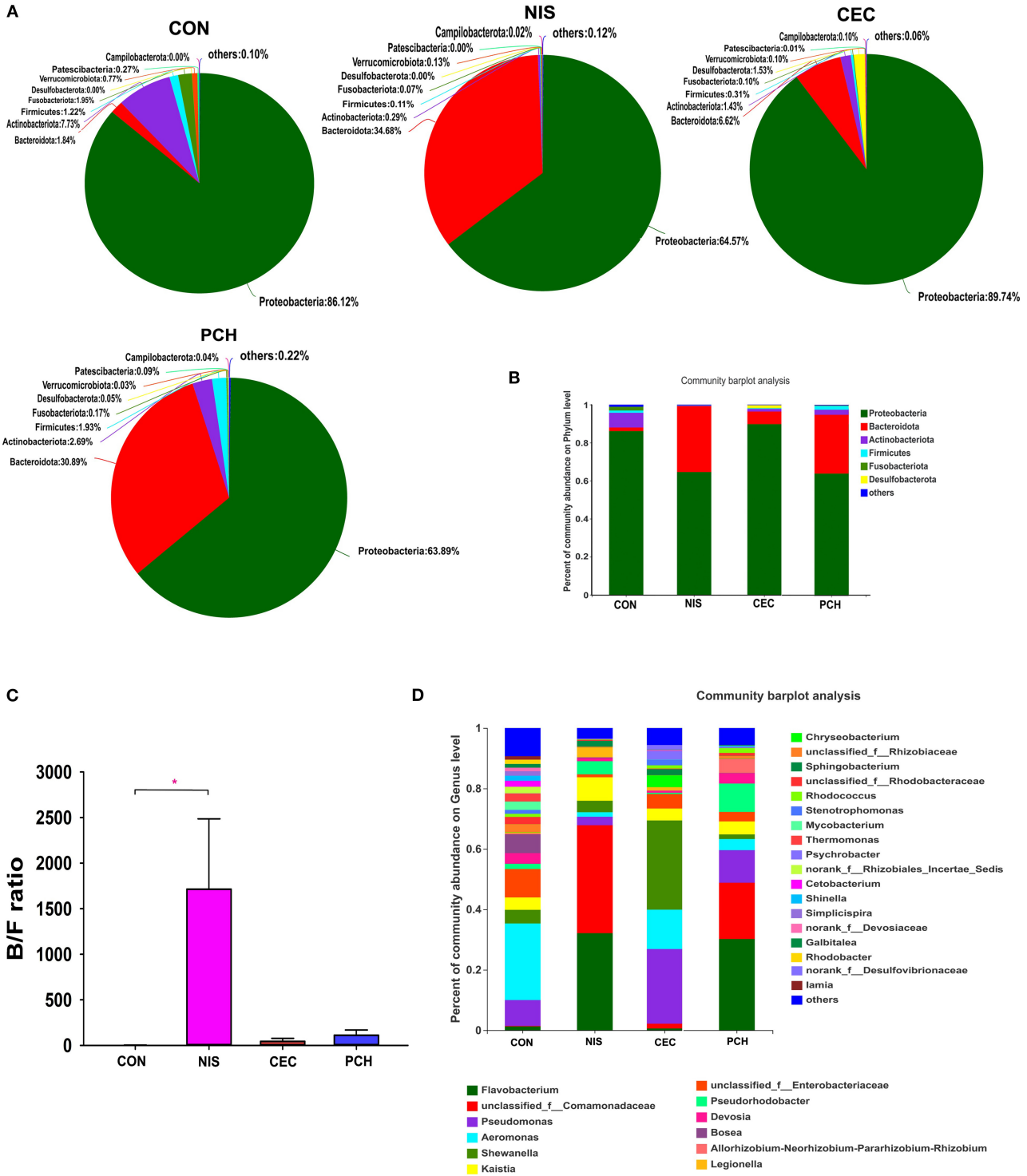

FIGURE 4 | Distribution of bacterial phyla and genera among the four groups. **(A)** Pie diagrams show the bacterial composition of the four groups at the phylum level. The relative abundance of bacterial phyla in each group is shown. **(B)** Column diagrams of distribution of bacterial phyla among the four groups. **(C)** Ratio of Bacteroidetes/Firmicutes (B/F) in the four groups. Data are expressed as mean with SD ($n = 6$). $p < 0.05$ was considered statistically significant ($^*p < 0.05$). **(D)** Column diagrams of distribution of bacterial genera among the four groups. "Others" refers to bacteria with <0.01% abundance.

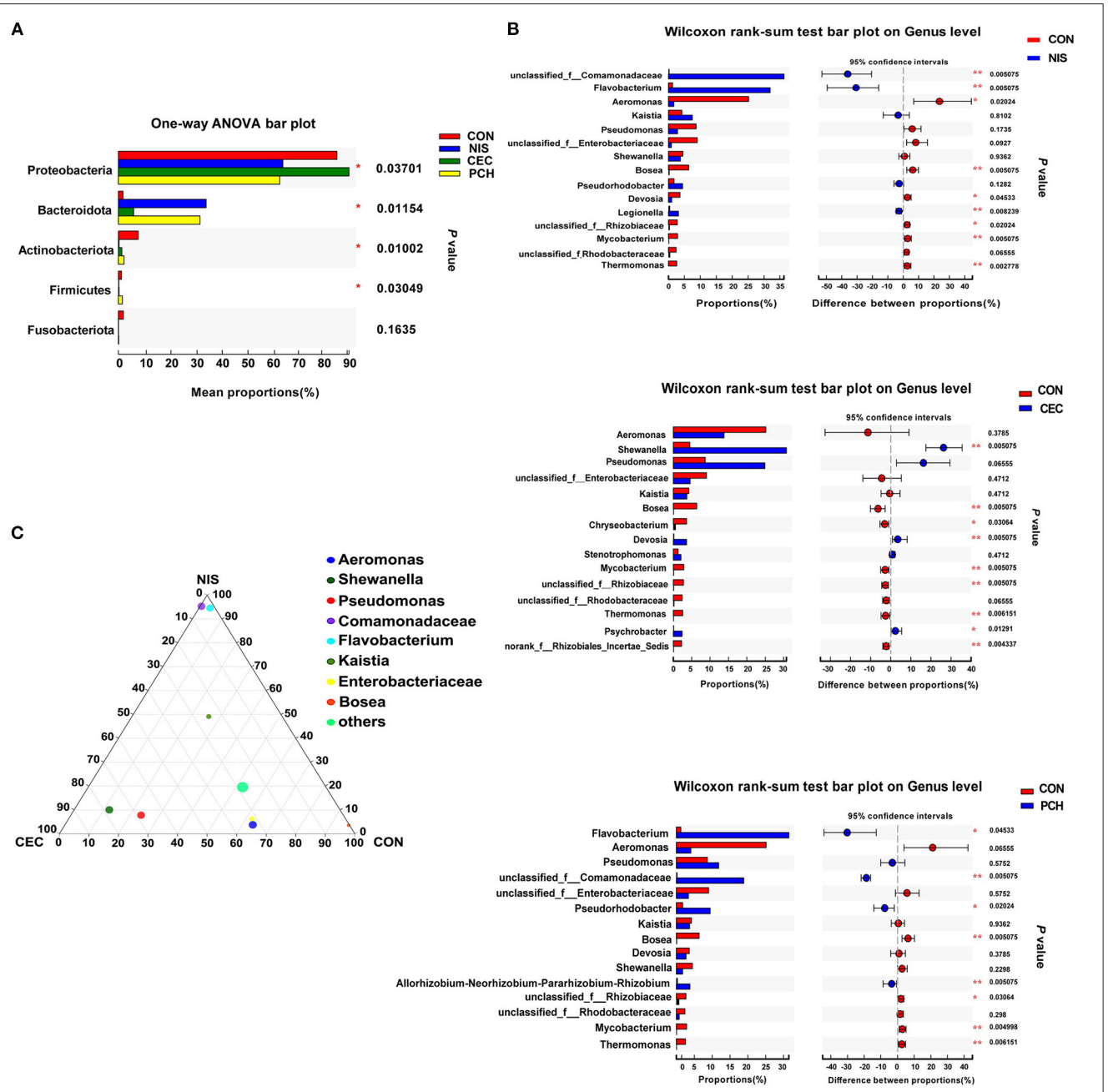

FIGURE 5 | Analysis of the differences in specific microbial taxa among the four groups. **(A)** The differences of microbial composition across the four groups at the phylum level. One-way ANOVA with a *post hoc* Tukey-kramer test was used for statistical analysis to determine significant difference among the four groups; **(B)** Wilcoxon rank-sum analysis of the differences between the control (CON) and the three experimental groups at the genus level. Data are presented as mean ± SD ($n = 6$). $p < 0.05$ was considered statistically significant (*$p < 0.05$, **$p < 0.01$). **(C)** Ternary plot analysis of differences in the main genera in CON, nisin (NIS), and cecropin (CEC) groups. Dot size indicates the relative abundance of the genera.

significantly decreased and increased, respectively, compared with that of the CON group.

DISCUSSION

Application of immunostimulants, including prebiotics (oligosaccharides, polysaccharides, and nutrients), probiotics, herbs, and AMPs as feed additives is occurring frequently in aquaculture (2). Studies have reported that supplementation with probiotics and prebiotics, herbs, and AMPs, individually or together (synbiotics) in the diet, could have beneficial effects on survival, growth, gut microbiota, immunity, and disease control in farmed fishes (32). However, in some cases, no significant differences in the growth or survival indices of

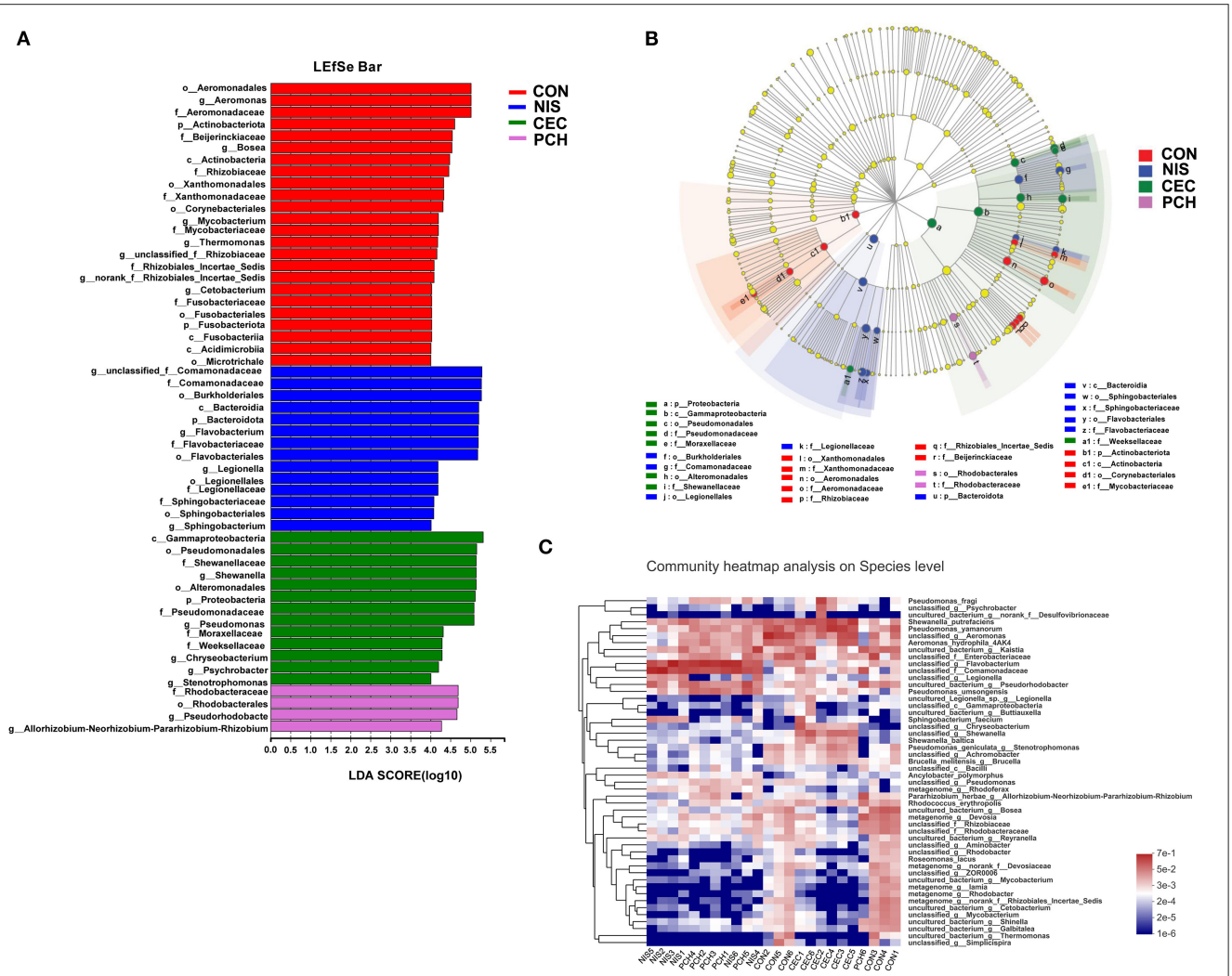

FIGURE 6 | LEfSe analysis of intestinal microbiota communities of the four groups. **(A)** Linear discriminant analysis (LDA) score in the four groups. Histogram showing differentially abundant taxa (LDA score > 4) in the gut microbiota of the four groups. The length of the column is proportional to the taxa abundance. **(B)** LDA effect size (LEfSe) analysis in the four groups. p, phylum; c, class; o, order; f, family; g, genus. **(C)** Heatmap of gut bacteria species from the four groups. The bacterial phylogenetic tree (shown on the left of the figure) was generated using the neighbor-joining method. The relative abundance values of bacterial species in different samples are depicted by color intensity, and the color legend corresponding to different values is to the right of the figure.

fish were detected at the end of the experimental trials, and overdoses of these substances may have negative effects on the performance of fishes (12, 33). The exact mechanisms of these dietary immunostimulants on fish health status are unknown. It has been speculated that prebiotics can affect immune parameters via the production of short-chain fatty acids (SCFAs) following gut microbial fermentation. SCFAs can regulate innate immune activities by binding to G protein-coupled receptors on immune cells (34). Herbs, which contain various bioactive compounds, have the ability to regulate many biological processes in fish, and some also demonstrate antimicrobial properties (18). Fish intestinal microbial communities are the main factors affecting the fermentability and functionality of the dietary immunostimulants. Therefore, it is critical to investigate the effects of immunostimulants on the intestinal microbial communities of specific fish species for their rational use in aquaculture.

AMPs that can perform immunomodulating functions, endotoxin neutralization, and induction of angiogenesis, are important components of the innate immune system of hosts and are widespread in nature (35). Various studies have investigated the effects of AMPs on growth, performance, antioxidant and immune responses, and disease resistance in poultry and livestock when used as feed additives, and many promising results have been obtained (36). It has been shown that the beneficial effects of AMPs on the growth performance of animals are mainly due to antimicrobial and immunomodulatory activities (37). A study by Ren et al. reported that dietary composite AMPs increased T-cell populations, stimulated the proliferation function of T cells, and decreased the percentage

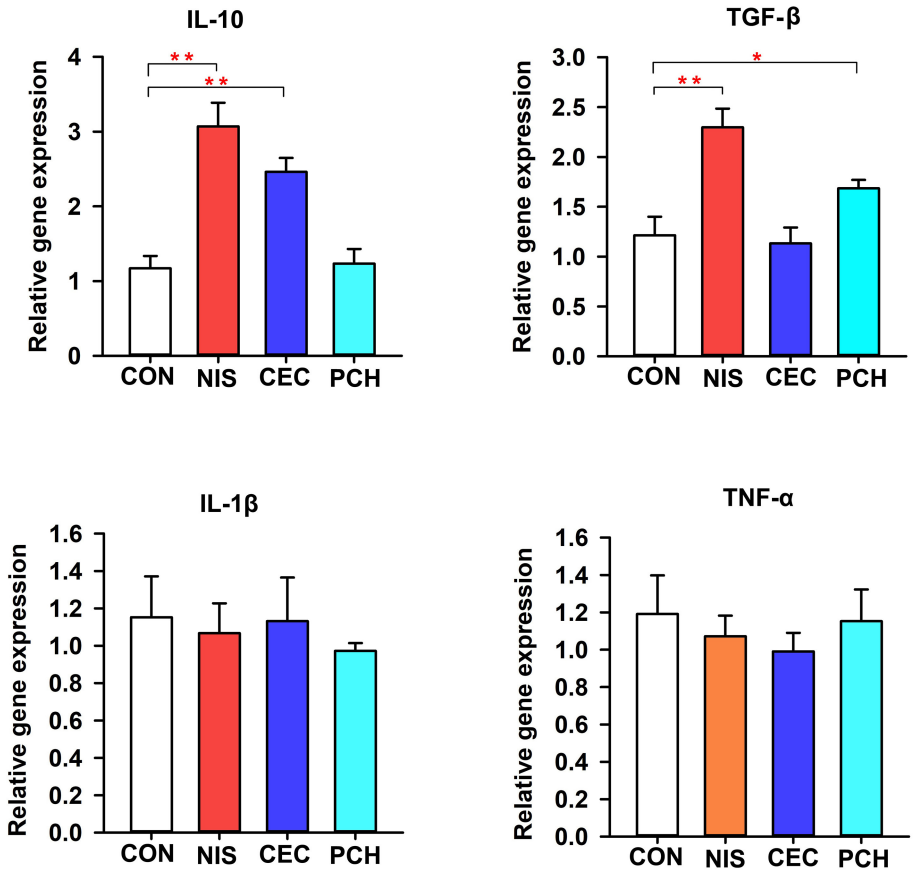

FIGURE 7 | Expression of immune-related genes in the intestine of the common carp in the four groups. The results were normalized against those of β-actin. Data are expressed as mean ± SD ($n = 6$). A significant difference compared with the control (CON) group is indicated by an asterisk. Statistical analysis was performed using one-way ANOVA with Dunnett's test (*$p < 0.05$, **$p < 0.01$).

of apoptotic spleen cells in weaning piglets (38). Shan et al. found that lactoferrin could improve the proliferation of spleen lymphocytes in the peripheral blood and effectively increased the concentration of serum antibodies and IL-2 levels in weaning piglets (39). AMPs generated from pig and rabbit systems can improve the intestinal mucosal immunity in broilers (40, 41). Dietary AMPs A3 and P5 enhance the total tract digestibility of weaning piglets and broilers toward crude protein and dry matter, and gross energy production (42). Wang et al. found that dietary AMP sublancin could increase villus height in the duodenum, as well as induce a higher villus-height-to-crypt-depth ratio in the jejunum of broilers (43). AMPs as feed additives can also improve the health of host animals by regulating the intestinal microbial ecology, including suppressing the growth of harmful microorganisms such as *Clostridium* and promoting the growth of beneficial microorganisms such as *Lactobacillus* and *Bifidobacterium* (44).

Compared with results observed in poultry and livestock, the effects of AMPs in aquaculture are understudied and may be more complicated owing to their reduced stability in water and direct interaction with the gut microecology in stomachless fish. Liu et al. reported that feeding grass carp with compound

TABLE 2 | Comparative analysis of digestive enzyme activities of common carp in the four groups.

Items	CON	NIS	CEC	PCH
Amylase (U/mg)	0.42 ± 0.07	0.36 ± 0.11	0.38 ± 0.11	0.43 ± 0.08
Protease (U/mg)	14.72 ± 1.96	31.09 ± 2.27[a]	22.99 ± 3.93[a]	15.02 ± 1.93
Lipase (U/mg)	25.51 ± 2.17	27.90 ± 4.44	20.66 ± 1.36[a]	32.26 ± 5.09[a]

[a] *Indicates significant differences compared with the CON group. Statistical analysis was performed using one-way ANOVA with Dunnett's test. ($n = 6$ fish for each group; $p < 0.05$).*

AMP-containing diets improved growth performance, as well as antioxidant and digestive capabilities, enhanced the expression of immune-related genes, and increased resistance to *Aeromonas hydrophila* challenge (12). Li et al. also claimed that AMPs supplemented into the diet can promote growth performance, improve oxidation resistance and immunity, increase digestive enzyme activity, and improve the intestinal morphology of juvenile largemouth bass (*Micropterus salmoides*) (24). AMP has been found to reduce serum triglyceride levels, improve immunity, and enrich the oxidation resistance of common

carp (45). Recently, Dai et al. reported that cecropin AD could improve intestinal immunity and enhance the disease resistance of juvenile turbot (*Scophthalmus maximus* L.) (46). Thus, these studies clearly demonstrate that AMPs have great application potential in aquaculture. A large variety of microbes with roles in nutrition, metabolism, and immunity can colonize the fish intestine. However, little is known about the effects of AMPs as feed additives on the gut microbiome of fish. Systematically addressing this issue may be helpful in revealing underlying mechanisms of the beneficial effects of AMPs on fish growth performance.

This study investigated the effects of two agriculturally important AMPs (nisin and cecropin) on the gut microbiome of common carp. Our results suggest that both nisin and cecropin alter the composition of the gut microbiome of common carp; however, the changes caused by these two AMPs are distinct from one another. The PCoA plot and hierarchical clustering tree revealed that the nisin group clustered away from the cecropin and control groups, whereas the cecropin group was located close to the control group in the PCoA plot and was clustered in the same branch of the tree (**Figure 3**). We speculate that the different effects of these two AMPs on the microbial communities of common carp may be attributed to their different antimicrobial spectra and mechanisms of action.

Chinese herbs have been used as traditional medicines to treat human diseases for thousands of years in East Asia. Various functional components from herbs, including minerals, alkaloids, flavonoids, vitamins, fatty acids, polysaccharides, and proteins, have been shown to have immunostimulatory, antitumor, antiviral, and antibacterial activities (2). The application of herbs with immune-stimulating functions in aquaculture has recently drawn increased attention. Several studies have demonstrated that herbs can enhance phagocytosis in fish. The phagocytic activity of blood leukocytes in crucian carp was enhanced after feeding with Chinese herbs (*I. indigotica, R. officinale*, *L. japonica,* and *A. paniculata*) (2). A mixture of *Astragalus* and *Lonicera* extracts increased the respiratory burst and phagocytic activities of blood phagocytes and plasma lysozyme activity in Nile tilapia, and increased resistance to *A. hydrophila* infection (47). Both *Angelica sinensis* and *A. membranaceus* showed the ability to activate the immune systems of rainbow trout, catla carp, Mozambique tilapia, common carp, and large yellow croaker (2). Studies on the effects of herbs on the gut microbiota community in fish are relatively limited. In this study, the effects of *P. chinense* on the gut microbiota of common carp were investigated, and it was found that it significantly altered the composition of the microbial community. The *P. chinense* group partially overlapped with the nisin group in the PCoA plot and was located in the same branch of the hierarchical clustering tree (**Figure 3**). This result indicates that *P. chinense* has a similar effect on the gut microbiota community of common carp to that of nisin.

The predominant bacterial phyla in common carp detected in this study were Proteobacteria, Bacteroidetes, Actinobacteria, Firmicutes, and Fusobacteriota, consistent with the results of previous study (48). After consuming nisin- and *P. chinense*-containing feed, the abundance of *Flavobacterium* was significantly increased in the gut microbiota community of common carp. *Flavobacterium* is widespread in soil and freshwater, and several species of this genus are known to cause diseases in freshwater fishes (49). The relative abundance of *Shewanella* was significantly increased in the cecropin group, compared with that of the control group. *Shewanella* is an opportunistic pathogen in fish and can damage the intestinal immune system of its host (50). The relative abundance of *Aeromonas* was reduced in the three experimental groups compared to that in the control group. Most of the 14 described species in *Aeromonas* genera have been associated with diseases, including bacterial enteritis, septicemia, and furunculosis (51). Based on these results, we conclude that nisin, cecropin, and *P. chinense* can alter the abundance of some pathogens, including opportunistic pathogens, in the gut microbial community of common carp.

In this study, the effects of nisin, cecropin, and *P. chinense* on the expression levels of four cytokine genes (TNF-α, IL-1β, IL10, and TGF-β) were also determined. Cytokines are key mediators of many biological processes, including tissue repair, blood cell production, cell growth, immune response, and inflammation (52). TNFα and IL-1β are typical proinflammatory cytokines, whereas TGFβ and IL10 are two anti-inflammatory cytokines. After consuming the nisin-, cecropin-, and *P. chinense*-containing feeds, the expression levels of IL-10 and TGF-β were significantly increased, which may indicate that these three substances have anti-inflammatory effects in the gut of common carp. Cecropin and *P. chinense* significantly increased the expression levels of IL-10 and TGF-β, respectively, whereas nisin upregulated the expression of both cytokines simultaneously. Similar effects of dietary AMPs and herbs on fish health have been reported by other research groups. For example, dietary turmeric has antistress, antioxidant, and anti-inflammatory effects in common carp (26). Dietary *Ginkgo biloba* extracts can upregulate the expression of antioxidant genes, immune-related genes, and anti-inflammatory cytokines IL-10 and TGF-β in hybrid grouper (53). Eucalyptol has also shown anti-inflammatory effects on common carp exposed to ambient copper (54). Expression levels of IL-10 and TGF-β are significantly upregulated in grass carp challenged with *A. hydrophila* after feeding diets supplemented with compound AMPs (12). However, in some cases, contradictory results are reported. For example, when supplemented as feed additive, *Rehmannia glutinosa* upregulates the expression of IL-1β, TNF-α, and iNOS, and downregulates the expression of IL-10 and TGF-β (25). Similarly, when guava leaves were added to the diet of *Labeo rohita*, expression levels of IL-1β and TNF-α were significantly increased, whereas levels of IL-10 and TGF-β were significantly decreased (55). These contradictory effects of immunostimulants on the expression levels of cytokines in fishes may have many causes. It has been shown that both AMPs and herbs are effectors of innate and adaptive immunity, capable of modulating pro- and anti-inflammatory responses, and that they also have chemotactic activity (9, 18). AMPs and herbs with different bioactive compounds may have different targets and mechanisms to regulate inflammatory responses. AMPs and herbs may also indirectly affect the inflammatory responses in the gut of fishes by altering the gut microbiota composition, which

is known to affect gut mucosal immunity. Our study supports the assertion that different AMPs and herbs have different effects on the gut microbial community of fishes. Additionally, the supplied concentration and experimental conditions may also affect the function of immunostimulants in inflammatory responses in fishes.

Although dietary supplementation of nisin, cecropin, and *P. chinense* did not produce any significant improvement in growth performance in this study, all three demonstrated the ability to alter specific digestive enzyme activities, which may mean that supplementation of these substances in feed can affect the digestive ability of common carp. Other studies with similar results have been reported. When supplemented at a concentration of 3 g/kg in the diet, aqueous extract of spade flower (*Hybanthus enneaspermus*) significantly improves the activities of amylase, lipase, and protease in rohu (56). Some digestive enzyme activities in the stomach and intestine of Japanese seabass were found to be significantly increased when dietary supplementation of a Chinese herbal medicine mixture was added (57). AMPs as feed additives may increase protease and lipase activity, as well as reduce the amylase activity in largemouth bass at specific concentrations (24). Notably, most of these studies describe only the effects of immunostimulants on the digestive enzyme activities, without underlying mechanism analysis. We speculate that immunostimulants as feed additives may affect digestive enzyme activity directly by regulating the corresponding gene expression or indirectly by altering the gut microbiota composition, which plays important roles in host nutrition. However, understanding the molecular mechanisms underlying the effects of supplemented immunostimulants on digestive enzyme activities requires future experiments to be conducted.

In summary, our current results suggest that nisin, cecropin, and *P. chinense*, when supplemented as feed additives, affect the diversity, abundance, and even the structure of the gut microbial community in common carp. Additionally, these three additives also show anti-inflammatory effects, and enhance specific digestive enzyme activity in the gut of common carp. For large-scale use of AMPs and Chinese herbs in aquaculture, further investigations into *in vitro* and *in vivo* toxicological tests, digestibility by fishes, and stability in the aquatic environment should be conducted. Additionally, considering that a given AMP or herb commonly shows various effects on different fish species, identifying the most effective substances for use in a specific fish species is also important.

DATA AVAILABILITY STATEMENT

The datasets presented in this study can be found in online repositories. The names of the repository/repositories and accession number(s) can be found in the article/**Supplementary Material**.

ETHICS STATEMENT

The animal study was reviewed and approved by Southwest Medical University Ethics Committee.

AUTHOR CONTRIBUTIONS

Experiments were conceived and designed by XG and performed by FK, PX, YY, LY, AG, JY, and JZ. Data were analyzed by XG. The initial draft of the manuscript was written by XG and critically revised by LL and QW. All authors have read and approved the final manuscript.

FUNDING

This work was supported by the China Postdoctoral Science Foundation (2020M683364), the Department of Science and Technology of Sichuan Province (2020YJ0129), the Collaborative Fund of Science and Technology Agency of Luzhou Government and Southwest Medical University (20YKDYYJC0030), and the Science Fund Project of Southwest Medical University (2019ZQN024 and 2020ZRQNA007).

ACKNOWLEDGMENTS

We would like to thank Editage (www.editage.cn) for English language editing.

SUPPLEMENTARY MATERIAL

The Supplementary Material for this article can be found online at: https://www.frontiersin.org/articles/10.3389/fnut.2021.729437/full#supplementary-material

REFERENCES

1. Hoseinifar SH, Hosseini M, Paknejad H, Safari R, Jafar A, Yousefi M, et al. Enhanced mucosal immune responses, immune related genes and growth performance in common carp (*Cyprinus carpio*) juveniles fed dietary *Pediococcus acidilactici* MA18/5M and raffinose. *Dev Comp Immunol*. (2019) 94:59–65. doi: 10.1016/j.dci.2019.01.009
2. Wang W, Sun J, Liu C, Xue Z. Application of immunostimulants in aquaculture: current knowledge and future perspectives. *Aquac Res*. (2017) 48:1–23. doi: 10.1111/are.13161
3. Hoseini SM, Yousefi M. Beneficial effects of thyme (*Thymus vulgaris*) extract on oxytetracycline-induced stress response, immunosuppression, oxidative stress and enzymatic changes in rainbow trout (*Oncorhynchus mykiss*). *Aquacult Nutr*. (2019) 25:298–309. doi: 10.1111/anu.12853
4. Yonar ME. The effect of lycopene on oxytetracycline-induced oxidative stress and immunosuppression in rainbow trout (*Oncorhynchus mykiss* W.). *Fish Shellfish Immunol*. (2012) 32:994–1001. doi: 10.1016/j.fsi.2012.02.012
5. Omoregie E, Oyebanji SM. Oxytetracycline-induced blood disorder in juvenile nile tilapia *Oreochromis niloticus* (Trewavas). *J World Aquacult Soc*. (2002) 33:377–82. doi: 10.1111/j.1749-7345.2002.tb00514.x
6. Choi WM, Mo WY, Wu SC, Mak NK, Bian ZX, Nie XP, et al. Effects of traditional Chinese medicines (TCM) on the immune response of grass carp (*Ctenopharyngodon idellus*). *Aquacult Int*. (2014) 22:361–77. doi: 10.1007/s10499-013-9644-7

7. Robinson TP, Bu DP, Carrique-Mas J, Fèvre EM, Gilbert M, Grace D, et al. Antibiotic resistance is the quintessential One Health issue. *Trans R Soc Trop Med Hyg*. (2016) 110:377–80. doi: 10.1093/trstmh/trw048
8. Casewell M, Friis C, Marco E, McMullin P, Phillips I. The European ban on growth-promoting antibiotics and emerging consequences for human and animal health. *J Antimicrob Chemother*. (2003) 52:159–61. doi: 10.1093/jac/dkg313
9. Wu L, Li F, Ran L, Gao Y, Xie P, Yang J, et al. Insight into the effects of nisin and cecropin on the oral microbial community of rats by high-throughput sequencing. *Front Microbiol*. (2020) 11:1082. doi: 10.3389/fmicb.2020.01082
10. Yi HY, Chowdhury M, Huang YD, Yu XQ. Insect antimicrobial peptides and their applications. *Appl Microbiol Biotechnol*. (2014) 98:5807–22. doi: 10.1007/s00253-014-5792-6
11. Paria A, Vinay T, Gupta SK, Choudhury TG, Sarkar B. Antimicrobial peptides: a promising future alternative to antibiotics in aquaculture. *World Aquacult*. (2018) 48:67–9. doi: 10.1159/000331009
12. Liu S, Wang J, Feng Y, Ye Q, Wen L, Xu G, et al. Effects of compound antimicrobial peptides on the growth performance, antioxidant and immune responses and disease resistance of grass carp (*Ctenopharyngodon idellus*). *Fish Shellfish Immunol*. (2020) 107:163–70. doi: 10.1016/j.fsi.2020.09.042
13. Ke F, Gao Y, Liu L, Zhang C, Wang Q, Gao X. Comparative analysis of the gut microbiota of grass carp fed with chicken faeces. *Environ Sci Pollut Res Int*. (2020) 27:32888–98. doi: 10.1007/s11356-020-09012-8
14. Józefiak D, Kierończyk B, Juśkiewicz J, Zduńczyk Z, Rawski M, Długosz J, et al. Dietary nisin modulates the gastrointestinal microbial ecology and enhances growth performance of the broiler chickens. *PLoS ONE. (*2013) 8:e85347. doi: 10.1371/journal.pone.0085347
15. Brady D, Grapputo A, Romoli O, Sandrelli F. Insect cecropins, antimicrobial peptides with potential therapeutic applications. *Int J Mol Sci*. (2019) 20:5862. doi: 10.3390/ijms20235862
16. Wen LF, He JG. Dose–response effects of an antimicrobial peptide, a cecropin hybrid, on growth performance, nutrient utilization, bacterial counts in the digesta and intestinal morphology in broilers. *Br J Nutr*. (2012) 108:1756–63. doi: 10.1017/S0007114511007240
17. Wu S, Zhang F, Huang Z, Liu H, Xie C, Zhang J, et al. Effects of the antimicrobial peptide cecropin AD on performance and intestinal health in weaned piglets challenged with *Escherichia coli*. *Peptides*. (2012) 35:225–30. doi: 10.1016/j.peptides.2012.03.030
18. Van Hai N. The use of medicinal plants as immunostimulants in aquaculture: a review. *Aquaculture*. (2015) 446:88–96. doi: 10.1016/j.aquaculture.2015.03.014
19. Reverter M, Bontemps N, Lecchini D, Banaigs B, Sasal P. Use of plant extracts in fish aquaculture as an alternative to chemotherapy: current status and future perspectives. *Aquaculture*. (2014) 433:50–61. doi: 10.1016/j.aquaculture.2014.05.048
20. Wang A, Li M, Huang H, Xiao Z, Shen J, Zhao Y, et al. A review of *Penthorum chinense* Pursh for hepatoprotection: traditional use, phytochemistry, pharmacology, toxicology and clinical trials. *J Ethnopharmacol*. (2020) 251:112569. doi: 10.1016/j.jep.2020.112569
21. Ding B, Ding Q, Zhang S, Jin Z, Wang Z, Li S, et al. Characterization of the anti-*Staphylococcus aureus* fraction from *Penthorum chinense* Pursh stems. *BMC Complement Altern Med*. (2019) 19:219. doi: 10.1186/s12906-019-2632-3
22. Yin J, Ren W, Wei B, Huang H, Li M, Wu X, et al. Characterization of chemical composition and prebiotic effect of a dietary medicinal plant *Penthorum chinense* Pursh. *Food Chem*. (2020) 319:126568. doi: 10.1016/j.foodchem.2020.126568
23. FAO. *The State of World Fisheries and Aquaculture 2020* (2020).
24. Li S, Chi S, Cheng X, Wu C, Xu Q, Qu P, et al. Effects of antimicrobial peptides on the growth performance, antioxidant and intestinal function in juvenile largemouth bass, *Micropterus salmoides*. *Aquacult Rep*. (2020) 16:100252. doi: 10.1016/j.aqrep.2019.100252
25. Wang J-L, Meng X-l, Lu R-h, Wu C, Luo Y-T, Yan X, et al. Effects of *Rehmannia glutinosa* on growth performance, immunological parameters and disease resistance to *Aeromonas hydrophila* in common carp (*Cyprinus carpio* L.). *Aquaculture*. (2015) 435:293–300. doi: 10.1016/j.aquaculture.2014.10.004
26. Rajabiesterabadi H, Hoseini SM, Fazelan Z, Hoseinifar SH, Doan HV. Effects of dietary turmeric administration on stress, immune, antioxidant and inflammatory responses of common carp (*Cyprinus carpio*) during copper exposure. *Aquacult Nutr*. (2020) 26:1143–53. doi: 10.1111/anu.13071
27. Bilen S, Filogh AM, Ali AB, Kenanoglu ON, Zoral MA. Effect of common mallow (*Malva sylvestris*) dietary supplementation on growth performance, digestive enzyme activities, haemotological and immune responses of common carp (*Cyprinus carpio*). *Aquacult Int*. (2020) 28:73–84. doi: 10.1007/s10499-019-00444-9
28. Hoseini SM, Mirghaed AT, Iri Y, Hoseinifar SH, Van Doan H, Reverter M. Effects of dietary Russian olive, *Elaeagnus angustifolia*, leaf extract on growth, hematological, immunological, and antioxidant parameters in common carp, *Cyprinus carpio*. *Aquaculture*. (2021) 536:736461. doi: 10.1016/j.aquaculture.2021.736461
29. Abdel-Latif HM, Abdel-Tawwab M, Khafaga AF, Dawood MA. Dietary oregano essential oil improved the growth performance via enhancing the intestinal morphometry and hepato-renal functions of common carp (*Cyprinus carpio* L.) fingerlings. *Aquaculture*. (2020) 526:735432. doi: 10.1016/j.aquaculture.2020.735432
30. Paray BA, Hoseini SM, Hoseinifar SH, Van Doan H. Effects of dietary oak (*Quercus castaneifolia*) leaf extract on growth, antioxidant, and immune characteristics and responses to crowding stress in common carp (*Cyprinus carpio*). *Aquaculture*. (2020) 524:735276. doi: 10.1016/j.aquaculture.2020.735276
31. Yuan JS, Reed A, Chen F, Stewart CN. Statistical analysis of real-time PCR data. *BMC Bioinformatics*. (2006) 7:85. doi: 10.1186/1471-2105-7-85
32. Hoseinifar SH, Van Doan H, Dadar M, Ringø E, Harikrishnan R. Feed additives, gut microbiota, and health in finfish aquaculture. In: Microbial Communities in Aquaculture Ecosystems. Springer (2019). p. 121–42. doi: 10.1007/978-3-030-16190-3_6
33. González-Félix ML, Gatlin DM, Urquidez-Bejarano P, de la Reé-Rodríguez C, Duarte-Rodríguez L, Sánchez F, et al. Effects of commercial dietary prebiotic and probiotic supplements on growth, innate immune responses, and intestinal microbiota and histology of *Totoaba macdonaldi*. *Aquaculture*. (2018) 491:239–51. doi: 10.1016/j.aquaculture.2018.03.031
34. Maslowski KM, Mackay CR. Diet, gut microbiota and immune responses. *Nat Immunol*. (2011) 12:5–9. doi: 10.1038/ni0111-5
35. Maróti G, Kereszt A, Kondorosi E, Mergaert P. Natural roles of antimicrobial peptides in microbes, plants and animals. *Res Microbiol*. (2011) 162:363–74. doi: 10.1016/j.resmic.2011.02.005
36. Wang J, Dou X, Song J, Lyu Y, Zhu X, Xu L, et al. Antimicrobial peptides: promising alternatives in the post feeding antibiotic era. *Med Res Rev*. (2019) 39:831–59. doi: 10.1002/med.21542
37. Mansour SC, Pena OM, Hancock RE. Host defense peptides: front-line immunomodulators. *Trends Immunol*. (2014) 35:443–50. doi: 10.1016/j.it.2014.07.004
38. Ren ZH, Yuan W, Deng HD, Deng JL, Dan QX, Jin HT, et al. Effects of antibacterial peptide on cellular immunity in weaned piglets. *J Anim Sci*. (2015) 93:127–34. doi: 10.2527/jas.2014-7933
39. Shan T, Wang Y, Wang Y, Liu J, Xu Z. Effect of dietary lactoferrin on the immune functions and serum iron level of weanling piglets. *J Anim Sci*. (2007) 85:2140–46. doi: 10.2527/jas.2006-754
40. Liu T, She R, Wang K, Bao H, Zhang Y, Luo D, et al. Effects of rabbit *Sacculus rotundus* antimicrobial peptides on the intestinal mucosal immunity in chickens. *Poult Sci*. (2008) 87:250–54. doi: 10.3382/ps.2007-00353
41. Bao H, She R, Liu T, Zhang Y, Peng KS, Luo D, et al. Effects of pig antibacterial peptides on growth performance and intestine mucosal immune of broiler chickens. *Poult Sci*. (2009) 88:291–97. doi: 10.3382/ps.2008-00330
42. Yoon JH, Ingale SL, Kim JS, Kim KH, Lee SH, Park YK, et al. Effects of dietary supplementation of antimicrobial peptide-A3 on growth performance, nutrient digestibility, intestinal and fecal microflora and intestinal morphology in weanling pigs. *Anim Feed Sci Technol*. (2012) 177:98–107. doi: 10.1016/j.anifeedsci.2012.06.009
43. Wang S, Zeng XF, Wang QW, Zhu JL, Peng Q, Hou CL, et al. The antimicrobial peptide sublancin ameliorates necrotic enteritis induced by *Clostridium perfringens* in broilers. *J Anim Sci*. (2015) 93:4750–60. doi: 10.2527/jas.2015-9284

44. Wang S, Zeng X, Yang Q, Qiao S. Antimicrobial peptides as potential alternatives to antibiotics in food animal industry. *Int J Mol Sci*. (2016) 17:603. doi: 10.3390/ijms17050603
45. Dong XQ, Zhang DM, Chen YK, Wang QJ, Yang YY. Effects of antimicrobial peptides (AMPs) on blood biochemical parameters, antioxidase activity, and immune function in the common carp (*Cyprinus carpio*). *Fish Shellfish Immunol*. (2015) 47:429–34. doi: 10.1016/j.fsi.2015.09.030
46. Dai J, Zheng J, Ou W, Xu W, Ai Q, Zhang W, et al. The effect of dietary cecropin AD on intestinal health, immune response and disease resistance of juvenile turbot (*Scophthalmus maximus* L.). *Fish Shellfish Immunol*. (2020) 100:117–25. doi: 10.1016/j.fsi.2020.02.052
47. Ardó L, Yin G, Xu P, Váradi L, Szigeti G, Jeney Z, et al. Chinese herbs (*Astragalus membranaceus* and *Lonicera japonica*) and boron enhance the non-specific immune response of Nile tilapia (*Oreochromis niloticus*) and resistance against *Aeromonas hydrophila*. *Aquaculture*. (2008) 275:26–33. doi: 10.1016/j.aquaculture.2007.12.022
48. Zhang Y, Zhang P, Shang X, Lu Y, Li Y. Exposure of lead on intestinal structural integrity and the diversity of gut microbiota of common carp. *Comp Biochem Physiol C Toxicol Pharmacol*. (2021) 239:108877. doi: 10.1016/j.cbpc.2020.108877
49. Stenholm AR, Dalsgaard I, Middelboe M. Isolation and characterization of bacteriophages infecting the fish pathogen *Flavobacterium psychrophilum*. *Appl Environ Microbiol*. (2008) 74:4070–78. doi: 10.1128/AEM.00428-08
50. Xiong J, Wang K, Wu J, Qiuqian L, Yang K, Qian Y, et al. Changes in intestinal bacterial communities are closely associated with shrimp disease severity. *Appl Microbiol Biotechnol*. (2015) 99:6911–19. doi: 10.1007/s00253-015-6632-z
51. Wu S, Wang G, Angert ER, Wang W, Li W, Zou H. Composition, diversity, and origin of the bacterial community in grass carp intestine. *PLoS ONE*. (2012) 7:e30440. doi: 10.1371/journal.pone.0030440
52. Hassan FI, Didari T, Khan F, Niaz K, Mojtahedzadeh M, Abdollahi M. A review on the protective effects of metformin in sepsis-induced organ failure. *Cell J*. (2020) 21:363. doi: 10.22074/cellj.2020.6286
53. Tan X, Sun Z, Chen S, Chen S, Huang Z, Zhou C, et al. Effects of dietary dandelion extracts on growth performance, body composition, plasma biochemical parameters, immune responses and disease resistance of juvenile golden pompano *Trachinotus ovatus*. *Fish Shellfish Immunol*. (2017) 66:198–206. doi: 10.1016/j.fsi.2017.05.028
54. Fazelan Z, Hoseini SM, Yousefi M, Khalili M, Hoseinifar SH, Van Doan H. Effects of dietary eucalyptol administration on antioxidant and inflammatory genes in common carp (*Cyprinus carpio*) exposed to ambient copper. *Aquaculture*. (2020) 520:734988. doi: 10.1016/j.aquaculture.2020.734988
55. Giri SS, Sen SS, Chi C, Kim HJ, Yun S, Park SC, et al. Effect of guava leaves on the growth performance and cytokine gene expression of *Labeo rohita* and its susceptibility to *Aeromonas hydrophila* infection. *Fish Shellfish Immunol*. (2015) 46:217–24. doi: 10.1016/j.fsi.2015.05.051
56. Giri SS, Jun JW, Sukumaran V, Park SC. Evaluation of dietary *Hybanthus enneaspermus* (Linn F. Muell.) as a growth and haemato-immunological modulator in *Labeo rohita*. *Fish Shellfish Immunol*. (2017) 68:310–7. doi: 10.1016/j.fsi.2017.07.009
57. Wang CY, Li ZB, Sun YZ, Chen Q, Li WJ, Huang YC, et al. Effects of Chinese herbal medicines mixture on growth performance digestive enzyme activity immune response of juvenile Japanese seabass, *Lateolabrax japonicus*. *Aquacult Nutr*. (2018) 24:683–93. doi: 10.1111/anu.12597

Conflict of Interest: The authors declare that the research was conducted in the absence of any commercial or financial relationships that could be construed as a potential conflict of interest.

frontiers in Nutrition

ORIGINAL RESEARCH
published: 04 November 2021
doi: 10.3389/fnut.2021.765414

The Association of Altered Gut Microbiota and Intestinal Mucosal Barrier Integrity in Mice With Heroin Dependence

Jiqing Yang[1,2,3,4], Pu Xiong[4,5], Ling Bai[3], Zunyue Zhang[4,5], Yong Zhou[4,5], Cheng Chen[4,5], Zhenrong Xie[4,5], Yu Xu[4,6], Minghui Chen[1,3], Huawei Wang[4], Mei Zhu[4,5], Juehua Yu[4,5] and Kunhua Wang[1,4,7]**

[1] Faculty of Life Science and Technology, Kunming University of Science and Technology, Kunming, China, [2] Department of Clinical Laboratory, The First Affiliated Hospital of Kunming Medical University, Kunming, China, [3] Medical School, Kunming University of Science and Technology, Kunming, China, [4] National Health Commission (NHC) Key Laboratory of Drug Addiction Medicine, First Affiliated Hospital of Kunming Medical University, Kunming, China, [5] Centre for Experimental Studies and Research, First Affiliated Hospital of Kunming Medical University, Kunming, China, [6] Department of Gastrointestinal Surgery, The First Affiliated Hospital of Kunming Medical University, Kunming, China, [7] Department of Administrative Affairs, Yunnan University, Kunming, China

OPEN ACCESS

Edited by:
Fengjiao Xin,
Institute of Food Science and Technology, Chinese Academy of Agricultural Science, China

Reviewed by:
Xiaoyu Hu,
Jilin University, China
Weiwei Ma,
Capital Medical University, China

***Correspondence:**
Juehua Yu
juehuayu@gmail.com
Kunhua Wang
wangkunhua1@163.com

Specialty section:
This article was submitted to Nutrition and Microbes, a section of the journal Frontiers in Nutrition

Received: 27 August 2021
Accepted: 30 September 2021
Published: 04 November 2021

Citation:
Yang J, Xiong P, Bai L, Zhang Z, Zhou Y, Chen C, Xie Z, Xu Y, Chen M, Wang H, Zhu M, Yu J and Wang K (2021) The Association of Altered Gut Microbiota and Intestinal Mucosal Barrier Integrity in Mice With Heroin Dependence. Front. Nutr. 8:765414. doi: 10.3389/fnut.2021.765414

The gut microbiota is believed to play a significant role in psychological and gastrointestinal symptoms in heroin addicts. However, the underlying mechanism remains largely unknown. We show here that heroin addicts had a decrease in body mass index (BMI) and abnormal serum D-lactic acid (DLA), endotoxin (ET) and diamine oxidase (DAO) levels during their withdrawal stage, suggesting a potential intestinal injury. The gut microbial profiles in the mouse model with heroin dependence showed slightly decreased alpha diversity, as well as higher levels of *Bifidobacterium* and *Sutterella* and a decrease in *Akkermansia* at genus level compared to the control group. Fecal microbiota transplantation (FMT) further confirmed that the microbiota altered by heroin dependence was sufficient to impair body weight and intestinal mucosal barrier integrity in recipient mice. Moreover, short-chain fatty acids (SCFAs) profiling revealed that microbiota-derived propionic acid significantly decreased in heroin dependent mice compared to controls. Overall, our study shows that heroin dependence significantly altered gut microbiota and impaired intestinal mucosal barrier integrity in mice, highlighting the role of the gut microbiota in substance use disorders and the pathophysiology of withdrawal symptoms.

Keywords: heroin dependence, gut microbiota, intestinal mucosal barrier integrity, SCFAs, mice

INTRODUCTION

As a chronic and relapsing brain disease (1, 2), heroin addiction is usually characterized by sensitization, dependence, and compulsive drug use (3, 4). Beyond neuropsychiatric disorders, our previous studies showed that heroin abuse is often associated with decreased appetite, constipation, nutritional and gastrointestinal symptoms that can lead to low abstinence rate and malnutrition or nutritional risks during the withdrawal period (5–7). More seriously, drug-induced intestinal barrier lesions and severe enterogenic infections or related death were observed in Rhesus monkeys (5) and methamphetamine treated mice (8). Notably, lower zona occludens-1 (ZO-1) immune positivity was observed in heroin abusers compared to healthy controls (9), indicating

that heroin affects the molecular integrity of tight junction (TJ) proteins, which correlates with gastrointestinal symptoms.

Although the mechanism of the gut microbiota in disease is not fully understood, the gut microbiota is a critical component of the brain-gut axis (10) potentially impacting behavior and mood (11), key modulators of host immunity (12), metabolic (13) and other diseases (14, 15). The role of gut dysbiosis is considered an essential factor in the development of drug addiction (10, 16). Furthermore, gastrointestinal disorders may be accompanied by gut microbiota dysbiosis (17). However, the association between gut microbiota and intestinal mucosa barrier function in the context of substance use disorder remains largely unknown. Further investigation is urgently needed to uncover the roles of intestinal microbiota in gastrointestinal symptoms in heroin addicts.

In this study, we investigated the serum indicators of intestinal mucosal barrier damage in heroin addicts during withdrawal stage and generated a mouse model mimicking heroin dependence. High-throughput sequencing of 16s rRNA gene and bioinformatic analysis was performed to determine the variations in gut microbiota in heroin dependent mice compared with saline-treated mice. To confirm the altered microbiota contributing to the intestinal mucosal barrier integrity, donor stool from mice with heroin dependence were transplanted into recipient mice by fecal microbiota transplantation (FMT). To assess intestinal mucosal barrier integrity, the serum level of DAO, DLA, and ET, as well as protein expression levels of Claudin-1 and ZO-1 were evaluated, respectively. The concentrations of metabolic products SCFAs in mouse fecal samples were analyzed using gas chromatography–mass spectrometry (GC-MS).

We show that heroin dependence causes substantial changes in the composition of the gut microbiota contributes to pathological changes of intestinal mucosal barrier function. Furthermore, it offers a deep insight into the function of the gut microbiota in heroin dependence induced digestive diseases and a new paradigm for addiction treatment.

MATERIALS AND METHODS

Study Populations and Ethics Statement

Thirty-eight male heroin addicts (age ranging from 18 to 58) from the hospital of the Longchuan Drug Rehabilitation Center in Dehong, China were recruited as the heroin group; 38 age-matched males with no heroin-use history were recruited as healthy controls (HCs). The inclusion criteria were: (1) male sex and aged between 18 and 58, (2) diagnosed with heroin dependence, and (3) in withdrawal stage. Participants were excluded if (1) severe neurological disorders, (2) severe chronic illnesses, infections, (3) antibiotic treatments (<7 days prior to study start), (4) refuse or inability to give informed consent. All participants provided written informed consent prior to study participation. The participants' age, gender, body weight, and height were collected. 2 ml of blood was drawn from each participant to measure intestinal mucosal barrier damage indicator.

Abbreviations: BMI, body mass index; DLA, D-lactic acid; DAO, diamine oxidase; EPM, elevated plus-maze test; ET, endotoxin; FMT, fecal microbiota transplantation; FST, forced swimming test; GC-MS, gas chromatography–mass spectrometry; LEfSe, linear discriminant analysis effect size; LDA, linear discriminant analysis; OCL-1, occludin-1; OFT, open-field test; OTUs, operational taxonomic units; PCA, principal component analysis; PLS-DA, partial least-squares discrimination analysis; SCFAs, short chain fatty acids; TJ, tight junction; TST, tail suspension test; ZO-1, zona occludens-1.

Animals

Male C57BL/6 SPF mice (6–8-week-old, weighing 20–25 g) were obtained from the Kunming Medical University Center for Laboratory Animals, housed individually under controlled temperature ($22 \pm 2^{\circ}$C) and humidity ($50 \pm 5\%$), and maintained on a 12/12 h light/dark cycle (lights on at 7 a.m.). The mice had free access to tap water and a standard mouse chow diet. Animals were deeply anesthetized with pentobarbital sodium (40 mg/kg, i.p.) then sacrificed, colonic tissues were perfused with 0.1 M PBS (pH 7.4, 37°C) followed by 4% (w/v) paraformaldehyde in 0.1 M PBS, prepared at 20 μm thickness by using a cryostat microtome (Leica CM 3500, Wetzlar, Germany). All experiments were conducted in accordance with the National Institutes of Health Guide for the Care and Use of Laboratory Animals.

Drugs

The Narcotics Department of Yunnan Provincial Public Security Administration generously supplied the diacetylmorphine HCl (heroin), and the heroin was freshly dissolved in 0.9% sterile saline for intraperitoneal (10 mg/kg).

Experimental Design

In order to generation the mouse model with heroin dependence, mice were randomly separated into two groups after 1 week of adaptation: (1) control group (0.2 ml saline i.p. $n = 10$); (2) heroin group (10 mg/kg heroin i.p. $n = 10$). The experimental design is showing in **Figure 1A**. Mice were treated with 10 mg/kg of heroin or saline for 21 continuous days. After 48 h withdrawal (day 24), fecal were collected and behavioral tests were performed. Mouse weight was periodically monitored every fourth day during the heroin treated, thus we collected the body weight on day 0–4–8–2–16–20–24, respectively. The intestinal mucosal integrity was investigated and heroin dependent mice were sacrificed at days 21 (Heroin-addicted) group and at days 24 (Heroin-withdrawal) group (**Figure 2A**).

Behavioral Locomotor Sensitization

Heroin-induced behavioral sensitization, which indicated addiction behavior, was measured using an open field test (OFT) and the ANY-maze software (Stoelting Co.) (18). Mice were placed individually in the corner of an open-field box (45 ×45 ×30 cm) and allowed to explore for 1 h in the OFT apparatus after heroin/saline treatment. The tracked plot and total distance traveled were collected and analyzed using a video tracking system (ANY-maze, Stoelting Co.).

Fecal Microbiota Transplantation (FMT)

We performed FMT as described previously (19, 20): fecal pellets (collected on day 24) from different mice in the corresponding group were resuspended together in PBS (1 fecal pellet/ml) for

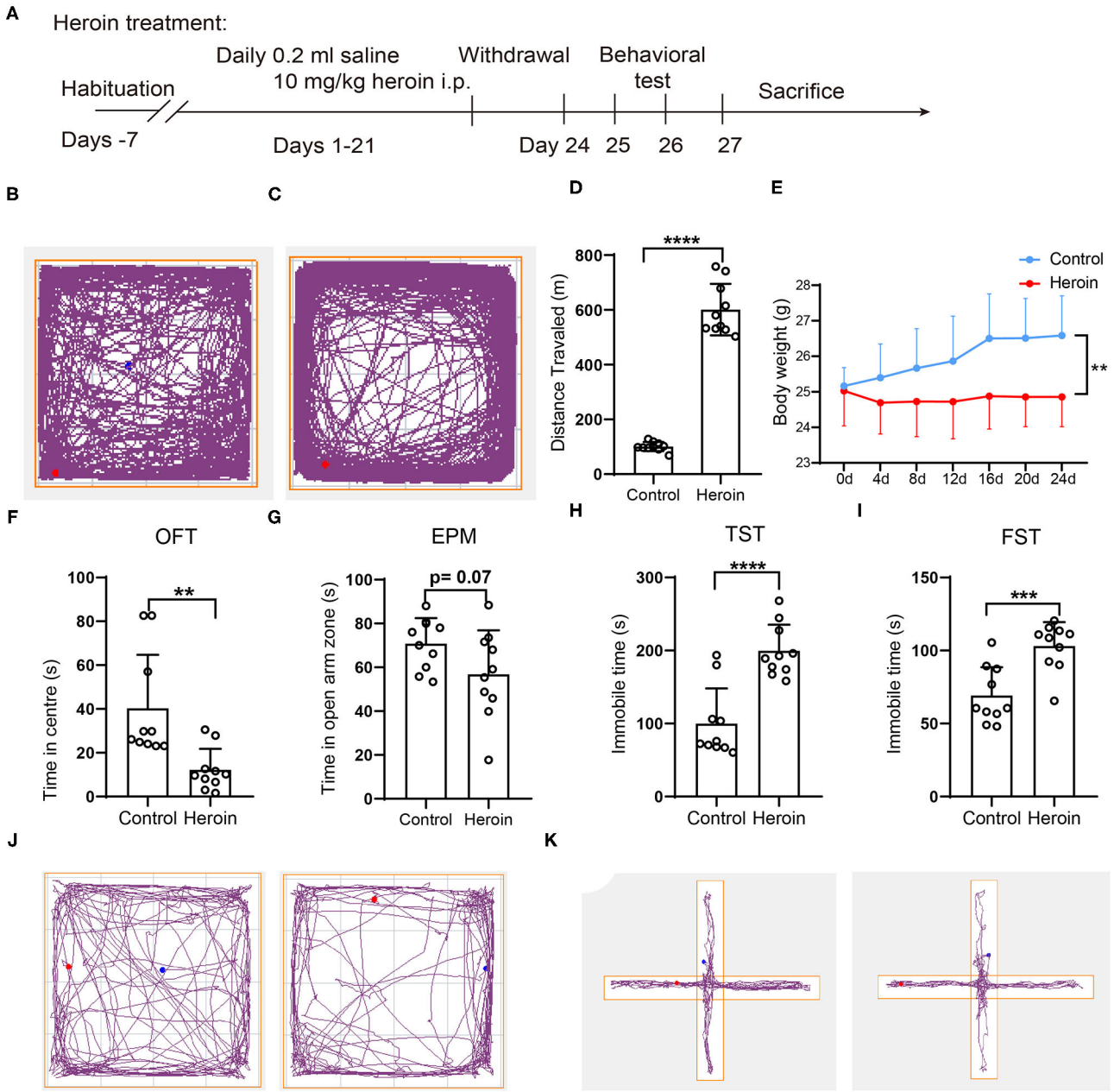

FIGURE 1 | Heroin-induced mouse behavior sensitization, neurobehavioral deficits, and body weight loss in C57/BL mice. **(A)** experimental design: C57/BL mice were administered an intraperitoneal (i.p.) injection of 10 mg/kg heroin for 21 days. After a 48-h withdrawal period, fresh fecal samples were collected for 16s rRNA sequencing, and cecal tissues were collected after sacrifice. **(B–D)** A 10 mg/kg heroin administration induced behavior sensitization. Track plots showing the position of the animal for 60-min tests where treatment with control **(B)** and heroin **(C)** (n =10); **(D)** Bar graphs show total distance traveled of the open field during the test. **(E)** Heroin- administrated mice showed reduced body weight compared to controls. **(F–K)** heroin-administrated mice exhibit anxiety and depression-like behavioral deficits: **(F)** time spent in the central area of the open field during the test; **(G)** time spent in open arms of the elevated plus maze; **(H)** Immobility time during the tail suspension test; **(I)** Immobility time in the forced swim test; **(J)**Track plots showing the position of the animal for 5-min tests in OFT where treatment with saline (left) and heroin (right); **(K)** Track plots showing the position of the animal for 5-min tests in EMP where treatment with saline (left) and heroin (right) (n = 10). The student's t-test was used to determine whether differences existed between the two groups, $^{**}p < 0.01$; $^{***}p < 0.001$; $^{****}p < 0.0001$. All data are expressed as the mean ± SD.

about 15 min, shaken and then centrifuged at 1,000 rpm, 4°C for 5 min. The suspension was centrifuged at 8,000 rpm, 4°C for 5 min to get total bacteria, then filtered twice in PBS. The final bacterial suspension was mixed with an equal volume of 40% sterile glycerol to a final concentration of 20%, then stored at −80°C until transplantation. The recipient mice (SPF male

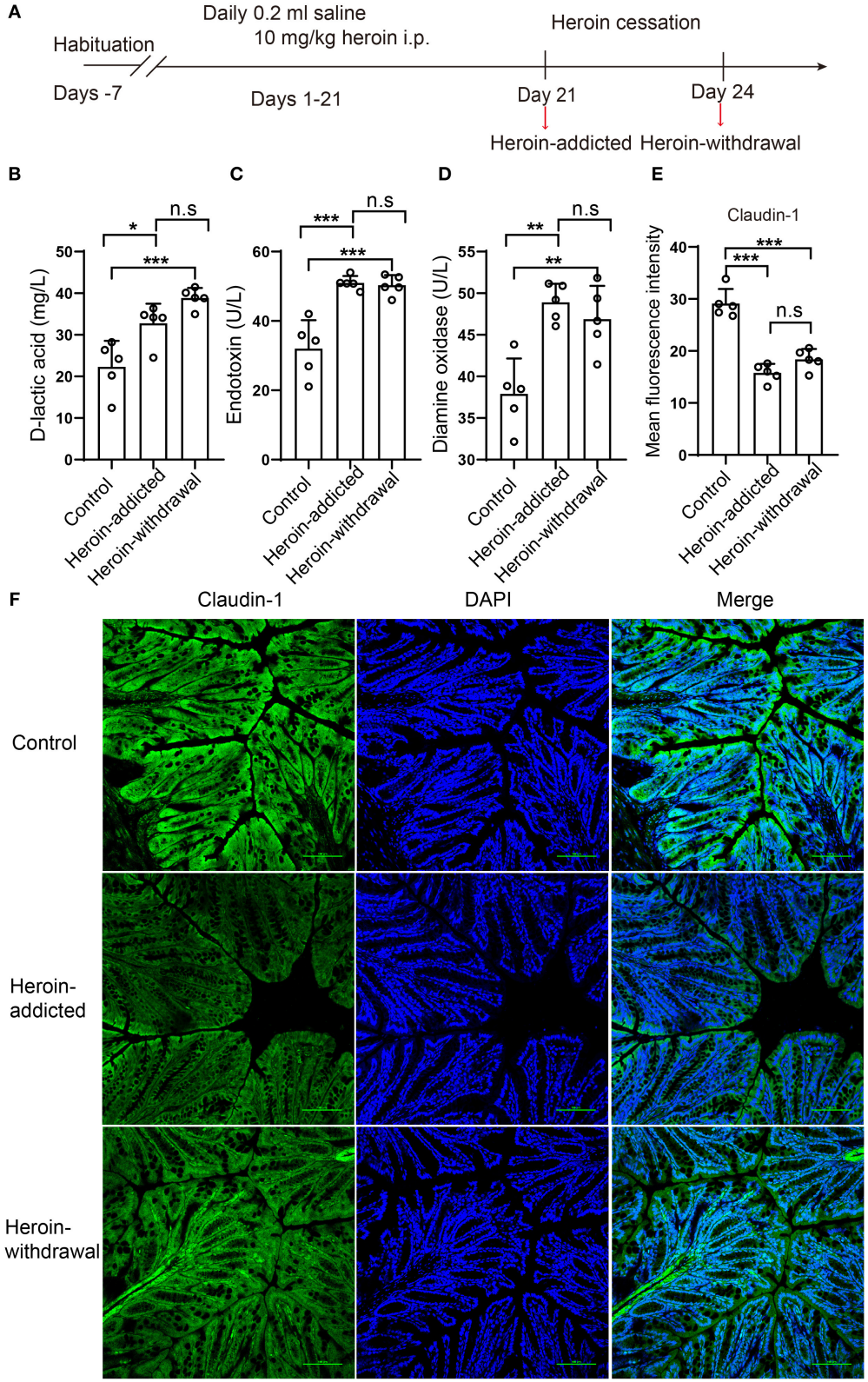

FIGURE 2 | Disrupted the intestinal mucosal integrity in mice with heroin dependence. **(A)** experimental design. The serum and colon tissues were collected on day 21 as heroin-addicted group, and after a 48-h withdrawal period (on day 24) as heroin-withdrawal group. **(B–D)** The serum levels of D-lactic acid (DLA), endotoxin (ET) and diamine oxidase (DAO) in heroin-addicted, heroin- withdrawal and control mice. **(E)** Immunofluorescence showed decreased expression levels of Claudin-1 in heroin-addicted and heroin-withdrawal groups. **(F)** Mean fluorescence intensity of Claudin-1 expression. All data are expressed as the mean ± SD $^{*}p < 0.05$; $^{**}p < 0.01$; $^{***}p < 0.001$ ($n = 5$ in each group).

C57/BL/6) were gavaged with 200 μl of the fecal slurry or PBS once a day for seven consecutive days. Body weight changes of recipient mice in pre-FMT and post-FMT were monitored, using pre-FMT body weight as baseline for FMT. A total of 30 mice were used in FMT experiment: donor mice (administrated with heroin for 21 days and collected fecal to prepare bacterial suspension $n = 10$), recipient mice: (gavaged with 200 μl of the fecal slurry $n = 10$, gavaged with 200 μl of PBS $n = 10$).

Open-Field Test (OFT)

The OFT assessed the effects of chronic psychological stress on anxious behavior. The mice were subjected to OFT for 5 min. The time spent in the center (inner 25% of the surface area) were recorded by ANY-maze software (Stoelting Co.) The open field arena was cleaned with 70% ethanol between each trial.

Elevated Plus-Maze Test (EPM)

The elevated plus-maze test was performed as previously described (21). The apparatus includes two open arms, two enclosed arms, and a central platform. The entire device was elevated 45 cm above the floor. A mouse was placed on the central platform and allowed to roam freely for 5 min. The time spent on open and closed arms were recorded.

Forced Swimming Test (FST)

A day before the test, a mouse was placed individually into a glass cylinder (20 cm height, 17 cm diameter) filled with water to a depth of 10 cm at 25°C for 5 min. During experimentation, subjects were placed individually in a filled glass cylinder for a period of 6 min and the total duration of immobility was measured for 5 min by ANY-maze software as indicative of depressive-like behavior. Motionless floating was considered immobile behavior (21).

Tail Suspension Test (TST)

The tail suspension test was conducted as described previously (21). Mouse was suspended 60 cm above the surface by adhesive the tip of the tail. Duration of immobility in a 6-min period was recorded by a video tracking system (ANY-maze, Stoelting Co.), which was indicative of depressive-like behavior.

Fecal Sample Collection and Microbial DNA Extraction

Fecal samples were collected from the control and heroin dependent mice, frozen immediately and stored at −80°C. Microbial DNA was extracted from fecal samples fusing the MagPure Stool DNA KFKit B (Magen, China). The quantity of genomic DNA was verified using the Qubit dsDNA BR Assay kit (Invitrogen, USA).

16S rRNA Gene Sequencing and Bioinformatic Analysis

16S rRNA gene sequencing procedure was performed by BGI (Shenzhen, China). Briefly, the V4 regions of the 16S rRNA gene in the DNA extracted from fecal samples were amplified using the following degenerate PCR primers: 515F (5′-GTGCCAGCMGCCGCGGTAA−3′), 806R (5′-GGACTACHVGGGTWTCTAAT-3′) and sequenced on the Illumina HiSeq2500 platform following the standard pipelines of Illumina and generating 2 × 250 bp paired-end reads. Taxonomic annotation was based on a customized version of SILVA reference database. Alpha and beta diversities were analyzed using QIIME. The relative abundance of bacteria was expressed as the percentage. Partial least-squares discrimination analysis (PLS-DA) was performed using the R package mix Omics, whereas principal coordinate analysis (PCoA) was performed using QIIME.

The Serum Levels of D-Lactic Acid (DLA), and Endotoxin (ET) and Diamine Oxidase (DAO)

The serum levels of DLA, ET, and DAO reflect intestinal mechanical barrier dysfunction, usually regarded as a very important evaluation of intestinal mucosal barrier damage (5). The indicators were determined by a combined test kit developed by the Institute of Biophysics, Chinese Academy of Sciences (Beijing Zhongsheng Jinyu Diagnostic Technology Co., Ltd.).

Immunofluorescence Staining

Expressions of Claudin-1 and ZO-1 were evaluated with immunofluorescence staining. Briefly, mouse colon tissue was fixed in 4% paraformaldehyde for 24 h, dehydrated using 30% sucrose, embedded in frozen section embedding agent and sliced (10-microns thick), permeabilized using 0.3% triton X-100 for 10 min, and blocked with 10% BSA for 60 min. The following primary antibodies was used: Claudin-1 (1:100, Abcam #ab15098), ZO-1 (1:200, Abcam #ab96587). The tissue sections were then incubated with the appropriate Anti-rabbit IgG (H+L) or F(ab')2 Fragment (Alexa Fluor® 488 Conjugate) (1:1000, CST#4412). Nuclei were stained with DAPI. The immunofluorescence quantification was analyzed by image J. Each experiment was repeated three times.

Detection of SCFAs in Fecal Samples

SCFAs contents were detected using MetWare (http://www.metware.cn/) based on the Agilent 7890B-7000D GC-MS/MS platform. As previously described (22), 20 mg of fecal samples were accurately weighed and placed in a 2-ml EP tube. A total of 1 ml of phosphoric acid (0.5% v/v) solution and a small steel ball were added to the EP tube. The mixture was grinded for 10 s, three times, then vortexed for 10 min and ultrasonicated for 5 min. A total of 0.1 mL supernatant was added to a 1.5-mL centrifugal tube after the mixture was centrifuged at 12,000 rpm for 10 min at 4°C and 0.5 mL MTBE (containing internal standard) solution was added to the centrifuge tube. The mixture was vortexed for 3 min and ultrasonicated for 5 min. Subsequently, the mixture was centrifuged at 12,000 rpm for 10 min at 4°C, and the supernatant was collected and used for GC-MS/MS analysis.

Statistical Analysis

The data were analyzed using the GraphPad Prism v.8 Software, data reported as means ± SD. Student's *t*-test and a Wilcoxon-test were performed to determine whether differences existed

TABLE 1 | The clinical information and intestinal barrier indicators of study population.

	HCs	Heroin	*p*-value
Subjects	$N = 38$	$N = 38$	NA
Sex	Male	Male	NA
Age (years)	34.44 ± 11.86	34.47 ± 8.40	0.122
BMI (Kg/m^2)	22.34 ± 2.60	21.02 ± 2.02	0.0162*
Diamine oxidase (U/L)	10.97 ± 3.24	13.54 ± 3.27	0.0009***
Exotoxin (U/L)	18.22 ± 3.41	20.83 ± 5.36	0.0135*
D-lactic acid (mg/L)	7.92 ± 4.21	10.36 ± 5.01	0.0247*

*The population demographics and serum levels of diamine oxidase (DAO), exotoxin (ET) and D-lactic acid (DLA) in heroin addicts and healthy controls (HCs). The results represent mean ± SD (p-values were calculated using unpaired t-test), *p < 0.05; ***p < 0.001.*

between the two groups. One-way ANOVA was used to compare between three or more groups. A p-value of <0.05 was considered statistically significant ($^*p < 0.05$; $^{**}p < 0.01$; $^{***}p < 0.001$; $^{****}p < 0.0001$). Notable non-significant differences were indicated in the figures by "n.s.," non-near significant ($0.05 < p < 0.1$) were indicated in the figures.

RESULTS

Subject Characteristics

A total of 76 participants (38 healthy controls and 38 heroin addicts) were included in the survey sample, and population demographics revealed that the distribution of the sample population by sex and age was not statistically different between the two groups (**Table 1**). The mean BMI was 22.34 ± 2.60 in the HCs, and 21.02 ± 2.02 in heroin addicts and there was a significant difference ($p < 0.05$) (low nutritional status) between the two groups. The serum levels of D-lactic acid (DLA), endotoxin (ET) and diamine oxidase (DAO) were the main indicators for evaluating the function of intestinal mucosal injury, intestinal wall permeability, and bacterial translocation (5). Compared to HCs, heroin addicts have a higher level of DAO, ET, and DLA (10.97 ± 3.24 U/L vs. 13.54 ± 3.27 $p < 0.0001$; 18.22 ± 3.41 U/L vs. 20.83 ± 5.36 U/L $p < 0.05$; 7.92 ± 4.21 mg/L vs. 10.36 ± 5.01 mg/L $p < 0.05$; respectively, **Table 1**). These results suggest a potential intestinal injury in the group of heroin addicts of withdrawal stage.

Generation of a Mouse Model With Heroin Dependence

After repeated 10 mg/kg heroin administrations for 14 days, the mouse model with heroin dependence was established and confirmed by behavior sensitization (**Figures 1A–D**). The total traveled distance collected in the OFT showed that heroin dependent mice traveled a significantly longer distance than control mice (101.09 ± 16.43 vs. 600.95 ± 93.86, $p < 0.0001$ **Figures 1B–D**), which was considered an addiction behavior (18). Data analysis showed that the body weight of the heroin dependent mice was significantly decreased relative to that of control mice (**Figure 1E**). Symptoms related to anxiety and/or depression were most often reported in drug withdrawal; herein, after 48 h withdrawal, anxiety and depression-like behaviors were evaluated by OFT, EMP, TST, and FST. The heroin dependent mice spent less time in the center of the open field ($p < 0.05$, **Figures 1F,J**) and decreased exploration of the open arms of the elevated-plus maze ($p = 0.07$, **Figures 1G,K**) during the 5-min test compared to mice that had received saline. For the TST and FST, heroin treated mice during withdrawal have reduced mobile time ($p < 0.0001$, **Figure 1H**) and swim time ($p < 0.001$, **Figure 1I**). Thus, mice with heroin dependence exhibited worse depressive and anxiety symptoms.

Disrupted the Intestinal Mucosal Integrity in Mice With Heroin Dependence

In our heroin-dependence mouse model, heroin-induced gut barrier dysfunction may occur at any time within the 21 days during heroin treatment or after the initiation of drug withdrawal. We thus compared the serum level of DLA, ET, and DAO, the expression of Claudin-1 at both day 21(Heroin-addicted stage) and at 48-h after initiation of withdrawal (Heroin-withdrawal stage) (**Figure 2A**). Compared to non-treated control mice, both heroin-addicted and heroin-withdrawal groups decreased the integrity of the intestinal mucosal barrier, as demonstrated by significant increases in the levels of serum DLA, ET, and DAO (**Figures 2B–D**), lower expression level of Claudin-1 (**Figures 2E,F**). These results were consistent with previous analysis in heroin addicts (**Table 1**). In addition, no significant differences were observed between the heroin-addicted and heroin-withdrawal groups ($p > 0.05$). For better mimicking the heroin dependence and withdrawal syndrome in patients, we decided to profile the microbiota in the heroin dependent mouse model undergoing withdrawal stage to explore the associations with intestinal mucosal integrity.

Discrepancy in the Gut Microbiota Structure and Diversity Between Heroin-Dependent and Control Groups

In general, greater bacterial diversity was considered beneficial to health; the gut microbiota in the heroin-dependent group was slightly decreased although no statistical differences were presented based on sob, chao, ace, Shannon, and simpson indices (**Figure 3A**). The fecal microbiota of the two groups could be divided into clusters according to community composition using Unweighted UniFracmetrics and clearly separated in

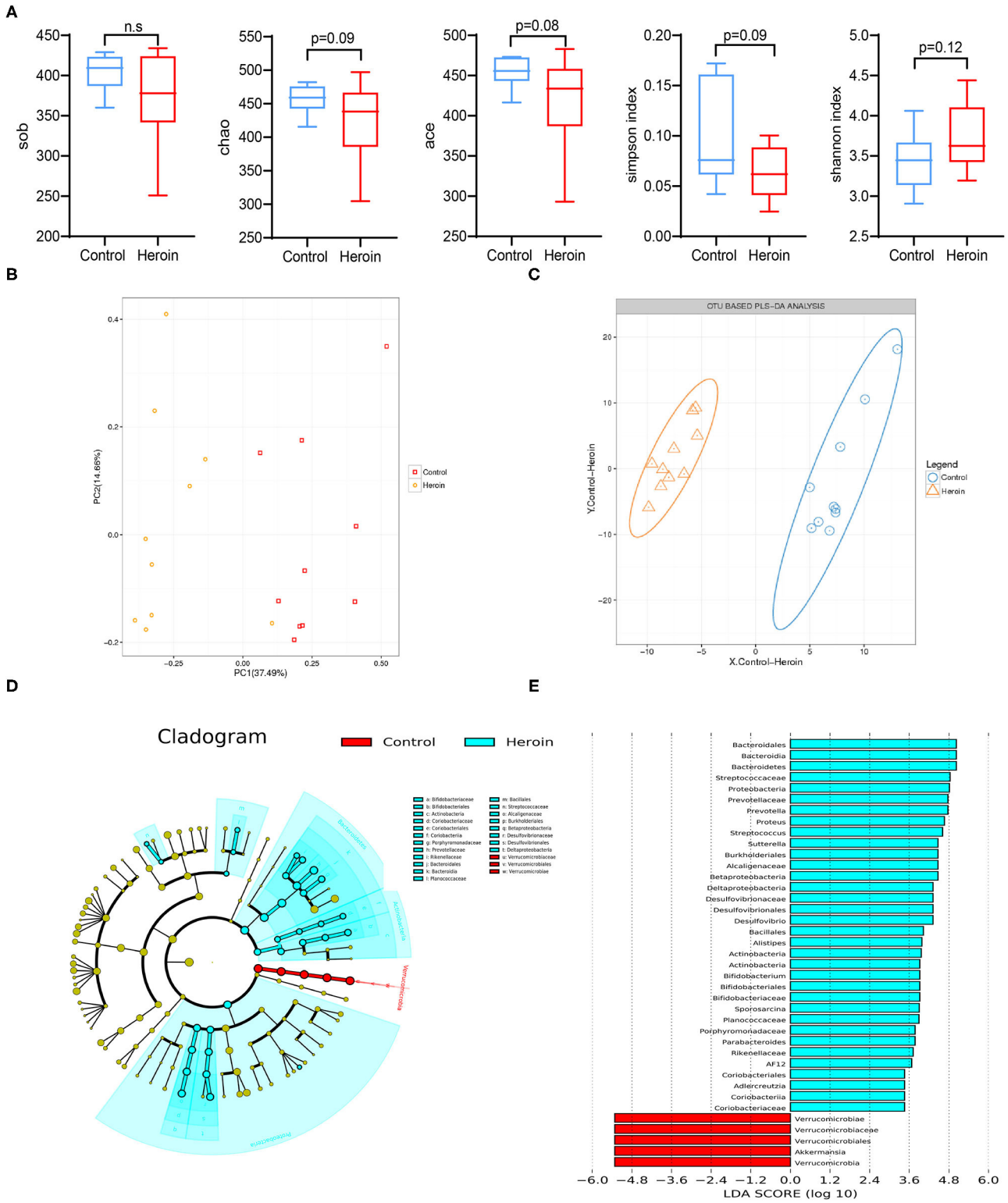

FIGURE 3 | Heroin administrated altered the gut microbiota structure and diversity. **(A)** Comparison of the alpha-diversity indices between the control and heroin groups based on the observed species, chao, ace, shannon, and simpson index. **(B)** Principal coordinate analysis (PCoA) of the samples using Unweighted-UniFrac from pyrosequencing. The red squares represent the control group, and the yellow dots represent the heroin administrated group. The fecal microbiotas of the two groups could be divided into clusters according to community composition using Unweighted UniFrac metrics and separated clearly using PCoA analysis. **(C)** Operational taxonomic unit (OUT)-based partial least-squares discrimination analysis (PLS-DA). **(D)** Linear discriminant analysis effect size (LEfSe) cladogram representing differentially abundant taxa. **(E)** Linear discriminant analysis (LDA) scores, as calculated by the LEfSe of differentially abundant taxa in the two groups. Cladogram showing differentially abundant taxonomic clades with an LDA score >2.0 among cases and controls.

the PCoA plot demonstrating the structural changes in the microbial communities (**Figure 3B**). The OUT-based PLS-DA analysis also showed apparent differences between the groups (**Figure 3C**). The linear discriminant analysis effect size (LEfSe) cladogram represents differentially abundant taxa (**Figure 3D**). *Bacteraidaceae*, *Prevatellaceae*, *Ruminococcaceae*, *Verrucomicrobia*, and *Akkerrnassia* were the key types that contributed to the difference in the microbiota composition between the two groups. The significant difference in bacterial abundance was compared using linear discriminant analysis (LDA). Moreover, the composition of the gut microbiota was significantly different from the two groups according to the LDA score (**Figure 3E**).

Heroin Dependence Altered Microbiota Composition in Mice

We identified the top microbiota (the relative abundance >0.01%, <0.01% were classified into 'others') at the family (**Figure 4A**) and genera (**Figure 4B**) levels in the heroin and control groups. At the family-level, the top microbiota includes S24-7, *Verrucomicrobiaceae*, *Lachnospiraceae*, *Paraprevotellaceae*, *Bacteroidaceae*, *Ruminococcaceae*, *Lactobacillaceae*, *Helicobacteraceae*, *Alcaligenaceae*, *Desulfovibrionaceae*, *Rikenellaceae*, *Prevotellaceae*, and *Erysipelotricchaceae* (**Figure 3A**). The relative abundances of *Verrucomicrobiaceae*, *Paraprevotellaceae*, and *Alcaligenaceae* differed between the two groups ($p < 0.05$). Mice with heroin dependence had a higher abundance of *Bifidobacteriaceae*, *Planococcaceae*, *Streptococcaceae*, *Desulfovibrionaceae* (the relative abundance of these bacteria <0.01%) compared to control mice (**Figure 4C**). At the genus-level, 11 genera were observed in the top microbiota of both groups (the relative abundance >0.01%) (**Figure 4B**), of these, *Akkermansia* was significantly decreased while *Bifidobacterium* and *Sutterella* were significantly enriched in the heroin group (**Figure 4D**). The remaining genera were not significantly enriched in either group (*Prevotella*, *Bacteroides*, *Lactobacillus*, *Oscillospira*, *Coprococcus*, *Ruminococcaceae*, *Turicibacter*, and *Helicobacter*). In addition, the level of *Bifidobacterium*, *Sporosarcina*, *Streptococcus*, and *Alistipes* (the relative abundance of these bacteria <0.01%) were increased more in heroin dependent group than that in the control group (**Figure 4D**).

Altered Gut Microbiota Is Associated With Impaired Intestinal Mucosal Barrier Integrity in Heroin Dependent Mice

To investigate whether heroin-dependent altered gut microbiota was sufficient to influence the integrity of the intestinal mucosal barrier in mice, the FMT experiments were performed (**Figure 5A**). Recipient mice receiving microbiota from heroin dependent mice showed a decreased body weight compared to mice that received FMT from controls (**Figure 5B**). Significant elevation of serum DAO ($p = 0.0305$) and ET ($p = 0.0476$) were observed in the FMT mice receiving microbiota from heroin dependent mice compared to control mice (**Figures 5C,D**), although the DLA levels increased was not statistically significant ($p = 0.36$, **Figure 5E**). The intestinal mucosal barrier integrity was crucial for intestinal homeostasis, and its function was maintained by intercellular TJs. Intestinal TJs, such as OCL and ZO-1 have been shown as the principal determinants of intestinal mucosal barrier integrity (23). Furthermore, we examined the expression and distribution of TJ proteins in the colon using immunofluorescence. As shown in **Figures 5F,G**, the expression of Claudin-1 and ZO-1 (**Supplementary Figure 1**) were decreased in both heroin dependence and FMT groups and these results indicated intestinal mucosal mechanical barrier impairment. Taken together, the results showed that heroin dependence induced intestinal mucosal barrier function impairment could be transmissible via gut microbiota in mice.

Analysis of Fecal Short-Chain Fatty Acids (SCFAs) in Mice

SCFAs are the primary products of microbial fermentation of undigested dietary carbohydrates especially acetate, propionate, and butyrate (24). Several reports highlighted the immunomodulatory capacities and the ability to strengthen epithelial barrier integrity (25, 26). The intestinal microbiota and their derived SCFAs are crucial to intestinal barrier integrity. Therefore, the levels of acetic acid, propionic acid, butyric acid, valeric acid, isobutyrate, and isovalerate in the fecal samples were analyzed by GC/MS. Acetic acid, butyric acid and propionic acid were the principal fecal SCFAs present in the mouse model, the concentrations of propionic acid significantly decreased in heroin dependence and FMT mice compared to control mice (**Figure 6**).

DISCUSSION

The microbiota-gut-brain axis were considered as the bidirectional system of communication between central nervous system (CNS) and the gastrointestinal tract (27). Many CNS diseases such as autism spectrum disorder, Parkinson's disease, and major depressive disorder are more susceptible to gastrointestinal symptoms disorder (28, 29), even more, gastrointestinal symptoms of individuals seems to strongly correlate with the severity of CNS diseases (28). Gastrointestinal ailments are the most frequent complications in heroin abusers, which not only aggravate the disease process, but even lead to low abstinence rate. The role of microbiota contribute more than 50% to the development of GI symptoms (30). In this study, a significant reduction in body weight was observed in heroin addicts and heroin dependent mice, as well as colonization with heroin dependence-altered microbiota by FMT. As body weight is commonly used to monitor the nutritional status, these results revealed that the gastrointestinal dysfunction-related decline in nutritional status was associated with heroin dependence.

According to the results of 16S rDNA sequencing, there were no significant differences in the alpha diversity, consistent with the results comparing cocaine users and non-users (31). At the genus level, *Akkermansia*, which belongs to the family of *Verrucomicrobia*, was significantly increased in the heroin

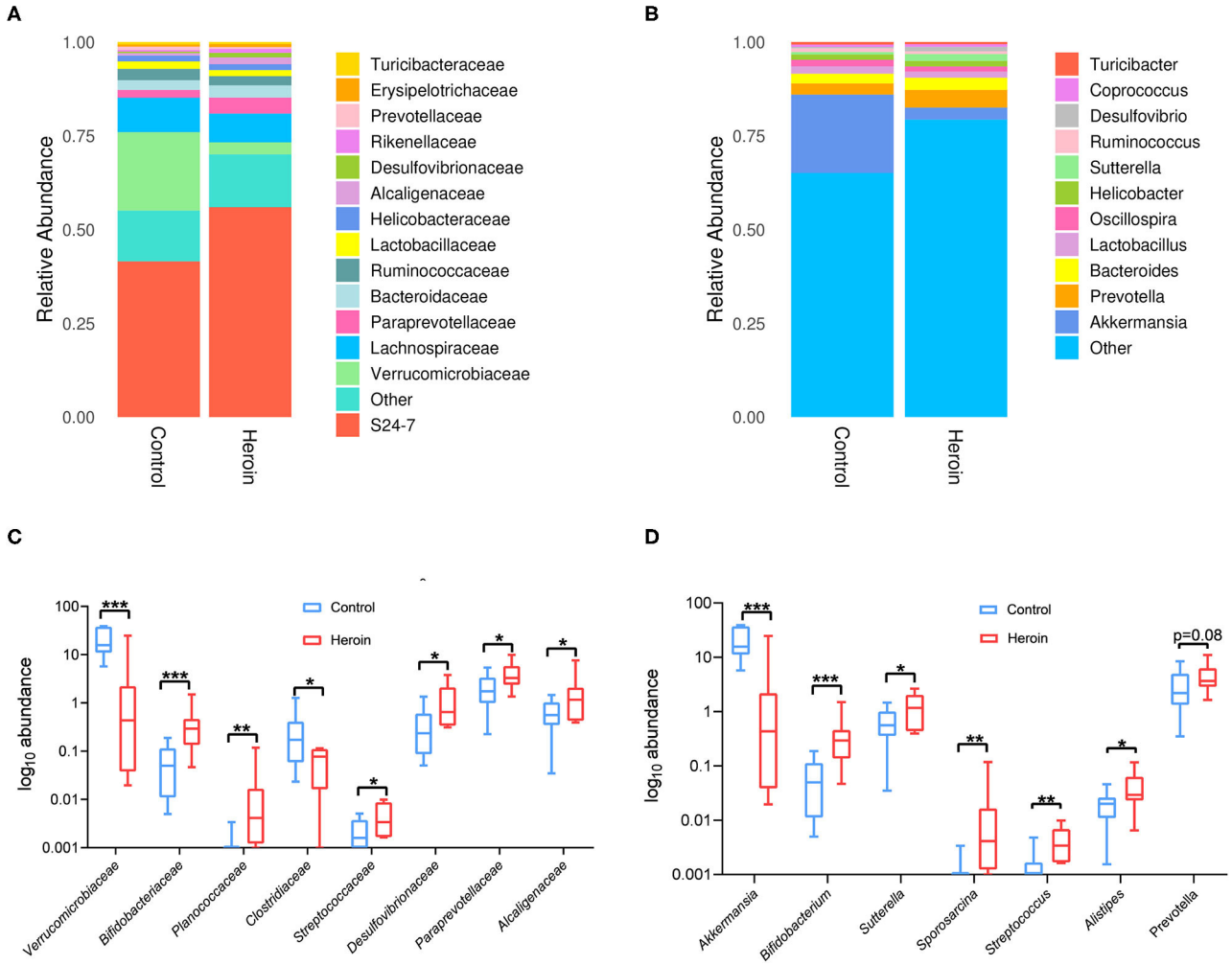

FIGURE 4 | Family and genus-level taxonomic distribution of intestinal microbiota and the top microbiota (the relative abundance >0.01%) at the family and genus levels in the control and heroin groups. **(A,B)** Bacterial community structures in the heroin administrated and control groups at the family **(A)** and genus levels **(B)**. Abundance is presented in terms of the percentage of the total effective bacterial sequences in each group. **(C,D)** All significantly different bacterial are listed in the heroin and control groups at the family **(C)** and genus levels **(D)**. Data are represented as boxplots, with median, minima, and maxima, statistical significance was calculated using Wilcoxon-test ($n = 10$) $^{*}p < 0.05$; $^{**}p < 0.01$; $^{***}p < 0.001$.

dependent mouse group (**Figures 4C,D**). Previous study suggested that higher body weight and lower *Akkermansia* abundance were found in the monosodium glutamate-induced abdominal obesity mice study (32), while in our present study lower *Akkermansia* abundance and lower weight were shown in heroin dependent mice. We speculate that Akkermansia may synergrise with other bacteria and involve in tighten intestinal barrier integrity, lipid storage, adipose tissue inflammation and insulin resistance. Therefore, it is reasonable to believe that the body weight loss was to some extent related to the change of *Verrucomicrobia*. In parallel, it has been shown in previous reports that the abundance of *Akkermansia* may directly exacerbate intestinal inflammation (33). Furthermore, *Akkermansia* was found to be involved in regulating inflammatory factors (34) and played an important anti-inflammatory role in the development of metabolic syndrome (35). Recent human studies have also shown that reduced *Akkermansia* were found in IBD patients (36, 37), and in children with autism spectrum disorder with a thinner GI mucus barrier (38). Mechanistically, *Akkermansia* may lead to dry stool and eventually intestinal mucosal barrier dysfunction by degrading intestinal mucin (32). Therefore, heroin dependence induced *Akkermansia* altering should trigger our more attention in clinical diagnosis and treatment. The relative abundance of *Bifidobacteriaceae* at family and genus levels were increased in mice with heroin dependence ($p < 0.001$, **Figures 4C,D**) compared with control mice. However, it is generally agreed that *Bifidobacteriaceae* is considered to be beneficial in humans and animals (39). A recent study showed that the *Bifidobacterium* were significantly elevated in early days while returned to

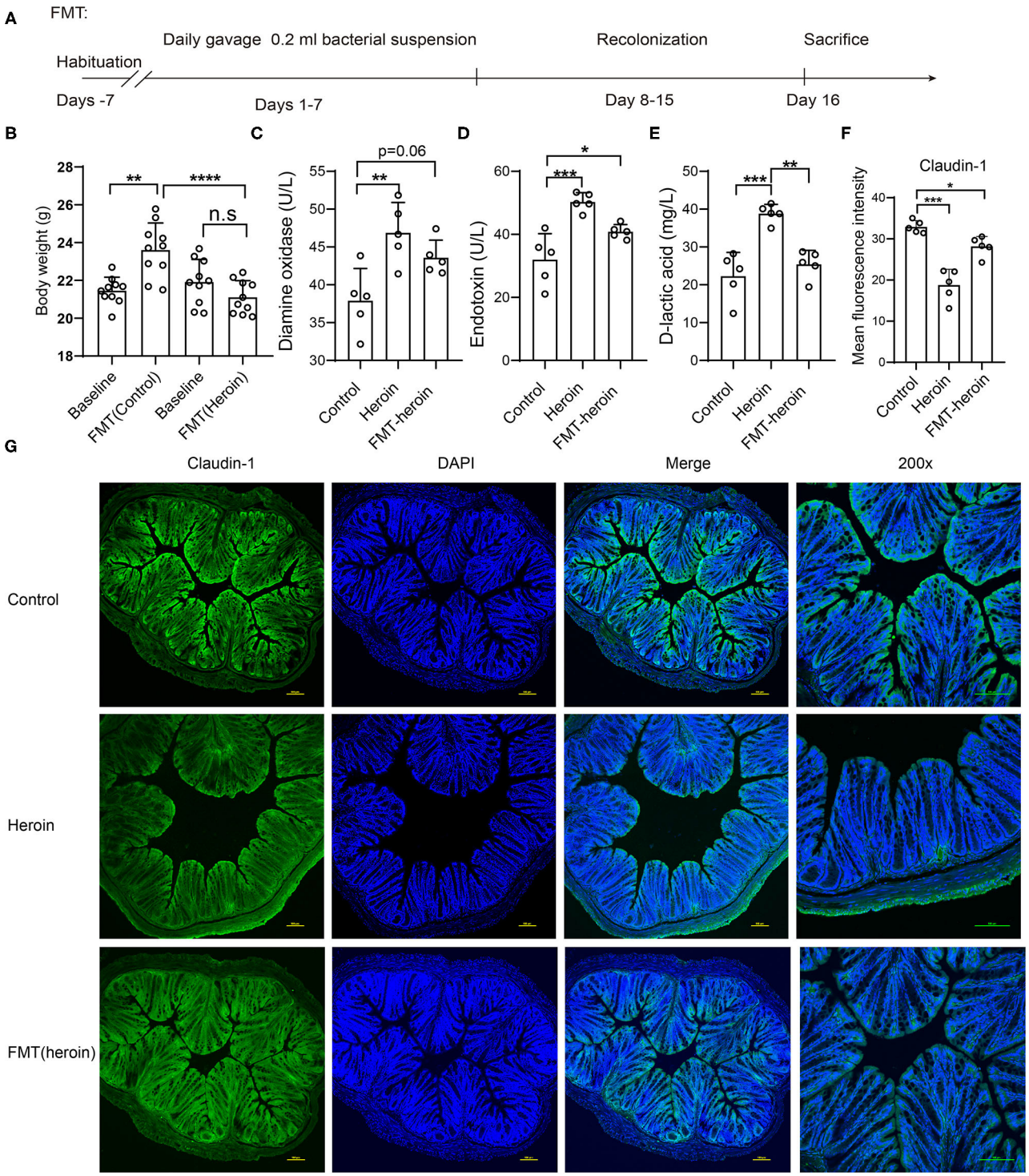

FIGURE 5 | Effect of FMT treatment on intestinal permeability and expression of tight junction proteins in mice. **(A)** Scheme of FMT experiment. **(B)** The body weight of pre-FMT and Post-FMT in receive control microbiota and heroin microbiota groups. **(C–E)** The serum levels of DLA, ET and DAO in control and FMT groups. **(F,G)** Immunofluorescence showed decreased expression levels of Claudin-1 in heroin and FMT groups. **(F)** Mean fluorescence intensity of Claudin-1 expression. **(G)** Example images. All data are expressed as the mean ± SD $^{*}p < 0.05$; $^{**}p < 0.01$; $^{***}p < 0.001$; $^{****}p < 0.0001$.

baseline levels after 7 days of methamphetamine cessation in rat model (40). Additionally, a higher level of *Bifidobacteriaceae* was found in major depressive disorder (41). These results align with our findings, and we speculated that increases in relative abundance of these gram-positive bacteria may act as a protective mechanism against heroin acute withdrawal,

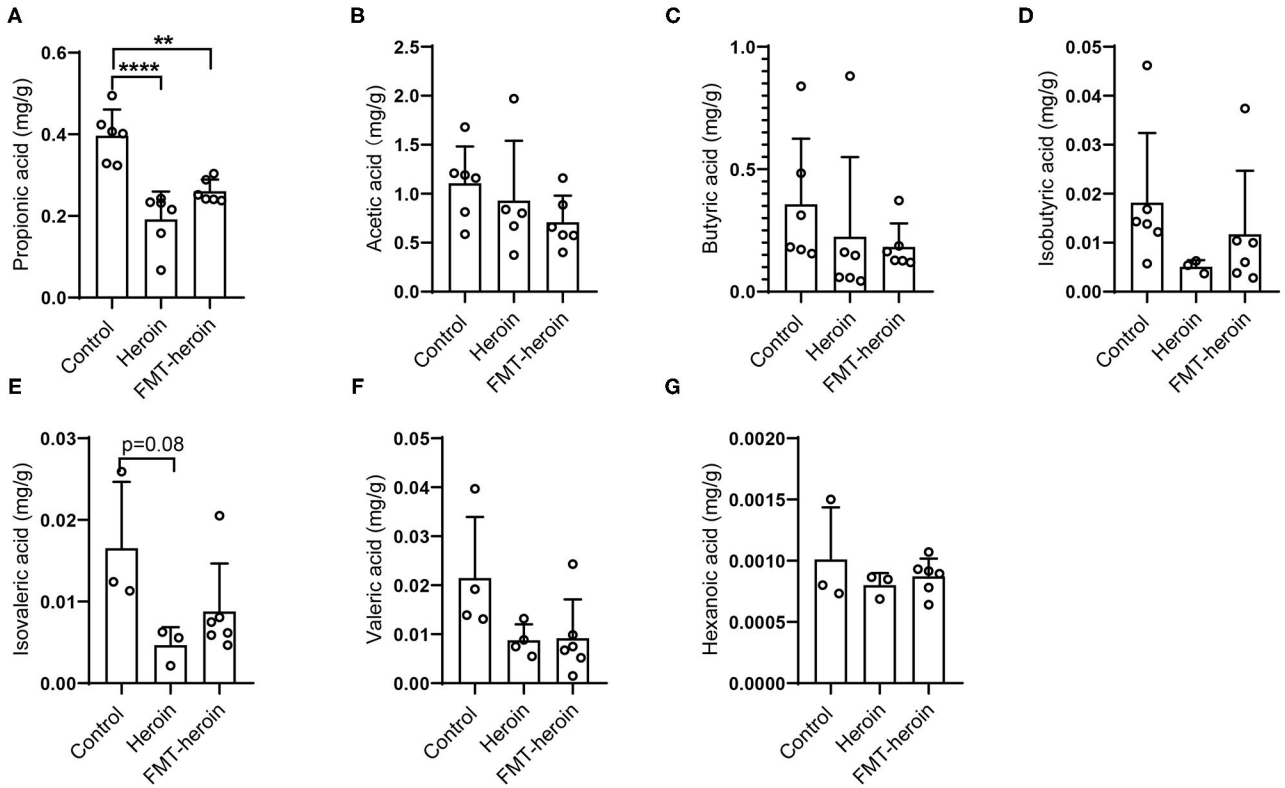

FIGURE 6 | Composition of short chain fatty acids in fecal samples of control, heroin-administrated and FMT treated mice. The levels of propionic acid were significantly altered in the heroin and FMT groups **(A)**. **(B–G)** Concentrations of the major SCFAs acetate, butyrate, isovaleric, isobutyric, valeric, hexanoic. All data are expressed as the mean ± SD ($n = 6$ per group). Statistically differences were analyzed with one-way ANOVA, $^{**}p < 0.01$; $^{****}p < 0.0001$.

alternatively, specific strains of *Bifidobacterium* may have inflammatory potential.

Sutterella is a genus of the family *Sutterellaceae* which belongs to the class *β-Proteobacteria*, have already proven that low levels are associated with gut immune homeostasis and high levels of IgA (42), meanwhile, low fecal IgA levels were attributed to the presence of high levels of *Sutterella* in a mouse model (43). *Sutterella* could impair the functionality of the intestinal antibacterial immune response, mainly it's capacity to limit intracellular bacterial species, rather than directly induce inflammation (44). Thus, *Sutterella* species are considered as commensals or bystanders in the context of gastrointestinal diseases (45, 46). Herein, we found that mice with heroin dependence exhibited an increased abundance of *Sutterella* which suggest intestinal barrier injury should be focused on. To date, the role of the *Prevotella* genus within the intestinal microbiota and its effects on the host are not entirely understood, whereas somewhat conflicting interpretations are available linking the *Prevotella* genus to health markers. Beneficial effects of some *Prevotella* strains in the gut have been reported, such as cardiovascular disease risk factor profile and glucose metabolism improvement (47, 48). Furthermore, *Prevotella* strain abundance has been found in healthy gut microbiota and was associated with plant-rich diets (49, 50). However, studies have also suggested a potential role of *Prevotella* species as intestinal pathobionts, as some strains promoted diseases, such as metabolic syndrome, obesity, inflammatory bowel disease or other inflammatory diseases (51). In mouse models, *Prevotella* enrichment was positively correlated with high risk of irritable bowel syndrome (IBD) and associated with higher susceptibility to chemically-induced colitis (52) by reducing interleukin (IL)-18 (53). Herein, as one of the top bacteria, *Prevotella* exhibited a relatively higher abundance, although the difference did not reach statistical significance ($p = 0.08$). In addition to the details described above, the altered bacterial such as *Desulfovibrio*, *Prevotella*, and *Oscillibacter* may utilize microbial exopolysaccharides synthesized by *Bifidobacterium* to produce SCFAs in the intestine (54).

The balance of gut microbiota helps to maintain the biological barrier of the intestine (55). Mice with heroin dependence exhibited several changes in bacterial, which might damage the integrity of the intestinal barrier. To further explore the role of microbiota in the intestinal barrier function, we performed FMT for subsequent studies. Consistent with our expectation, we observed the changes of intestinal mucosal barrier integrity and permeability (**Figures 5C–E**), further supported by immunofluorescence results of Claudin-1 and ZO-1 (**Figure 5F**, **Supplementary Figure 1**). FMT experiments suggest that the alteration of microbiota is closely related to the function change in the intestinal barrier.

In addition, SCFAs are the most critical and pleiotropic functional components of microbe-to-host signaling (56). It is now well-established that SCFAs modulate colonic motility by stimulating serotonin secretion from gut enterochromaffin cells (56, 57) and SCFAs are closely related to intestinal growth and barrier function (58). In the present study, we observed a significant decrease in the concentration of propionic acid in both heroin dependent mice and FMT mice (**Figure 6A**) compared to controls. Considering propionate can readily cross the gut-blood barrier and has potential health-promoting effects (59–61), we speculate that propionic acid may participate in TJ assembly by regulating TJ proteins and modulating the integrity of intestinal mucosal in mice.

In the current study, the strength of our work is that we utilized FMT mouse model to prove of concept that heroin dependence-altered microbiota is associated with disrupted intestinal mucosal integrity and permeability. However, there are some limitations. First, the results warrant further validation in other independent cohort studies with larger sample sizes. Second, there might be other subtle differences between undergoing heroin exposure and in withdrawal stage. Thus, additional animal models distinguishing between heroin-induced vs. withdrawal-induced damage to intestinal mucosal integrity and gut microbiota will be useful to determine the best timing for preventive intervention for heroin withdrawal management.

In summary, our study provides evidence showing that heroin dependence could alter gut microbiota and modulate mucosal barrier integrity, highlighting the role of the gut microbiota in substance use disorders and the pathophysiology of gastrointestinal disease.

DATA AVAILABILITY STATEMENT

The datasets presented in this study can be found in online repositories. The 16S rRNA gene sequencing data are available from NCBI Bioproject Accession number: PRJNA770289.

ETHICS STATEMENT

The studies involving human participants were reviewed and approved by the Clinical Research Ethics Committee, the First Affiliated Hospital of Kunming Medical University. The patients/participants provided their written informed consent to participate in this study. The animal study was reviewed and approved by the Animal Care and Use Committee of Kunming Medical University. Written informed consent was obtained from the owners for the participation of their animals in this study.

AUTHOR CONTRIBUTIONS

JY and KW: designed the experiments. JY, PX, LB, ZZ, YZ, CC, and ZX: recruited clinical participants and collected samples. YX, MC, MZ, and HW: animal behaviors and mice experiment. JY, KW, and ZZ: analyzed the 16S rRNA and metabolomics data. JY and ZZ: drafted the manuscript. All authors contributed to the article and approved the submitted version.

FUNDING

This work was supported by the National Natural Science Foundation of China (Nos. 3171101074, 81870458, and 31860306); Yunling Scholar (YLXL20170002); the Major project of Yunnan Provincial Bureau of Education (2020J0161; 2021J0234); Yunnan Engineering Technology Center of Digestive Disease (2018DH006); and Science and Technology Department of Yunnan Province (Nos. 202001AV070010, 2020DAMARA-004, and 2020DAMARA-005).

SUPPLEMENTARY MATERIAL

The Supplementary Material for this article can be found online at: https://www.frontiersin.org/articles/10.3389/fnut.2021.765414/full#supplementary-material

REFERENCES

1. Koob GF, Volkow ND. Neurocircuitry of addiction. *Neuropsychopharmacology*. (2010) 35:217–38. doi: 10.1038/npp.2009.110
2. Leshner AI. Addiction is a brain disease, and it matters. *Science*. (1997) 278:45–7. doi: 10.1126/science.278.5335.45
3. Hyman SE, Malenka RC. Addiction and the brain: the neurobiology of compulsion and its persistence. *Nat Rev Neurosci*. (2001) 2:695–703. doi: 10.1038/35094560
4. Nestler EJ. From neurobiology to treatment: progress against addiction. *Nat Neurosci*. (2002) 5(Suppl.):1076–9. doi: 10.1038/nn945
5. Shen S, Zhao J, Dai Y, Chen F, Zhang Z, Yu J, et al. Methamphetamine-induced alterations in intestinal mucosal barrier function occur via the microRNA-181c/ TNF-α/tight junction axis. *Toxicol Lett*. (2020) 321:73–82. doi: 10.1016/j.toxlet.2019.12.020
6. Xu Y, Xie Z, Wang H, Shen Z, Guo Y, Gao Y, et al. Bacterial diversity of intestinal microbiota in patients with substance use disorders revealed by 16S rRNA gene deep sequencing. *Sci Rep*. (2017) 7:3628. doi: 10.1038/s41598-017-03706-9
7. Zhao J, Shen S, Dai Y, Chen F, Wang K. Methamphetamine induces intestinal inflammatory injury via Nod-Like Receptor 3 Protein (NLRP3) inflammasome overexpression *in vitro* and *in vivo*. *Med Sci Monit*. (2019) 25:8515–26. doi: 10.12659/MSM.920190
8. Sun J, Chen F, Chen C, Zhang Z, Zhang Z, Tian W, et al. Intestinal mRNA expression profile and bioinformatics analysis in a methamphetamine-induced mouse model of inflammatory bowel disease. *Ann Transl Med*. (2020) 8:1669. doi: 10.21037/atm-20-7741
9. Moretti M, Belli G, Morini L, Monti MC, Osculati AMM, Visonà SD. Drug abuse-related neuroinflammation in human postmortem brains: an immunohistochemical approach. *J Neuropathol Exp Neurol*. (2019) 78:1059–65. doi: 10.1093/jnen/nlz084
10. Meckel KR, Kiraly DD. A potential role for the gut microbiome in substance use disorders. *Psychopharmacology*. (2019) 236:1513–30. doi: 10.1007/s00213-019-05232-0
11. Xu M, Xu X, Li J, Li F. Association between gut microbiota and autism spectrum disorder: a systematic review and meta-analysis. *Front Psychiatry*. (2019) 10:473. doi: 10.3389/fpsyt.2019.00473
12. Belkaid Y, Hand TW. Role of the microbiota in immunity and inflammation. *Cell*. (2014) 157:121–41. doi: 10.1016/j.cell.2014.03.011

13. Miller AW, Orr T, Dearing D, Monga M. Loss of function dysbiosis associated with antibiotics and high fat, high sugar diet. *ISME J*. (2019) 13:1379–90. doi: 10.1038/s41396-019-0357-4
14. Marchesi JR, Adams DH, Fava F, Hermes GD, Hirschfield GM, Hold G, et al. The gut microbiota and host health: a new clinical frontier. *Gut*. (2016) 65:330–9. doi: 10.1136/gutjnl-2015-309990
15. Dodiya HB, Forsyth CB, Voigt RM, Engen PA, Patel J, Shaikh M, et al. Chronic stress-induced gut dysfunction exacerbates Parkinson's disease phenotype and pathology in a rotenone-induced mouse model of Parkinson's disease. *Neurobiol Dis*. (2020) 135:104352. doi: 10.1016/j.nbd.2018.12.012
16. Skosnik PD, Cortes-Briones JA. Targeting the ecology within: the role of the gut-brain axis and human microbiota in drug addiction. *Med Hypotheses*. (2016) 93:77–80. doi: 10.1016/j.mehy.2016.05.021
17. Cao H, Liu X, An Y, Zhou G, Liu Y, Xu M, et al. Dysbiosis contributes to chronic constipation development via regulation of serotonin transporter in the intestine. *Sci Rep*. (2017) 7:10322. doi: 10.1038/s41598-017-10835-8
18. Su LY, Luo R, Liu Q, Su JR, Yang LX, Ding YQ, et al. Atg5- and Atg7-dependent autophagy in dopaminergic neurons regulates cellular and behavioral responses to morphine. *Autophagy*. (2017) 13:1496–511. doi: 10.1080/15548627.2017.1332549
19. Zhou ZL, Jia XB, Sun MF, Zhu YL, Qiao CM, Zhang BP, et al. Neuroprotection of fasting mimicking diet on MPTP-induced Parkinson's disease mice via gut microbiota and metabolites. *Neurotherapeutics*. (2019) 16:741–60. doi: 10.1007/s13311-019-00719-2
20. Schuijt TJ, Lankelma JM, Scicluna BP, de Sousa e Melo F, Roelofs JJ, de Boer JD, et al. The gut microbiota plays a protective role in the host defence against pneumococcal pneumonia. *Gut*. (2016) 65:575–83. doi: 10.1136/gutjnl-2015-309728
21. Jung EM, Moffat JJ, Liu J, Dravid SM, Gurumurthy CB, Kim WY. Arid1b haploinsufficiency disrupts cortical interneuron development and mouse behavior. *Nat Neurosci*. (2017) 20:1694–707. doi: 10.1038/s41593-017-0013-0
22. Zhao R, Chu L, Wang Y, Song Y, Liu P, Li C, et al. Application of packed-fiber solid-phase extraction coupled with GC-MS for the determination of short-chain fatty acids in children's urine. *Clin Chim Acta*. (2017) 468:120–5. doi: 10.1016/j.cca.2017.02.016
23. Zhuang Y, Wu H, Wang X, He J, He S, Yin Y. Resveratrol attenuates oxidative stress-induced intestinal barrier injury through PI3K/Akt-mediated Nrf2 signaling pathway. *Oxid Med Cell Longev*. (2019) 2019:7591840. doi: 10.1155/2019/7591840
24. González-Zancada N, Redondo-Useros N, Díaz LE, Gómez-Martínez S, Marcos A, Nova E. Association of moderate beer consumption with the gut microbiota and SCFA of healthy adults. *Molecules*. (2020) 25:4772. doi: 10.3390/molecules25204772
25. Curtasu MV, Tafintseva V, Bendiks ZA, Marco ML, Kohler A, Xu Y, et al. Obesity-related metabolome and gut microbiota profiles of Juvenile Göttingen minipigs-long-term intake of fructose and resistant starch. *Metabolites*. (2020) 10:456. doi: 10.3390/metabo10110456
26. Lucas S, Omata Y, Hofmann J, Böttcher M, Iljazovic A, Sarter K, et al. Short-chain fatty acids regulate systemic bone mass and protect from pathological bone loss. *Nat Commun*. (2018) 9:55. doi: 10.1038/s41467-017-02490-4
27. Du J, Zayed AA, Kigerl KA, Zane K, Sullivan MB, Popovich PG. Spinal cord injury changes the structure and functional potential of gut bacterial and viral communities. *mSystems*. (2021) 6:e01356-20. doi: 10.1128/mSystems.01356-20
28. Fattorusso A, Di Genova L, Dell'Isola GB, Mencaroni E, Esposito S. Autism spectrum disorders and the gut microbiota. *Nutrients*. (2019) 11:521. doi: 10.3390/nu11030521
29. Jiang H, Ling Z, Zhang Y, Mao H, Ma Z, Yin Y, et al. Altered fecal microbiota composition in patients with major depressive disorder. *Brain Behav Immun*. (2015) 48:186–94. doi: 10.1016/j.bbi.2015.03.016
30. Saulnier DM, Riehle K, Mistretta TA, Diaz MA, Mandal D, Raza S, et al. Gastrointestinal microbiome signatures of pediatric patients with irritable bowel syndrome. *Gastroenterology*. (2011) 141:1782–91. doi: 10.1053/j.gastro.2011.06.072
31. Volpe GE, Ward H, Mwamburi M, Dinh D, Bhalchandra S, Wanke C, et al. Associations of cocaine use and HIV infection with the intestinal microbiota, microbial translocation, and inflammation. *J Stud Alcohol Drugs*. (2014) 75:347–57. doi: 10.15288/jsad.2014.75.347
32. Zhao L, Zhu X, Xia M, Li J, Guo AY, Zhu Y, et al. Quercetin ameliorates gut microbiota dysbiosis that drives hypothalamic damage and hepatic lipogenesis in monosodium glutamate-induced abdominal obesity. *Front Nutr*. (2021) 8:671353. doi: 10.3389/fnut.2021.671353
33. Seregin SS, Golovchenko N, Schaf B, Chen J, Pudlo NA, Mitchell J, et al. NLRP6 protects Il10(-/-) mice from colitis by limiting colonization of *Akkermansia muciniphila*. *Cell Rep*. (2017) 19:2174. doi: 10.1016/j.celrep.2017.05.074
34. Everard A, Belzer C, Geurts L, Ouwerkerk JP, Druart C, Bindels LB, et al. Cross-talk between *Akkermansia muciniphila* and intestinal epithelium controls diet-induced obesity. *Proc Natl Acad Sci USA*. (2013) 110:9066–71. doi: 10.1073/pnas.1219451110
35. Routy B, Gopalakrishnan V, Daillère R, Zitvogel L, Wargo JA, Kroemer G. The gut microbiota influences anticancer immunosurveillance and general health. *Nat Rev Clin Oncol*. (2018) 15:382–96. doi: 10.1038/s41571-018-0006-2
36. Derrien M, Belzer C, de Vos WM. *Akkermansia muciniphila* and its role in regulating host functions. *Microb Pathog*. (2017) 106:171–81. doi: 10.1016/j.micpath.2016.02.005
37. Cheng Z, Zhao L, Dhall D, Ruegger PM, Borneman J, Frykman PK. Bacterial microbiome dynamics in post pull-through Hirschsprung-Associated Enterocolitis (HAEC): an experimental study employing the endothelin receptor B-null mouse model. *Front Surg*. (2018) 5:30. doi: 10.3389/fsurg.2018.00030
38. Martínez-González AE, Andreo-Martínez P. The role of gut microbiota in gastrointestinal symptoms of children with ASD. *Medicina*. (2019) 55:408. doi: 10.3390/medicina55080408
39. Bruyère J, Abada YS, Vitet H, Fontaine G, Deloulme JC, Cès A, et al. Presynaptic APP levels and synaptic homeostasis are regulated by Akt phosphorylation of huntingtin. *Elife*. (2020) 9:e56371. doi: 10.7554/eLife.56371.sa2
40. Forouzan S, Hoffman KL, Kosten TA. Methamphetamine exposure and its cessation alter gut microbiota and induce depressive-like behavioral effects on rats. *Psychopharmacology*. (2021) 238:281–92. doi: 10.1007/s00213-020-05681-y
41. Simpson CA, Diaz-Arteche C, Eliby D, Schwartz OS, Simmons JG, Cowan CSM. The gut microbiota in anxiety and depression - a systematic review. *Clin Psychol Rev*. (2021) 83:101943. doi: 10.1016/j.cpr.2020.101943
42. Kaakoush NO. *Sutterella* species, IgA-degrading bacteria in ulcerative colitis. *Trends Microbiol*. (2020) 28:519–22. doi: 10.1016/j.tim.2020.02.018
43. Moon C, Baldridge MT, Wallace MA, D CA, Burnham, Virgin HW, et al. Vertically transmitted faecal IgA levels determine extra-chromosomal phenotypic variation. *Nature*. (2015) 521:90–3. doi: 10.1038/nature14139
44. Hansen IS, Baeten DLP, den Dunnen J. The inflammatory function of human IgA. *Cell Mol Life Sci*. (2019) 76:1041–55. doi: 10.1007/s00018-018-2976-8
45. Hiippala K, Kainulainen V, Kalliomäki M, Arkkila P, Satokari R. Mucosal prevalence and interactions with the epithelium indicate commensalism of *Sutterella* spp. *Front Microbiol*. (2016) 7:1706. doi: 10.3389/fmicb.2016.01706
46. Mukhopadhya I, Hansen R, Nicholl CE, Alhaidan YA, Thomson JM, Berry SH, et al. A comprehensive evaluation of colonic mucosal isolates of *Sutterella wadsworthensis* from inflammatory bowel disease. *PLoS ONE*. (2011) 6:e27076. doi: 10.1371/journal.pone.0027076
47. Mancabelli L, Milani C, Lugli GA, Turroni F, Ferrario C, van Sinderen D, et al. Meta-analysis of the human gut microbiome from urbanized and pre-agricultural populations. *Environ Microbiol*. (2017) 19:1379–90. doi: 10.1111/1462-2920.13692
48. Wang Y, Ames NP, Tun HM, Tosh SM, Jones PJ, Khafipour E. High molecular weight barley β-glucan alters gut microbiota toward reduced cardiovascular disease risk. *Front Microbiol*. (2016) 7:129. doi: 10.3389/fmicb.2016.00129
49. Ley RE. Gut microbiota in 2015: prevotella in the gut: choose carefully. *Nat Rev Gastroenterol Hepatol*. (2016) 13:69–70. doi: 10.1038/nrgastro.2016.4
50. Geva-Zatorsky N, Sefik E, Kua L, Pasman L, Tan TG, Ortiz-Lopez A, et al. Mining the human gut microbiota for immunomodulatory organisms. *Cell*. (2017) 168:928–43.e11. doi: 10.1016/j.cell.2017.01.022
51. Larsen JM. The immune response to Prevotella bacteria in chronic inflammatory disease. *Immunology*. (2017) 151:363–74. doi: 10.1111/imm.12760

52. Su T, Liu R, Lee A, Long Y, Du L, Lai S, et al. Altered intestinal microbiota with increased abundance of prevotella is associated with high risk of diarrhea-predominant irritable bowel syndrome. *Gastroenterol Res Pract*. (2018) 2018:6961783. doi: 10.1155/2018/6961783
53. Iljazovic A, Roy U, Gálvez EJC, Lesker TR, Zhao B, Gronow A, et al. Perturbation of the gut microbiome by Prevotella spp. enhances host susceptibility to mucosal inflammation. *Mucosal Immunol*. (2021) 14:113–24. doi: 10.1038/s41385-020-0296-4
54. Zhang L, Song P, Zhang X, Metea C, Schleisman M, Karstens L, et al. Alpha-glucosidase inhibitors alter gut microbiota and ameliorate collagen-induced arthritis. *Front Pharmacol*. (2019) 10:1684. doi: 10.3389/fphar.2019.01684
55. Mager LF, Burkhard R, Pett N, Cooke NCA, Brown K, Ramay H, et al. Microbiome-derived inosine modulates response to checkpoint inhibitor immunotherapy. *Science*. (2020) 369:1481–9. doi: 10.1126/science.abc3421
56. Fukumoto S, Tatewaki M, Yamada T, Fujimiya M, Mantyh C, Voss M, et al. Short-chain fatty acids stimulate colonic transit via intraluminal 5-HT release in rats. *Am J Physiol Regul Integr Comp Physiol*. (2003) 284:R1269–76. doi: 10.1152/ajpregu.00442.2002
57. Yano JM, Yu K, Donaldson GP, Shastri GG, Ann P, Ma L, et al. Indigenous bacteria from the gut microbiota regulate host serotonin biosynthesis. *Cell*. (2015) 161:264–76. doi: 10.1016/j.cell.2015.02.047
58. Diao H, Jiao A, Yu B, He J, Zheng P, Yu J, et al. Beet pulp: an alternative to improve the gut health of growing pigs. *Animals*. (2020) 10:1860. doi: 10.3390/ani10101860
59. Al-Lahham SH, Peppelenbosch MP, Roelofsen H, Vonk RJ, Venema K. Biological effects of propionic acid in humans; metabolism, potential applications and underlying mechanisms. *Biochim Biophys Acta*. (2010) 1801:1175–83. doi: 10.1016/j.bbalip.2010.07.007
60. MacFabe DF, Cain NE, Boon F, Ossenkopp KP, Cain DP. Effects of the enteric bacterial metabolic product propionic acid on object-directed behavior, social behavior, cognition, and neuroinflammation in adolescent rats: relevance to autism spectrum disorder. *Behav Brain Res*. (2011) 217:47–54. doi: 10.1016/j.bbr.2010.10.005
61. Shultz SR, Aziz NA, Yang L, Sun M, MacFabe DF, O'Brien TJ. Intracerebroventricular injection of propionic acid, an enteric metabolite implicated in autism, induces social abnormalities that do not differ between seizure-prone (FAST) and seizure-resistant (SLOW) rats. *Behav Brain Res*. (2015) 278:542–8. doi: 10.1016/j.bbr.2014.10.050

Conflict of Interest: The authors declare that the research was conducted in the absence of any commercial or financial relationships that could be construed as a potential conflict of interest.

Publisher's Note: All claims expressed in this article are solely those of the authors and do not necessarily represent those of their affiliated organizations, or those of the publisher, the editors and the reviewers. Any product that may be evaluated in this article, or claim that may be made by its manufacturer, is not guaranteed or endorsed by the publisher.

frontiers in Nutrition

REVIEW
published: 10 November 2021
doi: 10.3389/fnut.2021.766606

Studies and Application of Sialylated Milk Components on Regulating Neonatal Gut Microbiota and Health

Yushuang Wang[1†], Xiaolei Ze[2†], Binqi Rui[1], Xinke Li[1], Nina Zeng[2], Jieli Yuan[1], Wenzhe Li[1], Jingyu Yan[3] and Ming Li[1]*

[1] College of Basic Medical Science, Dalian Medical University, Dalian, China, [2] Science and Technology Centre, By-Health Co., Ltd., Guangzhou, China, [3] Key Laboratory of Separation Science for Analytical Chemistry, Dalian Institute of Chemical Physics, Chinese Academy of Sciences (CAS), Dalian, China

Breast milk is rich in sialic acids (SA), which are commonly combined with milk oligosaccharides and glycoconjugates. As a functional nutrient component, SA-containing milk components have received increasing attention in recent years. Sialylated human milk oligosaccharides (HMOs) have been demonstrated to promote the growth and metabolism of beneficial gut microbiota in infants, bringing positive outcomes to intestinal health and immune function. They also exhibit antiviral and bacteriostatic activities in the intestinal mucosa of new-borns, thereby inhibiting the adhesion of pathogens to host cells. These properties play a pivotal role in regulating the intestinal microbial ecosystem and preventing the occurrence of neonatal inflammatory diseases. In addition, some recent studies also support the promoting effects of sialylated HMOs on neonatal bone and brain development. In addition to HMOs, sialylated glycoproteins and glycolipids are abundant in milk, and are also critical to neonatal health. This article reviews the current research progress in the regulation of sialylated milk oligosaccharides and glycoconjugates on neonatal gut microbiota and health.

Keywords: breast milk, sialic acids, oligosaccharides, glycoconjugates, new-born, gut microbiota

OPEN ACCESS

Edited by:
Fengjiao Xin,
Institute of Food Science and Technology, Chinese Academy of Agricultural Science (CAAS), China

Reviewed by:
Yanfeng Liu,
Jiangnan University, China
Xiangfang Zeng,
China Agricultural University, China

****Correspondence:***
Ming Li
vivianmarat@163.com

† These authors have contributed equally to this work

Specialty section:
This article was submitted to Nutrition and Microbes, a section of the journal Frontiers in Nutrition

Received: *29 August 2021*
Accepted: *18 October 2021*
Published: *10 November 2021*

Citation:
Wang Y, Ze X, Rui B, Li X, Zeng N, Yuan J, Li W, Yan J and Li M (2021) Studies and Application of Sialylated Milk Components on Regulating Neonatal Gut Microbiota and Health. Front. Nutr. 8:766606. doi: 10.3389/fnut.2021.766606

INTRODUCTION

Sialic acid (SA), known as N-acetylneuraminic acid (Neu5Ac), was originally isolated from bovine mandibular salivary gland mucin by a scientist named Blix. It is a negatively charged acidic monosaccharide containing nine carbon atoms, with a free carboxyl group at the anomeric carbon C2, and an N-acetyl group at C5 (1–3). More than 50 forms of SA have been found in nature, of which more than 15 have been identified in humans (4). SA is an essential functional sugar with multiple known roles (**Figure 1**), which are crucial for infant health, promoting the development of the brain and nervous system, and enhancing immunity. SA can also increase the absorption of minerals and vitamins in the intestinal tract and promote bone development (5). SA also demonstrates pharmaceutical value due to its anti-adhesion, antiviral, and anti-cancer properties, and plays a vital role in red stabilization and prevent blood component aggregation by its negative charge and hydrophilicity. SA also affects fertilization and plays an important role in biological recognition and diseases (2).

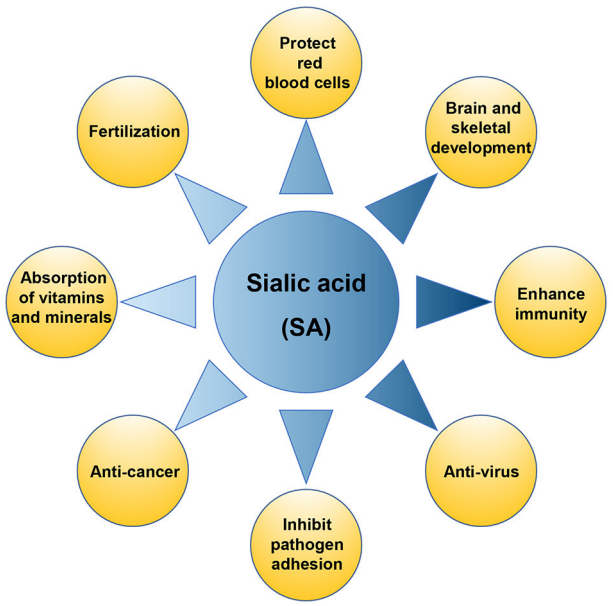

FIGURE 1 | The physiological function of sialic acid (SA).

SA is very abundant in human milk, as ∼70–83% of all SA are bound to human milk oligosaccharides (HMOs), 14–28% are bound to glycoproteins, and 0.2–0.4% to glycolipids, whereas the free form of SA is only 2–3% in human milk (6, 7). Recent studies showed that HMOs play an essential role in regulating neonatal intestinal microecology. Among these HMOs, ∼10–30% of oligosaccharides are sialylated (6, 8). In addition to HMOs, sialylated glycoproteins and glycolipids in milk are also abundant and critical to neonatal health (6), they were found regulate intestinal microbial ecosystem and prevent development of neonatal diseases by promoting probiotic growth and metabolism, inhibiting pathogen adhesion, inducing intestinal epithelial differentiation, promoting intestinal maturation, and optimizing immune function (6, 7, 9–11). Some recent studies also support the promoting effects of sialylated milk components on neonatal bone and brain development (12, 13).

Given the important role of intestinal gut microbes in infant nutrition and health, as well as the development of immune system, this article reviews the research progress in the regulation of sialylated milk oligosaccharides and glycoconjugates on neonatal gut microbiota and health. Although some of their effects on neonatal health have been reviewed in the past, the content has been incomplete and most of the discussion has focused on sialylated oligosaccharides. Here we focused on the regulation of sialylated milk components on neonatal gut microbiota, and updated new related researches for better understanding the important role of sialylated milk components in improving neonatal physiology and health through regulating neonatal gut microbiota.

Abbreviations: SA, Sialic acid; Neu5Ac, N-acetylneuraminic acid; HMOs, human milk oligosaccharides; Glc, glucose; Gal, galactose; GlcNAc, N-acetylglucosamine; Fuc, fucose; SL, sialyllactose; 3′-SL, 3′-sialyllactose; 6′-SL, 6′-sialyllactose; LSTa, LS-tetra-saccharide a; LSTb, LS-tetra-saccharide b; LSTc, LS-tera-saccharide c; DSLNT, disialyllacto-N-tetraose; SLN, sialyllactosamine; 3'-S-3-FL, 3'-sialyl-3-fucosyllactose; FUT2, fucosyltransferase-2; GDM, gestational diabetes mellitus; RSV, respiratory syncytial virus; AI, avian influenza; GBS, Group B Streptococcus; SCFAs, short chain fatty acids; SiabB2, exo-α-sialidase gene; NanH1 and NanH2, sialidase encoding genes; DMOs, donkey milk oligosaccharides; EGFR, epidermal growth factor receptor; EGF, epidermal growth factor; GDNF, glial-derived neurotrophic factor; PolySia, Polysialic acid; CREB, cAMP responsive element-binding protein; GPR35, G-protein coupled receptor 35; S-BMO, sialylated bovine milk oligosaccharides; mIns, myo-inositol; Glx, glutamate + glutamine; NAA, N-acetylaspartate; SI, scyllo-Inositol; KO, knockout; NEC, necrotizing enterocolitis; ETEC, enterotoxigenic Escherichia coli; EPEC, enteropathogenic Escherichia coli; UPEC, uropathogenic Escherichia coli; LF, lactoferrin; sIgA, secretory immunoglobulin A; HLF, human lactoferrin; BLF, bovine lactoferrin; Tregs, T regulatory cells; GMP, glycomacropeptide; OPN, Osteopontin; BSSL, Bile salt-stimulated lipase; MFGM, milk fat globule membrane; GAs, gangliosides; GM3, monosialoganglioside 3; GD3, disialoganglioside 3; HPLC, high performance liquid chromatography; HPAEC, high-performance anion-exchange chromatography; PAD, pulsed amperometry detection; LC-MS, liquid chromatography with mass spectrometry; MRM, multiple reaction monitoring; CE, capillary electrophoresis; NMR, nuclear magnetic resonance; nano-LC-chip-TOF, nano-liquid chromatography-chip-time of flight; HILIC, hydrophilic interaction chromatography; MS, mass spectrometry; SPE, solid-phase extraction; ESI-CID-MS/MS, Collision-induced dissociation tandem ESI-MS.

THE SIALYLATED COMPONENTS IN MILK

The Structures of Sialylated Milk Components

The Structures of Sialylated Milk Oligosaccharides

Human milk oligosaccharide is the most common solid component in breast milk, which is the third most abundant breast milk component, after lactose and lipids (14). It comprises D-glucose (Glc), D-galactose (Gal), N-acetylglucosamine (GlcNAc), L-fucose (Fuc), and Neu5Ac. So far, more than 200 HMO structures have been identified. These HMOs range from 3 to 32 monosaccharides in size and indigestible by the host (15). HMOs are divided into acidic and neutral oligosaccharides. Acidic oligosaccharides contain SA molecules, while neutral oligosaccharides do not (7). Neu5Ac is the only form of SA found in human milk, while milk of other mammals may also contain N-glycolylneuraminic acid (Neu5Gc)-bound oligosaccharides (16). Sialylated HMOs are mainly composed of 3′-sialyllactose (3′-SL), 6′-sialyllactose (6′-SL), LS-tetra-saccharide a (LSTa), LS-tetra-saccharide b (LSTb), LS-tera-saccharide c (LSTc), and disialyllacto-N-tetraose (DSLNT) (17, 18) (**Figure 2A**), and the concentration of them is about 1,000–3,300 mg/L in the colostrum and droped to about 135–2,150 mg/L in the matured human milk (**Table 1**). Among all sialylated HMOs, the content of sialyllactose (SL) is the highest, with an estimated concentration of 170–500 μg/mL for 6′-SL in mature breast milk (6, 22–24). SL play important roles in neonatal gut maturation, prevention of pathogen invasion, immune regulation, and prebiotic function (33).

The Structures of Sialylated Milk Glycoconjugates

Sialylated Glycoproteins in Milk

Researchers estimated that up to 70% of human milk proteins are glycosylated, and these proteins help shape the intestines and immune system of developing infants (34). The most abundant human milk glycoproteins include lactoferrin

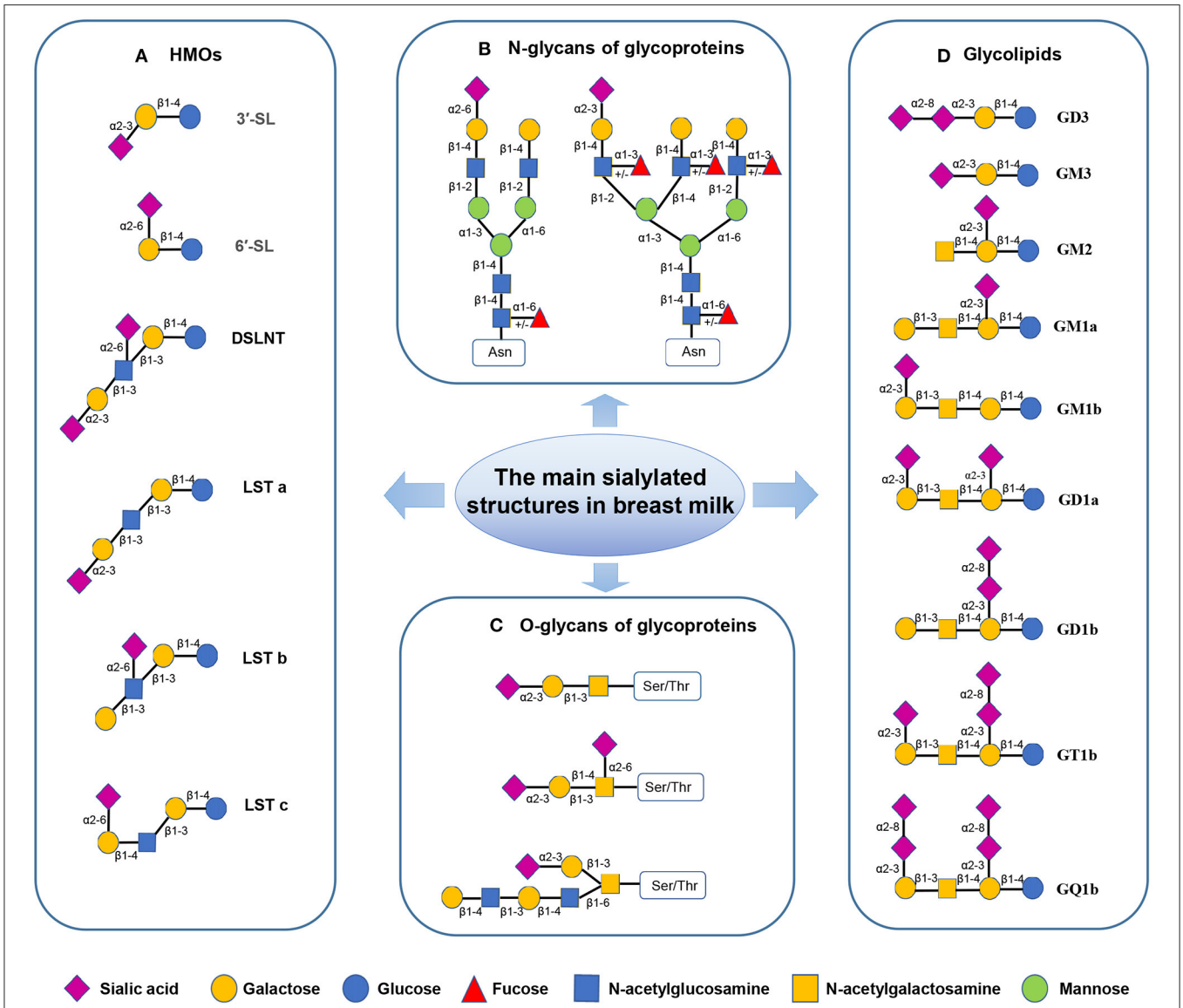

FIGURE 2 | The sialylated structures in breast milk (7, 17–20). (Monosaccharide key is shown at the bottom of the figure.) **(A)** Sialylated HMOs: lactose can be fucosylated or sialylated in different linkages to generate trisaccharides, such as 3′-SL and 6′-SL; The elongated chains can be sialylated by α2–3 or α2–6 linkages at the terminal positions forming structural isomers, such as DSLNT and LST. **(B)** Sialylated N-glycans of glycoproteins: The two most common structures in human milk N-glycome are presented; Asn-asparagine. **(C)** Sialylated O-glycans of glycoproteins; Ser-serine, Thr-threonine. **(D)** Gangliosides: In Svennerholm nomenclature, the capital letter "G" is used to denote the core saccharide of the "Ganglio" series, followed by the capital letters (M, D, T, Q) to indicate the total number of sialic acids. The following *Arabic numerals* (1–4) denote the length of the neutral core (21).

(LF, 17% of total protein), α-lactalbumin (17%), secretory immunoglobulin A (sIgA, 11%), and κ-casein (9%). The antipathogenic effects of human milk glycoproteins, such as LF, κ-casein, sIgA can be partly attributed to their sialylated glycan moieties (27).

Lactoferrin (LF)

LF is a highly sialylated iron-binding glycoprotein, which is the most abundant glycoprotein (80 KDa) in human milk, accounting for 1/4 of the total protein in human milk (35). Its concentration is highest in colostrum approximately 9.7 g/L and declines to 2–3 g/L in humans' mature milk (**Table 1**). LF concentration in mature bovine milk is 0.03 g/L−0.1 g/L, about 1/10 of that in human milk (28). Human lactoferrin (HLF) exhibits three potential N-glycosylation sites (Asn137, Asn478, and Asn623) (36, 37). In contrast, bovine lactoferrin (BLF) exhibits five (Asn233, Asn281, Asn368, Asn476, and Asn545). Alternatively, murine LF exhibits only one potential N-glycosylation site: Asn476. Glycans attached through N-glycosidic bonds may contribute to the functional activity of LF (38, 39). Researchers reported that HLF possesses multiple sialylated or fucosylated N-glycans

TABLE 1 | The concentrations of sialylated oligosaccharides and glycoconjugates in human milk.

Structures	Concentration in human milk (mg/L)			References
	Colostrum	Transitional	Mature	
Total Sialylated HMO	1,000–3,300	n.a.	135–2,150	(6)
6′-SL	250–1,300	n.a.	170–500	(6, 22–24)
3′-SL	90–350	n.a.	170 - 500	(6, 22–24)
DSLNT		78–2,500*		(25)
LSTa/b	n.a.	104 ± 46	31 ± 25	(26)
LSTc	n.a.	488 ± 224	11 ± 8	(26)
6′-SLN	n.a.	15 ± 15	5 ± 1	(26)
Total protein	8,000–10,000	n.a.	7,000–8,000	(27)
LF	9,700	n.a.	2,000–3,000	(28)
SIgA		6.51–1,359.61*		(29)
Mucins		729 ± 75*		(30)
κ-casein	450 ± 80	n.a.	1,050 ± 280	(31)
OPN	178.0 ± 17.9	n.a.	48.3 ± 10.2	(32)
BSSL		100–200*		(30)
Total GA	n.a.	21.18 ± 11.46	20.18 ± 9.75	(26)
GM3	n.a.	9.47 ± 8.37	18.62 ± 9.69	(26)
GD3	n.a.	11.71 ± 9.46	1.57 ± 2.24	(26)

*n.a. = Data not available. *The stages of breast milk samples were not indicated.*
Values (mg/L) are means ± standard deviation.

(**Figure 2B**), which exhibit highly branched complexes or hybrid or both (40).

κ-casein

κ-casein is another major glycoprotein in human milk, especially rich in the matured human milk (**Table 1**). It possesses seven O-glycosylation sites at its C-terminal (27). Its carbohydrate content is 40–60%, while bovine κ-casein carbohydrates are only ∼10% (41). Compared with bovine κ-casein, the glycan part of human κ-casein is rich in SA (6).

Secretory Immunoglobulin A (sIgA)

SIgA is a heavily glycosylated protein, built from "fucose, galactose, SA, and mannose residues." Moreover, monosaccharides, namely, GlcNAc is missing (42, 43). SIgA exhibits both N-linked and O-linked glycans (**Figure 2C**). More than 75% of the N-glycans in the J chain are sialylated, while <15% of the N-glycans in the H chain are sialylated (43). SIgA accounts for 80–90% of all immunoglobulins in human milk, with the highest concentrations found in premature mothers' colostrum and breast milk (**Table 1**).

Mucin

Mucin is an acidic glycoprotein with high molecular weight, ranging in size from 200 KDa to 2,000 KDa. Lactadherin is a mucin-related sialylated glycoprotein in the milk fat globule membrane (MFGM), which includes five N-linked glycosylation sites.

Osteopontin (OPN)

OPN is an acidic glycosylated protein with rich SA (44), which is found in high levels in breast milk (**Table 1**) but in low levels in milk and infant formula, and is an important immunoactive protein in breast milk. The glycosylation of OPN was dominated by O-glycan. Studies have shown that OPN plays an important role in improving immunity, promoting intestinal health and promoting cognitive development in infancy (45).

Bile Salt-Stimulated Lipase (BSSL)

BSSL is a highly glycosylated protein in human milk, with 10 potential O-linked glycosylation sites at the C-terminus of the protein, heavily decorated with carbohydrates including galactose, glucosamine, fucose, galactosamine and SA in molar ratios of 3:2:1:1:0.3, respectively (27). The concentration of BSSL in colostrum of GDM mothers was lower than that of normal mothers. BSSL helps infants digest fat early in life, and its levels are associated with breastfeeding (46). Purification and characterization of recombinant human bile salt-stimulated lipase expressed in milk of transgenic cloned cows (27).

Sialylated Glycolipids in Milk

Glycolipids of human milk are divided into neutral glycolipids-without SA and acidic glycolipids-containing SA (such as gangliosides). Gangliosides (GAs) are the most abundant in human milk glycolipids (**Table 1**) (47–50). Many types of GAs exist in breast milk, such as GD3, GM3, GM2, GM1a, GM1b, GD1a, GD1b, GT1b and GQ1b, among which monosialoganglioside 3 (GM3) and disialoganglioside 3 (GD3) are key (51) (**Figure 2D**). In breast milk, the content and distribution of GAs change during lactation and vary between

individuals. GD3 is the most abundant GA in colostrum, whereas GM3 is the main GA in mature milk (27). Milk GAs seem to prevent the adhesion of pathogens and improved the intestinal ecology of new-borns. GM3 is a receptor analog of intestinal cells, which can resist pathogens, such as enterotoxigenic and EPEC, and it has a protective role against infections (52).

Factors Affect the Levels of Sialylated Components in Milk

Sialylated oligosaccharides are a crucial component of HMOs, especially in the early stages of breast feeding, as they account for 20–30% of the total HMOs, and keep decreasing along with the extension of lactation process (53). The composition and concentration of HMOs vary among individual mothers and change during different lactation stages (54–56). The variation among different mothers is in part due to the genetic polymorphisms in fucosyltransferase-2 (FUT2) and FUT3, which encode the Secretor and Lewis genes, respectively. The polymorphisms in these genes altered the activities of fucosyltranserase and thus lead to distinct fucosylation patterns of HMOs (54, 55, 57, 58). However, the levels of sialylated HMOs were also found affected by mothers' secretor status. Xu et al. reported a higher content of sialylated HMOs in milk of non-secretor compared to milk of secretor mothers, they found that the sialylation level of secretory mothers is 26% lower than that of non-secretory mothers on the 120th day after birth (56, 59), while others found no difference (60, 61). In a study on the effects of breast milk oligosaccharides on iron and galactose oligosaccharide interventions in Kenyan infants, researchers found no significant anthropometric difference at baseline between infants of secretory and non-secretory mothers (61). Another study on stunted infants in Malawi found that non-secretory mothers of severely stunted infants exhibited lower concentrations of sialylated and fucosylated breast milk HMOs than those of non-secretory mothers of healthy infants (29). In addition to genetic factors, environmental factors such as geographic location and maternal nutritional status may also influence HMO concentration and composition (62–64). Preterm milk is another factor to affect HMOs concentration and composition. Alteration in concentration of sialylated HMOs were found in preterm milk, in particular the concentration of 3′-SL was elevated (65). Interestingly, HMOs were also detected in the serum of pregnant women and with increasing concentrations along with pregnancy (65). In a prospective longitudinal cohort study including 87 overweight or obese women, Jantscher-Krennand et al. (66) found that the sialylated HMOs, including 3′-SL and 3′-sialyllactosamine (3′-SLN), in serum of the pregnant women, were positively associated with fasting glucose level, suggesting that metabolism alterations during pregnancy may also affect HMOs pattern, and this influence may last till lactation to affect the infants. A previous study of our group (67) using mouse models with high-fat diet and streptozotocin-induced gestational diabetes mellitus (GDM) found that, there was a decreasing pattern in the concentration of milk oligosaccharides of GDM mice compared with that of the control mice, but with no significant statistic differences. However, the milk of GDM maternal mice contained significantly higher concentrations of fucosylated and sialylated N-glycans than the control mice. The alteration in milk glycobiome of GDM mice had direct effects on the intestinal microbiome of the offspring, which in turn affected their immune responses. Given this study is based on mouse models, which differs largely from human samples, future studies in the feature of HMOs of GDM mothers, as well as the pattern of glycoconjugates in human milk are urgently needed and will lay a foundation for the development of specific nutritional care for the GDM infants. In addition to HMOs, the levels of milk protein and lipids can also be affected by many maternal factors, including smoking, BMI, birth route, pregnancy weight gain, and energy intake during lactation. For example, Aksan et al. (68) have detected significant correlations between body weight, length, and head circumference, respectively, and OPN levels after one ($r = 0.442$, $p = < 0.001$; $r = -0.284$, $p = < 0.001$; $r = -0.392$, $p = < 0.001$) and 3 months ($r = 0.501$, $p = < 0.001$; $r = -0.450$, $p = < 0.001$; $r = -0.498$, $p = < 0.001$) of lactation.

TABLE 2 | The key technologies and methods for investigating sialylated oligosaccharides and glycoconjugates in milk.

Technologies and methods	References
Milk oligosaccharides	
High performance liquid chromatography, HPLC	(69)
High-performance anion-exchange chromatography, HPAEC	(70)
Pulsed amperometry detection, HPAE-PAD	(61)
Liquid chromatography with mass spectrometry and multiple reaction monitoring, LC-MS/MS-MRM	(71)
Capillary electrophoresis, CE	(72)
Nuclear magnetic resonance, NMR	(73)
Nano-liquid chromatography-chip-time of flight, Nano-LC-chip-TOF	(74)
Hydrophilic interaction chromatography, ESI-CID-MS/MS	(75, 76)
Collision-induced dissociation tandem ESI-MS, SPE-HILIC-MS	(75, 76)
Milk glycoconjugates	
Mass spectrometry, MS	(43)
HPLC	(43)
LC-ESI-MS/MS	(43)
Nano-LC-chip-TOF	(43, 52)
HPLC-MS	(77, 78)

Technologies and Methods of Investigating Sialylated Milk Components

The key technologies and methods of investigating sialylated oligosaccharides and glycocomplex in recent years are summarized in **Table 2**. The most common analytical method used to quantify HMOs were high performance liquid chromatography (HPLC) (69) with fluorescence detection and high-performance anion-exchange chromatography (HPAEC) (70) with pulsed amperometry detection (PAD) (61). Other methods involved LC-MS (liquid chromatography with mass spectrometry)/MRM (multiple reaction monitoring) (71),

CE (capillary electrophoresis) (72), NMR (nuclear magnetic resonance) (73), and nano-LC-chip-TOF (time of flight) (74) were also used to precisely detect the concentration and structures of the milk oligosaccharides. But for a long period, detection of acid milk oligosaccharides has been a technical problem. In recent years, Yan et al. (75, 76) developted a new method of solid-phase extraction (SPE) with hydrophilic interaction chromatography (HILIC) followed by mass spectrometry (MS) identification for the analysis of sialylated milk oligosaccharides. Collision-induced dissociation tandem ESI-MS (ESI-CID-MS/MS) is then used for sequence and sialic acid α2-3/α2-6 linkage analysis. For the detection of glycoconjugates in milk, the LC-MS method (43) was generally adopted. For example, the most common analytical methods for N-Glycans or O-Glycans were MS, HPLC, LC-ESI-MS/MS and Nano-LC-chip-TOF (43, 52). The ganglioside in breast milk was normally determined by HPLC-MS (77, 78).

EFFECTS OF SIALYLATED MILK COMPONENTS ON NEONATAL GUT MICROBIOTA AND HEALTH

Anti-infection

The Anti-infection Function of Sialylated Milk Oligosaccharides

The intestinal epithelium cells are covered by a large number of glycoproteins such as mucins. The glycans on these glycoproteins are major components of the gastrointestinal mucosa, and provide essential nutrients and ligands to induce host signaling to defense the invasion of pathological microorganisms and regulate the commensal microbiota. SA-containing glycans were found ubiquitously expressed by gastrointestinal epithelial cells (79–81). As the infection receptors, specific sugar residues, particularly sulfated or sialylated glycans on the mucosal surface can be recognized by many viruses. HMOs were found to prevent the colonization of viral pathogens through two proposed mechanisms. Firstly, as the structures of HMOs share homology with glycans on epithelial cell surface, they can prevent the early cellular attachment as soluble decoy receptors for virus or pathogens. For example, the sialic acid-α2,6 galactose (SA-α2,6Gal) epitope was found to be a receptor for human influenza virus (79) and the sialic acid-α2,3 galactose (SA-α2,3Gal) is a receptor for coxackievirus A24 (80). Another way is that HMOs bind to epithelial cell surface receptors to block viral adhesions (82). Therefore, supplement of SA-linked HMOs from mother's milk can protect intestinal cells of the infants from many viral infections, including influenza, rotavirus (83) and the respiratory syncytial virus (RSV). For example, an *in vitro* hemagglutination inhibition assessment of 3′-SL and 6′-SL against thirteen avian influenza (AI) viruses showed that 3′-SL can inhibit almost all subtypes of the tested AI viruses, whereas 6′-SL only exhibited anti-virus activity against few strains such as H1N1, H1N2, and H3N2. Further *in vivo* study found that administration of 3′-SL to H9N2-infected chickens resulted in elimination of the virus within 24 h post infection (84). The underlying mechanism is their ability to bind to haemagglutinin (HA) glycoprotein spikes of the influenza virus (85). Another study had proved that the combination of 3′-SL and 6′-SL was more effective than single application of each of them in binding to VP8* in a porcine rotavirus model. SA-containing HMO was also shown to inhibit rotavirus infectivity *in vitro* (86); however, both acidic and neutral HMOs were able to decreased NSP4 replication during acute rotavirus infectionin *situ*. Laucirica et al. (87) demonstrated that sialylated oligosaccharides can reduce the infectivity of human rotavirus, and they were considered as possible components to inhibit cholera toxin. The rabbit intestinal loop method was used to observe the effect of SL on cholera toxin-induced diarrhea. The results showed that SL was related to the inhibitory activity of milk against cholera toxin (88). In addition, application of 3′-SL has been shown to significantly decrease the cytokine level and RSV viral in airway epithelia (89).

Similar to the anti-virus activities, different sialylated HMOs can also selectively inhibit bacterial pathogens adhesion to sialylated receptors on the intestinal epithelium by direct binding (10). For example, sialylated HMOs have a strong inhibitory effect on hemagglutination induced by enterotoxigenic *Escherichia coli* (ETEC) and uropathogenic *Escherichia coli* (UPEC) (90). 3′-SL was found to bind to *Helicobacter pylori* and enteropathogenic *Escherichia coli* (EPEC) to inhibit their adhesion to human intestinal cells (HT-29, Caco-2) (38, 39, 91). Angeloni et al. (91) found that *in vitro*, 3′-SL reduced the expression of sialyltransferases ST3Gal1, ST3Gal2, and ST3Gal4, resulting in reduced glycosylation on the surface of Caco2 cells, thus reducing 50% reduction of EPEC adhesion. Further the study (92) found that 3′-SL also had an inhibitory effect on *Salmonella fyrisby*. 6′-SL has anti-adhesion effect on *Escherichia coli* O119, but on *Salmonella fyris*. And 6-SL has been shown to effectively inhibit pneumocyte invasion *Pseudomonas aeruginosa* strains. Acidic HMO components have an inhibitory effect on pathogens expressing specific fimbrial types, such as *Escherichia coli* expressing P and CFA fimbriae (92). In addition to *Escherichia coli*, *Streptococcus agalactiae* (Group B Streptococcus, GBS) is another leading cause of invasive bacterial infections in infants. Studies found that HMOs may function as an alternative substrate to modify a GBS component by impairing growth kinetics (93). A recent study demonstrated that sialylated variants of lacto-N-tetraose exert antimicrobial and antibiofilm action against GBS by increasing cellular permeability (94).

The Anti-infection Function of Sialylated Milk Glycoconjugates

The major sialylated glycopriteins in milk also possess the ability to inhibit the infection of both pathogenic bacteria and virus. LF is an antibacterial agent with a bacteriostatic effect on the neonatal intestinal mucosa. Its iron-chelating properties can prevent various pathogen growth dependent on iron proliferation (95, 96). The basis of these mechanisms of action is mainly attributed to the protein trunk; however, the N or O-glycans attached on LF protein may play a vital role. For instants, the SA residue on BLF was found to directly bind to Ca^{2+} ions that otherwise seem to stabilize LPS on the outer membrane of bacteria, and the SA portion of HLF can act in

a similar manner. In addition, LF can act as a decoy to bind to a variety of microbial pathogens, causing these pathogens to deviate from receptor sites on the surface of host cells (27). LF inhibits the adhesion of intestinal enteric to eukaryotic cell lines (96) and the adhesion inhibition of microorganisms to host cells. It exhibits direct cytotoxicity to bacteria, viruses, and fungi (97). Sialylated glycans of human milk κ-casein was found can inhibit the combination of *Streptococcus mutans* GS-5 to saliva-coated hydroxyapatite (98). After entering the intestine, κ-casein is cleaved by proteases to form glycomacropeptide (GMP), which exhibits antimicrobial properties. Casein GMP is the C-terminal part of κ-casein and locates on the 106–109th amino acid. GMP is present in both human and bovine milk (96, 99). κ-casein exhibits multifaceted protective effects on intestinal infection in infants. Researchers reported (27) that the probiotic effect of GMP may be because it contains Neu5Ac. For example, researchers showed that GMP with SA in bovine κ-casein can inhibit the adhesion of enterohemorrhagic *Escherichia coli* and *Salmonella enteritis* to Caco-2 cells. Further, κ-casein can inhibit pathogens' adhesion to the surface of gut cells in infants. Researchers reported (100) that GMP can inhibit splenocyte proliferation induced by concanavalin A and phytohemagglutinin. After neuraminidase digestion, GMP loses its inhibitory activity on mitogen-induced splenocyte proliferation, indicating that SA is the key to this phenomenon. However, after GMP digestion with trypsin and Streptomyces protease, the inhibitory effect was enhanced, indicating that the peptide chain was also involved. Together, studies suggest that κ-casein is crucial for protecting the infant intestinal tract. O-glycans of sIgA can bind to microorganisms, thereby inhibiting pathogens from adhering to the intestinal epithelium (101). Further, sIgA glycans containing SA can be used as bait to prevent pathogenic bacteria from binding to their glycosylated targets on the intestinal mucosa's surface (30, 101). sIgA can effectively inhibit the adhesion of S-fimbrial *Escherichia coli* by the specific interaction between sialylated N-and O-linked glycans and bacterial adhesins, thus, protecting new-borns from sepsis and meningitis caused by these pathogens (43, 101, 102). Also, the sIgA glycan plays a structural and functional role. For instance, sIgA is resistant to proteolytic digestion in the gut due to its glycan moiety attachment. Therefore, sIgA plays a vital role in protecting new-borns from pathogenic infection and promoting intestinal homeostasis. The antipathogenicity properties of lactadherin in human infants are mainly related to the prevention of rotavirus infection (27, 47). Sialylated glycans of milk mucins can bind to rotavirus and inhibit its replication both *in vitro* and *in vivo* (98). Mucin 1 and 4 are two key mucins identified in human MFGM, which can interact with microorganisms (27). The most researched mechanism is that the SA portion of mucin 1 interacts with pathogens, inhibiting pathogens' ability to bind to their sugar chain receptors on the surface of infant host cells. Therefore, mucin 1 exhibits an essential role in innate immune resistance against invasive microorganisms (30, 47). SA is one of the components of intestinal mucin glycans. When mucin is sialylated in the intestine, its molecular structure is more stable. It cannot be easily degraded by bacteria. In contrast, probiotics can increase the synthesis and secretion of mucin to improve intestinal mucosa's biological barrier function (103). *Ruminococcus gnavus* is human intestinal symbiotic bacteria, which can degrade mucin. Also, *Ruminococcus gnavus* ATCC 29149 binds to gut mucus through SA mediation (104). Presently, few studies exist on sialylated mucin in breast milk; therefore, its effect on infant intestinal microecology needs to be further studied in the future.

Promoting the Growth of Beneficial Bacteria

The Promoting Effects of Sialylated Milk Oligosaccharides on Beneficial gut Bacteria

Studies have found that sialylated HMOs play an important role in promoting the growth of beneficial bacteria. For instance, in an *in vitro* study by Zhuo et al. (10), to evaluate the response of individual bacteria to individual components of HMOS, each of 25 major strains isolated from the human gut microbiota was cultured with individual major fucosylated and other sialylated HMOs components. This allowed for an assessment of the effects of specific HMOs on the growth and metabolites of individual microorganisms. The results showed that supplementation with 6′-SL and 3′-SL promoted the growth of *Bifidobacterium lougum*, *Bacteriodes vulgatus*, and *Bacteroides thetaiotaomicron*. Among the 25 strains tested, these bacteria showed higher neuraminidase activity and produced a large amount of lactate or short-chain fatty acids (SCFAs) or both, which are beneficial for intestinal health and immune function in infants and young children (10, 105). An *in vivo* study also showed that addition of bovine derived oligosaccharide mixtures rich in 3′-SL and 6′-SL to infant formula led to changing in gut microbiota of infants (106). Animal studies showed that SL can improve intestinal dysbiosis and reduce anxiety through gut-brain axis (107). Supplementation of formula with SLs can also modulate gut-associated microbiota in neonatal pigs, which may have important health benefits for developing newborns (33).

The 6′-SL and 3′-SL in milk are partially hydrolyzed in the acidic conditions of the infant's stomach and the remaining SLs are utilized by intestinal bacteria such as *Bifidobacterium, Lactobacillus* and *Bacteroides vulgatus*. Kiyohara et al. isolated an exo-α-sialidase gene (SiabB2) from *Bifidobacterium bifidum* JCM1254 through expression cloning. Expression of SiabB2 in *Bifidobacterium longum* 105-A enabled this strain to degrade sialylated oligosaccharides present in human milk, suggesting that SiabB2 plays an essential role in the catabolism of sialylated HMOs by *Bifidobacterium bifidum* (108). *Bifidobacterium longum* subsp. *infantis* was found to express a sialidase that cleaves α2-6 and α2-3 linkages to utilize milk sialyloligosaccharides. Two-candidate sialidase encoding genes (NanH1 and NanH2) have been isolated from *Bifidobacterium longum* subsp. *infantis* ATCC15697 (109). Although NanH1 is the first sialidase-encoding gene that located in a cluster of genes that specialize in the catabolism of SA, the sialidase NanH2 from *Bifidobacterium bifidum* strains were found utilize HMO and degrade milk sialyloligosaccharides on their extracellular surface, but not NanH1, which suggested that NanH1 may be active for other sialylated glycans encountered in the infant's gut (109). A recent study of the consumption of HMOs by strains of

Bifidobacterium breve revealed that all of those tested strains can utilize sialylated lacto-N-tetraose (30). These results indicate that *Bifidobacterium* spp. play an important role in the utilization of sialylated HMOs.

The Promoting Effects of Sialylated Milk Glycoconjugates on the Growth of Beneficial Bacteria

Researchers have found that the abundance of *Bifidobacterium* and *Lactobacillus* in feces of breast-fed new-born was significantly correlated with fecal LF level (110). Expression of enzymes such as Endo-β-N-acetylglucosaminidases by infant-associated *Bifidobacterium* spp. was found to help them to release the complex N-glycans from LF, incubation of the bacterium with HLF or BLF led to the induction of genes associated to import and consumption of HMOs, suggesting linked regulatory mechanisms among these glycans. These findings indicate that HLF can promote the growth of beneficial bacteria and regulate intestinal homeostasis in neonates, thereby contributing to the establishment of a healthy intestinal microbiota profile (15, 111–114). Studies of κ-casein revealed that the GMP part of κ-casein can promote the growth of many beneficial microorganisms in the intestinal tract of infants, including *Bifidobacterium* and *Lactobacillus bifidum*, and thus preventing the colonization of pathogens (27). Some researchers also reported that supplementation of GAs in infant formula, with concentrations similar to those in human milk, can improve the intestinal ecology of premature infants by increasing the abundance of *Bifidobacterium* and reducing the content of *Escherichia coli*, suggesting that GAs play a significant role as prebiotics in the infant gut. In addition to these effects, a number of studies have also revealed that specific *Bifidobacteria* are able to catabolize GAs from milk. For example, *Bifidobacterium infantis* and *Bifidobacterium bifidum were found to* utilize the two milk GAs, GD3 and GM3, whereas *Bifidobacterium breve* did not utilize these GAs (52). And the important role of breast milk GAs in the establishment of intestinal *Bifidobacteria* has also been supported by clinical studies (16).

Promote the Intestinal Maturation and Mucosal Barrier Function of Neonates

Effects of Sialylated Milk Oligosaccharides on Intestinal Maturation and Mucosal Barrier Function of Neonates

The intestinal epithelial cells serve as a physical and biochemical barrier that separates the microbiota from the gut epithelium, and this mucosal barrier can as well-facilitate the communication between microbiota and immune system (115). The fermentation products of SLs from gut bacteria, especially from *Bifidobacterium* spp., are mainly lactate and SCFAs (10, 116). These products play important role in serving as nutrients for epithelial cells (117). For example, using adult and infant human epithelial cell lines and fecal batch cultures, Perdijk et al.'s study (11) found that, 6′-SL and 3′-SL can induce epithelial differentiation and wound repair, the effect may correlate with the upregulation of SCFAs production and increased abundance of *Bacteroides*, *Ruminococcs obeum*, *F. prausnitizii*.

In additon to in-direct effects on intestinal barriers through microbiota-metabolism, SLs have direct effects on intestinal epithelial cell proliferation and differentiation. As early as 2008, some *in vitro* studies have suggested that acidic milk oligosaccharides may inhibit the proliferation of intestinal epithelial cells and induce differentiation (118, 119). This effect is mediated via activation of the epidermal growth factor receptor (EGFR) by interaction of SLs with the carbohydrate moieties on this receptor (119). In the same year, Kuntz et al. (9) reported that 6′-SL directly affects the cell dynamics and promotes epithelial cell differentiation *in vitro*. A study (120) of donkey milk oligosaccharides (DMOs) found that 3′-SL and 6′-SL are the primary oligosaccharides in DMOs, they induce differentiation, promoted apoptosis and inhibited proliferation of HT-29, Caco-2 and human intestinal epithelial cells in a concentration-dependent manner, suggesting that DMOs promote maturation of intestinal epithelial cells. And theses effect was found associated with activation of the p38 pathway and cell cycle arrest at the G2/M phase. Recently, Yang et al. (121) explored the molecular and cellular mechanisms by SL intervention with intestinal maturation in neonatal piglets. They found that treatment of 3′-SL and 6′-SL to piglets can upregulate Ki-67 expression in ileum crypts, increase the width of ileum crypt, and reduce the incidence and severity of diarrhea. Their results showed that SL intervention upregulated the expression level of the glial-derived neurotrophic factor (GDNF) in the ileumof piglets, it also upregulated the mRNA expression level of ST8Sia IV, which is the key polysialyltransferase in the synthesis of Polysialic acid (PolySia)-NCAM. PolySia mediates binding to GDNF, activates Fyn, and increases the expression level of cAMP responsive element-binding protein (CREB) phosphorylation. GDNF promotes cell proliferation by upregulating the CREB, evidenced by the increase in the number and density of Ki-67 positive cells in the crypt. *In vivo* studies showed that CREB and its binding protein are required for the survival of intestinal stem cells, and that overexpression of CREB promotes cell proliferation. Further, SL intervention can significantly reduce the incidence and severity of diarrhea in early weaning of piglets. These results suggest that SL promotes intestinal maturation of neonatal piglets by up-regulating the synthesis of GDNF, Polysia and CREB interaction pathways. Another recent study by Natividad et al. (122) investigated the effects of six industrially available HMOs (2′-FL, 3′-SL, 6′-SL, LNnT, LNT and DFL) alone and in different combinations on epithelial barrier function by using an *in vitro* model of two intestinal epithelial cell lines, Caco-2 and HT29. The results showed tha the six HMOs blend dose-dependently limited the cytokine-induced FD4 translocation and decrease the epithelial permeability post challenge. Similarly, 3 and 5 HMO blends including 3′-SL and 6′-SL also conferred a significant protection against the challenge, which suggested that different abilities of specific HMOs in regulating the intestinal barrier and support the potential of complementing available HMOs combinations to promote intestinal health and protect against intestinal inflammatory diseases. Another *in vivo* study by Holscher et al. (123) also found that individual and combined treatment with 2′-FL, 3′-SL and 6′-SL inhibited the proliferation of small intestinal cell lines HT-29 and Caco-2Bbe, while they

enhanced differentiation of HT-29 and Caco-2Bbe cells. The combination of inhibition of proliferation and induction of differentiation suggests that sialylated HMOs may contribute specifically to the maturation of intestinal epithelial cells (91). Thus, the underlying mechanisms regarding the effects of sialylated HMOs on intestinal epithelial cells need to be further studied. A possible way to explain their effects is the directly activation of G-protein coupled receptor of cells by sialylated HMOs and in tern upregulated the signal transduction pathways downstream (124). Their results showed that one of the pathways by which HMO activates G-protein coupled receptor 35 (GPR35) is through a direct interaction of 6′-SL. GPR35 is a receptor that mediates pain and colitis attenuation. More recently, Tsukahara et al. (125) reported that the use of GPR35 agonists alleviated DSS-induced colitis in mice. They found that GPR35 agonists promoted *in vitro* intestinal epithelial cell migration, which may contribute to damage repair in colitis However, lack of GPR35 leads to a worsening outcome in DSS-induced experimental colitis, suggesting that GPR35 plays an important role in protecting colon inflammation (126). Another study has shown that GPR35 promotes the proliferation of intestinal epithelial cells (127). Therefore, it was proposed that sialylated HMOs may protect neonatal intestinal health by activating GPR35 through the interaction of 6′-SL.

Effects of Sialylated Milk Glycoconjugates on Intestinal Maturation and Mucosal Barrier Function of Neonates

It has been found that LF can reduce the abundance of *Escherichia coli* in colon and promote intestinal maturation, which protects piglets from early weaning diarrhea by up-regulated intestinal gene expression of brain-derived neurotrophic factors, ubiquitin carboxy-terminal hydrolase L1, and alkaline phosphatase activity (128). In addition, the formula containing BLF was found enhanced the proliferation, depth and area of jejunal crypt and the expression of β-catenin mRNA in piglets. The increased expression of β-catenin indicated that Wnt signal may partially mediate the stimulating effect of BLF on intestinal cell proliferation. These findings provide evidence that supporting the role of LF in neonatal intestinal growth and maturation (111). OPN is another milk glycocojugates that have been found to confer protection effects on intestinal maturation and mucosal barrier function of neonates. Based on the potential benefits of OPN in early life, the effects of OPN supplementation on growth, body composition, and intestinal transcriptome in raspus monkey pups were investigated by comparing different feeding patterns including breast milk, OPN formula, and regular formula (129). The results showed that although growth was similar in each group, the intestinal gene expression pattern (such as CUX1 and EGFR) was more similar in the breast milk and OPN formulations groups. In addition, studies have found that OPN in milk can promote the differentiation of intestinal epithelial cells (Caco-2), and stimulate intestinal immunity by upregulating the secretion of IL-18 by intestinal epithelial cells (Caco-2) (45). The possible mechanism by which OPN promotes intestinal health may be through changes in the expression of intestinal genes. For example (129), CUX1 is a protein-encoding gene whose expression product can bind to DNA to further regulate gene expression, influence cell morphological changes and differentiation, and also influence cell life cycle. These processes are crucial to the growth and development of the gut.

Immune Regulation

The Regulation of Sialylated Milk Oligosaccharides on Neonatal Immunity

In addition to regulating bacterial growth and inducing intestinal differentiation, acidic HMOs can affect cytokines' production and lymphocyte maturation. Bode et al. (130) found that acidic fraction of HMOs, mainly 3′-SL and 3′-sialyl-3-fucosyllactose (3′-S-3-FL) significantly inhibited leukocyte rolling and adhesion in a concentration-dependent manner, and therefore serve as anti-inflammatory components to contribute to the lower incidence of inflammatory diseases in human milk-fed infants. Another *in vitro* study (73) showed that acidic HMOs affect cytokine production and activation of cord blood derived T cells, which may influence lymphocyte maturation in breast-fed newborns. They were also found affecting the immune balance of Th1/Th2 by inhibiting the Th2 response of atopic patients, thus regulating the specific immune response of postnatal allergens (56, 90, 131).

3′-SL mediates anti-inflammatory properties by enhancing the expression of peptidoglycan recognition protein 3, a pathogen recognition receptor that has been shown *in vitro* to modulate the inflammatory response (6), and therefore reduce the levels of pro-inflammatory cytokines TNF-α and IL-8 mRNA in Caco-2 cells. It has been showed that supplementation of 3′-SL during infancy could affect bacterial colonization of the nouse intestine, and reduce the susceptibility to DSS-induced colitis during adulthood (132). In this model of colitis, the pro-inflammatory effect of 3′-SL was the direct stimulation of dendritic cells in mesenteric lymph nodes through Toll-like receptor 4, resulted in Th1 and Th17 cells expansion and the overproduction of pro-inflammatory cytokines (133). Although 3′-SL has a pro-inflammatory effect in model with DSS-induced colitis, it is considered to have a protective effect in other aspects (6).

Necrotizing enterocolitis (NEC) is a gut inflammatory disorder which is one of the leading causes of mortality and morbidity of preterm infants (134). Recent studies found that 2′-FL and 6′-SL protect the development of NEC in mouse and pig models by inhibiting the Toll-like receptor 4 signaling pathway. Most importantly, these findings suggest that the use of 2′-FL and 6′ -SL, either alone or in combination, may offer new avenues for prevention of this devastating disease (135). In addition to SL, studies found that another acidic HMO, with high structural specificity, namely DSLNT, can reduce NEC in neonatal rats, and its effect depends on the presence of two SAs (136). However, because the rat model exhibits its limitations, the need to confirm whether the results apply to human infants is paramount. If studies confirm the benefits of DSLNT for human infants, it will be an effective supplement that can be used to prevent or treat NEC in formula-fed infants (136). In a newly published cohort study of premature infants, a total of 80 mothers of preterm infants were sampled to measure DSLNT levels and found that the mothers of NEC infants had lower concentrations of DSLNT in their breast milk compared to the control group

(137). Further sequencing results of infants' gut microbiota showed that the relative abundance of beneficial bacteria (such as *Bifidobacterium*) was higher in the feces of preterm infants fed with high levels of DSLNT in breast milk, while the relative abundance of harmful bacteria represented by *Enterobacterium* was lower. These results suggest that DSLNT may be one of the nutritional strategies to help prevent NEC in premature infants. Further work is needed to determine whether DSLNT functions by regulating the microbiome or by acting directly on the host, for example by structure-specific receptor-mediated means to alter immune function and reduce inflammation (137).

The Regulation of Sialylated Milk Glycoconjugates on Neonatal Immunity

It was found that LF intervention in gilts can improve serum IgA and sIgA levels (36). Clinical trials confirmed that the potential application of BLF may be used to prevent nosocomial sepsis and NEC in premature infants (128). T regulatory cells' (Tregs) level in preterm infants was lower than that in full-term infants, and the level of Tregs increased under LF prevention. Although Treg cells participate in controlling the intestinal immune response of pathogens and strengthen the important role of BLF in controlling intestinal homeostasis (138, 139), however, in a randomized controlled trial of 2,203 infants (112), researchers found that supplementation of LF did not decrease the incidence rate of NEC or infection. In another randomized trial of low-birth-weight preterm infants in Canada (140), still, no clear answer exists to the benefits of BLF in reducing mortality or morbidity in low birth-weight infants. Considering the other beneficial effects of LF, these results of are disappointing; so, further randomized trials and researches that involves larger population of infants should be conducted. In terms of inflammation, LF was found to help reduce of the excessive immune response by blocking various pro-inflammatory cytokines, such as IL-1 β, IL-6, TNF-α, and IL-8, and inhibiting the activity of free radicals (97, 112), which suggested that HLF plays a vital role in balancing the intestinal microbiota and protection from neonatal inflammatory diseases.

sIgA is a key component in human milk for the regulation of neonatal immunity.The mother's milk provides the only source of sIgA for new-borns in the first month after birth and plays as the first immune defense line of human (15). It was found that the glycans on SIgA in breast milk play an important role in connecting innate and acquired immunity (43). In this study, Royle et al. found that the O-glycan regions on the heavy (H) chains and the SC N-glycans of human sIgA have adhesin-binding glycan epitopes including alpha2-6-linked SAs. These glycan epitopes provide sIgA with further bacteria-binding sites in addition to the four Fab-binding sites, thus enabling it to participate in both innate and adaptive immunity.

In a study measuring the biological activity of cow's milk OPN *in vivo* in a mouse model of OPN knockout (KO) (141), similar to wild-type mother-fed pups, pups fed by KO mothers showed inhibitory effects on LPS-induced TNF-α after bovine OPN supplementation, suggesting anti-inflammatory activity of milk OPN. The results of clinical trials have shown that infants fed with OPN-rich formula had less fever than those fed with standard formula. They had an increased proportion of T cells, and TNF-α levels were more similar to those of breast-fed infants, suggesting that OPN may be involved in the development and maturation of the infant's immune system (142). Breast milk OPN is likely to provide beneficial biological activity for breast-fed infants. The OPN active protein from milk is not readily hydrolyzed by the newborn's gastric juices, so most of the OPN active protein can enter the intestinal tract and perform further functions. Animal studies have shown that OPN active protein in milk can stimulate intestinal development and protect intestinal tract (129, 143). At present, *in vivo* studies on the correlation between OPN active protein and NEC are still very limited. Some scholars conducted a study on preterm piglets: the experimental group fed with OPN active protein formula underwent total parenteral nutrition for 2 days and enteral nutrition for 1.5 days. Results showed that OPN active protein formula feeding significantly reduced the disease severity of NEC in preterm piglets compared with conventional formula feeding (144). This also suggests that OPN active protein may have a potential protective effect on the occurrence of NEC in premature infants.

Since some studies showed that GAs may be involved in the activation of T cells and the differentiation of different lymphocyte subsets, the addition of human breast milk GAs or other sources of GAs to infant formula may play an important role in the proliferation, activation, and differentiation of neonatal immune cells, especially those from the intestinal tract (52). GAs can passively prevent infection in the form of "bait" and actively promote the maturity of the infant immune system by regulating immune cell functions and promoting the secretion of cytokines. In an animal experiment (145), scientists observed that in young mice fed GAs-rich milk powder, two cytokine-secreting cells, lamina propria lymphocytes and Pyle-collecting lymphoid, developed earlier and more in number than those in the control group. Another study (146) showed that young mice feed rich in GAs milk powder demonstrated higher levels of sIgA, a crucial immune factor in early life, suggesting better self-protection. In addition to immune protection, GAs are associated with maintaining immune homeostasis. In the early stage of life, new-borns are in a state of immune imbalance, tending to Th2 immunity; that is, it is easy to exhibit excessive immunity, thereby causing allergic reactions. Presently, GD3 can prevent over-immunity by inhibiting the proliferation of dendritic cell $CD4^+$ cells (147).

Promote Growth: Bone and Muscle Development

The Growth Promoting Effects of Sialylated Milk Oligosaccharides on Neonates

In addition to promote the maturation of intestinal barrier, sialylated HMOs were also found able to enhance liver, muscle metabolism by increasing nutrient utilization in undernourished infants (12, 148). A study in two Malawian birth cohorts revealed that the sialylated HMOs are significantly less abundant in milk (6-month-postpartum) of those Malawian mothers with severely stunted infants (148). This study also found that the sialylated bovine milk oligosaccharides (S-BMO) can promote

the augmentation of lean body mass gain of infants in a microbiota-dependent manner. Supplementation of S-BMOs to neonatal mice or gnotobiotic piglets enhanced their ability to utilize nutrients for anabolism, resulted in alteration of the bone morphology and metabolism of liver, muscle, and brain. Another study using mouse models revealed that 3′-SL can inhibit the degradation of cartilage, and upregulate the CO12a1 production to promote cartilage regeneration, which protects against osteoarthritic development in mice (149). By adding purified S-BMO with structures similar to those in human milk to the diet of young germ-free mice that were colonized with cultured bacterial strains from a 6-mo-old stunted infant, Cowardin et al. (12) found an increased femoral trabecular bone volume and cortical thickness, reduced osteoclasts and their bone marrow progenitors, and altered regulators of osteoclastogenesis and mediators of Th2 responses. Compare with the control mice, the S-BMO treated mice exhibited microbiota-dependent increase in cecal levels of succinate and in turn activated the tuft cell signaling pathway that linked to Th2 immune responses. A prominent fucosylated HMO, 2′-FL, failed to elicit these changes in bone biology, highlighting the structural specificity of the S-BMO effects. A mouse model study of collagen-induced arthritis showed that, 3′-SL could reduce the severity and incidence of arthritis, inhibit the formation of synovitis and pannus, and suppress cartilage destruction, which suggested that 3′-SL can serve as an inhibitor of p65 phosphorylation to ameliorate the progression of experimental rheumatoid arthritis (150).

The Growth Promoting Effects of Sialylated Milk Glycoconjugates on Neonates

Studies in infants and animals have proved that milk proteins significantly influence the growth and body composition of neonates (151). Human milk immunomodulatory proteins including LF and sIgA were found time-dependently and differentially associate with development of infant lean mass and adiposity during first 1 year of lactation (152). A rat study by Shama et al. (153) showed that treatment of a human milk-based protein concentrate contained 101 ± 6 g protein/kg in total and 5 ± 1 g lactoferrin/kg of milk solids supported the growth of weanling rats, suggested its potential use for preterm infants. Wu et al. (154) demonstrated that the formula containing hydrolyzed whey protein (hydrolyzed whey/intact casein = 63/37), could support the normal growth of healthy term infants, to a comparable extent to that of breast-fed infants during the first 3 months of life. Gridneva et al. investigated the relationships between infant/maternal body composition and human milk casein, whey and total protein during the first 12 months of lactation (155). Their results showed a differential effect of human milk casein on development of infant body composition during the first year of life, which suggested its potential application in improving outcome for the infants through interventions. Mucin is another source of a microbiological growth factor present in human milk, in the year of 1953, study of Tomarelli et al. (156) had proved that when fed with a basal diet of a composition including mucin approximating that of human milk resulted in increased growth of weanling rats. Interestingly, some studies suggested that milk components such as LF and OPN can form as a complex, which showed increased bioactivities that may possibly improve outcomes in formula-fed infants (157). BSSL in breast milk was also found to facilitate the ability of digestion and absorption of milk fat and promotes growth of small for gestational age preterm infants (158, 159).

Promote Brain Development and Cognition

Effects of Sialylated Milk Oligosaccharides on Brain and Cognition Development of Neonates

The neural cell membranes contain 20 times more SA than other types of membranes, suggesting that SA plays an important role in neural structure (160, 161). Therefore, whether SL has an effective role in promoting neurodevelopment by altering the concentration of important brain metabolites and neurotransmitters attracted many research attentions. In the year of 2016, Jacobi et al. (33) found that both 3′-SL and 6′-SL could increase the ganglisoside (GA) bound SA in the corpus callosum and cerebellum of piglets. And they can also enhance T-maze performance, increased expression level of mRNA glial fibrillary acidic protein gene encoding, and as well as the expression level of myelin basic protein and myelin-associated glycoprotein in piglets (121). In the year of 2019 (161), Wang et al. found a significant increasing effects of SL supplementation on the absolute levels of myo-inositol (mIns) and glutamate + glutamine (Glx) in piglets. They also detected significant positive correlations of brain N-acetylaspartate (NAA), total NAA, mIns, total choline, total creatine, scyllo-Inositol (SI) and glutathione with total white matter volume; Glu and SI with whole brain volume; and SI with whole brain weight respectively. Sialyllactosamine (SLN) and 3′-SL intake were closely correlated with the levels of brain Glu, mlns and Glx in the treatment groups only. This study provided *in vivo* evidences that sialylated milk oligosaccharides can affect neurotransmitters and alter the brain metabolites in piglets. In a recent study, Hauser et al. (13) explored the long-term consequences of selectively depriving mice of specific sialylated HMO during lactation using a gene knockout (KO) mouse model lacking 6′-SL synthesis-related genes. The study found that 6′-SL in breast milk is essential for cognitive development. When observing the microflora function, researchers found that the number of KEGG pathways that changed in St6Gal1 KO mice during lactation was much greater than that in adult mice. Thus, suggesting that the composition of St6Gal1 KO demonstrates a strong impact on the establishment of intestinal microbiota in the early stage of life, especially in weaning from a milk-based diet to a solid diet. However, further research is needed to clarify these aspects. Given the emerging "gut brain axis" and the important role of SL intervention in neonatal intestinal health and disease prevention, future studies will need to assess more precise and deeper molecular mechanisms (124). In addition, study in mice (107) revealed that supplementation of 6′-SL or 3′-SL can release anxiety during stressor tests, and prevent the gut dysbiosis resulting from stress, and help to maintaine normal numbers of doublecortin (DCX)$^+$ immature neurons. The above results suggested the important roles of SLs in ameliorating behavioral responses during stressor

exposure through effects on the microbiota dependent gut-brain axis.

Effects of Sialylated Milk Glycoconjugates on Brain and Cognition Development of Neonates

Emerging research in humans, rodents and piglets suggest that LF and other glycoproteins in milk may play unique roles in brain development and cognitive functions of infants (35, 162). For example, study of Chen et al. (35) in postnatal peglets found that LF supplementation can promote early neurodevelopment and cognition by upregulating the brain-derived neurotrophin factor (BDNF) signaling pathway and polysialylation. This study suggested that, as a SA-rich milk glycoprotein, the sialylated gloycans on LF may contributed significantly to this effect. A randomized, controlled trial carried by Li et al. (163) showed that infants receiving formula supplementated with bovine MFGM and lactoferrin for 1 year accelerated the neurodevelopmental profile and improved language subcategories at day 545. Oh et al. (164) studied the effects of glycated milk casein (Gc) fermented with *Lactobacillus rhamnosus* 4B15 (FGc) on the intestinal microbiota and physiological and behavioral properties in mice under chronic stress, and their results strongly suggested the protective effects of FGc targeting of intestinal microbiota for abnormal brain activity, which is consistent with the view that FGc plays an important role in regulating stress-related gut-brain axis disorders. Milk OPN was also found to increase the brain myelination and cognitive development in mice (165). In addition to glycoproteins, glycolipids in milk also contribute to the development of brain and congnition, as complex lipids are

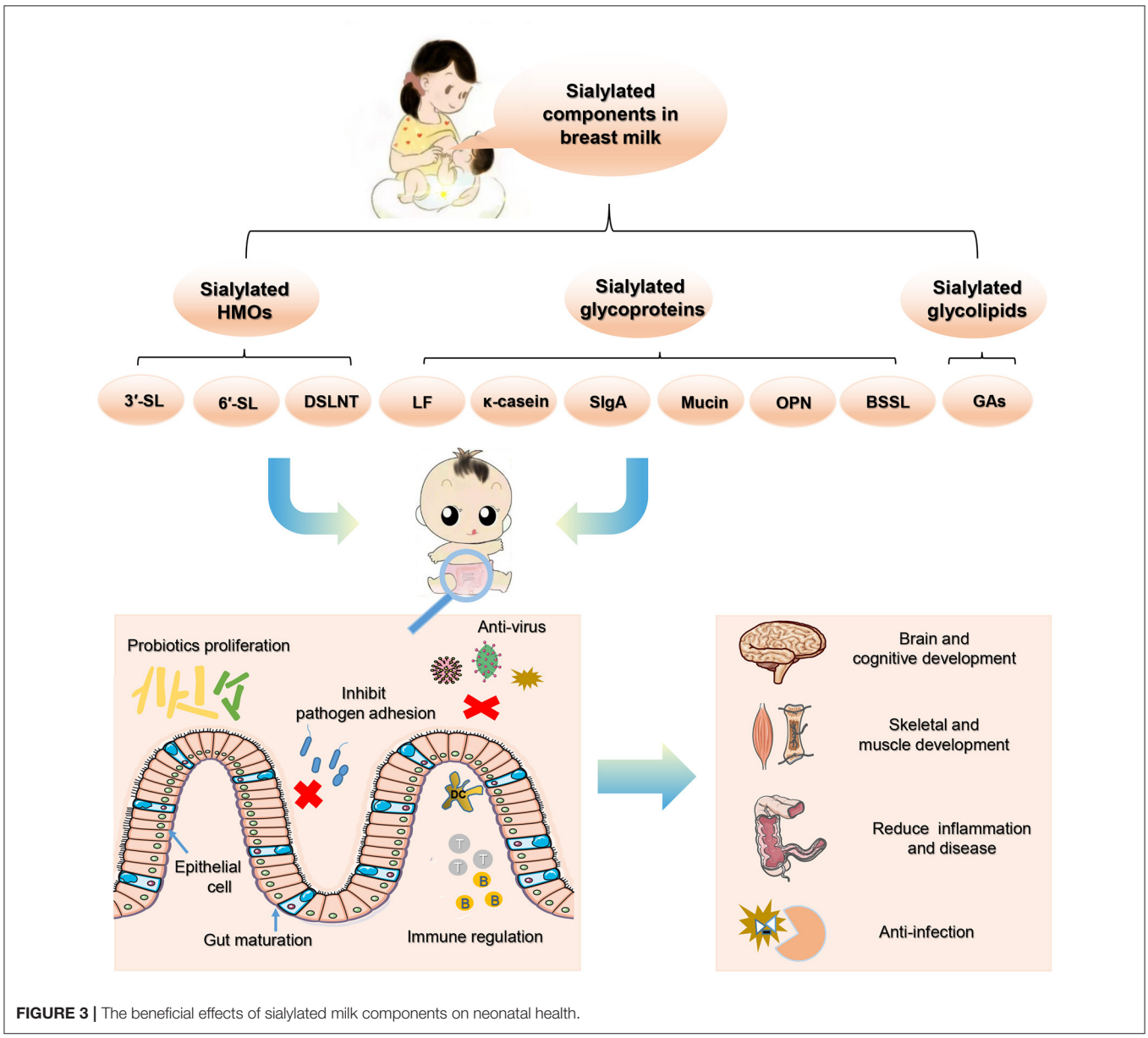

FIGURE 3 | The beneficial effects of sialylated milk components on neonatal health.

important constituents of the central nervous system. Studies have shown that supplementation with complex milk lipids (CML) in pregnancy may increase the level of fetal gangliosides (GA), with the potential to improve cognitive outcomes (166). For example, Liu et al. (167) have reported that early supplementation of phospholipids and gangliosides affects brain and cognitive development in neonatal piglets. A double-blind, randomized, controlled, parallel group clinical trial in which infants received the treatment or control product from 2 to 8 weeks of age until 24 weeks of age. Ganglioside supplementation using complex milk lipids significantly increased the scores for Hand and Eye coordination IQ, Performance IQ and General IQ (168).

FUTURE PERSPECTIVES

To sum up, sialylated milk components exert crucial probiotic and immunomodulatory effects on infant's gut. They play an important role in maintaining colonization resistance, inducing intestinal cell differentiation, promoting intestinal maturation, reducing inflammation, and promoting neonatal growth, all of which are considered to demonstrate significant health benefits to new-borns (**Figure 3**). As sialylated milk oligosaccharides and glycans exhibit local biological activities in the intestines to protect infants, a healthy establishment of the intestinal microbiota plays a key intermediate role to broaden the effects of sialylated milk components. However, most of these studies are based on animal experiments and *in vitro* studies, and in particular, the function of the sialylated glycan parts on milk glycoproteins and glycolipids on infants remain largely unknown. More supporting evidence of the beneficial effects of sialylated milk oligosaccharides and glycans on infant health will greatly promote the development and utilization of SA-containing microecological preparations. Their application to milk formula, healthy maternal and infant food, and medical purposes holds great potential.

AUTHOR CONTRIBUTIONS

YW and XZ wrote a draft version of the manuscript and drew figures. ML, XL, and BR contributed to the design of the review and did the literature search. NZ, WL, JYu, and JYa polished the manuscript and improved the English quality of the manuscript. ML contributed to revised the manuscript and were in charge of the final version of the manuscript. All authors were involved in the conception, preparation of the manuscript, and the final version of the manuscript has been read and approved by all the authors before its submission.

FUNDING

This research was funded by the National Natural Science Foundation of China (Nos. 31900920 and 22074143) and the Dalian Science and Technology Innovation Project (2020JJ27SN068). This work was also supported by Liaoning Provincial Program for Top Discipline of Basic Medical Sciences, China.

REFERENCES

1. Schauer R. Achievements and challenges of sialic acid research. *Glycoconj J.* (2000) 17:485–99. doi: 10.1023/A:1011062223612
2. Varki A. Sialic acids in human health and disease. *Trends Mol Med.* (2008) 14:351–60. doi: 10.1016/j.molmed.2008.06.002
3. Schauer R, Kamerling JP. Exploration of the sialic acid world. *Adv Carbohydr Chem Biochem.* (2018) 75:1–213. doi: 10.1016/bs.accb.2018.09.001
4. Kooner AS, Yu H, Chen X. Synthesis of N-Glycolylneuraminic acid (Neu5Gc) and its glycosides. *Front Immunol.* (2019) 10:2004. doi: 10.3389/fimmu.2019.02004
5. van Karnebeek CD, Bonafé L, Wen XY, Tarailo-Graovac M, Balzano S, Royer-Bertrand B, et al. NANS-mediated synthesis of sialic acid is required for brain and skeletal development. *Nat Genet.* (2016) 48:777–84. doi: 10.1038/ng.3578
6. ten Bruggencate SJ, Bovee-Oudenhoven IM, Feitsma AL, van Hoffen E, Schoterman MH. Functional role and mechanisms of sialyllactose and other sialylated milk oligosaccharides. *Nutr Rev.* (2014) 72:377–89. doi: 10.1111/nure.12106
7. Lis-Kuberka J, Orczyk-Pawiłowicz M. Sialylated oligosaccharides and glycoconjugates of human milk. The impact on infant and newborn protection, development and well-being. *Nutrients.* (2019) 11:306. doi: 10.3390/nu11020306
8. Ninonuevo MR, Park Y, Yin H, Zhang J, Ward RE, Clowers BH, et al. A strategy for annotating the human milk glycome. *J Agric Food Chem.* (2006) 54:7471–80. doi: 10.1021/jf0615810
9. Kuntz S, Rudloff S, Kunz C. Oligosaccharides from human milk influence growth-related characteristics of intestinally transformed and non-transformed intestinal cells. *Br J Nutr.* (2008) 99:462–71. doi: 10.1017/S0007114507824068
10. Yu ZT, Chen C, Newburg DS. Utilization of major fucosylated and sialylated human milk oligosaccharides by isolated human gut microbes. *Glycobiology.* (2013) 23:1281–92. doi: 10.1093/glycob/cwt065
11. Perdijk O, van Baarlen P, Fernandez-Gutierrez MM, van den Brink E, Schuren FHJ, Brugman S, et al. Sialyllactose and galactooligosaccharides promote epithelial barrier functioning and distinctly modulate microbiota composition and short chain fatty acid production *in vitro*. *Front Immunol.* (2019) 10:94. doi: 10.3389/fimmu.2019.00094
12. Cowardin CA, Ahern PP, Kung VL, Hibberd MC, Cheng J, Guruge JL, et al. Mechanisms by which sialylated milk oligosaccharides impact bone biology in a gnotobiotic mouse model of infant undernutrition. *Proc Natl Acad Sci USA.* (2019) 116:11988–96. doi: 10.1073/pnas.1821770116
13. Hauser J, Pisa E, Arias Vásquez A, Tomasi F, Traversa A, Chiodi V, et al. Sialylated human milk oligosaccharides program cognitive development through a non-genomic transmission mode. *Mol Psychiatry.* (2021) 26:2854–71. doi: 10.1038/s41380-021-01054-9
14. Plaza-Díaz J, Fontana L, Gil A. Human milk oligosaccharides and immune system development. *Nutrients.* (2018) 10:1038. doi: 10.3390/nu10081038
15. Thai JD, Gregory KE. Bioactive factors in human breast milk attenuate intestinal inflammation during early life. *Nutrients.* (2020) 12:581. doi: 10.3390/nu12020581
16. Zúñiga M, Monedero V, Yebra MJ. Utilization of host-derived glycans by intestinal lactobacillus and bifidobacterium species. *Front Microbiol.* (2018) 9:1917. doi: 10.3389/fmicb.2018.01917
17. Bode L. Human milk oligosaccharides: every baby needs a sugar mama. *Glycobiology.* (2012) 22:1147–62. doi: 10.1093/glycob/cws074
18. Zhang X, Liu Y, Liu L, Li J, Du G, Chen J. Microbial production of sialic acid and sialylated human milk oligosaccharides: advances and perspectives. *Biotechnol Adv.* (2019) 37:787–800. doi: 10.1016/j.biotechadv.2019.04.011

19. Smilowitz JT, Lebrilla CB, Mills DA, German JB, Freeman SL. Breast milk oligosaccharides: structure-function relationships in the neonate. *Annu Rev Nutr.* (2014) 34:143–69. doi: 10.1146/annurev-nutr-071813-105721
20. Triantis V, Bode L, van Neerven RJJ. Immunological effects of human milk oligosaccharides. *Front Pediatr.* (2018) 6:190. doi: 10.3389/fped.2018.00190
21. Schnaar RL. The biology of gangliosides. *Adv Carbohydr Chem Biochem.* (2019) 76:113–48. doi: 10.1016/bs.accb.2018.09.002
22. Seppo AE, Autran CA, Bode L, Järvinen KM. Human milk oligosaccharides and development of cow's milk allergy in infants. *J Allergy Clin Immunol.* (2017) 139:708–11.e705. doi: 10.1016/j.jaci.2016.08.031
23. Hobbs M, Jahan M, Ghorashi SA, Wang B. Current perspective of sialylated milk oligosaccharides in mammalian milk: implications for brain and gut health of newborns. *Foods.* (2021) 21;10:473. doi: 10.3390/foods10020473
24. Parschat K, Melsaether C, Jäpelt KR, Jennewein S. Clinical evaluation of 16-week supplementation with 5HMO-Mix in healthy-term human infants to determine tolerability, safety, and effect on growth. *Nutrients.* (2021) 13:2871. doi: 10.3390/nu13082871
25. Bao Y, Newburg DS. Capillary electrophoresis of acidic oligosaccharides from human milk. *Electrophoresis.* (2008) 29:2508–15. doi: 10.1002/elps.200700873
26. McJarrow P, Radwan H, Ma L, MacGibbon AKH, Hashim M, Hasan H, et al. Human milk oligosaccharide, phospholipid, and ganglioside concentrations in breast milk from United Arab emirates mothers: results from the MISC cohort. *Nutrients.* (2019) 11:2400. doi: 10.3390/nu11102400
27. Peterson R, Cheah WY, Grinyer J, Packer N. Glycoconjugates in human milk: protecting infants from disease. *Glycobiology.* (2013) 23:1425–38. doi: 10.1093/glycob/cwt072
28. Jahan M, Kracht S, Ho Y, Haque Z, Bhattachatyya BN, Wynn PC, et al. Dietary lactoferrin supplementation to gilts during gestation and lactation improves pig production and immunity. *PLoS ONE.* (2017) 12:e0185817. doi: 10.1371/journal.pone.0185817
29. Hogendorf A, Stańczyk-Przyłuska A, Sieniwicz-Luzeńczyk K, Wiszniewska M, Arendarczyk J, Banasik M, et al. Is there any association between secretory IgA and lactoferrin concentration in mature human milk and food allergy in breastfed children. *Med Wieku Rozwoj.* (2013) 17:47–52.
30. Liu B, Newburg DS. Human milk glycoproteins protect infants against human pathogens. *Breastfeed Med.* (2013) 8:354–62. doi: 10.1089/bfm.2013.0016
31. JLiao Y, Weber D, Xu W, Durbin-Johnson BP, Phinney BS, Lönnerdal B. Absolute quantification of human milk caseins and the whey/casein ratio during the first year of lactation. *J Proteome Res.* (2017) 16:4113–21. doi: 10.1021/acs.jproteome.7b00486
32. Jiang R, Lönnerdal B. Osteopontin in human milk and infant formula affects infant plasma osteopontin concentrations. *Pediatr Res.* (2019) 85:502–5. doi: 10.1038/s41390-018-0271-x
33. Jacobi SK, Yatsunenko T, Li D, Dasgupta S, Yu RK, Berg BM, et al. Dietary isomers of sialyllactose increase ganglioside sialic acid concentrations in the corpus callosum and cerebellum and modulate the colonic microbiota of formula-fed piglets. *J Nutr.* (2016) 146:200–8. doi: 10.3945/jn.115.220152
34. Zhu J, Dingess KA. The functional power of the human milk proteome. *Nutrients.* (2019) 11:1834. doi: 10.3390/nu11081834
35. Chen Y, Zheng Z, Zhu X, Shi Y, Tian D, Zhao F, et al. Lactoferrin promotes early neurodevelopment and cognition in postnatal piglets by upregulating the BDNF signaling pathway and polysialylation. *Mol Neurobiol.* (2015) 52:256–69. doi: 10.1007/s12035-014-8856-9
36. Albar AH, Almehdar HA, Uversky VN, Redwan EM. Structural heterogeneity and multifunctionality of lactoferrin. *Curr Protein Pept Sci.* (2014) 15:778–97. doi: 10.2174/1389203715666140919124530
37. O'Riordan N, Kane M, Joshi L, Hickey RM. Structural and functional characteristics of bovine milk protein glycosylation. *Glycobiology.* (2014) 24:220–36. doi: 10.1093/glycob/cwt162
38. Chaturvedi G, Tewari R, Mrigank, Agnihotri N, Vishwakarma RA, Ganguly NK. Inhibition of helicobacter pylori adherence by a peptide derived from neuraminyl lactose binding adhesin. *Mol Cell Biochem.* (2001) 228:83–9. doi: 10.1023/A:1013314604403
39. Simon PM, Goode PL, Mobasseri A, Zopf D. Inhibition of helicobacter pylori binding to gastrointestinal epithelial cells by sialic acid-containing oligosaccharides. *Infect Immun.* (1997) 65:750–7. doi: 10.1128/iai.65.2.750-757.1997
40. Nwosu CC, Aldredge DL, Lee H, Lerno LA, Zivkovic AM, German JB, et al. Comparison of the human and bovine milk N-glycome via high-performance microfluidic chip liquid chromatography and tandem mass spectrometry. *J Proteome Res.* (2012) 11:2912–24. doi: 10.1021/pr300008u
41. Rudloff S, Kunz C. Protein and nonprotein nitrogen components in human milk, bovine milk, and infant formula: quantitative and qualitative aspects in infant nutrition. *J Pediatr Gastroenterol Nutr.* (1997) 24:328–44. doi: 10.1097/00005176-199703000-00017
42. Hughes GJ, Reason AJ, Savoy L, Jaton J, Frutiger-Hughes S. Carbohydrate moieties in human secretory component. *Biochim Biophys Acta.* (1999) 143:486–93. doi: 10.1016/S0167-4838(99)00168-5
43. Royle L, Roos A, Harvey DJ, Wormald MR, van Gijlswijk-Janssen D, Redwan el-RM, et al. Secretory IgA N- and O-glycans provide a link between the innate and adaptive immune systems. *J Biol Chem.* (2003) 278:20140–53. doi: 10.1074/jbc.M301436200
44. Nemir M, Bhattacharyya D, Li X, Singh K, Mukherjee AB, Mukherjee BB. Targeted inhibition of osteopontin expression in the mammary gland causes abnormal morphogenesis and lactation deficiency. *J Biol Chem.* (2000) 275:969–76. doi: 10.1074/jbc.275.2.969
45. Jiang R, Lönnerdal B. Effects of milk osteopontin on intestine, neurodevelopment, and immunity. *Nestle Nutr Inst Workshop Ser.* (2020) 94:152–7. doi: 10.1159/000505067
46. Sha L, Zhou S, Xi Y, Li R, Li X. The level of bile salt-stimulated lipase in the milk of Chinese women and its association with maternal BMI. *J Biomed Res.* (2019) 34:122–8. doi: 10.7555/jbr.33.20180107
47. Newburg DS. Glycobiology of human milk. *Biochemistry.* (2013) 78:771–85. doi: 10.1134/S0006297913070092
48. Newburg DS, Chaturvedi P. Neutral glycolipids of human and bovine milk. *Lipids.* (1992) 27:923–7. doi: 10.1007/BF02535874
49. Newburg DS, Grave G. Recent advances in human milk glycobiology. *Pediatr Res.* (2014) 75:675–9. doi: 10.1038/pr.2014.24
50. Pan XL, Izumi T. Variation of the ganglioside compositions of human milk, cow's milk and infant formulas. *Early Hum Dev.* (2000) 57:25–31. doi: 10.1016/S0378-3782(99)00051-1
51. Nakano T, Sugawara M, Kawakami H. Sialic acid in human milk: composition and functions. *Acta Paediatr Taiwan.* (2001) 42:11–17.
52. Lee H, Garrido D, Mills DA, Barile D. Hydrolysis of milk gangliosides by infant-gut associated bifidobacteria determined by microfluidic chips and high-resolution mass spectrometry. *Electrophoresis.* (2014) 35:1742–50. doi: 10.1002/elps.201300653
53. Chaturvedi P, Warren CD, Altaye M, Morrow AL, Ruiz-Palacios G, Pickering LK, et al. Fucosylated human milk oligosaccharides vary between individuals and over the course of lactation. *Glycobiology.* (2001) 11:365–72. doi: 10.1093/glycob/11.5.365
54. Thurl S, Munzert M, Henker J, Boehm G, Müller-Werner B, Jelinek J, et al. Variation of human milk oligosaccharides in relation to milk groups and lactational periods. *Br J Nutr.* (2010) 104:1261–71. doi: 10.1017/S0007114510002072
55. Thurl S, Henker J, Siegel M, Tovar K, Sawatzki G. Detection of four human milk groups with respect to lewis blood group dependent oligosaccharides. *Glycoconj J.* (1997) 14:795–9. doi: 10.1023/A:1018529703106
56. Xu G, Davis JC, Goonatilleke E, Smilowitz JT, German JB, Lebrilla CB. Absolute quantitation of human milk oligosaccharides reveals phenotypic variations during lactation. *J Nutr.* (2017) 147:117–24. doi: 10.3945/jn.116.238279
57. Stahl B, Thurl S, Henker J, Siegel M, Finke B, Sawatzki G. Detection of four human milk groups with respect to Lewis-blood-group-dependent oligosaccharides by serologic and chromatographic analysis. *Adv Exp Med Biol.* (2001) 501:299–306. doi: 10.1007/978-1-4615-1371-1_37
58. Bai Y, Tao J, Zhou J, Fan Q, Liu M, Hu Y, et al. Fucosylated human milk oligosaccharides and N-Glycans in the milk of chinese mothers regulate the gut microbiome of their breast-fed infants during different lactation stages. *mSystems.* (2018) 3:e00206–18. doi: 10.1128/mSystems.00206-18
59. Azad MB, Robertson B, Atakora F, Becker AB, Subbarao P, Moraes TJ, et al. Human milk oligosaccharide concentrations are associated with multiple

fixed and modifiable maternal characteristics, environmental factors, and feeding practices. *J Nutr.* (2018) 148:1733–42. doi: 10.1093/jn/nxy175
60. Totten SM, Zivkovic AM, Wu S, Ngyuen U, Freeman SL, Ruhaak LR, et al. Comprehensive profiles of human milk oligosaccharides yield highly sensitive and specific markers for determining secretor status in lactating mothers. *J Proteome Res.* (2012) 11:6124–33. doi: 10.1021/pr300769g
61. Paganini D, Uyoga MA, Kortman GAM, Boekhorst J, Schneeberger S, Karanja S, et al. Maternal human milk oligosaccharide profile modulates the impact of an intervention with iron and galacto-oligosaccharides in kenyan infants. *Nutrients.* (2019) 11:2596. doi: 10.3390/nu11112596
62. Erney RM, Malone WT, Skelding MB, Marcon AA, Kleman-Leyer KM, O'Ryan ML, et al. Variability of human milk neutral oligosaccharides in a diverse population. *J Pediatr Gastroenterol Nutr.* (2000) 30:181–92. doi: 10.1097/00005176-200002000-00016
63. McGuire MK, Meehan CL, McGuire MA, Williams JE, Foster J, Sellen DW, et al. What's normal? Oligosaccharide concentrations and profiles in milk produced by healthy women vary geographically. *Am J Clin Nutr.* (2017) 105:1086–0. doi: 10.3945/ajcn.116.139980
64. Isganaitis E, Venditti S, Matthews TJ, Lerin C, Demerath EW, Fields DA. Maternal obesity and the human milk metabolome: associations with infant body composition and postnatal weight gain. *Am J Clin Nutr.* (2019) 110:111–20. doi: 10.1093/ajcn/nqy334
65. Austin S, De Castro CA, Sprenger N, Binia A, Affolter M, Garcia-Rodenas CL, et al. Human milk oligosaccharides in the milk of mothers delivering term versus preterm infants. *Nutrients.* (2019) 11:1282. doi: 10.3390/nu11061282
66. Jantscher-Krenn E, Treichler C, Brandl W, Schönbacher L, Köfeler H, van Poppel MNM. The association of human milk oligosaccharides with glucose metabolism in overweight and obese pregnant women. *Am J Clin Nutr.* (2019) 110:1335–43. doi: 10.1093/ajcn/nqz202
67. Zhou J, Wang Y, Fan Q, Liu Y, Liu H, Yan J, et al. High levels of fucosylation and sialylation of milk N-glycans from mothers with gestational diabetes mellitus alter the offspring gut microbiome and immune balance in mice. *FASEB J.* (2020) 34:3715–31. doi: 10.1096/fj.201901674R
68. Aksan A, Erdal I, Yalcin SS, Stein J, Samur G. Osteopontin levels in human milk are related to maternal nutrition and infant health and growth. *Nutrients.* (2021) 13:2670. doi: 10.3390/nu13082670
69. Lagström H, Rautava S, Ollila H, Kaljonen A, Turta O, Mäkelä J, et al. Associations between human milk oligosaccharides and growth in infancy and early childhood. *Am J Clin Nutr.* (2020) 111:769–78. doi: 10.1093/ajcn/nqaa010
70. Ayoub Moubareck C, Lootah M, Tahlak M, Venema K. Profiles of human milk oligosaccharides and their relations to the milk microbiota of breastfeeding mothers in Dubai. *Nutrients.* (2020) 12:1727. doi: 10.3390/nu12061727
71. Zhang W, Wang T, Chen X, Pang X, Zhang S, Obaroakpo JU, et al. Absolute quantification of twelve oligosaccharides in human milk using a targeted mass spectrometry-based approach. *Carbohydr Polym.* (2019) 219:328–33. doi: 10.1016/j.carbpol.2019.04.092
72. Bao Y, Zhu L, Newburg DS. Simultaneous quantification of sialyloligosaccharides from human milk by capillary electrophoresis. *Anal Biochem.* (2007) 370:206–14. doi: 10.1016/j.ab.2007.07.004
73. Spevacek AR, Smilowitz JT, Chin EL, Underwood MA, German JB, Slupsky CM. Infant maturity at birth reveals minor differences in the maternal milk metabolome in the first month of lactation. *J Nutr.* (2015) 145:1698–708. doi: 10.3945/jn.115.210252
74. Nijman RM, Liu Y, Bunyatratchata A, Smilowitz JT, Stahl B, Barile D. Characterization and quantification of oligosaccharides in human milk and infant formula. *J Agric Food Chem.* (2018) 66:6851–9. doi: 10.1021/acs.jafc.8b01515
75. Yan J, Ding J, Jin G, Yu D, Yu L, Long Z, et al. Profiling of sialylated oligosaccharides in mammalian milk using online solid phase extraction-hydrophilic interaction chromatography coupled with negative-ion electrospray mass spectrometry. *Anal Chem.* (2018) 90:3174–82. doi: 10.1021/acs.analchem.7b04468
76. Li J, Jiang M, Zhou J, Ding J, Guo Z, Li M, et al. Characterization of rat and mouse acidic milk oligosaccharides based on hydrophilic interaction chromatography coupled with electrospray tandem mass spectrometry. *Carbohydr Polym.* (2021) 259:117734. doi: 10.1016/j.carbpol.2021.117734
77. Ma L, MacGibbona AKH, Jan Mohamedb HJB, Loyb S, Rowanc A, McJarrowa P, et al. Determination of ganglioside concentrations in breast milk and serum from Malaysian mothers using a high performance liquid chromatography-mass spectrometry-multiple reaction monitoring method. *Int Dairy J.* (2015) 49:62–71. doi: 10.1016/j.idairyj.2015.05.006
78. Tan S, Chen C, Zhao A, Wang M, Zhao W, Zhang J, et al. The dynamic changes of gangliosides in breast milk and the intake of gangliosides in maternal and infant diet in three cities of China. *Int J Clin Exp Pathol.* (2020) 13:2870–88.
79. Yang B, Chuang H, Yang KD. Sialylated glycans as receptor and inhibitor of enterovirus 71 infection to DLD-1 intestinal cells. *Virol J.* (2009) 6:141. doi: 10.1186/1743-422X-6-141
80. Nilsson EC, Jamshidi F, Johansson SM, Oberste MS, Arnberg N. Sialic acid is a cellular receptor for coxsackievirus A24 variant, an emerging virus with pandemic potential. *J Virol.* (2008) 82:3061–8. doi: 10.1128/JVI.02470-07
81. Schnabl KL, Field C, Clandinin MT. Ganglioside composition of differentiated Caco-2 cells resembles human colostrum and neonatal rat intestine. *Br J Nutr.* (2009) 101:694–700. doi: 10.1017/S0007114508048289
82. Le Doare K, Holder B, Bassett A, Pannaraj PS. Mother's milk: a purposeful contribution to the development of the infant microbiota and immunity. *Front Immunol.* (2018) 9:361. doi: 10.3389/fimmu.2018.00361
83. Moore RE, Xu LL, Townsend SD. Prospecting human milk oligosaccharides as a defense against viral infections. *ACS Infect Dis.* (2021) 7:254–63. doi: 10.1021/acsinfecdis.0c00807
84. Pandey RP, Kim DH, Woo J, Song J, Jang SH, Kim JB, et al. Broad-spectrum neutralization of avian influenza viruses by sialylated human milk oligosaccharides: in vivo assessment of 3'-sialyllactose against H9N2 in chickens. *Sci Rep.* (2018) 8:2563. doi: 10.1038/s41598-018-20955-4
85. Zevgiti S, Zabala JG, Darji A, Dietrich U, Panou-Pomonis E, Sakarellos-Daitsiotis M. Sialic acid and sialyl-lactose glyco-conjugates: design, synthesis and binding assays to lectins and swine influenza H1N1 virus. *J Pept Sci.* (2012) 18:52–8. doi: 10.1002/psc.1415
86. Hester SN, Chen X, Li M, Monaco MH, Comstock SS, Kuhlenschmidt TB, et al. Human milk oligosaccharides inhibit rotavirus infectivity in vitro and in acutely infected piglets. *Br J Nutr.* (2013) 110:1233–42. doi: 10.1017/S0007114513000391
87. Laucirica DR, Triantis V, Schoemaker R, Estes MK, Ramani S. Milk oligosaccharides inhibit human rotavirus infectivity in MA104 cells. *J Nutr.* (2017) 147:1709–14. doi: 10.3945/jn.116.246090
88. Idota T, Kawakami H, Murakami Y, Sugawara M. Inhibition of cholera toxin by human milk fractions and sialyllactose. *Biosci Biotechnol Biochem.* (1995) 59:417–9. doi: 10.1271/bbb.59.417
89. Duska-McEwen G, Senft AP, Ruetschilling TL, Barrett EG, Buck RH. Human milk oligosaccharides enhance innate immunity to respiratory syncytial virus and influenza *in vitro*. *Food Sci Nutr.* (2014) 5:1387–98. doi: 10.4236/fns.2014.514151
90. Ray C, Kerketta JA, Rao S, Patel S, Dutt S, Arora K, et al. Human milk oligosaccharides: the journey ahead. *Int J Pediatr.* (2019) 2019:2390240. doi: 10.1155/2019/2390240
91. Angeloni S, Ridet JL, Kusy N, Gao H, Crevoisier F, Guinchard S, et al. Glycoprofiling with micro-arrays of glycoconjugates and lectins. *Glycobiology.* (2005) 15:31–41. doi: 10.1093/glycob/cwh143
92. Asadpoor M, Peeters C, Henricks PAJ, Varasteh S, Pieters RJ, Folkerts G, et al. Anti-pathogenic functions of non-digestible oligosaccharides *in vitro*. *Nutrients.* (2020) 12:1789. doi: 10.3390/nu12061789
93. Lin AE, Autran CA, Szyszka A, Escajadillo T, Huang M, Godula K, et al. Human milk oligosaccharides inhibit growth of group B Streptococcus. *J Biol Chem.* (2017) 292:11243–9. doi: 10.1074/jbc.M117.789974
94. Craft KM, Thomas HC, Townsend SD. Sialylated variants of lacto-N-tetraose exhibit antimicrobial activity against Group B Streptococcus. *Org Biomol Chem.* (2019) 17:1893–900. doi: 10.1039/C8OB02080A
95. Buescher ES. Anti-inflammatory characteristics of human milk: how, where, why. *Adv Exp Med Biol.* (2001) 501:207–22. doi: 10.1007/978-1-4615-1371-1_27

96. Pacheco AR, Barile D, Underwood MA, Mills DA. The impact of the milk glycobiome on the neonate gut microbiota. *Annu Rev Anim Biosci.* (2015) 3:419–45. doi: 10.1146/annurev-animal-022114-111112
97. Palmeira P, Carneiro-Sampaio M. Immunology of breast milk. *Rev Assoc Med Bras 1992.* (2016) 62:584–93. doi: 10.1590/1806-9282.62.06.584
98. Yolken RH, Peterson JA, Vonderfecht SL, Fouts ET, Midthun K, Newburg DS. Human milk mucin inhibits rotavirus replication and prevents experimental gastroenteritis. *J Clin Invest.* (1992) 90:1984–91. doi: 10.1172/JCI116078
99. Wang B, Brand-Miller J, McVeagh P, Petocz P. Concentration and distribution of sialic acid in human milk and infant formulas. *Am J Clin Nutr.* (2001) 74:510–5. doi: 10.1093/ajcn/74.4.510
100. Córdova-Dávalos LE, Jiménez M, Salinas E. Glycomacropeptide bioactivity and health: a review highlighting action mechanisms and signaling pathways. *Nutrients.* (2019) 11:598. doi: 10.3390/nu11030598
101. Arnold JN, Wormald MR, Sim RB, Rudd PM, Dwek RA. The impact of glycosylation on the biological function and structure of human immunoglobulins. *Annu Rev Immunol.* (2007) 25:21–50. doi: 10.1146/annurev.immunol.25.022106.141702
102. Schroten H, Stapper C, Plogmann R, Köhler H, Hacker J, Hanisch FG. Fab-independent antiadhesion effects of secretory immunoglobulin a on S-fimbriated escherichia coli are mediated by sialyloligosaccharides. *Infect Immun.* (1998) 66:3971–3. doi: 10.1128/IAI.66.8.3971-3973.1998
103. Hejdysz M, Kaczmarek SA, Rogiewicz A, Rutkowski A. Influence of graded dietary levels of meals from three lupin species on the excreta dry matter, intestinal viscosity, excretion of total and free sialic acids, and intestinal morphology of broiler chickens. *Ani Feed Sci Technol.* (2018). doi: 10.1016/j.anifeedsci.2018.01.015
104. Owen CD, Tailford LE, Monaco S, Šuligoj T, Vaux L, Lallement R, et al. Unravelling the specificity and mechanism of sialic acid recognition by the gut symbiont ruminococcus gnavus. *Nat Commun.* (2017) 8:2196. doi: 10.1038/s41467-017-02109-8
105. Kavanaugh DW, O'Callaghan J, Buttó LF, Slattery H, Lane J, Clyne M, et al. Exposure of bifidobacterium longum subsp. Infantis to milk oligosaccharides increases adhesion to epithelial cells and induces a substantial transcriptional response. *PLoS ONE.* (2013) 8:e67224. doi: 10.1371/journal.pone.0067224
106. Meli F, Puccio G, Cajozzo C, Ricottone GL, Pecquet S, Sprenger N, et al. Growth and safety evaluation of infant formulae containing oligosaccharides derived from bovine milk: a randomized, double-blind, noninferiority trial. *BMC Pediatr.* (2014) 14:306. doi: 10.1186/s12887-014-0306-3
107. Tarr AJ, Galley JD, Fisher SE, Chichlowski M, Berg BM, Bailey MT. The prebiotics 3'Sialyllactose and 6'Sialyllactose diminish stressor-induced anxiety-like behavior and colonic microbiota alterations: evidence for effects on the gut-brain axis. *Brain Behav Immun.* (2015) 50:166–77. doi: 10.1016/j.bbi.2015.06.025
108. Kiyohara M, Tanigawa K, Chaiwangsri T, Katayama T, Ashida H, Yamamoto K. An exo-alpha-sialidase from bifidobacteria involved in the degradation of sialyloligosaccharides in human milk and intestinal glycoconjugates. *Glycobiology.* (2011) 21:437–47. doi: 10.1093/glycob/cwq175
109. Sela DA, Li Y, Lerno L, Wu S, Marcobal AM, German JB, et al. An infant-associated bacterial commensal utilizes breast milk sialyloligosaccharides. *J Biol Chem.* (2011) 286:11909–18. doi: 10.1074/jbc.M110.193359
110. Garrido D, Nwosu C, Ruiz-Moyano S, Aldredge D, German JB, Lebrilla CB, et al. Endo-β-N-acetylglucosaminidases from infant gut-associated bifidobacteria release complex N-glycans from human milk glycoproteins. *Mol Cell Proteomics.* (2012) 11:775–85. doi: 10.1074/mcp.M112.018119
111. Vega-Bautista A, de la Garza M, Carrero JC, Campos-Rodríguez R, Godínez-Victoria M, Drago-Serrano ME. The impact of lactoferrin on the growth of intestinal inhabitant bacteria. *Int J Mol Sci.* (2019) 20:4707. doi: 10.3390/ijms20194707
112. ELFIN trial investigators group. Enteral lactoferrin supplementation for very preterm infants: a randomised placebo-controlled trial. *Lancet.* (2019) 393:423–33. doi: 10.1016/S0140-6736(18)32221-9
113. Mastromarino P, Capobianco D, Campagna G, Laforgia N, Drimaco P, Dileone A, et al. Correlation between lactoferrin and beneficial microbiota in breast milk and infant's feces. *Biometals.* (2014) 27:1077–86. doi: 10.1007/s10534-014-9762-3
114. Griffiths J, Jenkins P, Vargova M, Bowler U, Juszczak E, King A, et al. Enteral lactoferrin to prevent infection for very preterm infants: the ELFIN RCT. *Health Technol Assess.* (2018) 22:1–60. doi: 10.3310/hta22740
115. Yoo BB, Mazmanian SK. The enteric network: interactions between the immune and nervous systems of the gut. *Immunity.* (2017) 46:910–26. doi: 10.1016/j.immuni.2017.05.011
116. Moon JS, Joo W, Ling L, Choi HS, Han NS. In vitro digestion and fermentation of sialyllactoses by infant gut microflora. *J Funct Foods.* (2016) 21:497–506. doi: 10.1016/j.jff.2015.12.002
117. Iraporda C, Errea A, Romanin DE, Cayet D, Pereyra E, Pignataro O, et al. Lactate and short chain fatty acids produced by microbial fermentation downregulate proinflammatory responses in intestinal epithelial cells and myeloid cells. *Immunobiology.* (2015) 220:1161–9. doi: 10.1016/j.imbio.2015.06.004
118. Donovan SM. Human milk oligosaccharides - the plot thickens. *Br J Nutr.* (2009) 101:1267–9. doi: 10.1017/S0007114508091241
119. Kawashima N, Yoon SJ, Itoh K, Nakayama K. Tyrosine kinase activity of epidermal growth factor receptor is regulated by GM3 binding through carbohydrate to carbohydrate interactions. *J Biol Chem.* (2009) 284:6147–55. doi: 10.1074/jbc.M808171200
120. Wang J, Lei B, Yan J, Li J, Zhou X, Ren F, et al. Donkey milk oligosaccharides influence the growth-related characteristics of intestinal cells and induce G2/M growth arrest via the p38 pathway in HT-29 cells. *Food Funct.* (2019) 10:4823–33. doi: 10.1039/C8FO02584C
121. Yang C, Zhang P, Fang W, Chen Y, Zhang N, Qiao Z, et al. Molecular mechanisms underlying how sialyllactose intervention promotes intestinal maturity by upregulating GDNF through a CREB-dependent pathway in neonatal piglets. *Mol Neurobiol.* (2019) 56:7994–8007. doi: 10.1007/s12035-019-1628-9
122. Natividad JM, Rytz A, Keddani S, Bergonzelli G, Garcia-Rodenas CL. Blends of human milk oligosaccharides confer intestinal epithelial barrier protection *in Vitro*. *Nutrients.* (2020) 12:3047. doi: 10.3390/nu12103047
123. Holscher HD, Bode L, Tappenden KA. Human milk oligosaccharides influence intestinal epithelial cell maturation *In Vitro*. *J Pediatr Gastroenterol Nutr.* (2017) 64:296–301. doi: 10.1097/MPG.0000000000001274
124. Foata F, Sprenger N, Rochat F, Damak S. Activation of the G-protein coupled receptor GPR35 by human milk oligosaccharides through different pathways. *Sci Rep.* (2020) 10:16117. doi: 10.1038/s41598-020-73008-0
125. Tsukahara T, Hamouda N, Utsumi D, Matsumoto K, Amagase K, Kato S. G protein-coupled receptor 35 contributes to mucosal repair in mice via migration of colonic epithelial cells. *Pharmacol Res.* (2017) 123:27–39. doi: 10.1016/j.phrs.2017.06.009
126. Farooq SM, Hou Y, Li H, O'Meara M, Wang Y, Li C, et al. Disruption of GPR35 exacerbates dextran sulfate sodium-induced colitis in mice. *Dig Dis Sci.* (2018) 63:2910–22. doi: 10.1007/s10620-018-5216-z
127. Schneditz G, Elias JE, Pagano E, Zaeem Cader M, Saveljeva S, Long K, et al. GPR35 promotes glycolysis, proliferation, and oncogenic signaling by engaging with the sodium potassium pump. *Sci Signal.* (2019) 12:eaau9048. doi: 10.1126/scisignal.aau9048
128. Pammi M, Suresh G. Enteral lactoferrin supplementation for prevention of sepsis and necrotizing enterocolitis in preterm infants. *Cochrane Database Syst Rev.* (2017) 6:CD007137. doi: 10.1002/14651858.CD007137.pub5
129. Donovan SM, Monaco MH, Drnevich J, Kvistgaard AS, Hernell O, Lönnerdal B. Bovine osteopontin modifies the intestinal transcriptome of formula-fed infant rhesus monkeys to be more similar to those that were breastfed. *J Nutr.* (2014) 144:1910–9. doi: 10.3945/jn.114.197558
130. Bode L, Kunz C, Muhly-Reinholz M, Mayer K, Seeger W, Rudloff S. Inhibition of monocyte, lymphocyte, and neutrophil adhesion to endothelial cells by human milk oligosaccharides. *Thromb Haemost.* (2004) 92:1402–10. doi: 10.1160/TH04-01-0055
131. Eiwegger T, Stahl B, Haidl P, Schmitt J, Boehm G, Dehlink E, et al. Prebiotic oligosaccharides: in vitro evidence for gastrointestinal epithelial transfer and immunomodulatory properties. *Pediatr Allergy Immunol.* (2010) 21:1179–88. doi: 10.1111/j.1399-3038.2010.01062.x
132. Fuhrer A, Sprenger N, Kurakevich E, Borsig L, Chassard C, Hennet T. Milk sialyllactose influences colitis in mice through selective intestinal

bacterial colonization. *J Exp Med*. (2010) 207:2843–54. doi: 10.1084/jem.20101098
133. Kurakevich E, Hennet T, Hausmann M, Rogler G, Borsig L. Milk oligosaccharide sialyl(α2,3) lactose activates intestinal CD11c+ cells through TLR4. *Proc Natl Acad Sci USA*. (2013) 110:17444–9. doi: 10.1073/pnas.1306322110
134. De Fazio L, Beghetti I, Bertuccio SN, Marsico C, Martini S, Masetti R, et al. Necrotizing enterocolitis: overview on *in vitro* models. *Int J Mol Sci*. (2021) 22:6761. doi: 10.3390/ijms22136761
135. Sodhi CP, Wipf P, Yamaguchi Y, Fulton WB, Kovler M, Niño DF, et al. The human milk oligosaccharides 2'-fucosyllactose and 6'-sialyllactose protect against the development of necrotizing enterocolitis by inhibiting toll-like receptor 4 signaling. *Pediatr Res*. (2021) 89:91–101. doi: 10.1038/s41390-020-0852-3
136. Jantscher-Krenn E, Zherebtsov M, Nissan C, Goth K, Guner YS, Naidu N, et al. The human milk oligosaccharide disialyllacto-N-tetraose prevents necrotising enterocolitis in neonatal rats. *Gut*. (2012) 61:1417–25. doi: 10.1136/gutjnl-2011-301404
137. Masi AC, Embleton ND, Lamb CA, Young G, Granger CL, Najera J, et al. Human milk oligosaccharide DSLNT and gut microbiome in preterm infants predicts necrotising enterocolitis. *Gut*. (2020) 16:gutjnl-2020-322771. doi: 10.1136/gutjnl-2020-322771
138. Akin IM, Atasay B, Dogu F, Okulu E, Arsan S, Karatas HD, et al. Oral lactoferrin to prevent nosocomial sepsis and necrotizing enterocolitis of premature neonates and effect on T-regulatory cells. *Am J Perinatol*. (2014) 31:1111–20. doi: 10.1055/s-0034-1371704
139. Drago-Serrano ME, Campos-Rodríguez R, Carrero JC, de la Garza M. Lactoferrin: balancing ups and downs of inflammation due to microbial infections. *Int J Mol Sci*. (2017) 18:501. doi: 10.3390/ijms18030501
140. Asztalos EV, Barrington K, Lodha A, Tarnow-Mordi W, Martin A. Lactoferrin infant feeding trial_Canada (LIFT_Canada): protocol for a randomized trial of adding lactoferrin to feeds of very-low-birth-weight preterm infants. *BMC Pediatr*. (2020) 20:40. doi: 10.1186/s12887-020-1938-0
141. Jiang R, Lönnerdal B. Evaluation of bioactivities of bovine milk osteopontin using a knockout mouse model. *J Pediatr Gastroenterol Nutr*. (2020) 71:125–31. doi: 10.1097/MPG.0000000000002702
142. Lönnerdal B, Kvistgaard AS, Peerson JM, Donovan SM, Peng YM. Growth, nutrition, and cytokine response of breast-fed infants and infants fed formula with added bovine osteopontin. *J Pediatr Gastroenterol Nutr*. (2016) 62:650–7. doi: 10.1097/MPG.0000000000001005
143. Ek-Rylander B, Andersson G. Osteoclast migration on phosphorylated osteopontin is regulated by endogenous tartrate-resistant acid phosphatase. *Exp Cell Res*. (2010) 316:443–51. doi: 10.1016/j.yexcr.2009.10.019
144. Møller HK, Thymann T, Fink LN, Frokiaer H, Kvistgaard AS, Sangild PT. Bovine colostrum is superior to enriched formulas in stimulating intestinal function and necrotising enterocolitis resistance in preterm pigs. *Br J Nutr*. (2011) 105:44–53. doi: 10.1017/S0007114510003168
145. Vázquez E, Gil A, Rueda R. Dietary gangliosides positively modulate the percentages of Th1 and Th2 lymphocyte subsets in small intestine of mice at weaning. *Biofactors*. (2001) 15:1–9. doi: 10.1002/biof.5520150101
146. Greenspon J, Li R, Xiao L, Rao JN, Sun R, Strauch ED, et al. Sphingosine-1-phosphate regulates the expression of adherens junction protein E-cadherin and enhances intestinal epithelial cell barrier function. *Dig Dis Sci*. (2011) 56:1342–53. doi: 10.1007/s10620-010-1421-0
147. Brønnum H, Seested T, Hellgren LI, Brix S, Frøkiaer H. Milk-derived GM(3) and GD(3) differentially inhibit dendritic cell maturation and effector functionalities. *Scand J Immunol*. (2005) 61:551–7. doi: 10.1111/j.1365-3083.2005.01566.x
148. Charbonneau MR, O'Donnell D, Blanton LV, Totten SM, Davis JC, Barratt MJ, et al. Sialylated milk oligosaccharides promote microbiota-dependent growth in models of infant undernutrition. *Cell*. (2016) 164:859–71. doi: 10.1016/j.cell.2016.01.024
149. Jeon J, Kang LJ, Lee KM, Cho C, Song EK, Kim W, et al. 3'-Sialyllactose protects against osteoarthritic development by facilitating cartilage homeostasis. *J Cell Mol Med*. (2018) 22:57–66. doi: 10.1111/jcmm.13292
150. Kang LJ, Kwon ES, Lee KM, Cho C, Lee JI, Ryu YB, et al. 3'-Sialyllactose as an inhibitor of p65 phosphorylation ameliorates the progression of experimental rheumatoid arthritis. *Br J Pharmacol*. (2018) 175:4295–309. doi: 10.1111/bph.14486
151. Donovan SM. Human milk proteins: composition and physiological significance. *Nestle Nutr Inst Workshop Ser*. (2019) 90:93–101. doi: 10.1159/000490298
152. Gridneva Z, Lai CT, Rea A, Tie WJ, Ward LC, Murray K, et al. Human milk immunomodulatory proteins are related to development of infant body composition during the first year of lactation. *Pediatr Res*. (2021) 89:911–21. doi: 10.1038/s41390-020-0961-z
153. Shama S, Unger S, Pouliot Y, Doyen A, Suwal S, Pencharz P, et al. A human milk-based protein concentrate developed for preterm infants retains bioactive proteins and supports growth of weanling rats. *J Nutr*. (2021) 151:840–7. doi: 10.1093/jn/nxaa383
154. Wu SL, Ding D, Fang AP, Chen PY, Chen S, Jing LP, et al. Growth, gastrointestinal tolerance and stool characteristics of healthy term infants fed an infant formula containing hydrolyzed whey protein (63%) and intact casein (37%): a randomized clinical trial. *Nutrients*. (2017) 9:1254. doi: 10.3390/nu9111254
155. Gridneva Z, Tie WJ, Rea A, Lai CT, Ward LC, Murray K, et al. Human milk casein and whey protein and infant body composition over the first 12 months of lactation. *Nutrients*. (2018) 10:1332. doi: 10.3390/nu10091332
156. Tomarelli RM, Linden E, Durbin GT, Bernhart FW. The effect of mucin on the growth of rats fed simulated human milk. *J Nutr*. (1953) 51:251–9. doi: 10.1093/jn/51.2.251
157. Jiang R, Liu L, Du X, Lönnerdal B. Evaluation of bioactivities of the bovine milk lactoferrin-osteopontin complex in infant formulas. *J Agric Food Chem*. (2020) 68:6104–11. doi: 10.1021/acs.jafc.9b07988
158. Andersson EL, Hernell O, Bläckberg L, Fält H, Lindquist S. BSSL and PLRP2: key enzymes for lipid digestion in the newborn examined using the Caco-2 cell line. *J Lipid Res*. (2011) 52:1949–56. doi: 10.1194/jlr.M015685
159. Li X, Lindquist S, Lowe M, Noppa L, Hernell O. Bile salt-stimulated lipase and pancreatic lipase-related protein 2 are the dominating lipases in neonatal fat digestion in mice and rats. *Pediatr Res*. (2007) 62:537–41. doi: 10.1203/PDR.0b013e3181559e75
160. Wang B, Brand-Miller J. The role and potential of sialic acid in human nutrition. *Eur J Clin Nutr*. (2003) 57:1351–69. doi: 10.1038/sj.ejcn.1601704
161. Wang HX, Chen Y, Haque Z, de Veer M, Egan G, Wang B. Sialylated milk oligosaccharides alter neurotransmitters and brain metabolites in piglets: an *In vivo* magnetic resonance spectroscopic (MRS) study. *Nutr Neurosci*. (2019) 20:1–11. doi: 10.1080/1028415X.2019.1691856
162. Waworuntu RV, Hanania T, Boikess SR, Rex CS, Berg BM. Early life diet containing prebiotics and bioactive whey protein fractions increased dendritic spine density of rat hippocampal neurons. *Int J Dev Neurosci*. (2016) 55:28–33. doi: 10.1016/j.ijdevneu.2016.09.001
163. Li F, Wu SS, Berseth CL, Harris CL, Richards JD, Wampler JL, et al. Improved neurodevelopmental outcomes associated with bovine milk fat globule membrane and lactoferrin in infant formula: a randomized, controlled trial. *J Pediatr*. (2019) 215:24–31.e8. doi: 10.1016/j.jpeds.2019.08.030
164. Oh NS, Joung JY, Lee JY, Song JG, Oh S, Kim Y, et al. Glycated milk protein fermented with lactobacillus rhamnosus ameliorates the cognitive health of mice under mild-stress condition. *Gut Microbes*. (2020) 11:1643–61. doi: 10.1080/19490976.2020.1756690
165. Jiang R, Tran M, Lönnerdal B. Recombinant bovine and human osteopontin generated by chlamydomonas reinhardtii exhibit bioactivities similar to bovine milk osteopontin when assessed in mouse pups fed osteopontin-deficient milk. *Mol Nutr Food Res*. (2021) 65:e2000644. doi: 10.1002/mnfr.202000644
166. Huang S, Mo TT, Norris T, Sun S, Zhang T, Han TL, et al. The CLIMB (Complex Lipids In Mothers and Babies) study: protocol for a multicentre, three-group, parallel randomised controlled trial to investigate the effect of supplementation of complex lipids in pregnancy, on maternal ganglioside status and subsequent cognitive outcomes in the offspring. *BMJ Open*. (2017) 7:e016637. doi: 10.1136/bmjopen-2017-016637

167. Liu H, Radlowski EC, Conrad MS, Li Y, Dilger RN, Johnson RW. Early supplementation of phospholipids and gangliosides affects brain and cognitive development in neonatal piglets. *J Nutr.* (2014) 144:1903–9. doi: 10.3945/jn.114.199828
168. Gurnida DA, Rowan AM, Idjradinata P, Muchtadi D, Sekarwana N. Association of complex lipids containing gangliosides with cognitive development of 6-month-old infants. *Early Hum Dev.* (2012) 88:595–601. doi: 10.1016/j.earlhumdev.2012.01.003

Conflict of Interest: XZ and NZ are employed by By-Health Co. Ltd.

The remaining authors declare that the research was conducted in the absence of any commercial or financial relationships that could be construed as a potential conflict of interest.

Publisher's Note: All claims expressed in this article are solely those of the authors and do not necessarily represent those of their affiliated organizations, or those of the publisher, the editors and the reviewers. Any product that may be evaluated in this article, or claim that may be made by its manufacturer, is not guaranteed or endorsed by the publisher.

frontiers in Nutrition

ORIGINAL RESEARCH
published: 29 November 2021
doi: 10.3389/fnut.2021.774203

Soy Protein Alleviates Malnutrition in Weaning Rats by Regulating Gut Microbiota Composition and Serum Metabolites

Zuchen Wei[1,2†], *Nong Zhou*[2†], *Liang Zou*[3], *Zhenxing Shi*[1], *Baoqing Dun*[1*], *Guixing Ren*[1] *and Yang Yao*[1*]

[1] *Institute of Crop Science, Chinese Academy of Agricultural Sciences (CAAS), Beijing, China,* [2] *Laboratory for Green Cultivation and Deep Processing of Three Gorges Reservoir Area's Medicinal Herbs, College of Life Science and Engineering, The Chongqing Engineering, Chongqing Three Gorges University, Chongqing, China,* [3] *Key Laboratory of Coarse Cereal Processing, Ministry of Agriculture and Rural Affairs, Chengdu University, Chengdu, China*

OPEN ACCESS

Edited by:
Nuria Salazar, Institute of Dairy Products of Asturias (IPLA), Spain

Reviewed by:
Bhawani Chamlagain, University of Helsinki, Finland
Suman Kapila, National Dairy Research Institute (ICAR), India

***Correspondence:**
Baoqing Dun
dunbaoqing@caas.cn.com
Yang Yao
yaoyang@caas.cn

[†] *These authors have contributed equally to this work*

Specialty section:
This article was submitted to Nutrition and Microbes, a section of the journal Frontiers in Nutrition

Received: *11 September 2021*
Accepted: *19 October 2021*
Published: *29 November 2021*

Citation:
Wei Z, Zhou N, Zou L, Shi Z, Dun B, Ren G and Yao Y (2021) Soy Protein Alleviates Malnutrition in Weaning Rats by Regulating Gut Microbiota Composition and Serum Metabolites. Front. Nutr. 8:774203. doi: 10.3389/fnut.2021.774203

Dietary intervention with plant protein is one of the main methods that is used to lessen the symptoms of malnutrition. Supplementary soy protein to undernourished weaning rats for 6 weeks significantly increased their body weight gain. After the intervention, the level of total short-chain fatty acids (SCFAs) was restored to 1,512.7 μg/g, while the level was only 637.1 μg/g in the 7% protein group. The amino acids (valine, isoleucine, phenylalanine, and tryptophan) increased in the colon, and vitamin B_6 metabolism was significantly influenced in undernourished rats. The tryptophan and glycine-serine-threonine pathways were elevated, leading to an increase in the level of tryptophan and 5-hydroxytryptophan (5-HTP) in the serum. In addition, the relative abundance of *Lachnospiraceae*_NK4A136_group and *Lactobacillus* increased, while *Enterococcus* and *Streptococcus* decreased compared to undernourished rats. Overall, soy protein improved the growth of rats with malnutrition in early life by regulating gut microbiota and metabolites in the colon and serum.

Keywords: untargeted metabolomics, undernourished, microbiota, 16S rRNA, soy protein

INTRODUCTION

In 2018, stunting affected an estimated 21.9% of children under five (or 149 million), worldwide (1). Emerging views are of the opinion that an immature intestinal microbiota may cause severe malnutrition in children (2). The structure of the gut bacteria and their relative abundance in a healthy host are fixed with beneficial bacteria, such as *Lactobacilli* and *Bifidobacterium*. However, the structure of gut microbiota was vulnerable to the change of internal and external environment. Recently, some researchers demonstrated that bacteria in younger healthy children dominated their malnutrition, which suggests that the growth of the intestinal flora did not keep up with the development of the body (3). Bacteria, such as *Streptococcus* and *Enterococcus* dominated in the intestines of undernourished children and were defined as signs of immature intestines (4). Proteins were utilized by mature healthy intestinal microbes and produced short-chain fatty acids (SCFAs) to regulate tryptophan and 5-hydroxytryptamine (5-HT) in serum. These metabolites regulate host metabolism, appetite, and mood (5). However, there are limited studies on the correlation between serum metabolites and malnutrition.

Known as many reasons for malnutrition, diet is more effective than other factors in regulating the gut microbiota; thus, high-quality food is considered as one of the most effective ways for the treatment of malnutrition (6). Casein has been proven to carry innumerable nutritional values for humans, and it has long been used in the diets of infants to provide nutritional support (7). Casein can easily degrade in the small intestine, and is subsequently available for bacteria in the large intestine to increase the communities of *Lactobacilli* and *Bifidobacterium* while decreasing the counts of *Staphylococci, Coliforms,* and *Streptococci* (8–12). However, casein is not easily available to children in the undeveloped areas, especially in the remote areas (13, 14). Renewed interest mainly focuses on plant-derived protein, especially on soy protein, which is considered as an alternative nutrition for casein. In addition, accumulating studies demonstrated that the absorption of soy protein is more efficient in improving malnutrition than that of the consumption of the mixture of amino acids. In addition, soy protein has also been claimed to play positive roles in modulating the beneficial bacterial composition in the gut with increased communities of *Escherichia* and *Propionibacterium* (15, 16). It has been reported that food supplemented with soy protein alleviated malnutrition by changing the ratio of beneficial and "age-discriminatory" bacteria in the gut (14). Therefore, fostering gut microbiota may shed light on improving body weight and restoring health in undernourished children. Moreover, consuming targeted foods to facilitate the domination of beneficial microbes in the gut has been recommended (17).

However, few studies focus on finding whether soy protein can be used as a substitute for casein and whether the alleviation of malnutrition is interrelated with the regulation of intestinal flora. In this study, a comparison between casein and soy protein was performed in a malnourished rat model to shed light on whether soy protein could be substituted in a weaning-phase diet. The present study aimed to (i) compare the effects in an undernourished rat model using soy protein and casein, (ii) measure the contents of SCFAs and metabolites in the serum and colon, (iii) evaluate the change in the structure and relative abundance of gut microbiota using 16S rRNA gene sequencing, (iv) analyze the relationships among microbiota, apparent indicators, and metabolites (in serum and the colon).

MATERIALS AND METHODS

Materials and Chemicals

Normally ground soy protein (>95.2%) powder and casein (>95.2%) were obtained from Gushen Biological Technology Group Co., Ltd. (Dezhou, China). Insulin-like growth factor-1 (IGF-1)ELISA kits were commercially obtained from Abcam (Cambridge, MA, USA). Angiotensin-converting enzyme-2 (ACE 2) ELISA kits were purchased from Biorbyt (Princeton, New Jersey, USA). Acetate, propionate, butyrate, and standard valeric acid were bought from Sigma, Inc. (St. Louis, MO, USA). An E.N.Z.A.® Stool DNA isolation kit that was used to extract DNA was produced by Omega Bio-Tek, Inc. (Norcross, Georgia, USA). All other chemical reagents were of AR grade.

Abbreviations: CTG, control group; LPG, low protein group; CG, casein group; SPG, soy protein group; IGF-1, insulin-like growth factor-1; ACE 2, angiotensin-converting enzyme-2; SCFAs, short-chain fatty acids; 5-HTTP, 5-hydroxytryptophan.

Analysis of the Nutritional Value of Raw Materials Based on Amino Acids Score

Amino acids score (AAS) was determined as below:

$$\text{AAS\%} = \frac{\text{(\%) sample essential amino acid content}}{\text{(\%) recommended essential amino acids}}$$

The amino acids of the diet were evaluated using a Hitachi Limited Amino automatic analyzer (L-8900, Tokyo, Japan).

The Design of Animals and Experiment

Forty male Sprague-Dawley rats (SYXK (Beijing) 2018-0022) (4 weeks from birth, weighing 90.8 ± 4.24 g) were obtained from the Beijing Rital River Laboratory Animal Technology Company (Beijing, China). The malnutrition models were constructed according to the Brown method (18). Briefly, after 7 days of adaptation, 10 randomly distributed rats were categorized as a control group (CTG), and the other 30 rats categorized as a low protein group (LPG) were given a 7% protein diet. After 3 weeks, 30 rats in the malnutrition group (weight was decreased by 51.2% compared to the control rats) were randomly distributed into 3 groups ($n = 10$) as follows: LPG group, casein group (CG), and soy protein group (SPG). The body weight and tail length gain of the rats were measured every week. The experimental diets for each group are listed in **Table 1** (Jiangsu Xietong Pharmaceutical Bio-engineering Co., Ltd. Nanjing, China). During the experimental period, water and food were easily and adequately available for the rats. All rats were housed individually in cages placed at the room where temperature (22.3 ± 1°C) and humidity (50.2 ± 10%) were maintained stably with a 12 h light/dark cycle. On day 57 (the body weight had statistically increased in the SPG and CG compared to the LPG), each rat was sacrificed under anesthesia after 12 h of fasting, and blood was immediately obtained to prepare the serum stored at −80°C until analysis. The content of IGF-1 and ACE 2 in the serum were measured according to the instruction of the ELISA kits. The experiment was conducted in accordance with the European Community Guidelines for the Use of Experimental Animals and authorized by the Pony Testing International Group on Animal and Use.

SCFAs Analysis

The concentration of SCFAs was measured as described in a previous study (19) according to Shanghai Biotree Biotech Co., Ltd. (Shanghai, China) protocol. Fifty milligrams of colon contents were extracted with 1 mL ice-cold physiological saline, homogenized in a ball mill (4 min, 40 Hz) (Shanghaijingxin Experimental Technology, Shanghai, China), and then ultrasonically processed for 5 min in ice water. The supernatant obtained by centrifugation (5,000 rpm, 20 min, 4°C) was collected, and added to the mixture (9:1 v/v) containing

TABLE 1 | The composition of diets.

Component	CTG		LPG		CG		SPG	
	gm	kacl	gm	kacl	gm	kacl	gm	kacl
Casein/g	200	800	70	280	200	800	-	0
L-Cystine/g	3	12	3	12	3	12	3	12
Soy protein/g	-	-	-	-	-	-	245.4	982.2
Corn Starch/g	397.5	1,590	527.5	2,110	397.5	1,590	352.0	1,407.8
Maltodextrin 10/g	132	528	132	528	132	528	132	528
Sucrose/g	100	400	100	400	100	400	100	400
Cellulose, BW200/g	50	0	50	0	50	0	50	0
Lard/g	70	630	70	630	70	630	70	630
Vitamin Mix V10037/g	10	40	10	40	10	40	10	40
Mineral Mix S10022G/g	35	0	35	0	35	0	35	0
Choline Bitartrate/g	2.5	0	2.5	0	2.5	0	2.5	0
FD&C Red Dye #40/g	-	0	-	0	-	0	0.10	0
Total/g	1,000	4,000	1,000	4,000	1,000	4,000	1,000	4,000
Protein (%)	20.3	20.3	7.30	7.30	20.3	20.3	20.3	20.3
Carbohydrate (%)	64.0	64.0	77.0	77.0	70	64.0	64.0	64.0
Fat (%)	7.00	15.7	7.00	15.7	7.00	15.7	7.00	15.7
Total		100		100		100		100

CTG, Control group; LPG, low protein group; CG, casein group; SPG, soy protein group.

25% (w/v) of metaphosphoric acid. After centrifugation, the supernatant was transferred into a fresh vial for analysis. The supernatant (1 μL) was analyzed by an HP-FFAP capillary column (Agilent, Folsom, CA, USA). Using helium as the carrier gas, the initial temperature was set to 80°C (1 min), and subsequently increased to 200°C (in 5 min), then maintained (1 min) at 240°C. The injection and detector temperatures were 250 and 270°C, respectively. The electron impact energy was −70 eV. The mode of MS was set in Scan/SIM mode.

Untargeted Metabolomics

Sample of colon content (50 mg) was diluted in 1 mL of the extract solution (methanol: acetonitrile: water = 2:2:1, with isotopically-labeled internal standard mixture). After homogenization (35 HZ, 4 min) and sonication (5 min) in three times of repeated ice bath, the samples were incubated for 1 h (−40°C) and finally centrifuged (12,000 g, 15 min, 4°C). The supernatant was transferred to a fresh glass vial for analysis.

One hundred microliters of serum sample were mixed with 400 μL of solution (acetonitrile: methanol = 1:1) and vortexed (30 s), then sonicated (10 min, ice water bath), and subsequently incubated (1 h, −40°C) to precipitate proteins. After centrifugation (4°C, 12,000 rpm, 15 min), the supernatant was ready for analysis.

The quality control sample was prepared by mixing up all the samples with an equal aliquot. Liquid-chromatography tandem mass spectrometry (LC-MS/MS) analysis was conducted by a UHPLC system (Thermo Fisher, Waltham, MA, USA) equipped with BEH amide column (2.1 × 100 mm, 1.7 μm) connected to a Q Exactive HFX mass spectrometer (Thermo Fisher, Waltham, MA, USA). The flow was blended with 25 mmol/L of ammonium acetate and 25 mmol/L of ammonia hydroxide in water (pH = 9.7) (A) and acetonitrile (B). The injected sample was set at the temperature of 4°C, and the sample volume was set at 2 μL. An acquisition software consistently monitored the full scan MS spectrum. The electrospray ionization (ESI) source conditions were coded as follows: sheath gas flow rate and aux gas flow were 30 Arb and 25 Arb, respectively. Temperature was set at 350°C, and full MS resolution and MS/MS resolution were of 60,000 and 7,500. Collision energy was obtained with 10/30/60 in N-channel enhancement (NCE) mode, and spray voltage was found to be either 3.6 kV (positive) or −3.2 kV (negative).

16S rRNA Gene Sequences

On day 57, after sacrificing under anesthesia, the colon contents of the rats were collected from the respective groups. The analysis of 16S rRNA gene sequences was performed in the laboratory as per previous publication (19). After extracting total DNA by an E.N.Z.A.® Stool DNA isolation kit (Omega Bio-Tek, Inc. St. Louis, MO, USA), primers were programed according to the conserved regions, and subsequently, sequencing adapters were added to the ends of the primers (forward 5′-ACTCCTACGGGAGGCAGCA-3′ and reverse 5′-GGACTACHVGGGTWTCTAAT-3′). PCR amplification was performed, and the productions were cleaned, quantified, and homogenized to form a sequencing library. The built library was qualified by a library quality inspection and sequenced with an Illumina HiSeq 2500 system (Illumina In., CA, USA). The original image data obtained by Illumina HiSeq platforms were translated into sequenced reads, and stored in FASTQ (referred to as fq) file format. Trimmomatic v0.33 software

was first used to filter the raw reads obtained by sequencing; then, cutadapt 1.9.1 software was used to distinguish and cut the primer sequences. FLASH v1.2.7 software was applied to pass the overlapped splices of the high-quality reads of each sample, and clean reads were obtained from the resulting spliced sequence. The UCHIME v 4.2 software was employed to distinguish and cut the chimera sequence to produce the final effective data.

Statistical Analysis

Data were processed and finally expressed as the mean ± SD. GraphPad Prism 9 Software (San Diego, CA, USA) was used to analyze the differences among the four groups and transformed the data to a figure. For microbiota analyses, the Shannon index evaluated significant differences in the level of alpha diversity among the four groups. The abundance of operational taxonomic unit (OTU) was conducted to compare the changes of diversity among the four groups. The data of the gut microbiota in the levels of genus, host apparent indicators, and metabolites (in colon and serum) were analyzed to evaluate the correlations by Spearman's algorithm. The difference was considered significant if the $p < 0.05$.

RESULTS

Amino Acid Composition of Soy Protein and Casein

The amino acid profiles of different proteins are presented in **Table 2**. A total of 18 amino acids were detected, including 9 essential amino acids. The sulfur amino acids (methionine and cystine) and proline contents in casein reached 4.68 and 10.2%, respectively, while the corresponding values in soy protein were only 2.49 and 5.4%, respectively. However, compared with casein, soy protein was rich in arginine, alanine, glycine, and aspartic acid, and the total amount exceeded 86.8%. As shown in **Table 3**, the AAS of casein was above 100, which meets the requirements of FAO recommendations. Sulfur-containing amino acids were obviously the limiting amino acids in soy, which had the lowest percentage of all amino acids (2.49%). Tyrosine and phenylalanine, in soy protein and casein, had the highest AAS, reaching the values of 130.5 and 172.9, respectively. The following were the only two amino acids in soy with an AAS below 90: sulfur-containing amino acids (71.5) and lysine (87.4). The AAS is an important index for evaluating the quality of protein; it has been widely used to predict the potential ability of protein in food to provide indispensable amino acids.

TABLE 2 | Amino acid composition ($mg \cdot g^{-1}$ protein).

Amino acid	Soy protein	Casein
Tryptophan	7.94 ± 0.30^{b}	10.2 ± 0.27^{a}
Aspartic acid	89.4 ± 1.51^{a}	60.0 ± 2.05^{b}
Threonine	29.2 ± 0.31^{b}	34.2 ± 0.13^{a}
Serine	37.0 ± 2.26^{b}	41.5 ± 1.63^{a}
Glutamate	147.9 ± 2.33^{b}	182.9 ± 2.40^{a}
Proline	41.6 ± 0.71^{b}	91.8 ± 1.77^{a}
Glycine	32.1 ± 2.19^{b}	15.7 ± 2.55^{a}
Alanine	33.4 ± 1.13^{a}	25.7 ± 1.08^{b}
Cystine	8.84 ± 0.24^{b}	16.5 ± 0.57^{a}
Methionine	10.5 ± 0.34^{b}	25.5 ± 0.25^{a}
Valine	39.1 ± 0.41^{b}	57.0 ± 0.34^{a}
Isoleucine	38.2 ± 0.37^{b}	45.7 ± 0.35^{a}
Leucine	62.0 ± 0.34^{b}	78.0 ± 0.34^{a}
Tyrosine	25.2 ± 0.33^{b}	45.1 ± 0.43^{a}
Phenylalanine	43.2 ± 0.43^{a}	44.8 ± 0.36^{a}
Lysine	49.8 ± 0.62^{b}	69.0 ± 0.32^{a}
Histidine	20.6 ± 0.43^{a}	25.0 ± 0.37^{a}
Arginine	58.1 ± 2.19^{a}	31.1 ± 2.05^{b}

Data are presented as the mean ± SD (n = 3). The letters after the data indicate the statistical difference (p < 0.05).

TABLE 3 | The amino acid score (AAS) of dietary ingredients.

AAS (for infants/preschool children 2 yrs)	FAO (2013)	Soy protein	Casein
Threonine	31	94.2 ± 1.00^{b}	110.2 ± 5.59a
Methionine+Cystine	27	71.5 ± 2.13^{b}	155.8 ± 2.97^{a}
Isoleucine	32	119.2 ± 1.15^{b}	142.7 ± 1.08^{a}
Leucine	66	93.9 ± 0.51^{b}	118.1 ± 0.52^{a}
Phenylalanine+Tyrosine	52	130.5 ± 0.62^{b}	172.9 ± 1.51^{a}
Lysine	57	87.4 ± 1.09^{b}	121.0 ± 0.56^{a}
Histidine	20	103.1 ± 2.13^{b}	124.8 ± 1.86^{a}
Tryptophan	9	93.4 ± 3.47^{b}	120.3 ± 3.13^{a}
Valine	43	91.0 ± 0.96^{b}	132.5 ± 0.78^{a}

Data are presented as the mean ± SD (n = 3). The letters after the data indicate the statistical difference (p < 0.05).

Effects of Soy Protein on Body Weight, Tail Length, IGF-1, and ACE 2

The undernourished model induced by the protein-deficient diet (7% protein diet) showed a stunted growth in rats, as they reduced an average of 51.2% in body weight after 3 weeks, compared to CTG (**Figure 1A**). After 6 weeks of supplementary diets, the rats from the SPG and the CG significantly exhibited higher body weight gain ($p < 0.05$) than LPG, which increased by 64.9% in the SPG compared to those in the CG. At the same time, malnourished rats also had corresponding shorter tails. Results showed a similar growth trend performed in the length of the rat tail, with rats in the SPG and CG growing faster than rats in the LPG, and showed no statistical difference with CTG (**Figure 1B**).

Compared with those in the CTG, rats fed with low protein diet had lower IGF-1 and ACE 2 levels in the serum (**Figure 1C**). After the administration of supplementary diets (soy protein or casein protein) for 6 weeks, the IGF-1 levels in SPG and CG were elevated by 53.1 and 46.3%, respectively, compared to the LPG ($p < 0.05$). Additionally, the level of ACE 2 increased by 43.0 and 53.1% in the SPG and CG, respectively, compared to the LPG ($p < 0.05$) (**Figure 1C**).

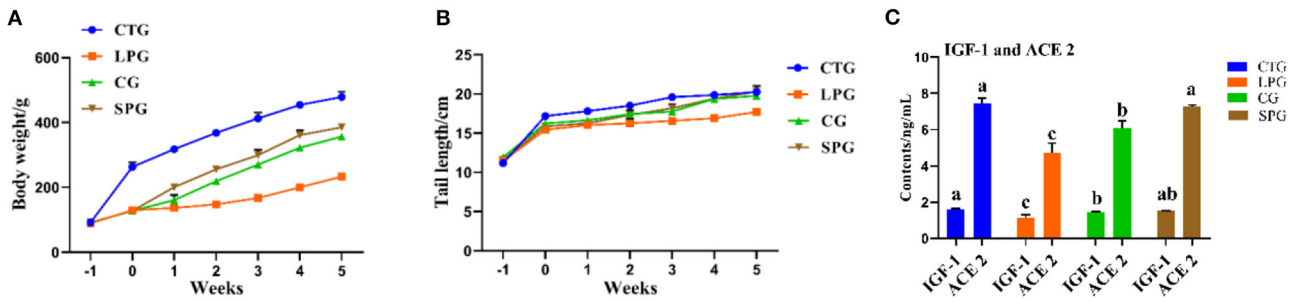

FIGURE 1 | Diet intervention alleviated the physiological condition of rats. **(A)** The body weight of rats. **(B)** The tail length of rats. **(C)** IGF-1 and ACE 2 contents in the serum. Data are presented as mean ± SEM. Different letters indicate statistical differences among the groups ($p < 0.05$). IGF-1, insulin-like growth factor-1; ACE 2, angiotensin-converting enzyme-2; CTG, control group; LPG, low protein group; CG, casein group; SPG, soy protein group.

Effects of Soy Protein on SCFAs and Colonic Metabolites

The concentration of total SCFAs and the acetate, propionate, butyrate, and valeric acid in the four groups varied significantly (**Figure 2A**). The LPG showed a dramatic decrease in the total level of SCFAs by 2.04-fold compared to CTG, while the SPG and the CG showed 1.37- and 1.86-fold increases compared to LPG (**Figure 2A**). In LPG, the levels of acetate, propionate, butyrate, and valeric acid decreased by 1.19, 1.96, 4.68, and 0.50-fold, respectively, compared to CTG (**Figure 2A**). Obviously, butyrate production was the most reduced in the LPG, while it was increased by 3.26- and 4.50-fold in the SPG and CG, respectively, compared to the LPG. Moreover, the levels of other SCFAs simultaneously increased after the administration of soy protein in the SPG.

A total of 1,054 metabolites were measured among the four groups. After analysis, 398 differentially expressed metabolites showed significant changes between CTG and LPG (VIP $>$ 1, $p < 0.05$) (**Figure 2B**), 257 differentially expressed metabolites between CG and LPG (VIP $>$ 1, $p < 0.05$) (**Figure 2C**), and 292 differentially expressed metabolites between SPG and LPG (VIP $>$ 1, $p < 0.05$) (**Figure 2D**). In these differentially expressed metabolites, valine was sharply decreased in the LPG by 74.7% compared to the CTG; however, it was restored to 80.6 and 91.2% in SPG and CG, respectively, compared to LPG (**Figure 2E**). The isoleucine, phenylalanine, and tryptophan also decreased by 81.1, 82.9, and 61.3%, respectively, in the LPG compared to that in CTG (**Figures 2F–H**), while alleviated after supplementary soy protein and casein.

The Kyoto Encyclopedia of Genes and Genomes (KEGG) was used to catch and map the metabolites in the colonic contents, and the results were analyzed through the enrichment pathway to show the enrichment of metabolites in the pathway. As shown in **Figure 2I**, the differentially expressed metabolites between CTG and LPG hit 23 metabolism pathways which included vitamin B_6 metabolism, valine, leucine, and isoleucine biosynthesis, phenylalanine, tyrosine, and tryptophan biosynthesis, pantothenate and CoA biosynthesis, cysteine and methionine metabolism, linoleic acid metabolism, and arginine and proline metabolism [$-\ln(p) > 1$]. Similarly, vitamin B_6 metabolism was significantly influenced in the SPG and CG compared to the LPG [$-\ln(p) > 1$] (**Figures 2J,K**). In addition, amino acid metabolism (tryptophan, tyrosine) and biosynthesis (tryptophan, tyrosine, isoleucine, leucine, valine, and phenylalanine) pathways were statistically changed among CTG, SPG, and CG compared to LPG.

Effects of Soy Protein on Metabolites in Serum

The metabolites in the serum measured by untargeted metabolomics based on MS/MS data are presented in **Figures 3A–C**. The LPG had 78 upregulated metabolites and 44 downregulated metabolites compared to CTG (**Figure 3A**), and the downregulated metabolites were mainly centralized in amino acid substances, such as tryptophan and threonine. However, the number of differentially expressed metabolites was reduced to 81 and 60 in the SPG and CG, respectively, compared to the CTG (**Figures 3B,C**).

The amount of tryptophan decreased by 266.1% in the LPG compared to CTG while restored in SPG and CG (**Figure 3D**) (VIP $>$ 1 and $p \leq 0.05$). Moreover, 5-hydroxy-tryptophan (5-HTP) showed significant changes in the results. In LPG, the content of 5-HTP was sharply decreased by 143.2, 82.2, and 31.5%, respectively, compared to CTG, SPG, and CG, respectively (**Figure 3E**). Since differences in amino acid substances among groups were observed, we conducted metabolic pathway analysis of the different metabolites (**Figures 3F–H**). Compared with the CTG, there were 6, 5, and 11 metabolite changes in the pathways of LPG, CG, and SPG, respectively, in which the amino acid metabolism pathway was involved as the main metabolite pathway. Through comprehensive analysis of the pathways where differential metabolites mainly gathered, key pathways that had higher correlation with the metabolites were determined. Five and three differentially expressed metabolites between the CTG and LPG hit the glycine-serine-threonine metabolism pathway and the tryptophan-metabolism pathway. However, these two metabolic pathways were restored among the CTG and the other two groups.

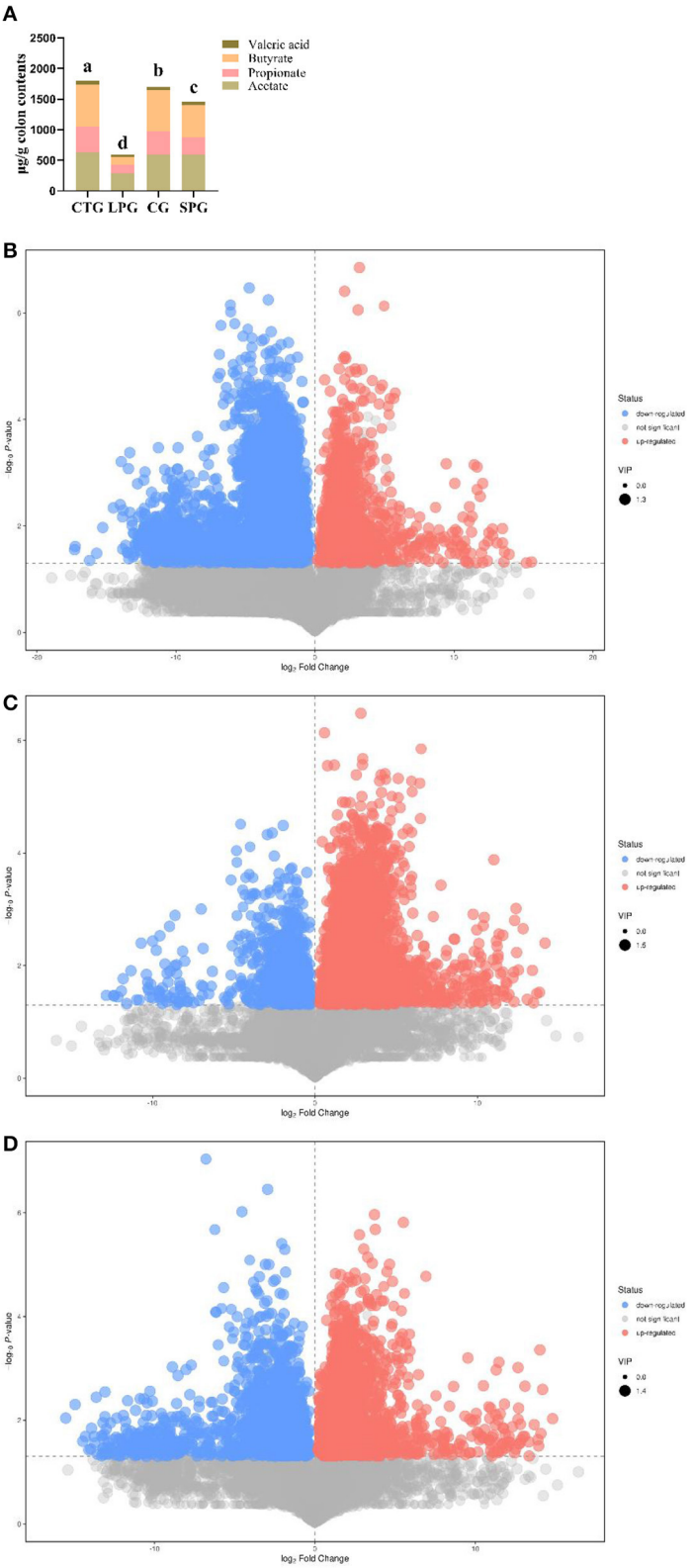

FIGURE 2 | Continued

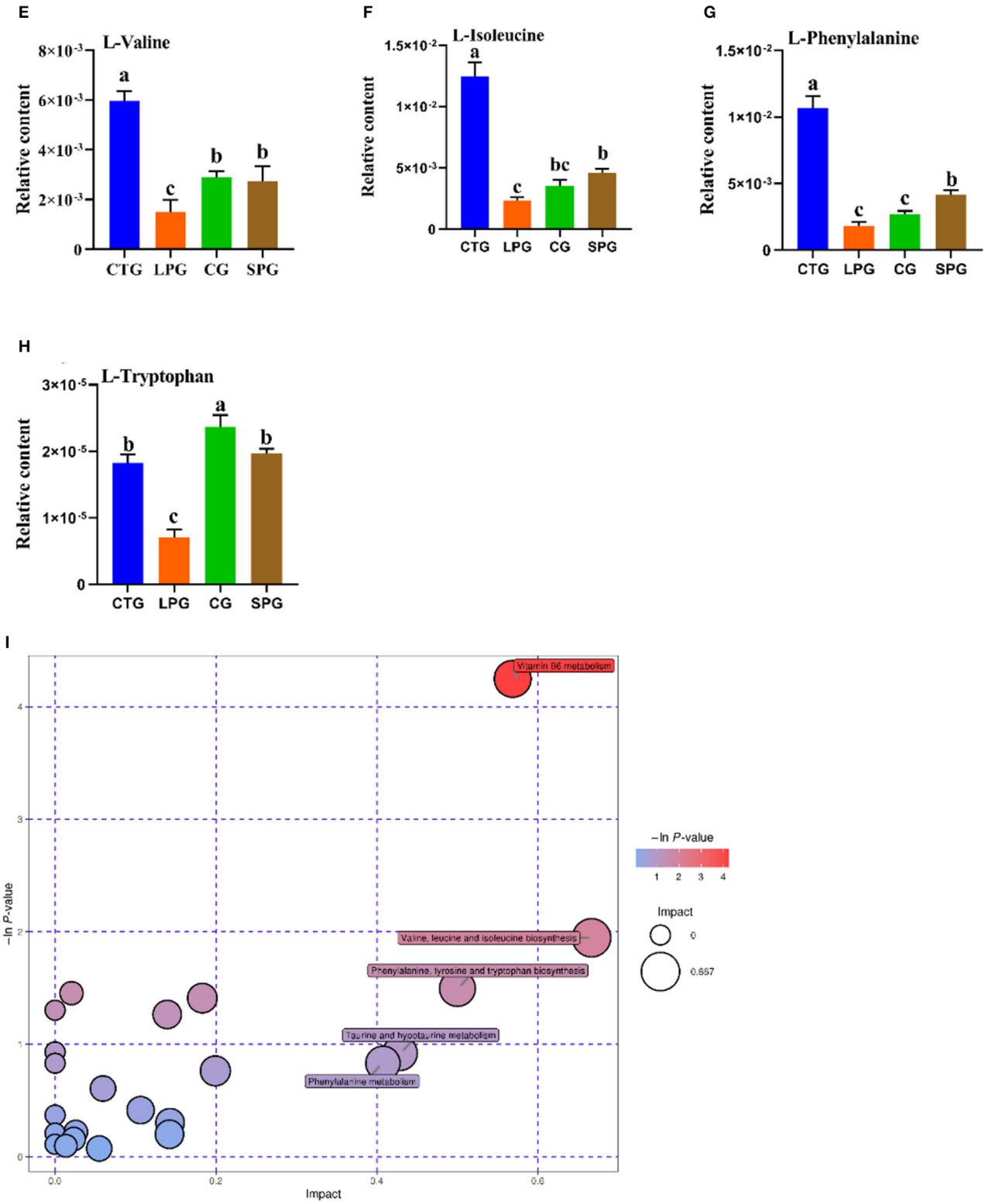

FIGURE 2 | Continued

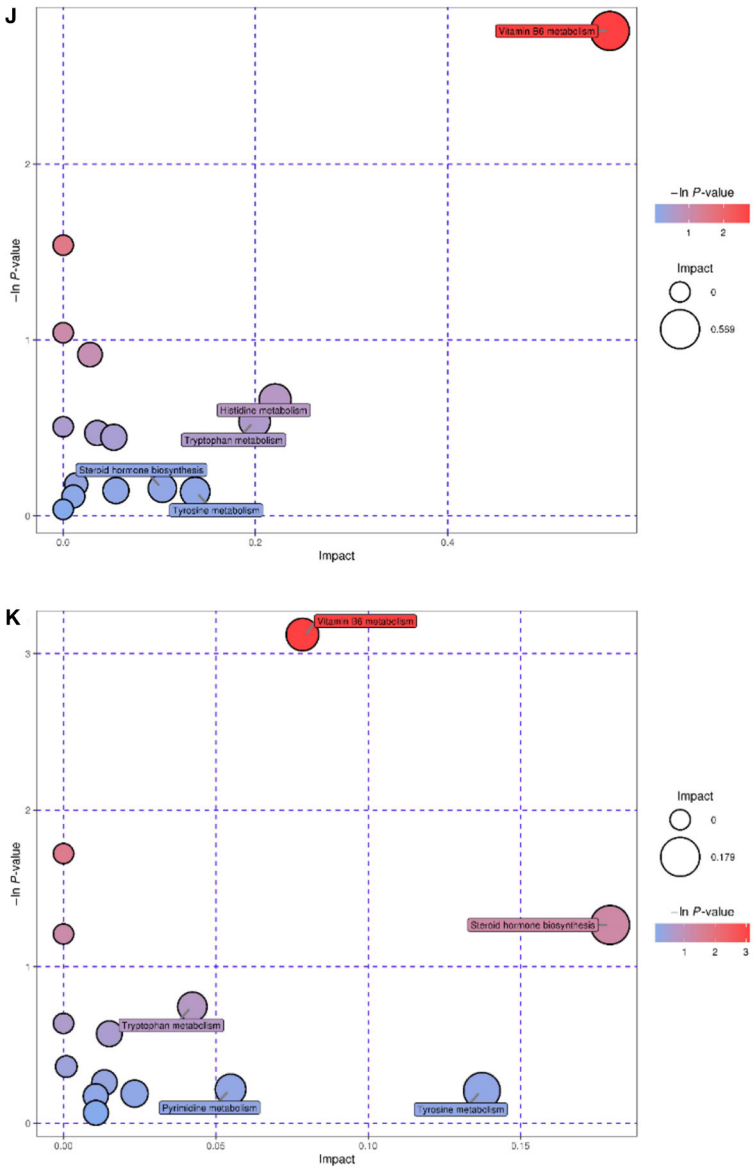

FIGURE 2 | Effect of diet intervention on the metabolites in the colon. **(A)** The contents of short-chain fatty acids (SCFAs). **(B)** The differentially expressed metabolites between LPG and CTG. **(C)** The differentially expressed metabolites between CG and LPG. **(D)** The differentially expressed metabolites between SPG and LPG. **(E)** The relative content of L-valine. **(F)** The relative content of L-isoleucine. **(G)** The relative content of L-phenylalanine. **(H)** The relative content of L-tryptophan. **(I)** Bobble plot of LPG to CTG. **(J)** The bobble plot of CG to LPG. **(K)** The bobble plot of SPG to LPG. Data are presented as mean ± SEM. Different letters indicate statistical differences among groups ($p < 0.05$). CTG, control group; LPG, low protein group; CG, casein group; SPG, soy protein group.

Effects of Soy Protein on Gut Microbiota

After sampling the colonic contents and sequencing in the V3–V4 regions using 16S rRNA, a total of 2,158,844 pairs of reads were obtained. With double-ended read quality control and splicing, a total of 2,148,662 purified reads were generated. At least 79,107 clean reads were obtained in each sample. Usearch software was used to cluster reads in the levels of 97.0% similarity (20), and subsequently obtained 487, 386, 479, and 481 OTUs in the CTG, LPG, SPG, and CG, respectively (**Figure 4A**). The significant reduction of OTUs in the LPG suggested that malnutrition caused a sharp decrease in the diversity of bacteria. Similarly, it reflected the richness of microbial communities, and the Shannon index was decreased dramatically in LPG compared to CTG (**Figure 4B**). However, the OTUs and the Shannon index were upgraded after the rats were supplemented with soy protein and casein, which suggested that the diversity of the species was restored (**Figures 2A,B**).

The changes in microbiota were shown in both the phylum and genus levels (**Figures 4C,D**). Belonging to the phylum level, *Firmicutes* dominated among the four groups. However, the

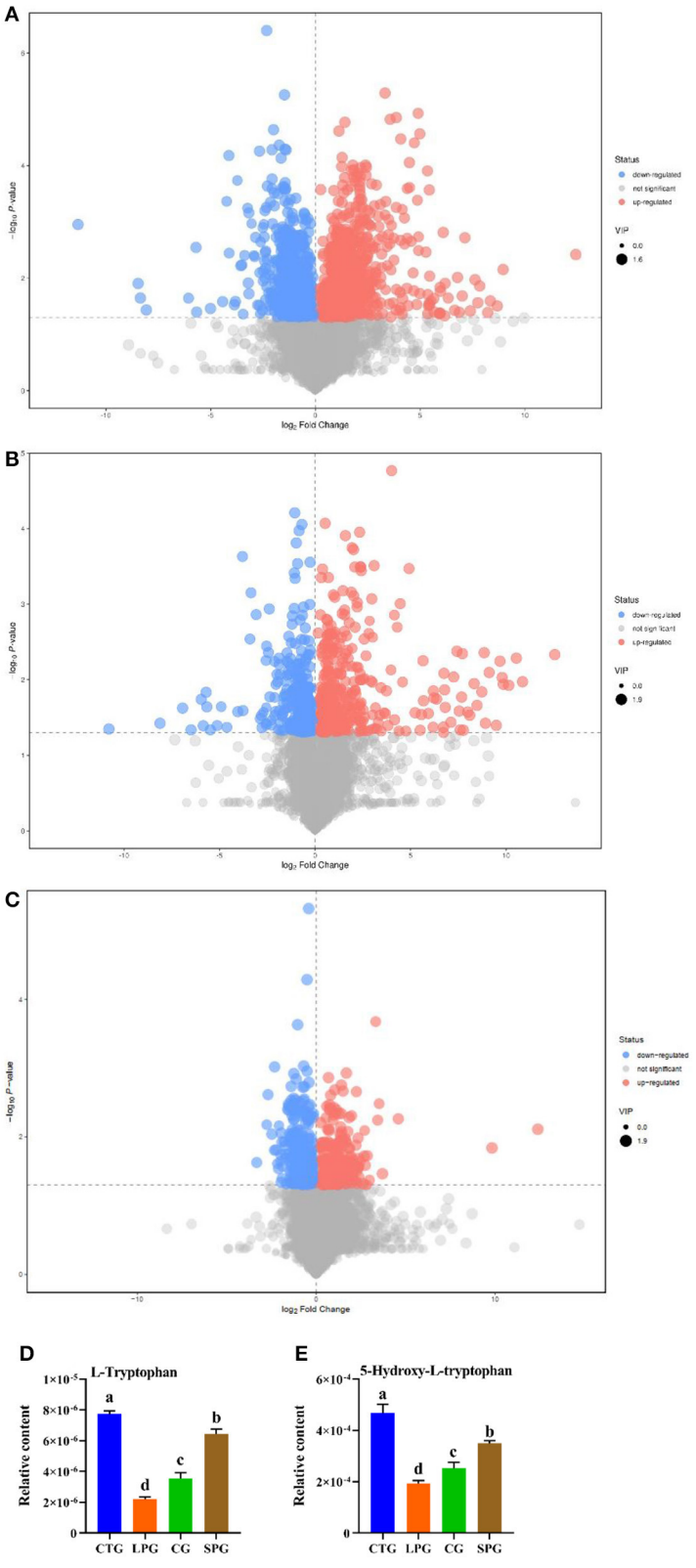

FIGURE 3 | Continued

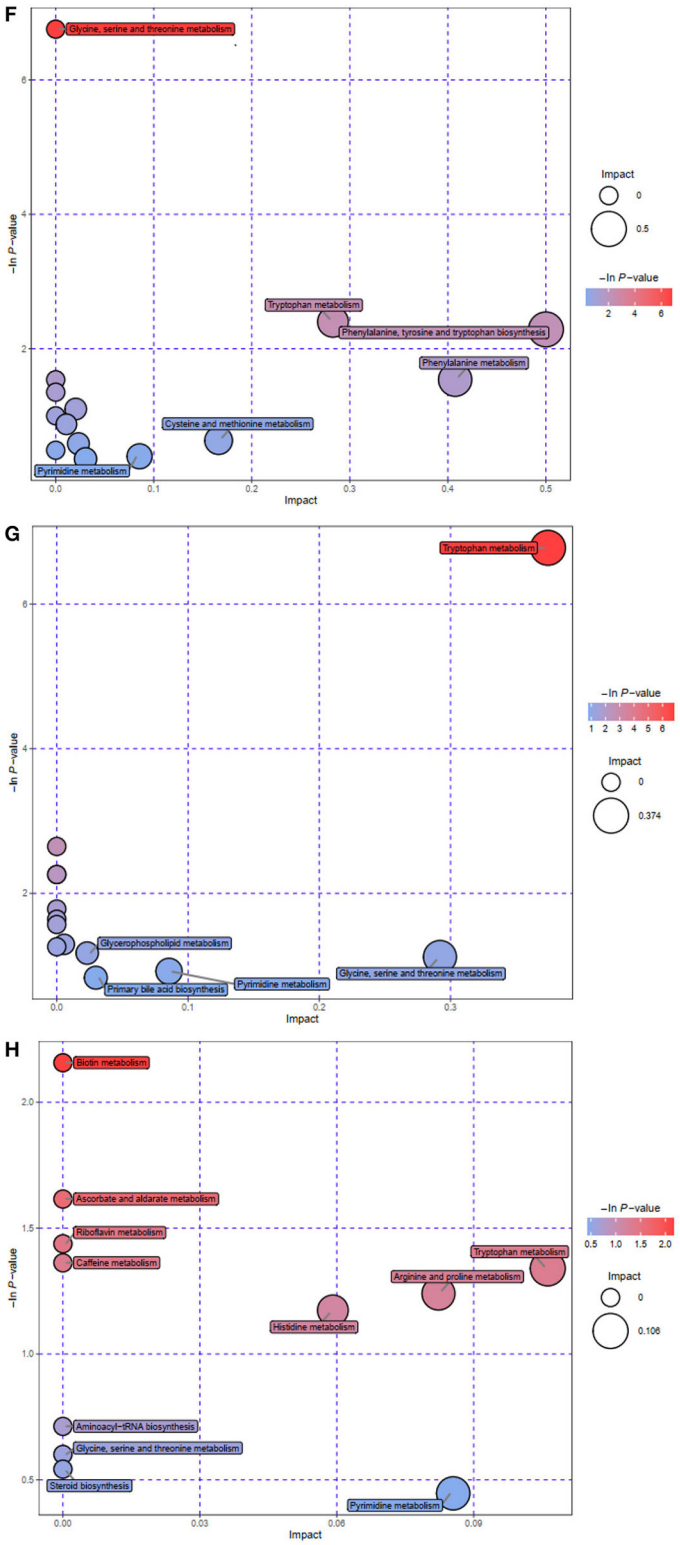

FIGURE 3 | Effect of diet intervention on the metabolites in serum. **(A)** The differentially expressed metabolites between LPG and CTG. **(B)** The differentially expressed metabolites between SPG and CTG. **(C)** The differentially expressed metabolites between CG and CTG. **(D)** The relative content of L-tryptophan. **(E)** The relative content of 5-hydroxy-L-tryptophan. **(F)** Bobble plot of LPG to CTG. **(G)** The bobble plot of SPG to CTG. **(H)** The bobble plot of CG to CTG. Data are presented as mean ± SEM. Different letters indicate statistical differences among the groups ($p < 0.05$). CTG, control group; LPG, low protein group; CG, casein group; SPG, soy protein group.

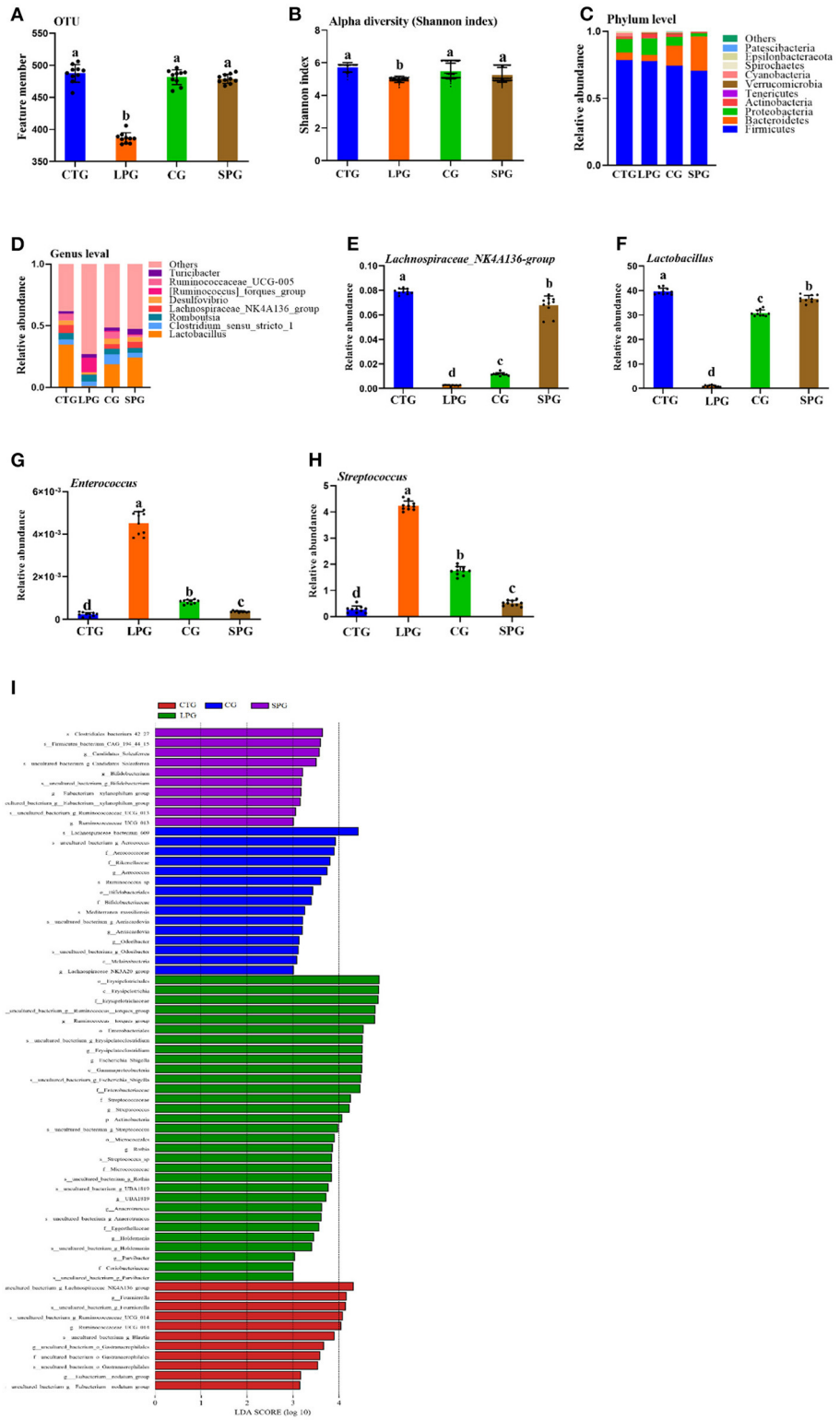

FIGURE 4 | Effect of diet intervention on the gut microbiota. **(A)** The amount of OTU based on 97.0% similarity. **(B)** Shannon index. **(C)** The change in the phylum level. **(D)** The change in the genus level. **(E)** The relative abundance of *Lachnospiraceae_NK4A136- group*. **(F)** The relative abundance of *Lactobacillus*. **(G)** The relative abundance of *Enterococcus*. **(H)** The relative abundance of *Streptococcus*. **(I)** LDA score of four diets on microbiota. Data are presented as mean ± SEM. Different letters indicate statistical differences among the groups ($p < 0.05$). OTU, operational taxonomic unit; CTG, control group; LPG, low protein group; CG, casein group; SPG, soy protein group.

ratio of *Bacteroidetes* varied significantly in different groups. *Bacteroidetes* increased significantly after the supplementation of soy protein and casein (**Figure 4C**). At the genus level, the groups, *Lactobacillus*, *Clostridium*_sensu_stricto_1, *Romboutsia*, *Lachnospiraceae*_NK4A136, *Desulfovibrio, Ruminococcaceae*_UCG-005, *[Ruminococcus]*_torques, and *Turicibacter* dominated in the CTG, SPG, and CG, respectively (**Figure 4D**). However, this trend was reversed in the LPG, with a sharp decrease in the counts of *Lactobacillus* and *Lachnospiraceae*_NK4A136_group and a dramatic rise in the relative abundance of *[Ruminococcus]*_torques_group. Based on the present study and previous conclusions by other scientists, four bacteria were selected for in-depth analysis. The relative abundance of *Lachnospiraceae*_NK4A136_group and *Lactobacillus* increased by 31.0-fold, 3.81-fold and by 3.52-fold, 27.0-fold in the SPG and CG, respectively (**Figures 4E,F**), while a reverse trend was observed in *Enterococcus* and *Streptococcus* compared to LPG (**Figures 4G,H**). Compared to LPG, *Enterococcus* and *Streptococcus* decreased by 11.0- and 4.52-fold in the SPG, and simultaneously, it was downregulated by 7- and 1.4-fold in the CG.

A linear discriminant analysis (LDA) column graph apparently showed a differential microbial among the four groups (**Figure 4I**). Sixty-seven OTUs were observed with significant alterations, including 11 in the CTG, 15 n the CG, and 10 in the SPG, respectively. Importantly, the LPG showed the most notable changes in the number of OTUs (31 OTUs). There were 5 OTUs, 15 OTUs, and 1 OTU in the CTG, LPG and CG, respectively, with LDA scores over 4. As a biomarker among groups, these OTUs were classified at the phylum level, and bacteria found in the LPG were assigned to four OTUs at the phylum level as follows: *Firmicutes*, *Bacteroidetes*, *Proteobacteria,* and *Actinobacteria*. Two OTUs were found in the CTG, 4 were found in the CG, and 2 were found in the SPG. However, *Firmicutes* dominated the biomarker bacteria among the four groups.

The Association Between Microbiota and Apparent Indicators

To test the influence of microbiota on rat growth and SCFA production, the Spearman's algorithm was used to carry out a correlation analysis. It was shown that there was a positive correlation among the targeted microbiota (*Lachnospiraceae*_NK4A136_group, *Phascolarctobacterium*, *Lactobacillus,* and *Alloprevotella*), body weight, and tail length (**Figure 5A**), while *Enterococcus*, *Streptococcus*, *Lachnospiraceae*_NK3A20_group, *Akkermansia*, *Erysipelatoclostridium,* and *Ruminococcus*_torques_group showed a negative correlation with body weight and tail length. In addition, the change of gut microbiota performed relationships with metabolites in the colon and serum. The alleviation of *Lachnospiraceae*_NK4A136_group, *Lactobacillus,* and *Phascolarctobacterium* were simultaneous with the increase of tryptophan (in the colon and serum), isoleucine (in colon), phenylalanine (in colon), valine (in colon), and 5-HTP (in serum) (**Figure 5B**). Therefore, an analysis was conducted between metabolites (in the colon and serum) and apparent indicators. It was evident that metabolites in the colon and serum were closely related to the growth of the rats in the malnutrition models (**Figure 5C**).

DISCUSSION

Many studies have demonstrated the beneficial functions of dietary intervention on undernutrition by restructuring the gut microbiota (4, 14). However, the potential of plant protein on alleviating growth deficits, and the effect played by gut microbiota and metabolites (in the colon and serum), is still unclear, impelling an urgent need to search for the mechanisms of how soy protein improves undernutrition in rats.

In the present study, supplementary soy protein alleviated the weight loss of weaning rats with undernutrition. Previous findings reported that supplementary soy flour in the diet improved body weight loss in undernourished piglets (4), while soy protein was first evidenced as a functional ingredient which performed extinguished effects on malnutrition in the present study. In addition, changes in the tail length of the rats showed a similar trend with the change in the body weight. In poor areas, deficiency of protein intake is one reason for the stunted growth. Therefore, high quality and efficient protein consumption were important to improve the linear growth of children in the developing countries (21). The amino acids of soy protein and casein in the present study are not completely similar to the previous study because of the difference in the purity and source of soy protein, but the ratio of the amino acids remained the same and the methionine and cystine were found to be the limiting amino acids in soy protein (22). A previous study confirmed that supplementary soy protein significantly improved the essential plasma amino acid concentrations in growth stunted rats which is evidenced in the present study (21). Although casein was higher than soy protein in AAS, soy protein improved the stunted growth better than casein.

A 6 week-diet intervention significantly restored the stunted growth induced by malnutrition. IGF-1, an indispensable factor in growth, is produced by the growth hormone secreted in the pituitary gland (23). ACE 2 plays an important role in regulating protein uptake, gut microbial ecology, and innate immunity (24). Our results demonstrated that the levels of IGF-1 and ACE 2 in LPG was statistically decreased in the serum, but the levels were restored after the intake of soy protein and casein. The decrease of IGF-1 and insufficient microbes in the gut happened simultaneously in mice (25). Similarly, the LPG showed low IGF-1 level and abnormal gut microbiota, while the supplementary soy protein improved this phenomenon. Soy protein is rich in amino acid composition and nutritional composition, but limited studies have reported the potential of soy protein in improving the malnutrition. More importantly, it has been observed that compared with protein derived from animals, plant-based crude protein has lower digestibility (26). Therefore, undigested protein residues can enter the colon as a substrate utilized by microbial to improve the intestinal health. A hypothesis was formed

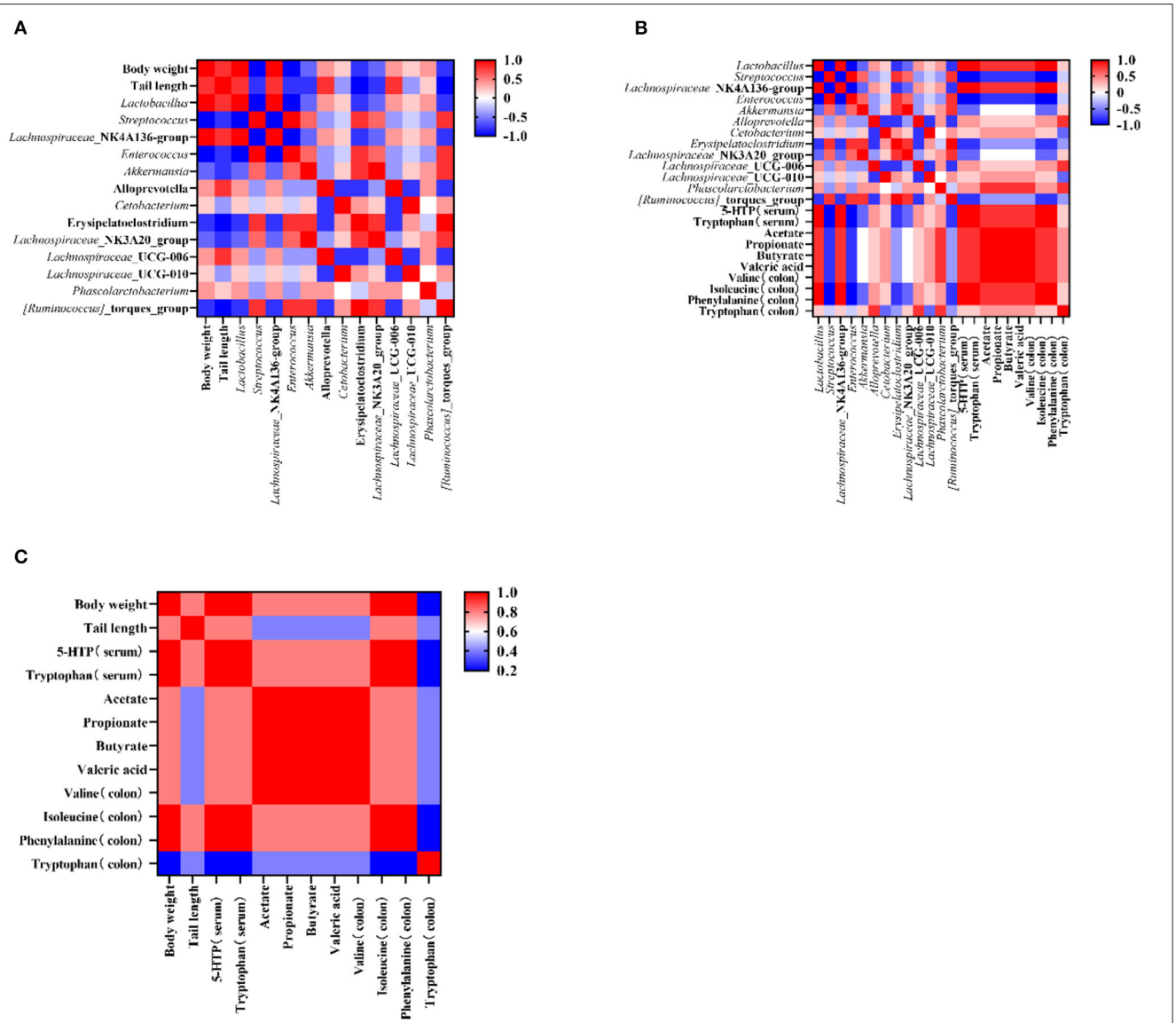

FIGURE 5 | The corelation among the targeted bacteria, apparent indicators, and metabolites (in the serum and the colon). **(A)** The corelation between targeted bacteria and apparent indicators. **(B)** The correlation between targeted bacteria and metabolites (in the colon and the serum). **(C)** The correlation between apparent indicators and metabolites (in the colon and the serum). Data are presented as mean ± SEM. Different letters indicate statistical differences among the groups ($p < 0.05$). CTG, control group; LPG, low protein group; CG, casein group; SPG, soy protein group.

regarding whether soy protein reshapes the gut microbiota, thus correcting malnutrition.

As an important metabolite (acetate, propionate, butyrate, and valeric acid) of microorganisms, the production of SCFAs was related to the effects of directed foods on gut microbiota, which applied protein and cellulose in the ingested diet (27). The total concentration and compositions of SCFAs among the four groups varied significantly. The CTG showed the highest concentration of SCFAs, while the LPG had the lowest concentration, which was similar to the previous study (27). Butyrate has been claimed to foster the proliferation of prebiotics in the gut and it played a unique role in reshaping the host metabolism and maintaining the integrity function of the intestine (28). A previous study claimed that the concentration of soy protein influenced the growth performance and the content of butyrate in broiler chicken through to day 42 of age (29). The sharp reduction in butyrate in the LPG was in accordance with the adverse influence in the gut microbiota, while the restoration and production of butyrate in the SPG also protected gut integrity. Acetate, propionate, and butyrate were dominant in the total SCFAs, while the butyrate content in the LPG was significantly reduced. This result suggests that dietary intervention caused changes in the contents of microbiota metabolites, and were simultaneous with the changes in the intestinal microbes. Overall,

soy protein increased the production of SCFAs and influenced gut microbiota, and subsequently alleviated malnutrition. However, changes of other metabolites in the colon coincided with SCFAs and gut microbiota.

The content of tryptophan decreased sharply in the colon in LPG, which indicated that the tryptophan biosynthesis and metabolism was damaged in malnutrition models. As aryl hydrocarbon receptor ligands, tryptophan catabolites played a unique role in the gut and immune system in the host (30). Therefore, the restoration of this metabolism and the content in the colon were critical in malnutrition improvement. At the same time, phenylalanine, isoleucine, and valine were also decreased in LPG which coincided with our previous results (31). Vitamin B_6 metabolism in the colon showed significant influence among LPG and other groups because the deficiency of tryptophan decreased the tryptophan-nicotinamide conversion rate, while subsequently influenced the vitamin B_6 metabolism (32). In addition, the disorder of Vitamin B_6 and low level of propionate and butyrate showed in LPG at the same time. Meanwhile, as a biomarker, *Lachnospiraceae*_NK4A136_group was observed to be a vitamin B_6 deficient group (33). Therefore, it is concluded that the change of metabolites in the colon was closely associated with the gut microbiota in alleviating undernutrition. Recent studies reported that changes of metabolites in the serum was related to the gut microbiota and SCFAs, which meant that the metabolites from the gut microbiota passed the gut barrier, and subsequently influenced the serum metabolites (28, 34).

Soy protein intake improved health in malnourished rats by influencing the gut microbiota, especially some signaling bacteria. Accumulating evidence has revealed that tryptophan, 5-HTP, and 5-HT (serotine) are important factors to maintain the intestinal balance (28, 30). Distress, loss of appetite, and other symptoms are usually associated as the signs of malnourishment in patients. As a neurotransmitter, 5-HT has been shown to affect the regulatory mechanisms of mood, appetite, etc., and it is associated with stress, anxiety, and depression (35). The results from untargeted metabolism analysis in the serum showed that the 5-HTP levels decreased sharply in the LPG, but its relative content was restored after diet intervention with soy protein and casein. A previous study reported that different diet proteins induced variable changes of 5-HTP and 5-HT in rats (36). In fact, diet soy protein showed higher tryptophan in the serum and higher 5-HTP in the hypothalamic, the hippocampal, and the cortical regions, compared to diet casein (36). Results were not completely the same with the present study, because the rats administered with soy protein in the present study were malnourished. However, the significant increase of 5-HTP in the serum evidenced a greater potential of soy protein in alleviating malnutrition. The 5-HTP could cross the blood-brain-barrier, and regulate the production of 5-HT. Thus, the reduction of 5-HTP in the serum might reveal the change of 5-HT in the brain. The difference of *Lactobacillus* levels between the CTG and LPG was also related to the change of 5-HT, because Liu et al. reported *Lactobacillus* genera on 5-HT synthesis (28).

The relative contents of tryptophan and the precursor of serotonin were significantly reduced in malnourished children which are consistent with our findings of a significant reduction of tryptophan levels in the LPG (24). Dietary supplementation with soy protein and casein alleviated this situation. Although the levels of serum 5-HTP and tryptophan in the SPG and CG did not reach the levels found in the normal rats, the SPG was still more effective than the CG which reported in a previous study that soy protein produced better 5-HTP and tryptophan in the serum than casein in the healthy rats (36). A recent study demonstrated that gut microbes produce 5-HT, 5-HTP, and indolealdehyde (IAld) *via* numerous other metabolic pathways, such as *Lactobacillus,* which converts tryptophan to IAld (28). Our research demonstrated a closer association between the decrease of gut microbiota and the downregulation of tryptophan metabolism in the LPG, while supplementary soy protein to undernourished rats regulated intestinal diversity and upregulated the tryptophan metabolism. Moreover, the glycine-serine-threonine metabolism pathway was significantly enriched among the four groups. In this pathway, compared to CTG, the LPG had hit the greatest number of differentially expressed metabolites (five), while the SPG and CG each had hit one. These data indicate that malnutrition caused by inefficient protein intake led to the disorder of the glycine-serine-threonine metabolism pathway.

The diversity and richness of the gut microbiota in LPG were statistically decreased which coincided with previous reports which showed that the change in the structure and relative content of gut microbiota was related to malnutrition (4). After supplementation with soy protein, the relative abundance of prebiotics, such as *Lachnospiraceae*_NK4A136_group and *Lactobacillus* in the gut increased, which was similar to a previous study in which Tamura et al. (27) observed changes in various bacteria after the intake of soy protein. Additionally, the relative abundance of *Streptococcus,* which was observed to be high in malnourished children (37), was much higher in the LPG and lower in the rats receiving soy protein. Therefore, the decrease of "age-discriminatory" bacteria indicated that the gut microbiota became more maturer and healthier. Moreover, the increase of the relative abundance of *Lactobacillus* and *Lachnospiraceae*_NK4A136_group led the host healthier because *Lactobacillus* terminated the adverse effects of chronic undernutrition in germ-free mice (25). All the bacteria observed in this study were related to intestinal health and maturation, as evidenced by previous studies (4, 28). Studies claimed that SCFAs performed beneficial effects on gut microbiota (28), and subsequently emerging views have focused on the relationship between gut microbiota and metabolites.

In the results of OMICS, fifty bacteria at the genus level were shown to be statistically correlated with the metabolites in the colon and serum, and found to have alleviated the growth defects; especially, the increase of *Lactobacillales, Alloprevotella,* and *Lachnospiraceae_NK4A136_group* kept up with the upregulation of beneficial substances, such as SCFAs and amino acids in the colon and serum. Many studies have found that SCFAs played crucial roles in the metabolites of the colon, serum, intestinal functions, and in growth development (34, 38). It is evident that the gut microbiota influenced the metabolites in the serum

and colon, and subsequently improves host health, such as attenuating undernutrition.

CONCLUSION

In the present study, soy protein intake positively influenced the physiological condition of rats by increasing the body weight, tail length, and serum bioinformation compared to undernourished rats. The change in the production of SCFAs revealed a change in the composition of gut microbiota. From the results of 16S rRNA sequencing, the relative abundances of four bacteria in the SPG and CG changed significantly compared to that in the LPG. Untargeted metabolic profiling showed that the metabolites of tryptophan and 5-HTP in malnourished rats changed significantly. The tryptophan metabolism and glycine-serine-threonine metabolism pathways were dramatically damaged in LPG but could be restored by supplementing the diet of soy protein. In the present study, we first reported the potential of soy protein in improving malnutrition evidenced by the changes of gut microbiota, SCFAs, colon, and serum metabolites. In addition, the bacteria of *Lachnospiraceae*_NK4A136_group, *Lactobacillus*, *Enterococcus*, and *Streptococcus* were closely related to malnutrition. More importantly, serum metabolites (tryptophan and 5-HTP), colon metabolites (SCFAs, valine, phenylalanine, isoleucine, and tryptophan), and metabolite pathways (tryptophan and glycine-serine-threonine in serum and vitamin B_6 and tryptophan in the colon) were shown for the first time, with a significant change during the period of improving malnutrition in early life. This study evidenced that soy protein supplementary is an effective dietary intervention that alleviates malnutrition. Soy protein, an inexpensive and easily obtained ingredient in the food industry, can be added to a supplemented food to reduce early childhood malnutrition.

DATA AVAILABILITY STATEMENT

The data presented in the study are deposited in the National Center for Biotechnology Information repository, accession number PRJNA774838.

ETHICS STATEMENT

The animal study was reviewed and approved by Beijing Municipal Science and Technology Commission.

AUTHOR CONTRIBUTIONS

ZW and NZ contributed equally to this work. ZW and NZ performed the majority of the experiments and wrote the manuscript. LZ and ZS contributed to the data analysis. BD, GR, and YY designed and supervised the study and checked the final manuscript. All authors contributed to the article and approved the submitted version.

FUNDING

This work was supported by the Central Public-interest Scientific Institution Basal Research Fund (Y2020PT30).

REFERENCES

1. Kangas ST, Kaestel P, Salpeteur C, Nikiema V, Talley L, Briend A, et al. Body composition during outpatient treatment of severe acute malnutrition: results from a randomised trial testing different doses of ready-to-use therapeutic foods. *Clin Nutr.* (2020) 39:3426–33. doi: 10.1016/j.clnu.2020.02.038
2. Kamil RZ, Murdiati A, Juffrie M, Nakayama J, Rahayu ES. Gut microbiota and short-chain fatty acid profile between normal and moderate malnutrition children in Yogyakarta, Indonesia. *Microorganisms.* (2021) 9:127. doi: 10.3390/MICROORGANISMS9010127
3. Pennisi E. Gut microbes may help malnourished children. *Science.* (2019) 365:109. doi: 10.1126/science.365.6449.109
4. Gehrig JL, Venkatesh S, Chang HW, Hibberd MC, Kung VL, Cheng J, et al. Effects of microbiota-directed foods in gnotobiotic animals and undernourished children. *Science.* (2019) 365:169. doi: 10.1126/science.aau4732
5. Fan Y, Pedersen O. Gut microbiota in human metabolic health and disease. *Nat Rev Microbiol.* (2021) 19:55–71. doi: 10.1038/s41579-020-0433-9
6. Luan Y, Fischer G, Wada Y, Sun L, Shi P. Quantifying the impact of diet quality on hunger and undernutrition. *J Clean Product.* (2018) 205:432–46. doi: 10.1016/j.jclepro.2018.09.064
7. Weinberg LG, Berner LA, Groves JE. Nutrient contributions of dairy foods in the United States, continuing survey of food intakes by individuals, 1994-1996, 1998. *J Am Diet Assoc.* (2004) 104:895–902. doi: 10.1016/j.jada.2004.03.017
8. Peled S, Livney YD. The role of dietary proteins and carbohydrates in gut microbiome composition and activity: a review. *Food Hydro.* (2021) 120:106911. doi: 10.1016/j.foodhyd.2021.106911
9. Pluske JR, Pethick DW, Hopwood DE, Hampson DJ. Nutritional influences on some major enteric bacterial diseases of pig. *Nutr Res Rev.* (2002) 15:333–71. doi: 10.1079/NRR200242
10. Hooper LV, Littman DR, Macpherson AJ. Interactions between the microbiota and the immune system. *Science.* (2012) 336:1268–3. doi: 10.1126/science.1223490
11. Hancock RE, Haney EF, Gill EE. The immunology of host defence peptides: beyond antimicrobial activity. *Nat Rev Immunol.* (2016) 16:321–34. doi: 10.1038/nri.2016.29
12. Morita T, Kasaoka S, Kiriyama S. Physiological functions of resistant proteins: proteins and peptides regulating large bowel fermentation of indigestible polysaccharide. *J AOAC Int.* (2004) 87:792–6. doi: 10.1093/jaoac/87.3.792
13. Donovan SM. Introduction to the special focus issue on the impact of diet on gut microbiota composition and function and future opportunities for nutritional modulation of the gut microbiome to improve human health. *Gut Microbes.* (2017) 8:75–81. doi: 10.1080/19490976.2017.1299309
14. Raman AS, Gehrig JL, Venkatesh S, Chang HW, Hibberd MC, Subramanian S, et al. A sparse covarying unit that describes healthy and impaired human gut microbiota development. *Science.* (2019) 365:4735. doi: 10.1126/science.aau4735
15. Deplancke B, Gaskins HR. Microbial modulation of innate defense: goblet cells and the intestinal mucus layer. *Am J Clin Nutr.* (2001). 73:1131S−41. doi: 10.1093/ajcn/73.6.1131S
16. Lozupone C, A, Stombaugh JI, Gordon JI, Jansson JK, Knight R. Diversity, stability and resilience of the human gut microbiota. *Nature.* (2012) 489:220–30. doi: 10.1038/nature11550
17. Velly H, Britton RA, Preidis GA. Mechanisms of cross-talk between the diet, the intestinal microbiome, and the undernourished host. *Gut microbes.* (2017) 8:98–112. doi: 10.1080/19490976.2016.1267888
18. Brown EM, Wlodarska M, Willing BP, Vonaesch P, Han J, Reynolds LA, et al. Diet and specific microbial exposure trigger features of environmental enteropathy in a novel murine model. *Nat Commun.* (2015) 6:7806. doi: 10.1038/ncomms8806

19. Shi ZX, Zhu YY, Teng C, Yao Y, Ren GX, Richel A. Anti-obesity effects of alpha-amylase inhibitor enriched-extract from white common beans (*Phaseolus vulgaris* L.) associated with the modulation of gut microbiota composition in high-fat diet-induced obese rats. *Food Funct.* (2020) 11:1624–34. doi: 10.1039/c9fo01813a
20. Edgar RC. UPARSE: highly accurate OTU sequences from microbial amplicon reads. *Nat Methods.* (2013) 10:996–8. doi: 10.1038/nmeth.2604
21. Furuta C, Murakami H. A novel concept of amino acid supplementation to improve the growth of young malnourished male rats. *Ann Nutr Metab.* (2018) 72:231–40. doi: 10.1159/000487603
22. Han SW, Chee KM, Cho SJ. Nutritional quality of rice bran protein in comparison to animal and vegetable protein. *Food Chem.* (2015) 172:766–9. doi: 10.1016/j.foodchem.2014.09.127
23. Thissen JP, Ketelslegers JM, Underwood LE. Nutritional regulation of the insulin-like growth factors. *Endocr Rev.* (1994) 15:80–101. doi: 10.1210/edrv-15-1-80
24. Hashimoto T, Perlot T, Rehman A, Trichereau J, Ishiguro H, Paolino M, et al. ACE2 links amino acid malnutrition to microbial ecology and intestinal inflammation. *Nature.* (2012) 487:477–81. doi: 10.1038/nature11228
25. Schwarzer M, Makki K, Storelli G, Machuca-Gayet I, Srutkova D, Hermanova P, et al. Lactobacillus plantarum strain maintains growth of infant mice during chronic undernutrition. *Science.* (2016) 351:854–7. doi: 10.1126/science.aad8588
26. He L, Han M, Qiao S, He P, Li D, Li N, et al. Soybean antigen proteins and their intestinal sensitization activities. *Curr Protein Pept Sc.* (2015) 16:613–21. doi: 10.2174/1389203716666150630134602
27. Tamura K, Sasaki H, Shiga K, Miyakawa H, Shibata S. The timing effects of soy protein intake on mice gut gicrobiota. *Nutrients.* (2019) 12:87. doi: 10.3390/nu12010087
28. Liu Z, Dai X, Zhang H, Shi R, Hui Y, Jin X, et al. Gut microbiota mediates intermittent-fasting alleviation of diabetes-induced cognitive impairment. *Nat Commun.* (2020) 11:855. doi: 10.1038/s41467-020-14676-4
29. Kiarie EG, Mohammadigheisar M, Kakhki RAM, Madsen MH. Impact of feeding modified soy protein concentrate in the starter phase on growth performance and gastrointestinal responses in broiler chickens through to day 42 of age. *Poult Sci.* (2021) 100:101147. doi: 10.1016/j.psj.2021.101147
30. Roager HM, Licht TR. Microbial tryptophan catabolites in health and disease. *Nat Commun.* (2018) 9:3294. doi: 10.1038/s41467-018-05470-4
31. Cogo E, Elsayed M, Liang V, Cooley K, Guerin C, Psihogios A, et al. Are supplemental branched-chain amino acids beneficial during the oncological peri-operative period: a systematic review and meta-analysis. *Integr Cancer Ther.* (2021) 20:1534735421997551. doi: 10.1177/1534735421997551
32. Shibata K. Organ co-relationship in tryptophan metabolism and factors that govern the biosynthesis of nicotinamide from tryptophan. *J Nutr Sci Vitaminol.* (2018) 64:90–8. doi: 10.3177/jnsv.64.90
33. Mayengbam S, Chleilat F, Reimer RA. Dietary vitamin B_6 deficiency impairs gut microbiota and host and microbial metabolites in rats. *Biomedicines.* (2020) 8:469. doi: 10.3390/biomedicines8110469
34. Liu XN, Li X, Xia B, Jin X, Zou QH, Zeng ZH, et al. High-fiber diet mitigates maternal obesity-induced cognitive and social dysfunction in the offspring via gut-brain axis. *Cell Metab.* (2021) 33:923–38. doi: 10.1016/j.cmet.2021.02.002
35. Taleb S. Tryptophan dietary impacts gut barrier and metabolic diseases. *Front Immunol.* (2019) 10:2113. doi: 10.3389/fimmu.2019.02113
36. Choi S, Disilvio B, Fernstrom MH, Fernstrom JD. Meal ingestion, amino acids and brain neurotransmitters: effects of dietary protein source on serotonin and catecholamine synthesis rates. *Physiol Behav.* (2009) 98:156–62. doi: 10.1016/j.physbeh.2009.05.004
37. Monira S, Nakamura S, Gotoh K, Izutsu K, Watanabe H, Alam NH, et al. Gut microbiota of healthy and malnourished children in bangladesh. *Front Microbiol.* (2011) 2:228. doi: 10.3389/fmicb.2011.00228
38. Zhou CH, Meng YT, Xu JJ, Fang X, Zhao JL, Zhou W, et al. Altered diversity and composition of gut microbiota in Chinese patients with chronic pancreatitis. *Pancreatology.* (2020) 20:16–24. doi: 10.1016/j.pan.2019.11.013

Conflict of Interest: The authors declare that the research was conducted in the absence of any commercial or financial relationships that could be construed as a potential conflict of interest.

Publisher's Note: All claims expressed in this article are solely those of the authors and do not necessarily represent those of their affiliated organizations, or those of the publisher, the editors and the reviewers. Any product that may be evaluated in this article, or claim that may be made by its manufacturer, is not guaranteed or endorsed by the publisher.

frontiers in Nutrition

ORIGINAL RESEARCH
published: 06 December 2021
doi: 10.3389/fnut.2021.764556

The High Level of Xylooligosaccharides Improves Growth Performance in Weaned Piglets by Increasing Antioxidant Activity, Enhancing Immune Function, and Modulating Gut Microbiota

*Jiaman Pang[1], Xingjian Zhou[1], Hao Ye[1,2], Yujun Wu[1], Zhenyu Wang[1], Dongdong Lu[1], Junjun Wang[1] and Dandan Han[1]**

[1] State Key Laboratory of Animal Nutrition, College of Animal Science and Technology, China Agricultural University, Beijing, China, [2] Adaptation Physiology Group, Department of Animal Sciences, Wageningen University and Research, Wageningen, Netherlands

OPEN ACCESS

Edited by:
Fengjiao Xin,
Institute of Food Science and Technology, Chinese Academy of Agricultural Science (CAAS), China

Reviewed by:
Jiashun Chen,
Hunan Agricultural University, China
Fang Chen,
Allegheny Veterinary Emergency Trauma & Specialty, United States

***Correspondence:**
Dandan Han
handandan@cau.edu.cn

Specialty section:
This article was submitted to Nutrition and Microbes, a section of the journal Frontiers in Nutrition

Received: 25 August 2021
Accepted: 26 October 2021
Published: 06 December 2021

Citation:
Pang J, Zhou X, Ye H, Wu Y, Wang Z, Lu D, Wang J and Han D (2021) The High Level of Xylooligosaccharides Improves Growth Performance in Weaned Piglets by Increasing Antioxidant Activity, Enhancing Immune Function, and Modulating Gut Microbiota. Front. Nutr. 8:764556. doi: 10.3389/fnut.2021.764556

The aim of this study was to investigate the effects of the high level of xylooligosaccharides (XOS) on growth performance, antioxidant capability, immune function, and fecal microbiota in weaning piglets. The results showed that 28 d body weight exhibited linear and quadratic increases ($P < 0.05$) with increasing dietary XOS level, as well as average daily feed intake (ADFI) on d 15–28, average daily gain (ADG) on d 15–28 and 1–28. There was a linear decrease ($P < 0.05$) between XOS levels and feed conversion rate (FCR) on d 1–14 and 1–28. Additionally, glutathione peroxidase (GSH-Px) showed a linear increase ($P < 0.05$), while the malondialdehyde (MDA) level decreased linearly and quadratically ($P < 0.05$) with the increasing dietary level of XOS. Moreover, the XOS treatments markedly increased the levels of immunoglobulin A (Ig A) (linear, $P < 0.05$; quadratic, $P < 0.05$), IgM (quadratic, $P < 0.05$), IgG (linear, $P < 0.05$), and anti-inflammatory cytokine interleukin-10 (IL-10) (quadratic, $P < 0.05$) in serum, while the IL-1β (linear, $P < 0.05$; quadratic, $P < 0.05$) and IL-6 (linear, $P < 0.05$) decreased with increasing level of XOS. Microbiota analysis showed that dietary supplementation with 1.5% XOS decreased ($P < 0.05$) the α-diversity and enriched ($P < 0.05$) beneficial bacteria including *Lactobacillus*, *Bifidobacterium*, and *Fusicatenibacter* at the genus level, compared with the control group. Importantly, linearly increasing responses ($P < 0.05$) to fecal acetate, propionate, butyrate, and total short-chain fatty acids (SCFAs) were observed with increasing level of XOS. Spearman correlation analyses found that *Lactobacillus* abundance was positively correlated with ADG, acetate, propionate, and IgA ($P < 0.05$), but negatively correlated with IL-1β ($P < 0.05$). *Bifidobacterium* abundance was positively related with ADFI, total SCFAs, IgG, and IL-10 ($P < 0.05$), as well as *g_Fusicatenibacter* abundance with ADFI, total SCFAs,

and IL-10. However, *Bifidobacterium* and *Fusicatenibacter* abundances were negatively associated with MDA levels ($P < 0.05$). In summary, dietary supplementation with XOS can improve the growth performance in weaning piglets by increasing antioxidant capability, enhancing immune function, and promoting beneficial bacteria counts.

Keywords: Xylooligosaccharides, weaning piglets, growth performance, antioxidant, immune function, fecal microbiota, short-chain fatty acids

INTRODUCTION

In modern swine production, weaning is a critical period for piglets to encounter multiple stressors including environmental, dietary, and social changes (1). Due to immunological and physiological immaturity, weaning results in stress syndromes in piglets including transient anorexia, unbalanced gut microbiota, increased diarrhea incidence, and decreased growth performance (2). China is the biggest porker producer and consumer in the world but about 24 million piglets die from diarrhea caused by bacterial infection after weaning each year (3, 4). Thus, antibiotics were widely applied to prevent pathogenic infection and promote growth in the postweaning period (5). However, the antibiotic growth promoters have been limited to being used in swine industry in China due to the adverse effects of antibiotics resistance and residue, which pose a great threat to human health and food security (3). To maintain piglet health during the weaning period and preserve public health, it is urgent to find and develop antibiotic alternatives.

The growing evidence suggested prebiotics as preferable alternatives to antibiotics (6). Prebiotics are non-digestible substrates that improve host health by selectively stimulating growth or activity of specific bacteria (7). At present, commercial prebiotics are mainly functional oligosaccharides, such as galactooligosaccharides (GOS), mannanoligosaccharides (MOS), fructooligosaccharides (FOS), and xylooligosaccharides (XOS) (5, 6). The XOS are produced from hydrolysis of xylan, which widely exist in plant cell wall and various agricultural waste or byproducts. The XOS are composed of 2–10 xylose monomers linked through β-(1,4) linkages with acidity and temperature stability, and non-toxicity (8–10). Many researches indicated that dietary supplementation of XOS improve the animal growth performance in weaning piglets and broiler chicken by enhancing immune functions, elevating antioxidant activity, increasing nutrient digestibility, and maintaining intestinal morphology and barrier (4, 11–14). In addition, some studies found that XOS are able to increase short-chain fatty acids (SCFAs) concentrations in broiler chicken or weaning piglets (4, 15), stimulate proliferation of *Lactobacillu*s, and inhibit the growth of *Escherichia coli* in weaning piglets (4, 16). Christensen et al. (17) found that *Bifidobacteriaceae* varied approximately 10,000-fold from 0.001 to 10.7% in rats after consumption of 10% XOS. However, the abundance of *Bifidobacterium* had no remarkable increase at the low dosage of XOS in pigs (4, 11, 18).

Whether the high level of XOS can promote *Bifidobacterium* microbiota in weaning piglets remains unknown. Meanwhile, the effects of the high level of XOS on growth performance, antioxidant capability, and immune function have not been fully studied in weaning piglets. Therefore, the objective of this study was to investigate the high level of XOS effects on growth performance, antioxidant capability, and anti-inflammatory action, and whether the high level of XOS promote *Bifidobacterium* abundance of weaned piglets.

MATERIALS AND METHODS

This work was approved by the Animal Ethics Committee of China Agricultural University.

Animals, Housing, and Experimental Design

A total of 192 piglets (Duroc × Landrace × Large White) weaned at 30 d of age with an average initial body weight (BW) of 7.50 ± 0.8 kg were randomly divided into four groups based on BW and sex. Each group had six replicate pens with eight piglets per pen. The control group piglets were fed with a control diet without the supplementation of XOS. The XOS-treated groups piglets were received dietary supplementation of 0.75% XOS, 1.5% XOS, and 3% XOS, respectively. The XOS (P70, 70%) were provided by Longlive Biotechnology Corporation (Shandong, China). The experimental period included two feeding phases: phase 1, from d 1 to d 14 postweaning; phase 2, from d 15 to d 28 postweaning. The dietary compositions and nutrient concentrations are presented in **Table 1**. All diets without antibiotics were formulated to meet the nutrient requirements of National Research Council (19). The pigs were housed in an environmentally controlled room with slatted plastic flooring. The environmental temperature was maintained at 26–28°C and relative humidity was controlled at 40–50%. The pigs were given *ad libitum* access to feed and water throughout the trial for 28 days.

Samples Collection

Individual pig BW was recorded at the initial of the weaning and on d 14 and d 28. Pen feed intake was also measured on d 14 and d 28 of this experiment. The average daily gain (ADG), average daily feed intake (ADFI), and feed conversion rate (FCR) were calculated. The feces of pigs were scored daily for diarrhea according to the following criteria: 1 = firm and well-form feces, 2 = soft and form feces, 3 = sloppy feces and mild diarrhea, and 4 = pasty and liquid diarrhea. The incidence of diarrhea was calculated for the first 7 d after weaning. The incidence of diarrhea was calculated as follows: Diarrhea incidence (%) =

TABLE 1 | Composition of the experimental diets (as-fed basis).

Items	Phase 1 (1–14 d), XOS (% of diet)				Phase 2 (15–28 d), XOS (% of diet)			
	Control (0)	0.75	1.5	3	Control (0)	0.75	1.5	3
Ingredient (%)								
Corn	61.95	60.65	59.15	56.70	67.16	65.76	64.41	62.06
Soybean meal 43%	10.00	10.00	10.00	10.00	15.00	15.00	15.00	15.00
Dehulled soybean meal 46%	5.00	5.20	5.50	5.90	2.00	2.30	2.50	2.90
Fish meal	5.00	5.00	5.00	5.00	3.00	3.00	3.00	3.00
Expanded soybean	6.00	6.00	6.00	6.00	6.00	6.00	6.00	6.00
Whey power	8.00	8.00	8.00	8.00	3.00	3.00	3.00	3.00
Soybean oil	0.40	0.75	1.20	1.75	0.40	0.75	1.15	1.60
XOS	0.00	0.75	1.50	3.00	0.00	0.75	1.50	3.00
$CaHPO_4$	1.15	1.15	1.15	1.15	1.10	1.10	1.10	1.10
Limestone	0.80	0.80	0.80	0.80	0.70	0.70	0.70	0.70
Salt	0.20	0.20	0.20	0.20	0.20	0.20	0.20	0.20
Primix[a]	0.50	0.50	0.50	0.50	0.50	0.50	0.50	0.50
L-Lys-HCl (78.8%)	0.61	0.61	0.61	0.61	0.55	0.55	0.55	0.55
DL-Met (98%)	0.12	0.12	0.12	0.12	0.12	0.12	0.12	0.12
L-Thr (98%)	0.22	0.22	0.22	0.22	0.22	0.22	0.22	0.22
L-Trp (98%)	0.05	0.05	0.05	0.05	0.05	0.05	0.05	0.05
Total	100.00	100.00	100.00	100.00	100.00	100.00	100.00	100.00
Calculated nutrient level (%)								
Digestible energy (MJ/kg)	14.44	14.41	14.41	14.42	14.45	14.42	14.40	14.42
Crude protein (%)	18.98	18.97	18.99	18.98	18.28	18.31	18.29	18.29
Total Ca (%)	0.91	0.91	0.91	0.91	0.75	0.75	0.75	0.75
Total *P* (%)	0.71	0.71	0.71	0.71	0.63	0.63	0.63	0.63
Lys (%)	1.35	1.35	1.35	1.36	1.24	1.25	1.25	1.26
Met (%)	0.40	0.40	0.40	0.40	0.38	0.38	0.38	0.38
Thr (%)	0.80	0.80	0.80	0.80	0.76	0.76	0.76	0.76
Trp (%)	0.23	0.23	0.23	0.23	0.22	0.22	0.22	0.22

[a] *The premix provided the following per kg of diets: VA 12,000 IU, VD_3 2,500 IU, VE 30 IU, VK_3 3 mg, VB_5 10 mg, VB_{12} 27.6 μg, niacin 30 mg, choline chloride 400 mg, Mn (as MnO) 40 mg, Fe (as $FeSO_4 \cdot H_2O$) 90 mg, Zn (as ZnO) 100 mg, Cu (as $CuSO_4 \cdot 5H_2O$) 8.8 mg, I (as KI) 0.35 mg, Se (Na_2SeO_3) 0.3 mg.*

(total number of pigs per pen with diarrhea)/(number of pigs per pen × 7 d) × 100%.

On d 28, eight pigs of each group were randomly selected (at least one pig per pen) to collect blood samples from precaval vein into 10 mL sterile tubes. The blood samples were centrifuged at 3,000 ×g at room temperature for 10 min to obtain serum, and stored at −80°C for further analysis. Fecal samples (one pig per pen) were collected into sterile tubes on d 28 and stored at −80°C for further analysis.

Biochemical and Immunological Parameters in Blood

Serum total protein (TP), albumin (ALB), albumin globulin ratio (A/G), alanine aminotransferase (ALT), aspartate aminotransferase (AST), blood urea nitrogen (BUN), and alkaline phosphatase (ALP) were measured using automatic biochemical analyzer (Hitachi 7020, Tokyo, Japan). The total superoxide dismutase (T-SOD) activity, catalase (CAT) activity, total antioxidant capacity (T-AOC), malondialdehyde (MDA) content, and glutathione peroxidase (GSH-Px) capacity in serum were measured using commercial kits (Jiancheng Co., Ltd, Nanjing, China). The activity of T-SOD was determined at 450 nm by the xanthine oxidase method. The CAT activity was determined at 405 nm by ammonium molybdate method. The T-AOC was determined at 405 nm by 2,2′-azinobis-(3-ethylbenzthiazoline-6-sulphonate) method. The MDA content was measured at 532 nm using the thiobarbituric acid method. The activity of GSH-Px was measured at 412 nm using 2,2′-dithiodibenzoic acid method. The levels of immunoglobulin A (IgA), IgG, IgM, interleukin-1β (IL-1β), IL-6, and IL-10 in serum were detected by commercial ELISA kits (Jiancheng Co., Ltd, Nanjing, China) according to manufacturer's instructions.

Analysis of Microbiota in Feces

The total bacterial DNA of the feces was extracted using the QIAamp Fast DNA Stool Mini Kit (Qiagen, Germany) following the manufacturer's protocol. The V3–V4 hypervariable regions of bacteria 16S rDNA were amplified with universal primers 338F (ACTCCTACGGGAGGCAGCAG) and 806R (GGACTACHVGGGTWTCTAAT). The purified PCR products were equimolarly combined and paired-end sequenced on the Illumina Miseq platform (Illumina, San Diego, CA, USA).

TABLE 2 | Specific bacteria primers used in this study.

Primer	Forward 5′ → 3′	Reverse 5′ → 3′	Reference
Total bacteria	ACTCCTACGGGAGGCAGCAG	ATTACCGCGGCTGCTGG	(20)
Bifidobacterium spp.	CGCGTCCGGTGTGAAAG	CTTCCCGATATCTACACATTCCA	
Lactobacillus spp.	GAGGCAGCAGTAGGGAATCTTC	GGCCAGTTACTACCTCTATCCTTCTTC	
E. coli	CATGCCGCGTGTATGAAGAA	CGGGTAACGTCAATGAGCAAA	
Salmonella spp.	CCTTTCTCCATCGTCCTGAA	TGGTGTTATCTGCCCGACCA	(21)

The raw reads were demultiplexed and quality filtered by Quantitative Insights Into Microbial Ecology (QIIME) (version 1.9) software with the following criteria: (i) the reads were truncated at any site receiving an average quality score of <20 over a 50 bp sliding window, and the truncated reads shorter than 50 bp were discarded, reads containing ambiguous characters were also discarded; (ii) only overlapping sequences longer than 10 bp and the reads without more than two nucleotide mismatches in the primer were assembled. The remaining sequences with 97% similarity were clustered into the same operational taxonomic units (OTUs) using UPARSE (version 7.1) and chimeric sequences were removed. The taxonomy of each OTU representative sequence was analyzed by Ribosomal Database Project (RDP) classifier against the SILVA 16S rRNA gene database using confidence threshold of 70%. The analysis of the α-diversity was calculated by the MOTHUR program. For the β-diversity, principal coordinate analysis (PCoA) was performed based on Bray-Curtis distances. The data were analyzed on the Majorbio I-Sanger cloud platform (www.i-sanger.com).

Quantification of Specific Bacteria in Feces

The total bacterial DNA of feces was isolated as described above. The absolute copy numbers of specific bacteria were calculated as previously described (22). The primers were listed in **Table 2**.

Determination of SCFAs in Feces

The concentrations of SCFAs, including lactate, acetate, propionate, and butyrate in the feces were determined using Ion Chromatograph. Briefly, 0.5 g of feces was weighed and dissolved in 10 mL distilled water, homogenized using ultrasound for 30 min at room temperature, and centrifuged at 5,000 ×g for 10 min to obtain the supernatants. The supernatants were diluted 10× and filtered using 0.22 μm membranes before being detected by high-performance ion chromatography system (DIONEX ICS-3000; Thermo Fisher, USA). The injection volume was 25 μL and the flow rate was 1.0 mL/min (23).

Statistical Analysis

All the data were performed using Statistics Analysis System (SAS) 9.4 version (Cary, NC, United States). Data statistical significances were analyzed by one-way ANOVA for multiple groups. Statistical differences among the treatments were separated by Duncan's multiple tests method. The data of two groups were analyzed by unpaired Student's *t*-test. The incidence of diarrhea was analyzed by χ^2 test. The differential bacteria were identified by using linear discriminant analysis (LDA) effect size (LEfSe) analysis. The level of statistical significance was $P \leq 0.05$, whereas $0.05 < P < 0.1$ was considered as a trend of significant difference. Data are presented as means ± SEM.

RESULTS

Effects of XOS Supplementation on Growth Performance in Weaning Piglets

The dietary supplementation with the high level of XOS had no effects ($P > 0.05$) on 14 d BW, ADG on d 1–14, ADFI on d 1–14, and FCR on d 15–28 and 1–28 (**Table 3**). However, supplementation with XOS significantly increased ADG on d 15–28 and 1–28 ($P < 0.05$). Similarly, 28 d BW in 1.5% and 3% XOS groups had higher than the control group ($P < 0.05$), as well as ADFI on d 15–28. Notably, 1.5% XOS group markedly increased ($P < 0.05$) ADFI on d 1–28 compared with other groups, but there were no differences among the other groups ($P > 0.05$). Compared with the control group, the FCR on d 1–14 was markedly decreased in the 3% XOS group ($P < 0.05$). In addition, linear and quadratic increases ($P < 0.05$) were observed between different XOS levels and 28 d BW, as well as ADG on d 15–28 and 1–28, and ADFI on d 15–28 (**Table 3**), with the highest ($P < 0.05$) at the supplemental level of 1.5% XOS. ADFI on d 1–14 and 1–28 exhibited quadratic increases ($P < 0.05$) with the increasing dietary level of XOS. There was a linear decrease ($P < 0.05$) between the dietary XOS levels and FCR on d 1–14 and 1–28, with the lowest FCR ($P < 0.05$) on d 1–14 at the level of 3% XOS (**Table 3**).

Effects of XOS Supplementation on Diarrhea Incidence of Weaning Piglets

There was a decreasing trend for the incidence of diarrhea between the pigs fed with the control diet and the 3% XOS diet. However, dietary supplementation with 0.75% XOS and 1.5% XOS significantly decreased ($P < 0.05$) the diarrhea incidence compared with the control group in weaning piglets (**Table 3**).

Effects of XOS Supplementation on Serum Biochemical Parameters and Antioxidant Indictors in Weaning Piglets

The serum biochemical parameters on d 28 are presented in **Table 4**. The XOS treatments had no effects on serum biochemical parameters on d 28 in weaning pigs (**Table 4**).

The serum T-SOD, CAT, T-AOC, GSH-PX, and MDA were measured to evaluate the effects of XOS on antioxidant capability (**Table 5**). The results showed that dietary supplementation with XOS failed to affect T-SOD, CAT, and T-AOC activities ($P >$

TABLE 3 | The effects of XOS supplementation on growth performance of weaning piglets.

Items	XOS (% of diet)					*P*-valve		
	Control (0)	0.75	1.5	3	SEM	Diet	Liner	Quadratic
Initial BW (kg)	7.50	7.52	7.53	7.50	0.10	0.999		
14 d BW (kg)	10.77	10.85	11.32	11.08	0.12	0.364	0.272	0.292
28 d BW (kg)	16.30^{c}	16.84^{bc}	17.70^{a}	17.17^{ab}	0.14	0.001	0.007	0.003
d 1–14								
ADG (g/d)	233.99	238.18	270.34	256.29	5.86	0.093	0.093	0.157
ADFI (g/d)	341.01	355.23	378.74	338.97	6.75	0.131	0.878	0.029
FCR	1.46^{a}	1.50^{a}	1.40^{ab}	1.33^{b}	0.02	0.037	0.011	0.511
d 15–28								
ADG (g/d)	394.79^{c}	427.91^{b}	455.75^{a}	434.82^{ab}	5.68	< 0.001	0.001	< 0.001
ADFI (g/d)	690.92^{c}	717.22^{bc}	797.56^{a}	738.90^{b}	10.15	< 0.001	0.007	< 0.001
FCR	1.75	1.68	1.75	1.70	0.02	0.400	0.510	0.932
d 1–28								
ADG (g/d)	314.39^{c}	333.05^{b}	363.05^{a}	345.56^{b}	4.53	< 0.001	< 0.001	< 0.001
ADFI (g/d)	515.97^{b}	536.23^{b}	588.15^{a}	538.94^{b}	7.44	0.001	0.099	0.001
FCR	1.64	1.61	1.62	1.56	0.01	0.147	0.032	0.838
Diarrhea incidence (%)	12.50^{a}	6.25^{b}	7.74^{b}	8.33^{ab*}		0.035		

BW, body weight; ADG, average daily gain; ADFI, average daily feed intake; FCR, feed conversion rate.
*Values with different letter superscripts mean significant difference ($P < 0.05$) in a row, while with no letter superscripts mean no significant difference ($P > 0.05$). *indicates a trend of significance ($0.05 \leq P < 0.1$). The same as below. N = 6 for each group.*

TABLE 4 | The effects of XOS supplementation on serum biochemical parameters of weaning piglets.

Items	XOS (% of diet)					*P*-valve		
	Control (0)	0.75	1.5	3	SEM	Diet	Liner	Quadratic
TP (g/L)	47.36	49.20	49.45	48.59	0.60	0.632	0.603	0.247
ALB (g/L)	35.94	36.31	35.71	35.81	0.51	0.981	0.847	0.981
GLB (g/L)	11.43	12.89	12.28	12.78	0.52	0.743	0.487	0.666
A/G	3.46	3.00	3.12	2.85	0.18	0.694	0.320	0.746
ALT (U/L)	40.06	44.95	39.39	39.44	1.15	0.258	0.437	0.541
AST (U/L)	43.25	41.85	44.53	39.13	2.15	0.851	0.545	0.657
ALP (U/L)	415.39	383.53	392.40	378.14	15.63	0.853	0.495	0.757
BUN (mmol/L)	2.73	2.83	2.59	2.51	0.13	0.829	0.434	0.626

TP, total protein; ALB, albumin; GLB, globulin; A/G, albumin to globulin ratio; ALT, alanine aminotransferase; AST, aspartate aminotransferase; ALP, alkaline phosphatase; BUN, blood urea nitrogen; n = 6–8 for each group.

0.05) except for GSH-Px and MDA ($P < 0.05$). Compared with the control group, both 1.5 and 3% XOS groups significantly increased the GSH-Px level. However, the XOS treatments significantly declined ($P < 0.05$) the MDA level compared with the control group, and the diet supplemented with 1.5% XOS ($P < 0.05$) had the lowest MDA concentration among the four groups. Besides, the GSH-Px showed a linear increase ($P < 0.05$) with the increasing dietary level of XOS, but MDA levels decreased linearly and quadratically ($P < 0.05$).

Effects of XOS Supplementation on Immunological Function and Inflammatory Cytokines in Weaning Piglets

The serum levels of IgM, IgG, IgA, IL-1β, IL-6, and IL-10 were determined to evaluate the effects of XOS on immune status. As shown in **Table 6**, quadratic responses ($P < 0.05$) in serum levels of IgM and IL-10 were observed with the increasing supplemental XOS level. Addition of 0.75% XOS and 1.5% XOS had higher ($P < 0.05$) level of IgM than the control group. 1.5% XOS group also significantly increased IL-10 level compared with control group ($P < 0.05$). There were linear responses in serum levels of IgG and IL-6 ($P < 0.05$) with the increasing supplemental XOS level in the diets. Compared with the control group, 1.5 and 3% XOS groups significantly increased ($P < 0.05$) the IgG concentration in serum. However, the XOS-treated pigs remarkedly decreased ($P < 0.05$) serum level of IL-6, while no differences ($P > 0.05$) were found in XOS treatments. Additionally, IL-1β showed linear and quadratic ($P < 0.05$) responses with the increasing level of XOS in the diets, with the lowest ($P < 0.05$) serum concentration of IL-1β at the supplemental level of 1.5% XOS. Moreover, the XOS treatments significantly increased ($P < 0.05$) the level of IgA compared with

TABLE 5 | The effects of XOS supplementation on antioxidant activities of weaning piglets.

Items	XOS (% of diet)					*P*-valve		
	Control (0)	0.75	1.5	3	SEM	Diet	Liner	Quadratic
T-SOD (U/mL)	135.11	135.11	140.03	138.62	1.61	0.634	0.357	0.597
CAT (U/mL)	2.20	2.18	2.76	2.44	0.15	0.479	0.426	0.387
T-AOC (mmol/L)	0.23	0.24	0.25	0.24	0.004	0.317	0.406	0.162
GSH-Px (U/mL)	284.06^{b}	293.75^{ab}	312.19^{a}	317.58^{a}	4.65	0.030	0.005	0.355
MDA (nmol/mL)	3.86^{a}	3.37^{b}	2.70^{c}	3.25^{b}	0.11	0.001	0.017	0.001

SOD, superoxide dismutase; CAT, catalase; GSH-Px, glutathione peroxidase; T-AOC, total antioxidant capacity; MDA, malondialdehyde. N = 6–8 for each group. Values with different letter superscripts mean significant difference (P < 0.05) in a row, while with no letter superscripts mean no significant difference (P > 0.05).

TABLE 6 | The effects of XOS supplementation on immunological function and inflammatory cytokines of weaning piglets.

Items	XOS (% of diet)					*P*-valve		
	Control (0)	0.75	1.5	3	SEM	Diet	Liner	Quadratic
IgM (g/L)	0.82^{b}	0.92^{a}	0.94^{a}	0.87^{ab}	0.02	0.011	0.488	0.001
IgG (g/L)	6.18^{b}	6.48^{ab}	7.05^{a}	7.21^{a}	0.14	0.029	0.006	0.350
IgA (g/L)	0.85^{c}	1.00^{b}	1.15^{a}	1.15^{a}	0.03	<0.001	<0.001	0.016
IL-1β (pg/mL)	21.74^{a}	20.20^{ab}	16.20^{c}	18.89^{b}	0.52	<0.001	0.008	0.001
IL-6 (pg/mL)	97.01^{a}	80.21^{b}	78.53^{b}	84.13^{b}	2.03	0.001	0.005	0.101
IL-10 (pg/mL)	22.91^{b}	26.02^{b}	30.50^{a}	23.51^{b}	0.75	<0.001	0.779	<0.001

IgM, immunoglobulin M, IgG, immunoglobulin G, IgA, immunoglobulin A, IL-1β, interleukin-1β, IL-6, interleukin-6, IL-10, interleukin-10. N = 7–8 for each group. Values with different letter superscripts mean significant difference (P < 0.05) in a row, while with no letter superscripts mean no significant difference (P > 0.05).

TABLE 7 | The effects of XOS supplementation on fecal microbial diversity of weaning piglets.

Items	Control	1.5% XOS	SEM	*P*-value
Sobs	330.00	313.67	9.05	0.392
Shannon	4.18	3.59	0.13	0.011
Simpson	0.04	0.09	0.01	0.026
Ace	347.35	333.95	7.30	0.384
Chao	356.77	340.55	7.85	0.324

Fecal microbial α-diversity indices were analyzed by unpaired Student's t-test (n = 6).

control groups. The different levels of XOS showed linear and quadratic ($P < 0.05$) effects on IgA.

Effects of XOS Supplementation on Fecal Microbiota in Weaning Piglets

Next, the microbiota of fecal samples in the control group and 1.5% XOS group was analyzed. As shown in **Table 7**, the alpha diversity was evaluated. The Shannon index had a significant decrease ($P < 0.05$) in the 1.5% XOS group compared with the control group, whereas the Simpson index had a significant increase in the 1.5% XOS group ($P < 0.05$). However, there were no impacts of 1.5% XOS on Sobs ($P > 0.05$), Ace, and Chao indices compared with the control group.

Bata-diversity was assessed using PCoA plots based on Bray-Curtis distances. The fecal microbiota composition in the 1.5% XOS group could obviously separate from the control group ($P < 0.05$, **Figure 1A**). At the phylum level, *Firmicutes*, *Bacteroidota*, and *Actinobacteriota* predominated in feces (**Figure 1B**). At the genus level, *Lactobacillus* was dominant in both groups (**Figure 1C**). The relative abundances of *Lactobacillus* and *Bifidobacterium* were remarkedly increased ($P < 0.05$) in the 1.5% XOS group (**Figure 1D**), while the relative abundances of *g_Clostridia_UCG-014*, *g__Ruminococcus*, *g__norank_f__Ruminococcaceae*, and *g__norank_f__Eubacterium_coprostanoligenes_group* in the 1.5% XOS group were markedly lower ($P < 0.05$) than the control group (**Figure 1D**). The differential bacteria were identified by using linear discriminant analysis (LDA) effect size (LEfSe). A dietary supplemented with 1.5% XOS was associated with increased relative abundances of *Lactobacillus*, *Bifidobacterium*, and *Fusicatenibacter* at the genus level in weaning piglets (**Figure 1E**, LDA score >2).

Quantification of Specific Bacteria in Feces

Compared with the control group, the pigs fed with a diet addition of 1.5% XOS markedly increased ($P < 0.05$) the copy numbers of *Bifidobacterium* and *Lactobacillus* in feces (**Figure 2**). However, 1.5% XOS did not differ ($P > 0.05$) the total bacteria, *Salmonella,* and *E. coli* (**Figure 2**).

Effects of XOS Supplementation on Fecal SCFAs

The fecal SCFAs concentrations in response to different dosages of XOS supplementation on d 28 are shown in **Table 8**. Linearly increasing responses ($P < 0.05$) to the fecal acetate, propionate,

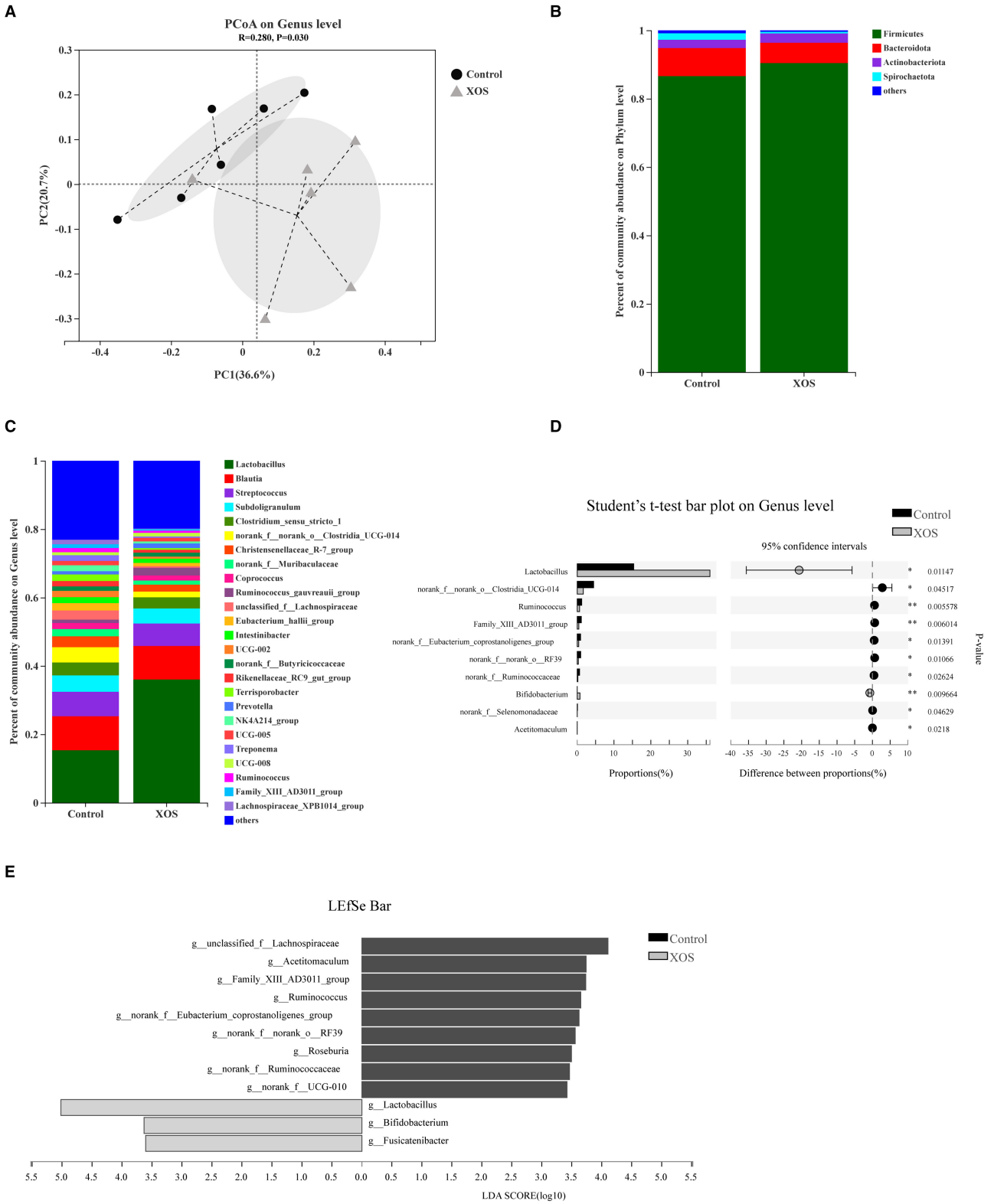

FIGURE 1 | Dietary supplementation with xylooligosaccharides (XOS) modulates the composition of fecal microbiota. **(A)** Principal coordinate analysis (PCoA) on genus level based on Bray-Curtis distances. Composition of bacterial communities **(B)** at the phylum level and **(C)** at the genus level. **(D)** Differential bacteria at the genus level. **(E)** Linear discriminant analysis (LDA) effect size (LEfSe) analysis screened biomarker of microbial community after addition of XOS. $^{*}P < 0.05$ and $^{**}P < 0.01$, $n = 6$ for each group.

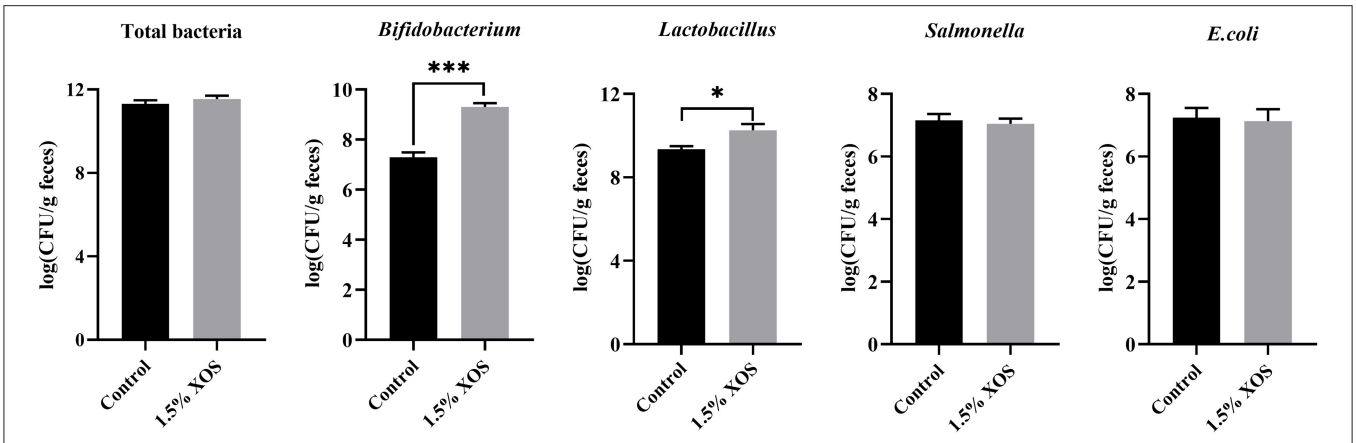

FIGURE 2 | Effect of XOS on specific bacteria in feces. Data are presented as means + SEM. *$P < 0.05$ and ***$P < 0.001$, $n = 6$ for each group.

TABLE 8 | The effects of dietary supplementation with XOS on SCFAs concentration in feces of weaning piglets.

Items	XOS (% of diet)					*P*-valve		
	Control (0)	0.75	1.5	3	SEM	Diet	Liner	Quadratic
Acetate (mmol/kg)	130.80^{b}	149.10^{ab}	151.63^{ab}	165.18^{a}	4.23	0.026	0.004	0.458
Propionate (mmol/kg)	76.38^{b}	91.09^{ab}	90.64^{ab}	99.92^{a}	2.90	0.025	0.006	0.379
Butyrate (mmol/kg)	43.16^{b}	59.67^{a}	61.85^{a}	68.97^{a}	3.20	0.020	0.005	0.517
Total SCFAs (mmol/kg)	250.34^{b}	299.86^{a}	304.12^{a}	334.08^{a}	9.39	0.007	0.001	0.373

SCFAs, short-chain fatty acids; SEM, standard error of the means.

Total SCFAs include acetate, prorate, and butyrate (n = 6 for each group). Values with different letter superscripts mean significant difference (P < 0.05) in a row, while with no letter superscripts mean no significant difference (P > 0.05).

butyrate, and total SCFAs were observed with the increasing supplemental XOS level. A dietary supplemented with 3% XOS had higher ($P < 0.05$) concentrations of acetate and propionate in feces than the control group, while there were no differences among in control, 0.75%, and 1.5% XOS groups or among the XOS treatments. Besides that, the supplementation of XOS markedly increased ($P < 0.05$) concentrations of butyrate and total SCFAs in feces compared with the control group, but no differences were noted in the XOS-treated groups ($P > 0.05$).

Correlation of Fecal Microbiota With Serum Parameters, SCFAs, and Growth Performance

As shown in **Figure 3**, the genus *Lactobacillus* abundance was positively correlated with ADG, acetate, propionate, and IgA ($P < 0.05$), but negatively correlated with IL-1β ($P < 0.05$). The genus *Bifidobacterium* was positively related with ADFI, total SCFAs, IgG, and IL-10 ($P < 0.05$), as well as *g_Fusicatenibacter* abundance with ADFI, total SCFAs, and IL-10 ($P < 0.05$). However, the genus *Bifidobacterium* and *Fusicatenibacter* abundances were negatively associated with MDA ($P < 0.05$). Meanwhile, the genus *Bifidobacterium* abundance was negatively associated with IL-1β and IL-6 ($P < 0.05$). The genus *g_Ruminococcus*, *g__Family_XIII_AD3011_group*, and *g__norank_f__norank_o__RF39* were negatively correlated with ADG, acetate, propionate, and butyrate. In addition, there was a positive correlation between *g_Ruminococcus* and MDA level ($P < 0.05$), while a remarkable negative correlation was found between *g_Ruminococcus* and total SCFAs, and IL-10 levels ($P < 0.05$). There were similar results for *g__Family_XIII_AD3011_group*, *g__norank_f__norank_o__RF39,* and *g__norank_f__Eubacterium_coprostanoligenes_group*. Moreover, a positive correlation was observed between *g__norank_f__norank_o__RF39* abundance and IL-6 ($P < 0.05$), as well as *Clostridia_UCG-014*, *g__Family_XIII_AD3011_group*, *g__norank_f__norank_o__RF39* abundance, and IL-1β level.

DISCUSSIONS

Recently, the XOS as functional food are widely used in animal diets for improving animal growth performance, enhancing the quality of animal products, and regulating intestinal health (24). However, the abundance of *Bifidobacterium* did not show a remarkable increase at the low dosage of XOS in weaning pigs or growing pigs (4, 11, 18). In the present study, we investigated the effects of the high level of XOS on growth performance, antioxidant capability, and anti-inflammatory action, and whether the high level of XOS promotes *Bifidobacterium* abundance of weaning piglets. We

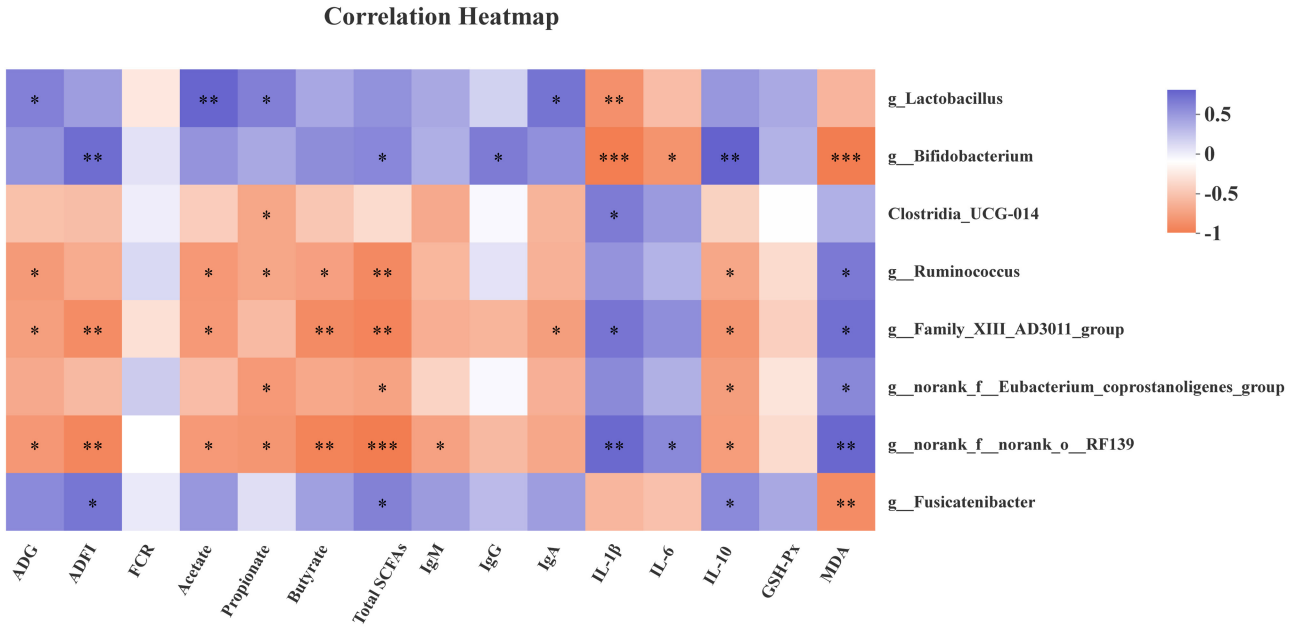

FIGURE 3 | Correlation heatmap between microbiota and antioxidant capability, immune function, growth performance, and fecal SCFAs. Spearman correlations were applied. ADG, average daily gain; ADFI, average daily feed intake; FCR, feed conversion rate; Total SCFAs, total short-chain fatty acids; GSH-Px, glutathione peroxidase; MDA, malondialdehyde. Total SCFAs = acetate + propionate + butyrate. *$P < 0.05$, **$P < 0.01$, and ***$P < 0.001$.

found that the diet supplemented with 1.5% XOS significantly increased final BW, ADG, and ADFI during d 15–28 and the whole study period. Moreover, 28 d BW exhibited linear and quadratic responses ($P < 0.05$) with the increasing dietary XOS level, as well as ADFI on d 15–28, ADG on d 15–28 and 1–28, with the highest at the level of 1.5% XOS. As the dietary XOS level increased, ADFI on d 1–14 and 1–28 increased quadratically. Besides, the FCR on d 1–14 and 1–28 decreased linearly with increasing level of XOS in the diets. The 3% XOS group piglets had a lower ADFI and ADG than the 1.5% XOS group, which due to an excessive level of XOS may affect the dietary palatability. The previous studies showed that supplementation of XOS improved animal growth performance. Chen et al. (4, 13) found that an addition of 500 mg/kg XOS significantly increased BW, ADG, and decreased FCR in weaning piglets. Similarly, a dietary supplementation with 400 mg/kg XOS also increased final BW and ADG in nursery pigs, while ADFI and FCR were not affected (12). Additionally, a dietary supplementation of 250 mg/kg XOS markedly increased ADG and ADFI for weaning piglets (25). The difference between our findings and previous reports might be attributable to the dosage of XOS.

It has been reported that oligosaccharides may influence serum biochemical parameters (26). Our results showed that either the high level or the low level of XOS failed to affect serum biochemical parameters in weaning pigs. Consistently, the previous studies indicated that serum biochemical parameters were not altered in XOS-treated weaning pigs or limited effect in XOS-treated nursery pigs (11, 12, 27).

The CAT, SOD, and GSH-Px as the main antioxidant enzymes in the antioxidant protection system play a vital role in scavenging free radicals, reducing and eliminating oxidative damage. The serum T-AOC is an important indicator for evaluating the overall function of antioxidant capability *in vivo*. The MDA is considered as a biomarker for lipid peroxidation under the oxidative stress status. In this study, serum GSH-Px concentration increased linearly with increasing supplemental XOS level in weaning pigs. In addition, there were linear and quadratic responses between serum MAD level and XOS, with the lowest at the 1.5% XOS. The XOS had no impact on serum T-SOD, CAT, and T-AOC in our findings. Consistently, dietary addition of 400 mg/kg XOS markedly declined the serum MDA level and increased a trend of GSH-Px (12). Chen et al. (13) also reported that piglets fed with the diet of 500 mg/kg XOS had higher T-SOD and CAT levels on day 28, whereas the MDA level was lower than the control group. Moreover, T-SOD, T-AOC, and CAT levels exhibited quadratic increases with different dietary XOS levels on day 28, but the level of MDA was decreased quadratically. A recent report also found that maternal supplementation of 500 mg/kg XOS in diet had a lower level of MDA in sucking pigs, while did not affect the SOD, T-AOC, and CAT activity (28). These results indicated that XOS improvement of growth performance of weaned piglets might be related to increasing the antioxidant capability.

The immunoglobulins, including IgG, IgM, and IgA involve host immune response and protect against pathogens and virus infection. The previous studies showed that XOS can elevate the serum level of IgG in nursery pigs and IgM in broilers (12, 29). Notably, with the level of XOS increased, the serum IgA had a linear increase and IgM showed linear and quadratic responses in laying hens (30). Besides, 500 mg/kg XOS increased the concentration of serum IgG on day 28 in weaning piglets, and serum IgG concentration showed a quadratic effect with

increasing XOS level in diet (13). Similarly, our results found that a dietary supplementation of 0.75 and 1.5% XOS significantly increased the serum IgM concentration in weaning piglets compared with the control group. Additionally, 1.5% and 3% XOS had higher levels of IgG than the control group. Moreover, the serum level of IgA was increased later in XOS-treated pigs. Numerous studies indicated that XOS can alleviate inflammatory status in animals. Sow supplementation of 500 mg/kg XOS decreased serum IL-1β, IL-6, IL-2, and Tumor Necrosis Factor (TNF)-α levels in sucking piglets (28). In the present study, 1.5 and 3% XOS significantly decreased the serum IL-1β compared with the control group. The XOS-treated piglets had a lower serum level of IL-6 than the vehicle group. Furthermore, anti-inflammatory cytokine IL-10 was markedly increased in the 1.5% XOS group. Notably, the effects of XOS supplementation could depend on the dosage, since Yin et al. (11) found XOS at 100 mg/kg only decreased the serum IFN-γ in weaning piglets, but had no impacts on IL-1β, IL-6, and IL-10. Hansen et al. (31) reported that a diet supplemented with 10% XOS downregulated the IFN-γ and IL-1β in mice. Importantly, XOS suppressed the pro-inflammatory cytokines, IL-1β, IL-6, and TNF-α secretion from RAW265.7 macrophages stimulated with lipopolysaccharide in the pretreatment model (32). The possible mechanism responsible for the beneficial effects is that XOS can enhance immune function and decrease the inflammatory status in weaning piglets.

It has been widely demonstrated that XOS can modulate gut microbiota composition by selectively stimulating beneficial bacteria. Thus, the microbiota composition of fecal samples was analyzed by 16S rRNA gene sequencing. The result found that 1.5% XOS significantly decreased the Shannon index and increased the Simpson index, indicating dietary supplementation of XOS decreased the diversity of gut microbiota community. Similarly, the addition of 250 mg/kg XOS significantly decreased the Shannon index during growing fatty pigs (16). The XOS decreased α-diversity Chao1 and Shannon indices in high-fat diet-induced mice as well (33). The α-diversity decrease might result from increasing the relative abundances of *Lactobacillus* and *Bifidobacterium* in XOS-treated pigs. The PCoA plots based on Bray-Curtis distances were a clear separation between XOS and control groups, which is similar to that reported by Pan et al. (16). It has been reported that XOS can promote counts of *Lactobacillus* in weaning piglets (4, 16), while the low level of XOS failed to stimulate the abundance of *Bifidobacterium* (4, 11, 18, 34). In the current study, the abundances of *Lactobacillus* and *Bifidobacterium* were markedly increased in 1.5% XOS-treated pigs using l6S rRNA gene sequencing, as well as by qPCR. Notably, 1.5% XOS elevated the relative *Bifidobacterium* abundance approximately 35-fold from 0.021 to 0.74%. The high level of XOS did not markedly vary *Bifidobacterium* abundance in weaning piglets compared to rodents (17), probably due to the differences of microbial stability and physiological backgrounds between animal species. Holman et al. (35) analysis of core microbiota in the swine gut revealed that *Clostridium*, *Blautia*, *Lactobacillus*, *Prevotella*, *Ruminococcus*, *Roseburia*, the RC9 gut group, and *Subdoligranulum* were considered as core microbiota but the relative abundance of *Bifidobacterium* in fecal samples remained low (<0.35%). Moreover, the XOS treatments linearly increased the fecal acetate, propionate, butyrate, and total SCFAs levels in weaning piglets. Chen et al. (4) also found that the dietary supplementation of 500 mg/kg XOS elevated the acetate, propionate, butyrate, and total SCFAs concentrations in the cecum of piglets. Furthermore, the *Lactobacillus*, *Bifidobacterium*, and *Fusicatenibacter* were regarded as biomarkers in XOS-treated pigs identified by LEfSe analysis (LDA > 2). Collectively, the high level of XOS can alter the fecal microbiota composition and increase the concentrations of SCFAs by promoting the beneficial bacteria.

The growing evidence has shown that *Lactobacillus* and *Bifidobacterium* are associated with SCFAs production, antioxidant activity, and host inflammatory status (36–39). Thus, spearman correlations between bacteria and antioxidant, immune function, growth performance, and fecal SCFAs were performed. The *Lactobacillus* exhibited positive correlations with ADG, acetate, propionate, and serum IgA level, but a negative correlation with serum IL-1β level. The *Bifidobacterium* was positively associated with ADFI, total SCFAs, IgG, and IL-10, while negatively associated with levels of IL-1β, IL-6, and MDA in serum. The recent reports indicated that *Fusicatenibacter* is a SCFAs-producing bacteria, which closely related to host health, such as Parkinson's disease, ulcerative colitis (40–44). The *Fusicatenibacter* suppresses intestinal inflammation and is positively associated with SCFAs production (41). Consistently, there were positive correlations between *Fusicatenibacter* and ADFI, total SCFAs, and IL-10 level, while a negative correlation was observed between *Fusicatenibacter* and MDA in our findings. However, the bacteria with higher abundances in the control group, like *g_Ruminococcus*, *g__Family_XIII_AD3011_group*, and *g__norank_f__norank_o__RF39*, were in negative relations with ADG, ADFI, SCFAs, and IL-10, and in positive relations with IL-1β and MDA.

CONCLUSIONS

In conclusion, our results indicated that XOS supplementation improved the growth performance, increased antioxidant capability, enhanced immune function, and decreased body inflammatory status and incidence of diarrhea in weaning piglets, which could be contributed to the modulation of gut microbiota community, especially by increasing the abundances of *Lactobacillus*, *Bifidobacterium*, and *Fusicatenibacter*. However, the high level of XOS did not sharply the relative abundance of *Bifidobacterium* in feces. The optimum level of XOS supplementation was 1.5% for weaning piglets in this study.

DATA AVAILABILITY STATEMENT

The datasets presented in this study can be found in online repositories. The names of the repository/repositories and accession number(s) can be found below: NCBI SRA; PRJNA762151.

ETHICS STATEMENT

The animal study was reviewed and approved by Animal Ethics Committee of China Agricultural University.

AUTHOR CONTRIBUTIONS

JP wrote the manuscript. JP, XZ, YW, and DL performed the experiments. HY revised the manuscript. ZW analyzed the data. JW obtained financial support and oversaw this study. JP, DH, and JW designed the research. All authors contributed to the article and approved the submitted version.

FUNDING

This research was funded by the National Natural Science Foundation of China (31972596, 31630074, 31902170), the Beijing Municipal Natural Science Foundation (S170001), the China Agriculture Research System (CARS-35), and the Fundamental Research Funds for the Central Universities (2021TC089).

ACKNOWLEDGMENTS

The experiments were conducted at the swine research unit of China Agricultural University (Chengde, China).

REFERENCES

1. Campbell JM, Crenshaw JD, Polo J. The biological stress of early weaned piglets. *J Anim Sci Biotechnol.* (2013) 4:19. doi: 10.1186/2049-1891-4-19
2. Gresse R, Chaucheyras-Durand F, Fleury MA, Van De Wiele T, Forano E, et al. Gut microbiota dysbiosis in postweaning piglets: Understanding the keys to health. *Trends Microbiol.* (2017) 25:851–73. doi: 10.1016/j.tim.2017.05.004
3. Collignon P, Voss A. China, what antibiotics and what volumes are used in food production animals? *Antimicrob Resist Infect Control.* (2015) 4:16. doi: 10.1186/s13756-015-0056-5
4. Chen Y, Xie Y, Zhong R, Liu L, Lin C, Xiao L, et al. Effects of xylo-oligosaccharides on growth and gut microbiota as potential replacements for antibiotic in weaning piglets. *Front Microbiol.* (2021) 12:641172. doi: 10.3389/fmicb.2021.641172
5. Barton MD. Impact of antibiotic use in the swine industry. *Curr Opin Microbiol.* (2014) 19:9–15. doi: 10.1016/j.mib.2014.05.017
6. Cunningham M, Azcarate-Peril MA, Barnard A, Benoit V, Grimaldi R, Guyonnet D, et al. Shaping the future of probiotics and prebiotics. *Trends Microbiol.* (2021) 29:667–85. doi: 10.1016/j.tim.2021.01.003
7. Gibson GR, Roberfroid MB. Dietary modulation of the human colonic microbiota: introducing the concept of prebiotics. *J Nutr.* (1995) 125:1401–12. doi: 10.1093/jn/125.6.1401
8. Gao Y, Zhang S, Li C, Xiao L, Shen J, Yin J. Acute and subchronic toxicity of xylo-oligosaccharide in mice and rats. *Toxicol Mech Methods.* (2012) 22:605–10. doi: 10.3109/15376516.2012.706837
9. Gao Y, Wang Y, Li Y, Han R, Li C, Xiao L, et al. Repeated sub-chronic oral toxicity study of xylooligosaccharides (XOS) in dogs. *Regul Toxicol Pharmacol.* (2017) 86:379–85. doi: 10.1016/j.yrtph.2017.04.009
10. Amorim C, Silverio SC, Prather KLJ, Rodrigues LR. From lignocellulosic residues to market: Production and commercial potential of xylooligosaccharides. *Biotechnol Adv.* (2019) 37:107397. doi: 10.1016/j.biotechadv.2019.05.003
11. Yin J, Li F, Kong X, Wen C, Guo Q, Zhang L, et al. Dietary xylo-oligosaccharide improves intestinal functions in weaned piglets. *Food Funct.* (2019) 10:2701–9. doi: 10.1039/C8FO02485E
12. Hou Z, Wu D, Dai Q. Effects of dietary xylo-oligosaccharide on growth performance, serum biochemical parameters, antioxidant function, and immunological function of nursery piglets. *Rev Bras Zootecn.* (2020) 49:e20190170. doi: 10.37496./rbz4920190170
13. Chen Y, Xie Y, Zhong R, Han H, Liu L, Chen L, et al. Effects of graded levels of xylo-oligosaccharides on growth performance, serum parameters, intestinal morphology, and intestinal barrier function in weaned piglets. *J Anim Sci.* (2021) 99:1–8. doi: 10.1093./jas/skab183
14. Wang Q, Wang XF, Xing T, Li JL, Zhu XD, Zhang L, et al. The combined impact of xylo-oligosaccharides and gamma-irradiated Astragalus polysaccharides on growth performance and intestinal mucosal barrier function of broilers. *Poult Sci.* (2021) 100:100909. doi: 10.1016/j.psj.2020.11.075
15. Craig AD, Khattak F, Hastie P, Bedford MR, Olukosi OA. Xylanase and xylo-oligosaccharide prebiotic improve the growth performance and concentration of potentially prebiotic oligosaccharides in the ileum of broiler chickens. *Br Poult Sci.* (2020) 61:70–8. doi: 10.1080/00071668.2019.1673318
16. Pan J, Yin J, Zhang K, Xie P, Ding H, Huang X, et al. Dietary xylo-oligosaccharide supplementation alters gut microbial composition and activity in pigs according to age and dose. *AMB Express.* (2019) 9:134. doi: 10.1186/s13568-019-0858-6
17. Christensen EG, Licht TR, Leser TD, Bahl MI. Dietary xylo-oligosaccharide stimulates intestinal *Bifidobacteria* and *Lactobacilli* but has limited effect on intestinal integrity in rats. *BMC Res Notes.* (2014) 7:660. doi: 10.1186/1756-0500-7-660
18. Sutton TA, O'neill HVM, Bedford MR, Mcdermott K, Miller HM. Effect of xylanase and xylo-oligosaccharide supplementation on growth performance and faecal bacterial community composition in growing pigs. *Anim Feed Sci Tech.* (2021) 274:114822–33. doi: 10.1016./j.anifeedsci.2021.114822
19. National Research Council (NRC). (2012). Nutrient Requirements of Swine. 11th rev. ed. Washington DC: National Academies Press.
20. Chen H, Mao X, He J, Yu B, Huang Z, Yu J, et al. Dietary fibre affects intestinal mucosal barrier function and regulates intestinal bacteria in weaning piglets. *Br J Nutr.* (2013) 110:1837–48. doi: 10.1017/S0007114513001293
21. Cohen HJ, Mechanda SM, Lin W. PCR amplification of the fimA gene sequence of *Salmonella* Typhimurium, a specific method for detection of *Salmonella* spp. *Appl Environ Microbiol.* (1996) 62:4303–8. doi: 10.1128/aem.62.12.4303-4308.1996
22. Li N, Huang S, Jiang L, Dai Z, Li T, Han D, et al. Characterization of the early life microbiota development and predominant *Lactobacillus* species at distinct gut segments of low- and normal-birth-weight piglets. *Front Microbiol.* (2019) 10:797. doi: 10.3389/fmicb.2019.00797
23. He B, Li T, Wang W, Gao H, Bai Y, Zhang S, et al. Metabolic characteristics and nutrient utilization in high-feed-efficiency pigs selected using different feed conversion ratio models. *Sci China Life Sci.* (2019) 62:959–70. doi: 10.1007/s11427-018-9372-6
24. Baker JT, Duarte ME, Holanda DM, Kim SW. Friend or Foe? Impacts of dietary xylans, xylooligosaccharides, and xylanases on intestinal health and growth performance of monogastric animals. *Animals (Basel).* (2021) 11:609. doi: 10.3390/ani11030609
25. Ding H, Zhao X, Azad MaK, Ma C, Gao Q, et al. Dietary supplementation with *Bacillus subtilis* and xylo-oligosaccharides improves growth performance and intestinal morphology and alters intestinal microbiota and metabolites in weaned piglets. *Food Funct.* (2021) 12:5837–49. doi: 10.1039/D1FO00208B
26. Chen Q, Liu M, Zhang P, Fan S, Huang J, Yu S, et al. Fucoidan and galactooligosaccharides ameliorate high-fat diet-induced dyslipidemia in rats by modulating the gut microbiota and bile acid metabolism. *Nutrition.* (2019) 65:50–9. doi: 10.1016/j.nut.2019.03.001
27. Liu JB, Cao SC, Liu J, Xie YN, Zhang HF. Effect of probiotics and xylo-oligosaccharide supplementation on nutrient digestibility, intestinal health and noxious gas emission in weanling pigs. *Asian-Australas J Anim Sci.* (2018) 31:1660–9. doi: 10.5713/ajas.17.0908

28. Ma C, Gao Q, Zhang W, Zhu Q, Tang W, Blachier F, et al. Supplementing synbiotic in sows' diets modifies beneficially blood parameters and colonic microbiota composition and metabolic activity in suckling piglets. *Front Vet Sci.* (2020) 7:575685. doi: 10.3389/fvets.2020.575685
29. Luo D, Li J, Xing T, Zhang L, Gao F. Combined effects of xylo-oligosaccharides and coated sodium butyrate on growth performance, immune function, and intestinal physical barrier function of broilers. *Anim Sci J.* (2021) 92:e13545. doi: 10.1111/asj.13545
30. Ding XM Li DD, Bai SP, Wang JP, Zeng QF, Su ZW, et al. Effect of dietary xylooligosaccharides on intestinal characteristics, gut microbiota, cecal short-chain fatty acids, and plasma immune parameters of laying hens. *Poult Sci.* (2018) 97:874–81. doi: 10.3382/ps/pex372
31. Hansen CH, Frøkiær H, Christensen AG, Bergström A, Licht TR, Hansen AK, et al. Dietary xylooligosaccharide downregulates IFN-γ and the low-grade inflammatory cytokine IL-1β systemically in mice. *J Nutr.* (2013) 143:533–40. doi: 10.3945/jn.112.172361
32. Chen HH, Chen YK, Chang HC, Lin SY. Immunomodulatory effects of xylooligosaccharides. *Food Sci Technol Res.* (2012) 18:195–9. doi: 10.3136/fstr.18.195
33. Long J, Yang J, Henning SM, Woo SL, Hsu M, Chan B, et al. Xylooligosaccharide supplementation decreases visceral fat accumulation and modulates cecum microbiome in mice. *J Funct Foods.* (2019) 52:138–46. doi: 10.1016/j.jff.2018.10.035
34. Zhou J, Wu S, Qi G, Fu Y, Wang W, Zhang H, et al. Dietary supplemental xylooligosaccharide modulates nutrient digestibility, intestinal morphology, and gut microbiota in laying hens. *Anim Nutr.* (2021) 7:152–62. doi: 10.1016/j.aninu.2020.05.010
35. Holman DB, Brunelle BW, Trachsel J, Allen HK. Meta-analysis to define a core microbiota in the swine gut. *mSystems.* (2017) 2:e00004–17. doi: 10.1128./mSystems.00004-17
36. Hidalgo-Cantabrana C, Delgado S, Ruiz L, Ruas-Madiedo P, Sánchez B, Margolles A. *Bifidobacteria* and their health-promoting effects. *Microbiol Spectr.* (2017) 5:BAD-0010-2016. doi: 10.1128./microbiolspec.BAD-0010-2016
37. Zhang Z, Lv J, Pan L, Zhang Y. Roles and applications of probiotic *Lactobacillus* strains. *Appl Microbiol Biotechnol.* (2018) 102:8135–43. doi: 10.1007/s00253-018-9217-9
38. Nowak A, Paliwoda A, Błasiak J. Anti-proliferative, pro-apoptotic and anti-oxidative activity of *Lactobacillus* and *Bifidobacterium* strains: a review of mechanisms and therapeutic perspectives. *Crit Rev Food Sci Nutr.* (2019) 59:3456–67. doi: 10.1080/10408398.2018.1494539
39. Markowiak-Kopeć P, Slizewska K. The effect of probiotics on the production of short-chain fatty acids by human intestinal microbiome. *Nutrients.* (2020) 12:1107–29. doi: 10.3390./nu12041107
40. Takada T, Kurakawa T, Tsuji H, Nomoto K. Fusicatenibacter saccharivorans gen. nov, sp nov, isolated from human faeces. *Int J Syst Evol Microbiol.* (2013) 63:3691–6. doi: 10.1099/ijs.0.045823-0
41. Takeshita K, Mizuno S, Mikami Y, Sujino T, Saigusa K, Matsuoka K, et al. A single species of Clostridium subcluster XIVa decreased in ulcerative colitis patients. *Inflamm Bowel Dis.* (2016) 22:2802–10. doi: 10.1097/MIB.0000000000000972
42. Jin M, Kalainy S, Baskota N, Chiang D, Deehan EC, Mcdougall C, et al. Faecal microbiota from patients with cirrhosis has a low capacity to ferment non-digestible carbohydrates into short-chain fatty acids. *Liver Int.* (2019) 39:1437–47. doi: 10.1111/liv.14106
43. Yuan Y, Zhao G, Ji H, Peng B, Huang Z, Jin W, et al. Changes in the gut microbiota during and after commercial helium-oxygen saturation diving in China. *Occup Environ Med.* (2019) 76:801–7. doi: 10.1136/oemed-2019-106031
44. Qiu X, Zhao X, Cui X, Mao X, Tang N, Jiao C, et al. Characterization of fungal and bacterial dysbiosis in young adult Chinese patients with Crohn's disease. *Therap Adv Gastroenterol.* (2020) 13:1756284820971202. doi: 10.1177/1756284820971202

Conflict of Interest: The authors declare that the research was conducted in the absence of any commercial or financial relationships that could be construed as a potential conflict of interest.

Publisher's Note: All claims expressed in this article are solely those of the authors and do not necessarily represent those of their affiliated organizations, or those of the publisher, the editors and the reviewers. Any product that may be evaluated in this article, or claim that may be made by its manufacturer, is not guaranteed or endorsed by the publisher.

frontiers in Nutrition

ORIGINAL RESEARCH
published: 16 December 2021
doi: 10.3389/fnut.2021.738707

Effects of Dietary Protein Levels on Fecal Amino Acids Excretion and Apparent Digestibility, and Fecal and Ileal Microbial Amino Acids Composition in Weaned Piglets

Zhenguo Yang [1,2†], Huan Deng [1,2†], Tianle He [1,2†], Zhihong Sun [1,2], Ziema Bumbie Gifty [1,2], Ping Hu [1,2], Zebing Rao [1,2] and Zhiru Tang [1,2*]*

[1] Laboratory for Bio-Feed and Molecular Nutrition, College of Animal Science and Technology, Southwest University, Chongqing, China, [2] Chongqing Key Laboratory of Herbivore Science, Chongqing, China

OPEN ACCESS

Edited by:
Xi Ma,
China Agricultural University, China

Reviewed by:
Suman Kapila,
National Dairy Research Institute (ICAR), India
Shusong Wu,
Hunan Agricultural University, China

***Correspondence:**
Zhenguo Yang
guoguo00002@163.com
Zhiru Tang
tangzhiru2326@sina.com

†These authors have contributed equally to this work

Specialty section:
This article was submitted to Nutrition and Microbes, a section of the journal Frontiers in Nutrition

Received: 20 July 2021
Accepted: 25 October 2021
Published: 16 December 2021

Citation:
Yang Z, Deng H, He T, Sun Z, Gifty ZB, Hu P, Rao Z and Tang Z (2021) Effects of Dietary Protein Levels on Fecal Amino Acids Excretion and Apparent Digestibility, and Fecal and Ileal Microbial Amino Acids Composition in Weaned Piglets. Front. Nutr. 8:738707. doi: 10.3389/fnut.2021.738707

Background and Aims: The purpose of this study was to determine the effects of low protein diets with the same Lys, Met + Cys, Thr, and Trp levels as in high protein diets on the fecal amino acid excretion and apparent digestibility, and ileal and fecal microbial amino acids composition in weaned piglets.

Methods: Fifty-four 21-day-old Duroc × Landrace × Yorkshire weaned piglets were randomly divided into three groups and fed with corn-soybean meal basal diets, in which the crude protein (CP) content was 20% (H-CP), 17% (M-CP), and 14% (L-CP), respectively. The experiment included a 7-day adaptation period and a 45-day trial period. Six piglets in each group were randomly slaughtered on days 10, 25, and 45 of the trial period, and the intestinal contents, intestinal mucosa, and feces were collected.

Results: The results showed that the interaction between feeding time and dietary CP levels was reflected in the apparent digestibility of dietary CP and amino acid (AA) ($p < 0.01$). With the increase of age, the apparent digestibility of CP and AA were increased ($p < 0.01$). With the increase of CP levels, the excretion of nitrogen (N) was decreased ($p < 0.01$), whereas the flow of microbial AA in the ileum and feces were increased ($p < 0.01$). The interaction between feeding time and dietary CP levels was also reflected in the composition of AA in the ileum and stool of piglets ($p < 0.01$). The proportion of His, Lyr, Met, Cys, and Ser was lower than the average, whereas the proportion of Phe, Leu, Pro, Ala, Glu, and Asp was higher than the average. With the increase of age, the AA content of microorganisms increased ($p < 0.01$).

Conclusion: All in all, this work revealed the changes of N, CP, and AA excretion and digestibility of feces and microorganisms of piglets under the combined action of different dietary protein levels and different feeding times, and also the changes of AA composition of intestinal microorganisms and AA composition of microorganisms.

Keywords: low protein diet, intestinal microorganism, amino acids, apparent digestibility, weaned piglets

INTRODUCTION

The shortage of protein feed resources and the environmental pollution caused by N emissions were two difficult problems to be solved urgently in the piglets' industry nowadays (1). A low protein diet with an AA balance could effectively alleviate these two problems and be gradually applied to different growth stages of piglets. From the economic and environmental point of view, reducing dietary CP and supplementing crystalline AA were effective strategies for the piglets' industry to reduce costs and pollution (2, 3). It was reported that for every 1% reduction of CP in the diet, the total N excretion was reduced by about 8% (4). According to the above theory and the NRC recommendation, reducing the dietary CP level by 2–4%, according to the NRC recommendation, and adding appropriate synthetic AA could not only meet the protein demand of animals but also effectively reduce N emission (5). The researchers lowered feed CP levels according to theoretical values and added crystalline Lys, Try, Thr, and Met to the feed and found that such a combination did not cause a decline in the growth performance of the piglets (6). Dai et al. (7) also pointed that this AA could make up for the lack of feed protein. Therefore, to maximize the saving of protein resources and alleviate pollution, the critical point of dietary CP levels should be determined and the best AA balance model should be designed.

Ignoring the effect of intestinal microorganisms on protein digestion and metabolism, most traditional nutrition studies focused on the intake of protein, AA patterns, and protein utilization of piglets themselves (8). The microorganisms in piglet intestines were mainly anaerobes and facultative anaerobes, of which Bacteroides account for more than 90%, which played an important role in maintaining body health and improving immunity, absorption, and metabolism of nutrients (9). Dietary proteins and AA which could not be digested in the small intestine (together with nitrogenous substances such as digestive enzymes and mucus secreted by the small intestine) were used by microorganisms to synthesize bacterial proteins after entering the intestine or degrade metabolites such as ammonia, hydrogen sulfide, biogenic amines, phenols, and indole compounds (10). The decrease of dietary protein level in growing piglets increased the relative abundance of intestinal microflora (11). The intestinal microorganisms of porcine metabolized some essential AA (such as Lys and Thr) and some conditionally essential AA, and the metabolism of some specific AA required the interaction of some specific microorganisms (7). Therefore, intestinal bacteria colonized their hosts in the process of N metabolism.

However, there was no in-depth research on the metabolism of AA and proteins by intestinal microorganisms. There were few reports about the effect of CP level on the AA composition of intestinal bacteria. Therefore, the experiment was conducted to study the effects of dietary protein levels on the apparent digestibility of CP and AA and the AA composition of intestinal microorganisms in piglets. Thus, this study provided a scientific theoretical basis for further understanding the digestion and absorption of protein in the intestinal tract of piglets, reducing N emissions, and changing the supply mode of N nutrients by gastrointestinal microorganisms. The objectives of the present work were to investigate whether the same levels of Lys, Met + Cys, Thr, and Trp in the L-CP diet and the H-CP diet affected fecal amino acid excretion, apparent digestibility, and microbial amino acid composition in ileum and feces of weaned piglets.

TABLE 1 | Ingredient composition of experimental diets in weaned piglets (g/kg, DM basis).

Ingredients	14%CP	17%CP	20%CP
Corn	71.80	66.50	63.70
Soybean meal	13.40	18.80	19.80
Whey powder	4.40	4.30	4.30
Fish meal	1.50	4.00	9.00
Soybean oil	4.10	2.60	0.80
L-Lys·HCl	0.88	0.62	0.38
DL-Met	0.27	0.19	0.10
L-Thr	0.33	0.21	0.09
L-Trp	0.08	0.04	0.01
Monocalcium phosphate	1.15	0.74	0.00
Limestone	0.79	0.70	0.52
Salt	0.30	0.30	0.30
Premix	1.00	1.00	1.00
Total	100.00	100.00	100.00
Nutritional level (based on chemical analysis)			
DM (MJ/kg)	14.60	14.60	14.60
CP	14.14	17.32	20.27
Lys	1.26	1.25	1.26
Met + Cys	0.63	0.65	0.62
Thr	0.76	0.75	0.76
Trp	0.20	0.20	0.20
Arg	0.71	0.93	1.09
His	0.30	0.37	0.44
Ileu	0.46	0.60	0.71
Leu	1.11	1.32	1.52
Phe	0.56	0.70	0.81
Val	0.54	0.64	0.72
Ca, %	0.70	0.71	0.69
Available *P*, %	0.53	0.55	0.57
EAA	6.29	7.18	7.91
NEAA	6.84	8.40	9.74
EAA/NEAA	0.90	0.85	0.80

In addition to digestive energy data, the remaining nutrients are measured values.

MATERIALS AND METHODS

Animals, Experimental Design, and Diets

Fifty four Duroc × Landrace × Yorkshire barrows (initial BW = 5.55 ± 0.49 kg, 21-day-old) were obtained from a local

Abbreviations: YSE, Yucca Schidigera Extract; CU, Candida Utilis; CON, control; RA, relative abundance; GLU, glucose; BUN, blood urea nitrogen; T-SOD, total superoxide dismutase; CAT, catalase; T-CHO, total cholesterol; AST, aspartate aminotransferase; MDA, transforming growth factor-β; ALT, alanine transaminase; T-AOC, total antioxidant capacity; ADG, average daily gain; ADFI, average daily feed intake.

commercial swine farm. All piglets were raised separately in 24 ± 1°C steel metabolic crates. Fifty-four piglets were randomly divided into three groups, with 18 piglets in each group and each piglet was a repeat. The experiment lasted for 45 days according to three dietary protein levels (14, 17, and 20%). The diets for piglets were prepared according to various nutrients recommended by NRC (12). They were allowed to eat and drink freely in a mechanically ventilated temperature-controlled room at 24 ± 1°C. The formula of the diet is shown in **Table 1**. All experimental procedures were approved by the License of Experimental Animals (SYXK 2014-0002) of the Animal Experimentation Ethics Committee of Southwest University, Chongqing, China.

Measurements and Sampling

On days 10, 25, and 45 of the experiment, six piglets were randomly selected from each group to collect feces, and then intravenous anesthesia with pentobarbital sodium (50 mg/kg BW) was used to collect blood. In addition, the digestive juice at the end of the ileum was collected with sterilized plastic bags. The samples were stored at 4°C for microbial separation and chemical analysis. A summary of the centrifugation protocol is given in **Figure 1**. The samples for chemical analysis were stored at −20°C (6).

Chemical Analyses

The feces were dried to a constant mass in a forced bellow at 95°C, and other digestive juice samples were fractionated by 250 RCF for 15 min at 4°C differential centrifugation. The determination of total N and AA composition follows the method proposed by predecessors (9, 10).

Data Treatment and Statistical Analysis

The endogenous indicator acid insoluble ash (AIA) was determined to calculate the apparent digestibility of dry matter, CP, and total AA. The formula is as follows: 1-bc/ad, where *a* denotes the content of DM, CP, or AA in diets (%); *b* denotes the content of dry matter (DM), CP, or AA in feces (%); *c* denotes the content of AIA in diet (%); and *d* denotes the content of AIA in feces (%). AA compositions were the content of single AA in TAA. The basic statistics of the data were carried out by Microsoft Excel 2020, the routine indexes were analyzed by SAS two-way ANOVA and significance test, and the measured data were analyzed by single factor ANOVA and significance test by SAS statistical software. The results were expressed by mean ± SEM, $p < 0.05$. The difference was significant.

RESULTS

Fecal N Excretion and Digestibility

As shown in **Table 2**, the excretion and digestibility of DM, CP, TN, total protein N (TPN), and total non-protein N (TNN) of piglets were increased with the increase of dietary protein levels on days 10 and 25 ($p < 0.01$). The excretion and digestibility of DM, CP, TN, TPN, and TNN of L-CP and H-CP were higher than those in the M-CP group on day 45 ($p < 0.01$). The excretion and digestibility of DM, CP, TN, TPN, and TNN of L-CP and H-CP were higher than those in the M-CP group on day 45 ($p < 0.01$). The excretion of microbial total N (MTN), microbial protein N (MPN), and microbial non-protein N (MNN) of piglets in the H-CP group were higher than those in the L-CP group and M-CP group on day 10 ($p < 0.01$). The excretion of MTN, MPN, and MNN in the M-CP group

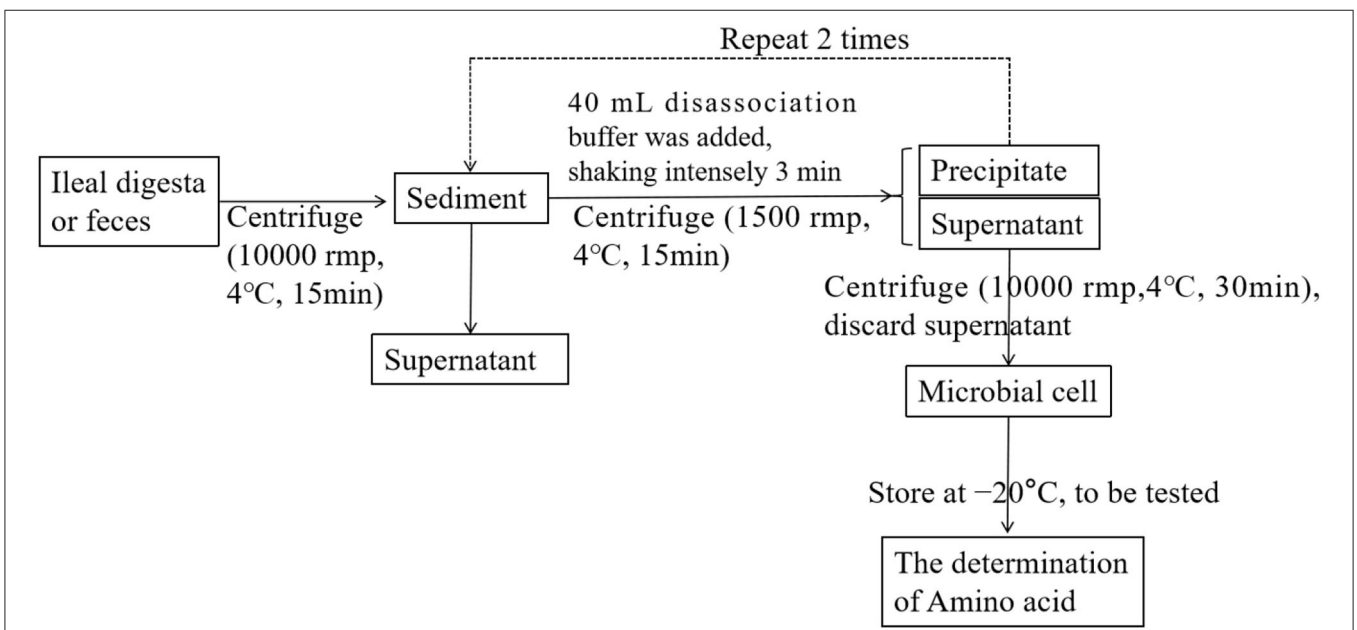

FIGURE 1 | Schematic diagram of the processing of the digesta samples.

TABLE 2 | Effects of dietary different protein levels on N excretion in feces and its apparent digestibility of piglets.

Time (d)	Items	DM-D (%)	CP-flow (mg/g DM)	CP-D (%)	TN (mg/g DM)	TN-D (%)	TPN (mg/g DM)	TPN-D (%)	TNN (mg/g DM)	TNN-D (%)	MTN (mg/g DM)	MPN (mg/g DM)	MNN (mg/g DM)
10 d	L-CP	85.0	261	69.6	41.8	69.6	36.7	76.5	5.1	58.5	0.67	0.59	0.09
	M-CP	83.7	282	70.9	45.1	70.9	40.1	74.3	5.0	54.7	1.34	1.23	0.11
	H-CP	89.6	302	82.6	48.3	82.6	42.8	84.4	5.5	75.4	2.12	1.86	0.26
25 d	L-CP	88.9	236	79.7	37.8	79.7	33.4	84.1	4.4	73.6	0.44	0.39	0.05
	M-CP	88.8	271	80.8	43.4	80.8	38.0	83.5	5.4	66.0	0.94	0.84	0.11
	H-CP	89.1	279	83.3	44.6	83.3	39.1	85.5	5.5	73.8	0.61	0.51	0.11
45 d	L-CP	91.2	228	84.2	36.6	84.2	31.0	88.3	5.6	77.2	1.35	1.17	0.17
	M-CP	88.6	208	84.1	33.3	84.1	28.1	88.4	5.2	75.6	1.86	1.67	0.19
	H-CP	90.0	224	87.8	35.9	87.8	30.7	90.5	5.2	81.5	1.63	1.44	0.19
SEM	Days	0.38	3.0	0.59	0.48	0.59	0.47	0.49	0.07	0.63	0.018	0.015	0.005
	CP	0.38	3.0	0.59	0.48	0.59	0.47	0.49	0.07	0.63	0.018	0.015	0.005
	Days × CP	0.66	5.2	1.03	0.8	1.03	0.8	0.85	0.12	1.09	0.028	0.025	0.008
P-Value	Days	<0.01	<0.01	<0.01	<0.01	<0.01	<0.01	<0.01	0.08	<0.01	<0.01	<0.01	<0.01
	CP	<0.01	<0.01	<0.01	<0.01	<0.01	<0.01	<0.01	<0.01	<0.01	<0.01	<0.01	<0.01
	Days × CP	<0.01	<0.01	<0.01	<0.01	<0.01	<0.01	<0.01	<0.01	<0.01	<0.01	<0.01	<0.01

L-CP, piglets fed a maize-soybean meal diet containing 14% CP; M-CP, piglets fed a maize-soybean meal diet containing 17% CP; H-CP piglets fed a maize-soybean meal diet containing 20% CP; SEM, standard error means; DM, dry matter; CP, crude protein; TN, total nitrogen, TPN, total protein nitrogen; TNN, total non-protein nitrogen; MTN, microbial total nitrogen; MPN, microbial protein nitrogen; MNN, microbial non-protein nitrogen. The same is in the following tables.

TABLE 3 | Effects of dietary protein levels on the TAA excretion (mg/g DM) and apparent digestibility (%) of piglets.

Time (d)	Items	TAA (+M)	TAA-D (+M, %)	NEAA (+M)	NEAA-D (+M, %)	EAA (+M)	EAA-D (+M, %)	E/NE (+M)	TAA (–M)	TAA-D (–M, %)	NEAA (–M)	NEAA-D (–M, %)	EAA (–M)	EAA-D (–M)	EAA/NEAA (–M)
10 d	L-CP	226	76.5	111	78.0	115	77.3	1.04	222.2	76.9	109.3	75.98	112.8	77.7	1.03
	M-CP	251	74.3	120	76.5	131	74.4	1.09	243.8	75.1	117.5	74.91	126.6	75.2	1.08
	H-CP	270	84.4	132	84.5	138	83.8	1.05	258.4	85.2	126.9	88.72	131.5	84.6	1.04
25 d	L-CP	207	84.1	102	85.0	105	84.7	1.03	204.5	84.2	101.4	83.52	103.2	84.9	1.02
	M-CP	236	83.5	117	84.3	119	84.1	1.02	231.2	83.9	114.3	83.31	116.3	84.4	1.02
	H-CP	243	85.5	118	85.6	125	84.8	1.06	239.4	85.7	116	86.40	123.5	85.0	1.06
45 d	L-CP	195	88.3	105	87.3	90	88.3	0.86	187.6	88.5	101.9	86.90	85.6	90.0	0.84
	M-CP	179	88.4	87	88.8	92	89.2	1.06	169.0	88.1	82.3	87.83	86.7	88.3	1.05
	H-CP	194	90.5	97	90.5	97	90.4	1.00	184.7	90.1	92.5	90.33	92.2	89.9	1.00
SEM	Days	3	0.49	1.4	0.49	1.70	0.50		3.0	0.48	1.7	0.49	1.8	0.48	
	CP	3	0.49	1.4	0.49	1.70	0.50		3.0	0.48	1.4	0.49	1.7	0.48	
	Days × CP	5.2	0.85	2.4	0.84	3	0.86		5.1	0.83	2.4	0.85	2.9	0.83	
P-value	Days	<0.01	<0.01	<0.01	<0.01	<0.01	<0.01	<0.01	<0.01	<0.01	<0.01	<0.01	<0.01	<0.01	<0.01
	CP	<0.01	<0.01	<0.01	<0.01	<0.01	<0.01	<0.01	<0.01	<0.01	<0.01	<0.01	<0.01	<0.01	<0.01
	Days × CP	<0.01	<0.01	<0.01	<0.01	0.06	<0.01	<0.01	<0.01	<0.01	<0.01	<0.01	<0.01	<0.01	<0.01

was higher than those in the L-CP group and H-CP group on days 25 and 45 ($p < 0.01$). The excretion of MTN, MTN, and MNN at day 25 was lower than those on days 10 and 45 ($p < 0.01$). The interaction effects between feeding time and dietary protein level (Days × CP) were as follows: CP ($p < 0.01$); total N (TN) ($p < 0.01$); TPN ($p < 0.01$); total non-protein N (TNN) ($p < 0.01$); MTN ($p < 0.01$); MPN ($p < 0.01$); and MNN ($p < 0.01$).

Fecal Total AA Excretion and Apparent Digestibility

As shown in **Table 3**, the excretion of total AA (TAA), essential AA (EAA), and non-essential AA (NEAA) decreased with the increase of feeding days of piglets ($p < 0.01$), and the digestibility of TAA, EAA, and NEAA increased with the prolongation of feeding time ($p < 0.01$). The excretion of TAA, EAA, NEAA, TAA (–M), NEAA (–M), and EAA (–M) increased with the

TABLE 4 | Effects of dietary protein levels on the excretion of the amino acid in feces of piglets (mg/g DM).

Time (d)	Items	Asp	Ser	Glu	Gly	Ala	Pro	Tyr	Thr	Cys	Val	Met	Ile	Leu	Phe	Lys	His	Arg
10 d	L-CP	22.4	7.1	30.3	13.7	23.1	15.1	8.2	12.4	3.5	15.5	3.2	13.8	24.9	12.2	10.5	4.5	6.1
	M-CP	23.0	8.3	32.7	17.3	24.7	14.3	9.0	11.6	3.8	18.8	4.4	16.4	29.1	14.2	12.0	4.6	7.2
	H-CP	24.9	11.8	35.6	18.6	26.7	14.4	9.5	12.1	5.0	19.1	4.0	17.0	31.4	14.0	12.2	5.0	8.6
25 d	L-CP	19.5	5.8	28.7	14.2	22.1	12.6	5.8	7.8	4.9	15.6	3.3	13.3	23.9	11.1	9.9	3.9	5.0
	M-CP	22.6	7.6	31.6	16.9	24.8	13.5	7.7	10.2	3.7	17.7	3.5	15.5	26.4	11.9	11.4	4.2	6.5
	H-CP	22.5	9.2	30.6	17.7	24.4	13.5	8.3	10.0	8.4	17.8	4.1	15.1	26.7	12.4	11.6	4.1	6.7
45 d	L-CP	13.7	6.3	37.6	16.4	23.4	7.5	5.1	7.5	7.0	11.5	3.7	10.1	16.7	8.6	9.0	5.1	5.6
	M-CP	15.9	5.9	22.8	13.4	19.7	9.4	6.1	7.5	3.6	14.3	2.2	12.1	20.5	9.9	8.1	3.4	4.5
	H-CP	18.0	6.3	37.7	15.4	19.7	12.2	6.7	8.6	3.4	14.5	2.7	12.5	20.9	10.2	9.1	3.3	4.8
SEM	Days	0.4	0.2	0.5	0.3	0.3	0.3	0.2	0.2	0.4	0.2	0.1	0.3	0.5	0.2	0.2	0.1	0.2
	CP	0.4	0.2	0.5	0.3	0.3	0.3	0.2	0.2	0.4	0.2	0.1	0.3	0.5	0.2	0.2	0.1	0.2
	Days × CP	0.70	0.4	0.9	0.5	0.60	0.50	0.4	0.30	0.67	0.4	0.2	0.4	0.83	0.3	0.3	0.2	0.3
P-value	Days	<0.01	<0.01	<0.01	<0.01	<0.01	<0.01	<0.01	<0.01	0.02	<0.01	<0.01	<0.01	<0.01	<0.01	<0.01	<0.01	<0.01
	CP	<0.01	<0.01	<0.01	<0.01	0.33	<0.01	<0.01	<0.01	<0.01	<0.01	0.33	<0.01	<0.01	<0.01	<0.01	0.05	<0.01
	Days × CP	0.23	<0.01	<0.01	<0.01	<0.01	<0.01	0.6	<0.01	<0.01	0.46	<0.01	0.57	0.25	0.58	<0.01	<0.01	<0.01

TABLE 5 | Effects of dietary protein levels on the AA apparent digestibility in feces of piglets (%).

Time (d)	Items	Asp	Ser	Glu	Gly	Ala	Pro	Tyr	Thr	Cys	Val	Met	Ile	Leu	Phe	Lys	His	Arg
10 d	L-CP	71.5	84.1	80.2	72.3	65.3	76.4	69.5	74.3	74.5	70.3	83.7	69.8	76.1	75.9	80.0	87.0	89.3
	M-CP	76.7	79.8	79.0	64.2	60.8	77.1	64.4	74.0	69.9	61.3	92.1	62.7	68.8	70.4	76.4	86.0	87.2
	H-CP	84.9	84.0	87.9	81.5	78.3	88.9	76.5	83.9	80.4	81.1	86.7	79.5	82.1	83.8	85.7	90.8	91.8
25 d	L-CP	81.8	90.3	86.1	78.9	75.6	85.5	83.9	88.2	73.5	75.0	87.5	78.5	83.0	83.9	86.1	91.9	93.5
	M-CP	84.3	87.3	86.0	76.0	73.3	85.3	79.1	84.3	79.6	87.3	95.7	75.9	80.7	83.0	84.6	91.2	92.1
	H-CP	86.0	87.2	89.2	81.5	79.2	89.3	79.1	86.3	66.4	77.9	86.3	81.2	84.2	85.0	85.8	92.6	93.4
45 d	L-CP	91.6	90.4	86.5	80.0	85.4	93.9	87.7	91.2	68.6	87.6	82.6	87.6	89.1	88.9	91.3	89.9	94.4
	M-CP	89.0	90.0	91.2	83.5	84.2	91.4	84.7	89.3	83.2	83.1	92.7	83.6	86.7	87.7	91.2	92.8	95.1
	H-CP	91.0	91.0	92.8	86.6	86.2	91.5	86.1	89.8	87.3	87.3	92.1	87.4	89.8	90.3	91.9	94.6	96.1
SEM	Days	0.59	0.5	0.43	0.65	0.77	0.5	0.85	0.64	1.69	0.68	0.65	0.74	0.56	0.58	0.47	0.44	0.25
	CP	0.59	0.5	0.43	0.65	0.77	0.5	0.85	0.64	1.69	0.68	0.65	0.74	0.56	0.58	0.47	0.44	0.25
	Days × CP	1.03	0.86	0.74	1.12	1.33	0.87	1.48	1.1	2.93	1.17	1.13	1.28	0.96	1.01	0.82	0.76	0.43
P-value	Days	<0.01	<0.01	<0.01	<0.01	<0.01	<0.01	<0.01	<0.01	0.03	<0.01	0.04	<0.01	<0.01	<0.01	<0.01	<0.01	<0.01
	CP	<0.01	<0.01	<0.01	<0.01	<0.01	<0.01	<0.01	<0.01	0.03	<0.01	<0.01	<0.01	<0.01	<0.01	<0.01	<0.01	<0.01
	Days × CP	<0.01	0.04	<0.01	<0.01	<0.01	<0.01	<0.01	<0.01	<0.01	<0.01	<0.01	<0.01	<0.01	<0.01	<0.01	0.01	<0.01

increase of dietary protein level on days 10 and 20 ($p < 0.01$). The digestibility of TAA, EAA, and NEAA in the H-CP group was higher than those in the L-CP group and M-CP group ($p < 0.01$). The digestibility of TAA, EAA, and NEAA in the M-CP group was lower than those in L-CP and H-CP groups at days 10 and 25 ($p < 0.01$). The digestibility of TAA, EAA, and NEAA in the L-CP group was lower than those in M-CP and H-CP groups at day 45 ($p < 0.01$). Interestingly, the change law of the above results is similar after the AA part of the microbes were removed from feces AA. The interaction effects between feeding time and dietary protein level (Days × CP) were as follows: TAA ($p < 0.01$), TAA digestibility ($p < 0.01$), NEAA ($p < 0.01$), NEAA digestibility ($p < 0.01$), EAA digestibility ($p < 0.0l$), TAA (–M) ($p < 0.01$), TAA digestibility (–M) ($p < 0.01$), NEAA (–M) ($p < 0.01$), NEAA digestibility (–M) ($p < 0.01$), EAA (–M) ($p < 0.01$), and EAA digestibility (–M) ($p < 0.01$).

Fecal AA Excretion and Apparent Digestibility

As shown in **Table 4**, the excretion of all amino acids in piglets, except Cys, decreased with the increase of feeding time ($p < 0.01$). The excretion of Asp, Pro, Val, Ile, Leu, Try, Phe, and Lys increased with the increase of dietary protein level ($p < 0.01$). The excretion of Asp, Ser, Glu, Gly, Ala, Cys, Val, Ile, Leu, Lys, Phe, Lys, and Arg increased with the increase of dietary protein level on day 10 ($p < 0.01$). The excretion of Asp, Ser, Gly, Ala, Thr, Cys, Val, Met, Ile, Leu, Try, Phe, Lys, and Arg increased with the increase of dietary protein level on day 25 ($p < 0.01$). The excretion of Asp, Pro, Thr, Val, Ile, Leu, Try, and Phe increased with the increase of dietary protein level ($p < 0.01$) on day 45. The interaction effects between feeding time and dietary protein level (Days × CP) were as follows: Try ($p < 0.01$), Glu ($p < 0.01$), glycine (Gly) ($p < 0.01$), Ala ($p < 0.01$), Pro ($p < 0.01$), Thr ($p < 0.01$), Cys ($p < 0.01$), Met ($p < 0.01$), Lys ($p < 0.01$), His ($p < 0.01$), and Arg ($p < 0.01$) in the feces of piglets.

As can be seen from **Table 5**, the apparent digestibility of Ala, Ile, Leu, Tyr, Phe, and Lys of piglets in the M-CP group was lower than that of the L-CP group and H-CP group ($p < 0.01$). The apparent digestibility of Met was higher than that in the other two groups. The apparent digestibility of Asp, Glu, Gly, Ala, Pro, Thr, Cys, Val, Ile, Leu, Tyr, Phe, Lys, His, and Arg in the H-CP group was higher than those in the L-CP group and M-CP group on day 10 ($p < 0.01$). The apparent digestibility of fecal Cys, Val, and Met in the M-CP group were higher than that in the L-CP group and H-CP group ($p < 0.01$), and the remaining amino acids were lower than those in the other two groups on day 25 ($p < 0.01$). The apparent digestibility of Glu, Gly, Cys, Met, His, and Arg increased with the increase of dietary protein level ($p < 0.01$), and the apparent digestibility of the remaining amino acids in the M-CP group was lower than those in the L-CP group and H-CP group on day 45 ($p < 0.01$). The interaction effects between feeding time and dietary protein level (Days × CP) were as follows: Asp ($p < 0.01$), Glu ($p < 0.01$), Gly ($p < 0.01$), Ala ($p < 0.01$), Pro ($p < 0.01$), Thr ($p < 0.01$), Cys ($p < 0.01$), Val ($p < 0.01$), Met ($p < 0.01$), Ile ($p < 0.01$), Leu ($p < 0.01$), Tyt ($p < 0.01$), Phe ($p < 0.01$), Lys ($p < 0.01$), His ($p < 0.01$), and Arg

TABLE 6 | Effects of dietary protein levels on the microbe AA excretion in feces of piglets (mg/g DM).

Time (d)	Items	Asp	Ser	Glu	Gly	Ala	Pro	Tyr	Thr	Cys	Val	Met	Ile	Leu	Phe	Lys	His	Arg	TAA	NEAA	EAA	EAA/NEAA
10 d	L-CP	0.315	0.145	0.435	0.216	0.376	0.173	0.165	0.156	0.025	0.320	0.058	0.260	0.312	0.255	0.205	0.108	0.168	3.70	1.66	2.03	1.22
	M-CP	0.617	0.253	0.710	0.535	0.265	0.362	0.302	0.365	0.063	0.706	0.065	0.563	0.795	0.456	0.428	0.213	0.336	7.03	2.74	4.29	1.38
	H-CP	0.765	0.438	1.340	0.712	1.406	0.516	0.565	0.690	0.052	0.985	0.310	0.728	1.011	0.683	0.626	0.265	0.522	11.61	5.19	6.43	1.32
25 d	L-CP	0.213	0.118	0.265	0.150	0.263	0.087	0.083	0.223	0.010	0.172	0.018	0.153	0.240	0.136	0.136	0.070	0.085	2.44	1.10	1.34	1.29
	M-CP	0.680	0.155	0.658	0.346	0.670	0.168	0.150	0.268	0.020	0.297	0.097	0.335	0.498	0.266	0.280	0.135	0.232	5.25	2.67	2.58	1.25
	H-CP	0.352	0.132	0.352	0.216	0.330	0.108	0.125	0.230	0.035	0.198	0.048	0.241	0.295	0.17	0.155	0.090	0.12	3.20	1.48	1.71	1.23
45 d	L-CP	0.698	0.343	0.792	0.633	0.628	0.176	0.395	0.462	0.052	0.348	0.160	0.677	0.395	0.593	0.467	0.270	0.346	7.35	3.27	5.08	1.25
	M-CP	1.045	0.355	1.233	0.702	1.168	0.362	0.408	0.533	0.105	0.758	0.170	0.702	1.108	0.628	0.505	0.253	0.395	10.04	4.86	5.57	1.15
	H-CP	0.853	0.351	1.212	0.532	1.030	0.308	0.350	0.470	0.077	0.593	0.153	0.545	1.070	0.553	0.405	0.187	0.312	9.00	4.29	4.72	1.10
SEM	Days	0.011	0.012	0.016	0.009	0.018	0.008	0.014	0.012	0.004	0.013	0.005	0.090	0.014	0.009	0.008	0.006	0.01	0.044	0.057	0.011	
	CP	0.011	0.012	0.016	0.009	0.018	0.008	0.014	0.012	0.004	0.013	0.005	0.090	0.014	0.009	0.008	0.006	0.01	0.044	0.057	0.011	
	Days × CP	0.020	0.020	0.027	0.016	0.032	0.014	0.024	0.021	0.007	0.022	0.009	0.016	0.024	0.016	0.015	0.011	0.017	0.161	0.075	0.098	
P-value	Days	<0.01	<0.01	<0.01	<0.01	<0.01	<0.01	<0.01	<0.01	<0.01	<0.01	<0.01	<0.01	<0.01	<0.01	<0.01	<0.01	<0.01	<0.01	<0.01	0.04	<0.01
	CP	<0.01	<0.01	<0.01	<0.01	<0.01	<0.01	<0.01	<0.01	<0.01	<0.01	<0.01	<0.01	<0.01	<0.01	<0.01	<0.01	<0.01	<0.01	<0.01	<0.01	<0.01
	Days × CP	<0.01	<0.01	<0.01	<0.01	<0.01	<0.01	<0.01	<0.01	0.010	<0.01	<0.01	<0.01	<0.01	<0.01	<0.01	<0.01	<0.01	<0.01	<0.01	<0.01	<0.01

($p < 0.01$) in piglet feces. At the level of feeding time, except for Cys and Met, the apparent digestibility of AA in feces increased significantly with the increase of feeding time ($p < 0.01$).

Fecal Microbial AA Excretion

As shown in **Table 6**, the excretion of AA of fecal microorganisms of piglets on day 25 was lower than that on day 10 and day 45 ($p < 0.01$), and the excretion of TAA and NEAA of fecal microorganisms of piglets on day 25 was higher than that on days 10 and 45 ($p < 0.0$l). There was no significant difference in fecal microbial EAA excretion with the increase of feeding time ($p > 0.05$). The AA excretion of fecal microorganisms of piglets in the L-CP group was lower than that in the M-CP group and H-CP group ($p < 0.01$). The excretion of fecal microorganisms TAA, EAA, and NEAA increased with the increase of CP levels on day 10 ($p < 0.01$), and the excretion of TAA, EAA, and NEAA of the M-CP group were significantly higher than that of L-CP and H-CP on the day 25 ($p < 0.01$). Generally speaking, the emission of EAA was greater than that of NEAA. The interaction effects between feeding time and dietary protein level (Days × CP) were as follows: Asp ($p < 0.01$), Ser ($p < 0.01$), Glu ($p < 0.01$), Gly ($p < 0.01$), Ala ($p < 0.01$), Pro ($p < 0.01$), Thr ($p < 0.01$), Cys ($p < 0.01$), Val ($p < 0.01$), Met ($p < 0.01$), Ile ($p < 0.01$), Leu ($p < 0.01$), Tyr ($p < 0.01$), Phe ($p < 0.01$), Lys ($p < 0.01$), His ($p < 0.01$), and Arg ($p < 0.01$) in piglet feces.

The excretion of amino acids except for Cys and Ile of fecal microorganisms increased with the increase of dietary protein level on day 10 ($p < 0.01$). The excretion of amino acids except for Cys and His of feces microbial in the M-CP group was higher than that in L-CP and H-CP ($p < 0.01$), and the excretion of microbial AA in L-CP was the lowest on day 25. The fecal excretion of amino acids except for Ser, Glu, Cys, Met, Ile, Leu, Tyr, and His of fecal microorganisms of piglets in the M-CP group was higher than that in the L-CP group and H-CP group ($p < 0.01$).

Effects of Different Protein Levels on Microbial AA Composition in Feces and Ileum of Piglets

As shown in **Tables 7**, **8**, the number of microbial AA increased with the increase of piglet age. The EAA/NEEA of Ile chyme and feces decreased with the increase of dietary CP ($p < 0.01$). The protein nutrition patterns of Asp, Ala, Glu, and Leu in the AA composition of ileum and feces of piglets were more obvious. The proportion of His, Tyr, Met, Cys, and Ser was lower than the average level, while the proportion of Phe, Leu, Pro, Ala, Glu, and Asp were higher than the average level. The interaction effects between feeding time and dietary protein level (Days × CP) were was reflected in Asp ($p < 0.01$), Glu ($p < 0.01$), Ala ($p < 0.01$), Pro ($p < 0.01$), Cys ($p < 0.01$), Val ($p < 0.01$), Met ($p < 0.01$), Ile ($p < 0.01$), Tyr ($p < 0.01$), Phe ($p < 0.01$), Lys ($p < 0.01$), His ($p < 0.01$), and Arg ($p < 0.01$) in ileum and feces of piglets.

TABLE 7 | Effects of dietary protein levels on the microbial bacteria AA form in feces of piglets (%).

Time (d)	Items	Asp	Ser	Glu	Gly	Ala	Pro	Tyr	Thr	Cys	Val	Met	Ile	Leu	Phe	Lys	His	Arg	TAA	NEAA	EAA	NEAA/EAA
10 d	L-CP	8.56	3.93	11.76	5.87	10.25	4.62	4.36	4.27	0.67	8.67	1.55	7.050	8.52	6.92	5.57	2.90	4.54	100.00	45.0	55.0	1.22
	M-CP	8.33	3.43	9.62	7.23	8.49	4.87	4.06	4.92	0.84	10.05	0.88	7.630	10.73	6.18	5.80	2.91	4.55	100.00	42.0	58.0	1.38
	H-CP	6.60	3.80	11.54	6.15	12.13	4.45	4.88	5.94	0.44	8.31	2.69	6.300	8.72	5.89	5.41	2.30	4.47	100.00	44.7	55.3	1.32
25 d	L-CP	8.82	4.87	10.92	6.17	10.79	3.54	3.38	9.25	0.52	7.13	0.79	6.240	9.90	5.61	5.65	2.86	3.57	100.00	45.1	54.9	1.29
	M-CP	8.93	3.41	10.90	7.56	9.19	3.67	3.16	5.89	0.44	6.44	2.05	7.330	10.98	5.90	6.12	2.93	5.09	100.00	43.7	56.3	1.25
	H-CP	11.04	4.13	11.04	6.80	10.20	3.3	3.84	7.31	1.13	6.26	1.44	7.610	9.15	5.36	4.89	2.89	3.62	100.00	46.5	53.5	1.23
45 d	L-CP	9.54	4.64	10.79	8.62	8.53	2.4	5.38	6.27	0.72	4.73	0.99	9.180	5.33	8.09	6.38	3.69	4.72	100.00	44.5	55.5	1.25
	M-CP	10.01	3.41	11.80	6.72	11.20	3.46	3.91	5.13	1.01	7.26	1.67	6.710	10.62	6.05	4.83	2.42	3.80	100.00	46.6	53.4	1.15
	H-CP	9.49	3.91	13.47	5.89	11.46	3.42	3.88	5.20	0.85	6.58	1.70	6.070	11.92	6.15	4.51	2.06	3.45	100.00	47.6	52.4	1.10
SEM	Days	0.19	0.14	0.16	0.13	0.23	0.11	0.17	0.16	0.05	0.17	0.07	0.11	0.24	0.12	0.15	0.10	0.12		0.28	0.28	
	CP	0.19	0.14	0.16	0.13	0.23	0.11	0.17	0.16	0.05	0.17	0.07	0.11	0.24	0.12	0.15	0.10	0.12		0.28	0.28	
	Days × CP	0.32	0.24	0.27	0.23	0.40	0.19	0.30	0.28	0.09	0.29	0.11	0.19	0.41	0.20	0.20	0.17	0.21		0.49	0.49	
P-value	Days	<0.01	0.12	<0.01	<0.01	0.59	<0.01	<0.01	<0.01	0.02	<0.01	<0.01	0.09	0.06	<0.01	0.20	0.32	<0.01		<0.01	<0.01	<0.01
	CP	0.9	<0.01	<0.01	<0.01	<0.01	0.01	0.02	<0.01	0.08	<0.01	<0.01	<0.01	<0.01	<0.01	<0.01	<0.01	<0.01		<0.01	<0.01	<0.01
	Days × CP	<0.01	0.36	<0.01	<0.01	<0.01	<0.01	<0.01	<0.01	<0.01	<0.01	<0.01	<0.01	<0.01	<0.01	<0.01	<0.01	<0.01		<0.01	<0.01	<0.01

TABLE 8 | Effects of dietary protein levels on the microbial bacteria AA form in ileum of piglets (%).

Time (d)	Items	Asp	Ser	Glu	Gly	Ala	Pro	Tyr	Thr	Cys	Val	Met	Ile	Leu	Phe	Lys	His	Arg	TAA	NEAA	EAA	EAA/NEAA
10 d	L-CP	9.41	3.64	11.61	5.46	7.23	3.93	4.52	5.26	0.46	7.44	0.41	7.19	13.41	7.17	4.78	3.32	4.78	100.0	42.3	58.7	1.39
	M-CP	9.89	3.39	11.47	7.05	6.42	3.88	4.11	5.64	0.46	6.70	0.28	6.69	12.59	7.33	5.47	3.46	5.19	100.0	42.1	57.9	1.38
	H-CP	8.76	3.60	12.05	8.05	7.25	4.98	3.47	4.92	0.44	8.68	0.40	6.81	12.19	6.46	4.75	2.99	4.22	100.00	44.7	55.3	1.24
25 d	L-CP	9.44	4.65	10.23	5.52	5.96	5.48	4.09	4.87	0.48	6.47	0.68	6.41	13.71	8.14	3.86	4.67	5.35	100.00	41.3	58.7	1.42
	M-CP	11.27	3.95	12.80	6.39	6.35	4.75	3.60	4.72	0.26	7.87	0.38	8.00	12.65	7.16	3.67	2.59	3.63	100.00	45.5	54.5	1.20
	H-CP	10.72	4.76	12.58	7.23	6.06	7.26	2.91	4.93	0.27	7.40	0.22	6.73	12.31	7.46	4.02	2.77	2.38	100.00	48.6	51.4	1.06
45 d	L-CP	10.92	4.25	9.77	5.82	6.53	4.93	2.96	5.02	0.48	7.34	0.63	8.32	12.03	8.51	4.10	4.62	3.74	100.00	42.2	57.8	1.37
	M-CP	10.37	5.43	11.96	6.43	7.07	4.57	3.04	4.67	0.55	6.28	0.35	6.27	12.60	6.46	4.82	4.37	3.14	100.00	47.5	52.5	1.11
	H-CP	10.80	6.15	12.58	7.53	7.80	4.44	3.87	5.37	0.42	6.47	0.47	7.08	10.09	6.34	3.86	2.77	3.13	100.00	49.3	50.7	1.03
SEM	Days	0.15	0.11	0.22	0.16	0.14	0.12	0.12	0.12	0.02	0.21	0.01	0.12	0.18	0.13	0.09	0.09	0.08		0.30	0.30	0.02
	CP	0.15	0.11	0.22	0.16	0.14	0.12	0.12	0.12	0.02	0.21	0.01	0.12	0.18	0.13	0.09	0.09	0.08		0.30	0.30	0.02
	Days × CP	0.26	0.19	0.38	0.28	0.28	0.24	0.20	0.21	0.04	0.36	0.02	0.21	0.31	0.23	0.16	0.16	0.14		0.52	0.52	0.03
P-value	Days	<0.01	<0.01	0.387	0.12	<0.01	<0.01	<0.01	0.04	<0.01	0.01	<0.01	0.15	0.03	0.05	<0.01	<0.01	<0.01		<0.01	<0.01	<0.01
	CP	<0.01	<0.01	<0.01	<0.01	0.04	<0.01	0.03	0.93	0.01	0.14	<0.01	0.04	<0.01	<0.01	<0.01	<0.01	<0.01		<0.01	<0.01	<0.01
	Days × CP	<0.01	<0.01	<0.01	0.35	<0.01	<0.01	<0.01	0.03	<0.01	<0.01	<0.01	<0.01	0.06	<0.01	<0.01	<0.01	<0.01		<0.01	<0.01	<0.01

DISCUSSION

Apparent Digestibility of CP and AA

Research showed that the composition of dietary nutrients could directly affect the secretion of digestive enzymes in piglets (11). Griffiths reported that high protein levels could significantly affect the activity of digestive enzymes in the intestines of piglets (13). The secretion of digestive enzymes directly restricted the absorption and utilization of dietary CP, and so different dietary CP levels could lead to differences in fecal CP, AA, fecal CP digestibility, and AA digestibility of piglets. In this experiment, the apparent digestibility of CP and AA were increased linearly with the increase of dietary CP levels. When the CP levels increased to 20%, the measured indexes and the corresponding apparent digestibility increased significantly. It could be seen that increasing the dietary protein level in an appropriate range would directly affect the digestion and metabolism of nutrients such as dry matter, CP and AA in piglets.

In this study, the digestibility of dry matter, CP, and N increased significantly with the increase of feeding time, and H-CP was significantly higher than that of the L-CP group and M-CP group. The reasons were the following points: first, the intestinal development of piglets was not perfect, the secretion of digestive enzymes is less, the digestive system of piglets tended to mature after 45 days, and the secretion of all kinds of digestive enzymes tended to be stable. Secondly, properly increasing the dietary protein level and balanced AA level was beneficial for the absorption and utilization of the digestive tract of piglets. Some studies had shown that endogenous N could affect the apparent digestibility of intestinal N. When the dietary protein content was low, because of the increasing proportion of endogenous protein, the apparent digestibility of CP was decreased. In addition, protease was a kind of dietary protein metabolic enzyme, and the dietary protein level could directly affect the protease activity in the digestive tract. Within a certain range of protein levels, the apparent digestibility of CP was positively correlated with dietary protein levels (14), which was consistent with the results of this study.

There was not a simple linear relationship between CP apparent digestibility and dietary CP content. The study of Silva and Perera (15) pointed out that with the increase of dietary protein level, the apparent digestibility of dietary protein increased at first and then decreased. The results showed that there is an optimal concentration range for protein utilization. The digestibility of protein would not be ideal if the protein level was below or above the concentration range, that is, the protein digestibility would not be ideal on day 45. There was no such change in the results of this study, and the reason for the difference might be that the protein level in the study did not exceed the optimal range and belonged to the rising zone. At the same time, weaned piglets were in a special physiological period, and the utilization of protein level at this stage remains to be further studied.

The differences in dietary N digestion and utilization of piglets under different CP levels led to differences in N excretion

(16, 17). In this study, within the range of 14–20% CP the apparent N digestibility of piglets increased linearly with the increase of CP levels, and the total N excretion increased with the increase of dietary CP levels and feeding time, which was consistent with the conclusions of other scholars (18). The apparent biological value of protein was mainly affected by the deposition ability of N nutrients and the degree of dietary protein balance, which reflected the utilization degree of N nutrients in piglets. The protein balance of the three diets used in this experiment was the same, and so the apparent biological value mainly depended on the ability of piglets to deposit N nutrients absorbed from the diet. When the dietary protein level was lower than the needs of the body, the piglets would make adaptive adjustments in order to improve the utilization efficiency of N nutrients absorbed in the diet and increase the deposition of N nutrients.

Effects of Different Protein Levels on Microbial AA Composition in Feces and Ileum of Piglets

AAs played a very important role in animal nutrition and physiology (19). However, there was a lack of knowledge about the utilization and metabolism of AA in intestinal microorganisms. The results of human-like microorganisms *in vitro* culture showed that the rapidly fermented AA of human-like microorganisms was Lys, Arg, Thr, His, Glu, and Asp (20). The addition of fermentable carbohydrates to the culture system could reduce the decarboxylation of AA and the formation of amines by bacteria (21). The study also showed that the bacteria of Clostridium, Bacteroides, and Prepfococo were the main AA fermentation bacteria in the human intestine (22). Studies on fistula piglets had shown that Lys, Phe, and branched-chain AA synthesized by bacteria in the intestinal cavity can be absorbed by the small intestine and large intestine (23). However, these findings did not explain the high level of net utilization of AA in the intestine (24). So far, the metabolic pathway of dietary AA, especially essential AA, in the intestinal cavity was not clear (25). The study also showed that the bacteria of Clostridium, Bacteroides, and Prepfococo were the main AA fermentation bacteria in the human intestine (26). Studies on fistula pigs had shown that lysine, phenylalanine, and branched chain AA synthesized by bacteria in the intestinal cavity could be absorbed by the small intestine and large intestine (27, 28). However, these findings did not explain the high level of net utilization of AA in the intestine (27). So far, the metabolic pathway of dietary AA, especially essential AA, in the intestinal cavity was not clear (29). In this experiment, the proportion of microbial AA in piglet feces was only 1–5%, and the response of intestinal microorganisms Asp, Ala, Glu, and Leu to the N nutrition model was more obvious. In the AA composition of intestinal microorganisms, it was found that there were similarities between ileum and rectum: the proportion of His, Tyr, Met, Cys, and Ser was lower than the average level. The proportion of Phe, Leu, Pro, Ala, Glu, and Asp was higher than the average level.

CONCLUSIONS

To sum up, this study revealed some scientific problems, such as the changes of N, CP, and AA excretion and digestibility of feces and microorganisms of piglets at different feeding times, the changes of AA composition of intestinal microorganisms, the changes in AA composition of microorganisms, the mechanism of enzyme activity, and the mechanism of enzyme activity affecting the changes of biogenic amines. The purpose of this work was to provide a theoretical basis for the follow-up research on how gastrointestinal microorganisms and gastrointestinal digestion and metabolism change the mode of N supply.

DATA AVAILABILITY STATEMENT

The original contributions presented in the study are included in the article/supplementary material, further inquiries can be directed to the corresponding author/s.

ETHICS STATEMENT

The animal study was reviewed and approved by Sciences Animal Ethics Committee of Chinese Academy of Sciences (Hunan, China; Ethic approval number: SYXK 2014-0002).

AUTHOR CONTRIBUTIONS

ZT and ZY designed the whole experiment and verified the validity of experiment and checked the results. HD and TH performed the experiment, including chemical analysis, and statistical analysis. ZY and TH worked on the manuscript. ZS, ZG, PH, and ZR participated in the experiment design and gave valuable advice. All of the authors have read and approved the final version of this manuscript.

FUNDING

This study was funded in part by the National Natural Science Foundation of China (31902167 and 31772610), Fundamental Research Funds for the Central Universities (XDJK2020C019), Chongqing Natural Science Foundation (Basic Research and Frontier Exploration Special Project) General Project (cstc2019jcyj-msxmX0524 and cstc2021jcyj-msxmX0966), Research project on educational and teaching reform in Southwest University (2019JY017), National Program on Key Basic Research Project of China (2013CB127303), and the National Science Foundation for postdoctoral scientists of China (2018M640895).

ACKNOWLEDGMENTS

We thank Professor De Wu and Professor Guozhong Dong for their insightful suggestions on experimental design.

REFERENCES

1. Kendall DC, Gaines AM, Kerr BJ, Allee GL. True ileal digestible tryptophan to lysine ratios in ninety- to one hundred twenty-five-kilogram barrows. *J Anim Sci.* (2007) 85:3004–12. doi: 10.2527/jas.2007-0013
2. Chen H, Yi X, Zhang G, Lu N, Chu L, Thacker PA, et al. Studies on reducing nitrogen excretion: I. Net energy requirement of finishing pigs maximizing performance and carcass quality fed low crude protein diets supplemented with crystalline amino acids. *J Anim Sci Biotechnol.* (2011) 2:84–93. doi: 10.3382/ps.0310700
3. Kerr B. Dietary manipulation to reduce environmental impact. In: *Proceedings of the 9th International Symposium on Digestive Physiology in Pigs* (Banff, AB) (2003).
4. Shriver JA, Carter SD, Sutton AL, Richert BT Senne BW, Pettey LA. Effects of adding fiber sources to reduced-CP, amino acids-supplemented diets on nitrogen excretion, growth performance, and carcass traits of finishing pigs. *J. Anim Sci.* (2003) 81:492–502. doi: 10.1046/j.1439-0396.2003.00411.x
5. Shi B, Liu J, Sun Z, Li TJ, Zhu, WW, Tang Z. The effects of different dietary crude protein level on faecal crude protein and amino acid flow and digestibility in growing pigs. *J Appl Anim Res.* (2016) 46:74–80. doi: 10.1080/09712119.2016.1260570
6. Yang, Z, He T, Bumbie G, Hu H, Chen QJ, Lu C, et al. Effects of dietary crude protein levels on fecal crude protein, amino acids flow amount, fecal and ileal microbial amino acids composition and amino acid digestibility in growing pigs. *Animals.* (2020) 10:2092–105. doi: 10.3390/ani10112092
7. Dai ZL, Zhang J, Wu G, Zhu WY. Utilization of amino acids by bacteria from the pig small intestine. *Amino Acids.* (2010) 39:1201–15. doi: 10.1007/s00726-010-0556-9
8. Zhou J, Wang Y, Zeng X, Zhang T, Li P, Yao B, et al. Effect of antibiotic-free, low-protein diets with specific amino acids compositions on growth and intestinal flora in weaned pigs. *Food Funct.* (2020) 11:493–507. doi: 10.1039/C9FO02724F
9. Horwitz W. Official methods of analysis of the association of official analytical chemists. In: *Association of Official Analytical Chemists*. 17th ed. (Arlington, VA) (2000). p. 1059–60.
10. Moughan PJ, Hodgkinson SM. The enzyme hydrolysed protein method for the determination of endogenous ileal nitrogen and amino acids flows-a modification. *Anim Feed Sci Technol.* (2003) 108:207–14. doi: 10.1016/S0377-8401(03)00130-5
11. Zhao Y, Tian G, Chen D, Zheng P, Yu B. Dietary protein levels and amino acid supplementation patterns alter the composition and functions of colonic microbiota in pigs. *Anim Nutr.* (2020) 6:143–51. doi: 10.1016/j.aninu.2020.02.005
12. *National Research Council*. Washington, DC: National Research Council (2012).
13. Griffiths D W, Moseley G. The effect of diets containing field beans of high or low polyphenolic content on the activity of digestive enzymes in the intestines of rats. *J Sci Food Agric.* (2010) 31:255–9. doi: 10.1002/jsfa.27403 10307
14. Nieto R, Miranda A, García M, Aguilera JF. The effect of dietary protein content and feeding level on the rate of protein deposition and energy utilization in growing Iberian pigs from 15 to 50kg body weight. *British J Nutr.* (2002) 88:39–49. doi: 10.1079/BJN2002591
15. Silva SSD, Perera M. Effect of dietary protein level and salinity with further observations on variability in daily digestibility. *Agriculture.* (1984) 38:293–306. doi: 10.1016/0044-8486(84)90334-X
16. Li TQ, Hao YJ, An RY, Gao YJ. Effect of dietary protein level on digestibility of Amur Sturgeon larvae. *Freshw Fish.* (2002) 5:51–4. (In Chinese). doi: 10.3969/j.issn.1000-6907.2002.05.020
17. Zhang B, Wang C, Liu H, Liu J, Liu H. Effects of dietary protein level on growth performance and nitrogen excretion of dairy heifers. *Asian Austral J Anim Sci.* (2016) 30:386–91. doi: 10.5713/ajas.16. 0214
18. Li Y, Wei H, Li F, Guo Q, Duan Y, Yin Y. Effects of low-protein diets supplemented with branched-chain amino acids on lipid metabolism in white adipose tissue of piglets. *J Agric Food Chem.* (2017) 65:2839–48. doi: 10.1021/acs.jafc.7b00488
19. Duan J, Jie Y, Ren W, Liu T, Cui Z, Huang X, et al. Dietary supplementation with L-glutamate and L-aspartate alleviates oxidative stress in weaned piglets challenged with hydrogen peroxide. *Amino Acids.* (2016) 48:53–64. doi: 10.1007/s00726-015-2065-3
20. Yin J, Li T, He J. Long-term effect of lysine restriction on liver global proteins, meat quality, and blood biochemical parameters in pigs. *Protein Peptide Lett.* (2018) 25:405–16. doi: 10.2174/0929866525666180406 142451
21. Li Y, Yin J, Han H, Liu G, Deng D, Kim SW, et al. Metabolic and proteomic responses to long-term protein restriction in a pig model. *J Agr Food Chem.* (2018) 66:12571–9. doi: 10.1021/acs.jafc.8b05305
22. Zheng P, Song Y, Tian Y, Zhang H, Yu B, He J, et al. Dietary arginine supplementation affects intestinal function by enhancing antioxidant capacity of a nitric oxide-independent pathway in low-birth-weight piglets. *J Nutr.* (2018) 148:1751–9. doi: 10.1093/jn/nxy198
23. Yin J, Ying Y, Han H, Liu ZJ, Zeng XF, Li T, et al. Long-term effects of lysine concentration on growth performance, intestinal microbiome, and metabolic profiles in a pig model. *Food Funct.* (2018) 9:4153–63. doi: 10.1039/C8FO00973B
24. Scott KP, Gratz SW, Sheridan PO, Flint HJ, Duncan SH. The influence of diet on the gut microbiota. *Pharmacol Res.* (2013) 69:52–60. doi: 10.1016/j.phrs.2012.10.020
25. David LA, Maurice CF, Carmody RN, Gootenberg DB, Button JE, Wolfe BE, et al. Diet rapidly and reproducibly alters the human gut microbiome. *Nature.* (2014) 505:559–63. doi: 10.1038/nature12820
26. Metges C. Contribution of microbial amino acids to amino acids homeostasis of the host. *J Nutr.* (2000) 130:1857–64S. doi: 10.1093/jn/130.7.1857S
27. Torrallardona D, Harris CI, Fuller MF. Pigs' gastrointestinal microflora provide them with essential amino acids. *J Nutr.* (2003) 133:1127–31. doi: 10.1093/jn/133.4.1127
28. Torrallardona D, Harris CI, Fuller MF. Lysine synthesized by the gastrointestinal microflora of pigs is absorbed, mostly in the small intestine. *AJP Endocrinol Metab.* (2003) 284:E1177–80. doi: 10.1152/ajpendo.00465.2002
29. Wu G. Amino acids: metabolism, functions, and nutrition. *Amino Acids.* (2009) 37:1–17. doi: 10.1007/s00726-009-0269-0

Conflict of Interest: The authors declare that the research was conducted in the absence of any commercial or financial relationships that could be construed as a potential conflict of interest.

frontiers in Nutrition

ORIGINAL RESEARCH
published: 28 December 2021
doi: 10.3389/fnut.2021.787055

Low Doses of Sucralose Alter Fecal Microbiota in High-Fat Diet-Induced Obese Rats

*Minchun Zhang†, Jie Chen†, Minglan Yang†, Cheng Qian, Yu Liu, Yicheng Qi, Rilu Feng, Mei Yang, Wei Liu and Jing Ma**

Department of Endocrinology and Metabolism, Renji Hospital, School of Medicine, Shanghai Jiao Tong University, Shanghai, China

Artificial sweeteners (AS) have been widely used as sugar substitutes to reduce calorie intake. However, it was reported that high doses of AS induced glucose intolerance via modulating gut microbiota. The objective of this study was to investigate the effects of lower doses of sucralose on fecal microbiota in obesity. Eight weeks after high-fat diet (HFD), the male Sprague Dawley rats were randomly divided into four groups (6 in each group) and administrated by a daily gavage of 2 ml normal saline (CON), 0.54 mM sucralose (N054), 0.78 mM sucralose (N078), and 324 mM sucrose (S324), respectively. After 4 weeks, fecal samples were obtained and analyzed by 16S ribosomal RNA gene sequencing. The richness and diversity of fecal microbiota were not changed by sucralose or sucrose. Both 0.54 mM (0.43 mg) and 0.78 mM (0.62 mg) sucralose tended to reduce the beneficial bacteria, *Lactobacillaceae* and *Akkermansiaceae.* The relative abundance of family *Acidaminoccaceae* and its genus *Phascolarctobacteriam* were increased after 0.54 mM sucralose. In functional prediction, 0.54 mM sucralose increased profiles of carbohydrate metabolism, whereas 0.78 mM sucralose enhanced those of amino acid metabolism. The lower doses of sucralose might alter the compositions of fecal microbiota. The effects of sucralose in different dosages should be considered in the future study.

Keywords: artificial sweeteners, sucralose, fecal microbiota, obesity, 16S ribosomal RNA gene analysis

OPEN ACCESS

Edited by:
Fengjiao Xin,
Institute of Food Science and Technology, Chinese Academy of Agricultural Science (CAAS), China

Reviewed by:
Isabelle Mack,
University of Tübingen, Germany
Jose Luiz de Brito Alves,
Federal University of Paraíba, Brazil

****Correspondence:***
Jing Ma
majing@renji.com

†These authors have contributed equally to this work

Specialty section:
This article was submitted to Nutrition and Microbes, a section of the journal Frontiers in Nutrition

Received: *30 September 2021*
Accepted: *01 December 2021*
Published: *28 December 2021*

Citation:
Zhang M, Chen J, Yang M, Qian C, Liu Y, Qi Y, Feng R, Yang M, Liu W and Ma J (2021) Low Doses of Sucralose Alter Fecal Microbiota in High-Fat Diet-Induced Obese Rats. Front. Nutr. 8:787055. doi: 10.3389/fnut.2021.787055

INTRODUCTION

Obesity has emerged as a major public health challenge affecting over 650 million adults worldwide. It increases the risks of type 2 diabetes, cardiovascular diseases, and even certain cancers (1). Table sugars contribute to the weight gain and thereby risks for metabolic disorders (2, 3). Therefore, artificial sweeteners (AS) are widely used as sugar substitutes to provide intensive sweet taste without extra calorie.

The US Food and Drug Administration (FDA) provided the acceptable daily intake (ADI) levels of 6 kinds of AS including saccharin, aspartame, acesulfame potassium (Ace-K), sucralose, neotame, and advantame (4). However, the effects of AS on glucose homeostasis remain controversial. Some studies demonstrated the benefits of AS exposure (5), whereas others showed that AS were associated with the incidence of obesity and type 2 diabetes (6–8).

The plausible mechanisms underlying the metabolic effects of AS are not fully understood. Given that most AS pass through the gastrointestinal tract without being absorbed or digested, they may directly alter the gut microbiota which plays crucial roles in the pathogenesis of metabolic diseases (9, 10). Suez et al. reported that saccharin in ADI dose (5 mg/kg body weight) induced glucose intolerance by modulating gut microbiota in mice and healthy subjects (11). The transplantation of saccharin-exposed feces induced glucose intolerance in germ-free mice (11). Another, it was indicated that administration of sucralose at dosages of 1.1–11 mg/kg reduced beneficial fecal bacteria and elevated fecal pH, intestinal p-glycoprotein, and cytochrome p-450 in rats (12). It should be noticed that the doses of AS in most studies were far beyond levels of daily consumption.

Sucralose is derived from sucrose with replacement of three hydrogen–oxygen groups by three chlorine atoms. In this process, the sweetness of sucralose is dramatically intensified to about 600 times of sucrose (13). About 85% of sucralose is excreted without being absorbed or digested in the gastrointestinal tract (13). Previous studies showed that a single dose of sucralose had no effects on blood glucose in health subjects (14) and patients with type 2 diabetes (15). However, it has been reported that sucralose exerted strong bacteriostatic effects *in vitro* and altered the structures of microbial communities in normal rodents (16). It remains unclear whether sucralose particularly in low doses can modulate the gut microbiota compared with natural sugars. We therefore aimed to evaluate the potential effects of different concentrations of sucralose and sucrose on fecal microbiota in high-fat diet (HFD)-induced obese rats.

MATERIALS AND METHODS

Animals

Male Sprague Dawley (SD) rats (4 weeks old) were fed with sterile food and water under specific pathogen-free (SPF) conditions with 12-h dark–light cycle, controlled temperature (20–23°C), and settled humidity (40–60%) (Laboratory Animal Resources, Chinese Academy of Sciences). After adapting to the environment for 1 week, the rats were fed with an *ad libitum* HFD (45% fat) or normal chow diet (NCD, 10% fat) correspondingly for 8 weeks. Rats on HFD weighed 20% more than those on the NCD group were considered as obesity. The protocol of this study was approved by the Institutional Animal Care and Use Committee of Shanghai Laboratory Animal Center, Chinese Academy of Sciences on January 8, 2018.

Abbreviations: ABC, ATP-binding cassette; Ace-K, Acesulfame potassium; ADI, Acceptable daily intake; ANOVA, Analysis of variance; AS, Artificial sweeteners; ATP, Adenosinetriphosphate; COMP, Component; CON, Control; DNA, Deoxyribonucleic acid; FDA, Food and Drug Administration; HFD, High-fat diet; KEGG, Kyoto Encyclopedia of Genes and Genomes; LDA, Linear discriminant analysis; LEfSe, Linear discriminant analysis effect size; OTU, Operational taxonomic units; PCoA, Principal coordinates analysis; PCR, Polymerase chain reaction; PERMANOVA, Permutational multivariate ANOVA; PICRUSt, Phylogenetic Investigation of Communities by Reconstruction of Unobserved States; PLS-DA, Partial least squares-discriminant analysis; RNA, Ribonucleic acid; SCFAs, Short-chain fatty acids; SD, Sprague Dawley; SPF, Specific pathogen-free.

Treatment

The 24 obese rats were randomly divided into 4 groups (6 in each group): normal saline (control group, CON), 0.54 mM sucralose (N054, Sigma-Aldrich, MO, USA), 0.78 mM sucralose (N078), and 324 mM sucrose (S324, Sigma-Aldrich, MO, USA). Rats were intragastric administrated with 2 ml certain solution at a fixed time every day for 4 weeks (17). The doses translated to human were 0.11 mg/kg (N054), 0.16 mg/kg (N078), and 56.20 mg/kg (S324) according to the body surface area (18).

Fecal Sample Collection

At the end of treatment, fecal samples were collected after 12-h fasting. Each rat was hold in hands and received abdominal massage until fresh pellets were collected in a 1.5-ml sterile freezing tube. The tubes were placed immediately in liquid nitrogen and moved to −80°C refrigerator.

DNA Extraction, PCR Amplification, and 16S rRNA Gene Sequencing

DNA extraction, PCR amplification, and 16S rRNA sequencing were performed as described in previous study (19). In short, total genomic DNAs of stool samples were extracted using the EZNA soil DNA Kit (Omega Bio-Tek, Norcross, GA, USA). Genes of the 16S rRNA V3–V4 regions were amplified by specific 338F and 806R primers with thermocycler polymerase chain reaction (PCR) system (GeneAmp 9700, ABI, USA). The extracted and purified amplicons were sequenced using Illumina MiSeq platform (Illumina, San Diego, USA).

Statistical Analyses

All data were included in the analysis. Bioinformatic analyses were performed by the Majorbio I-Sanger Cloud Platform (https://cloud.majorbio.com/) and SPSS Statistics v.23 software (IBM). Alpha diversity indices were applied to analyze the richness and diversity of samples, including Sobs, ACE, Chao1, Shannon, and Simpson. Unsupervised principal coordinates analysis (PCoA) and supervised partial least squares-discriminant analysis (PLS-DA) were performed to explore the similarities or dissimilarities of each sample. Permutational multivariate ANOVA (PERMANOVA) was calculated on the base of Bray–Curtis.

Differences in the relative abundance of taxa among groups were analyzed using the Kruskal–Wallis rank sum test with Tukey–Kramer *post-hoc* analysis. Correlation network according to Spearman's correlation analysis was used to determine the interactions of bacterial community. The linear discriminant analysis (LDA) effect size (LEfSe) algorithm differentiated microbial features for biomarker discovery. Only taxa with absolute LDA (log10) scores >2.0 and a p value of 0.05 were presented in this study. Metabolic functions were predicted using Phylogenetic Investigation of Communities by Reconstruction of Unobserved States (PICRUSt).

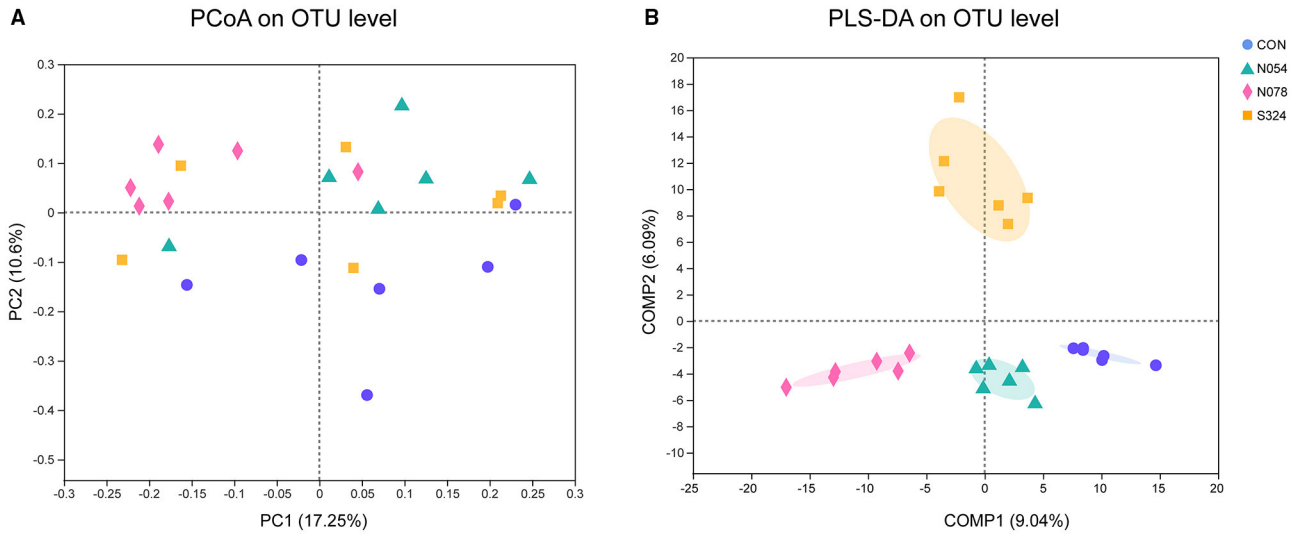

FIGURE 1 | Beta diversity analysis in four groups with unsupervised and classification methods. **(A)** Principal coordinates analysis (PCoA). Bray–Curtis distances and permutational multivariate analysis of variance (PERMANOVA) were performed. $p = 0.001$ and p adjust $= 0.001$. **(B)** Partial least squares discriminant analysis (PLS-DA). Each sample was represented by a dot ($n = 6$). CON, control group; N054, 0.54 mM sucralose; N078, 0.78 mM sucralose; S324, 324 mM sucrose.

RESULTS

Characteristics of Bacterial Diversity and Clustering

In the analysis of alpha diversity, neither sucralose nor sucrose altered the community richness (Sobs, ACE, Chao1 index) or diversity (Shannon, Simpson index) of fecal microbiota (**Supplementary Table S1**). The PCoA plot revealed that most samples treated by 0.78 mM sucralose clustered in a distinct group compared with CON, N054, and S324 groups (PERMANOVA, $p = 0.001$ and p adjust $= 0.001$). It was also confirmed by the supervised PLS-DA on OTU level. Each of the four groups showed a specific cluster (COMP1 9.04% and COMP2 6.09%), suggesting that they had different bacterial structures (**Figure 1**). The results of weighted unifrac and unweighted unifrac were similar to PCoA based on Bray–Curtis (**Supplementary Figures S1A,S1B**).

Alterations of Core Microbial Composition Induced by Sucralose and Sucrose

On phylum level, 0.54 mM sucralose increased the relative abundance of *Firmicutes* but decreased that of *Bacteroidetes*. 0.78 mM sucralose decreased the relative abundance of *Firmicutes* but increased that of *Bacteroidetes* (**Figures 2A,B**). The ratio of *Firmicutes* to *Bacteroidetes* in N054 was higher than that in N078 (**Supplementary Figure S2**). No differences were detected in the ratio of *Bacteroidetes* to *Proteobacteria*. Notably, both 0.54 and 0.78 mM sucralose reduced the relative abundance of *Verrucomicrobia*.

To describe the alterations of bacterial communities, the relative abundance of families was detected (**Figures 2C,D**). The beneficial bacteria, *Lactobacillaceae* and *Akkermansiaceae,* tended to be lower in both 0.54 and 0.78 mM sucralose, compared with control and sucrose groups (**Figure 2D**). These concentrations of sucralose increased the relative abundance of *Barnesiellaceae*, whereas they decreased that of *Streptococcaceae*. Sucralose and sucrose consistently upregulated *Christensenellaceae* and downregulated *Micrococcaceae* and *Eubacteriaceae*. 0.54 mM sucralose significantly reduced the relative abundance of *Muribaculaceae* but increased that of *Acidaminococcaceae*. LEfSe analysis showed that genus *Phascolarctobacterium*, belonged to the family *Acidaminococcaceae,* was enriched in N054 group. Family *Muribaculaceae* (S24-7) was enriched in N078 group (**Figure 3**) and it was negatively correlated with the change of body weight (**Supplementary Figure S3**). The family *Akkermansiaceae* and genus *Akkermansia* of *Verrucomicrobia* phylum were significantly enriched in S324 group (**Figure 3**).

In the network graph of interacting families in N054 group (**Supplementary Figure S4**), *Akkermansiaceae* was positively correlated with *Christensenellaceae*, *Barnesiellaceae*, *Veillonellaceae,* and *norank Gastranaerophilales* and it had a negative correlation with *Acidaminococcaceae*. The most abundant family *Muribaculaceae* had a positive interaction with *Bifidobacteriaceae* and negative interactions with *Deferribacteraceae* and *Burkholderiaceae*.

Effects of Predicted Metabolic Functions of Fecal Microbiota

PICRUSt and LEfSe were used to determine the changes in predicted functional composition (**Figure 4**). At KEGG level 3, ATP-binding cassette (ABC) transporters and the carbohydrate metabolism were enhanced by N054 group. The exposure of 0.78 mM sucralose increased the functional profiles related to metabolism including amino acid-related enzymes, energy metabolism, alanine, aspartate and glutamate metabolism,

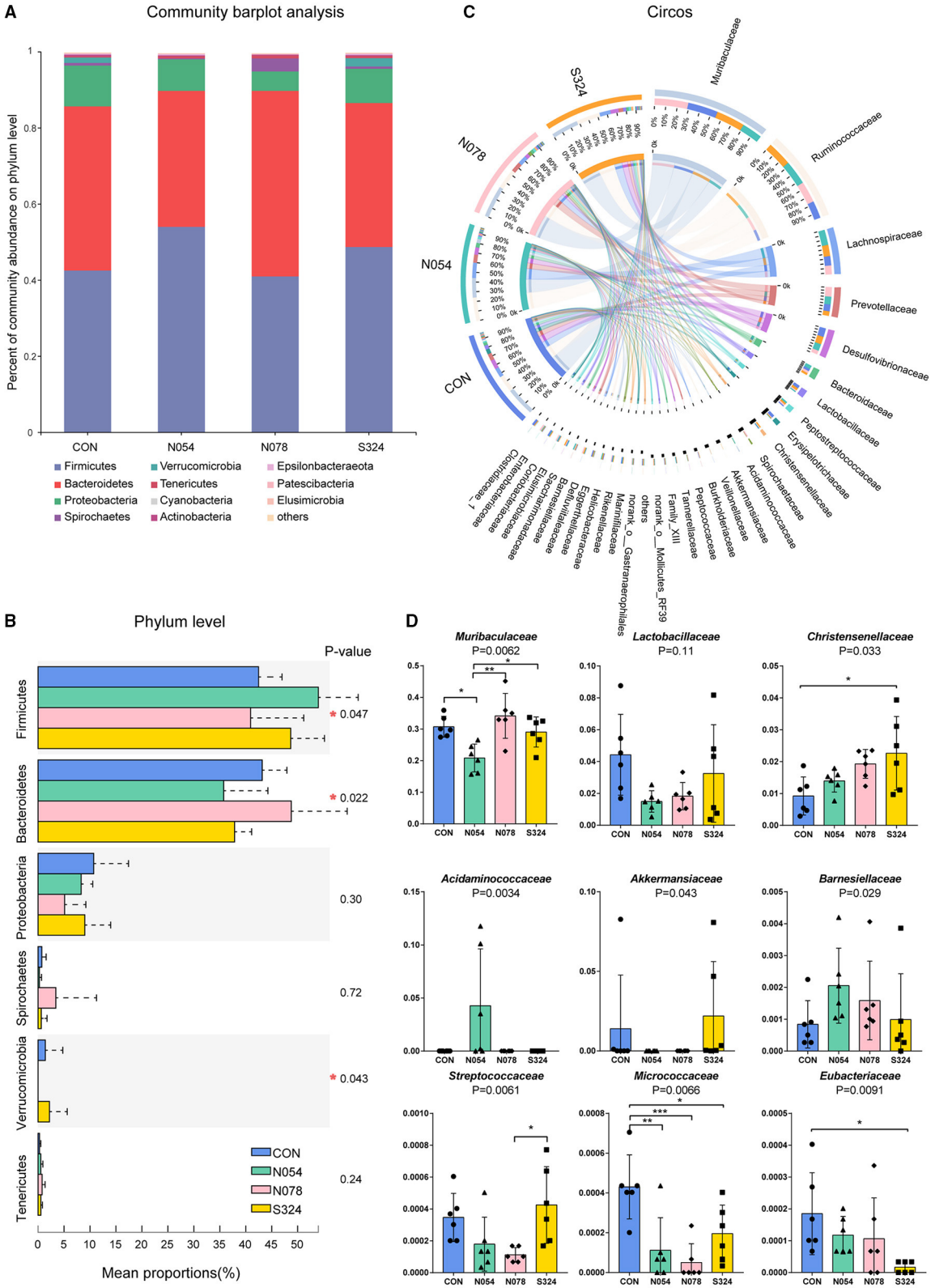

FIGURE 2 | Main bacterial communities of different taxonomies. **(A)** Community bar plot of the domain phyla. **(B)** Relative abundant of the domain phyla of four groups. **(C)** Circos plot showing the relationship between microbial families and samples. **(D)** Relative abundance of core bacterial families. Kruskal–Wallis rank sum test with Tukey–Kramer *post-hoc* analysis was performed ($n = 6$). Mean ± standard error. $^{*}p < 0.05$, $^{**}p \leq 0.01$, $^{***}p \leq 0.001$.

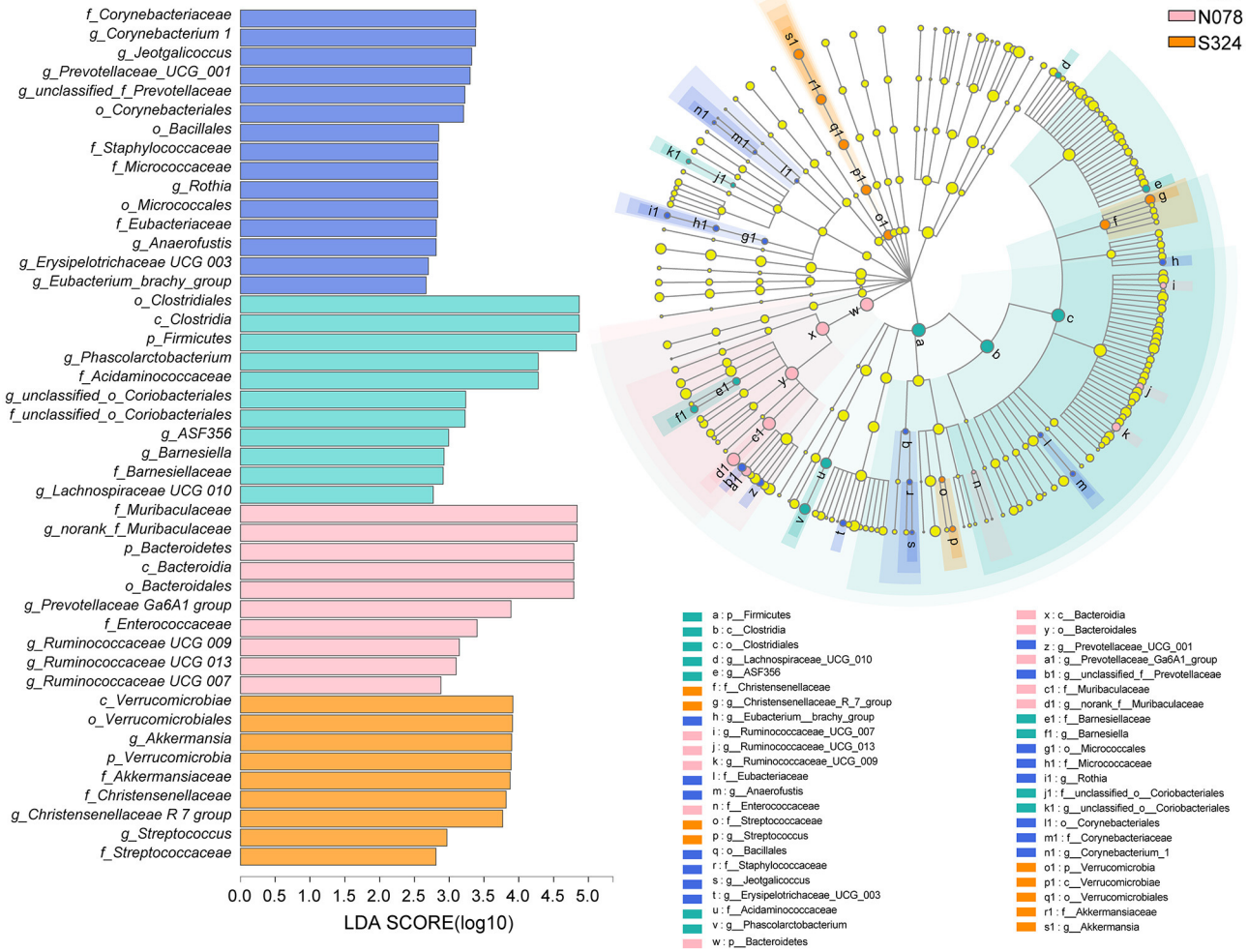

FIGURE 3 | LDA effect size (LEfSe) analysis based on genus level among four groups. **(A)** LEfSe bar plot demonstrating the significant bacterial differences. **(B)** Cladogram indicating the phylogenetic distribution of fecal microbiota with phyla in the outermost and genera in the innermost ring. Multiple comparison strategy was all-against-all ($n = 6$). Only LDA score >2.0 is shown.

pantothenate and CoA biosynthesis, and vitamin B6 metabolism. The biosynthesis of fatty acid was related to the 324 mM sucrose intervention.

DISCUSSION

In this study, we demonstrated 4-week low doses of sucralose (0.54 and 0.78 mM) altered the compositions and metabolic functions of fecal microbiota in obese rats. The richness and diversity of fecal microbiota were not changed by the sucralose and sucrose. Previous *in vitro* studies found that sucralose exerted bacteriostatic effects in a dose-dependent manner *via* inhibiting the invertase and sucrose permease of bacteria (16). However, sucralose did not reduce the overall richness and diversity of intestinal bacteria *in vivo* which was consistent with our results (16). It was probably due to the wide variety of microorganisms and their complex interactions with each other (20).

Beta diversity was used to explore the differences and similarities of microbial compositions among samples. Few studies investigated the impacts of AS on beta diversity. There was a study found that neotame changed the beta diversity after 4-week intervention on CD-1 mice (21). We presented that 0.54 mM (∼0.43 mg) and 0.78 mM (∼0.62 mg) sucralose groups had different clusters. It indicates that even the low doses of sucralose significantly altered the structures of fecal microbiota.

Firmicutes and *Bacteroidetes* were the two most abundant phyla, accounting for over 90% of the gut microbiota (22). We observed that 0.54 mM sucralose increased the relative abundance of *Firmicutes* and decreased that of *Bacteroidetes,* whereas 0.78 mM sucralose exerted the opposite effects. Notably, it was reported that sucralose did not alter the levels of

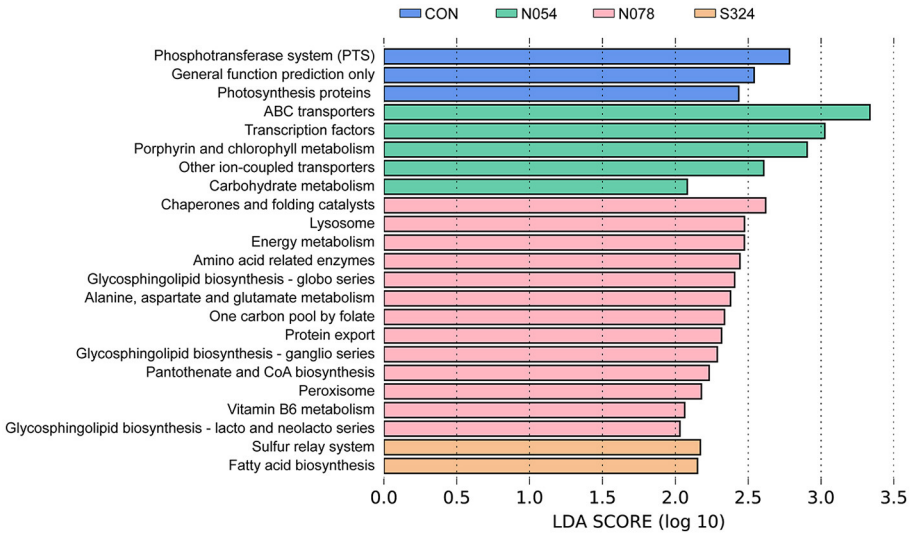

FIGURE 4 | LEfSe analysis on predictive functions of KEGG level 3 identified *via* PICRUSt. A Log LDA >2.0 was considered as significant difference. KEGG, Kyoto Encyclopedia of Genes and Genomes; PICRUSt, Phylogenetic Investigation of Communities by Reconstruction of Unobserved States.

Firmicutes nor *Bacteroidetes* in human (780 mg/d, 7 days) (23) nor mice studies (1.5 and 15 mg/kg body weight, 8 weeks) (24). Nevertheless, when sucralose was consumed with HFD simultaneously, there were obvious changes in *Firmicutes* and *Bacteroidetes.* A recent study also highlighted the intake of sucralose with carbohydrate impaired insulin sensitivity and glucose metabolism (25). Given the widely use of AS in obese patients, the interaction between AS and HFD warrants further study.

We presented that sucralose had no effects on phylum *Proteobacteria* level in HFD rats, which was consistent with the previous study (16). It was reported that *Proteobacteria* was elevated after the commercial sucralose (Splenda) dosage in a Crohn's disease model (SAMP mice) and the related control (AKR/J mice) (26). In fact, the higher level of *Proteobacteria* was closely related to inflammation, and it increased in the models of immune system dysfunction (27). Therefore, the effect of sucralose on *Proteobacteria* needs to be further clarified.

Our results highlighted that both 0.54 and 0.78 mM sucralose tended to reduce the relative abundance of beneficial bacteria *Lactobacillaceae* and *Akkermansiaceae,* which could improve metabolic symptoms via various mechanisms. Notably, *Lactobacillus* were reduced by 39.1% after a 12-week intervention of Splenda in healthy rats (12). The reduction of *Lactobacillus* was also confirmed in acesulfame potassium-treated mice (28). *Akkermansia Muciniphila,* a mucin-degrading bacterium, was lower in human or animal models with obesity and type 2 diabetes (29). Bian et al. observed that the abundance of *Akkermansia* was not changed during 3-month supplementation of sucralose but it was increased after further 3-month consumption in healthy mice (30). In our study, a 4-week administration with sucralose reduced *Akkermansiaceae* of obese rats. The underlying mechanisms are poorly understood. It is noteworthy that the osmolarities of solutions were different, which could mediate gastrointestinal motility directly and further affect community composition of intestinal flora (31). *Akkermansia* was decreased in anorexia nervosa after refeeding, the latter being accompanied by normal bowel movements (32). Although in our previous study, sucralose (0.4 mM nor 4 mM) had no effect on gastric emptying rate in healthy humans (14), its potential effects on gut microbiota are still unclear. Gastrointestinal tract transit times need to be investigated in future research.

In this study, sucralose at the dose of 0.78 mM increased family *Muribaculaceae* (S24-7), which was enriched in obesity-resistant mice (33). Sucralose and sucrose consistently upregulated *Christensenellaceae*, and the latter was inversely related to host body mass index (BMI) in several studies (34). Bian et al. showed the similar change after 6-month supplementation with sucralose into the drinking water (30). Another, *Eubacteriaceae, Barnesiellaceae*, *Streptococcaceae,* and *Micrococcaceae* were not closely correlated with metabolic disorder at present.

We demonstrated that the family *Acidaminoccaceae* was negatively associated with *Akkermansiaceae* in the network analysis. The genus *Phascolarctobacteriam*, belonging to family *Acidaminoccaceae,* was strongly correlated with metabolic dysfunction including weight gain and glucose intolerance (35). We found that *Phascolarctobacteriam* was enriched in the 0.54 mM sucralose group. *Phascolarctobacterium* could ferment carbohydrate and produced short-chain fatty acids such as acetate and propionate (36). It was consistent with our functional prediction that carbohydrate metabolism was enhanced in 0.54 mM sucralose dosage.

In accordance with the changes in bacterial compositions, we provided evidence that sucralose in doses of 0.54 and 0.78 mM changed functional profiles of fecal microbiota related to the metabolism of carbohydrates and amino acids. Gut

microbial metabolite from daily diet was linking to the development of obesity and insulin resistance (37). Sucralose was previously showed to alter the metabolism of some amino acids and their derivatives (30). Additionally, Suez et al. (11) reported that the consumption of saccharin in ADI dosage increased the pathway genes related to glycosaminoglycan and other glycan. We presented that the dose of sucralose was an important factor to gut microbiota. Particularly, 0.54 mM sucralose (∼2.2% of FDA ADI dosage) enhanced the ABC transporters and carbohydrate metabolism, whereas the exposure of 0.78 mM sucralose (∼3.2% of ADI dosage) was more related to the amino acid metabolism. We previously indicated that 0.78 mM instead of 0.54 mM sucralose lowered the blood glucose level of HFD-induced obese rats (17). It should be noticed that the different effects of these sucralose dosages on gut microbiota might be partly responsible for the distinct energy metabolism. Thus, AS might have complex effects on fecal microbiota, taste receptors, and gut hormone secretion.

There are some limitations that should be considered. First, this study focused on the obesity condition, and the fecal microbiota of the rats with NCD were not detected. Second, the use of 16S rRNA gene sequencing rather than metagenomic sequencing limited the detection of bacterial taxonomy and functions. Nonetheless, we preliminary observed the changes in compositions and predicted functions caused by sucralose and sucrose. The different strains and the potential mechanisms should be further explored *in vitro* and *in vivo*. Finally, given glucose homeostasis was maintained by multiple organs, the weak connection of biochemical variables and fecal microbiota is also a limitation of this study.

In conclusion, our study demonstrated that 4-week dosages of sucralose (0.54 and 0.78 mM) changed the compositions of fecal microbiota in HFD-induced obese rats. Lower doses of sucralose (0.54 and 0.78 mM) tended to reduce the beneficial bacteria, *Lactobacillaceae* and *Akkermansiaceae*. Furthermore, 0.54 mM sucralose increased the predictive functions of carbohydrates and the consumption of 0.78 mM sucralose was related to amino acid metabolism. The effects of sucralose on energy metabolism might vary with dosages and intervention period. The metabolic effects of sucralose in different dosages should be considered in the future study.

DATA AVAILABILITY STATEMENT

The datasets presented in this study can be found in online repositories. The names of the repository/repositories and accession number(s) can be found below: NCBI [accession: PRJNA773931].

ETHICS STATEMENT

The animal study was reviewed and approved by Ethics Committee of Renji Hospital Affiliated to Shanghai Jiaotong University.

AUTHOR CONTRIBUTIONS

MZ did the data analysis and prepared the manuscript. JC wrote the manuscript. MiY collected the samples and did the fecal DNA extraction. CQ, YL, YQ, and RF performed the animal experiments. MeY checked the data analysis. WL contributed to the study design. JM was the guarantor of this study to ensure the accuracy and integrity of the data. All authors contributed to the article and approved the submitted version.

FUNDING

This study was supported by the Shanghai Pujiang Program (2019PJD027), Shanghai Medicine and Health Development Foundation (SHMHDF, DMRFP_I_06), Shanghai Municipal Education Commission—Gaofeng Clinical Medicine Grant Support (20181807), 2019 management and construction project of hospital (CHDI-2019-A-01), and the National Natural Science Foundation of China (81800747).

SUPPLEMENTARY MATERIAL

The Supplementary Material for this article can be found online at: https://www.frontiersin.org/articles/10.3389/fnut.2021.787055/full#supplementary-material

Supplementary Figure S1 | PCoA. **(A)** Weighted unifrac. **(B)** Weighted unifrac. Each sample was represented by a dot ($n = 6$). CON, control group; N054, 0.54 mM sucralose; N078, 0.78 mM sucralose; S324, 324 mM sucrose.

Supplementary Figure S2 | Ratio of the domain phyla and body weight of rats. **(A)** Ratio of *Firmicutes* to *Bacteroidetes*. **(B)** Ratio of *Bacteroidetes* to *Proteobacteria*. Kruskal–Wallis rank sum test ($n = 6$). **(C)** Body weight before and after diet-induced obesity. NCD, normal chow diet; HFD, high-fat diet. **(D)** Body weight of rats during treatment period. Mean ± standard error of mean.

Supplementary Figure S3 | Correlation heatmap of fecal microbiota with biochemical variables. Spearman correlation analysis between the top 30 most abundant bacterial families and biochemical variables related to glucose homeostasis. GLP-1, glucagon-like peptide-1; GIP, gastric inhibitory peptide; AUC, area under curve during intragastric glucose tolerance test; HOMA-IR, homeostatic model assessment for insulin resistance (HOMA-IR). $^*p < 0.05$.

Supplementary Figure S4 | Network analysis of the top 50 abundant families in 0.54 mM sucralose group. Spearman's correlation analysis was used and a connection between two nodes stands for significant ($p \geq 0.5$ and $p < 0.5$). The red color means positive correlation and green means negative correlation.

Supplementary Table S1 | Alpha diversity of fecal microbiota in four groups.

REFERENCES

1. Calle EE, Kaaks R. Overweight, obesity and cancer: epidemiological evidence and proposed mechanisms. *Nat Rev Cancer*. (2004) 4:579–91. doi: 10.1038/nrc1408
2. Malik VS, Popkin BM, Bray GA, Despres JP, Hu FB. Sugar-sweetened beverages, obesity, type 2 diabetes mellitus, and cardiovascular disease risk. *Circulation*. (2010) 121:1356–64. doi: 10.1161/CIRCULATIONAHA.109.876185
3. Vos MB, Kaar JL, Welsh JA, Van Horn LV, Feig DI, Anderson CAM, et al. Added sugars and cardiovascular disease risk in children: a scientific statement from the American Heart Association. *Circulation*. (2017) 135:e1017–34. doi: 10.1161/CIR.0000000000000439

4. Rother KI, Conway EM, Sylvetsky AC. How non-nutritive sweeteners influence hormones and health. *Trends Endocrinol Metab*. (2018) 29:455–67. doi: 10.1016/j.tem.2018.04.010
5. Johnson RK, Lichtenstein AH, Anderson CAM, Carson JA, Després JP, Hu FB, et al. Low-calorie sweetened beverages and cardiometabolic health: a science advisory from the American Heart Association. *Circulation*. (2018) 138:e126–40. doi: 10.1161/CIR.0000000000000569
6. Imamura F, O'Connor L, Ye Z, Mursu J, Hayashino Y, Bhupathiraju SN, et al. Consumption of sugar sweetened beverages, artificially sweetened beverages, and fruit juice and incidence of type 2 diabetes: systematic review, meta-analysis, and estimation of population attributable fraction. *BMJ*. (2015) 351:h3576. doi: 10.1136/bmj.h3576
7. Swithers SE. Artificial sweeteners produce the counterintuitive effect of inducing metabolic derangements. *Trends Endocrinol Metab*. (2013) 24:431–41. doi: 10.1016/j.tem.2013.05.005
8. Gardener H, Elkind MSV. Artificial sweeteners, real risks. *Stroke*. (2019) 50:549–51. doi: 10.1161/STROKEAHA.119.024456
9. Greenhill C. Gut microbiota: not so sweet–artificial sweeteners can cause glucose intolerance by affecting the gut microbiota. *Nat Rev Endocrinol*. (2014) 10:637. doi: 10.1038/nrendo.2014.167
10. Valdes AM, Walter J, Segal E, Spector TD. Role of the gut microbiota in nutrition and health. *BMJ*. (2018) 361:k2179. doi: 10.1136/bmj.k2179
11. Suez J, Korem T, Zeevi D, Zilberman-Schapira G, Thaiss CA, Maza O, et al. Artificial sweeteners induce glucose intolerance by altering the gut microbiota. *Nature*. (2014) 514:181–6. doi: 10.1038/nature13793
12. Abou-Donia MB, El-Masry EM, Abdel-Rahman AA, McLendon RE, Schiffman SS. Splenda alters gut microflora and increases intestinal p-glycoprotein and cytochrome p-450 in male rats. *J Toxicol Environ Health Part A*. (2008) 71:1415–29. doi: 10.1080/15287390802328630
13. AlDeeb OA, Mahgoub H, Foda NH. Sucralose. *Profiles Drug Subst Excip Relat Methodol*. (2013) 38:423–62. doi: 10.1016/B978-0-12-407691-4.00010-1
14. Ma J, Bellon M, Wishart JM, Young R, Blackshaw LA, Jones KL, et al. Effect of the artificial sweetener, sucralose, on gastric emptying and incretin hormone release in healthy subjects. *Am J Physiol Gastrointest Liver Physiol*. (2009) 296:G735–9. doi: 10.1152/ajpgi.90708.2008
15. Mezitis NH, Maggio CA, Koch P, Quddoos A, Allison DB, Pi-Sunyer FX. Glycemic effect of a single high oral dose of the novel sweetener sucralose in patients with diabetes. *Diab Care*. (1996) 19:1004–5. doi: 10.2337/diacare.19.9.1004
16. Wang QP, Browman D, Herzog H, Neely GG. Non-nutritive sweeteners possess a bacteriostatic effect and alter gut microbiota in mice. *PLoS ONE*. (2018) 13:e0199080. doi: 10.1371/journal.pone.0199080
17. Qian C, Qi Y, Feng R, Yang M, Zhang M, Liu W, et al. Sucralose can improve glucose tolerance and upregulate expression of sweet taste receptors and glucose transporters in an obese rat model. *Eur J Nutr*. (2020) 60:1809–17. doi: 10.1007/s00394-020-02375-1
18. Reagan-Shaw S, Nihal M, Ahmad N. Dose translation from animal to human studies revisited. *FASEB J*. (2008) 22:659–61. doi: 10.1096/fj.07-9574LSF
19. Zhang M, Feng R, Yang M, Qian C, Wang Z, Liu W, et al. Effects of metformin, acarbose, and sitagliptin monotherapy on gut microbiota in Zucker diabetic fatty rats. *BMJ Open Diab Res Care*. (2019) 7:e000717. doi: 10.1136/bmjdrc-2019-000717
20. Tremaroli V, Bäckhed F. Functional interactions between the gut microbiota and host metabolism. *Nature*. (2012) 489:242–9. doi: 10.1038/nature11552
21. Chi L, Bian X, Gao B, Tu P, Lai Y, Ru H, et al. Effects of the artificial sweetener neotame on the gut microbiome and fecal metabolites in mice. *Molecules*. (2018) 23:367. doi: 10.3390/molecules23020367
22. Qin J, Li R, Raes J, Arumugam M, Burgdorf KS, Manichanh C, et al. A human gut microbial gene catalogue established by metagenomic sequencing. *Nature*. (2010) 464:59–65. doi: 10.1038/nature08821
23. Thomson P, Santibanez R, Aguirre C, Galgani JE, Garrido D. Short-term impact of sucralose consumption on the metabolic response and gut microbiome of healthy adults. *Br J Nutr*. (2019) 122:856–62. doi: 10.1017/S0007114519001570
24. Uebanso T, Ohnishi A, Kitayama R, Yoshimoto A, Nakahashi M, Shimohata T, et al. Effects of low-dose non-caloric sweetener consumption on gut microbiota in mice. *Nutrients*. (2017) 9:560. doi: 10.3390/nu9060560
25. Dalenberg JR, Patel BP, Denis R, Veldhuizen MG, Nakamura Y, Vinke PC, et al. Short-term consumption of sucralose with, but not without, carbohydrate impairs neural and metabolic sensitivity to sugar in humans. *Cell Metab*. (2020) 31:493–502.e7. doi: 10.1016/j.cmet.2020.01.014
26. Rodriguez-Palacios A, Harding A, Menghini P, Himmelman C, Retuerto M, Nickerson KP, et al. The artificial sweetener splenda promotes gut proteobacteria, dysbiosis, and myeloperoxidase reactivity in Crohn's disease-like ileitis. *Inflamm Bowel Dis*. (2018) 24:1005–20. doi: 10.1093/ibd/izy060
27. Rizzatti G, Lopetuso LR, Gibiino G, Binda C, Gasbarrini A. Proteobacteria: a common factor in human diseases. *Biomed Res Int*. (2017) 2017:9351507. doi: 10.1155/2017/9351507
28. Bian X, Chi L, Gao B, Tu P, Ru H, Lu K. The artificial sweetener acesulfame potassium affects the gut microbiome and body weight gain in CD-1 mice. *PLoS ONE*. (2017) 12:e0178426. doi: 10.1371/journal.pone.0178426
29. Depommier C, Everard A, Druart C, Plovier H, Van Hul M, Vieira-Silva S, et al. Supplementation with Akkermansia muciniphila in overweight and obese human volunteers: a proof-of-concept exploratory study. *Nat Med*. (2019) 25:1096–103. doi: 10.1038/s41591-019-0495-2
30. Bian X, Chi L, Gao B, Tu P, Ru H, Lu K. Gut Microbiome response to sucralose and its potential role in inducing liver inflammation in mice. *Front Physiol*. (2017) 8:487. doi: 10.3389/fphys.2017.00487
31. Vandeputte D, Falony G, Vieira-Silva S, Tito RY, Joossens M, Raes J. Stool consistency is strongly associated with gut microbiota richness and composition, enterotypes and bacterial growth rates. *Gut*. (2016) 65:57–62. doi: 10.1136/gutjnl-2015-309618
32. Mack I, Cuntz U, Grämer C, Niedermaier S, Pohl C, Schwiertz A, et al. Weight gain in anorexia nervosa does not ameliorate the faecal microbiota, branched chain fatty acid profiles, and gastrointestinal complaints. *Sci Rep*. (2016) 6:26752. doi: 10.1038/srep26752
33. Cao W, Chin Y, Chen X, Mi Y, Xue C, Wang Y, et al. The role of gut microbiota in the resistance to obesity in mice fed a high fat diet. *Int J Food Sci Nutr*. (2020) 71:453–63. doi: 10.1080/09637486.2019.1686608
34. Waters JL, Ley RE. The human gut bacteria Christensenellaceae are widespread, heritable, and associated with health. *BMC Biol*. (2019) 17:83. doi: 10.1186/s12915-019-0699-4
35. Lecomte V, Kaakoush NO, Maloney CA, Raipuria M, Huinao KD, Mitchell HM, et al. Changes in gut microbiota in rats fed a high fat diet correlate with obesity-associated metabolic parameters. *PLoS ONE*. (2015) 10:e0126931. doi: 10.1371/journal.pone.0126931
36. Wu F, Guo X, Zhang J, Zhang M, Ou Z, Peng Y. Phascolarctobacterium faecium abundant colonization in human gastrointestinal tract. *Exp Ther Med*. (2017) 14:3122–6. doi: 10.3892/etm.2017.4878
37. Canfora EE, Meex RCR, Venema K, Blaak EE. Gut microbial metabolites in obesity, NAFLD and T2DM. *Nat Rev Endocrinol*. (2019) 15:261–73. doi: 10.1038/s41574-019-0156-z

Conflict of Interest: The authors declare that the research was conducted in the absence of any commercial or financial relationships that could be construed as a potential conflict of interest.

frontiers in Nutrition

ORIGINAL RESEARCH
published: 03 January 2022
doi: 10.3389/fnut.2021.783688

Early-Life Nutrition Interventions Improved Growth Performance and Intestinal Health via the Gut Microbiota in Piglets

Chengzeng Luo[1,2†], *Bing Xia*[1,3†], *Ruqing Zhong*[1*], *Dan Shen*[1], *Jiaheng Li*[1], *Liang Chen*[1] *and Hongfu Zhang*[1]

[1] State Key Laboratory of Animal Nutrition, Institute of Animal Science, Chinese Academy of Agricultural Sciences, Beijing, China, [2] College of Animal Science, Xinjiang Agricultural University, Urumqi, China, [3] College of Animal Science and Technology, Northwest A&F University, Xianyang, China

OPEN ACCESS

Edited by:
Fengjiao Xin,
Institute of Food Science and Technology, Chinese Academy of Agricultural Science (CAAS), China

Reviewed by:
Xin Wu,
Chinese Academy of Sciences (CAS), China
Md. Abul Kalam Azad,
Institute of Subtropical Agriculture, Chinese Academy of Sciences (CAS), China

***Correspondence:**
Ruqing Zhong
zhongruqing@caas.cn

[†] These authors have contributed equally to this work

Specialty section:
This article was submitted to Nutrition and Microbes, a section of the journal Frontiers in Nutrition

Received: 26 September 2021
Accepted: 29 November 2021
Published: 03 January 2022

Citation:
Luo C, Xia B, Zhong R, Shen D, Li J, Chen L and Zhang H (2022) Early-Life Nutrition Interventions Improved Growth Performance and Intestinal Health via the Gut Microbiota in Piglets. Front. Nutr. 8:783688. doi: 10.3389/fnut.2021.783688

Intestinal infections in piglets are the main causes of morbidity before and after weaning. Studies have not explored approaches for combining pre-weaning and post-weaning nutritional strategies to sustain optimal gut health. The current study thus sought to explore the effects of early-life nutrition interventions through administration of synthetic milk on growth performance and gut health in piglets from 3 to 30 days of age. Twelve sows were randomly allocated to control group (**CON**) and early-life nutrition interventions group (**ENI**). Piglets were fed with the same creep diet from 7 days of age *ad libitum.* Piglets in the ENI group were provided with additional synthetic milk from Day 3 to Day 30. The results showed that early-life nutrition interventions improved growth performance, liver weight, spleen weight, and reduced diarrhea rate of piglets after weaning ($P < 0.05$). Early-life nutrition interventions significantly upregulated expression of ZO-1, *Occludin*, *Claudin4*, *GALNT1*, *B3GNT6,* and *MUC2* in colonic mucosa at mRNA level ($P < 0.05$). Early-life nutrition interventions reduced activity of alkaline phosphatase (AKP) in serum and the content of lipopolysaccharides (LPS) in plasma ($P < 0.05$). The number of goblet cells and crypt depth of colon of piglets was significantly higher in piglets in the ENI group relative to that of piglets in the CON group ($P < 0.05$). The relative mRNA expression levels of *MCP-1*, *TNF-α*, *IL-1β,* and *IL-8,* and the protein expression levels of TNF-α, IL-6, and IL-8 in colonic mucosa of piglets in the ENI group were lower compared with those of piglets in the CON group ($P < 0.05$). Relative abundance of *Lactobacillus* in colonic chyme and mucosa of piglets in the ENI group was significantly higher relative to that of piglets in the CON group ($P < 0.05$). Correlation analysis indicated that abundance of *Lactobacillus* was positively correlated with the relative mRNA expression levels of *ZO-1*, *Claudin4,* and *GALNT1,* and it was negatively correlated with the level of *MCP-1* in colonic chyme and mucosa. In summary, the findings of this study showed that early-life nutrition interventions improved growth performance, colonic barrier, and reduced inflammation in the colon by modulating composition of gut microbiota in piglets. Early-life nutrition

intervention through supplemental synthetic milk is a feasible measure to improve the health and reduce the number of deaths of piglets.

Keywords: early-life nutrition interventions, growth performance, intestinal barrier, inflammatory cytokines, short-chain fatty acids (SCFAs), gut microbiota

INTRODUCTION

Stress is a major cause of death in piglets. Approximately 10 million piglets die each year due to stress all over the world (1). Piglets are subjected to a number of stressors, such as an abrupt separation from the sow, transportation and handling stress, social hierarchy stress, comingling with pigs from other litters, and a different physical environment (room, building, farm, and water supply) during pre- and post-weaning periods (2). Changes in food are also an important source of stress. Creep feed is often provided to piglets in swine industries to improve post-weaning growth performance of piglets and improve acclimatization of piglets to solid feed before weaning. The process of dietary gradual transition from sow milk to solid feed is an important stressor for piglets owing to the significant differences between creep feed and sow milk (3). Piglets are subjected to bear risk of viruses and pathogens from solid feed, resulting in intestinal diseases, especially diarrhea (3). Moreover, dietary transition often leads to disorder in digestive function, which in turn causes low growth performance (4). Notably, low-birth-weight piglets may die easier in the transition period (5).

Gut microbiome plays a fundamentally significant role in the health of the host (6). Increase in the abundance of beneficial intestinal microflora can reduce occurrence of stress caused by sudden dietary transition by reducing the frequency of diarrhea and intestinal inflammation in the host (7). Studies report that nutritional interventions can modulate the abundance of intestinal microbes, and reduce the risk of gastrointestinal infections (3). Early-life nutrition intervention in piglets has been widely explored in recent years. Several studies have explored effects of oral supplementation, including prebiotics and functional amino acids, for neonatal piglets and the findings show that these oral supplementations increase abundance and colonization of beneficial bacteria, and improve gut health of the host (8). For example, dietary supplementation with 1% amino acid blend improved intestinal functions, and reduced incidence of diarrhea in piglets (9). Moreover, yeast glycoprotein supplementation increases relative abundance of *Lactobacillus* in the colon of piglets (10). In addition, synthetic milk modulates mucosal immunology and abundance of microbiota in neonatal piglets (11). Notably, synthetic milk reduces the abundance of *Escherichia* and diarrhea frequency in piglets after weaning (7). Therefore, early-life nutritional intervention has significant potential in reducing the risk of gastrointestinal infections in piglets. Furthermore, it promotes growth performance in piglets (12). Tan et al. (13) reported that pigs with high-feed efficiency exhibit large numbers of beneficial bacteria in their gut.

Moreover, synthetic milk plays a nutritional role in piglets. Milk production in sows may not satisfy the demand of piglets when litters comprise more piglets relative to the number of productive sow teats. Therefore, some piglets face severe starvation stress during lactation which ultimately result in poor growth performance or even death (14). Piglets should thus be supplied with additional nutritional interventions to improve growth performance. A previous study reported that administration of synthetic milk increased body weight of weaning piglets by 18% (8). In addition, synthetic milk significantly reduces pre-weaning mortality (15). However, only a limited number of studies have explored effects of nutritional interventions on intestinal microbes and growth performance. Moreover, previous studies reported a wide variation in the timing of administration of the supplements, the category of piglets, the type of supplements, and supplementation dosage (3). Therefore, further studies should explore pre-weaning and post-weaning nutritional strategies that sustain optimal growth performance and intestinal health throughout the weaning process for piglets. The present study thus proposes the hypothesis: early-life nutrition interventions improve growth performance and intestinal health by modulating gut microbiota abundance in piglets. This study thus sought to explore the effects of early-life nutrition interventions on growth performance and gut health of piglets, through determination of body weight, diarrhea rate, weight of visceral organs, effect on intestinal barrier, expression levels of inflammatory cytokines in the colon, profiles of microbial metabolites, and colonic microbiota composition.

MATERIALS AND METHODS

Ethics Statement

All procedures in the current study including animal experiments and sample collection were approved by the Experimental Animal Welfare and Ethical Committee of the Institute of Animal Science, Chinese Academy of Agricultural Sciences (No. IAS2020-104).

Experimental Design

A total of 12 healthy sows (3–4 years old, 5th−6th parity) obtained from a commercial farm (Henan, China) along with their litters were assigned to two groups: the control group (**CON**) and the early-life nutrition intervention group (**ENI**). Each group comprised a total of 6 sows, and 11 piglets were selected from each litter. The piglets among the two groups had similar initial body weight (initial BW $= 1.73 \pm 0.03$ kg). All sows with suckling piglets were separately housed in closed farrowing pens and provided with similar commercial diets and water *ad libitum*. The environment of the pigpens was kept clean, ventilated, and regularly disinfected.

All piglets were fed with the same standard creep diet (**Table 1**) from 7 to 30 days of age. Newborn piglets in the CON group

TABLE 1 | Composition and nutrient levels of diets[a].

Ingredient composition, %	Diet CON
Corn	57.00
Full-fat soybean	6.00
Soybean meal	20.00
Fish meal	5.00
Dried whey	5.00
Soybean oil	1.00
CaHPO4	0.50
NaCl	0.30
Limestone	0.51
Choline chloride	0.09
Lysine HCl	0.40
Met	0.10
Thr	0.10
Glucose	1.50
Suger	1.50
Premix[b]	1.00
Nutrient levels, %	
DE (MJ/kg)	14.44
CP	20.68
Lys	1.18
Met	0.37
Total Ca	0.70
Total P	0.55

[a] *DE, digestible energy; CP, crude protein.*

[b] *The premix provided the following per kg of diets: VA: 18,000 IU; VD3: 4500 IU; VE 22.5 mg; VK3: 4.5 mg; VB1: 4.32 mg; VB2: 12 mg; VB6: 4.86 mg; VB12: 0.03 mg; nicotinamide: 41.58 mg; calcium pantothenate: 33.12 mg; folic acid: 1.764 mg; biotim: 0.48 mg; Cu: 20 mg; Fe: 140 mg; Zn: 140 mg; Mn: 40 mg; I: 0.5 mg; Se: 0.3 mg.*

The synthetic milk was added to the ENI group based on the standard creep diets. The proximate composition of the synthetic milk (% dry matter): crude protein, 19.50%; crude lipid, 17.50%; crude ash, 6.00%; crude fiber, 0.00%; calcium, 0.60%; phosphorus, 0.60%; potassium, 1.40%; sodium, 0.50%; Lys, 1.90%; Met+Cys, 0.95%; Thr, 1.00%; Trp, 0.32%.

were only fed with the standard creep diet. Newborn piglets in the ENI group were provided with additional synthetic milk, a supplementary for breast milk from Day 3 to Day 30 of age. All piglets were weaned on Day 21. Piglets in the ENI group were allowed free access to synthetic milk before 22 days of age, whereas the amount of synthetic milk was reduced from 22 to 30 days. Piglets were fed with synthetic milk through feeders. The synthetic milk and feeders were purchased from Libaowei Nutrition Technology Co., Ltd (Guangdong, China). Synthetic milk was treated with ultrahigh temperature methods. Details on the feeding mode and the nutritional constituents of the synthetic milk are presented in **Figure 1A** and **Table 1**, respectively. The living weight of all piglets was recorded on Day 3, 21 and Day 30 of age. Incidence of diarrhea of piglets was recorded every day during the experimental period and the diarrhea rate was calculated as follows: Diarrhea rate (%) = (the number of piglets with diarrhea × diarrhea days) / (total number of piglets × total observational days) × 100 (16).

Sample Collection

Four piglets randomly selected from each group were weighed at the end of the experiment (Day 30 of the pigs' age). Blood samples of 5 ml were collected from the anterior vena cava of the piglets. Blood samples were coagulated for 30 min, then serum was obtained by centrifugation at 3,000 g for 10 min at ambient temperature. Furthermore, plasma was collected using heparin as an anticoagulant, and the plasma sample was centrifuged for 10 min at 3,000 g. The piglets were euthanized under anesthesia after collection of blood samples. The length of the colon and the whole intestine was determined. Further, the weight of livers and spleen was determined. Samples of colonic chyme and mucosa were collected, immediately transferred to liquid nitrogen, and stored at −80°C for subsequent analysis. Colon tissue samples were fixed in Carnoy's solution.

Genes Expression Analysis

Total RNA was extracted using TRIzol reagent (Ambion, UT) from colonic mucosa samples. RNA integrity was by electrophoresis using 1.0% agarose gel. Nano Drop® ND-1000 spectrophotometer (Nano-Drop Technologies, Wilmington, DE) was used to determine quality of RNA. cDNA was synthesized from RNA using a reverse transcription kit. cDNA samples were stored at −20°C for quantitative real-time PCR (qRT-PCR). All primers were designed by the National Center for Biotechnology Information (NCBI). Primer sequences are presented in **Table 2**. Primers were purchased from Sangon Biotech (Shanghai, China). qRT-PCR assays were performed using TB Green Premix Ex Taq (TaKaRa, Kusatsu, Japan) at a final volume of 20 μL containing 10 μl of 2 × Top Green qPCR SuperMix (TransStart®, Beijing, China), and 7.8 μl of ddH_2O, 0.4 μl of each primer, 1 μl of diluted cDNA, and 0.4 μl of Passive Reference Dye (50×). x*ZO-1*, *Claudin4*, *Occludin*, *TNF-α*, *IL-1β*, *MCP-1*, *IL-8*, *GALNT1*, *B3GNT6*, *MUC2* mRNA expression levels were explored in colonic mucosa. Expression levels of the target genes were normalized to the housekeeping genes *β-actin* and *GAPDH* as endogenous controls. qRT-PCR reaction was programmed as follows: 94°C for 30 s, and followed by 40 cycles for 5 s at 94°C, 30 s at 60°C and 10 s at 72°C. Relative expression levels of all genes were determined using the $2^{-\Delta\Delta CT}$ method (17).

AKP, LPS, and ELISA

AKP activity in serum was determined using commercial reagent kits (Nanjing Jiancheng Bioengineering Institute, Nanjing, China). LPS level in plasma was determined using the commercially available Tachypleus amebocyte lysate kit (Chinese Horseshoe Crab Reagent Manufactory Co., Ltd, Xiamen, China) following the quantitative Chromogenic Limulus Amebocyte Lysate assay method.

Protein expression levels of IL-8, IL-6, and TNF-α proteins in the colonic mucosa were determined using ELISA assay kits (Invitrogen, Carlsbad, CA) according to the manufacturer's protocol. A microplate reader (BioTek-ELx808, BioTek Instruments, Inc., Texas) was used to read the protein bands.

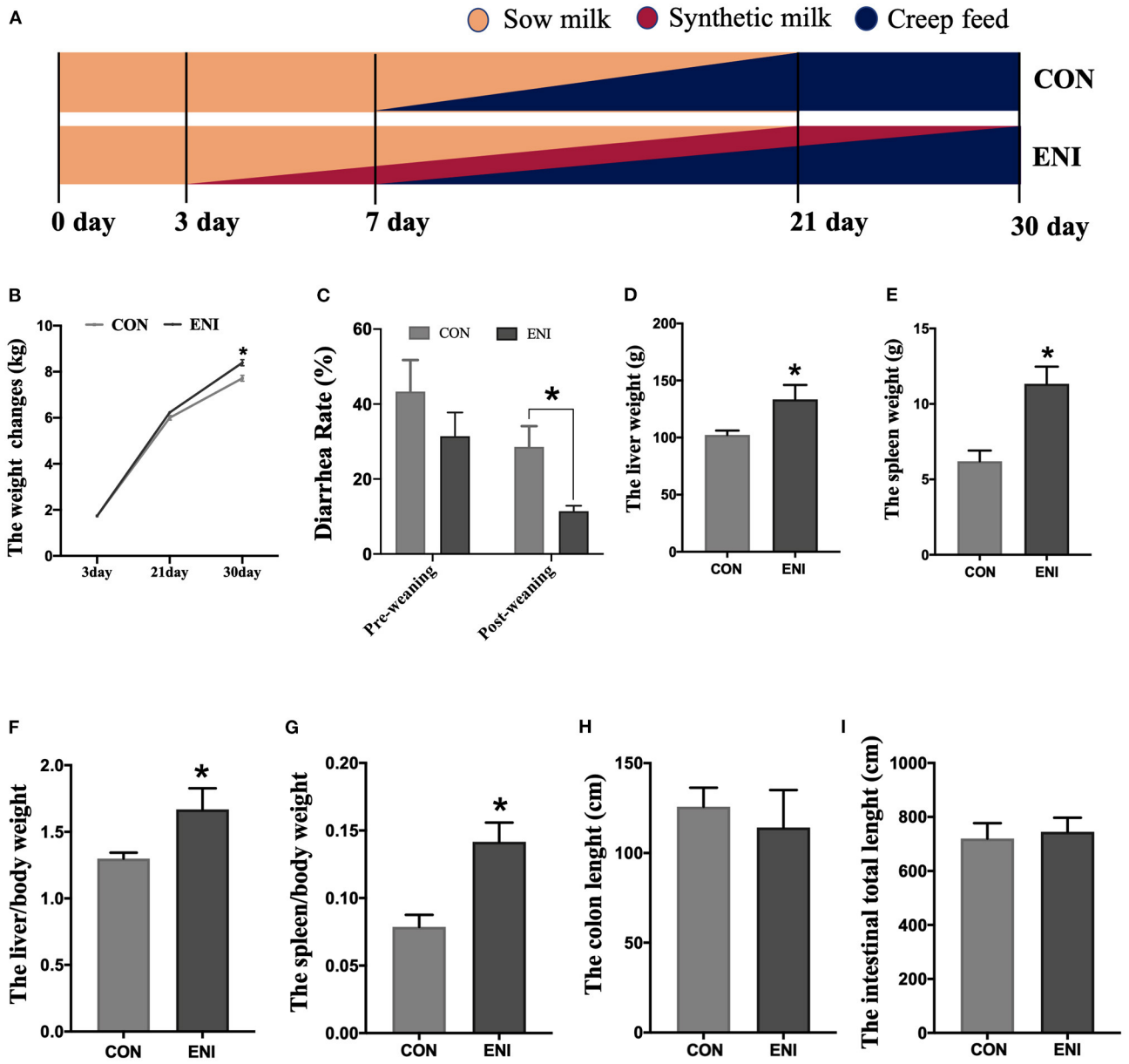

FIGURE 1 | Effects of early-life nutrition interventions on growth performance and visceral organs in piglets. CON, control group, ENI, early-life nutrition interventions group. **(A)** The feeding mode diagram. **(B)** The weight changes of piglets at 3, 21, and 30 days of age in each group. **(C)** The diarrhea rate of pre-weaning and post-weaning of piglets. **(D)** The liver weight of piglets in each group. **(E)** The spleen weight of piglets in each group. **(F)** The relative weights of liver to living body weight. **(G)** The relative weights of spleen to living body weight. **(H)** The length of colon in each group. **(I)** The length of whole intestine. Data are expressed as mean ± SEM ($n = 4$). The independent-samples t-test was used to compare data between two groups. $^*P < 0.05$.

Tissue Sample and Intestinal Morphology Analysis

Colon tissue was immersed and fixed with Carnoy's solution for 24 h. Colon samples were then removed from formalin and embedded in paraffin. Subsequently, the paraffin blocks were sectioned to obtain 5 μm thick sections using a semi-automatic microtome (LONGSHOU, China). Sections were stained with hematoxylin and eosin (H&E) stain (18), and viewed under an optical microscope. The crypt depth was determined following a method described by Wang et al. (19).

Further, 5 μm thick sections were obtained as described above and analyzed using the PAS-AB kit (Beijing Solarbio Technology Co., Ltd, Beijing, China) instructions. Sections were viewed under an optical microscope, and the amount of goblet cells was determined using a method reported by Cantero-Recasens et al. (20).

TABLE 2 | The nucleotide sequences of primer.

Target gene	Forward sequence (5′ - 3′)	Reverse sequence (5′ - 3′)
ZO-1	CTCCAGGCCCTTACCTTTCG	GGGGTAGGGGTCCTTCCTAT
Claudin4	CAACTGCGTGGATGATGAGA	CCAGGGGATTGTAGAAGTCG
Occludin	CAGGTGCACCCTCCAGATTG	TATGTCGTTGCTGGGTGCAT
TNF-α	TAAGGGCTGCCTTGGTTCAG	AGAGGTTCAGCGATGTAGCG
IL-1β	ATTCAGGGACCCTACCCTCTC	CTTCTCCACTGCCACGATGA
MCP1	AAACGGAGACTTGGGCACAT	GCAAGGACCCTTCCGTCATC
IL-8	TACGCATTCCACACCTTTC	GGCAGACCTCTTTTCCATT
GALNT1	GAGCCCAGTGATGGATGGAT	GGGAACACTTGGCCTTTCAG
B3GNT6	CTGGAGTGTTGTCCAGCCAT	AGCTAAGGAGCAGCGTCAAG
MUC2	CGCATGGATGGCTGTTTCTG	ATTGCTCGCAGTTGTTGGTG
GAPDH	GGGCATGAACCATGAGAAGT	GGGCATGAACCATGAGAAGT
β-actin	GCGTAGCATTTGCTGCATGA	GCGTGTGTGTAACTAGGGGT

Analysis of SCFAs Levels

Approximately 0.1 g of colonic chyme and mucosa samples were separately obtained from each sample. The samples were suspended in 1 mL of ddH_2O in 1.5-mL screw capped vials for analysis of concentration of SCFAs. Concentrations of SCFAs were determined by gas chromatography as described by Wu et al. (21).

DNA Extraction, 16S RRNA Gene Amplification, Sequencing and Analysis

Approximately 0.5–1 g of colonic chyme and colonic mucosa samples were separately obtained from each sample, and microbial community genomic DNA was extracted using E.Z.N.A.® soil DNA Kit (D5625-02, Omega Bio-Tek Inc., Norcross, GA) according to the manufacturer's instructions. Genomic DNA samples were stored at −80°C for subsequent analysis. Purity and DNA concentration were determined through 1% agarose gel electrophoresis and NanoDrop2000 spectrophotometer (Thermo Fisher Scientific, Waltham, MA), respectively. V3-V4 regions of bacterial 16S rRNA gene were amplified using the following primer set: 338F (5'-ACTCCTACGGGAGGCAGCAG-3') and 806R (5'-GGACTACHVGGGTWTCTAAT-3'). The reaction system was comprised of 4 μl of 5 × FastPfu Buffer, 2 μl of 2.5 mM dNTPs, 0.8 μl of each primer (5 μM), 0.4 μl of FastPfu polymerase and 10 μl of DNA template. The reactions were performed using GeneAmp® 9700 thermal cycler (Applied Biosystems, Foster City, CA). Amplification process was as follows: denaturation for 3 min at 95°C followed by 27 cycles of 95°C for 30 s, 55°C for 30 s, 72°C for 45 s, and a final extension of 10 min at 72°C. The amplified fragments were analyzed by electrophoresis on a 2% agarose gel. The products were then purified with AxyPrep DNA Gel Extraction Kit (Axygen Bioscience, CA) according to the manufacturer's instructions. Raw microbial sequence data were analyzed and processed at the Majorbio Bio-Pharm Technology Co. Ltd. (Shanghai, China). Sequences were analyzed and assigned to operational taxonomic units (OTUs; 97% identity). The alpha-diversity whose coverage is based on the Chao and Shannon index within each sample was determined by QIIME tool (Version 174 1.7.0) (22). Beta diversity was evaluated by computing the unweighted Unifrac distance and visualized using principal coordinates analysis (PCoA) plots. LDA effect size (LEfSe) was used to explore biomarkers that exhibited statistical differences. The datasets presented in this study were submitted to the NCBI Sequence Read Archive (SRA) database. The name of the repository and accession number is [PRJNA779481].

Statistical Analysis

Growth performance, organs weight, intestinal length and morphology, colonic permeability, mRNA expression, and concentrations of SCFAs data were subjected to analysis of variance using SPSS (23.0) software. Student's *t*-test was used to determine differences between two groups. The results were presented as means ± SEM. The relationships among the intestinal barrier, inflammatory cytokines, and bacterial species were explored using Pearson's correlation analysis and a correlation matrix was generated. Figures were generated using GraphPad 8.0 software. * was used to indicate a statistically significant difference ($P < 0.05$), and ** indicated a highly significant difference ($P < 0.01$). The *P* values ranging from 0.05 to 0.1 were also recorded.

RESULTS

Body Weight, Diarrhea Rate, and Organ Development in Piglets

The results showed that the body weight of piglets in both groups gradually increased from Day 3 to Day 30. The body weight of piglets in the ENI group was significantly higher relative to that of piglets in the CON group at the age of 30 ($P < 0.05$) (**Figure 1B**). Diarrhea rate of piglets in the ENI group was lower compared with the rate of piglets in the CON group, and the difference was statistically significant at the post-weaning stage ($P < 0.05$) (**Figure 1C**). Piglets in the ENI group had higher liver and spleen weight and higher relative weights of liver and spleen to living body weight compared with those of piglets in the control group ($P < 0.05$) (**Figures 1D–G**). The colon of piglets in the CON group was longer relative to that of piglets in the ENI

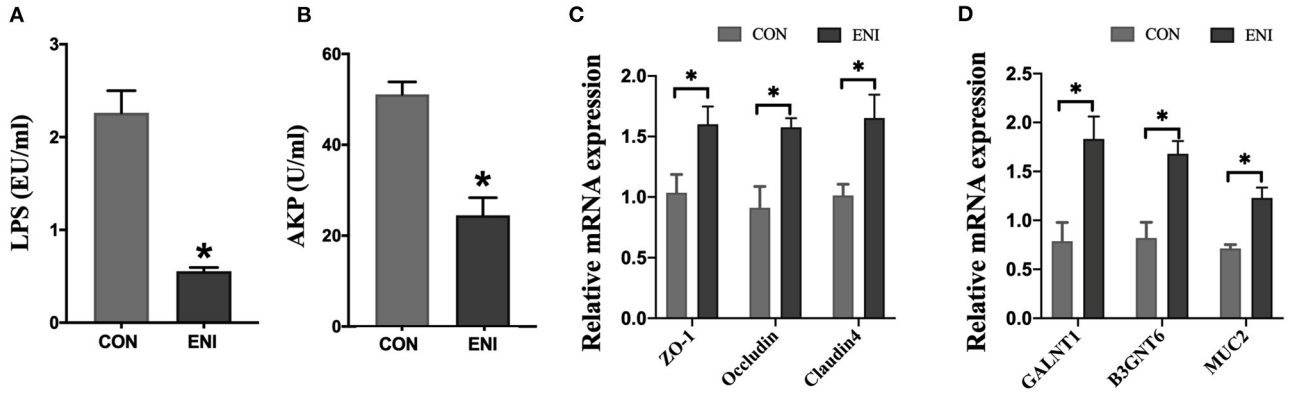

FIGURE 2 | Effects of early-life nutrition interventions on the intestinal barrier of the colon in piglets. CON, control group, ENI, early-life nutrition interventions group. **(A)** The content of LPS in plasma. **(B)** The activity of AKP in serum. **(C)** The mRNA expression levels of ZO-1, Occludin, and Claudin4 in the colon. **(D)** The mRNA expression levels of GALNT1, B3GNT6, and MUC2 in the colon. Data are expressed as mean ± SEM ($n = 4$). The independent-samples t-test was used to compare data between two groups. $^*P < 0.05$.

group, however, the differences were not statistically significant (**Figures 1H,I**).

Intestinal Morphology and Intestinal Barrier of Colonic Mucosa in Piglets

The results showed that the activity of AKP in serum and the level of LPS in plasma of piglets in the ENI group were significantly lower compared with those of piglets in the CON group ($P < 0.05$) (**Figures 2A,B**). The findings indicated that early-life nutrition intervention significantly upregulated expression of *ZO-1*, *Occludin*, *Claudin4*, *GALNT1*, *B3GNT6,* and *MUC2* genes in colonic mucosa at the mRNA level (**Figures 2C,D**).

Analysis of intestinal morphology did not show any noticeable pathologic changes in the two groups; however, the number of goblet cells and crypt depth of piglets was significantly higher in the ENI group compared with that of the CON group ($P < 0.05$) (**Figures 3A–C**).

Intestinal Inflammation in Colonic Mucosa of Piglets

Relative mRNA expression levels of MCP-1, TNF-α, IL-1β, and IL-8 in the ENI group were lower relative to those in the CON group, however, only the difference in relative mRNA expression level of MCP-1 was statistically significant ($P < 0.05$) (**Figure 4A**). Protein expression levels of inflammatory cytokines (TNF-α ($P = 0.066$), IL-6, and IL-8) in the colonic mucosa showed a similar trend as the relative mRNA expression levels of inflammatory cytokines (**Figure 4B**).

Concentrations of SCFAs in Colonic Mucosa and Chyme

Concentrations of acetic acid, propionic acid, isobutyric acid, butyric acid, and valeric acid in colonic mucosa and colonic chyme of piglets in the ENI group were higher relative to those of piglets in the CON group (**Figures 5A–D,F**), however, the differences were not statistically significant. Concentration of isovaleric acid in colonic chyme of piglets in the ENI group was lower compared with that of piglets in the CON group, however, the difference was not statistically significant (**Figure 5E**).

Composition of Gut Microbes in Colonic Chyme and Mucosa Samples From Piglets

Fresh colonic chyme and colonic mucosa were obtained from piglets, and 16 s rRNA gene sequencing analysis was performed to explore the effects of early-life nutrition interventions on the structures and composition of the gut microbiota. The findings showed no significant difference in Chao index and Shannon index in colonic mucosa between the two group (**Figures 6C,D**). However, Chao index and Shannon index in colonic chyme of piglets in the CON group were higher compared with those of piglets in the ENI group ($P < 0.05$) (**Figures 6A,B**). PCoA analysis showed significant differences in phylum and genus composition between ENI and CON groups (**Figures 6E–H**).

Microbial community composition at the phylum and genus level of the two groups is presented in **Figures 7A,B,E,F**. The results showed that colonic chyme samples comprised 6 major phyla including *Firmicutes, Actinobacteria, Bacteroidota, Proteobacteria, Spirochaetota,* and *Campilobacterota* (**Figure 7A**). The findings showed that colonic mucosa samples mainly comprised *Desulfobacterota, Deferribacterota, Firmicutes, Actinobacteria, Bacteroidota, Proteobacteria, Spirochaetota,* and *Campilobacterota* at the phylum level **(Figure 7E)**. The proportion of *Firmicutes* in colonic chyme was higher in the ENI group compared with that in the CON group, whereas the proportion of *Bacteroidota* in colonic chyme was higher in the CON group relative to that in the ENI group ($P < 0.05$) **(Figure 7C)**. Notably, the proportion of the top 6 bacteria in colonic mucosa was not significantly different between the two groups **(Figure 7G)**.

Composition of the gut microbiota in the colonic chyme and colonic mucosa was further analyzed at the genus level. The proportion of *Catenibacterium* in colonic chyme was significantly

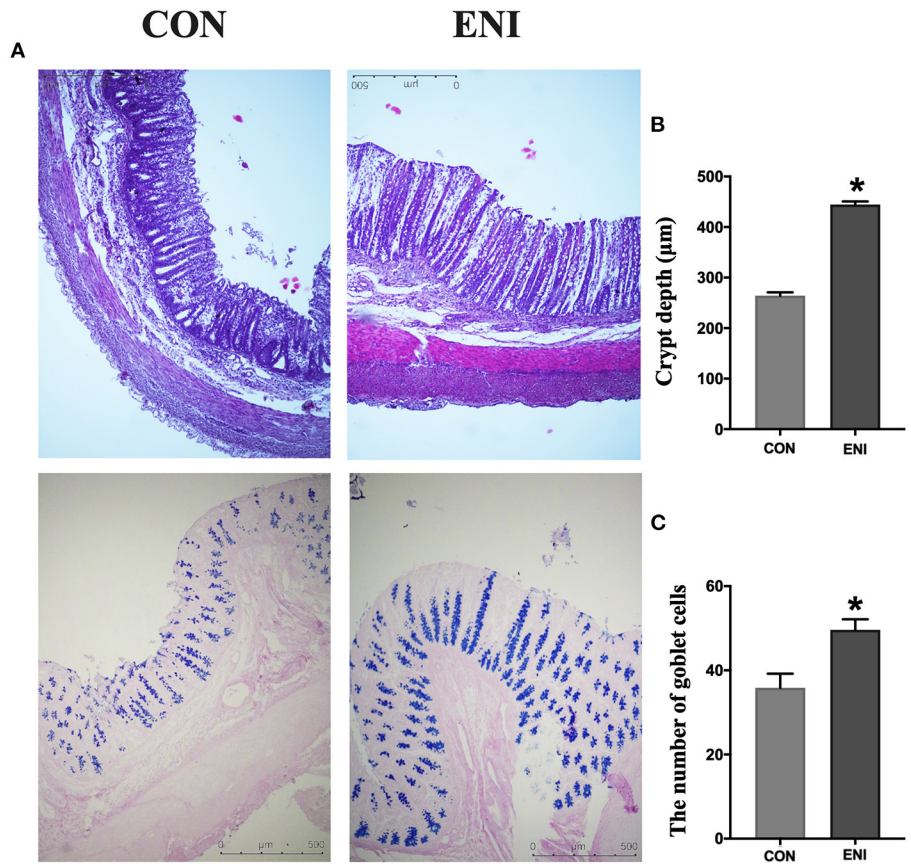

FIGURE 3 | Effects of early-life nutrition interventions on the morphology of the colon and the number of goblet cells. CON, control group, ENI, early-life nutrition interventions group. **(A)**. HE and PAS staining of colon tissue. **(B)** The crypt depth of the colon. **(C)** The number of goblet cells of the colon. Data are expressed as mean ± SEM ($n = 4$). The independent-samples t-test was used to compare data between two groups. *$P < 0.05$.

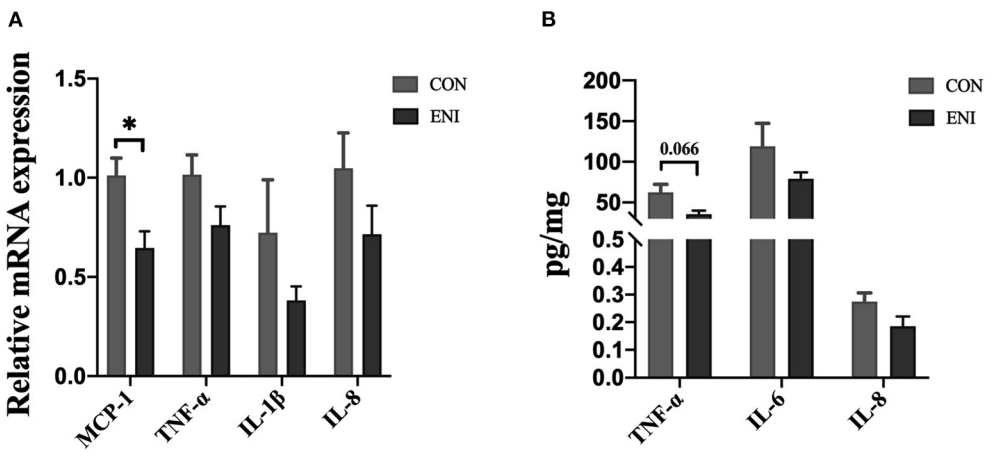

FIGURE 4 | Effects of early-life nutrition interventions on inflammation in the piglet colon. CON, control group, ENI, early-life nutrition interventions group. **(A)** The mRNA expression levels of MCP-1, TNF-α, IL-1β, and IL-8 in colon. **(B)** The protein expression levels of TNF-α, IL-6, and IL-8 in piglets. Data are expressed as mean ± SEM ($n = 4$). The independent-samples *t*-test was used to compare data between two groups. *$P < 0.05$.

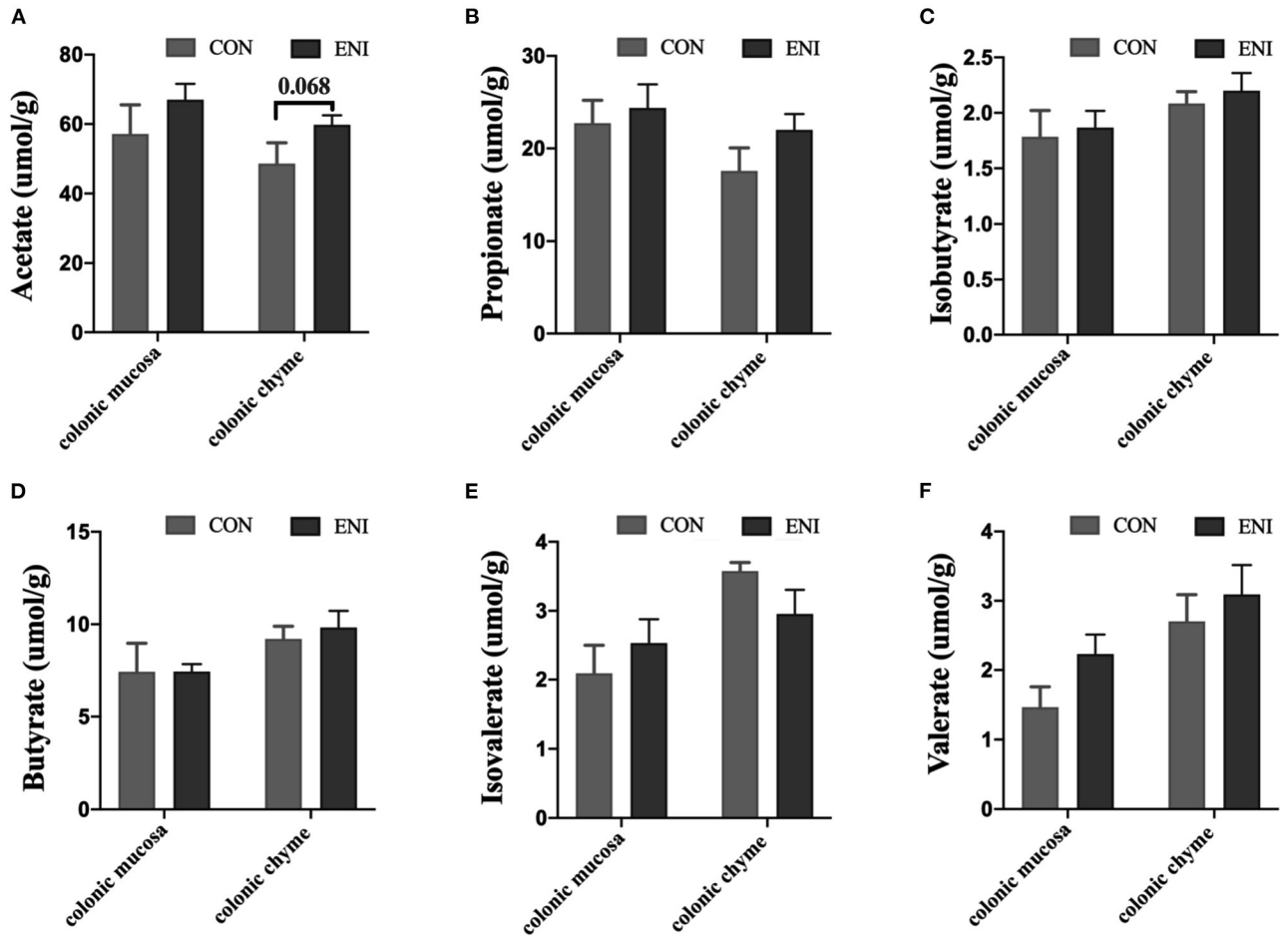

FIGURE 5 | Effects of early-life nutrition interventions on concentrations of SCFAs in the colonic mucosa and colonic chyme. CON, control group, ENI, early-life nutrition interventions group. **(A)** Acetate acid. **(B)** Propionic acid. **(C)** Isobutyric acid. **(D)** Butyric acid. **(E)** Isovaleric acid. **(F)** Valeric acid. Data are expressed as mean ± SEM ($n = 4$). The independent-samples t-test was used to compare data between two groups. $^*P < 0.05$.

higher in the ENI group ($P < 0.05$), whereas the proportion of *norank-f-Muribaculaceae* in colonic chyme was lower in the ENI group compared with that of the CON group ($P < 0.05$) **(Figure 7D)** The proportion of the top 10 bacteria in colonic mucosa was not significantly different between the two groups **(Figure 7H)**. LEfSe analysis was performed and presented as LDA score ≥2.0 to further explore the differences in microbiota composition between the two groups. The results showed that 61 biomarkers (blue bar) were enriched in colonic chyme in the CON group compared with the levels in the ENI group. Notably, LEfSe analysis showed that only 5 biomarkers (red bar) were enriched in colonic chyme of the ENI group, including *Lachnospiraceae, Lachnospirales, Firmicutes, Lactobacillaceae,* and *Lactobacillus* **(Figure 8A)**. Analysis of colonic mucosa showed a total of 23 biomarkers in the CON and ENI groups. The results showed that piglets in the ENI group had a higher composition of microbiota compared with that in the CON group **(Figure 8B)**. Notably, *Lactobacillus* was enriched in colonic mucosa and chyme.

Relationship Among Intestinal Microbiota, Intestinal Barrier and Immune-Related Indexes

The potential association among intestinal microbiota, intestinal barrier, and immune-related indexes in colonic chyme and mucosa was explored. The results showed that the proportion of *Lactobacillus* in colonic chyme was negatively correlated with the relative mRNA expression level of *MCP-1 and* was positively correlated with the relative mRNA expression levels of *ZO-1*, *Claudin4,* and *GALNT1* **(Figure 9A)**. The proportion of *Escherichia-Shigella* was positively correlated with the relative mRNA expression level of *IL-8*. Moreover, proportions of *Parabacteroides* and *Actinobacillus* were positively correlated with the relative mRNA expression level of *IL-1β*, whereas the proportion of *Clostridium-sensu-stricto-6* was negatively correlated with the relative mRNA expression levels of *ZO-1* and *Occludin*.

Correlation analysis of the intestinal microbiota, intestinal barrier, and immune-related indexes in colonic mucosa showed

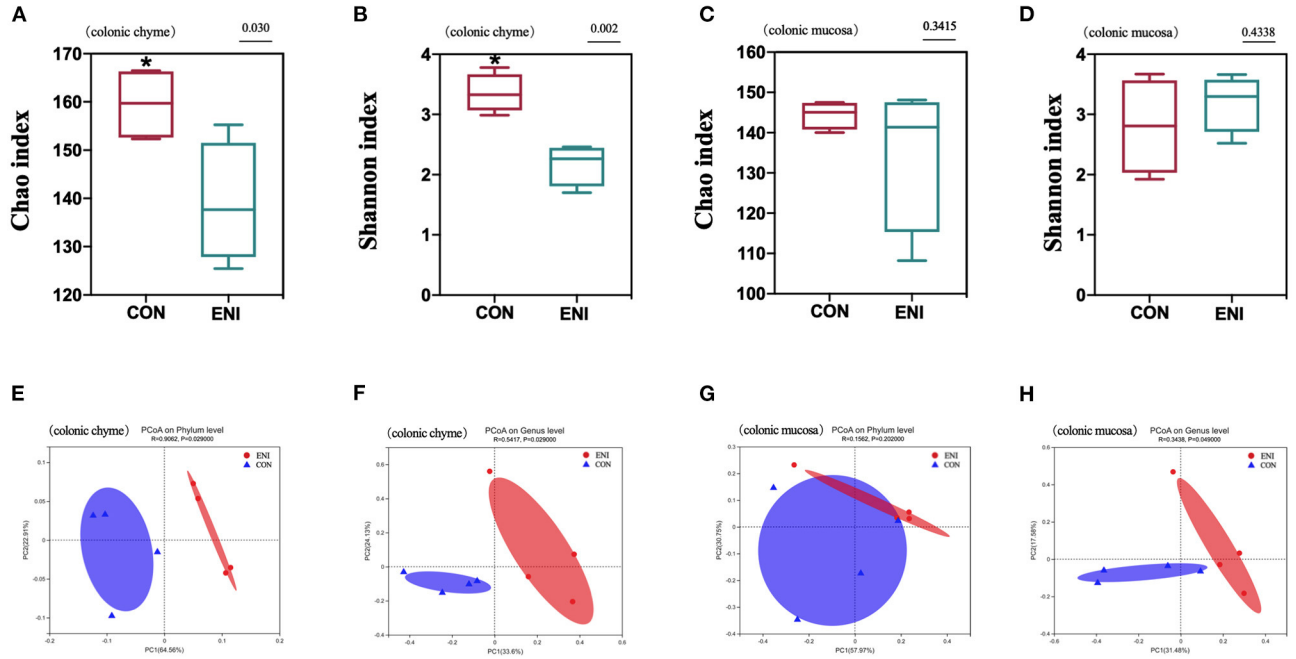

FIGURE 6 | The analysis of gut microbiota diversity in the colonic chyme and colonic mucosa of piglets. CON, control group, ENI, early-life nutrition interventions group. **(A)** The Chao index of microbiota in colonic chyme. **(B)** The Shannon index of microbiota in colonic chyme. **(C)** The Chao index of microbiota in colonic mucosa. **(D)** The Shannon index of microbiota in colonic mucosa. **(E)** PCoA analysis of microbiota in colonic chyme at the phylum level. **(F)** PCoA analysis of microbiota in colonic chyme at the genus level. **(G)** PCoA analysis of microbiota in colonic mucosa at the phylum level. **(H)** PCoA analysis of microbiota in colonic mucosa at the genus level. Data are expressed as mean ± SEM ($n = 4$). The independent-samples *t*-test was used to compare data between two groups. $^*P < 0.05$.

similar results to those of colonic chyme (**Figure 9B**). The results showed that the proportion of *Lactobacillus* was negatively correlated with the relative mRNA expression level of *MCP-1*, and was positively correlated with the relative mRNA expression levels of *ZO-1*, *Claudin4,* and *GALNT1*. The proportion of *Escherichia-Shigella* was positively correlated with the relative mRNA expression levels of *IL-8*. The proportion of *Parabacteroides* was positively correlated with the relative mRNA expression level of *IL-1β* (**Figure 10**).

DISCUSSION

Previous studies report that dietary changes can alter the composition of gut microbes in suckling piglets and these changes can be adjusted by early-life nutrition interventions (3, 23). For example, Sugiharto et al. (11) reported that provision of synthetic milk to suckling piglets improved the gut microbiome composition, as well as increased concentration of SCFAs in the colon. Similar findings were observed in the present study. The proportion of *Firmicutes* and *Bacteroidetes* was significantly different between the ENI and CON groups. Studies report that change in microbiota composition is significantly associated with diet composition. A diet rich in protein and fat increases the ratio of *Firmicutes* to *Bacteroides* in the intestines of animals or humans (24). The synthetic milk used in the current study contained high crude protein and crude fat content, which may be an important reason for the increase in *Firmicutes* proportion in the intestine and a decrease in *Bacteroides* proportion. Most previous studies mainly focused on microbiota composition in chyme and fecal samples, and only a few studies explored the composition of mucosa-associated microbiota (25). Changes in mucosa-associated microbiota may have significant effects on host growth and development (25). Therefore, microbiome composition in chyme and mucosa was explored and a significant difference was observed between the two sites, both at phylum and genus levels. This disparity can be attributed to different substrate availability, and rapid decrease in oxygen gradient from the outer mucosal layer to the lumen (26, 27). Although the microbiome composition was different in chyme and mucosa samples in this study, *Lactobacillus* was the dominant genus in the ENI group. *Lactobacillus* genus is commonly found in food and intestinal tracts and is a typical probiotic with significant beneficial effects on gut health. *Lactobacillus* effectively inhibits colonization of harmful bacteria in the intestine (28). A high proportion of *Lactobacillus* can be attributed to administration of early-life nutritional interventions, resulting in low proportions of harmful bacteria, such as *Escherichia-Shigella, Actinobacillus, Clostridium-sensu-stricto-6, Pasteurellaceae,* and *Parabacteroides*.

The period from birth to 30 days old is a transition period during which the piglet diet is changed from sow milk to solid foods, and this period represents a delicate moment for piglets (29, 30). Weaned piglets are more likely to suffer from body

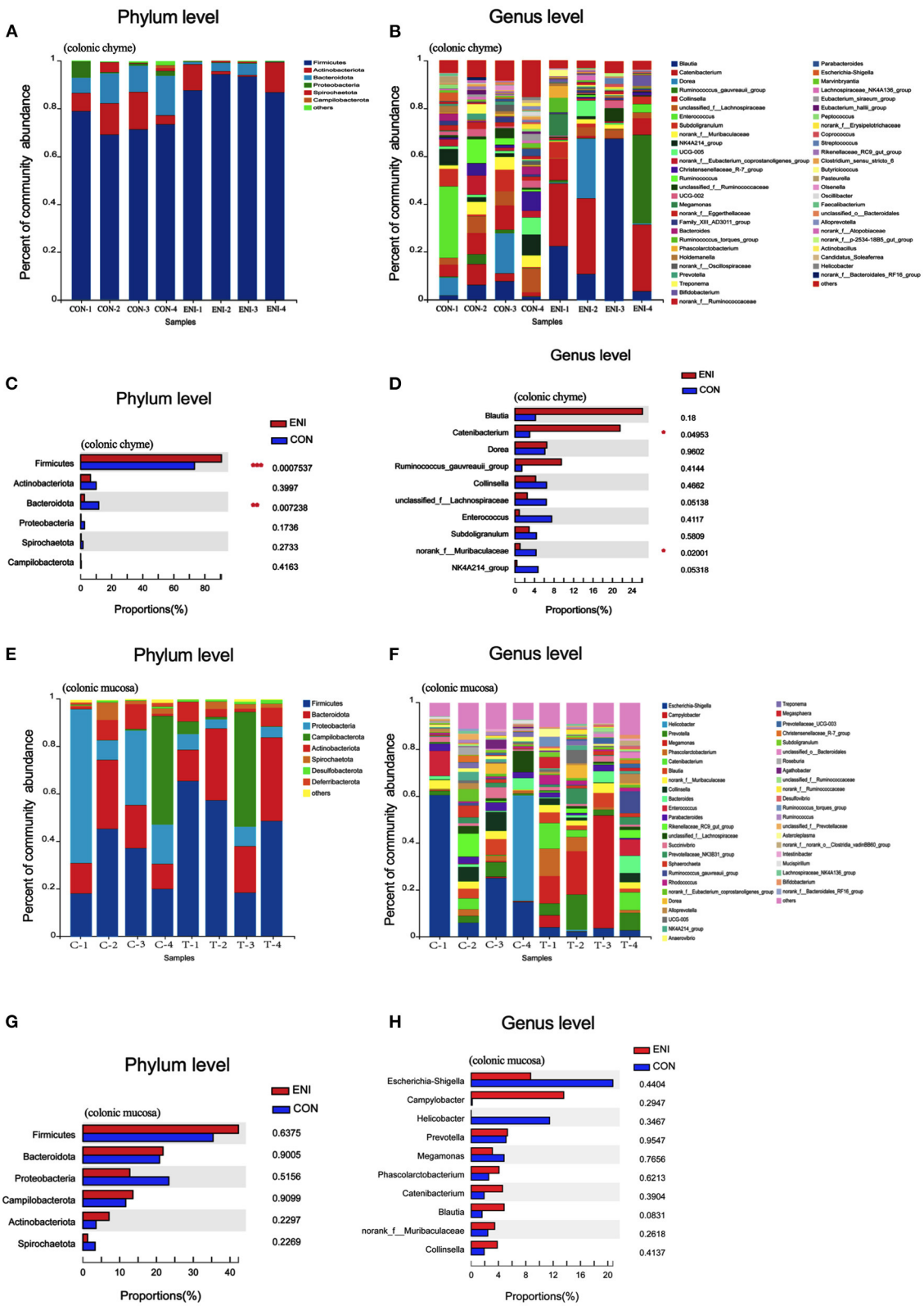

FIGURE 7 | Gut microbiota community composition in the colonic chyme and colonic mucosa of piglets. CON, control group, ENI, early-life nutrition interventions group. **(A)** The relative abundances of microbiota in colonic chyme at the phylum level. **(B)** The relative abundances of microbiota in colonic chyme at the genus level. *(Continued)*

FIGURE 7 | (C) The top 6 bacteria in colonic chyme at the phylum level statistical comparison of the relative abundances. **(D)** The top 10 bacteria in colonic chyme at the genus level statistical comparison of the relative abundances. **(E)** The relative abundances of microbiota in colonic mucosa at the phylum level. **(F)** The relative abundances of microbiota in colonic mucosa at the genus level. **(G)** The top 6 bacteria in colonic mucosa at the phylum level statistical comparison of the relative abundances. **(H)** The top 10 bacteria in colonic mucosa at the genus level statistical comparison of the relative abundances. Data are expressed as mean ± SEM ($n = 4$). The independent-samples t-test was used to compare data between two groups. $^*P < 0.05$.

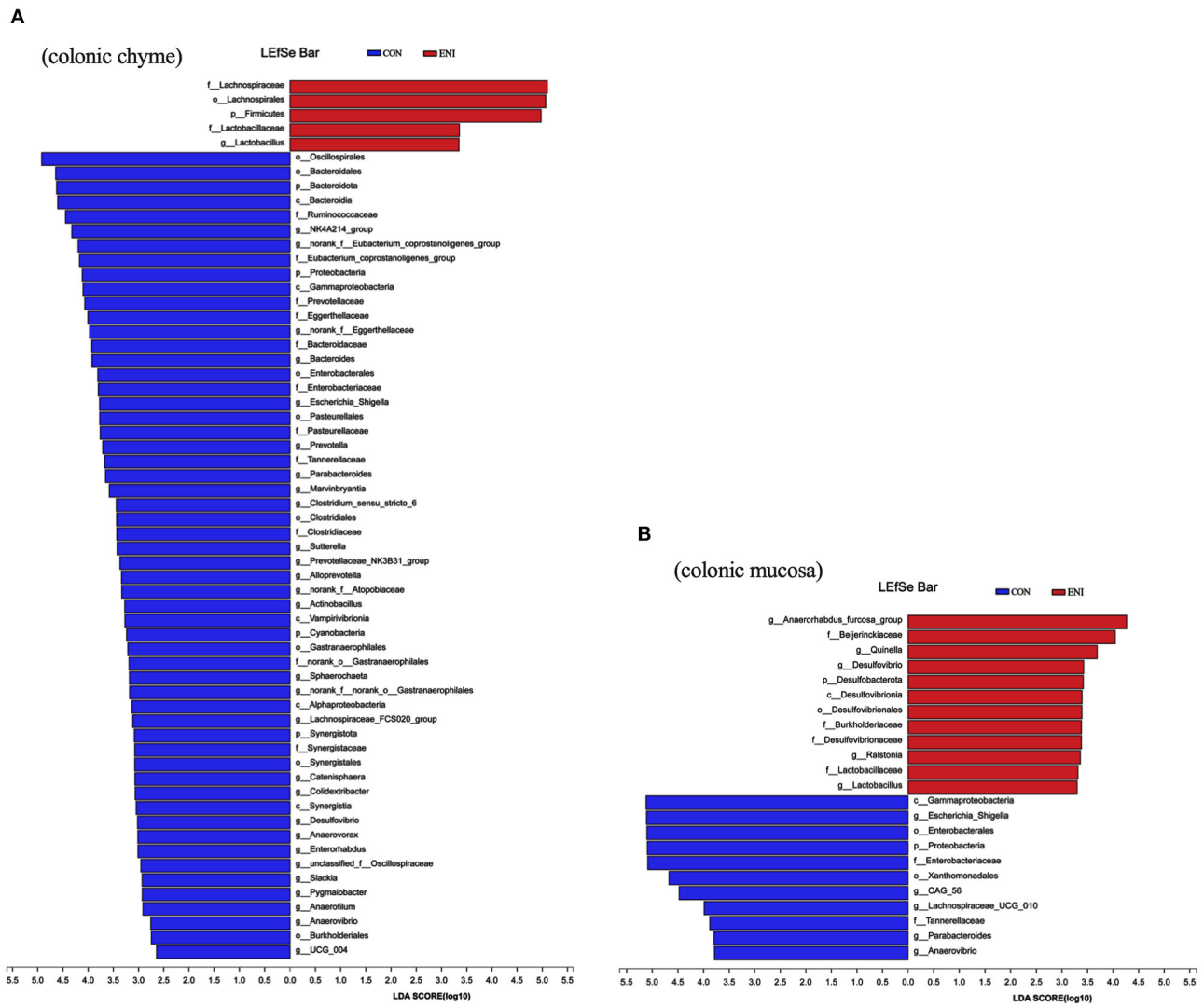

FIGURE 8 | The differentially abundant taxa among the two groups by LEfSe analysis. CON: control group, ENI: early-life nutrition interventions group. **(A)** LEfSe analysis of microbiota in colonic chyme. **(B)** LEfSe analysis of microbiota in colonic mucosa.

weight loss, appetite slough, and digestive function disorder during this period (31). Several studies have been conducted to explore the changes that occur during this period as they affect production in the pig industry (32). Studies report that supplementation of additional formula milk improves growth performance, and reduces incidence of pre-weaning and post-weaning diarrhea of piglets (7), and the findings show that gut microbiota play a key role in these changes. The findings of the present study showed that early-life nutrition interventions improve body weight gain and reduce diarrhea incidence at pre-weaning and post-weaning periods of piglets. Early-life nutrition interventions significantly increased the ratio of liver to body weight and ratio of spleen to body weight. The ratio of liver to body weight is widely used as a parameter for general assessment of liver size or regrowth. The spleen is a major hematopoietic tissue, and the increased ratio of spleen

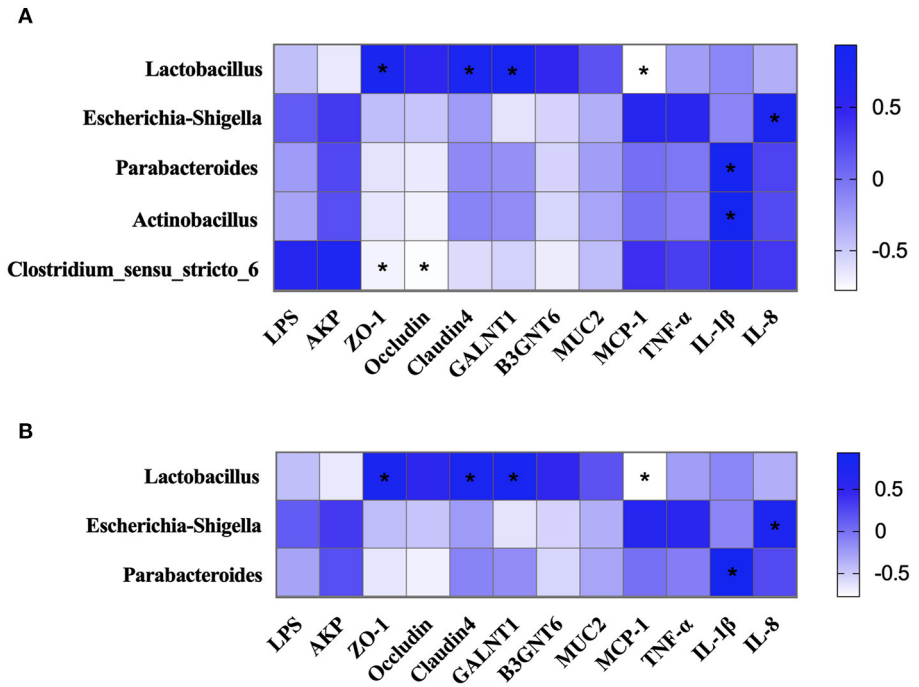

FIGURE 9 | The correlation of intestinal microbiota, intestinal barrier, and immune-related indexes. **(A)** The correlation of intestinal microbiota, intestinal barrier, and immune-related indexes in colonic chyme. **(B)** The correlation of intestinal microbiota, intestinal barrier, and immune-related indexes in colonic mucosa. *$P < 0.05$.

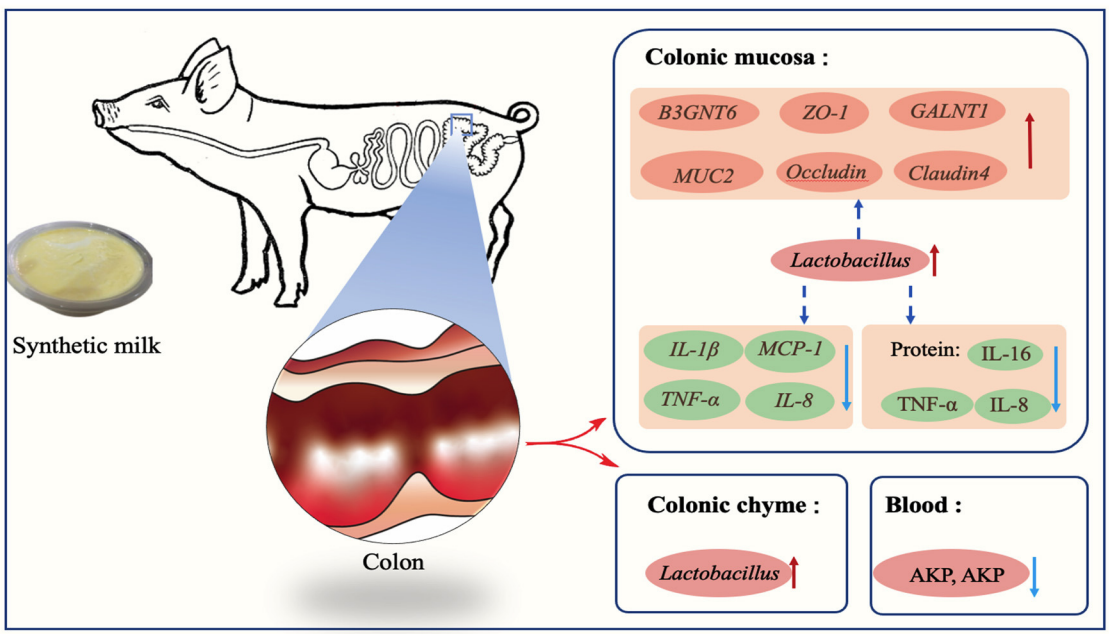

FIGURE 10 | Early-life nutrition interventions improved growth performance and intestinal health via the gut microbiota in piglets: a possible mechanism.

to body weight is correlated with the hematopoietic function of the spleen (33). This finding indicates that the condition of the piglets improved after administration of early-life nutrition interventions. *Lactobacillus* was enriched in colonic mucosa and chyme of piglets. These findings indicate that early-life nutrition interventions supported growth of beneficial bacteria in the gut

before and after weaning thus reducing the risk of gastrointestinal infections, and improved body weight of piglets (3). Moreover, the proportion of *Firmicutes* was increased, whereas the proportion of *Bacteroidetes* was significantly decreased in the ENI group relative to that of the CON group. Previous studies report that the ratio of *Firmicutes* to *Bacteroidetes* is an indicator of obesity (34). *Firmicutes* are more efficient in absorbing energy compared with *Bacteroidetes*, thus they promote more efficient absorption of calories resulting in weight gain (35). This finding partially explains the observation that piglets in the ENI group exhibited better growth performance compared with the CON group. In addition, studies report that milk substitutions improve feed intake of piglets (36), which is often used as a measure of growth performance (37). Therefore, increase in the weight of piglets in the ENI group can be attributed to improved feed intake induced by the early-life nutrition interventions.

The intestine is one of the largest organs in organisms and plays a role in defending other organs against harmful agents, and plays key roles in digestion and absorption of dietary nutrients in the body (38). Nutrients are received from the outside to the intestine to support the life of animals, and various harmful pathogens and toxins may attack the host through the intestine (39). The intestinal barrier plays an important role in life activities and prevents these harmful substances from penetrating the intestinal tissue (40). The results in the current study showed that the relative mRNA expression levels of tight junction proteins, barrier defense-related proteins, and key glycosyltransferases were higher in piglets in the ENI group relative to the levels in piglets in the CON group. High expression levels of these markers implied that synthetic milk improves the gut barrier function, and maintains the intestine at a relatively healthy level (41). Previous studies used milk as a substitute for sow milk and the findings showed that it improved intestinal function and upregulated expression of tight junction proteins. For example, Jin et al. (42) reported that milk supplementation changes mRNA expression levels of *ZO-1, Occludin,* and *Claudin-1*. The synthetic milk may potentially harbor specific growth factors which improved expression of tight junction proteins (42). Moreover, *Lactobacillus* may have upregulated gene expression of tight junction proteins (43). Previous studies report that *Lactobacillus* plays a key role in positively protecting the gut barrier (44). Pearson correlation analysis was conducted to explore the relationships among the abundances of major gut flora with the expression of tight junction proteins. Abundance of *Lactobacillus* was positively correlated with expression levels of tight junction proteins explored in the present study. The *MUC2* gene plays an important role in intestinal barrier protection and is produced and secreted by intestinal goblet cells (45). Several factors regulate the secretory processes of *MUC2* including cytokines, toxins, microbiota-metabolites, and microbes such as *Lactobacillus* (46). The findings of the current study showed that early-life nutrition interventions increased the abundance of *Lactobacillus* in the colon. The production and secretion of *MUC2* may have been stimulated by *Lactobacillus* (47). Abundance of *Lactobacillus* was positively correlated with the relative mRNA expression levels of *MUC2*. Furthermore, early-life nutrition interventions downregulated expression of inflammatory cytokines in the present study. This was attributed to increased expression of *MUC2,* and decreased enteric leakiness which in turn reduced contact of intestinal epithelial cells with harmful substances, and ultimately decreased frequency of inflammation (48). Previous human and animal studies indicated that LPS is a strong inducer of proinflammatory cytokines, and is produced by harmful microorganisms (49). LPS stimulation upregulates expression of *TNF-α*, *MCP-1,* and *IL-10* (50). In the present study, Pearson correlation analysis showed that abundances of *Escherichia-Shigella, Parabacteroides, Actinobacillus,* and *Clostridium-sensu-stricto-6* were positively correlated with expression levels of inflammatory cytokines. The lower inflammatory cytokines of piglets in the ENI group can be attributed to the effects of the early-life nutrition interventions that reduced abundances of proinflammatory bacteria such as *Escherichia-Shigella* (51). Previous studies indicate that intestinal crypt hyperplasia can cause a series of intestinal disorders (52). The crypt depth of the colon was increased by early-life nutritional intervention in the present trial. Although similar results were reported by Greeff et al. (8), the study did not fully explore the mechanism underlying increase in crypt length. Further studies should be conducted to explain this phenomenon.

CONCLUSION

In summary, early-life nutrition interventions through administration of synthetic milk increased growth performance, improved gut health, and reduced the diarrhea rate of piglets in the present study. Intestinal microbes, mainly beneficial bacteria such as *Lactobacillus*, play an important role in these changes. Implementation of this approach and further studies can improve pig production through reduction of antimicrobial infections thus improving mortality and morbidity of piglets.

DATA AVAILABILITY STATEMENT

The datasets presented in this study can be found in online repositories. The names of the repository/repositories and accession number(s) can be found below: https://www.ncbi.nlm.nih.gov; PRJNA779481.

ETHICS STATEMENT

The animal study was reviewed and approved by Experimental Animal Welfare and Ethical Committee of the Institute of Animal Science, Chinese Academy of Agricultural Sciences. Written informed consent was obtained from the owners for the participation of their animals in this study.

AUTHOR CONTRIBUTIONS

CL and BX designed the experiment. CL, BX, DS, and JL carried out the experiment. CL, BX, and JL wrote the manuscript. RZ, LC, and HZ revised the manuscript. All authors contributed to the article and approved the submitted version.

FUNDING

This research was supported by the Agricultural Science and Technology Innovation Program (CAAS-ZDRW202006-02, ASTIPIAS07) and Central Public-Interest Scientific Institution Basal Research Fund (No. 2021-YWF-ZYSQ-01).

REFERENCES

1. Syrovnev GI, Mykytyuk VV, Khmeleva EV. The presence of a potential patient of *Colibacterisis* in the population of pigs of local selection of ukrainian meat breed. *J Anim Breed Genet.* (2020) 59:115–23. doi: 10.31073/abg.59.13
2. Campbell JM, Crenshaw JD, Polo J. The biological stress of early weaned piglets. *J Anim Sci Biotechnol.* (2013) 4:19. doi: 10.1186/2049-1891-4-19
3. Huting AMS, Middelkoop A, Guan X, Molist F. Using nutritional strategies to shape the gastro-intestinal tracts of suckling and weaned piglets. *Animals.* (2021) 11:402. doi: 10.3390/ani11020402
4. Vente-Spreeuwenberg M, Verdonk J, Bakker G, Beynen AC, Verstegen M. Effect of dietary protein source on feed intake and small intestinal morphology in newly weaned piglets. *Livest Prod Sci.* (2004) 86:169–77. doi: 10.1016/S0301-6226(03)00166-0
5. Croxen MA, Finlay B. Molecular mechanisms of *Escherichia coli* pathogenicity. *Nat Rev Microbiol.* (2010) 8:26–38. doi: 10.1038/nrmicro2265
6. Milani C, Duranti S, Bottacini F, Casey E, Turroni F, Mahony J, et al. The first microbial colonizers of the human gut: composition, activities, and health implications of the infant gut microbiota. *Microbiol Mol Biol Rev.* (2017) 81:e00036–17. doi: 10.1128/MMBR.00036-17
7. Shi C, Zhu Y, Niu Q, Wang J, Wang J, Zhu W. The changes of colonic bacterial composition and bacterial metabolism induced by an early food introduction in a neonatal porcine model. *Curr Microbiol.* (2018) 75:745–51. doi: 10.1007/s00284-018-1442-z
8. de Greeff A, Resink JW, van Hees HM, Ruuls L, Klaassen GJ, Rouwers SM, et al. Supplementation of piglets with nutrient-dense complex milk replacer improves intestinal development and microbial fermentation. *J Anim Sci.* (2016) 94:1012–9. doi: 10.2527/jas.2015-9481
9. Yi D, Li B, Hou Y, Wang L, Zhao D, Chen H, et al. Dietary supplementation with an amino acid blend enhances intestinal function in piglets. *Amino Acids.* (2018) 50:1089–100. doi: 10.1007/s00726-018-2586-7
10. Qin L, Ji W, Wang J, Li B, Hu J, Wu X. Effects of dietary supplementation with yeast glycoprotein on growth performance, intestinal mucosal morphology, immune response and colonic microbiota in weaned piglets. *Food Funct.* (2019) 10:2359–71. doi: 10.1039/C8FO02327A
11. Sugiharto S, Poulsen AS, Canibe N, Lauridsen C. Effect of bovine colostrum feeding in comparison with milk replacer and natural feeding on the immune responses and colonisation of enterotoxigenic *Escherichia coli* in the intestinal tissue of piglets. *Br J Nutr.* (2015) 113:923–34. doi: 10.1017/S0007114514003201
12. Uryu H, Tsukahara T, Ishikawa H, Oi M, Otake S, Yamane I, et al. Comparison of productivity and fecal microbiotas of sows in commercial farms. *Microorganisms.* (2020) 8:1469. doi: 10.3390/microorganisms8101469
13. Tan Z, Wang Y, Yang T, Ao H, Chen S, Xing K, et al. Differences in gut microbiota composition in finishing Landrace pigs with low and high feed conversion ratios. *Antonie Van Leeuwenhoek.* (2018) 111:1673–85. doi: 10.1007/s10482-018-1057-1
14. Rutherford KMD, Baxter EM, D'Eath RB, Turner SP, Arnott G, Roehe R. The welfare implications of large litter size in the domestic pig I: biological factors. *Anim Welfare.* (2013) 22:199–218. doi: 10.7120/09627286.22.2.199
15. Novotni-Dankó G, Balogh P, Huzsvai L, Gyori Z. Effect of feeding liquid milk supplement on litter performances and on sow back-fat thickness change during the suckling period. *Arch Anim Breed.* (2015) 58:229–35. doi: 10.5194/aab-58-229-2015
16. Yu J, Song Y, Yu B, He J, Zheng P, Mao X, et al. Tannic acid prevents post-weaning diarrhea by improving intestinal barrier integrity and function in weaned piglets. *J Anim Sci Biotechnol.* (2020) 11:87. doi: 10.1186/s40104-020-00496-5
17. Cheng L, Yi W, Sheng T, Yi L, Cheng Y, Cun C, et al. Effects of replacing fish meal with mussel (*Cristaria plicata*) meat on growth, digestive ability, antioxidant capacity and hepatic IGF-I gene expression in juvenile Ussuri catfish (*Pseudobagrus ussuriensis*). *Aquac Res.* (2019) 50:826–35. doi: 10.1111/are.13953
18. Zhong G, Shao D, Wang Q, Tong H, Shi S. Effects of dietary supplemented of γ-amino butyric acid on growth performance, blood biochemical indices and intestinal morphology of yellow-feathered broilers exposed to a high temperature environment. *Ital J Anim Sci.* (2020) 24:431–8. doi: 10.1080/1828051X.2020.1747953
19. Wang M, Zhang S, Zhong R, Wan F, Zhang H. Olive fruit extracts supplement improve antioxidant capacity via altering colonic microbiota composition in mice. *Front Nut.* (2021) 8:645099. doi: 10.3389/fnut.2021.645099
20. Cantero-Recasens G, Butnaru CM, Valverde MA, Naranjo JR, Brouwers N, Malhotra V. KChIP3 coupled to Ca(2+) oscillations exerts a tonic brake on baseline mucin release in the colon. *Elife.* (2018) 7:e39729. doi: 10.7554/eLife.39729.016
21. Wu W, Xie J, Zhang H. Dietary fibers influence the intestinal SCFAs and plasma metabolites profiling in growing pigs. *Food Funct.* (2016) 7:4644–54. doi: 10.1039/C6FO01406B
22. Qin S, Guan S, Mei Z, Shi J, Xu C, Hao J, et al. Dietary fucoidan improves metabolic syndrome in association with increased *Akkermansia* population in the gut microbiota of high-fat diet-fed mice-ScienceDirect. *J Funct Foods.* (2017) 28:138–46. doi: 10.1016/j.jff.2016.11.002
23. Zheng L, Duarte ME, Sevarolli Loftus A, Kim SW. Intestinal health of pigs upon weaning: challenges and nutritional intervention. *Front Vet Sci.* (2021)8:628258. doi: 10.3389/fvets.2021.628258
24. Magne F, Gotteland M, Gauthier L, Zazueta A, Pesoa S, Navarrete P, et al. The *Firmicutes/Bacteroidetes* ratio: a relevant marker of gut dysbiosis in obese patients? *Nutrients.* (2020)12:1474. doi: 10.3390/nu12051474
25. Bishnu, Adhikari, Woo S, Kim, Min Y, Kwon. Characterization of microbiota associated with digesta and mucosa in different regions of gastrointestinal tract of nursery pigs. *Int J Mol Sci.* (2019)20:1630. doi: 10.3390/ijms20071630
26. Zhao W, Wang Y, Liu S, Huang J, He M. The dynamic distribution of porcine microbiota across different ages and gastrointestinal tract segments. *PLoS ONE.* (2015)10:e0117441. doi: 10.1371/journal.pone.0117441
27. Albenberg L, Esipova TV, Judge CP, Bittinger K, Wu GD. Correlation between intraluminal oxygen gradient and radial partitioning of intestinal microbiota in humans and mice. *Gastroenterology.* (2014)147:1055–63. doi: 10.1053/j.gastro.2014.07.020
28. Keita N, Yasuyuki S, Kazuki Y, Tsutomu K, Shinji T, Yuji Y, et al. *Lactobacillus gasseri* SBT2055 reduces infection by and colonization of *Campylobacter jejuni*. *PLoS ONE.* (2014) 9:e108827. doi: 10.1371/journal.pone.0108827
29. Sang IL, Kim IH. Nucleotide-mediated SPDEF modulates TFF3-mediated wound healing and intestinal barrier function during the weaning process. *Sci Rep.* (2018) 8:4827. doi: 10.1038/s41598-018-23218-4
30. Baldassarre ME, Mauro AD, Caroli M, Schettini F, Laforgia N. Premature birth is an independent risk factor for early adiposity rebound: longitudinal analysis of BMI data from birth to 7 years. *Nutrients.* (2020) 12:3654. doi: 10.3390/nu12123654
31. Zhang S, Jung JH, Kim HS, Kim BY, Kim IH. Influences of phytoncide supplementation on growth performance, nutrient digestibility, blood profiles, diarrhea scores and fecal microflora shedding in weaning pigs. *Asian-Australas J A Sci.* (2012) 25:1309–15. doi: 10.5713/ajas.2012.12170
32. Liao S, Tang S, Chang M, Qi M, Li J, Tan B, et al. Chloroquine downregulation of intestinal autophagy to alleviate biological stress in early-weaned piglets. *Animals.* (2020) 10:290. doi: 10.3390/ani10020290

33. Macková NO, Fedorocko P. Effect of liposomal muramyl tripeptide phosphatidylethanolamine and indomethacin on hematopoietic recovery in irradiated mice. *Physiol Res.* (2002) 51:511–21. doi: 10.1086/338285
34. Zou Y, Ju X, Chen W, Yuan J, Wang Z, Aluko RE, et al. Rice bran attenuated obesity via alleviating dyslipidemia, browning of white adipocytes and modulating gut microbiota in high-fat diet-induced obese mice. *Food Funct.* (2020) 11:2406–17. doi: 10.1039/C9FO01524H
35. Koliada A, Syzenko G, Moseiko V, Budovska L, Puchkov K, Perederiy V, et al. Association between body mass index and *Firmicutes*/*Bacteroidetes* ratio in an adult Ukrainian population. *BMC Microbiol.* (2017) 17:120. doi: 10.1186/s12866-017-1027-1
36. van Oostrum M, Lammers A, Molist F. Providing artificial milk before and after weaning improves postweaning piglet performance. *J Anim Sci.* (2016) 94:429–32. doi: 10.2527/jas.2015-9732
37. Baktavachalam GB, Delaney B, Fisher TL, Ladics GS, Layton RJ, Locke ME, et al. Transgenic maize event TC1507: global status of food, feed, and environmental safety. *Gm Crops Food.* (2015) 6:80–102. doi: 10.1080/21645698.2015.1054093
38. Tanaka T, Tahara-Hanaoka S, Nabekura T, Ikeda K, Jiang S, Tsutsumi S, et al. PPARβ/δ activation of CD300a controls intestinal immunity. *Sci Rep.* (2014) 4:5412. doi: 10.1038/srep05412
39. Sullivan ZA, Khoury-Hanold W, Lim J, Smillie C, Biton M, Reis BS, et al. gd T cells regulate the intestinal response to nutrient sensing. *Science.* (2021) 371:eaba8310. doi: 10.1126/science.aba8310
40. Scapigliati G. Functional aspects of fish lymphocytes. *Dev Comp Immunol.* (2013) 41:200–8. doi: 10.1016/j.dci.2013.05.012
41. Bennet S, Trnblom H. Editorial: increased expression of nerve growth factor correlates with visceral hypersensitivity and impaired gut barrier function in diarrhoea-predominant irritable bowel syndrome. *Aliment Pharmacol Ther.* (2017) 45:567–68. PMID: 28074514 doi: 10.1111/apt.13902
42. Jin J, Zhang L, Jia J, Chen Q, Chen Q. Jejunal inflammatory cytokines, barrier proteins and microbiome-metabolome responses to early supplementary feeding of Bamei suckling piglets. *BMC Microbiol.* (2020) 20:169. doi: 10.1186/s12866-020-01847-y
43. Chang CH, Teng PY, Lee TT, Yu B. Effects of multi-strain probiotic supplementation on intestinal microbiota, tight junctions, and inflammation in young broiler chickens challenged with *Salmonella enterica subsp. enterica*. *Asian-Australas J Anim Sci.* (2020) 33:1797–808. doi: 10.5713/ajas.19.0427
44. Kembra AS, Tariful I, Paige J, Naima MM. Systematic review of beef protein effects on gut microbiota: Implications for health. *Adv Nutr.* (2020) 12:102–14. doi: 10.1093/advances/nmaa085
45. Meng X, Wang W, Lan T, Yang W, Yu D, Fang X, et al. A purified aspartic protease from *Akkermansia Muciniphila* plays an important role in degrading Muc2. *Int J Mol Sci.* (2019) 21:72. doi: 10.3390/ijms21010072
46. Thai P, Loukoianov A, Wachi S, Wu R. Regulation of airway mucin gene expression. *Annu Rev Physiol.* (2008) 70:405–29. doi: 10.1146/annurev.physiol.70.113006.100441
47. Mack DR, Michail S, Wei S, Mcdougall L, Hollingsworth MA. Probiotics inhibit enteropathogenic *E.* coli adherence in vitro by inducing intestinal mucin gene expression. *Am J Physiol.* (1999) 276:941. doi: 10.1152/ajpgi.1999.276.4.G941
48. Cani PD. Human gut microbiome: hopes, threats and promises. *Gut.* (2018) 67:1716–25. doi: 10.1136/gutjnl-2018-316723
49. Pandur E, Tamási K, Pap R, Jánosa G, Sipos K. Distinct effects of *Escherichia coli*, *Pseudomonas aeruginosa* and *Staphylococcus aureus* cell wall component-induced inflammation on the iron metabolism of THP-1 cells. *Int J Mol Sci.* (2021) 22:1497–508. doi: 10.3390/ijms22031497
50. Turnbull IR. DAP12 (KARAP) amplifies inflammation and increases mortality from endotoxemia and septic peritonitis. *J Exp Mede.* (2005) 202:363–9. doi: 10.1084/jem.20050986
51. Cui M, Xiao H, Li Y, Zhang S, Dong J, Wang B, et al. Sexual dimorphism of gut microbiota dictates therapeutics efficacy of radiation injuries. *Adv Sci.* (2019) 6:1901048. doi: 10.1002/advs.201901048
52. Spreeuwenberg M, Verdonk J, Gaskins HR, Verstegen M. Small intestine epithelial barrier function is compromised in pigs with low feed intake at weaning. *J Nutr.* (2001) 131:1520–7. doi: 10.1093/jn/131.5.1520

Conflict of Interest: The authors declare that the research was conducted in the absence of any commercial or financial relationships that could be construed as a potential conflict of interest.

Publisher's Note: All claims expressed in this article are solely those of the authors and do not necessarily represent those of their affiliated organizations, or those of the publisher, the editors and the reviewers. Any product that may be evaluated in this article, or claim that may be made by its manufacturer, is not guaranteed or endorsed by the publisher.

frontiers in Nutrition

ORIGINAL RESEARCH
published: 05 January 2022
doi: 10.3389/fnut.2021.813757

Intestinal Microbiota and Serum Metabolic Profile Responded to Two Nutritional Different Diets in Mice

Zhifeng Wu[1†], Wei Cheng[1†], Zhenyu Wang[2], Shuaifei Feng[1], Huicong Zou[1], Xiang Tan[1], Yapeng Yang[1], Yuqing Wang[1], Hang Zhang[1], Miaomiao Dong[1], Yingping Xiao[3], Shiyu Tao[1*] and Hong Wei[1*]*

[1] College of Animal Sciences and Technology, Huazhong Agricultural University, Wuhan, China, [2] State Key Laboratory of Animal Nutrition, College of Animal Science and Technology, China Agricultural University, Beijing, China, [3] State Key Laboratory for Managing Biotic and Chemical Threats to the Quality and Safety of Agro-products, Institute of Agro-product Safety and Nutrition, Zhejiang Academy of Agricultural Sciences, Hangzhou, China

OPEN ACCESS

Edited by:
Nuria Salazar,
Spanish National Research Council (CSIC), Spain

Reviewed by:
Xiaokang Ma,
Hunan Agricultural University, China
Yulan Liu,
Wuhan Polytechnic University, China

***Correspondence:**
Yingping Xiao
xiaoyp@zaas.ac.cn
Shiyu Tao
sytao@mail.hzau.edu.cn
Hong Wei
weihong63528@163.com

[†] These authors have contributed equally to this work and share first authorship

Specialty section:
This article was submitted to Nutrition and Microbes, a section of the journal Frontiers in Nutrition

Received: 12 November 2021
Accepted: 14 December 2021
Published: 05 January 2022

Citation:
Wu Z, Cheng W, Wang Z, Feng S, Zou H, Tan X, Yang Y, Wang Y, Zhang H, Dong M, Xiao Y, Tao S and Wei H (2022) Intestinal Microbiota and Serum Metabolic Profile Responded to Two Nutritional Different Diets in Mice. Front. Nutr. 8:813757. doi: 10.3389/fnut.2021.813757

There is an interaction and bidirectional selection between dietary intake and gut microbiota due to the different efficiency of nutrients in the gut. The nutritional composition of germ-free (GF) diets differs significantly from specific pathogen-free (SPF) diets. There is, however, no data revealing how SPF animals from the same microbial background respond to them and if they affect the host. We examined the growth of SPF mice on the GF diet and found that it reduced body weight, intestinal length and intestinal morphology. Interestingly, the GF diet increased the level of pro-inflammatory bacteria in the gut of SPF mice, including Proteobacteria, *Burkholderiaceae*, *Alloprevotella* and *Parasutterella*. Furthermore, GF diets caused significant increases in malondialdehyde (MDA), IL-1β, IL-6, and D-lactate levels in the serum of SPF mice and significantly altered their serum metabolic profile, especially amino acid metabolism. In conclusion, GF diets are not suitable for the growth and development of SPF mice. These findings, based on the role of gut microbiota in diet selection, provide new insights into the scientific and rational use of experimental animal diets.

Keywords: germ-free diet, nutrient, microbiota, metabolism, gut development

INTRODUCTION

Diets are composed of different types and levels of nutrients, which act differently and can cause considerable changes in the organism. In detail, nutrient deficiencies or excesses affect hormones, metabolic pathways, gene expression, and the composition and function of gut microbes, altering the physiology of the host and having a major impact on growth, reproduction, and metabolism (1). For example, high dietary fat can disrupt the intestinal barrier and lead to inflammation, which is associated with the development of many diseases such as metabolic disorders and cancer (2–4). In animals, specific components of the diet such as dietary fiber enhance sow performance and improve piglet growth through the gut microbiota (5, 6). Therefore, the selection of diets with different nutrient contents and types in animal experiments may lead to bias in the baseline data of the experimental animals themselves due to different nutrient supply and animal needs, thus affecting the scientificity and rationality of the experimental data (7, 8).

The gut microbiota is the largest symbiont community in the body and is considered as an additional organ which closely related to immunity, nutrient absorption and metabolism and other

physiological functions (9, 10). The gut microbiota uses nutrients from the diet as substrates for metabolism, and different microbes utilize the same diet differently. In turn, diet regulates the structure of the gut microbiota, so that different diets lead to microbial differences in the same host background (11). Such diet-microbiota interactions have beneficial or detrimental effects on the host by directly altering the microbial structure or by indirectly altering microbial metabolites (12). Microorganisms in the gut produce a large number of small molecules through primary and secondary metabolic pathways, many of which are dependent on the host's diet. The most widely studied of these are short-chain fatty acids (13). Short-chain fatty acids are produced by fermentation of indigestible foods by gut microorganisms and play an important role in providing energy, maintaining intestinal health, and fighting inflammation (14–16). Several studies have shown the correlation between gut microbiota and host physiological functions. Anaerobic bacteria in the intestine form a biological barrier to maintain the normal function of the intestinal mucosa. The intestinal barrier serves as a physical and immune defense against toxins, food antigens, and harmful microbes in the intestinal lumen (17, 18). Intestinal microbial dysbiosis leads to the impaired intestinal barrier. Furthermore, dysbiosis of the gut microbiota causes alterations of metabolites, which translocate from the gut across a disrupted intestinal barrier to affect various metabolic organs, leading to metabolic inflammation and oxidative stress and ultimately to disease (19, 20).

In addition to the regulation of host physiological functions, the gut microbiota ferments certain components of the diet to produce nutrients the host needs such as vitamin K, biotin, pantothenic acid, and pyridoxine (21). As one of the most important experimental models for studying gut microbiota, germ-free (GF) animals do not have the ability to synthesize these nutrients (22, 23). Unlike specific pathogen-free (SPF) animals, which do not have specific pathogens but a complete gut microbiota, GF animals do not contain any microorganisms in their bodies. Therefore, in contrast to SPF animals, the ability of GF animals to utilize nutrients is compromised (24). The GF and SPF diets are recognized as diets that are suitable for two different animals and meet their respective nutritional requirements. Based on the different physiological characteristics and nutritional needs of GF and SPF animals, the composition of their diets is different. For example, The GF diet should be as low in fiber as possible and nutrients such as vitamins, minerals, and amino acids should be supplemented additionally compared to the SPF diet (24, 25). Our laboratory has been studying the diets of GF animals and has formulated diets that meet the growth and reproductive needs of GF mice (26). The GF diet has a higher nutritional content than the SPF diet, both as previously reported and in the formulas we have created.

Based on the comparison and speculation of the nutrient composition of the two different diets, we propose the scientific hypothesis that the gut microbiota in the same host context can lead to microbial selectivity for diet due to differences in nutrient preferences, thus causing differences in a range of physiological functions in the host. Therefore, in this study, we used SPF mice of the same host microbial background (same strain) as animal models to investigate the response of the gut microbiota to the different diets and the differences in metabolism, gut development, inflammatory and oxidative status and growth due to the different response profiles.

METHODS AND MATERIALS

Mice

Sixteen 3-week-old male SPF Kunming (KM) mice were purchased from the Experimental Animal Center of Huazhong Agricultural University (Wuhan, China). Mice were housed in a pathogen-free colony (temperature, 25 ± 2°C; relative humidity, 45–60%; lighting cycle, 12 h/day; light hours 06:30–18:30) with free access to food and water. All animal experiments and sample collection procedures were approved by the Institutional Animal Care and Use Committee of Huazhong Agricultural University, Hubei, China. All experimental methods in this study were carried out following the Guide for the Care and Use of Laboratory Animals at Huazhong Agricultural University. The animal experiment ethics number for this study is HZAUMO-2021-0187.

Experiment Design and Sample Collections

Mice from the same genetic and microbiological background were divided randomly into 2 groups ($n = 8$/group): (i) mice were fed SPF diet; (ii) mice were fed GF diet. The SPF diet (lot number: 21053113) was purchased in Keao Xieli Feed Co., Ltd. (Beijing, China). The GF diet is manufactured according to our specially designed formula and sterilized by 50 kGy of Co60-γ irradiation to completely kill the microorganisms (27, 28). The GF and SPF diets had the same ingredients but different ratios, and both were tested for the nutrient content according to standards before starting to feed the mice. **Table 1** lists the composition and content of both diets. After 7 weeks, mice were sacrificed to collect the duodenum, jejunum, and ileum after the mice were euthanized with CO_2 inhalation followed by cervical dislocation to ensure death. Full blood samples of mice were collected by extirpating eyeballs. The serum was prepared as follows: the whole blood was left at room temperature for 60 min and then centrifuged (3,500 rpm, 15 min) to remove any remaining insoluble material. The serum is then stored at −80°C. The lengths of the small intestine and colon were measured and the duodenum, jejunum and ileum segments obtained were fixed in 4% paraformaldehyde for hematoxylin-eosin staining. Before sacrifice, fresh feces from each mouse were collected for the microbial sequencing. Measurement of mice weight at the beginning of the experiment (3 weeks old) and before sampling (10 weeks old).

Hematological Parameters Testing

Whole blood was collected in 5 mL EDTA anticoagulation tubes. Hematology analyzer VETSCAN HM5 (Abaxis, Inc., Union City, CA, USA) was used to test hematological parameters. The following hematological parameters were measured: white blood cell (WBC), lymphocyte count (LYM), monocyte count (MON), neutrophil count (NEU), red blood cell (RBC), hemoglobin (HGB), hematocrit (HCT), mean cell volume (MCV), mean

TABLE 1 | Ingredient composition of the GF diet and SPF diet.

	Nutrient levels	GF diet	SPF diet		Nutrient levels	GF diet	SPF diet
Nutrient level	Crude protein, g/kg	227.10	231.00	Amino acid	Lysine, g/kg	9.50	13.90
	Crude fat, g/kg	66.50	48.00		Tryptophan, g/kg	1.20	2.50
	Crude fiber, g/kg	22.00	41.00		Arginine, g/kg	12.60	12.00
	Crude ash, g/kg	55.50	70.00		Leucine, g/kg	14.25	17.60
	Moisture, g/kg	69.00	79.00		Isoleucine, g/kg	6.00	11.00
	Energy, Kcal/kg	3820.00	3440.00		Threonine, g/kg	8.00	9.00
Vitamins	Vitamin A, IU/kg	9555.00	20000.00		Valine, g/kg	9.40	11.90
	Vitamin D, IU/kg	1445.00	1667.00		Histidine, g/kg	4.35	5.60
	Vitamin E, mg/kg	82.70	182.00	Minerals	Calcium, g/kg	10.70	12.10
	Vitamin K, mg/kg	2.03	8.00		Total phosphorus, g/kg	11.40	7.90
	Vitamin B1, mg/kg	8.05	20.23		Natrium, g/kg	0.09	2.83
	Vitamin B2, mg/kg	12.60	20.00		Magnesium, g/kg	2.30	2.80
	Vitamin B6, mg/kg	10.80	15.00		Potassium, g/kg	0.70	8.20
	Vitamin B12, mg/kg	0.03	0.03		Copper, mg/kg	18.00	12.41
	Niacin, mg/kg	58.80	70.00		Iron, mg/kg	156.0	158.6
	Pantothenic Acid, mg/kg	25.30	25.00		Manganese, mg/kg	426.50	88.10
	Biotin, mg/kg	0.16	0.30		Zinc, mg/kg	138.00	50.70
	Folic Acid, mg/kg	4.62	10.0		Iodine, mg/kg	0.03	0.90

cell hemoglobin (MCH), mean cell hemoglobin concentration (MCHC), red cell distribution width (RDW), platelet count (PLT), mean platelet volume (MPV), thrombocytosis (PCT) and platelet distribution width (PDW). The lymphocyte ratio (LYM%), monocyte ratio (MON%) and neutrophil ratio (NEU%) were calculated from the above assay values.

Hematoxylin-Eosin Staining and Analysis

After fixation with 4% paraformaldehyde for 24 h, the duodenum, jejunum, and ileum samples were embedded in paraffin, sectioned and stained with hematoxylin for histological analysis. Determination of villus height and crypt depth were performed using CaseViewer software (version 220 2.2) at 200× magnification. Three tissue sections from each mouse were coded and examined by 2 professionals to prevent observer bias.

Growth, Intestinal Permeability, Immune and Oxidative Stress Markers Testing

The ELISA kits (Shanghai Enzyme-linked Biotechnology, Shanghai, China) were used to detect various types of indicators in serum including growth-related hormones, inflammatory factors, oxidative stress indicators, and intestinal barrier indicators, according to the manufacturer's instructions. Growth-related hormones included Growth hormone (GH) and Insulin-like growth factor 1 (IGF-1). Inflammatory cytokines included tumor necrosis factors-α (TNF-α), interleukin-1β (IL-1β), interleukin-6 (IL-6), and interleukin-8 (IL-8), oxidative stress indicators included superoxide dismutase (SOD) and malondialdehyde (MDA), diamine oxidase (DAO) and D-lactate (D-LA) were indicators of intestinal permeability. Besides, two immunoglobulins, Immunoglobulin A (IgA) and Immunoglobulin G (IgG) were also measured in serum.

Bacterial DNA Extraction, 16S rRNA Gene Amplification and Sequencing

Fecal samples were collected and immediately frozen at −80°C. Total DNA was extracted from each fecal specimen by using the QIAamp R Fast DNA Stool Mini Kit (Qiagen Ltd., Germany) following the manufacturer's instructions. The V3–V4 region of the 16S rRNA gene was amplified with primers: 338F (5′-ACTCCTACGGGAGGCAGCA-3′) and 806R (5′-GGACTACHVGGGTWTCTAAT-3′). The amplified products were detected using agarose gel electrophoresis (2% agarose), recovered by AxyPrep DNA Gel Recovery Kit (Axygen Biosciences, Union City, CA, United States), and then quantified by Qubit 2.0 Fluorometer (Thermo Fisher Scientific, Waltham, MA, United States) to pool into equimolar amounts. Paired-end library was constructed using NEXTFLEX Rapid DNA-Seq (Bioo Scientific, Austin, TX, USA) and MiSeq Reagent Kit v3 (Illumina, San Diego, CA, USA) were used for sequencing. Amplicon libraries were sequenced on the Illumina MiSeq 2500 platform (Illumina, San Diego, CA, USA) for paired-end reads of 250 bp. The raw reads were deposited into the NCBI Sequence Read Archive database (accession number: PRJNA768608): https://dataview.ncbi.nlm.nih.gov/object/PRJNA768608. The specific information of the raw sequencing data were listed in **Supplementary Table S1**.

Detection of Serum Metabolomics

The untargeted metabolomics profiling was performed on XploreMET platform (Metabo-Profile, Shanghai, China). Briefly, samples were thawed and centrifuged to separate the fragments. Mix 50 μl of sample and 10 μl of internal standard and add 175 μL of pre-cooled methanol/chloroform. After centrifugation 200 μl of supernatant was transferred to an autosampler vial

(Agilent Technologies, Foster City, CA, USA). The sample was evaporated using a CentriVap vacuum concentrator (Labconco, Kansas City, MO, USA) to remove the chloroform and the sample was further freeze-dried. Dried samples were derivatized with 50 μL of methoxylamine (20 mg/mL pyridine) for 2 h at 30°C, followed by the addition of 50 μL of MSTFA (N-methyl-N-(trimethylsilyl)trifluoroacetamide) with 1% trimethylchlorosilane (TMCS) containing fatty acid methyl ester (FAMEs) as a retention index at 37°C. The samples were left for a further 1 h at 5°C using the sample preparation head. In the meantime, the derivatized samples were injected with a sample injection tip. Each sample was introduced onto a time-of-flight mass spectrometry (GC-TOF/MS) system (Pegasus) with an Agilent 7890B gas chromatograph for GC-TOFMS analysis.

Statistical Analysis

16S raw sequencing reads were demultiplexed according to sample-specific barcode (6–8 nucleotides) and imported into the QIIME2 platform (version 2020.2) (29). Quality control and denoising were performed simultaneously using DADA2 with default parameters to generate ASVs (30). All ASVs were classified against the silva 132 database by naïve Bayes classifier constructed by scikit-learn software (31). α-and β-diversity were calculated using the vegan package (version 2.5-6) inside R. PCoA was performed using weighted Bray-Curtis distance metrics. PERMANOVA was used to evaluate factors shaping microbiota by using the adonis function of the "vegan" package (999 permutations). Differential taxa were identified by LefSe (32) and function prediction was performed with PICRUSt2 (version 2.4.1) (33).

The metabolomics raw data were processed using ChromaTOF (V4.71, Leco Corp., St. Joseph, MO, USA) for automatic baseline denoising and smoothing, peak picking, deconvolution, and peak alignment. Compound identification was performed by comparing MS similarity and FAMES retention index distances with reference standards in JiaLib. Statistical analysis includes multivariate statistical analysis such as principal component analysis (PCA), partial least squares discriminant analysis (PLS-DA), etc., and univariate statistical analysis including Student *t*-test, Mann-Whitney-Wilcoxon

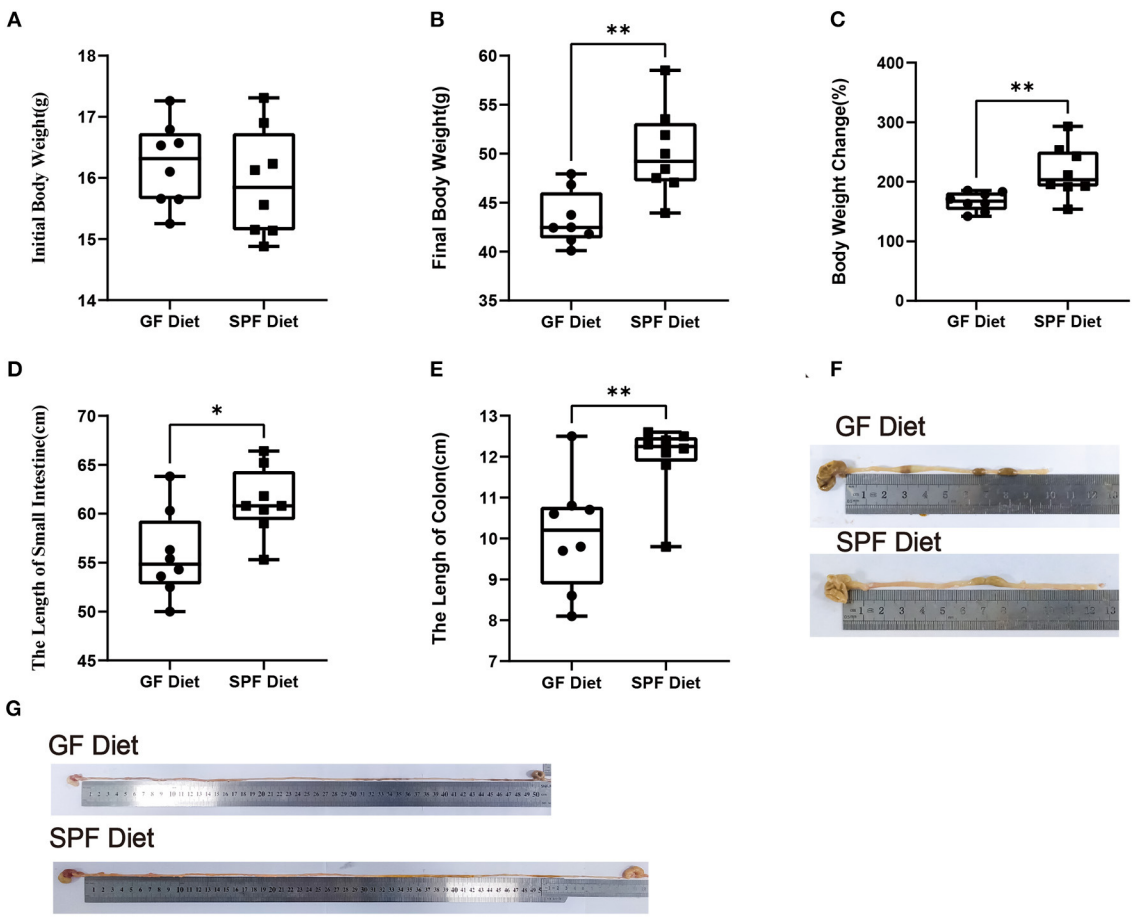

FIGURE 1 | Effect of GF diet on body weight and small intestine and colon length of SPF mice. **(A)** Initial body weight, **(B)** Final body weight, **(C)** Body weight change (%), **(D)** Small intestinal length, **(E)** Colonic length, **(F)** Colonic illustrate, and **(G)** Small intestinal illustrate. The unpaired *t*-test was used to determine whether differences existed between the two groups, $^{*}P < 0.05$, $^{**}P < 0.01$. All data are shown as mean ± SEM ($n = 8$).

(*U*-test), etc. All *P*-values were adjusted for false discovery rate (FDR). Statistical algorithms were performed using the widely used statistical analysis package in R Studio (http://cran.r-project.org/).

The differential bacteria and metabolites screened by lefSe were combined according to the group and imported into R. Rcorr function was used to calculate the Pearson correlation coefficient and *P*-value. The differential bacteria were classified by group and metabolites were classified by class, and the classified data were imported into R for heat mapping using the "Pheatmap" package (1.0.8).

All data were presented as means ± SEM. Data were tested for normal distribution and statistical significance was assessed by the independent sample *t*-test using SPSS (SPSS version 20.0 for Windows; SPSS Inc., Chicago, IL, USA) software. Data were considered statistically significant when $P < 0.05$.

RESULTS

GF Diet Intake Reduces Body Weight and Shortens the Length of the Small Intestine and Colon in SPF Mice

In the present experiment, the initial body weights of the SPF diet and GF diet group were almost identical ($P > 0.05$; **Figure 1A**). Compared with SPF diet mice, GF diet mice had significantly lower final body weight and rate of weight change ($P < 0.01$; **Figures 1B,C**) and significantly shorter lengths of the small intestine ($P < 0.05$; **Figures 1D,G**) and colon ($P < 0.01$ **Figures 1E,F**).

GF Diet Intake Causes Deterioration of Intestinal Morphology in SPF Mice

To investigate the effect of the GF diet on the intestinal morphology of mice, the duodenum, jejunum and ileum were stained with HE (**Figures 2A–C**). Compared with SPF Diet, the villi length of the duodenum, jejunum and ileum of GF diet mice was significantly lower ($P < 0.05$; **Figures 2D–F**). The crypt depth of ileum was reduced ($P < 0.05$; **Figure 2I**) and there was no change in duodenal and jejunal crypt depth ($P > 0.05$; **Figures 2G,H**). No difference in villi length/crypt depth ratio in duodenum, jejunum and ileum ($P > 0.05$; **Figures 2J–L**).

GF Diet Intake Alters Hematological Parameters in SPF Mice

Hematological parameters were examined using anticoagulated blood from mice on the GF diet and SPF diet groups. The results revealed that LYM% and RDWs were significantly lower and MON, MON% and NEU% were significantly higher in the GF

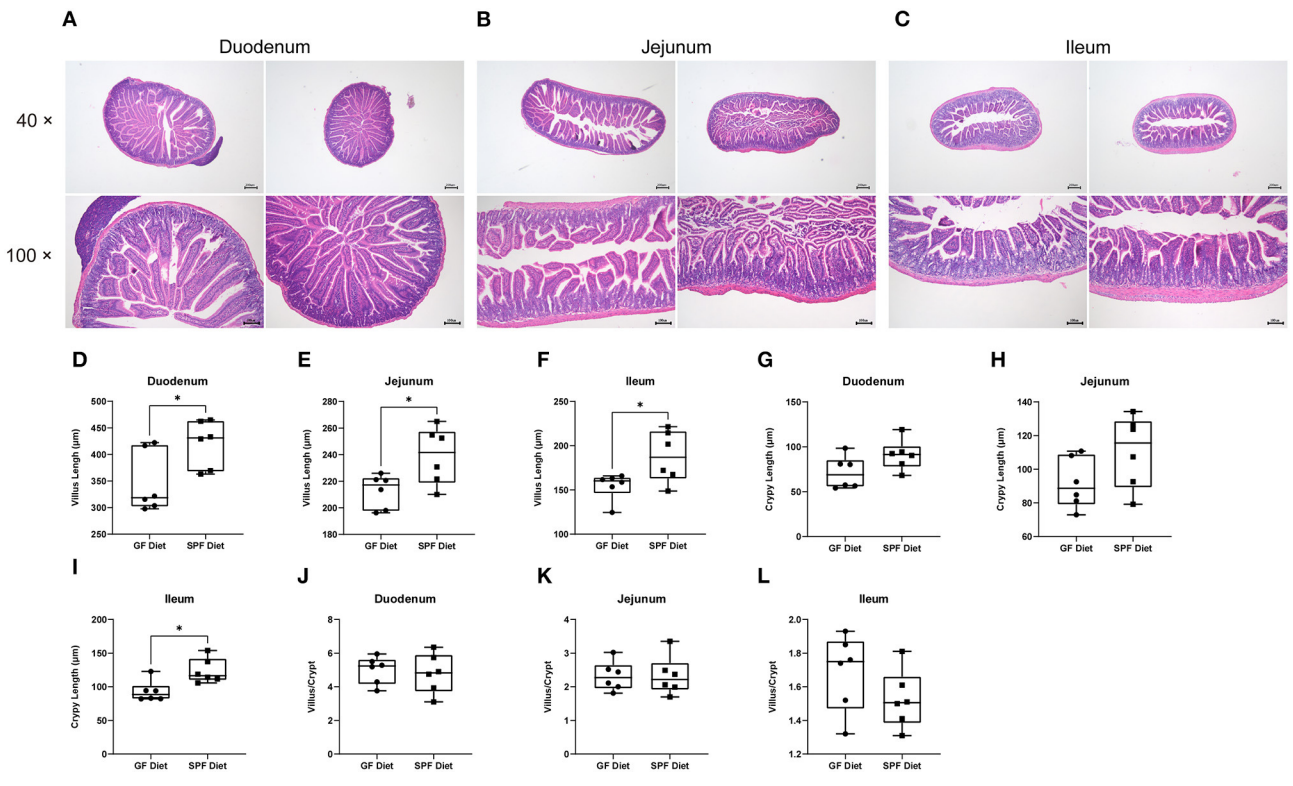

FIGURE 2 | Effect of GF diet on intestinal morphology of SPF mice. Hematoxylin and eosin staining of **(A)** Duodenum, **(B)** Jejunum, and **(C)** Ileum. **(D)** Villus length of duodenum. **(E)** Villus length of jejunum, **(F)** Villus length of ileum, **(G)** Crypt length of duodenum. **(H)** Crypt length of jejunum, **(I)** Crypt length of ileum, **(J)** Villus/Crypt analysis of duodenum. **(K)** Villus/Crypt analysis of jejunum, **(L)** Villus/Crypt analysis of ileum. The unpaired *t*-test was used to determine whether differences existed between the two groups, $^*P < 0.05$. Data are shown as mean ± SEM ($n = 6$).

TABLE 2 | Effect of GF diet and SPF diet on hematological parameters in mice.

Index/unit	GF diet	SPF diet	*P*-value
WBC/10^9/L	3.40 ± 1.77	3.45 ± 1.26	0.948
LYM/10^9/L	2.15 ± 1.67	2.52 ± 0.81	0.589
LYM%/%	57.73 ± 18.46	73.50 ± 4.70	0.030
MON/10^9/L	0.23 ± 0.11	0.13 ± 0.02	0.328
MON%/%	8.23 ± 4.44	4.21 ± 1.40	0.034
NEU/10^9/L	1.02 ± 0.36	0.80 ± 0.49	0.029
NEU%/%	34.06 ± 14.4	22.26 ± 5.45	0.048
RBC/10^{12}/L	9.10 ± 2.58	10.74 ± 1.48	0.139
HGB/g/dl	11.20 ± 4.08	13.59 ± 1.55	0.144
HCT/%	42.40 ± 13.06	51.58 ± 5.78	0.090
MCV/fl	46.63 ± 3.46	48.13 ± 2.59	0.343
MCH/pg	12.00 ± 1.83	12.73 ± 1.10	0.353
MCHC/g/dl	25.81 ± 3.83	26.38 ± 1.62	0.708
RDWc/%	19.00 ± 0.76	19.48 ± 1.56	0.452
RDWs/fl	33.21 ± 1.93	35.36 ± 1.29	0.020
PLT/10^9/L	509.88 ± 145.31	569.88 ± 175.30	0.468
MPV/fl	7.45 ± 1.23	6.98 ± 0.33	0.309
PCT/%	0.39 ± 0.17	0.40 ± 0.13	0.884
PDWc/%	33.14 ± 3.45	31.39 ± 2.58	0.270
PDWs/fl	11.83 ± 4.05	10.08 ± 2.05	0.294

WBC, White blood cell; LYM, Lymphocyte count; LYM%, Lymphocyte ratio; MON, Monocyte count; MON%, Monocyte ratio; NEU, Neutrophil count; NEU%, Neutrophil ratio; RBC, Red blood cell; HGB, Hemoglobin; HCT, Hematocrit; MCV, Mean cell volume; MCH, Mean cell hemoglobin; MCHC, Mean cell hemoglobin concentration; RDWc, Red cell distribution width (CV), RDWs, Red cell distribution width (SD); PLT, Platelet count; MPV, Mean platelet volume; PCT, Phrombocytosis; PDWc, Platelet distribution width (CV); PDWs, Platelet distribution width (SD).

diet group compared to the mice in the SPF diet group ($P < 0.05$; **Table 2**), with no differences in WBC, LYM, NEU, RBC, HGB, HCT, MCV, MCH, MCHC, RDWc, PLT, MPV, PCT, PDWc, and PDWs ($P > 0.05$; **Table 2**).

GF Diet Intake Alters Intestinal Permeability and Induces Inflammatory Responses

To investigate the effects of the GF diet on growth, immunity, inflammation, oxidative stress, and intestinal permeability in SPF mice, we measured the serum parameters. The levels of MDA, IL-1β, IL-6, and D-lactate were found to be significantly higher in the GF diet mice than in the SPF diet ($P < 0.05$; **Figures 3A–D**), while the remaining indicators were not statistically different ($P > 0.05$; **Figures 3E–L**).

GF Diet Intake Changes the Fecal Microbiota of SPF Mice

Feces from two groups of mice were collected to examine the differences in fecal microbiota between the GF diet and SPF diet group. Assessment of microbiota composition and diversity of mouse fecal samples by deep sequencing of the V3–V4 region of the 16S rRNA gene. A total of 844,103 high-quality 16S rRNA gene sequences were obtained from 16 fecal samples. The average number of high-quality sequences generated per sample was 52,756. The microbial α-diversity in the fecal samples of both groups is shown in **Figure 4A**. The observed fecal microbial species, Chao1, ACE, Shannon, Simpson, and J indices did not change significantly between the SPF diet and GF diet group ($P > 0.05$; **Figure 4A**). PCoA based on Bray-Curtis distance showed that the structure of the fecal microbial community was similar in both groups of mice (**Figure 4B**). The relative abundance of fecal microbiota levels indicated that Firmicutes, Bacteroidetes, and Actinobacteria were predominant in the feces of both groups of mice (**Figure 4C**). At the genus level, as shown in **Figure 4D**, *Lactobacillus*, *uncultured bacterium*, *Bifidobacterium*, and *Bacteroides* were the dominant genera in both groups of mice (**Figure 4D**). Using LefSe analysis of gut microbial abundance in all samples, bacteria with $P < 0.05$ and LDA > 2.0 were screened, and we identified 16 different levels of differential bacteria ($P < 0.05$; **Table 3**). At the phylum level, the abundance of Firmicutes was reduced and Actinobacteria and Proteobacteria were increased in the GF diet group. At the genus level, the relative abundances of *Negativibacillus*, *Alloprevotella*, *Parasutterella*, *uncultured bacterium*, and *Bifidobacterium* were significantly elevated and *Ruminiclostridium* and *Enterococcus* were significantly reduced in the feces of the GF diet group compared with those from the SPF diet group (**Figure 4E**). Besides, at other different levels, the abundance of *Gammaproteobacteria*, *Betaproteobacteriales*, *Burkholderiaceae*, and *gut metagenome* increased significantly in the GF diet group, while *uncultured rumen bacterium* and *Lactobacillus gasseri* decreased significantly (**Figure 4E**).

Next, we used PICRUSt2 to assess the functional content of the microbiota based on the 16S data. A total of 14 Kyoto Encyclopedia of Genes and Genomes (KEGG) Orthology including related to Metabolism and Environmental Information Processing showed differences between GF diet and SPF diet group ($P < 0.05$; **Supplementary Table S2**). A significantly higher production capacity of biosynthesis of amino acids, biosynthesis of secondary metabolites, biosynthesis of antibiotics, metabolic pathways, phenylalanine, tyrosine and tryptophan biosynthesis, 2-Oxocarboxylic acid metabolism, cysteine and methionine metabolism and histidine metabolism was observed in the GF diet group. However, compared with the SPF diet group, phosphotransferase system (PTS), starch and sucrose metabolism, glycolysis/gluconeogenesis, amino sugar and nucleotide sugar metabolism, fructose and mannose metabolism, the two-component system showed significantly lower in the GF diet group (**Figure 4F**).

GF Diet Intake Changes Metabolic Profiles of Serum in SPF Mice

Serum from both groups of mice was collected for non-targeted metabolomic analysis on the GC-TOF/MS platform and a total of 144 metabolites were identified. The classes of metabolites identified and the number of metabolites in each class were shown in **Figure 5A**. The main metabolites detected were amino acids (42.07%), carbohydrates (16.51%), organic acids (13.53%), and fatty acids (11.22%). PCA was used to observe within- and between-group sample variability and possible outliers. The PCA score plot found a significant difference between the GF diet and SPF diet groups, indicating that the different

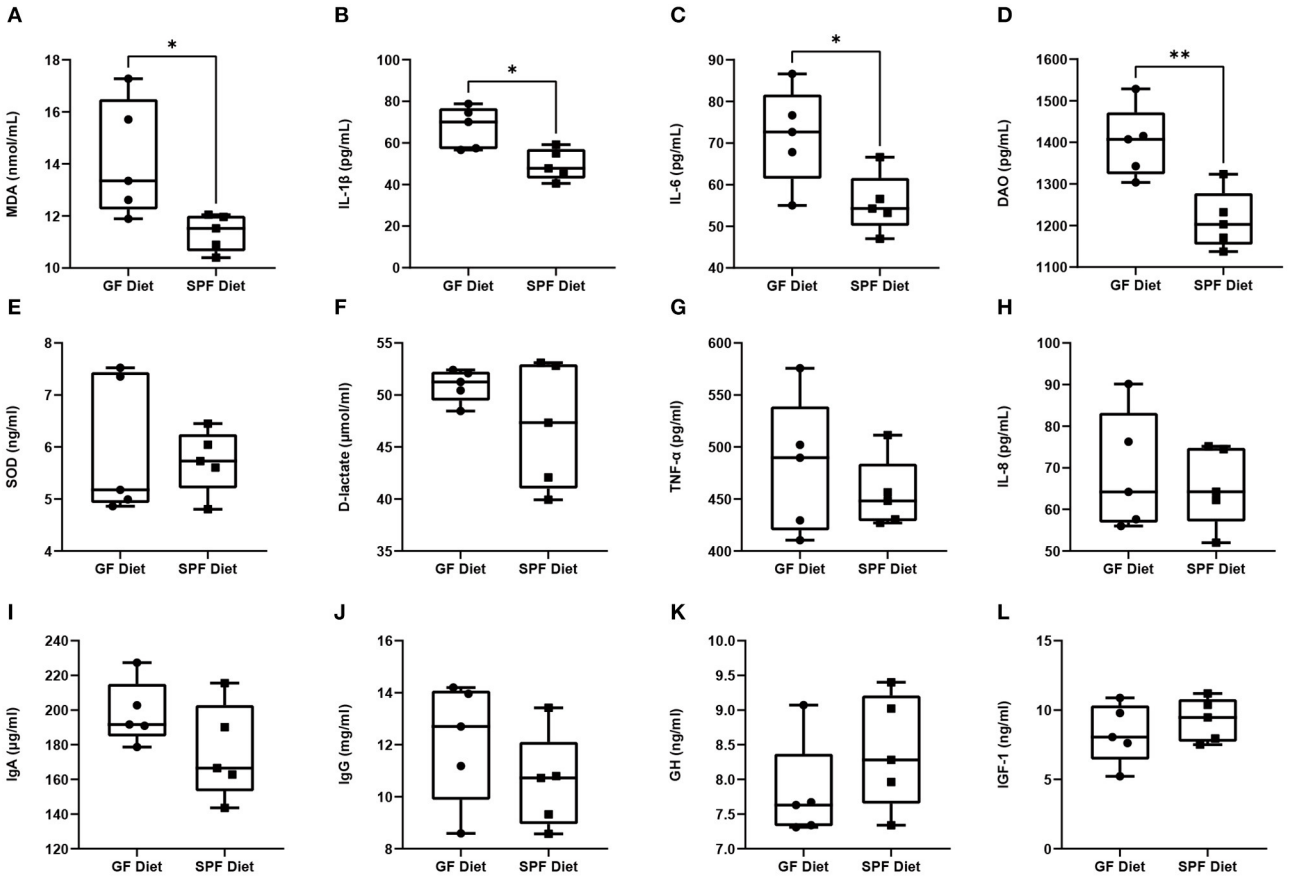

FIGURE 3 | Effect of GF diet on intestinal permeability, inflammatory response, oxidative stress, hormones and immune factors. **(A)** Malondialdehyde (MDA), **(B)** Interleukin-1β (IL-1β), **(C)** Interleukin-6 (IL-6), **(D)** Diamine oxidase (DAO), **(E)** Superoxide dismutase (SOD), **(F)** D-lactate (D-LA), **(G)** Tumor necrosis factors-α (TNF-α), **(H)** Interleukin-8 (IL-8), **(I)** Immunoglobulin A (IgA), **(J)** Immunoglobulin G (IgG), **(K)** Growth hormone (GH), and **(L)** Insulin-like growth factor 1 (IGF-1) contents in serum of SPF mice. Values are presented as mean ± SEM ($n = 5$). Statistical significance was calculated using unpaired *t*-test, $^{*}P < 0.05$; $^{**}P < 0.01$.

dietary treatments had a significant effect on serum metabolites (**Figure 5B**). Analysis of the various metabolites in the two groups of samples revealed significant differences in nucleotide and vitamin-related metabolites ($P < 0.05$; **Figure 5C**) and extremely significant differences in indole-related metabolites ($P < 0.01$; **Figure 5C**). Single and multidimensional tests were used to obtain the differential metabolites between the two groups and a total of 39 differential metabolites were identified ($P < 0.05$, **Table 4**). The major differential metabolites among the different dietary treatments were amino acids and carbohydrates, followed by organic acids and fatty acids, and others (**Figure 5D**).

For amino acids, the GF diet significantly increased the content of valine, leucine, and aminoadipic acid ($P < 0.05$) and extremely significantly increased the content of alpha-Aminobutyric acid ($P < 0.01$), while significantly decreasing the content of histidine, tryptophan and pipecolic acid ($P < 0.05$) and extremely significantly decreasing the content of serine and taurine ($P < 0.01$) compared with the SPF diet group. For carbohydrates, all metabolites were significantly higher ($P < 0.05$) in the GF diet group compared to the SPF diet group, except for mannitol, which was significantly lower in the GF diet group ($P < 0.05$). For organic Acids, similar to carbohydrates, all metabolites were elevated in the GF diet group except for lactic acid ($P < 0.05$). For fatty acids, all metabolites were increased in the GF diet group compared to the SPF diet ($P < 0.05$).

Through pathway analysis, all metabolites were mapped onto 32 KEGG metabolic pathways (**Supplementary Table S3**). Removing the pathways with an impact value of 0, 27 KEGG metabolic pathways were finally identified including amino acid metabolism (14 metabolites), carbohydrate metabolism (7 metabolites), metabolism of cofactors and vitamins (2 metabolites), metabolism of other amino acids (2 metabolites), lipid metabolism (2 metabolites), and nucleotide metabolism (2 metabolites) (**Figure 5E**).

Correlations Between Gut Microbiota and Metabolites, Hematological Parameters, and Intestinal Length

Next, we screened for differential metabolites by different classes and investigated potential associations between all levels of differential gut microbiota and metabolites, hematological

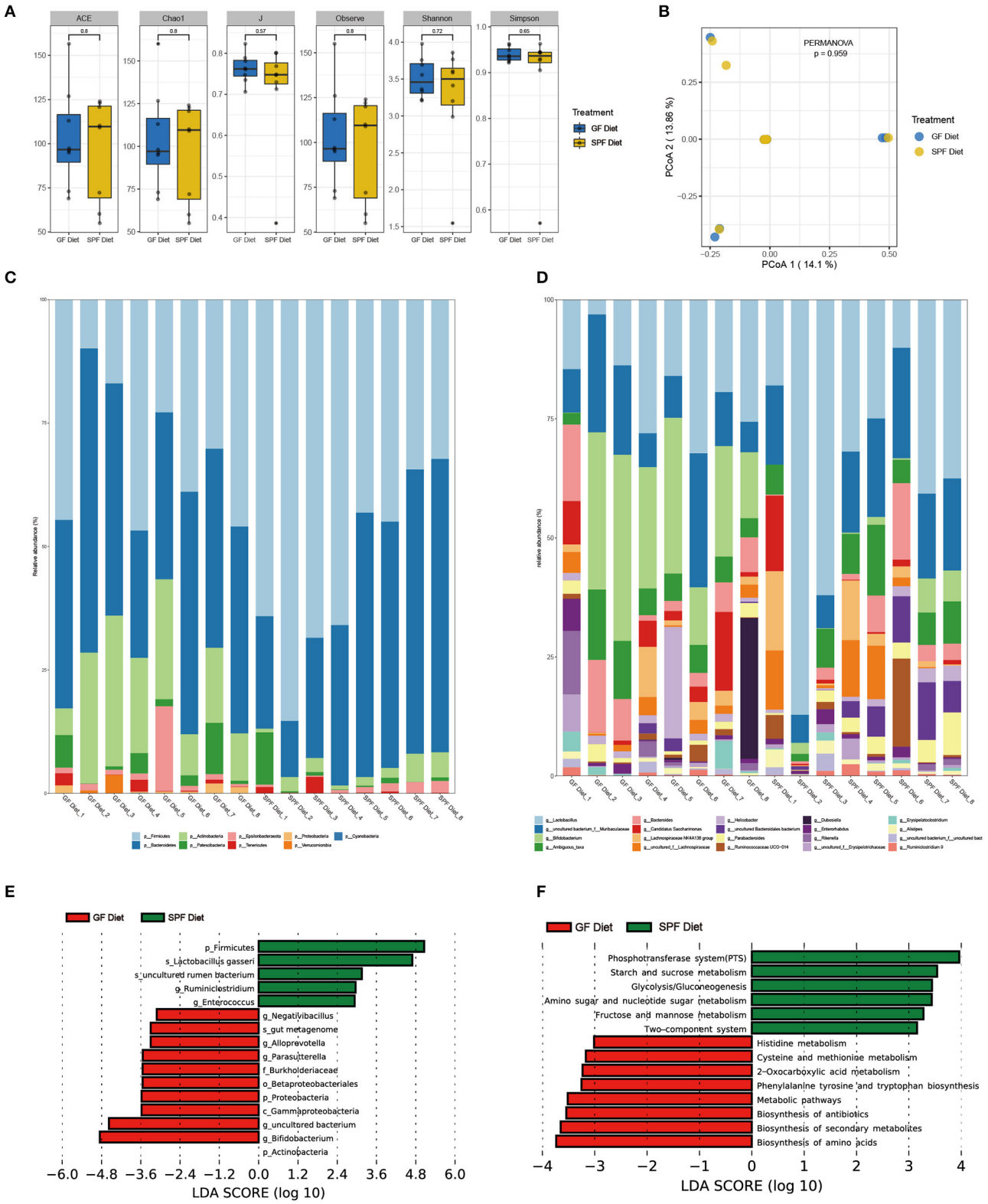

FIGURE 4 | Effect of GF diet on fecal microbial community of SPF mice. **(A)** Fecal microbial α-diversity. **(B)** Principal coordinates analysis (PCoA) based on the total OTUs. The phylum **(C)** and the genus **(D)** in relative abundance of the fecal microbiota. **(E)** Identification of differential bacterial taxa by LefSe tool (LDA score > 2.0). The length of the column is proportional to the taxa abundance. **(F)** Assess the functional content of microbiota.

TABLE 3 | All levels of differential bacteria in the feces between the GF diet group and the SPF diet group.

Microbial taxa	LDA	Enrichment	*P*-value
p_Actinobacteria	4.865	GF diet	0.001
p_Firmicutes	5.055	SPF diet	0.046
p_Proteobacteria	3.575	GF diet	0.013
c_Gammaproteobacteria	3.577	GF diet	0.007
o_Betaproteobacteriales	3.541	GF diet	0.027
f_Burkholderiaceae	3.541	GF diet	0.027
g_Alloprevotella	3.295	GF diet	0.027
g_Bifidobacterium	4.852	GF diet	0.008
g_Enterococcus	2.931	SPF diet	0.011
g_Negativibacillus	3.112	GF diet	0.027
g_Parasutterella	3.540	GF diet	0.027
g_Ruminiclostridium	2.960	SPF diet	0.027
g_unculted bacterium	4.571	GF diet	0.036
s_gut metagenome	3.295	GF diet	0.027
s_Lactobacillus gasseri	4.692	SPF diet	0.027
s_uncultured rumen bacterium	3.152	SPF diet	0.008

p, Phylum; c, Class; o, Order; f, Family; g, Genus; s, Species.

parameters and intestinal length. As shown in the heatmap in **Figure 6**, Actinobacteria and *Bifidobacterium* ware significantly positively related to leucine, aminoadipic acid, threonic acid, fructose 6-phosphate, glucose 6-phosphate, myristic acid, 11Z-Eicosenoic acid, Behenic acid 3-Hydroxybutyric acid, DHA and glycolic acid while significantly negatively related to taurine, tryptophan, mannitol, and xanthosine. Moreover, another bacterium that significantly affects metabolites is *Alloprevotella*, which was significantly positively to glucose 6-phosphate, DHA, Glycolic acid and 2-Hydroxybutyric acid while significantly negatively related to taurine, histidine, tryptophan, and mannitol. For hematological parameters, Several bacteria from Proteobacteria (*Parasutterella*, *Burkholderiaceae*, *Betaproteobacteriales*, *Gammaproteobacteria*) were significantly positively correlated with MON% and negatively correlated with RDWs. For intestinal length, *Negativibacillus* was significantly negatively related to the length of the small intestine and colon.

DISCUSSION

Extensive studies of the gut microbiota have shown that diet can regulate the composition and function of the microbial community in the intestine (11, 34–36). Furthermore, diet drives the metabolism of the gut microbiota, making metabolites a link between diet and different physiological states (13, 37, 38). A notable example is that high-fat diet can alter the microbiota structure and metabolic profile of mice, leading to an inflammatory response and impairment of intestinal barrier function (3, 4). In our study, we measured the actual nutrient content in GF and SPF diets. Although we added more nutritional ingredients to the GF diet, we found that the nutrient content of the GF diet was lower than that of the SPF diet. This is because high dose irradiation leads to nutrient loss in the GF diet. Consistent with previous reports, we found that irradiation led to a reduction in vitamins, amino acids, and some minerals in the GF diet (27, 28, 39).

Diets with different nutrient contents lead to differences in the microbiota and metabolic profile of the organism (7, 40). In the present study, we observed differences in gut microbiota and serum metabolism in SPF mice due to GF diet. For gut microbiota, the relative abundance of Firmicutes was reduced and the abundance of Bacteroidetes was increased in the GF diet group. This is possibly due to the low fiber content of the GF diet. Previous studies have shown that the fiber content of the diet correlates with the ratio of Firmicutes/Bacteroidetes, with the lower the fiber content, the higher the Firmicutes/Bacteroidetes ratio (41). Furthermore, we found that the abundance of several inflammation-associated microbiotas was significantly upregulated in the GF diet group, including Proteobacteria, *Burkholderiaceae*, *Alloprevotella*, and *Parasutterella*. Studies have previously shown that Proteobacteria and *Parasutterella* are associated with dysbiosis of the gut microbiota and chronic inflammation of the gut (42–44). *Burkholderiaceae* is associated with the development of Inflammatory bowel disease (IBD) (45) and *Alloprevotella* associated with metabolic disorders due to unhealthy diet (46). These suggested that the GF diet affects the intestine by increasing harmful bacteria in the gut. By metabolomic analysis, we found that the GF diet resulted in different metabolic patterns in the serum. For specifically affected metabolites, the GF diet increased the content of alpha-aminobutyric acid, valine, leucine, and aminoadipic acid compared with the SPF diet. Increased levels of alpha-aminobutyric acid are thought to be a marker for a range of diseases (47, 48). Valine and leucine are branched-chain amino acids (BCAA) and recent studies have reported a role for BBCA in the development of diseases such as type 2 diabetes (T2D), IBD, and cardiovascular disease (49, 50). Moreover, we observed differences in the KEGG metabolic pathway between the GF diet and SPF diet groups mainly in amino acid metabolism. Besides the low amino acid content observed in GF diet, amino acid imbalance may also have a detrimental effect on SPF mice. Amino acid imbalance causes many diseases of the body (51). Recent studies have shown that imbalance of amino acids, especially the ratio of BCAA to non-BCAA (especially tryptophan and threonine) altered the whole-body metabolism in mice (52). Further analysis revealed that Actinobacteria, *Bifidobacterium*, *Negativibacillus*, *Alloprevotella*, and *gut metagenom* were negatively related to the abundance of Taurine, Histidine, and Tryptophan, while Actinobacteria and *Bifidobacterium* were positively correlated with several BCAAs. This suggests that alterations in specific bacteria disrupt the amino acid balance and thus lead to changes in the metabolic profile.

MON are circulating white blood cells that are important in both innate and adaptive immunity and play a major role in immune defense, inflammation and tissue remodeling (53). The numbers of MON increase during acute infection and inflammation (54). We found an increase in the number of MON in the GF diet group. We also measured several serum indicators

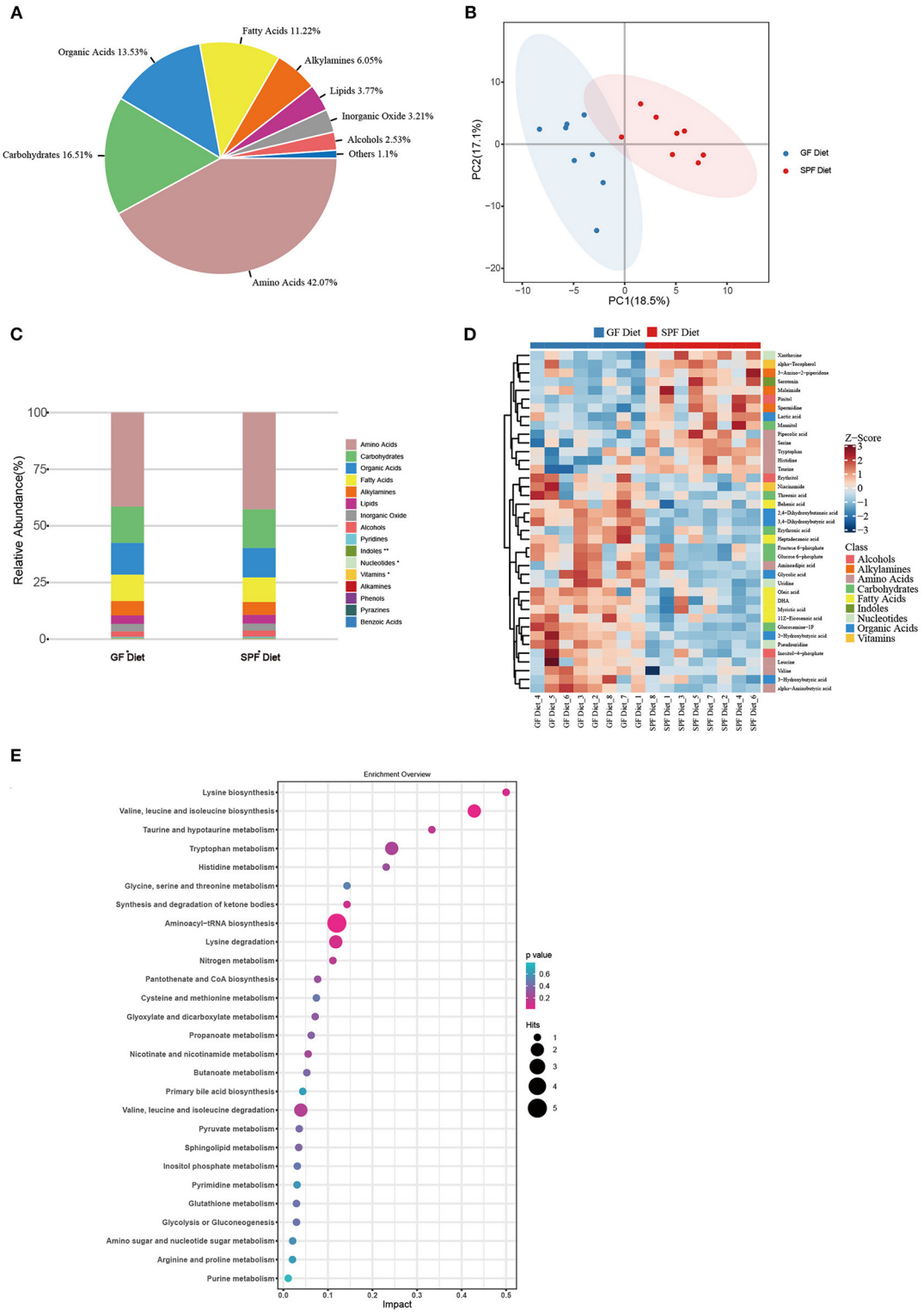

FIGURE 5 | Effect of GF diet on metabolic profiles of serum in SPF mice. **(A)** Distribution of metabolite classes. **(B)** Principal component analysis (PCA) score plot of all samples. **(C)** Distribution of the relative abundance of metabolites of each Class in different groups. **(D)** Heatmap of the potential biomarkers. The relative abundance values of metabolites in different samples are depicted by color intensity. **(E)** Pathway analysis bubble plot. The horizontal coordinate is the extent to which the pathway is affected, and the number of differential metabolites in the pathway is represented by graphs of different sizes. The *P*-values calculated by the enrichment analysis are described in terms of color intensity.

TABLE 4 | Altered metabolites in the serum between GF diet and SPF diet groups.

Metabolite	Class	GF diet	SPF diet	*P*-value
alpha-Aminobutyric acid	Amino acids	4.40 ± 1.36	2.27 ± 0.43	0.003
Valine	Amino acids	292.13 ± 51.84	202.03 ± 77.99	0.010
Leucine	Amino acids	311.77 ± 53.72	266.14 ± 19.39	0.028
Serine	Amino acids	81.38 ± 24.34	123.96 ± 15.43	0.002
Taurine	Amino acids	208.34 ± 134.03	358.64 ± 28.76	0.005
Aminoadipic acid	Amino acids	1.52 ± 0.50	1.02 ± 0.35	0.050
Histidine	Amino acids	16.75 ± 14.61	33.27 ± 8.73	0.025
Tryptophan	Amino acids	215.32 ± 18.35	235.34 ± 15.87	0.047
Pipecolic acid	Amino acids	7.93 ± 2.17	12.16 ± 3.08	0.011
Threonic acid	Carbohydrates	3.41 ± 0.89	2.58 ± 0.33	0.028
Erythronic acid	Carbohydrates	51.74 ± 13.75	37.79 ± 8.90	0.044
Glucosamine-1P	Carbohydrates	1.75 ± 0.31	0.84 ± 0.19	0.000
Mannitol	Carbohydrates	18.70 ± 2.89	24.21 ± 4.39	0.017
Fructose 6-phosphate	Carbohydrates	1.42 ± 0.34	0.93 ± 0.43	0.033
Glucose 6-phosphate	Carbohydrates	2.71 ± 0.73	1.53 ± 0.72	0.009
Myristic acid	Fatty acids	10.02 ± 1.18	7.55 ± 2.43	0.036
Heptadecanoic acid	Fatty acids	6.91 ± 1.09	5.14 ± 0.83	0.005
Oleic acid	Fatty acids	187.58 ± 31.14	146.53 ± 22.40	0.007
11Z-Eicosenoic acid	Fatty acids	3.88 ± 0.73	2.65 ± 0.51	0.003
DHA	Fatty acids	1.92 ± 0.14	1.30 ± 0.48	0.010
Behenic acid	Fatty acids	0.56 ± 0.08	0.44 ± 0.08	0.019
Lactic acid	Organic acids	365.47 ± 52.72	440.38 ± 49.46	0.016
Glycolic acid	Organic acids	29.80 ± 7.16	20.71 ± 2.71	0.010
2-Hydroxybutyric acid	Organic acids	7.68 ± 2.16	3.16 ± 0.68	0.000
3-Hydroxybutyric acid	Organic acids	477.18 ± 147	306.36 ± 105.92	0.027
3,4-Dihydroxybutyric acid	Organic acids	1.35 ± 0.20	0.69 ± 0.12	0.000
2,4-Dihydroxybutanoic acid	Organic acids	12.09 ± 1.49	5.88 ± 0.80	0.000
Erythritol	Alcohols	3.32 ± 0.49	2.84 ± 0.29	0.047
Pinitol	Alcohols	0.16 ± 0.05	0.55 ± 0.20	0.000
Inositol-4-phosphate	Alcohols	22.02 ± 2.79	18.63 ± 2.30	0.027
Maleimide	Alkylamines	9.19 ± 1.73	11.42 ± 2.05	0.046
3-Amino-2-piperidone	Alkylamines	3.89 ± 1.31	5.83 ± 1.47	0.021
Spermidine	Alkylamines	0.22 ± 0.10	0.46 ± 0.14	0.004
Pseudouridine	Nucleotides	6.46 ± 0.92	4.24 ± 0.44	0.000
Uridine	Nucleotides	0.80 ± 0.28	0.39 ± 0.16	0.007
Xanthosine	Nucleotides	0.07 ± 0.02	0.12 ± 0.03	0.002
Niacinamide	Vitamins	14.94 ± 2.77	23.49 ± 4.68	0.022
alpha-Tocopherol	Vitamins	4.40 ± 1.36	2.27 ± 0.43	0.010
Serotonin	Indoles	292.13 ± 51.84	202.03 ± 77.99	0.001

related to inflammation and found significantly higher levels of IL-1β and IL-6 in the GF diet group. IL-1β and IL-6 are key mediators of the inflammatory response (55). IL-1β affects T cell maturation and the proliferation of B cells. Besides, IL-1β promotes the expression of several inflammatory molecules such as nitric oxide and phospholipase A2 (56, 57). IL-6 is involved in the regulation of the acute phase response to injury and infection. Its dysregulation is associated with the development of various diseases such as IBD, multiple sclerosis and various cancers (58). Our data showed that IL-1β and IL-6 levels were significantly increased in the serum of GF diet mice. The RDW reflects the degree of heterogeneity of erythrocyte volume. The increase in RDW reflects a severe disruption of erythrocyte homeostasis and may be attributable to a variety of underlying metabolic abnormalities such as oxidative stress, inflammation, malnutrition and erythrocyte ruptured (59). We found RDW was significantly increased in the GF diet group of mice. Another indicator of oxidative stress observed to be significantly increased in the GF diet group was MDA. MDA is a metabolic product of free radical-induced peroxidation of unsaturated fatty acids in biological membranes, and its level reflects the degree of lipid peroxidation in the body and indirectly the degree of cellular

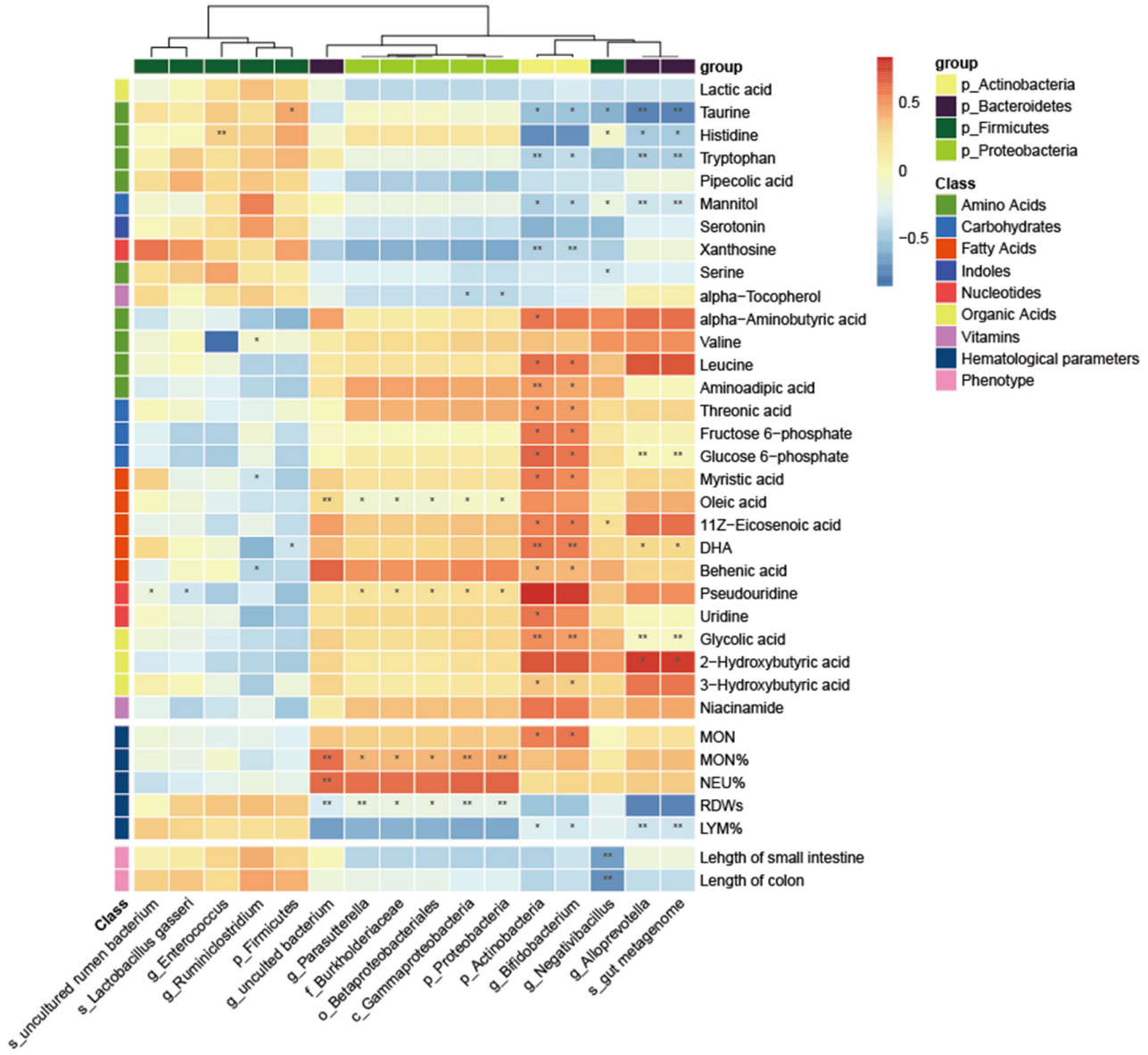

FIGURE 6 | Correlation heatmap between the differential microbiota and specific metabolites, hematological parameters and intestinal length. The Pearson correlation coefficient was used to examine the correlation. $^{*}P < 0.05$, $^{**}P < 0.01$.

damage (60, 61). Through correlation analysis, we found that these indicators correlated with the abundance of Proteobacteria. The altered abundance of Proteobacteria is one of the features of gut microbial dysbiosis, and its elevated abundance leads to intestinal epithelial dysfunction and intestinal inflammation (62, 63). These results suggest that the GF diet leads to inflammation and oxidative stress in the organism by increasing the abundance of Proteobacteria in the gut.

In the present study, we found intestinal dysplasia and impairment of intestinal barrier function in mice from the GF diet group. The length of the small intestine and colon in the mice from the GF diet group was extremely significantly shortened. The small intestine is the main digestive organ of the body and is the primary site for nutrient absorption. Villi expand the surface area of the intestine and help the body to absorb nutrients from food. Therefore, a decrease in the length of the villi is associated with decreased nutrient absorption, weight gain and fat accumulation in animals (64). We observed a significant negative correlation between *Negativibacillus* and small intestinal and colonic length. *Negativibacillus* is a pathogenic bacteria associated with gut dysbiosis or pediatric Crohn's disease (65, 66). D-LA, a chemical marker of the intestinal barrier, is present at low levels in healthy individuals, and levels of D-LA increase when the intestinal barrier is disrupted (67). A significant increase in

the serum concentrations of D-LA was observed in mice from GF diet, suggesting that GF diet intake induced an increase in intestinal permeability in mice.

Weight loss in SPF mice is attributed to inflammation, intestinal dysplasia and oxidative stress following GF diet intake. The intake of GF diet altered the gut microbiota and serum metabolic profile of mice, and the increase of harmful bacteria in the gut led to damage of the intestinal barrier function (68). Current research suggests that disruption of intestinal barrier function leads to increased intestinal permeability, which facilitates the transport of harmful substances and pathogens to the bloodstream, leading to inflammation and oxidative stress (69, 70). Pathophysiology of various diseases associated with inflammation and oxidative stress. Oxidative stress can promote inflammation, conversely, inflammatory processes also promote oxidative stress and injury. Both of them can cause injury to cells and contribute to a diverse set of pathologies (71, 72). Overall, diet altered the gut microbiota, leading to damage to the intestinal barrier and inflammation, ultimately disrupting the healthy physiological state of the mice.

CONCLUSIONS

In the present study, we found considerable differences in nutrient content between the GF and SPF diets and due to the special nutritional composition, the GF diet altered the structure of the gut microbiota, increased pro-inflammatory bacteria in the gut such as Proteobacteria, *Burkholderiaceae*, *Alloprevotella*, and *Parasutterella*. In addition, the GF diet altered the serum metabolic profile especially amino acid metabolism in SPF mice. Furthermore, the GF diet was found to cause a significant increase in levels of MDA, IL-1β, IL-6, and D-lactate in the serum and these indicators in the serum indicated that the GF diet destroyed the intestinal barrier, leading to inflammatory responses and oxidative stress, which ultimately led to weight loss in SPF mice. These results are helpful to enhance our understanding of the effects of different nutrient composition diets on host physiological status through the gut microbiota, and also provide new ideas for the scientific selection of diets for experimental animals.

DATA AVAILABILITY STATEMENT

The datasets presented in this study can be found in online repositories. The names of the repository/repositories and accession number(s) can be found in the article/**Supplementary Materials**.

ETHICS STATEMENT

The animal study was reviewed and approved by Scientific Ethics Committee of Huazhong Agricultural University.

AUTHOR CONTRIBUTIONS

ZWu, WC, and ST designed the experiments. ZWu, XT, YW, and MD carried out the experiments and collected the samples. YY and HZ performed the analysis of samples. ZWa, SF, and HZ analyzed the 16S rRNA and metabolomics data. ZWu drafted the manuscript. ST, YX, and HW revised the manuscript. All authors contributed to the article and approved the submitted version.

FUNDING

This work was supported by the National Nature Science Foundation of China (31902189) and the Fundamental Research Funds for the Central Universities (2662020DKQD004, 2662019PY012).

SUPPLEMENTARY MATERIAL

The Supplementary Material for this article can be found online at: https://www.frontiersin.org/articles/10.3389/fnut.2021.813757/full#supplementary-material

REFERENCES

1. Freire R. Scientific evidence of diets for weight loss: different macronutrient composition, intermittent fasting, and popular diets. *Nutrition.* (2019) 69:110549. doi: 10.1016/j.nut.2019.07.001
2. Me N, Bee Ling T. Effect of high-fat diets on oxidative stress, cellular inflammatory response and cognitive function. *Nutrients.* (2019) 11:1–22. doi: 10.3390/nu11112579
3. Tan R, Dong H, Chen Z, Jin M, Yin J, Li H, et al. Intestinal microbiota mediates high-fructose and high-fat diets to induce chronic intestinal inflammation. *Front Cell Infect Microbiol.* (2021) 11:654074. doi: 10.3389/fcimb.2021.654074
4. Yang J, Wei H, Zhou Y, Szeto C-H, Li C, Lin Y, et al. High-fat diet promotes colorectal tumorigenesis through modulating gut microbiota and metabolites. *Gastroenterology.* (2022) 162:135–49.e2. doi: 10.1053/j.gastro.2021.08.041
5. Kiros T, Derakhshani H, Pinloche E, D'Inca R, Marshall J, Auclair E, et al. Effect of live yeast *Saccharomyces cerevisiae* (Actisaf Sc 47) supplementation on the performance and hindgut microbiota composition of weanling pigs open. *Sci Rep.* (2018) 8:5315. doi: 10.1038/s41598-018-23373-8
6. Liu B, Zhu X, Cui Y, Wang W, Liu H, Li Z, et al. Consumption of dietary fiber from different sources during pregnancy alters sow gut microbiota and improves performance and reduces inflammation in sows and piglets. *mSystems.* (2021) 6:e00591-20. doi: 10.1128/mSystems.00591-20
7. Dalby M, Ross A, Walker A, Morgan P. Dietary uncoupling of gut microbiota and energy harvesting from obesity and glucose tolerance in mice. *Cell Rep.* (2017) 21:1521–33. doi: 10.1016/j.celrep.2017.10.056
8. Omary MB, Cohen DE, Gut E-O, Jalan R, Low MJ, Nathanson MH, et al. Not all mice are the same: standardization of animal research data presentation. *J Hepatol.* (2016) 64:894–95. doi: 10.1002/hep.28608
9. Lynch S, Pedersen O. The human intestinal microbiome in health and disease. *N Engl J Med.* (2016) 375:2369–79. doi: 10.1056/NEJMra1600266
10. Sommer F, Bäckhed F. The gut microbiota—masters of host development and physiology. *Nat Rev Microbiol.* (2013) 11:227–38. doi: 10.1038/nrmicro2974
11. Wu G, Chen J, Hoffmann C, Bittinger K, Chen Y-Y, Keilbaugh S, et al. Linking long-term dietary patterns with gut microbial enterotypes. *Science.* (2011) 334:105–8. doi: 10.1126/science.1208344
12. Koh A, De Vadder F, Kovatcheva-Datchary P, Bäckhed F. From dietary fiber to host physiology: short-chain fatty acids as key bacterial metabolites. *Cell.* (2016) 165:1332–45. doi: 10.1016/j.cell.2016.05.041
13. Sonnenburg J, Bäckhed F. Diet–microbiota interactions as moderators of human metabolism. *Nature.* (2016) 535:56–64. doi: 10.1038/nature18846

14. Raman M, Ambalam P, Doble M. Short-chain fatty acids. In: Raman M, Ambalam P, Doble M, editors. *Probiotics and Bioactive Carbohydrates in Colon Cancer Management*. New Delhi: Springer India (2016). p. 97–115.
15. Morrison D, Preston T. Formation of short chain fatty acids by the gut microbiota and their impact on human metabolism. *Gut Microbes.* (2016) 7:1–12. doi: 10.1080/19490976.2015.1134082
16. van der Hee B, Wells JM. Microbial regulation of host physiology by short-chain fatty acids. *Trends Microbiol.* (2021) 29:700–12. doi: 10.1016/j.tim.2021.02.001
17. Takiishi T, Morales C, Câmara N. Intestinal barrier and gut microbiota: shaping our immune responses throughout life. *Tissue Barriers.* (2017) 5:e1373208. doi: 10.1080/21688370.2017.1373208
18. Ghosh S, Whitley CS, Haribabu B, Jala VR. Regulation of intestinal barrier function by microbial metabolites. *Cell Mol Gastroenterol Hepatol.* (2021) 11:1463–82. doi: 10.1016/j.jcmgh.2021.02.007
19. Tilg H, Zmora N, Adolph T, Elinav E. The intestinal microbiota fuelling metabolic inflammation. *Nat Rev Immunol.* (2019) 20:40–54. doi: 10.1038/s41577-019-0198-4
20. Tomasello G, Mazzola M, Leone A, Sinagra E, Zummo G, Farina F, et al. Nutrition, oxidative stress and intestinal dysbiosis: influence of diet on gut microbiota in inflammatory bowel diseases. *Biomed Papers.* (2016) 160:461–6. doi: 10.5507/bp.2016.052
21. LeBlanc JG, Milani C, Savoy G, Sesma F, Van Sinderen D, Ventura M. Bacteria as vitamin suppliers to their host: a gut microbiota perspective. *Curr Opin Biotechnol.* (2012) 24:160–8. doi: 10.1016/j.copbio.2012.08.005
22. Li J, Wei H. Establishment of an efficient germ-free animal system to support functional microbiome research. *Sci China Life Sci.* (2019) 62:1400–3. doi: 10.1007/s11427-019-9832-9
23. Al-Asmakh M, Zadjali F. Use of germ-free animal models in microbiota-related research. *J Microbiol Biotechnol.* (2015) 25:1583–8. doi: 10.4014/jmb.1501.01039
24. Wostmann BS. The germfree animal in nutritional studies. *Annu Rev Nutr.* (1981) 1:257–79. doi: 10.1146/annurev.nu.01.070181.001353
25. Uzbay T. Germ-free animal experiments in the gut microbiota studies. *Curr Opin Pharmacol.* (2019) 49:6–10. doi: 10.1016/j.coph.2019.03.016
26. Lin L, Song J, Li J, Zuo X, Wei H, Yang C, et al. Imaging the *in vivo* growth patterns of bacteria in human gut microbiota. *Gut Microbes.* (2021) 13:1960134. doi: 10.1080/19490976.2021.1960134
27. Caulfield C, Cassidy J, Kelly J. Effects of gamma irradiation and pasteurization on the nutritive composition of commercially available animal diets. *J Am Assoc Lab Anim Sci.* (2008) 47:61–6.
28. Aquino K. *Sterilization by Gamma Irradiation*. In: Adrovic F, editor. Gamma Radiation. Intech Open (2012). p. 172–202.
29. Bolyen E, Rideout JR, Dillon MR, Bokulich NA, Abnet CC, Al-Ghalith GA, et al. Reproducible, interactive, scalable and extensible microbiome data science using QIIME 2. *Nat Biotechnol.* (2019) 37:852–7. doi: 10.1038/s41587-019-0209-9
30. Callahan BJ, McMurdie PJ, Rosen MJ, Han AW, Johnson AJ, Holmes SP. DADA2: high-resolution sample inference from illumina amplicon data. *Nat Methods.* (2016) 13:581–3. doi: 10.1038/nmeth.3869
31. Pedregosa F, Varoquaux G, Gramfort A, Michel V, Thirion B, Grisel O, et al. Scikit-learn: machine learning in python. *J Mach Learn Res*. (2011) 12:2825–30.
32. Segata N, Izard J, Waldron L, Gevers D, Miropolsky L, Garrett WS, et al. Metagenomic biomarker discovery and explanation. *Genome Biol.* (2011) 12:R60. doi: 10.1186/gb-2011-12-6-r60
33. Douglas GM, Maffei VJ, Zaneveld JR, Yurgel SN, Brown JR, Taylor CM, et al. PICRUSt2 for prediction of metagenome functions. *Nat Biotechnol.* (2020) 38:685–8. doi: 10.1038/s41587-020-0548-6
34. David L, Maurice C, Carmody R, Gootenberg D, Button J, Wolfe B, et al. Diet rapidly and reproducibly alters the gut microbiome. *Nature.* (2013) 505:559–63. doi: 10.1038/nature12820
35. Cotillard A, Kennedy S, Kong L, Prifti E, Pons N, Le Chatelier E, et al. Dietary intervention impact on gut microbial gene richness. *Nature.* (2013) 500:585–90. doi: 10.1038/nature12480
36. Walker A, Ince J, Duncan S, Webster L, Holtrop G, Ze X, et al. Dominant and diet-responsive groups of bacteria within the human colonic microbiota. *ISME J.* (2011) 5:220–30. doi: 10.1038/ismej.2010.118
37. Asnicar F, Berry S, Valdes A, Nguyen L, Piccinno G, Drew D, et al. Microbiome connections with host metabolism and habitual diet from 1,098 deeply phenotyped individuals. *Nat Med.* (2021) 27:321–32. doi: 10.1038/s41591-020-01183-8
38. Nicolas G, Chang P. Deciphering the chemical lexicon of host–gut microbiota interactions. *Trends Pharmacol Sci.* (2019) 40:430–45. doi: 10.1016/j.tips.2019.04.006
39. Kilcast D. Effect of irradiation on vitamins. *Food Chem.* (1994) 49:157–64. doi: 10.1016/0308-8146(94)90152-X
40. Galiè S, Gavilán JG, Camacho-Barcia L, Atzeni A, Muralidharan J, Papandreou C, et al. Effects of the mediterranean diet or nut consumption on gut microbiota composition and fecal metabolites and their relationship with cardiometabolic risk factors. *Mol Nutr Food Res.* (2021) 65:2000982. doi: 10.1002/mnfr.202000982
41. García-Mantrana I, Selma-Royo M, Baena C, Collado MC. Shifts on gut microbiota associated to mediterranean diet adherence and specific dietary intakes on general adult population. *Front Microbiol.* (2018) 9:890. doi: 10.3389/fmicb.2018.00890
42. Chen C, Li F, Wei W, Wang Z, Dai J, Hao L, et al. The metagenome of the female upper reproductive tract. *Giga Sci.* (2018) 7:giy107. doi: 10.1093/gigascience/giy107
43. Huang C, Chen J, Wang J, Zhou H, Lu Y, Lou L, et al. Dysbiosis of intestinal microbiota and decreased antimicrobial peptide level in paneth cells during hypertriglyceridemia-related acute necrotizing pancreatitis in rats. *Front Microbiol.* (2017) 8:776. doi: 10.3389/fmicb.2017.00776
44. Rizzatti G, Lopetuso L, Gibiino G, Binda C, Gasbarrini A. Proteobacteria: a common factor in human diseases. *BioMed Res Int.* (2017) 2017:1–7. doi: 10.1155/2017/9351507
45. Sim W, Wagner J, Cameron DJS, Catto-Smith A, Bishop R, Kirkwood CD. Novel burkholderiales 23S rRNA genes identified in ileal biopsy samples from children: preliminary evidence that a subtype is associated with perianal Crohn's disease. *J Clin Microbiol.* (2010) 48:1939–42. doi: 10.1128/JCM.02261-09
46. Dong Z, Liu Y, Pan H, Wang H, Wang X, Xu X, et al. The effects of high-salt gastric intake on the composition of the intestinal microbiota in Wistar rats. *Med Sci Monitor.* (2020) 26:e922160. doi: 10.12659/MSM.922160
47. Effros R. Alpha aminobutyric acid, an alternative measure of hepatic injury in sepsis? *Transl Res.* (2011) 158:326–7. doi: 10.1016/j.trsl.2011.07.003
48. Nair M, Yao D, Chen C, Pieters M. Serum metabolite markers of early Mycoplasma hyopneumoniae infection in pigs. *Vet Res.* (2019) 50:1–10. doi: 10.1186/s13567-019-0715-2
49. White P, Newgard C. Branched-chain amino acids in disease. *Science.* (2019) 363:582–3. doi: 10.1126/science.aav0558
50. Xie D, Li F, Pang D, Zhao S, Zhang M, Ren Z, et al. Systematic metabolic profiling of mice with dextran sulfate sodium-induced colitis. *J Inflammation Res.* (2021) 14:2941–53. doi: 10.2147/JIR.S313374
51. Roth E, Druml W. Plasma amino acid imbalance: dangerous in chronic diseases? *Curr Opin Clin Nutr Metabolic Care.* (2010) 14:67–74. doi: 10.1097/MCO.0b013e328341368c
52. Solon-Biet S, Cogger V, Pulpitel T, Wahl D, Clark X, Bagley E, et al. Branched-chain amino acids impact health and lifespan indirectly via amino acid balance and appetite control. *Nat Metab.* (2019) 1:532–45. doi: 10.1038/s42255-019-0059-2
53. Kratofil R, Kubes P, Deniset J. Monocyte conversion during inflammation and injury. *Arterioscler Thromb Vasc Biol.* (2016) 37:ATVBAHA.116.308198. doi: 10.1161/ATVBAHA.116.308198
54. Furth R. Monocyte production during inflammation. *Compar Immunol Microbiol Infect Dis.* (1985) 8:205–11. doi: 10.1016/0147-9571(85)90045-1
55. Boshtam M, Asgary S, Kouhpayeh S, Shariati L, Khanahmad H. Aptamers against pro- and anti-inflammatory cytokines: a review. *Inflammation.* (2017) 40:340–9. doi: 10.1007/s10753-016-0477-1
56. Gupta P, Barthwal M. IL-1 β genesis: the art of regulating the regulator. *Cell Mol Immunol.* (2018) 15:998–1000. doi: 10.1038/s41423-018-0054-7

57. Lopez-Castejon G, Brough D. Understanding the mechanism of IL-1β secretion. *Cytokine Growth Factor Rev.* (2011) 22:189–95. doi: 10.1016/j.cytogfr.2011.10.001
58. Tanaka T, Narazaki M, Kishimoto T. IL-6 in inflammation, immunity, and disease. *Cold Spring Harb Perspect Biol.* (2014) 6:a016295. doi: 10.1101/cshperspect.a016295
59. Salvagno GL, Sanchis-Gomar F, Picanza A, Lippi G. Red blood cell distribution width: A simple parameter with multiple clinical applications. Critical Reviews in *Crit Rev Clin Lab Sci*. (2015) 52:86–105. doi: 10.3109/10408363.2014.992064
60. Jové M, Mota-Martorell N, Pradas I, Martín-Gari M, Ayala V, Pamplona R. The advanced lipoxidation end-product malondialdehyde-lysine in aging and longevity. *Antioxidants.* (2020) 9:1132. doi: 10.3390/antiox9111132
61. Marnett L, Buck J, Tuttle M, Basu A, Bull A. Distribution of oxidation of malondialdehyde in mice. *Prostaglandins.* (1985) 30:241–54. doi: 10.1016/0090-6980(85)90188-1
62. Litvak Y, Byndloss M, Tsolis R, Baumler A. Dysbiotic proteobacteria expansion: a microbial signature of epithelial dysfunction. *Curr Opin Microbiol.* (2017) 39:1–6. doi: 10.1016/j.mib.2017.07.003
63. Hamilton A. *Proteus* spp. as putative gastrointestinal pathogens. *Clin Microbiol Rev.* (2018) 31:e00085-17. doi: 10.1128/CMR.00085-17
64. Taylor SR, Ramsamooj S, Liang RJ, Katti A, Pozovskiy R, Vasan N, et al. Dietary fructose improves intestinal cell survival and nutrient absorption. *Nature*. (2021) 597:263–7. doi: 10.1038/s41586-021-03827-2
65. Wang Y, Gao X, Zhang X, Xiao F, Hu H, Li X, et al. Microbial and metabolic features associated with outcome of infliximab therapy in pediatric Crohn's disease. *Gut Microbes.* (2021) 13:1–18. doi: 10.1080/19490976.2020.1865708
66. Tang S, Zhong R, Yin C, Su D, Xie J, Chen L, et al. Exposure to high aerial ammonia causes hindgut dysbiotic microbiota and alterations of microbiota-derived metabolites in growing pigs. *Front Nutr.* (2021) 8:689818. doi: 10.3389/fnut.2021.689818
67. Ji J, Gu Z, Li H, Su L, Liu Z. Cryptdin-2 predicts intestinal injury during heatstroke in mice. *Int J Mol Med.* (2017) 41:137–46. doi: 10.3892/ijmm.2017.3229
68. Sharkey K, Beck P, McKay D. Neuroimmunophysiology of the gut: advances and emerging concepts focusing on the epithelium. *Nat Rev Gastroenterol Hepatol.* (2018) 15:1. doi: 10.1038/s41575-018-0051-4
69. Grosheva I, Zheng D, Levy M, Polansky O, Lichtenstein A, Golani O, et al. High-throughput screen identifies host and microbiota regulators of intestinal barrier function. *Gastroenterology*. (2020) 159:1807–23. doi: 10.1053/j.gastro.2020.07.003
70. König J, Wells J, Cani P, García-Ródenas C, MacDonald T, Mercenier A, et al. Human intestinal barrier function in health and disease. *Clin Transl Gastroenterol.* (2016) 7:e196. doi: 10.1038/ctg.2016.54
71. Chatterjee S. Chapter Two - Oxidative Stress, Inflammation, and Disease. In: Dziubla T, Butterfield DA, editors. *Oxidative Stress and Biomaterials*. Academic Press (2016). p. 35–58.
72. Bander Z, Nitert M, Mousa A, Naderpoor N. The gut microbiota and inflammation: an overview. *Int J Environ Res Public Health.* (2020) 17:7618. doi: 10.3390/ijerph17207618

Conflict of Interest: The authors declare that the research was conducted in the absence of any commercial or financial relationships that could be construed as a potential conflict of interest.

frontiers in Nutrition

ORIGINAL RESEARCH
published: 17 January 2022
doi: 10.3389/fnut.2021.815922

Hydroxytyrosol Benefits Boar Semen Quality via Improving Gut Microbiota and Blood Metabolome

Hui Han[1,2†], Ruqing Zhong[1†], Yexun Zhou[1,2], Bohui Xiong[1], Liang Chen[1], Yue Jiang[1], Lei Liu[1], Haiqing Sun[3], Jiajian Tan[3], Fuping Tao[4], Yong Zhao[1] and Hongfu Zhang[1*]*

[1] State Key Laboratory of Animal Nutrition, Institute of Animal Sciences, Chinese Academy of Agricultural Sciences, Beijing, China, [2] Precision Livestock and Nutrition Unit, Gembloux Agro-Bio Tech, University of Liège, Gembloux, Belgium, [3] YangXiang Joint Stock Company, Guigang, China, [4] Hangzhou Viablife Biotech Co., Ltd., Hangzhou, China

Semen quality is one of the most important factors for the success of artificial insemination which has been widely applied in swine industry to take the advantages of the superior genetic background and higher fertility capability of boars. Hydroxytyrosol (HT), a polyphenol, has attracted broad interest due to its strong antioxidant, anti-inflammatory, and antibacterial activities. Sperm plasma membrane contains a large proportion of polyunsaturated fatty acids which is easily impaired by oxidative stress and thus to diminish semen quality. In current investigation, we aimed to explore the effects of dietary supplementation of HT on boar semen quality and the underlying mechanisms. Dietary supplementation of HT tended to increase sperm motility and semen volume/ejaculation. And the follow-up 2 months (without HT, just basal diet), the semen volume was significantly more while the abnormal sperm was less in HT group than that in control group. HT increased the "beneficial microbes" *Bifidobacterium*, *Lactobacillus*, *Eubacterium, Intestinimonas, Coprococcus, and Butyricicoccus*, however, decreased the relative abundance of "harmful microbes" *Streptococcus*, *Oscillibacter*, *Clostridium_sensu_stricto*, *Escherichia*, *Phascolarctobacterium*, and *Barnesiella*. Furthermore, HT increased plamsa steroid hormones such as testosterone and its derivatives, and antioxidant molecules while decreased bile acids and the derivatives. All the data suggest that HT improves gut microbiota to benefit plasma metabolites then to enhance spermatogenesis and semen quality. HT may be used as dietary additive to enhance boar semen quality in swine industry.

Keywords: hydroxytyrosol, boar, semen quality, gut microbiota, blood metabolome

OPEN ACCESS

Edited by:
Fengjiao Xin, Laboratory of Biomanufacturing and Food Engineering, Institute of Food Science and Technology, Chinese Academy of Agricultural Science (CAAS), China

Reviewed by:
Jetty Chung-Yung Lee, The University of Hong Kong, Hong Kong SAR, China
Yan Lin, Sichuan Agricultural University, China
Fengjie Huang, Shanghai Jiao Tong University, China

***Correspondence:**
Yong Zhao
yzhao818@hotmail.com; yong.zhao@murdoch.edu.au
Hongfu Zhang
zhanghongfu@caas.cn

† These authors have contributed equally to this work

Specialty section:
This article was submitted to Nutrition and Microbes, a section of the journal Frontiers in Nutrition

Received: *16 November 2021*
Accepted: *23 December 2021*
Published: *17 January 2022*

Citation:
Han H, Zhong R, Zhou Y, Xiong B, Chen L, Jiang Y, Liu L, Sun H, Tan J, Tao F, Zhao Y and Zhang H (2022) Hydroxytyrosol Benefits Boar Semen Quality via Improving Gut Microbiota and Blood Metabolome. Front. Nutr. 8:815922. doi: 10.3389/fnut.2021.815922

INTRODUCTION

Artificial insemination (AI) has been extensively used in swine industry in order to take the advantages of the superior genetic background and higher fertility capability of boars and sows (1–4). The application of AI is restricted to the semen quality, which can be influenced by multiple factors including the boar itself (e.g., age) and the environment factors (e.g., temperature and light) (1–4). Sperm plasma membrane contains a large proportion of polyunsaturated fatty acids (PUFA), which is easily impaired by oxidative stress and thus to diminish semen quality (1, 2). Increasing evidence suggests the potential to use nutritional interventions to enhance antioxidant capacity for

improving boar semen quality (3, 4). *In vitro* studies found that supplementation with exogenous antioxidants, such as rosmarinic acid, polysaccharide, and skim milk could improve boar sperm quality by alleviating oxidative stress during the cryopreservation (5–7). Moreover, a lot of evidence from *in vivo* studies also illustrated that dietary supplementation with antioxidants improved the boar semen quality. For example, dietary supplementation of L-arginine and lysine improved boar semen quality by increasing antioxidant capacity (3, 4).

Hydroxytyrosol (HT), a polyphenol, is extracted from olive leaves and oil. HT has attracted broad interest due to its strong antioxidant, anti-inflammatory, and antibacterial activities (8, 9). HT exhibited antioxidant capacity by scavenging oxidant chemical species and promoting the expressions of antioxidant enzymes via activating nuclear factor E2-related factor 2 (Nrf2) signaling (8). Furthermore, Wei et al. reported that HT increased bacterial membrane permeabilization and then interacted with DNA, which collectively inhibited bacterial growth (10). Our recent study also showed that olive fruit extracts enriching HT exhibited strong antioxidant effects by benefiting gut microbiota in mice (11). Moreover, our previous study found that improved gut microbiota was able to ameliorate sperm quality by modulating the plasma metabolomes and small intestinal function in mice (12, 13). To search the effective strategies to improve sperm quality and enhance the production of swine production, current investigation was designed to explore the effects of dietary supplementation of HT on the boar semen quality and the underlying mechanisms.

TABLE 1 | Composition and nutrient analysis of basal diet.

Ingredient	Content, %
Corn	35.15
Barley	24.83
wheat	15.82
Rice bran meal	9.40
Soybean meal	7.90
Soybean oil	2.00
L-lysine	0.40
Methionine	0.14
Threonine	0.24
Ground limestone	1.44
Monocalcium phosphate	1.21
Sodium chloride	0.48
Premix*	1.00
Total	100
Nutrient, %	
Calculated NE, kcal/kg	2.24
Crude protein, %	14.50
Crude fat, %	3.22
Crude ash, %	6.18
Crude fiber, %	4.15

*Premix provided the following minerals per kilogram: 17 mg Cu, 160 mg Fe, 140 mg Zn, 50 mg Mn, 0.50 mg I, 0.50 mg Se, and 0.22 mg Cr.

MATERIALS AND METHODS

Boars and Experimental Design

All animal procedures were approved by the Animal Care and Use Committee of the Institute of Animal Sciences of Chinese Academy of Agricultural Sciences (IAS2021-67). A total of 20 healthy boars (Duroc) aged from 31 to 33 months were selected in this study at the artificial insemination center of Yangxiang Joint Stock Company (Guangxi, China) (1). Boar feeding conditions have been previously reported (2). All boars were randomly divided into 2 groups ($n = 10$ per group). Boars in the control group (Con) were fed with a commercially prepared corn and soybean meal-based diet (**Table 1**), and boars in the HT supplement group (HT) were fed with a basal diet supplemented with 20 mg/kg body weight of HT. The dose of HT was adopted according to our previous mice experiment (11). The boars received two meals at 11:00 and 17:00 and the total feed intake amounts were 2.5 kg (1.25 kg per meal) every day. HT was mixed with the diet when the boars received the first meal and HT was taken almost completely by the boars each day. HT (purity > 99%) was kindly donated by Viablife Biotech Co., Ltd. (Hangzhou, China). The boars were housed in individual crates and HT was supplied for 60 days (**Figure 1A**).

Semen samples were collected by gloved-hand techniques. After collection, four semen parameters were assessed: semen volume, sperm concentration, sperm motility, and abnormal sperm rate, according to the reported methods (1, 14). Blood samples were collected into ethylenediamine tetraacetic acid (EDTA) plasma tubes by venipuncture from the hindlimb vein of boars during ejaculations. Each blood sample was then centrifuged at 3,000 × g for 10 min at 4°C to obtain a plasma sample and subsequently stored at −80°C until analysis. Each boar's rectum was massaged to stimulate defecation, and then fresh feces were collected and stored at −80°C for subsequent microbiota analysis (1).

The follow-up long term beneficial effects of HT on boar semen quality were determined. After HT supplementation, all the boars were fed with basal diet (without HT supplementation). The semen was collected every 5 days and the semen quality was analyzed. The long-term analysis was for 2 months (**Figure 1A**).

Evaluation of Spermatozoa Motility Using a Computer-Assisted Sperm Analysis System

Spermatozoa motility and concentration, and abnormal sperm rate were determined by the computer-assisted sperm assay (CASA) method according to World Health Organization guidelines and our previous reports (ML-210JZ, Nanning SongJing TianLun Biological Technology Co., LTD, Nanning, China) (15–18).

Morphological Observations of Spermatozoa

Boar sperm was stained with Eosin Y (1%) (15–17). Spermatozoa abnormalities were then viewed using an optical microscope and were classified into head or tail morphological abnormalities: two

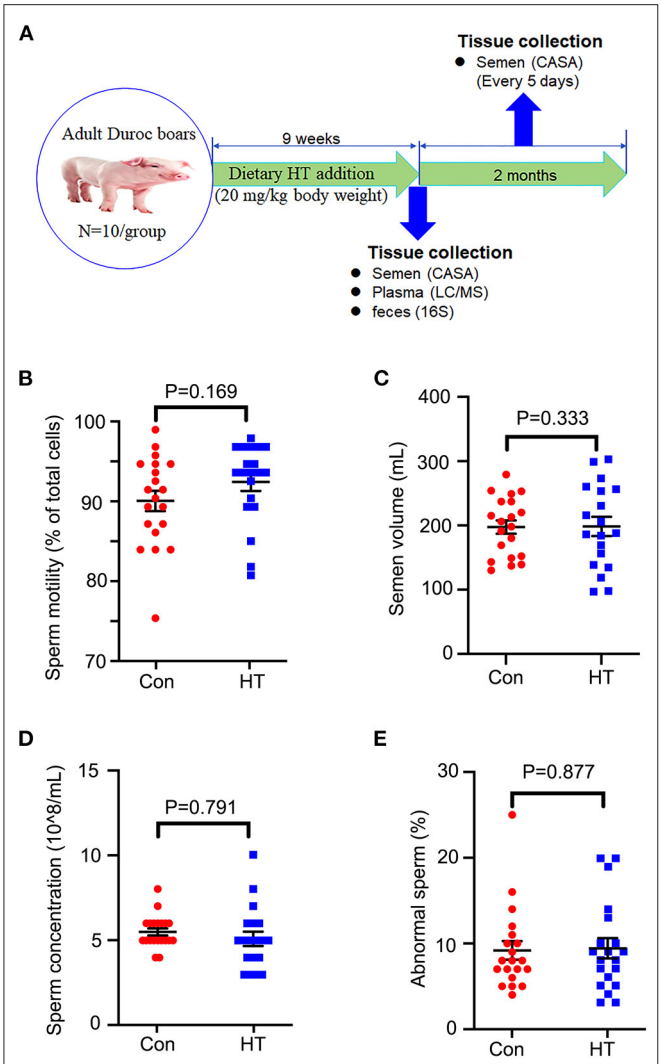

FIGURE 1 | Effects of HT on the semen quality. **(A)** Study design. **(B)** Sperm motility. **(C)** Semen volume. **(D)** Sperm concentration. **(E)** Abnormal sperm. Data were expressed as the mean ± SEM.

heads, two tails, blunt hooks, and short tails. The examinations were repeated three times, and 500 spermatozoa per animal were scored.

Boar Feces Microbiota Sequencing

Total genome DNA from feces was extracted using E.Z.N.A.R Stool DNA Kit (Omega Biotek Inc, USA). The V3-V4 region of the bacterial 16S rRNA gene was amplified using a specific primer (338F, 5'-ACTCCTACGGGAGGCAGCAG-3'; 806R, 5'-GGACTACHVGGGTWTCTAAT-3'). Then the library was sequenced on the Illumina HiSeq 2500 platform and 300 bp paired-end reads were generated at the Novo gene. The sequences were analyzed and assigned to operational taxonomic units (OTUs; 97% identity). OUT abundance information was normalized using a standard of sequence number corresponding to the sample with the least sequences (12, 13).

Plasma Metabolites Determined by LC-MS/MS

The metabolites were detected as reported in our early study (19). Briefly, boar plasma was collected and maintained at −80°C. LC-MS/MS analysis with ACQUITY UPLC and AB Sciex Triple TOF 5600 (LC/MS) was applied (19). Before LC-MS/MS analysis, the serum samples (100 μl) were precipitated with 10 μl methanol (0.3 mg/ml L-2-Chlorophe) on ice and processed to remove proteins. All samples were then centrifuged at 13,000 g for 10 min at 4°C and the supernatants were injected onto a ACQUITY UPLC HSS T3 column, which was at a flow rate of 0.35 ml/min with 2 μl mobile phase. MS analyses were conducted using electrospray ionization in the positive and negative ion models. Using full scan analysis. Progenesis QI v. 2.3 (Nonlinear Dynamics, Newcastle, UK) was applied to normalize the peaks. Human Metabolome Database (HMDB), Lipidmaps (v. 2.3), and METLIN software were applied to qualify the data. Furthermore, the data were analyzed with SIMCA software (v. 14.0, Umetrics, Umeå, Sweden) and KEGG database (https://www.kegg.jp/) was applied for the pathway enrichment analysis (19).

Detection of Protein Levels and Location in Spermatozoa Using Immunofluorescence Staining

Microscope slides loaded with boar sperm cells were incubated with 2% Triton X-100 for 1 h at room temperature. Then the samples were blocked for non-specific binding by incubating in 1% BSA with 1% goat serum for 30 min at room temperature. After washing, the cells were incubated with appropriate diluted primary antibodies (anti-Catsper, 1:100; anti-p-ERK, 1:100; anti-PKA, 1:100; anti-ZAG, 1:100) at 4°C overnight and then stained with secondary antibodies (Alexa Flour 546 goat-anti-rabbit IgG) at 1:200 dilution in PBS for 30 min at room temperature. Cell nuclei were counterstained with DAPI. All the samples were observed at room temperature using Leica Laser Scanning Confocal Microscope (LEICA TCS SP% II, Germany) (17).

Determination of Protein Levels by Western Blotting

Proteins was isolated from sperm cells using RIPA buffer containing protease and phosphate inhibitors (Sangong Biotech, Ltd, Shanghai, China). Total protein concentration was measured using BCA kit (Beyotime Institute of Biotechnology, Shanghai, Chain) according to the manufacture's instruction. Fifty microgram protein was loaded onto 10% polyacrylamide gels and transferred to polyvinylidene fluoride (PVDF) PVDF membrane. The membranes were blocked for 1 h at room temperature in TBST buffer containing 5% non-fat milk. Then the membranes were incubated overnight at 4°C with the primary antibodies (Novex® by life technologies, USA) at a dilution of 1:500 prepares in blocking solution. The control samples were incubated with actin antibody. After washed 3 times, the membranes were incubated with secondary donkey anti-goat IgG-HRP (Beyotime Institute of Biotechnology, Shanghai, P.R. China) or goat anti-rabbit IgG-HRP (Novex® by

life technologies, USA) for 1 h at room temperature. finally, the blots were imaged following three washes (12, 13, 17).

Statistical Analysis

All statistical analyses were performed by using the student's *t*-test (SPSS 21 software). Spearman correlation analysis between the relative abundance of gut microbiota and plasma metabolites using GraphPad Prism 7.0. Data are expressed as the mean ± SEM. *P*-value <0.05 was considered significant.

Data Availability

The microbiota raw sequencing data generated in this study has been uploaded to the NCBI SRA database with the accession number PRJNA779574.

RESULTS

Effects of HT on Semen Quality

The semen quality was analyzed by using the semen obtained from the last two collections before the end of the experiment. Compared to control group, dietary supplementation of HT tended to increase sperm motility and semen volume/ejaculation even though not significantly (**Figures 1B,C**). However, HT did not alter sperm concentration or abnormal rate (**Figures 1D,E**).

Effects of HT on the Protein Expression of Important Genes Related to Sperm Quality

Compared to control group, dietary supplementation of HT increased the protein levels of important genes related to sperm quality such as *Catsper*, *p-ERK*, *PKA*, *p-AKT*, and *ZAG* by IHF staining analysis (**Figures 2A,B**; $P < 0.05$). The data were confirmed by the WB analysis of *Catsper*, *Gelsolin*, and *PKA* (**Figures 2C,D**; $P < 0.05$) which suggested that HT improved sperm quality by enhancing the protein expression of important genes related to sperm quality.

Improvement of HT on Fecal Microbiota

The results showed that dietary supplementation of HT had no significant effects on the α-diversity of fecal microbiota,

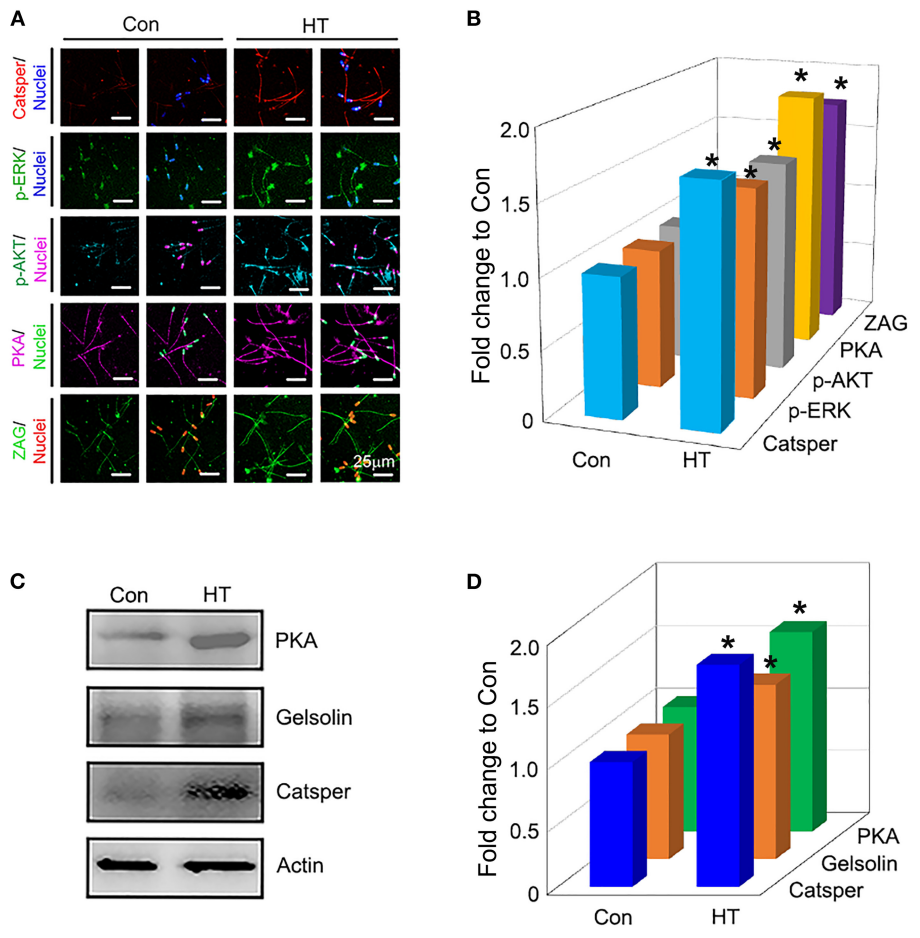

FIGURE 2 | Effects of HT on the protein expression of important genes related to sperm quality. **(A)** Immunofluorescence staining (IHF) of Catsper, p-ERK, p-ERK, PKA, and ZAG. **(B)** Quantitative data for IHF staining (Fold change to Con). **(C)** Western blotting (WB) of PKA, Gelsolin, and Catsper. **(D)** Quantitative data for WB staining (Fold change to Con). *$P < 0.05$.

which was characterized by ACE, Chao1, Simpson, and Shannon indexes (**Supplementary Figure 1A**). There were 1,109 common OTUs for both Con and HT groups (**Supplementary Figure 1B**). Moreover, the Con group and HT group contained specific 93 and 77 OTUs, respectively (**Supplementary Figure 1B**).

The microbial structure was different between HT group and Con group by PCoA analysis (**Supplementary Figure 1C**). At the phylum level, HT tended to reduce the relative abundance of *Bacteroidetes* and to increase the relative abundance of *Actinobacteria* (**Figure 3A**; **Supplementary Figure 1E**). At the order level, HT tended to decrease the level of *Bacteroidales* and to increase the relative abundance of *Bifidobacteriales* (**Figure 3B**; **Supplementary Figure 1F**). Moreover, at the family level, HT had the tendency to decrease the relative abundance of *Prevotellaceae* (**Figure 3C**; **Supplementary Figure 1G**). At the genus level, HT tended to increase the relative abundance of "beneficial microbes" *Bifidobacterium*, *Lactobacillus*, *Eubacterium, Intestinimonas, Coprococcus, and Butyricicoccus* (**Figures 3D,E**; **Supplementary Figure 1H**), however, to decrease the relative abundance of "harmful microbes" *Streptococcus*, *Oscillibacter*, *Clostridium_sensu_stricto*, *Escherichia*, *Phascolarctobacterium*, and *Barnesiella* (**Figures 3D,F**; **Supplementary Figure 1H**) (12). LDA effect size (LEfSe) analysis of the taxonomic alterations revealed that the content of some microbiota was different between HT group and control group (**Supplementary Figure 1D**).

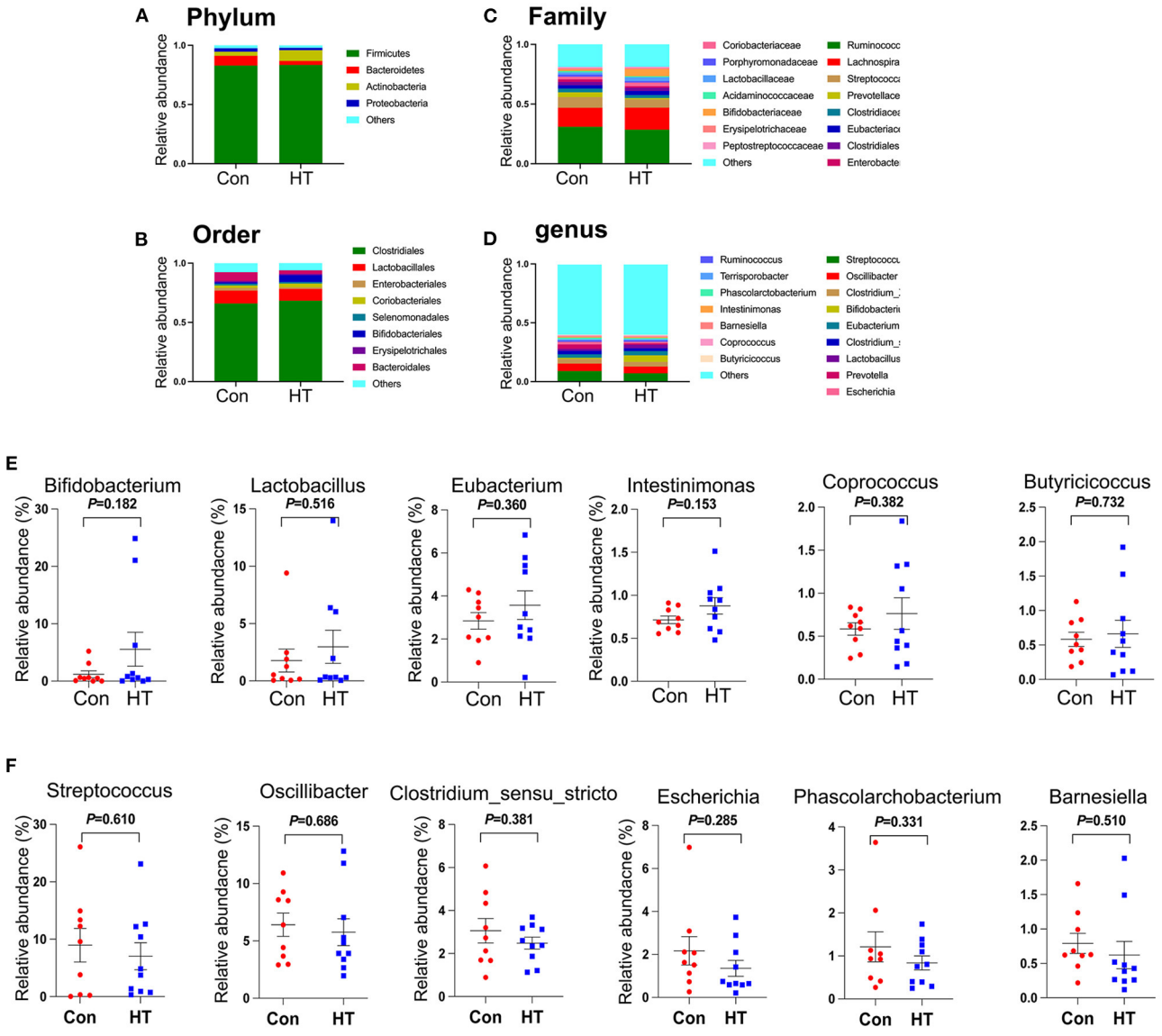

FIGURE 3 | Effects of HT on the fecal microbial composition. **(A)** The relative amount of microbiota in feces at Phylum level. **(B)** The relative amount of microbiota in feces at Order level. **(C)** The relative amount of microbiota in feces at Family level. The relative amount of microbiota in feces at Genus level **(D–F)**. Data were expressed as the mean ± SEM.

Effects of HT Supplement on the Plasma Metabolites

Compared to control group, HT significantly changed boar plasma metabolites indicated by the plot from the partial least squares discriminant analysis (PLS-DA) (**Supplementary Figure 2A**). There were 16 significantly changed metabolites between the HT and Con groups (**Supplementary Figure 2B**). The potential metabolic pathways of the changed metabolites were determined by KEGG pathway analysis. The results showed that the changed metabolites were involved in sphingolipid metabolism, Fc gamma R-mediated phagocytosis, apelin signaling pathway, choline metabolism in cancer, calcium signaling pathway, phospholipase D signaling pathway, tuberculosis, sphingolipid signaling pathway, and insulin resistance signaling pathways (**Supplementary Figure 2C**). It is very interesting to notice that HT increased plasma level of steroid hormones and their derivatives (**Figures 4A–F**), especially testosterone

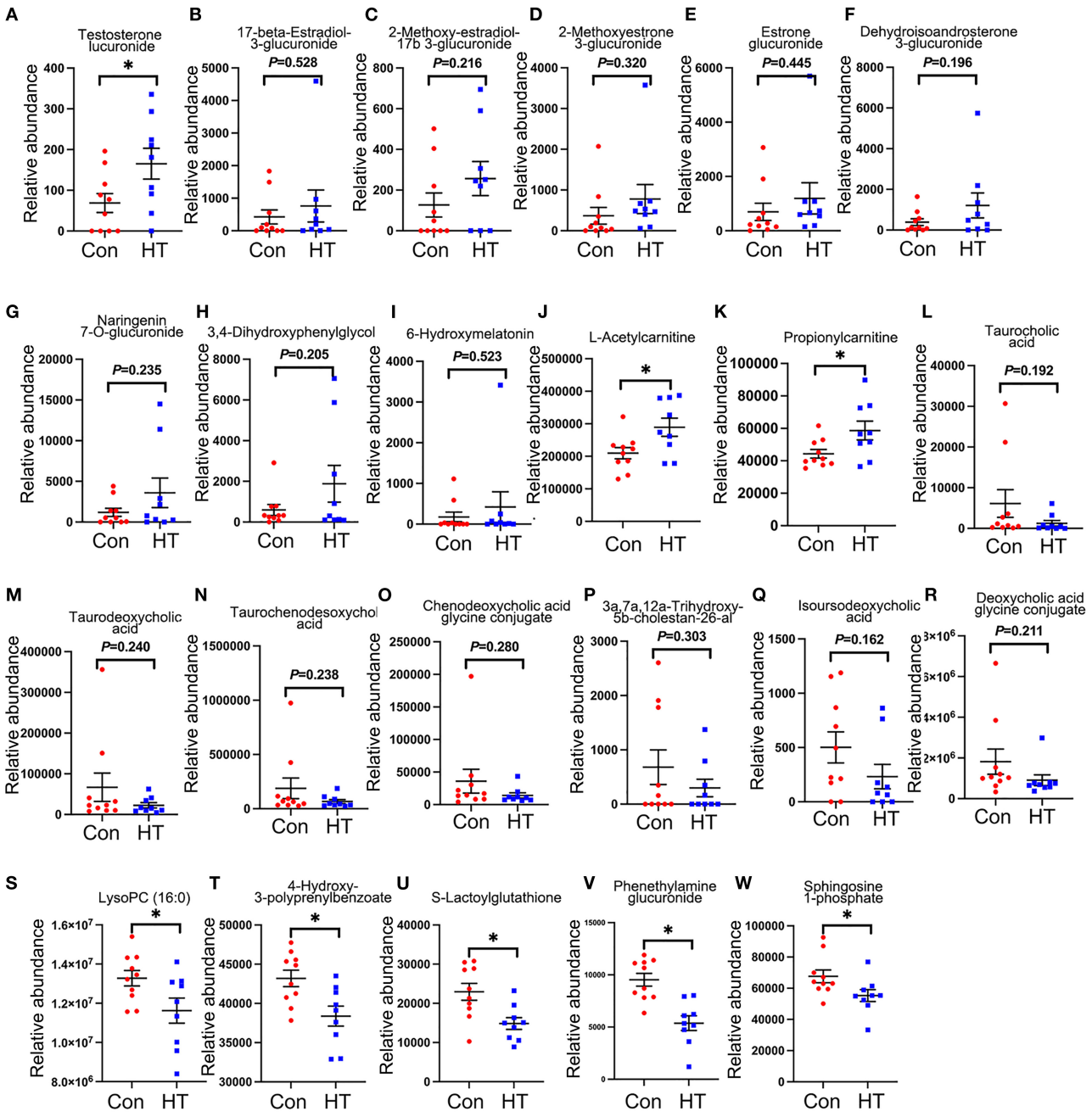

FIGURE 4 | HT-induced alterations in plasma metabolites. **(A–W)** The relative quantification of plasma metabolites. Data were expressed as the mean ± SEM. *P < 0.05.

glucuronide (**Figure 4A**). And HT tended to increase the plasma levels of flavonoids: Naringenin 7-O-glucuronide, and 3,4-Dihydroxyphenylglycol (**Figures 4G,H**). Moreover, it is very interesting that melatonin metabolite 6-hydroxymelatonin, L-Acetylcarnitine and Propionylcarnitine were also elevated by HT in boar plasma although not significantly (**Figures 4I–K**). However, HT decreased plasma levels of bile acids: taurocholic, taurodeoxycholic acid, taurochenodesoxycholic acid, chenodeoxycholic acid glycine conjugate, 3a,7a,12a-Trihydroxy-5b-cholestan-26-al, isoursodeoxycholic acid, and deoxycholic acid glycine conjugate (**Figures 4L–R**). Furthermore, HT tended to decrease plasma LysoPC (16:0), 4-Hydroxy-3-polyprenylbenzoate, Phenethylamine glucuronide and Sphingosine 1-phosphate (**Figures 4S–W**).

Correlation of Fecal Microbiota, Plasma Metabolites, and/or Sperm Quality

There was very good correlation between fecal microbiota and plasma metabolites, between plasma metabolites and semen parameters, and between fecal microbiota and semen parameters (the average of semen quality of each boar obtained from the last two collections before the end of the experiment) by the spearman correlation analysis (**Figure 5**). As shown in **Figure 5A**, the fecal *Lactobacillus* and *Bifidobacterium* were positively correlated with the plasma naringenin 7-O-glucuronide; while *Streptococcus* and *Escherichia* were negatively correlated with the plasma 3,4-dihydroxyphenylglycol and naringenin 7-O-glucuronide; *Coprococcus* was negatively correlated with plasma taurocholic, taurodeoxycholic acid, taurochenodesoxycholic acid, chenodeoxycholic acid glycine conjugate. Plasma LysoPC (16:0), S-lactoylglutathione, phenethylamine glucuronide, 4-hydroxy-3-polyprenylbenzoate, and ethyl glucuronide were negatively correlated with sperm motility (**Figure 5B**); while plasma gamma-glutamyl leucine, lithocholate 3-O-glucuronide, estrone glucuronide, and gamma-glutamylleucine were positively correlated with sperm motility (**Figure 5B**). Moreover, there was a significantly positive association between the sperm motility and the fecal *Ruminococcus* and a significantly negative association between the sperm volume and the fecal *Streptococcus* and *Escherichia* (**Figure 5C**).

Long-Term Beneficial Effects of HT on Semen Quality

HT had a long-term beneficial effect on boar semen quality by the increase in the semen volume and the decrease in the percentage of abnormal sperm in the follow-up 2 months analysis (without HT supplementation) (**Figures 6A,B**). However, HT did not change sperm concentration and motility in the follow-up determination (**Figures 6C,D**).

DISCUSSION

Previous studies have reported that dietary supplementation of antioxidants, such as lysine and L-arginine could improve sperm quality in boars (3, 4). Our recent study found that HT had antioxidant effects via modulating gut microbiota and enhancing the expressions of antioxidant enzymes in mice (11). In current investigation, we found that dietary supplementation of HT tended to increase the semen quality, which may be associated with the alterations in gut microbiota and plasma metabolites.

Accumulating evidence suggests that gut microbiota involves in various perspectives of host health (20, 21). Moreover, previous studies have well-established the causal relationship between the gut microbiota and sperm quality in both animal models and humans (1, 12, 13, 22, 23). Polyphenols, including HT, can be metabolized by gut microbiota in the colon and on the other hand HT can modify gut microbiota (24, 25). HT enhanced the relative abundance of *Actinobacteria*, *Prevotellaceae_UCG-001*, and *Lactobacillus johnsoniiin* in mice (26, 27). Similarly, in current study, we found that HT tended to increase the relative abundance of *Lactobacillus*, which has been shown to have the ability to improve sperm motility in zebrafish (28, 29). Moreover, it has been shown that the increase in the relative abundance of *Bacteroides* and *Prevotella* was associated with higher circulating endotoxin and decreased spermatogenesis (22). HT decreased the relative amount of *Prevotella* and *Bacteroides* in current study. We previously found that alginate oligosaccharides (AOS) could enhance the sperm motility and concentration by the increase in the relative abundance of *Bifidobacteriales* in mice (12). In current study, we found that HT tended to increase the relative abundance of *Bifidobacteriales*. Collectively, our data suggested that HT had the potential to improve spermatogenesis and sperm motility by benefiting gut microbiota.

Our previous study has shown that improved gut microbiota can enhance sperm quality by altering circulating metabolome (12). In current investigation, dietary supplementation of HT altered plasma metabolites by the increase in steroid hormones, antioxidant molecules, and many others. Testosterone and its derivatives play vital roles in spermatogenesis which were increased by HT in boar plasma. L-carnitine plays an important role in improving sperm motility and has been used to treat infertility due to its strong anti-oxidant and anti-inflammatory effects in men and animal models (30–33). It has been shown that epididymis has high level of L-carnitine (32). Interestingly, in current investigation, HT enhanced the plasma level of propionyl-L-carnitine, which is a derivate of L-carnitine and can enhance cellular content of L-carnitine (34). Additionally, in this study, we found that HT enhanced the plasma levels of flavonoids and riboflavin. It has been shown that flavonoids and flavanone metabolites, such as naringenin 7-O-glucuronide and 3,4-dihydroxyphenylglycol, had powerful antioxidant ability, thus they may contribute to improved sperm quality and function (35–38). 6-Hydroxymelatonin (increased by HT) is one of the metabolites of melatonin and has been shown to have strong antioxidant activity (39). Thus, we speculate that HT might improve sperm quality by enhancing the antioxidant capacity of boars. Furthermore, various studies have reported that bile acids can cause oxidative stress by promoting the production of oxygen free radicals from mitochondria (40). Moreover, bile acids contribute to infertility by activating farnesoid X receptor and G-protein-coupled bile acid receptor expressed in sperm, which then influence glucose and lipid metabolism and lead to abnormal sperm (41, 42). In current study, plasma levels of several bile acids and their derivates were decreased by HT.

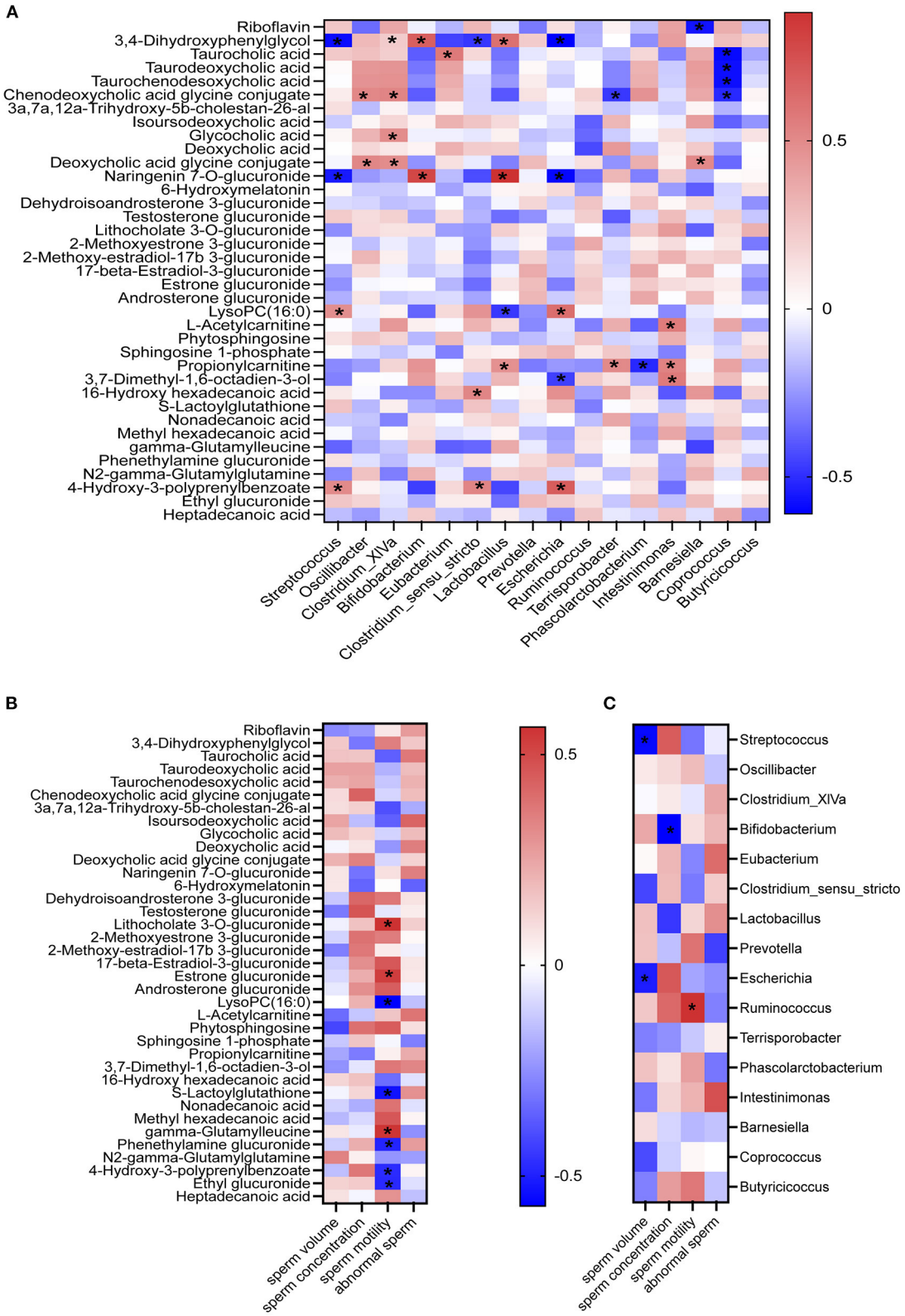

FIGURE 5 | Correlations. Correlations between fecal microbiota and plasma metabolites **(A)**; between plasma metabolites and semen quality parameters **(B)**; and between fecal microbiota and semen quality parameters **(C)** by Pearson correlation analyses. $^{*}P < 0.05$.

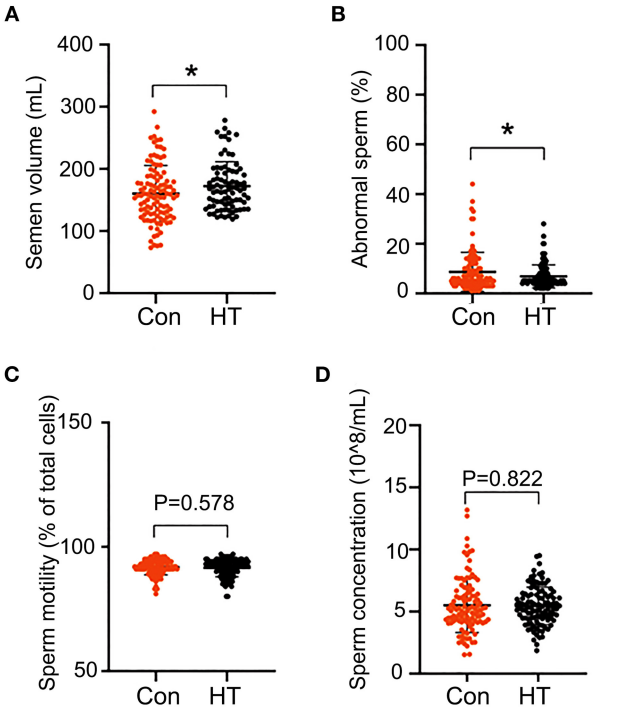

FIGURE 6 | Long-term effects of HT on semen quality. After HT supplementation, semen quality was determined every 5 days for 2 months (no HT supplementation). **(A)** Semen volume. **(B)** Abnormal sperm. **(C)** Sperm motility. **(D)** Sperm concentration. Data were expressed as the mean ± SEM. *$P < 0.05$.

Furthermore, there was a positive correlation between the plasma level of propionyl-L-carnitine and the relative abundance of *Lactobacillus*. Gut microbiota, including *Lactobacillus*, regulates the L-carnitine metabolism (43, 44). Collectively, these data demonstrated that HT might have the potential to improve plasma metabolome to benefit spermatogenesis.

Indeed, HT improved spermatogenesis by the increase in the protein levels of important genes (*PKA*, *p-AKT*, *p-ERK*, *Catsper*, *ZAG*, and *Gelsolin*) for spermatogenesis and sperm quality. Cation channel of sperm (Catsper) is the primary spermatozoan calcium ion channel and plays an essential role in male fertility via modulating sperm tail calcium entry and sperm hyperactivated motility (45). It has been reported that the cyclic adenosine monophosphate (cAMP) dependent protein kinase (protein kinase A, PKA), AKT, and ERK signaling are involved in modulating the sperm maturation, capacitation, and motility (46, 47). Zn-alpha2-glycoprotein (ZAG) can promote sperm motility via cAMP/PKA signaling pathway (48). Notably, in current study, HT increased the protein levels of these genes which suggested HT enhancing spermatogenesis.

The underlying mechanisms of HT improving semen quality is that it benefits gut microbiota to improve plamsa metabolites then to enhance spermatogenesis and semen quality. The data were confirmed by the follow-up long-term analysis. After the feeding period, all the boars were fed a basal diet (without HT supplementation) and semen samples were collected and analyzed every 5 days for 2 months. HT increased semen volume while decreased the percentage of abnormal sperm in the follow-up 2 months. In summary, HT improves boar semen quality via the benefiting on gut microbiota and plamsa metabolome. HT may be applied as dietary additive to improve boar semen quality in swine industry.

DATA AVAILABILITY STATEMENT

The datasets presented in this study can be found in online repositories. The names of the repository/repositories and accession number(s) can be found in the article/**Supplementary Material**.

ETHICS STATEMENT

The animal study was reviewed and approved by the Animal Care and Use Committee of the Institute of Animal Sciences of Chinese Academy of Agricultural Sciences (IAS2021-67).

AUTHOR CONTRIBUTIONS

YZha and HZ designed the experiment. HH, RZ, YZho, BX, LC, LL, HS, JT, and FT conducted the experiment and analyzed the data. HZ and YZha wrote and edited the manuscript. All authors contributed to the article and approved the submitted version.

FUNDING

This research was supported by the Agricultural Science and Technology Innovation Program (CAAS-ZDRW202006-02, ASTIPIAS07) and the State Key Laboratory of Animal Nutrition (2004DA125184G2102).

ACKNOWLEDGMENTS

We thank the investigators and staff of The Beijing Genomics Institute (BGI) and Shanghai LUMING Biotechnology CO., LCD for technical support.

SUPPLEMENTARY MATERIAL

The Supplementary Material for this article can be found online at: https://www.frontiersin.org/articles/10.3389/fnut.2021.815922/full#supplementary-material

Supplementary Figure 1 | Effects of HT on the fecal microbial diversity. **(A)** α-diversity with chao1, ACE, Shannon, and Simpson indexes. **(B)** Venn diagram of OUT. **(C)** PCoA of OUT. **(D)** Phylum level. **(E)** Order level. **(F)** Family level; **(G)** Genus level.

Supplementary Figure 2 | Effects of HT on plasma metabolites. **(A)** OPLS-DA. **(B)** Heatmap of altered serum metabolites. **(C)** KEGG enriched pathways of altered plasma metabolites.

Supplementary Table 1 | Primary antibody information.

Supplementary Data Set 1 | Plasma metabolites.

REFERENCES

1. Guo L, Wu Y, Wang C, Wei H, Tan J, Sun H, et al. Gut microbiological disorders reduce semen utilization rate in duroc boars. *Front Microbiol.* (2020) 11:581926. doi: 10.3389/fmicb.2020.581926
2. Wu YH, Lai W, Liu ZH, Wei HK, Zhou YF, Tan JJ, et al. Serum and seminal plasma element concentrations in relation to semen quality in Duroc boars. *Biol Trace Elem Res.* (2019) 189:85–94. doi: 10.1007/s12011-018-1459-y
3. Chen JQ, Li YS, Li ZJ, Lu HX, Zhu PQ, Li CM. Dietary l-arginine supplementation improves semen quality and libido of boars under high ambient temperature. *Animal.* (2018) 12:1611–20. doi: 10.1017/S1751731117003147
4. Dong HJ, Wu D, Xu SY, Li Q, Fang ZF, Che LQ, et al. Effect of dietary supplementation with amino acids on boar sperm quality and fertility. *Anim Reprod Sci.* (2016) 172:182–9. doi: 10.1016/j.anireprosci.2016.08.003
5. He Y, Li D, Zhang W, Tian X, Pang W, Du R, et al. Boar sperm quality and oxidative status as affected by rosmarinic acid at 17 °C. *Trop Anim Health Prod.* (2020) 52:2169–77. doi: 10.1007/s11250-020-02246-1
6. Ren Z, Shaoyong W, Li Q, Ma L, Xiao J, Jiao J, et al. Effects of Isatis root polysaccharide on boar sperm quality during liquid storage and in vitro fertilization. *Anim Reprod Sci.* (2019) 210:106178. doi: 10.1016/j.anireprosci.2019.106178
7. Namula Z, Sato Y, Kodama R, Morinaga K, Luu VV, Taniguchi M, et al. Motility and fertility of boar semen after liquid preservation at 5°C for more than 2 weeks. *Anim Sci J.* (2013) 84:600–6. doi: 10.1111/asj.12049
8. Bertelli M, Kiani AK, Paolacci S, Manara E, Kurti D, Dhuli K, et al. Hydroxytyrosol: a natural compound with promising pharmacological activities. *J Biotechnol.* (2020) 309:29–33. doi: 10.1016/j.jbiotec.2019.12.016
9. Karković Marković A, Torić J, Barbarić M, Jakobušić Brala C. Hydroxytyrosol, tyrosol and derivatives and their potential effects on human health. *Molecules.* (2019) 24:2001. doi: 10.3390/molecules24102001
10. Wei J, Wang S, Pei D, Qu L, Li Y, Chen J, et al. Antibacterial activity of hydroxytyrosol acetate from olive leaves (Olea Europaea L.). *Nat Prod Res.* (2018) 32:1967–70. doi: 10.1080/14786419.2017.1356830
11. Wang M, Zhang S, Zhong R, Wan F, Chen L, Liu L, et al. Olive fruit extracts supplement improve antioxidant capacity via altering colonic microbiota composition in mice. *Front Nutr.* (2021) 8:645099. doi: 10.3389/fnut.2021.645099
12. Zhang P, Feng Y, Li L, Ge W, Yu S, Hao Y, et al. Improvement in sperm quality and spermatogenesis following faecal microbiota transplantation from alginate oligosaccharide dosed mice. *Gut.* (2021) 70:222–5. doi: 10.1136/gutjnl-2020-320992
13. Zhao Y, Zhang P, Ge W, Feng Y, Li L, Sun Z, et al. Alginate oligosaccharides improve germ cell development and testicular microenvironment to rescue busulfan disrupted spermatogenesis. *Theranostics.* (2020) 10:3308–24. doi: 10.7150/thno.43189
14. Wu YH, Guo LL, Liu ZH, Wei HK, Zhou YF, Tan JJ, et al. Microelements in seminal and serum plasma are associated with fresh semen quality in Yorkshire boars. *Theriogenology.* (2019) 132:88–94. doi: 10.1016/j.theriogenology.2019.04.002
15. Zhang W, Zhao Y, Zhang P, Hao Y, Yu S, Min L, et al. Decrease in male mouse fertility by hydrogen sulfide and/or ammonia can be inheritable. *Chemosphere.* (2018) 194:147–57. doi: 10.1016/j.chemosphere.2017.11.164
16. Zhang P, Zhao Y, Zhang H, Liu J, Feng Y, Yin S, et al. Low dose chlorothalonil impairs mouse spermatogenesis through the intertwining of estrogen receptor pathways with histone and DNA methylation. *Chemosphere.* (2019) 230:384–95. doi: 10.1016/j.chemosphere.2019.05.029
17. Zhao Y, Zhang W, Liu X, Zhang P, Hao Y, Li L, et al. Hydrogen sulfide and/or ammonia reduces spermatozoa motility through AMPK/AKT related pathways. *Sci Rep.* (2016) 6:37884. doi: 10.1038/srep37884
18. WHO. *WHO Laboratory Manual for the Examination and Processing of Human Semen*. 5th ed. Cambridge: Cambridge University Press (2010).
19. Zhang P, Liu J, Xiong B, Zhang C, Kang B, Gao Y, et al. Microbiota from alginate oligosaccharide dosed mice successfully mitigated small intestinal mucositis. *Microbiome.* (2020) 8:112. doi: 10.1186/s40168-020-00886-x
20. Han H, Jiang Y, Wang M, Melaku M, Liu L, Zhao Y, et al. Intestinal dysbiosis in nonalcoholic fatty liver disease (NAFLD): focusing on the gut-liver axis. *Crit Rev Food Sci Nutr.* (2021) 1–18. doi: 10.1080/10408398.2021.1966738
21. Han H, Yi B, Zhong R, Wang M, Zhang S, Ma J, et al. From gut microbiota to host appetite: gut microbiota-derived metabolites as key regulators. *Microbiome.* (2021) 9:162. doi: 10.1186/s40168-021-01093-y
22. Ding N, Zhang X, Zhang XD, Jing J, Liu SS, Mu YP, et al. Impairment of spermatogenesis and sperm motility by the high-fat diet-induced dysbiosis of gut microbes. *Gut.* (2020) 69:1608–19. doi: 10.1136/gutjnl-2019-319127
23. Lundy SD, Sangwan N, Parekh NV, Selvam MKP, Gupta S, McCaffrey P, et al. Functional and taxonomic dysbiosis of the gut, urine, and semen microbiomes in male infertility. *Eur Urol.* (2021) 79:826–36. doi: 10.1016/j.eururo.2021.01.014
24. Tuck KL, Freeman MP, Hayball PJ, Stretch GL, Stupans, I. The in vivo fate of hydroxytyrosol and tyrosol, antioxidant phenolic constituents of olive oil, after intravenous and oral dosing of labeled compounds to rats. *J Nutr.* (2001) 131:1993–6. doi: 10.1093/jn/131.7.1993
25. Visioli F, Galli C, Bornet F, Mattei A, Patelli R, Galli G, et al. Olive oil phenolics are dose-dependently absorbed in humans. *FEBS Lett.* (2000) 468:159–60. doi: 10.1016/S0014-5793(00)01216-3
26. Liu Z, Wang N, Ma Y, Wen, D. Hydroxytyrosol improves obesity and insulin resistance by modulating gut microbiota in high-fat diet-induced obese mice. *Front Microbiol.* (2019) 10:390. doi: 10.3389/fmicb.2019.00390
27. Wang N, Ma Y, Liu Z, Liu L, Yang K, Wei Y, et al. Hydroxytyrosol prevents PM(2.5)-induced adiposity and insulin resistance by restraining oxidative stress related NF-κB pathway and modulation of gut microbiota in a murine model. *Free Radic Biol Med.* (2019) 141:393–407. doi: 10.1016/j.freeradbiomed.2019.07.002
28. Valcarce DG, Riesco MF, Martínez-Vázquez JM, Robles, V. Diet supplemented with antioxidant and anti-inflammatory probiotics improves sperm quality after only one spermatogenic cycle in zebrafish model. *Nutrients.* (2019) 11:843. doi: 10.3390/nu11040843
29. Valcarce DG, Riesco MF, Martínez-Vázquez JM, Robles, V. Long exposure to a diet supplemented with antioxidant and anti-inflammatory probiotics improves sperm quality and progeny survival in the zebrafish model. *Biomolecules.* (2019) 9:338. doi: 10.3390/biom9080338
30. Abd-Elrazek AM, Ahmed-Farid OAH. Protective effect of L-carnitine and L-arginine against busulfan-induced oligospermia in adult rat. *Andrologia.* (2018) 50:1–8. doi: 10.1111/and.12806
31. Micic S, Lalic N, Djordjevic D, Bojanic N, Bogavac-Stanojevic N, Busetto GM, et al. Double-blind, randomised, placebo-controlled trial on the effect of L-carnitine and L-acetylcarnitine on sperm parameters in men with idiopathic oligoasthenozoospermia. *Andrologia.* (2019) 51:e13267. doi: 10.1111/and.13267
32. Mongioi L, Calogero AE, Vicari E, Condorelli RA, Russo GI, Privitera S, et al. The role of carnitine in male infertility. *Andrology.* (2016) 4:800–7. doi: 10.1111/andr.12191
33. Reuter SE, Evans AM. Carnitine and acylcarnitines: pharmacokinetic, pharmacological and clinical aspects. *Clin Pharmacokinet.* (2012) 51:553–72. doi: 10.1007/BF03261931
34. Ferrari R, Merli E, Cicchitelli G, Mele D, Fucili A, Ceconi C. Therapeutic effects of L-carnitine and propionyl-L-carnitine on cardiovascular diseases: a review. *Ann N Y Acad Sci.* (2004) 1033:79–91. doi: 10.1196/annals.1320.007
35. Anacleto SL, Milenkovic D, Kroon PA, Needs PW, Lajolo FM, Hassimotto NMA. Citrus flavanone metabolites protect pancreatic-β cells under oxidative stress induced by cholesterol. *Food Funct.* (2020) 11:8612–24. doi: 10.1039/D0FO01839B
36. Kuang W, Zhang J, Lan Z, Deepak R, Liu C, Ma Z, et al. SLC22A14 is a mitochondrial riboflavin transporter required for sperm oxidative phosphorylation and male fertility. *Cell Rep.* (2021) 35:109025. doi: 10.1016/j.celrep.2021.109025
37. Saedisomeolia A, Ashoori M. Riboflavin in human health: a review of current evidences. *Adv Food Nutr Res.* (2018) 83:57–81. doi: 10.1016/bs.afnr.2017.11.002
38. Tvrdá E, Debacker M, Duračka M, Kováč J, Bučko O. Quercetin and naringenin provide functional and antioxidant protection to stored boar semen. *Animals.* (2020) 10:1930. doi: 10.3390/ani10101930
39. Maharaj DS, Walker RB, Glass BD, Daya S. 6-Hydroxymelatonin protects against cyanide induced oxidative stress in rat brain homogenates. *J Chem Neuroanat.* (2003) 26:103–7. doi: 10.1016/S0891-0618(03)00034-6

40. Bomzon A, Holt S, Moore K. Bile acids, oxidative stress, and renal function in biliary obstruction. *Semin Nephrol.* (1997) 17:549–62.
41. Baptissart M, Vega A, Martinot E, Pommier AJ, Houten SM, Marceau G, et al. Bile acids alter male fertility through G-protein-coupled bile acid receptor 1 signaling pathways in mice. *Hepatology.* (2014) 60:1054–65. doi: 10.1002/hep.27204
42. Malivindi R, Santoro M, De Rose D, Panza S, Gervasi S, Rago V, et al. Activated-farnesoid X receptor (FXR) expressed in human sperm alters its fertilising ability. *Reproduction.* (2018) 156:249–59. doi: 10.1530/REP-18-0203
43. Kim M, Kim M, Kang M, Yoo HJ, Kim MS, Ahn YT, et al. Effects of weight loss using supplementation with *Lactobacillus* strains on body fat and medium-chain acylcarnitines in overweight individuals. *Food Funct.* (2017) 8:250–61. doi: 10.1039/C6FO00993J
44. Ussher JR, Lopaschuk GD, Arduini A. Gut microbiota metabolism of L-carnitine and cardiovascular risk. *Atherosclerosis.* (2013) 231:456–61. doi: 10.1016/j.atherosclerosis.2013.10.013
45. Lishko PV, Kirichok Y, Ren D, Navarro B, Chung JJ, Clapham DE. The control of male fertility by spermatozoan ion channels. *Annu Rev Physiol.* (2012) 74:453–75. doi: 10.1146/annurev-physiol-020911-153258
46. Baro Graf C, Ritagliati C, Stival C, Luque GM, Gentile I, Buffone MG, et al. Everything you ever wanted to know about PKA regulation and its involvement in mammalian sperm capacitation. *Mol Cell Endocrinol.* (2020) 518:110992. doi: 10.1016/j.mce.2020.110992
47. Li X, Luo T, Li H, Yan N. Sphingomyelin synthase 2 participate in the regulation of sperm motility and apoptosis. *Molecules.* (2020) 25:4231. doi: 10.3390/molecules25184231
48. Qu F, Ying X, Guo W, Guo Q, Chen G, Liu Y, et al. The role of Zn-alpha2 glycoprotein in sperm motility is mediated by changes in cyclic AMP. *Reproduction.* (2007) 134:569–76. doi: 10.1530/REP-07-0145

Conflict of Interest: HS and JT were employed by company YangXiang Joint Stock Company. FT was employed by company Hangzhou Viablife Biotech Co., Ltd.

The remaining authors declare that the research was conducted in the absence of any commercial or financial relationships that could be construed as a potential conflict of interest.

The handling editor declared a shared affiliation with the authors HH, RZ, YZ, BX, LC, YJ, and LL at the time of review.

Publisher's Note: All claims expressed in this article are solely those of the authors and do not necessarily represent those of their affiliated organizations, or those of the publisher, the editors and the reviewers. Any product that may be evaluated in this article, or claim that may be made by its manufacturer, is not guaranteed or endorsed by the publisher.

frontiers in Nutrition

ORIGINAL RESEARCH
published: 20 January 2022
doi: 10.3389/fnut.2021.803691

Lentinan Supplementation Protects the Gut–Liver Axis and Prevents Steatohepatitis: The Role of Gut Microbiota Involved

Xiaoying Yang[1†], Mingxuan Zheng[1†], Menglu Zhou[1†], Limian Zhou[1†], Xing Ge[1], Ning Pang[2], Hongchun Li[3,4], Xiangyang Li[1], Mengdi Li[1], Jun Zhang[5], Xu-Feng Huang[6], Kuiyang Zheng[1] and Yinghua Yu[1,6]*

[1] Jiangsu Key Laboratory of Immunity and Metabolism, Department of Pathogen Biology and Immunology, Xuzhou Medical University, Xuzhou, China, [2] Tianjin Third Central Hospital, Tianjin, China, [3] Medical Technology Institute, Xuzhou Medical University, Xuzhou, China, [4] Department of Laboratory Medicine, Affiliated Hospital of Xuzhou Medical University, Xuzhou, China, [5] Affiliated Hospital of Liaoning University of Traditional Chinese Medicine, Shenyang, China, [6] School of Medicine, Illawarra Health and Medical Research Institute (IHMRI), University of Wollongong, Wollongong, NSW, Australia

OPEN ACCESS

Edited by:
Xi Ma,
China Agricultural University, China

Reviewed by:
Peixin Fan,
University of Florida, United States
Michael Müller,
University of East Anglia, United Kingdom

***Correspondence:**
Yinghua Yu
yinghua@uow.edu.au

[†]These authors have contributed equally to this work and share first authorship

Specialty section:
This article was submitted to Nutrition and Microbes, a section of the journal Frontiers in Nutrition

Received: *28 October 2021*
Accepted: *20 December 2021*
Published: *20 January 2022*

Citation:
Yang X, Zheng M, Zhou M, Zhou L, Ge X, Pang N, Li H, Li X, Li M, Zhang J, Huang X-F, Zheng K and Yu Y (2022) Lentinan Supplementation Protects the Gut–Liver Axis and Prevents Steatohepatitis: The Role of Gut Microbiota Involved. Front. Nutr. 8:803691. doi: 10.3389/fnut.2021.803691

The microbiota–gut–liver axis has emerged as an important player in developing nonalcoholic steatohepatitis (NASH), a type of nonalcoholic fatty liver disease (NAFLD). Higher mushroom intake is negatively associated with the prevalence of NAFLD. This study examined whether lentinan, an active ingredient in mushrooms, could improve NAFLD and gut microbiota dysbiosis in NAFLD mice induced by a high-fat (HF) diet. Dietary lentinan supplementation for 15 weeks significantly improved gut microbiota dysbiosis in HF mice, evidenced by increased the abundance of phylum Actinobacteria and decreased phylum Proteobacteria and Epsilonbacteraeota. Moreover, lentinan improved intestinal barrier integrity and characterized by enhancing intestinal tight junction proteins, restoring intestinal redox balance, and reducing serum lipopolysaccharide (LPS). In the liver, lentinan attenuated HF diet-induced steatohepatitis, alteration of inflammation–insulin (NFκB-PTP1B-Akt-GSK3β) signaling molecules, and dysregulation of metabolism and immune response genes. Importantly, the antihepatic inflammation effects of lentinan were associated with improved gut microbiota dysbiosis in the treated animals, since the Spearman's correlation analysis showed that hepatic LPS-binding protein and receptor (Lbp and Tlr4) and pro- and antiinflammatory cytokine expression were significantly correlated with the abundance of gut microbiota of phylum Proteobacteria, Epsilonbacteraeota and Actinobacteria. Therefore, lentinan supplementation may be used to mitigate NAFLD by modulating the microbiota–gut–liver axis.

Keywords: mushroom, NAFLD, gut-liver axis, oxidative stress, gut microbiota, β-glucan

INTRODUCTION

Nonalcoholic fatty liver disease (NAFLD), one of the most common liver diseases worldwide, affects up to 30% of the adult population (1). Nonalcoholic steatohepatitis (NASH), a more severe form of NAFLD, is defined by the presence of steatosis with inflammation and progressive fibrosis, ultimately leading to cirrhosis or hepatocellular carcinoma (2). Recently, evidence for cross talk

among the gut microbiota, the liver, the immune system, and energy metabolism has emerged, indicating that the microbiota is an important player in the development of NASH (3).

Compelling evidence links NASH with the alteration of the gut microbiome and intestinal barrier integrity. For example, the diversity and composition of gut microbiota significantly alter in the animal model and patients with NASH (4, 5). The tight junction proteins, including zonula occludens-1 (ZO-1) and occludin, decrease in the proximal small intestine of NASH mice (6). The gut integrity is disrupted by a redox imbalance in the intestine (7–10). Reactive oxygen species (ROS), such as nitric oxide (NO) and its generating enzyme inducible NO synthase (iNOS), induce the dysfunction and loss of tight junction of intestinal epithelial cells (7–9). In contrast, antioxidant enzymes, such as haem oxygenase 1 (HO-1), NAD(P)H quinone dehydrogenase 1 (NQO1), and glutamate-cysteine ligase catalytic subunit (Gclc), play important roles in maintaining intestinal barrier integrity (10). The transcription factor of these antioxidant enzymes, nuclear factor erythroid 2-related factor 2 (Nrf2), ameliorates intestinal barrier dysfunction induced by lipopolysaccharide (LPS, present in the outer membrane of gram-negative bacteria) (11). Therefore, gut microbiota dysbiosis and redox imbalance may disrupt gut integrity and lead to overtranslating the gut bacteria-derived toxin, such as LPS, into the port vein, thereby promoting inflammatory responses in the liver.

Lipopolysaccharide and its downstream pathway significantly contribute to hepatic inflammation in NAFLD (12, 13). LPS binds to its binding protein (Lbp), a 60-kDa acute-phase protein, to elicit immune responses by presenting the LPS to toll-like receptor 4 (Tlr4, important cell surface pattern receptor) (14, 15). Activation of Tlr4 subsequently induces proinflammatory responses, including the activation of nuclear factor kappa B (NFκB) and the increase in proinflammatory cytokines (TNFα, IL-6, and IL-1β) expression (14, 15). NFκB is also a transcription factor that increases protein tyrosine phosphatase 1B (PTP1B, encoded by the ptpn1 gene) (16), leading to insulin resistance. It is reported that patients with NASH have upregulation of hepatic Tlr4 mRNA and increased serum LPS (hyperendotoxinemia) (17). Therefore, the alteration of the gut–liver axis mediated by gut microbiota metabolite, LPS, may play a critical role in the development and progression of NASH.

Mushrooms have been used as food and medicinal resources for millennia (18). A clinical study has reported that higher mushroom intake was negatively associated with the NAFLD prevalence among adults (19). It is speculative that the active ingredient in mushrooms, such as β-glucan, contributes to the beneficial effect. Lentinan from shiitake mushroom, a β(1,3)/β(1,6)-glucan, has a β(1,3) backbone branched with short β(1,6)-linked side chains. In comparison, the β-glucans in cereal are primarily in β(1,4) linkages separating shorter stretches of β(1,3) structure. The mixed-linkage β(1,3)/β(1,4)-glucan (MLG) of cereal is the specific hydrolysis by the MLG utilization locus (MLGUL) of some gut microbiota, such as *Bacteroides ovatus* (20), resulting in compositional and functional shifts in the gut microbiota (21, 22). Recently, it has been reported that lentinan, β(1,3)/β(1,6)-glucans of mushroom, alleviates LPS-induced intestinal injury through modulating the composition and metabolites of intestinal microbiota in piglet (23). However, lentinan's potential effects and mechanism on the gut–liver axis in NAFLD represent a gap in the current research.

In this study, using the high-fat (HF) diet-induced NASH mouse model, we examined the effects of lentinan on gut microbiota, gut redox balance, and tight junction proteins, and also lipid deposition, NFκB/PTP1B signaling of endotoxin LPS, macrophage infiltration, and transcriptome regulation of immune and metabolic response in the liver.

MATERIALS AND METHODS

Materials

Lentinan (**Figure 1A**) of purity >98% was purchased from Yuanye Biological Technology Co., Ltd (Shanghai, China). Details of sources of antibodies and other reagents used are shown in the **Supplementary Data**.

Animals and Treatment

Male C57BL/6J mice aged 9 weeks were purchased from the Experimental Animal Center of Xuzhou Medical University [Xuzhou, China, SCXK (Su) 2015-0009], housed, and maintained in a 12-h light/dark photoperiod with unrestricted water and food. All animal care and experiments were carried out under protocols approved by the ethics committee of Xuzhou Medical University. After habituation to the laboratory environment for 1 week, the mice were randomly divided into four groups ($N = 10$ per group): (1) mice fed a low-fat (LF) diet (5% fat by weight) as a control (LF) group; (2) mice fed the LF diet supplemented with lentinan (500 mg/Kg in diet) as the LFL group; (3) mice receiving the HF diet (31.5% fat by weight) as the HF group; and (4) mice fed the HF diet supplemented with lentinan (500 mg/Kg in diet) as the HFL group. The detailed information of LF and HF diets is in **Supplementary Table S1**. The consumption of 500 mg/Kg lentinan in the diet is equivalent to dose of ∼60 mg/kg body weight for mice, which was decided according to an effective dose of β-glucan at 30 mg/kg in reduction of blood glucose in rats (24) and transferred by dose translation formula between mice and rats (25). Lentinan (98%) was purchased from Yuanye Biological Technology Co., Ltd (Shanghai, China). Mice were administered the three diets for 15 weeks. Body weight and food intake were measured on the last day of each week. After 13 weeks of feeding, an intraperitoneal glucose tolerance test (GTT) was performed as detailed below. Mice were then euthanized after 15 weeks of feeding. The data of body weight, energy intake, liver weight, and GTT were collected from 10 mice per group. After the mice

Abbreviations: AUC, area under curve; DEGs, differentially expressed genes; Gclc, glutamate-cysteine ligase catalytic subunit; GTT, glucose tolerance test; HF, high-fat diet; HFL, high-fat diet supplemented with lentinan; HO-1, haem oxygenase 1; iNOS, inducible NO synthase; INSR, insulin receptor; Lbp, lipopolysaccharide-binding protein; LF, low-fat diet; LPS, lipopolysaccharide; Mcp1, monocyte chemoattractant protein-1; NAFLD, nonalcoholic fatty liver; NFκB, nuclear factor kappa B; NQO1, NAD(P)H quinone dehydrogenase 1; Nrf2, nuclear factor-E2-related factor 2; PTP1B, protein tyrosine phosphatase 1B; ROS, reactive oxygen species; Tlr4, toll-like receptor 4; TNFα, tumor necrosis factor alpha; ZO-1: zonula occludens-1.

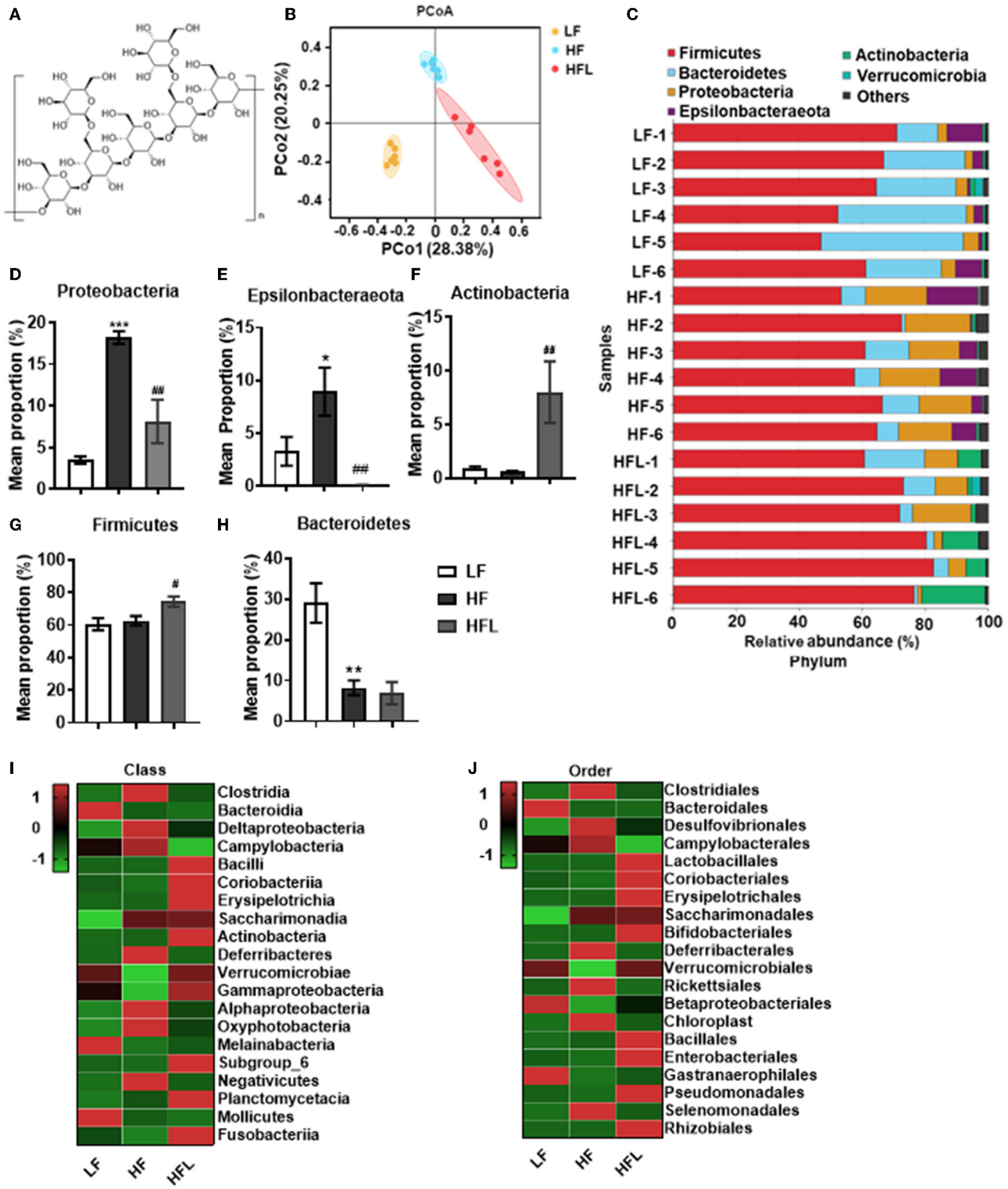

FIGURE 1 | Lentinan improved HF diet-induced dysbiosis. Cecal contents microbiota composition was analyzed by 16S RNA sequencing. **(A)** The chemical structure of lentinan. **(B)** PCoA of community dissimilarity. **(C)** The taxonomic composition analysis at phylum levels among three groups. **(D–H)** Relative abundance of phylum. Proteobacteria **(D)**, Epsilonbacteraeota **(E)**, Actinobacteria **(F)**, Firmicutes **(G)**, and Bacteroidetes **(H)**. **(I,J)** The top 20 bacteria in relative abundance at the levels of class **(I)** and order **(J)** in three groups. The color of spots in the left panel of heatmap represents the Z-scores, demonstrating that all groups were represented by the Z-scores as the relative abundance levels [Z score = (actual relative abundances of a species in a specific group – mean relative abundance of the three groups)/standard deviation]. Values are means ± SEM ($n = 6$). $^{*}p < 0.05$, $^{**}p < 0.01$, $^{***}p < 0.001$ vs. LF mice; $^{\#}p < 0.05$, $^{\#\#}p < 0.01$ vs. HF mice.

were sacrificed ($n = 6$ mice per group), blood was collected to detect serum LPS levels; fresh tissues of liver and intestine were collected to perform qPCR and western blot; cecum contents were collected for gut microbiota analysis. In addition, after mice were perfused with paraformaldehyde ($n = 4$ mice per group), the liver and intestinal tissues were collected for oil red O staining, Hematoxylin and eosin (H&E) staining, immunohistochemistry, and immunofluorescence.

Glucose Tolerance Test

The GTT was performed as we have previously described (26). The detailed methods are described in the **Supplementary Data**.

RNA-Sequencing Analysis

RNA sample preparation and sequencing: Total RNA was extracted from livers of mice in LF, HF, and HFL groups (three mice in each group) using TRIzol reagent kit (Invitrogen, Carlsbad, California, USA). Subsequently, the mRNA was enriched by oligo (dT) beads. The enriched mRNA was fragmented with fragmentation buffer and reverse-transcribed into cDNA with random primers. Second-strand cDNA was synthesized by DNA polymerase I, RNase H, dNTP, and buffer. The cDNA fragments were purified with a QiaQuick PCR extraction kit (Qiagen 28104), end repaired, poly(A) added, and ligated to Illumina sequencing adapters. The ligation products were size selected by agarose gel electrophoresis, PCR amplified and sequenced using Illumina HiSeq 4000 by CapitalBio Technology Co., Ltd (China).

Gene-level differential expression analyses: Differential expression genes (DEGs) analysis for mRNA was performed using R package edge R. DEGs with |log2(fold change)| value >1 and $p < 0.05$, considered as significantly modulated (27), were retained for further analysis. The KEGG pathway enrichment analysis was performed for DEGs using the Database for Annotation, Visualization, and Integrated Discovery (DAVID) (28). The protein–protein interaction (PPI) network of the proteins encoded by the DEGs was searched using the STRING database and Cytoscape software (29).

LPS Determination

The serum concentration of LPS was determined using a chromogenic end-point TAL kit. The absorbance was measured at 545 nm using a spectrophotometer, with measurable concentrations ranging from 0.1 to 1.0 EU/ml. All samples for LPS measurements were performed in duplicate.

Oil Red O Staining

Oil red O staining was used to examine hepatic lipid accumulation as described previously (30). The detailed methods are provided in the **Supplementary Data**.

Hematoxylin and Eosin Staining

The H&E staining detection and histological assessment are described in the **Supplementary Data**.

Immunohistochemistry

The immunohistochemistry methods for hepatic F4/80 and intestinal iNOS detection and quantification are provided in the **Supplementary Data**.

Immunofluorescence

Jejunum segments were immunostained as described previously (31). The detailed methods are described in the **Supplementary Data**.

Western Blotting

Western blot assays were performed as described previously (32). The methods are depicted in the **Supplementary Data**.

Quantitative RT-PCR Analysis

Total RNA was extracted with RNA Isolator Total RNA Extraction Reagent (Vazyme, China) from the liver and jejunum, before reverse-transcription to cDNA using a high-capacity cDNA reverse transcription kit (Takara, Japan). qPCR was performed using the TransStart® Top Green qPCR SuperMix (TransGen, China) and determined on a real-time PCR detection system (Roche LightCycler480, Switzerland). The mRNA levels for specific genes were calculated using the formula $2(-\Delta\Delta Ct)$ and normalized by β-actin mRNA levels. All primers are listed in **Supplementary Table S2**.

Gut Microbiota Analysis

DNA extraction, PCR amplification, and 16S rRNA gene sequencing: After 15 weeks of feeding, the cecum contents of mice were collected. Microbial DNA was extracted using the HiPure Stool DNA Kit (Magen, Guangzhou, China) according to the protocol recommended by the manufacturer. V3–V4 region of 16s rRNA genes was amplified by PCR with the primers 341-F, 5'-CCT ACGGGNGGCWGCAG-3' and 806-R, 5'-GGACTACHVGGG TATCTAAT-3' (33), and the amplification procedure was as follows: Initial denaturation at 94°C for 2 min, followed by denaturation at 98°C for 10 s, annealing at 65°C for 30 s, and extension at 68°C for 30 s. This round was repeated for 30 cycles, followed by a final extension at 68°C for 5 min. PCRs were performed in triplicate, and the reaction system was composed of 5 ml of 10 × KOD buffer, 5 ml of 2 mM dNTPs, 3 ml of 25 mM MgSO4, 1.5 ml of each primer (10 mM), 1 ml of KOD polymerase, and 100 ng of template DNA, with 50 ml in total. After amplification, the products were purified using the AxyPrep DNA Gel Extraction Kit (Axygen Biosciences, Union City, CA, USA) and quantified using ABI StepOnePlus Real-Time PCR System (Life Technologies, Foster City, USA). Purified products were pooled in equimolar and paired-end sequenced (PE250) on an Illumina platform according to the standard protocols.

Sequence data processing: To get high-quality clean reads, raw reads containing more than 10% of unknown nucleotides-(N) and reads with <60% of bases with a quality value (Q-value) >20 were removed using FASTP (version 0.18.0) (34). Paired-end clean reads were merged as raw tags using FLSAH (version 1.2.11) (35) with a minimum overlap of 10 bp and mismatch error rates of 2%. Noisy sequences of raw tags were filtered

by QIIME (version 1.9.1) (36) pipeline under specific filtering conditions (37) to obtain high-quality clean tags. The filtering conditions were as follows: (1) break raw tags from the first low-quality base site where the number of bases in the continuous low-quality value (the default quality threshold is $\leq$3) reaches the set length (the default length is three); (2) then, filter tags whose continuous high-quality base length was <75% of the tag length. The clean tags were searched against the reference database (http://drive5.com/uchime/uchime_download.html) to perform reference-based chimera checking using the UCHIME algorithm. After chimeric tags were removed, the final effective tags were used for further analysis.

Bioinformatic analysis: The clean tags were clustered into operational taxonomic units (OTUs) of $\geq$97% similarity using UPARSE (version 9.2.64) pipeline (38). The α-diversity indices evaluating gut microbial community richness (the Ace and Chao1 estimators) and community diversity (the Shannon estimator) were calculated using Mothur (39). Principal coordinate analysis (PCoA) based on Bray–Curtis distance and permutational multivariate analysis of variance (PERMANOVA) was performed to compare the global microbiota composition after the intervention in each group at phylum, genus, and OTU levels, respectively. The difference in abundant taxa was detected by the linear discriminant analysis (LDA) effect size (LEfSe) algorithm, which emphasizes statistical significance, biological consistency, and effect relevance (40). Differences with log 10 LDA scores (absolute values) >3.0 and $p < 0.05$ were considered significant (41). The functional potential of the gut microbial communities was estimated by the PICRUSt12 algorithm (42). In univariate analysis of gut microbiota and predicted KEGG biochemical pathways in each group, a paired *t*-test or a Wilcoxon matched-pairs test was adopted and *p*-values were adjusted for multiple comparisons using the Benjamini–Hochberg false discovery rate.

Statistical Analysis

Statistical analysis was performed using SPSS (version 20, IBM Corporation, Chicago, IL, USA). All data were tested for normality by applying the Shapiro–Wilk normality test. If normality was given, the one-way analysis of variance (ANOVA) was performed, followed by the *post-hoc*, Tukey's test for comparisons among the groups. Correlations between gut bacterial abundance and serum LPS and its binding protein and receptor in the liver and also hepatic proinflammatory and antiinflammatory cytokines were calculated using Spearman's correlation analysis. Differences were considered significant when $p < 0.05$ and marked with * or # ($^{*}p < 0.05$, $^{**}p < 0.01$, $^{***}p < 0.001$, $^{\#}p < 0.05$, $^{\#\#}p < 0.01$, $^{\#\#\#}p < 0.001$). Values are expressed as the mean ± standard error of means (SEM).

RESULTS

Dietary Lentinan Supplementation Improved Gut Microbiota Dysbiosis in HF Mice

Gut microbiota dysbiosis plays an important role in NAFLD onset and progression (43, 44). Here, by 16S rRNA gene sequencing analysis, we investigated the gut microbiota after the HF diet with or without lentinan (**Figure 1A**) supplementation for 15 weeks. Principal coordinate analysis (PCoA) of microbiota showed a clear cluster separation among the LF, HF, and HFL groups (**Figure 1B**), whereas the LF diet-fed mice with lentinan supplementation had a similar cluster with the LF mice (**Supplementary Figure S1A**). The HF mice showed a decrease in gut microbial community richness (the Chao1 and Ace estimators) and community diversity (the Shannon estimator) (all $p < 0.05$, **Supplementary Figures S1B–D**), whereas lentinan prevented the reduction of gut microbial community richness (all $p < 0.05$, **Supplementary Figures S1B,C**). Among the LF, HF, and HFL groups, the difference in the relative abundance of microbiota at phylum was shown in **Supplementary Figure S1E**. Specifically, the gut microbiota of these three groups was mainly dominated by Firmicutes, Bacteroidetes, Proteobacteria, Epsilonbacteraeota, and Actinobacteria at the phylum level (**Figure 1C**), in which Proteobacteria and Epsilonbacteraeota increased (both $p < 0.05$, **Figures 1D,E**), and Bacteroidetes decreased in the HF group ($p < 0.05$, **Figure 1H**). Importantly, lentinan supplementation reduced the abundance of Proteobacteria and Epsilonbacteraeota and increased Actinobacteria and Firmicutes (all $p < 0.05$, **Figures 1D–G** and **Supplementary Figure S1E**). At the class level, Clostridia, Bacteroidia, Deltaproteobacteria, Campylobacteria, and Bacilli were dominant bacterial (**Supplementary Figure S1F**), in which Clostridia, Deltaproteobacteria, and Campylobacteria were deceased in the HF mice with lentinan supplementation compared with that of the HF group (**Figure 1I**). At the order level, Clostridiales, Bacteroidales, Desulfovibrionales, Campylobacterales, and Lactobacillales accounted for the majority of gut microbiota (**Supplementary Figure S1G**). Compared with HF mice, supplementation of lentinan decreased the relative abundance of Clostridiales, Desulfovibrionales, and Campylobacterales and increased Lactobacillales (**Figure 1J**).

Furthermore, in HF mice, the low taxa belonging to phylum Proteobacteria, including class Deltaproteobacteria, order Desulfovibrionales, and family Desulfovibrionaceae, were all significantly increased (**Figures 2A–C** and **Supplementary Figures S1F–H**). Phylum Epsilonbacteraeota's lower taxa, including class Campylobacteria, order Campylobacterales, family Helicobacteraceae, and genus *Helicobacter*, were significantly increased in HF mice (**Figures 2D–G** and **Supplementary Figures S1F–I**). Importantly, lentinan prevented HF-induced alterations in these microbiota belonging to the phylum Proteobacteria and Epsilonbacteraeota. Notably, bacteria belonging to Actinobacteria, order Bifidobacteriales, family Bifidobacteriaceae, and genus *Bifidobacterium* were elevated significantly in HF mice with lentinan supplementation (**Figures 2H–J** and **Supplementary Figures S1G–I**). LDA effect size (LEfSe) showed that the lower taxa bacteria of the phylum Epsilonbacteraeota, such as order Campylobacterales, class Campylobacteria, family Helicobacteraceae, and genus *Helicobacter*, belonging to phylum Proteobacteria were enriched in the HF group (**Figure 2K**). In HFL mice, bacteria belonging to order Bifidobacteriales, family Bifidobacteriaceae, and genus *Bifidobacterium* were elevated. In addition, genus

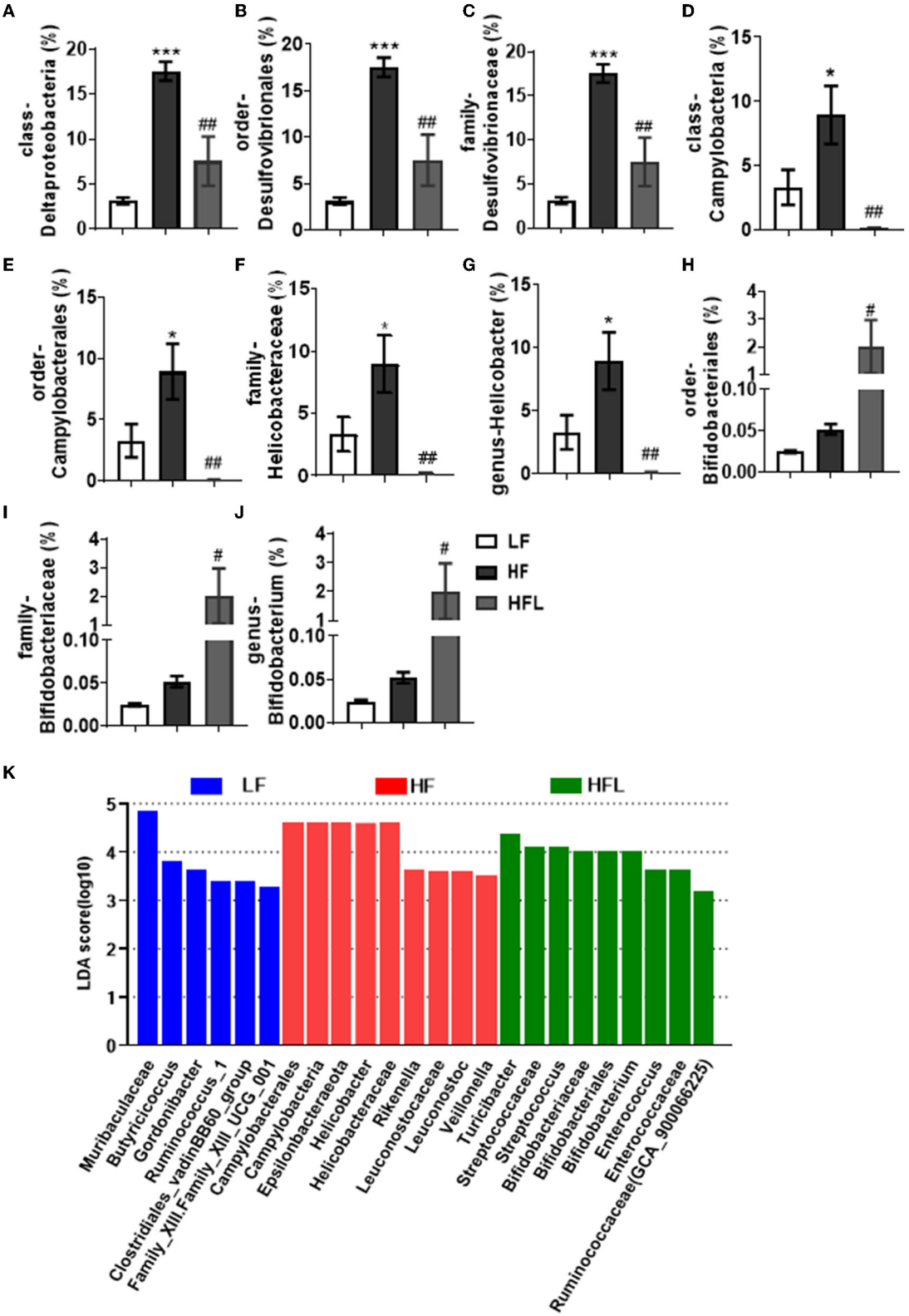

FIGURE 2 | Lentinan restored the HF-induced compositional shift of gut microbial community. **(A–K)** Comparison of the representative taxonomic abundance of class Deltaproteobacteria **(A)**, order Desulfovibrionales **(B)**, family Desulfovibrionaceae **(C)**, class Campylobacteria **(D)**, order Campylobacterales **(E)**, family Helicobacteraceae **(F)**, genus *Helicobacter* **(G)**, order Bifidobacteriales **(H)**, family Bifidobacteriaceae **(I)**, and genus *Bifidobacterium* **(J)**. **(K)** LEfSe results of mice gut microbiomes. Values are means ± SEM ($n = 6$). $^{*}p < 0.05$, $^{***}p < 0.001$ vs. LF mice; $^{\#}p < 0.05$, $^{\#\#}p < 0.01$ vs. HF mice.

TABLE 1 | Predicted KEGG functional pathway differences at level 2 inferred from 16S rRNA gene sequence using PICRUSt after LF, HF and HFL diet.

KO functional categories		LF	HF	HFL	LF vs. HF	HF vs. HFL
Level One	**Level Two**				***p*-value**	***p*-value**
Metabolism	Carbohydrate Metabolism	12.062 ± 0.232	11.862 ± 0.335	12.522 ± 0.228	—	0.001
	Amino Acid Metabolism	10.842 ± 0.321	10.431 ± 0.181	10.421 ± 0.264	0.016	—
	Nucleotide Metabolism	4.562 ± 0.153	4.408 ± 0.12	4.608 ± 0.188	—	0.042
	Enzyme Families	2.569 ± 0.025	2.476 ± 0.052	2.528 ± 0.063	0.005	—
	Glycan Biosynthesis and Metabolism	2.683 ± 0.217	2.414 ± 0.151	2.108 ± 0.165	0.020	0.010
	Metabolism of Other Amino Acids	1.655 ± 0.033	1.551 ± 0.025	1.639 ± 0.075	0.003	0.008
	Biosynthesis of Other Secondary Metabolites	1.037 ± 0.044	0.947 ± 0.035	0.982 ± 0.043	0.002	—
Genetic Information Processing	Transcription	3.424 ± 0.117	3.483 ± 0.144	3.631 ± 0.077	—	0.044
Environmental Information Processing	Signal Transduction	2.139 ± 0.247	2.44 ± 0.193	2.04 ± 0.254	0.041	0.010
	Signaling Molecules and Interaction	0.194 ± 0.003	0.179 ± 0.011	0.212 ± 0.03	—	0.007
Cellular Processes	Cell Motility	3.629 ± 0.992	4.453 ± 0.691	3.155 ± 0.716	—	0.014
	Transport and Catabolism	0.415 ± 0.045	0.335 ± 0.034	0.306 ± 0.047	0.005	—
Human Diseases	Metabolic Diseases	0.106 ± 0.011	0.094 ± 0.004	0.103 ± 0.008	—	0.025
Organismal Systems	Environmental Adaptation	0.201 ± 0.011	0.221 ± 0.010	0.199 ± 0.007	0.002	0.001
	Nervous System	0.111 ± 0.004	0.103 ± 0.002	0.109 ± 0.004	0.001	0.010
	Immune System	0.105 ± 0.012	0.094 ± 0.006	0.092 ± 0.006	0.044	—
	Digestive System	0.023 ± 0.006	0.015 ± 0.003	0.014 ± 0.004	0.016	—
	Excretory System	0.02 ± 0.005	0.011 ± 0.004	0.012 ± 0.004	0.003	—
	Circulatory System	0.009 ± 0.008	0.015 ± 0.011	0 ± 0.001	—	0.007

Values are mean (%) ± standard deviation (%). n = 6. KEGG, Kyoto Encyclopedia of Genes and Genomes; PICRUSt, Phylogenetic Investigation of Communities by Reconstruction of Unobserved States; KO, KEGG Ortholog; LF, low-fat diet; HF, high-fat diet; HFL, HF diet supplemented with lentinan.

Turicibacter, family Streptococcaceae, genus *Streptococcus*, genus *Enterococcus*, family Enterococcaceae, and genus *Ruminococcaceae* (GCA_900066225) were also increased in HFL mice. Moreover, KEGG functional orthologs predicted potential functional interactions between the gut microbiota and host among the LF, HF, and HFL group in 19 functional orthologs at level two (**Table 1**). Totally, 12 functional orthologs were significantly altered in the HF group compared with the LF group. Compared with the HF group, the lentinan supplementation was associated with microbial functional shifts in 12 functional orthologs, including carbohydrate metabolism, nucleotide metabolism, glycan biosynthesis and metabolism, metabolism of other amino acids, transcription, signal transduction, and so on.

Dietary Lentinan Supplementation Improved Hyperendotoxinemia, Tight Junction Proteins, and Redox Imbalance in the Jejunum of HF Mice

Gut microbiota alteration can promote the endotoxinemia and alteration of intestinal barrier integrity (45). After identifying the capacity of lentinan to prevent gut dysbiosis, we next examined the serum LPS and the tight junction proteins, occludin and ZO-1 in the jejunum. The serum LPS level was significantly increased in the HF fed mice, whereas lentinan inhibited the elevation of serum LPS in the mice fed by HF diet, but not by LF diet ($p < 0.01$, **Figure 3A**). Meanwhile, the mRNA expressions of the tight junction proteins, occludin and ZO-1, were significantly lower in the jejunum of HF diet-fed mice compared with LF and HFL groups (all $p < 0.05$, **Figure 3B**). In line with these findings in transcription level, the protein levels of the tight junction proteins were significantly increased in the mice with lentinan supplementation (all $p < 0.05$, **Figure 3C**). The HF mice showed reduced immunofluorescence staining of both occludin and ZO-1, whereas clear and uniform positive staining of the tight junction proteins was found in the epithelium of jejunum in LF and HFL groups (**Figure 3D**), suggesting that intestinal barrier integrity was improved by lentinan supplementation.

Given that redox imbalance is the major factor for intestinal barrier dysfunction (7–10), we next investigated the effects of lentinan supplementation on antioxidants and oxidative stress markers in the jejunum. The expression of antioxidants Nrf2, HO-1, NQO1, and Gclc was decreased in the HF group, whereas lentinan supplementation significantly prevented the decrease in antioxidants induced by the HF diet (all $p < 0.05$, **Figures 3E,F**). Moreover, lentinan significantly inhibited the HF diet-mediated increments of iNOS protein (all $p < 0.05$, **Figures 3E–G**). These findings suggest lentinan supplementation attenuated redox imbalance in the intestine of HF mice.

Dietary Lentinan Supplementation Prevented HF Diet-Induced Hepatosteatosis and Hepatic Inflammation

Following lentinan improving gut microbiota, redox balance, and tight junction proteins, we further examined the effects of lentinan on hepatic lipid deposition and macrophage infiltration.

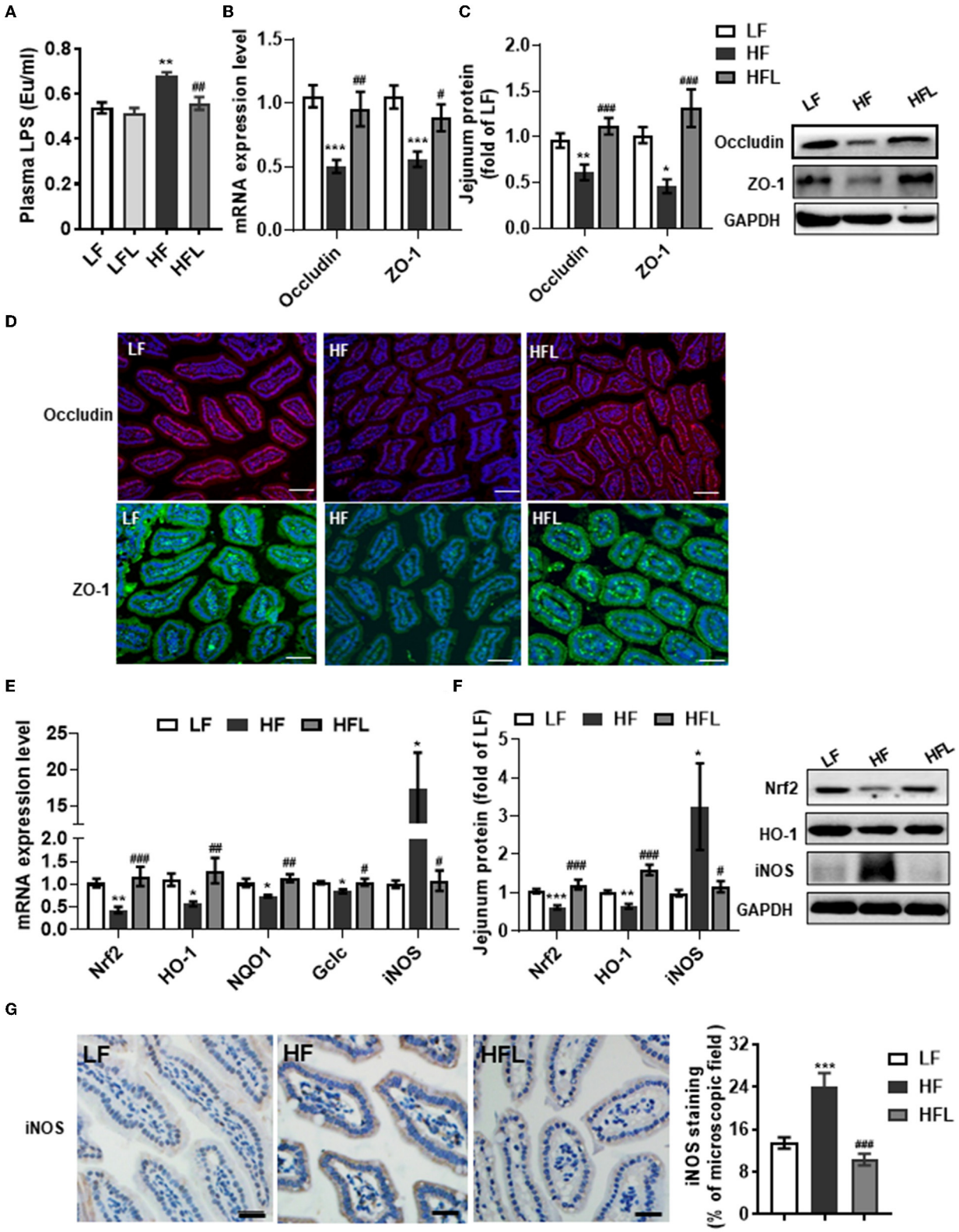

FIGURE 3 | Lentinan improved intestinal barrier integrity and oxidative stress in the jejunum in HF mice. **(A)** Serum LPS levels. **(B)** The mRNA levels of occludin and ZO-1 in the jejunum. **(C)** Protein levels of occludin and ZO-1 in the jejunum. **(D)** Immunofluorescence staining of occludin and ZO-1 proteins in the jejunum sections. **(E)** The mRNA levels of Nrf2, HO-1, NQO1, Gclc, and iNOS in the jejunum. **(F)** Protein levels of Nrf2, HO-1, and iNOS in the jejunum. **(G)** iNOS protein staining of

(Continued)

FIGURE 3 | jejunum sections and quantification of iNOS protein after staining. Values are means ± SEM ($n = 6$). $^{*}p < 0.05$, $^{**}p < 0.01$, $^{***}p < 0.001$ vs. LF mice; $^{\#}p < 0.05$, $^{\#\#}p < 0.01$, $^{\#\#\#}p < 0.001$ vs. HF mice. Scale bar: 50 μM.

With oil red O and H&E staining, the hepatocytes of the HF group contained larger cytoplasmic lipid droplets ($p < 0.001$, **Figures 4A,B**) and were enlarged with ballooning ($p < 0.001$, **Figures 4C,D**), compared with LF mice. These alterations in hepatic cellular morphology were significantly prevented by lentinan supplementation. Moreover, we found that the number of F4/80-positive cells (macrophage marker) was higher in HF mice compared with LF mice and HFL mice (both $p < 0.05$, **Figures 4E,F**), indicating that lentinan suppressed macrophage infiltration induced by HF diet. Importantly, lentinan supplementation reduced the mRNA expression of macrophage-related gene CD68 and CD11c (the marker of proinflammatory M1 type macrophages), but increased the mRNA expression of CD206 (the marker of antiinflammatory M2 type macrophages) (all $p < 0.05$, **Figure 4G**), suggesting that the M1 macrophage polarization was inhibited by lentinan. Furthermore, lentinan supplementation inhibited the mRNA of the proinflammatory cytokines and chemokines, TNFα, IL-1β, IL-6, and monocyte chemoattractant protein-1 (Mcp1) compared with HF mice (all $p < 0.05$, **Figure 4H**) and increased the expression of antiinflammatory cytokines, IL-10, and arginase I (Arg1) (both $p < 0.05$, **Figure 4H**). Moreover, the mRNA expressions of Lbp and Tlr4 (the LPS-binding protein and cell surface pattern recognition receptors) were significantly higher in the liver of HF mice compared to LF mice and HFL mice ($p < 0.05$, **Figure 4H**), which is consistent with the increase in serum LPS levels in the HF group described previously (**Figure 3A**).

The Spearman's correlation analysis was used to investigate the relationship between gut bacterial abundance and serum LPS and its binding protein and receptor in the liver and also hepatic proinflammatory and antiinflammatory cytokines (**Figure 4I**). Phylum Proteobacteria and its down taxa (class Deltaproteobacteria, order Desulfovibrionales, and family Desulfovibrionaceae), and also phylum Epsilonbacteraeota and its down taxa (class Campylobacteria, order Campylobacterales, family Helicobacteraceae and genus *Helicobacter*), were positively correlated with LPS, Lbp, Tlr4, and proinflammatory cytokines, whereas negatively correlated with antiinflammatory cytokines, IL-10, and Arg1. Phylum Actinobacteria and its down taxa (order Bifidobacteriales, family Bifidobacteriaceae, and genus *Bifidobacterium*) were negatively correlated with Tlr4 and positively correlated with IL-10. Therefore, these findings suggest that lentinan in attenuation of HF diet-induced hepatic inflammation was associated with the improvement of gut microbiota profile.

Dietary Lentinan Supplementation Improved Glucose Intolerance and Hepatic NFκB-PTP1B-Akt-GSK3β Signaling Pathway in HF Mice

Hepatic inflammation contributes to insulin resistance and abnormal glucose metabolism (46). Next, we determined whether lentinan could improve glucose metabolism. In the GTT test, lentinan decreased the blood glucose level at 60-, 90-, and 120-min time points (all $p < 0.05$, **Figure 5A**). The glucose area under curve (AUC) was markedly higher in HF mice than in LF, LFL, and HFL mice (both $p < 0.01$, **Figure 5B**). Consistently, mRNA expression of insulin receptor (INSR) was significantly lower in livers of HF mice than that in the other two groups (both $p < 0.001$, **Figure 5C**). PTP1B is a mediator of the proinflammatory (NFκB) signaling pathway in dysregulation of insulin (pAkt-pGSK3β) signaling cascade (47). We found that lentinan significantly decreased the total and phosphorylated protein levels of NFκB subunit p65 and also PTP1B protein level in livers of HF mice (all $p < 0.001$, **Figure 5D**). Furthermore, the phosphorylation levels of Akt and GSK3β significantly decreased in HF diet-fed mice, whereas lentinan reversed the reduction in these two insulin signaling molecules (both $p < 0.05$, **Figure 5D**). These results showed that lentinan improved glucose intolerance and retrieved the insulin Akt-GSK3β signaling pathway in HF mice. In addition, we observed that after the HF diet for 15 weeks, the mice had significantly higher body weight, body weight gain, energy intake, and liver weight compared with LF diet-fed mice, and lentinan supplementation prevented these changes (**Supplementary Table S3**). However, these metabolic indexes of LFL mice were not significantly altered compared with LF group (**Supplementary Table S3**).

Dietary Lentinan Supplementation Modulated Hepatic Transcriptome Related to Metabolism and Immune Response

To gain comprehensive profiles of lentinan supplementation on the hepatic metabolisms and inflammation at the transcriptome level, RNA-sequencing (RNA-seq) of liver tissues of HF and HFL groups was performed, followed by differentially expressed genes (DEGs) screening analysis. Consequently, lentinan supplementation modulated a total of 749 genes, including 408 upregulated genes and 341 downregulated genes (**Figures 6A,B**). Within the organismal system, 48 genes were significantly altered in the immune system, the most affected system (**Figure 6C**). In metabolism pathways, there were 146 genes altered, including 24 in lipid metabolism, 8 in glycan biosynthesis and metabolism, and 13 in carbohydrate metabolism. The top 20 KEGG pathways associated with DEGs are shown in **Supplementary Table S4**. Of these, the energy metabolism and immune response-related pathways were significantly affected in the liver of mice with lentinan supplementation, such as PI3K-Akt signaling pathway, metabolic pathways, arachidonic acid metabolism, and cytokine–cytokine receptor interaction. The PPI network was constructed to clarify the interaction of DEGs involved in hepatic lipid metabolism, carbohydrate metabolism, immune system, and PTP1B-Akt signaling affected by lentinan. The results demonstrated that the complex interaction network of immune and metabolism was significantly intervened by the lentinan supplementation (**Figure 6D**). The connectivity degree

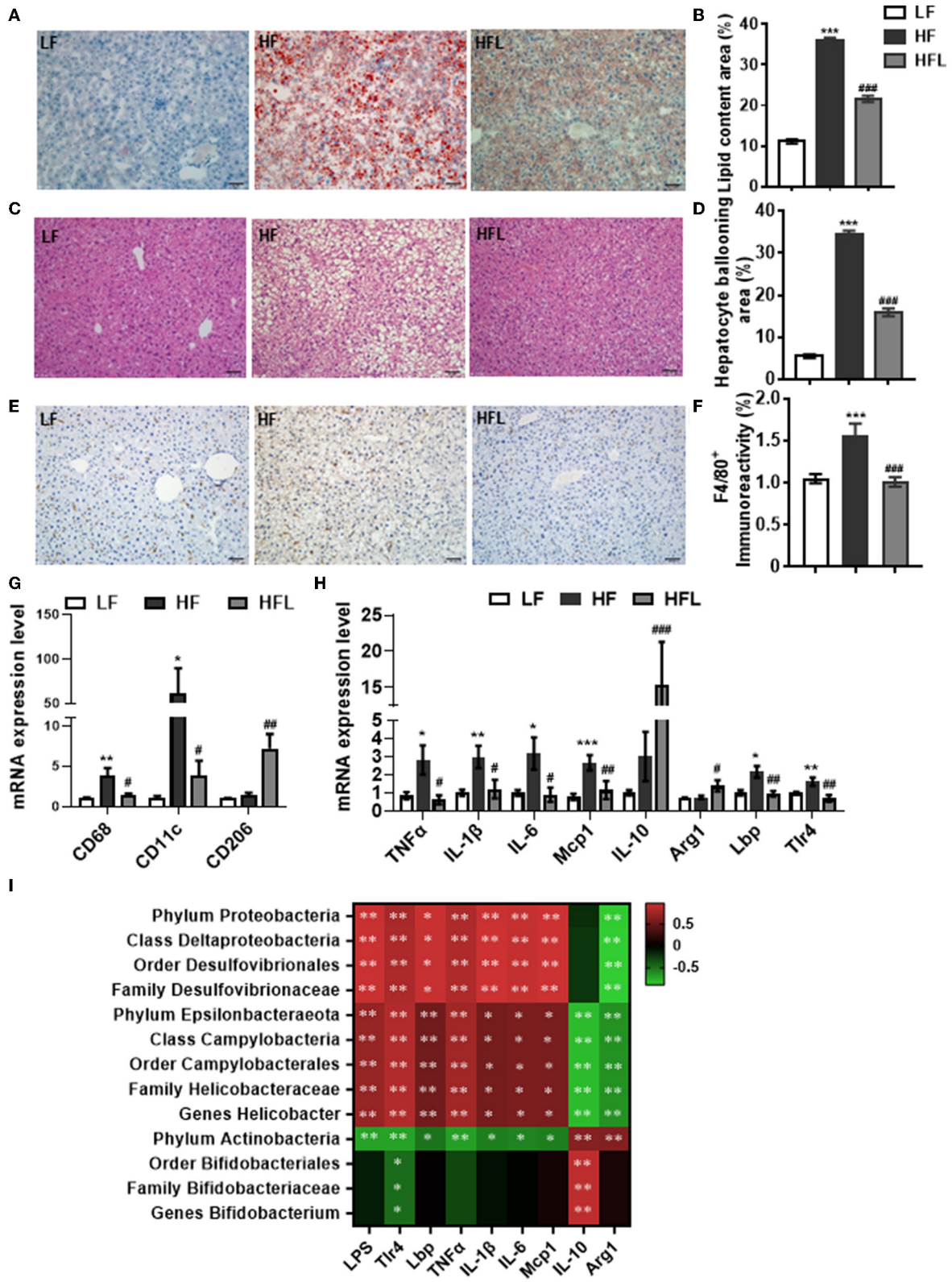

FIGURE 4 | Lentinan prevented HF diet-induced hepatic lipid deposition, macrophage infiltration, and hepatic inflammation. **(A)** Oil red O staining of liver sections. **(B)** Quantification of hepatic lipid area after Oil red O staining. **(C)** H&E staining of liver sections. **(D)** Quantification of hepatic ballooning after H&E staining. **(E)** F4/80 protein staining of liver sections. **(F)** Densitometric analysis of F4/80 staining. **(G)** CD68, CD11c, and CD206 mRNA levels in liver tissues of mice. **(H)** The mRNA levels

(Continued)

FIGURE 4 | of TNFα, IL-1β, IL-6, Mcp1, IL-10, Arg1, Lbp, and Tlr4 in liver tissues. **(I)** Correlation between specific gut microbiota, serum LPS, its binding protein and receptor in the liver, and hepatic proinflammatory and antiinflammatory cytokine expression. Values are means ± SEM ($n = 6$). $^{*}p < 0.05$, $^{**}p < 0.01$, $^{***}p < 0.001$ vs. LF mice; $^{\#}p < 0.05$, $^{\#\#}p < 0.01$, $^{\#\#\#}p < 0.001$ vs. HF mice.

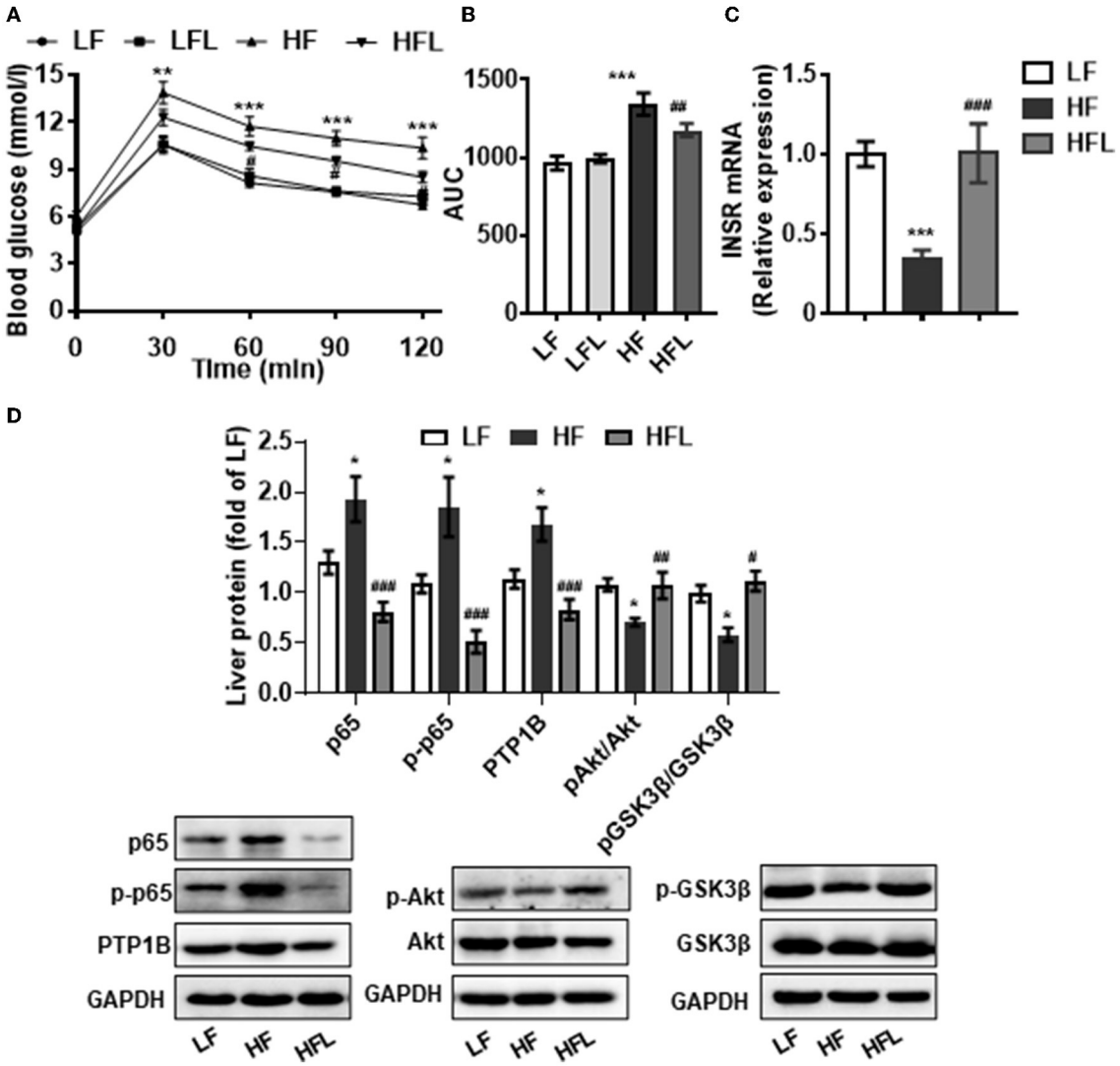

FIGURE 5 | Lentinan improved glucose intolerance and NFκB-PTP1B-Akt-GSK3β signaling pathway in the liver of HF mice. **(A)** Blood glucose levels during GTT performed on week 13 and **(B)** area under the curve (AUC). **(C)** Hepatic INSR mRNA levels. **(D)** Protein levels of p65, p-p65, PTP1B, p-Akt/Akt, and p-GSK3β/GSK3β in liver tissues. Values are means ± SEM ($n = 6$). $^{*}p < 0.05$, $^{**}p < 0.01$, $^{***}p < 0.001$ vs. LF mice; $^{\#}p < 0.05$, $^{\#\#}p < 0.01$, $^{\#\#\#}p < 0.001$ vs. HF mice.

of PTP1B-Akt signaling with the PPI network was 38, indicating that PTP1B-Akt is a key node with a higher centrality value in the interaction network regulated by lentinan in HF diet-fed mice. Furthermore, we confirmed the mRNA expression of 10 DEGs by qPCR (**Figure 6E**).

DISCUSSION

In this study, we demonstrated that chronic dietary supplementation of lentinan attenuated gut microbiota alteration, intestinal tight junction deficit, and redox imbalance induced by a HF diet. In the liver, lentinan suppressed steatohepatitis and improved endotoxemia (LPS) and its downstream NFκB-PTP1B-Akt-GSK3β (inflammation–insulin) signaling pathway. Furthermore, Spearman's correlation analysis revealed that the gut phylum Proteobacteria, Epsilonbacteraeota, and Actinobacteria, and also their next level taxa, were correlated with LPS-related-binding protein and receptor, and inflammatory cytokines in the liver. Previous animal and epidemiological studies suggest that mushroom intake has beneficial effects for steatohepatitis and NALFD (48–50). For example, in a large population-based study (a cross-sectional

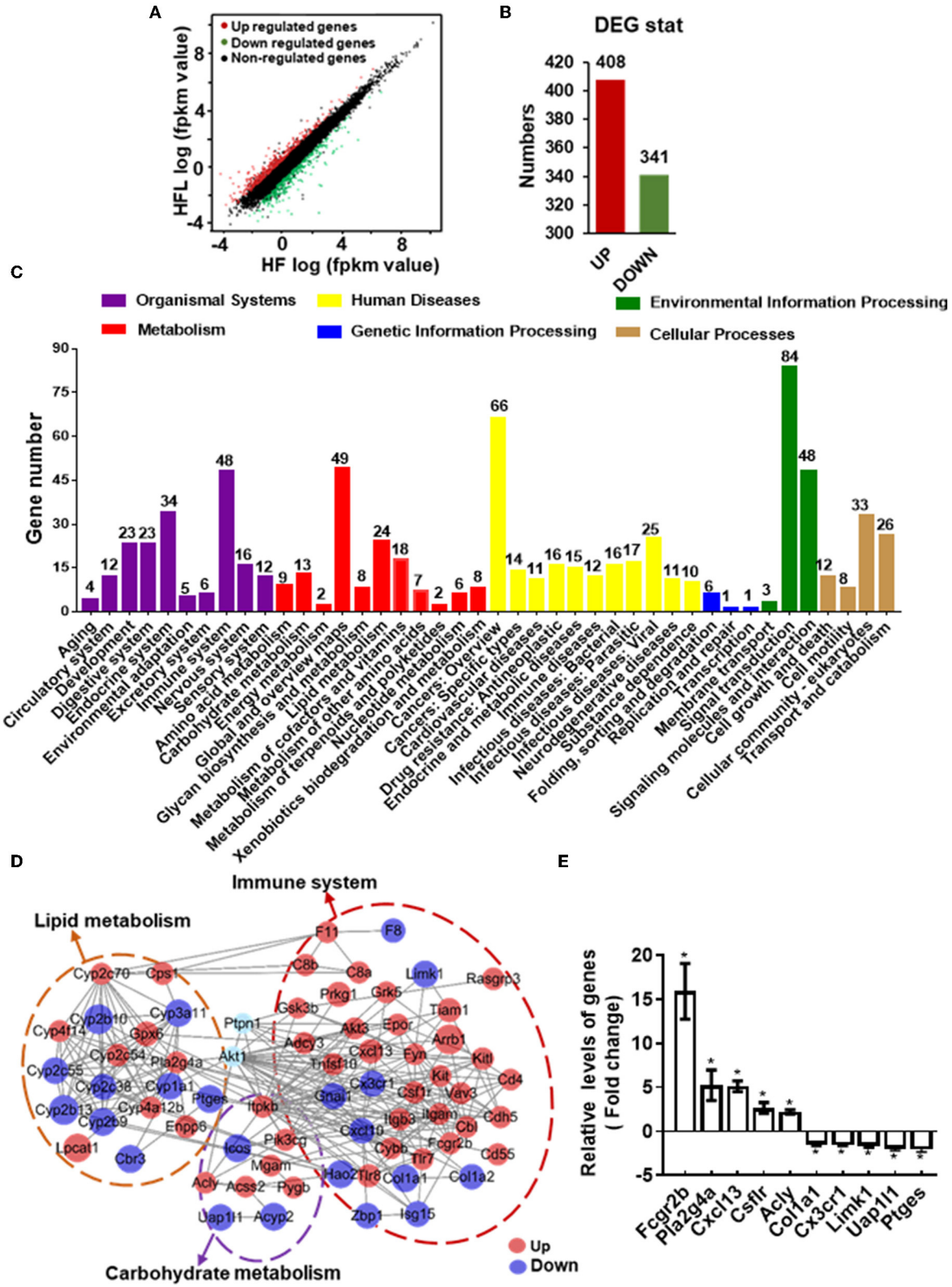

FIGURE 6 | Lentinan modulated hepatic transcriptome for immune and metabolism. **(A)** Scatter plots of genes in pairwise of the HFL group vs. the HF group. The x-axis and y-axis present gene expression levels. **(B)** The number of differentially expressed genes (DEGs). **(C)** KEGG pathway classification of DEGs for the HFL group vs. the HF group. All second-level categories are grouped in top categories in different colors ($n = 3$). **(D)** PPI network by string analysis of DEGs involved in lipid

(Continued)

FIGURE 6 | metabolism, carbohydrate metabolism, immune system, and PTP1B-Akt signaling. The line indicates interaction evidence of nodes. Orange represents upregulation, and blue represents downregulation in the HFL mice by comparison with the HF mice. **(E)** qPCR analysis of the mRNA of some altered genes in the PPI network. Values are means ± SEM ($n = 6$). *$p < 0.05$, vs. HF mice.

study of 24,236 adults), a high intake of mushrooms is associated with a low prevalence of NAFLD (50). However, the detailed mechanisms of mushroom in improving NAFLD have not been investigated. Here, importantly, our findings of lentinan (the main ingredient of mushroom) in benefits to the gut–liver axis suggest that lentinan as a prebiotic contributes to mushroom consumption in preventing western-style diets induced NAFLD.

Previous clinical studies have reported that the richness and diversity of gut microbiota are decreased in patients with NAFLD (51, 52). Furthermore, at the phylum level, the proportion of Bacteroidetes is decreased in patients with NAFLD (53). The progression of NAFLD is correlated with an increase in Proteobacteria (52). In this study, in the HF diet-induced NAFLD mouse model, we found that both the richness and the diversity were decreased in the gut microbiota. At phylum levels, the abundance of Bacteroidetes was decreased, whereas the Proteobacteria was increased in HF diet-fed mice. Therefore, the findings of our mouse study further suggest that overconsumption of dietary fat contributes to gut microbiota dysbiosis (in richness, diversity, and composition) in the NAFLD. Importantly, in this study, supplementation of lentinan prevented HF diet-induced gut microbiota alteration in richness and composition. At phylum levels, lentinan ameliorated the elevation of the Proteobacteria and Epsilonbacteraeota induced by a HF diet. Moreover, lentinan increased the abundance of Actinobacteria and Firmicutes at phylum levels. With LDA analysis, lentinan supplementation promoted bacteria that belongs to the phylum Actinobacteria, including order Bifidobacteriales, family Bifidobacteriaceae, and genus *Bifidobacterium*. These bacteria have been reported to be probiotics to improve lipid metabolism and inhibit the progression of NAFLD (54, 55). Therefore, lentinan in improving the gut microbiota richness and composition in the above probiotics may contribute to the prevention of NAFLD induced by the HF diet.

In this study, lentinan supplementation promoted the probiotics for gut health, such as genus *Bifidobacterium.* It is reported that microbiomes belonging to the genus *Bifidobacterium* are associated with decreased intestinal permeability of infants (56), and the administration of *Bifidobacterium infantis* increases the tight junction proteins, occludin and claudin four, in the intestine of a neonatal mouse model of necrotizing enterocolitis (57). The probiotics in *Bifidobacterium* improving gut integrity have been considered due to their potentials in reducing oxidative stress. For example, *Bifidobacterium lactis HN019* supplemented in milk reduces nitric oxide metabolites levels in patients with metabolic syndrome (58). A yogurt enriched with *Bifidobacterium lactis* decreases malondialdehyde (a prooxidant biomarker) in patients with diabetes mellitus type two (59). Importantly, we found that lentinan supplementation significantly attenuated the alterations in oxidative stress marker iNOS and antioxidants Nrf2, HO-1, NQO1, and Gclc in the small intestinal tissue induced by the chronic HF diet. Overall, these findings suggest that lentinan supplementation in promoting probiotics, such as genus *Bifidobacterium,* contributes to attenuating cellular redox imbalance and intestinal barrier disruption.

In this study, we found a dramatic reduction in tight junction proteins (occludin and ZO-1) in the jejunum of HF mice. It is reported that the intensity of ZO-1 staining is significantly lower in the duodenum of patients with NAFLD with increased intestinal permeability (60). The abnormality of intestine permeability is related to the increased bacterial overgrowth prevalence in the small intestine of these patients (60). Interestingly, in this study, we revealed that the bacteria of phylum Proteobacteria and Epsilonbacteraeota were significantly increased in the small intestine of NAFLD mice induced by the HF diet. Proteobacteria is a major source of translocated antigen LPS from the gut (61, 62). It is reported that LPS exposure causes oxidative stress in the gut (63). NO/iNOS system mediates LPS-induced barrier dysfunction in the intestine, evidenced by that the administration of NOS inhibitor attenuates LPS-induced tight junction disruption in the ileum and colon of mice (9). Therefore, the increased Proteobacteria and its derived LPS may contribute to gut barrier dysfunction and redox imbalance. In addition, some bacteria of phylum Epsilonbacteraeota, such as order Campylobacterales, genus *Campylobacter,* and genus *Helicobacter*, are tolerant of bile acids and promote hepatic inflammation (64). Flagellins and other 19 proteins of *Campylobacter jejuni* are associated with the bile adaptation (65). The intragastrical inoculation of *Helicobacter hepaticus* induces chronic hepatitis and fibrosis in mice with the activation of p65 in the liver (66). Therefore, the above findings suggest that the bile resistance property of bacteria in phylum Epsilonbacteraeota may allow them to colonize the bile and liver to promote chronic hepatitis in the NAFLD mice induced by the HF diet. Importantly, we found that lentinan supplementation improved tight junction proteins (occludin and ZO-1) deficits in the small intestine and concurrently decreased the proportion of phylum Proteobacteria and Epsilonbacteraeota and serum LPS in HF diet-fed mice. Therefore, lentinan in the prevention of the dysbiosis of Proteobacteria, overtranslocation of its derived metabolite LPS into blood circulation and the inhibition of bile-resistant Epsilonbacteraeota may be involved in the improvement of gut barrier dysfunction and hepatic inflammation induced by chronic HF diet.

The liver is an important immunological organ, in which the immune system is activated after exposure to gut microbiome-derived factors, such as LPS (13, 67). We found that LPS-binding protein and cell surface pattern recognition receptor, Lbp and Tlr4, were significantly increased in the liver of mice fed the HF diet. Consistently, in a clinical study, Tlr4 mRNA

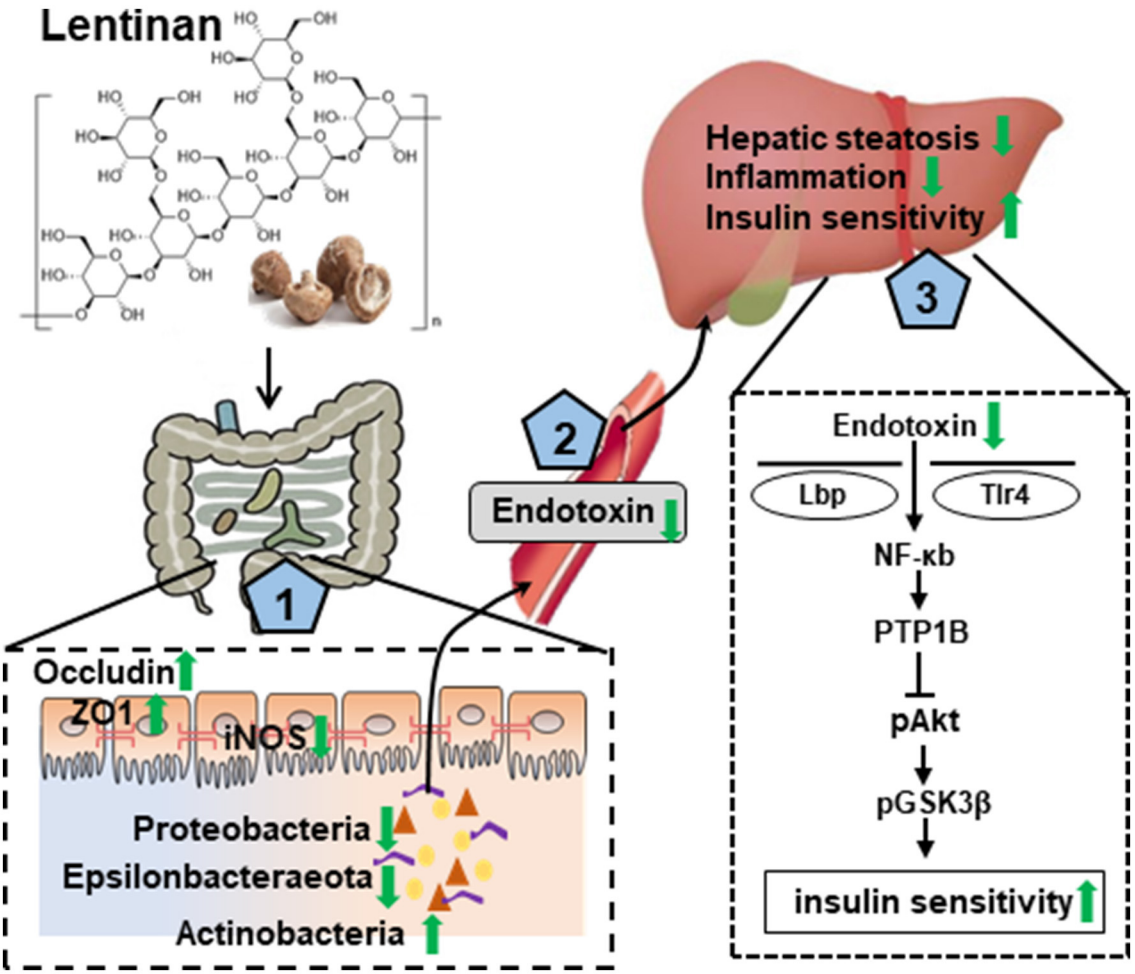

FIGURE 7 | Graphical summary of the protective effect of lentinan on the development of NAFLD *via* the gut–liver axis. Lentinan showed conservation of appropriate intestinal microbiota composition, resetting cellular redox balance (activation of antioxidants and inhibition of iNOS), and increasing tight junction proteins for gut epithelial integrity (1), which contribute to reduce endotoxin translocation into circulation and liver (2) and thereby to mitigate the adverse consequences of HF consumption, that is, hepatic steatosis and inflammation, and insulin resistance (3). Green arrows represent lentinan's effects.

expression is upregulated in hepatic biopsy tissue of patients with NASH with increased serum LPS (17). Tlr4 triggers the initial activation of the NFκB signaling pathway, which is necessary for the transcription of proinflammatory cytokines (TNFα, IL-6, and IL-1β) and overexpression of PTP1B (the inhibitor of insulin signaling) (15, 68). In this study, we found that the HF diet promoted steatohepatitis and glucose intolerance in mice, which had M1 proinflammatory macrophage polarization, elevated NFκB and PTP1B level and impaired insulin Akt-GSK3β signaling pathway in the liver. Importantly, supplementation with lentinan attenuated these adverse effects induced by the HF diet. Furthermore, the RNA-seq profile of the liver transcriptome followed by the KEGG pathways analysis also confirmed that the PI3K-Akt signaling pathway and cytokine–cytokine receptor interaction in the liver were significantly affected by lentinan. Consistently, the PPI network analysis showed that PTP1B and Akt1 are vital nodes in the network among metabolism and the immune system. In addition, the KEGG pathway analysis suggests that lentinan significantly modulated the arachidonic acid metabolism pathway, which is reported to be involved in the development and progression of NAFLD (69). However, the detailed mechanism of the arachidonic acid pathway involving lentinan improving NAFLD requires further investigation. Furthermore, according to the current mice study, supplementation of 368 mg lentinan per day may attenuate the NAFLD in humans. However, clinical trials would be required to determine the optimum dose in future human studies.

CONCLUSION

In summary, this study with the NAFLD mouse model induced by the HF diet, chronic lentinan supplementation preserved the conservation of gut microbiota in richness and appropriate composition. Remarkably, lentinan supplementation promoted genus *Bifidobacterium* (important for intestinal barrier integrity

and redox balance) and inhibited the proliferation and growth of bacteria belonging to the phylum Proteobacteria (a major source of translocated antigen LPS) and bile-resistant Epsilonbacteraeota. Lentinan supplementation enhanced tight junction proteins and reset cellular redox balance (activation of antioxidants and inhibition of iNOS) in the small intestine and also improved steatohepatitis and NFκB-PTP1B-Akt-GSK3β (inflammation–insulin) signaling pathway in the liver. In addition to highlight the mechanisms underlying lentinan in improving NAFLD through the gut–liver axis (**Figure 7**), the findings of this study suggest increasing intake of mushroom ingredient, lentinan, could be a plausible strategy to mitigate the adverse effects of western-style diets on the gut microbiota and gut–liver axis in NAFLD.

DATA AVAILABILITY STATEMENT

RNA-Seq analysis raw reads were deposited into the NCBI Sequence Read Archive (SRA) database, accession number PRJNA784639. All 16S rRNA raw data were submitted to the NCBI Sequence Read Archive (SRA) database with the accession number PRJNA784743.

ETHICS STATEMENT

The animal study was reviewed and approved by the Ethics Committee of Xuzhou Medical University.

AUTHOR CONTRIBUTIONS

XY and YY: conceptualization and funding acquisition. MZhe: methodology and data curation. XG, MZho, LZ, XL, ML, and HL: validation. MZhe, JZ, and NP: formal analysis. XY: investigation. XY and MZhe: writing—original draft preparation. YY and KZ: writing, reviewing, and editing. X-FH and YY: visualization. All authors contributed to the article and approved the submitted version.

FUNDING

The study was funded by the National Natural Science Foundation of China (81870854, 82071184, and 81800718), the Natural Science Foundation of the Jiangsu Higher Education Institutions of China (18KJB310015 and 19KJA560003), the Natural Science Foundation of Jiangsu Province (No. BK20211055), the Jiangsu Shuangchuang Program, the Priority Academic Program Development of Jiangsu Higher Education Institutions (PAPD) in 2014, the Starting Foundation for Talents of Xuzhou Medical University (D2018006 and D2018003), and the Jiangsu Graduate Innovation Program (No. KYCX20_2469 and No. KYCX21_2637).

SUPPLEMENTARY MATERIAL

The Supplementary Material for this article can be found online at: https://www.frontiersin.org/articles/10.3389/fnut.2021.803691/full#supplementary-material

REFERENCES

1. Musso G, Cassader M, Gambino R. Non-alcoholic steatohepatitis: emerging molecular targets and therapeutic strategies. *Nat Rev Drug Discov.* (2016) 15:249–74. doi: 10.1038/nrd.2015.3
2. Tiniakos DG, Vos MB, Brunt E.M. Nonalcoholic fatty liver disease: pathology and pathogenesis. *Annu Rev Pathol.* (2010) 5:145–71. doi: 10.1146/annurev-pathol-121808-102132
3. Tripathi A, Debelius J, Brenner DA, Karin M, Loomba R, Schnabl B, et al. The gut–liver axis and the intersection with the microbiome. *Nat Rev Gastroenterol Hepatol.* (2018) 15:397–411. doi: 10.1038/s41575-018-0011-z
4. Schnabl DA. Interactions between the intestinal microbiome and liver diseases. *Gastroenterology.* (2014) 146:1513–24. doi: 10.1053/j.gastro.2014.01.020
5. Mokhtari Z, Gibson DL, Hekmatdoost A. Nonalcoholic fatty liver disease, the gut microbiome, and diet. *Adv Nutr.* (2017) 8:240–52. doi: 10.3945/an.116.013151
6. Sellmann C, Degen C, Jin CJ, Nier A, Engstler AJ, Hasan Alkhatib D, et al. Oral arginine supplementation protects female mice from the onset of non-alcoholic steatohepatitis. *Amino Acids.* (2017) 49:1215–25. doi: 10.1007/s00726-017-2423-4
7. Grishin A, Bowling J, Bell B, Wang J, Ford HR. Roles of nitric oxide and intestinal microbiota in the pathogenesis of necrotizing enterocolitis. *J Pediatr Surg.* (2016) 51:13–7. doi: 10.1016/j.jpedsurg.2015.10.006
8. Rao R. Oxidative stress-induced disruption of epithelial and endothelial tight junctions. *Front Biosci.* (2008) 13:7210–26. doi: 10.2741/3223
9. Han X, Fink MP, Yang R, Delude RL. Increased iNOS activity is essential for intestinal epithelial tight junction dysfunction in endotoxemic mice. *Shock.* (2004) 21:261–70. doi: 10.1097/01.shk.0000112346.38599.10
10. Nam ST, Hwang JH, Kim DH, Park MJ, Lee IH, Nam HJ, et al. Role of NADH: quinone oxidoreductase-1 in the tight junctions of colonic epithelial cells. *BMB Reports.* (2014) 47:494–9. doi: 10.5483/BMBRep.2014.47.9.196
11. Zhang S, Zhou Q, Li Y, Zhang Y, Wu Y. MitoQ modulates lipopolysaccharide-induced intestinal barrier dysfunction via regulating Nrf2 signaling. *Mediators Inflamm.* (2020) 2020:3276148. doi: 10.1155/2020/3276148
12. Patouraux S, Rousseau D, Bonnafous S, Lebeaupin C, Luci C, Canivet CM, et al. CD44 is a key player in non-alcoholic steatohepatitis. *J Hepatol.* (2017) 67:328–38. doi: 10.1016/j.jhep.2017.03.003
13. Carpino G, Del Ben M, Pastori D, Carnevale R, Baratta F, Overi D, et al. Increased liver localization of lipopolysaccharides in human and experimental NAFLD. *Hepatology.* (2020) 72:470–85. doi: 10.1002/hep.31056
14. Zhu J, Zhang Y, Shen Y, Zhou H, Yu X. Lycium barbarum polysaccharides induce toll-like receptor 2- and 4-mediated phenotypic and functional maturation of murine dendritic cells via activation of NF-κB. *Mol Med Rep.* (2013) 8:1216–20. doi: 10.3892/mmr.2013.1608
15. Hiroki T, Shino T, Kanae K, Yohei K, Sao K, Ippo U, et al. Lipopolysaccharide (LPS)-binding protein stimulates CD14-dependent toll-like receptor 4 internalization and LPS-induced TBK1-IKKε-IRF3 axis activation. *J Biol Chem.* (2018) 293:10186–201. doi: 10.1074/jbc.M117.796631
16. Pardo V, González-Rodríguez Á, Guijas C, Balsinde J M, Valverde Á. Opposite cross-talk by oleate and palmitate on insulin signaling in hepatocytes through macrophage activation. *J Biol Chem.* (2015) 290:11663–77. doi: 10.1074/jbc.M115.649483
17. Sharifnia T, Antoun J, Verriere TGC, Suarez G, Wattacheril J, Wilson KT, et al. Hepatic TLR4 signaling in obese NAFLD. *Am J Physiol Gastrointest Liver Physiol.* (2015) 309:G270–8. doi: 10.1152/ajpgi.00304.2014
18. Wasser SP. Medicinal mushrooms as a source of antitumor and immunomodulating polysaccharides. *Appl Microbiol Biotechnol.* (2002) 60:258–74. doi: 10.1007/s00253-002-1076-7

19. Zhang S, Gu Y, Lu M, Fu J, Zhang Q, Liu L, et al. Association between edible mushroom intake and the prevalence of newly diagnosed non-alcoholic fatty liver disease: results from the TCLSIH Cohort Study in China. *Br J Nutr*. (2019) 121:1–8. doi: 10.1017/S000711451800301X
20. Tamura K, Hemsworth GR, Déjean G, Rogers TE, Pudlo NA, Urs K, et al. Molecular mechanism by which prominent human gut bacteroidetes utilize mixed-linkage beta-glucans, major health-promoting cereal polysaccharides. *Cell Rep*. (2017) 21:417–30. doi: 10.1016/j.celrep.2017.09.049
21. Butt MS, Tahir-Nadeem M, Khan MKI, Shabir R, Butt MS. Oat: unique among the cereals. *Eur J Nutr*. (2008) 47:68–79. doi: 10.1007/s00394-008-0698-7
22. Wang Y, Ames NP, Tun HM, Tosh SM, Jones PJ, Khafipour E. High molecular weight barley β-glucan alters gut microbiota toward reduced cardiovascular disease risk. *Front Microbiol*. (2016) 7:129. doi: 10.3389/fmicb.2016.00129
23. Wang X, Wang W, Wang L, Yu C, Zhang G, Zhu H, et al. Lentinan modulates intestinal microbiota and enhances barrier integrity in a piglet model challenged with lipopolysaccharide. *Food Funct*. (2019) 10:479–89. doi: 10.1039/C8FO02438C
24. de Sales Guilarducci J, Marcelino B, Konig I, Orlando T, Varaschin M, Pereira LJD, et al. Accharomyces cerevisiae therapeutic effects of different doses of prebiotic (isolated from S) in comparison to n-3 supplement on glycemic control, lipid profiles and immunological response in diabetic rats. *Diabetol Metab Syndr*. (2020) 12:69. doi: 10.1186/s13098-020-00576-6
25. Reagan-Shaw S, Nihal M. Dose translation from animal to human studies revisited. *FASEB J*. (2008) 22:659–61. doi: 10.1096/fj.07-9574LSF
26. Liu Y, Fu X, Lan N, Li S, Zhang J, Wang S, et al. Luteolin protects against high fat diet-induced cognitive deficits in obesity mice. *Behav Brain Res*. (2014) 267:178–88. doi: 10.1016/j.bbr.2014.02.040
27. Huang S, Pang L, Wei CJ. Identification of a four-gene signature with prognostic significance in endometrial cancer using weighted-gene correlation network analysis. *Front Genet*. (2021) 12:678780. doi: 10.3389/fgene.2021.678780
28. Dennis G, Sherman B, Hosack D, Yang J, Gao W, Lane H, et al. DAVID: database for annotation, visualization, integrated discovery. *Genome Biol*. (2003) 4:P3. doi: 10.1186/gb-2003-4-9-r60
29. Szklarczyk D, Morris J, Cook H, Kuhn M, Wyder S, Simonovic M, et al. The STRING database in 2017: quality-controlled protein-protein association networks, made broadly accessible. *Nucleic Acids Research*. (2017) 45:D362–8. doi: 10.1093/nar/gkw937
30. Zhou CH, Liu LL, Wu YQ, Song Z, Xing SH. Enhanced expression of salusin-beta contributes to progression of atherosclerosis in LDL receptor deficient mice. *Can J Physiol Pharmacol*. (2012) 90:463–71. doi: 10.1139/y2012-022
31. Martin-Venegas R, Brufau MT, Guerrero-Zamora AM, Mercier Y, Geraert PA, Ferrer R. The methionine precursor DL-2-hydroxy-(4-methylthio)butanoic acid protects intestinal epithelial barrier function. *Food Chem*. (2013) 141:1702–9. doi: 10.1016/j.foodchem.2013.04.081
32. Wang H, Zhu YY, Wang L, Teng T, Zhou M, Wang SG, et al. Mangiferin ameliorates fatty liver via modulation of autophagy and inflammation in high-fat-diet induced mice. *Biomed Pharmacother*. (2017) 96:328–35. doi: 10.1016/j.biopha.2017.10.022
33. Guo M, Wu F, Hao G, Qi Q, Li R, Li N, et al. Bacillus subtilis improves immunity and disease resistance in rabbits. *Front Immunol*. (2017) 8:354. doi: 10.3389/fimmu.2017.00354
34. Chen S, Zhou Y, Chen Y, Gu J. Fastp: an ultra-fast all-in-one FASTQ preprocessor. *Bioinformatics*. (2018) 34:i884–90. doi: 10.1093/bioinformatics/bty560
35. Magoč T, Salzberg SL. FLASH: fast length adjustment of short reads to improve genome assemblies. *Bioinformatics*. (2011) 27:2957–63. doi: 10.1093/bioinformatics/btr507
36. Caporaso JG, Kuczynski J, Stombaugh J, Bittinger K, Bushman FD, Costello EK, et al. QIIME allows analysis of high-throughput community sequencing data. *Nat Methods*. (2010) 7:335–6. doi: 10.1038/nmeth.f.303
37. Bokulich NA, Subramanian S, Faith JJ, Gevers D, Gordon JI, Knight, et al. Quality-filtering vastly improves diversity estimates from Illumina amplicon sequencing. *Nat Methods*. (2013) 10:57–9. doi: 10.1038/nmeth.2276
38. Edgar RC. UPARSE: highly accurate OTU sequences from microbial amplicon reads. *Nat Methods*. (2013) 10:996–8. doi: 10.1038/nmeth.2604
39. Schloss PD, Westcott SL, Ryabin T, Hall JR, Hartmann M, Hollister EB, et al. Introducing mothur: open-source, platform-independent, community-supported software for describing and comparing microbial communities. *Appl Environ Microbiol*. (2009) 75:7537–41. doi: 10.1128/AEM.01541-09
40. Segata N, Izard J, Waldron L, Gevers D, Miropolsky L, Garrett WS, et al. Metagenomic biomarker discovery and explanation. *Genome Biology*. (2011) 12:R60. doi: 10.1186/gb-2011-12-6-r60
41. Sung JJY, Coker OO, Chu E, Szeto CH, Luk STY, Lau HCH, et al. Gastric microbes associated with gastric inflammation, atrophy and intestinal metaplasia 1 year after helicobacter pylori eradication. *Gut*. (2020) 69:1572–80. doi: 10.1136/gutjnl-2019-319826
42. Langille MG, Zaneveld J, Caporaso JG, McDonald D, Knights D, Reyes JA, et al. Predictive functional profiling of microbial communities using 16S rRNA marker gene sequences. *Nat Biotechnol*. (2013) 31:814–21. doi: 10.1038/nbt.2676
43. Kirpich IA, Marsano LS, McClain CJ. Gut-liver axis, nutrition, and non-alcoholic fatty liver disease. *Clin Biochem*. (2015) 48:923–30. doi: 10.1016/j.clinbiochem.2015.06.023
44. Ni Y, Ni L, Zhuge F, Fu Z. The gut microbiota and its metabolites, novel targets for treating and preventing non-alcoholic fatty liver disease. *Mol Nutr Food Res*. (2020) 64:e2000375. doi: 10.1002/mnfr.202000375
45. Gomes AC, Hoffmann C, Mota JF. The human gut microbiota: metabolism and perspective in obesity. *Gut Microbes*. (2018) 9:308–25. doi: 10.1080/19490976.2018.1465157
46. Brenachot X, Ramadori G, Ioris R, Veyrat-Durebex C, Altirriba J, Aras E, et al. Hepatic protein tyrosine phosphatase receptor gamma links obesity-induced inflammation to insulin resistance. *Nat Commun*. (2017) 8:1820. doi: 10.1038/s41467-017-02074-2
47. Tian J, Liao X, Wang Y, Si X, Shu C, Gong E, et al. Identification of cyanidin-3-arabinoside extracted from blueberry as a selective protein tyrosine phosphatase 1B inhibitor. *J Agric Food Chem*. (2019) 67:13624–34. doi: 10.1021/acs.jafc.9b06155
48. Iñiguez M, Pérez-Matute P, Villanueva-Millán MJ, Recio-Fernández E, Roncero-Ramos I, Pérez-Clavijo M, et al. Agaricus bisporus supplementation reduces high-fat diet-induced body weight gain and fatty liver development. *J Physiol Biochem*. (2018) 74:635–46. doi: 10.1007/s13105-018-0649-6
49. Nagao K, Inoue N, Inafuku M, Shirouchi B, Morooka T, Nomura S, et al. Mukitake mushroom (Panellus serotinus) alleviates nonalcoholic fatty liver disease through the suppression of monocyte chemoattractant protein 1 production in db/db mice. *J Nutr Biochem*. (2010) 21:418–23. doi: 10.1016/j.jnutbio.2009.01.021
50. Zhang S, Gu Y, Lu M, Fu J, Zhang Q, Liu L, et al. Association between edible mushroom intake and the prevalence of newly diagnosed non-alcoholic fatty liver disease: results from the tianjin chronic low-grade systemic inflammation and health cohort study in China. *Br J Nutr*. (2020) 123:104–12. doi: 10.1017/S0007114519002605
51. Kim H-N, Joo E-J, Cheong HS, Kim Y, Kim H-L, Shin H, et al. Gut microbiota and risk of persistent nonalcoholic fatty liver diseases. *J Clin Med*. (2019) 8:1089. doi: 10.3390/jcm8081089
52. Caussy C, Tripathi A, Humphrey G, Bassirian S, Singh S, Faulkner C, et al. A gut microbiome signature for cirrhosis due to nonalcoholic fatty liver disease. *Nat Commun*. (2019) 10:1406. doi: 10.1038/s41467-019-09455-9
53. Mouzaki M, Comelli EM, Arendt BM, Bonengel J, Fung SK, Fischer SE, et al. Intestinal microbiota in patients with nonalcoholic fatty liver disease. *Hepatology*. (2013) 58:120–7. doi: 10.1002/hep.26319
54. Li C, Nie SP, Zhu KX, Ding Q, Li C, Xiong T, et al. Lactobacillus plantarum NCU116 improves liver function, oxidative stress and lipid metabolism in rats with high fat diet induced non-alcoholic fatty liver disease. *Food Funct*. (2014) 5:3216–23. doi: 10.1039/C4FO00549J
55. Hye AK, Jeon-Kyung K, Jae-Young K, Se-Eun J, Joo HM, Dong-Hyun K. Lactobacillus plantarum LC27 and Bifidobacterium longum LC67 simultaneously alleviate high-fat diet-induced colitis, endotoxemia, liver steatosis, and obesity in mice. *Nutr Res*. (2019) 67:78–89. doi: 10.1016/j.nutres.2019.03.008
56. Underwood MA, German JB, Lebrilla CB, Mills DA. Bifidobacterium longum subspecies infantis: champion colonizer of the infant gut. *Pediatr Res*. (2015) 77:229–35. doi: 10.1038/pr.2014.156

57. Bergmann KR, Liu SXL, Tian R, Kushnir A, Turner JR, Li H-L, et al. Bifidobacteria stabilize claudins at tight junctions and prevent intestinal barrier dysfunction in mouse necrotizing enterocolitis. *Am J Pathol.* (2013) 182:1595–606. doi: 10.1016/j.ajpath.2013.01.013
58. Bernini LJ, Simão ANC, de Souza CHB, Alfieri DF, Segura LG, Costa GN, et al. Effect of bifidobacterium lactis HN019 on inflammatory markers and oxidative stress in subjects with and without the metabolic syndrome. *Br J Nutr.* (2018) 120:645–52. doi: 10.1017/S0007114518001861
59. Ejtahed HS, Mohtadi-Nia J, Homayouni-Rad A, Niafar M, Asghari-Jafarabadi M, Mofid V. Probiotic yogurt improves antioxidant status in type 2 diabetic patients. *Nutrition.* (2012) 28:539–43. doi: 10.1016/j.nut.2011.08.013
60. Miele L, Valenza V, La Torre G, Montalto M, Cammarota G, Ricci, et al. Increased intestinal permeability and tight junction alterations in nonalcoholic fatty liver disease. *Hepatology.* (2009) 49:1877–87. doi: 10.1002/hep.22848
61. Needham BD, Carroll SM, Giles DK, Georgiou G, Whiteley M, Trent MS. Modulating the innate immune response by combinatorial engineering of endotoxin. *Proc Natl Acad Sci USA*. (2013) 110:1464–9. doi: 10.1073/pnas.1218080110
62. Vatanen T, Kostic AD, d'Hennezel E, Siljander H, Franzosa EA, Yassour M, et al. Variation in microbiome LPS immunogenicity contributes to autoimmunity in humans. *Cell.* (2016) 165:842–53. doi: 10.1016/j.cell.2016.04.007
63. Wu QJ, Wang YQ, Qi YX. The protective effect of procyanidin against LPS-induced acute gut injury by the regulations of oxidative state. *SpringerPlus.* (2016) 5:1645. doi: 10.1186/s40064-016-3306-y
64. Okoli AS, Wadstrom T, Mendz GL. Minireview: bioinformatic study of bile responses in *Campylobacterales*. *FEMS Immunol Med Microbiol.* (2007) 49:101–23. doi: 10.1111/j.1574-695X.2006.00194.x
65. Fox E, Raftery M, Goodchild A, Mendz GJ. Campylobacter jejuni response to ox-bile stress. *FEMS Immunol Med Microbiol*. (2007) 49:165–72. doi: 10.1111/j.1574-695X.2006.00190.x
66. Cao S, Zhu L, Zhu C, Feng J, Yin J, Lu J, et al. Helicobacter hepaticus infection-induced IL-33 promotes hepatic inflammation and fibrosis through ST2 signaling pathways in BALB/c mice. *Biochem Biophys Res Commun.* (2020) 525:654–61. doi: 10.1016/j.bbrc.2020.02.139
67. Konturek PC, Harsch IA, Konturek K, Schink M, Konturek T, Neurath MF, et al. Gut−liver axis: how do gut bacteria influence the liver? *Med Sci.* (2018) 6:79. doi: 10.3390/medsci6030079
68. Zabolotny J, Kim Y, Welsh L, Kershaw E, Neel B, Kahn B. Protein-tyrosine phosphatase 1B expression is induced by inflammation *in vivo*. *J Biol Chem.* (2008) 283:14230–41. doi: 10.1074/jbc.M800061200
69. Ma K, Chen Y, Liang X, Miao J, Zhao Q. Inhibition of 5-lipoxygenase inhibitor zileuton in high-fat diet-induced nonalcoholic fatty liver disease progression model. *Iran J Basic Med Sci.* (2017) 20:1207–12. doi: 10.22038/IJBMS.2017.9482

Conflict of Interest: The authors declare that the research was conducted in the absence of any commercial or financial relationships that could be construed as a potential conflict of interest.

Publisher's Note: All claims expressed in this article are solely those of the authors and do not necessarily represent those of their affiliated organizations, or those of the publisher, the editors and the reviewers. Any product that may be evaluated in this article, or claim that may be made by its manufacturer, is not guaranteed or endorsed by the publisher.

frontiers in Nutrition

ORIGINAL RESEARCH
published: 25 February 2022
doi: 10.3389/fnut.2022.848392

Low Dose of Sucralose Alter Gut Microbiome in Mice

Zibin Zheng[1,2†], Yingping Xiao[2†], Lingyan Ma[2], Wentao Lyu[2], Hao Peng[1,2], Xiaorong Wang[3], Ying Ren[1] and Jinjun Li[3*]*

[1] Hubei Key Laboratory of Animal Nutrition and Feed Science, Wuhan Polytechnic University, Wuhan, China, [2] State Key Laboratory for Managing Biotic and Chemical Threats to the Quality and Safety of Agro-Products, Institute of Agro-Product Safety and Nutrition, Zhejiang Academy of Agricultural Sciences, Hangzhou, China, [3] Institute of Food Sciences, Zhejiang Academy of Agricultural Sciences, Hangzhou, China

Sucralose is a non-nutritive artificial sweetener (NNS) used in foods or beverages to control blood glucose levels and body weight gain. The consumption of NNS has increased in recent years over the world, and many researches have indicated long-term sucralose administration altered the gut microbiome composition of mice. These studies all focus on the US Food and Drug Administration (FDA) defined acceptable daily intake (ADI), approximately 5 mg/kg BW/day for human. In our study, mice were given with T1-4 (0.0003, 0.003, 0.03, and 0.3 mg/mL) of sucralose, respectively, Control group mice were given normal water. In particular, 0.3 mg/mL of sucralose was equal to the ADI (5 mg/kg BW/day). After 16 weeks, all mice were weighted and sacrificed, the liver of each mouse was isolated and weighed, segments of jejunum, ileum and colon were collected for H&E-stained. The contents of jejunum, ileum, cecum and colon were collected for 16S rRNA gene sequencing. The results showed sucralose administration affects the intestinal barrier function evidenced by distinct lymphocyte aggregation in ileum and colon while not change the mice body weight. The 16S rRNA gene sequencing of the mice gut microbiome suggested sucralose administration significantly changed the composition of gut microbiota, especially in T1 and T4 group. For example, a reduction of probiotics abundance (*Lachnoclostridium* and *Lachnospiraceae*) was found in cecum of T4 group mice compared with Control group. On the other hand, *Allobaculum*, which was reported positively correlated with diabetes, was increased in the T1 and T4 group. In addition, the potential pathogens, including *Tenacibaculum*, *Ruegeria*, *Staphylococcus* were also increased in jejunum, ileum and colon by sucralose administration in T1 and T4 group. These new findings indicate that low dose of sucralose (T1) alter gut microbiome in mice, and these adverse health effects are equal to ADI level (T4). Overall, our study provides guidance and suggestions for the use of sucralose in foods and beverages.

Keywords: sucralose, low dose, gut microbiome, mice, intestinal barrier

OPEN ACCESS

Edited by:
Tingtao Chen,
Nanchang University, China

Reviewed by:
Andrew William Moran,
University of Liverpool,
United Kingdom
Na Li,
Beijing University of Chinese Medicine, China

***Correspondence:**
Ying Ren
ranee1974@163.com
Jinjun Li
lijinjun@zaas.ac.cn

† These authors share first authorship

Specialty section:
This article was submitted to Nutrition and Microbes, a section of the journal Frontiers in Nutrition

Received: *04 January 2022*
Accepted: *02 February 2022*
Published: *25 February 2022*

Citation:
Zheng Z, Xiao Y, Ma L, Lyu W, Peng H, Wang X, Ren Y and Li J (2022) Low Dose of Sucralose Alter Gut Microbiome in Mice. Front. Nutr. 9:848392. doi: 10.3389/fnut.2022.848392

INTRODUCTION

Global consumption of sugar-free foods is increasing. Non-nutritional sweeteners (NNS) added to beverages and foods are defined as sweetener with higher sweetness and lower calorie content than caloric or nutritional sweeteners (such as sucrose or corn syrup) (1). Sucralose also named trichlorogalactosucrose and TGS, is a NNS, zero-calorie artificial

sweetener (2). It is a substitute for chlorinated sugar, and its sweetness is 600 times than sucrose, because of its low production cost, high thermal stability and solubility, sucralose has become an important sugar substitute in foods and beverage (3, 4). US Food and Drug Administration (FDA) defined acceptable daily intake (ADI) approximately 5 mg/kg BW/day for human (5, 6). The adverse health effects of sucralose have been highly argued over the years. For example, a large number of early studies have shown that most of the ingested sucralose will not be absorbed and metabolized by the body, and it will not change with gut peristalsis (7, 8). However, researches have confirmed that sucralose can change the composition of gut microbiome, inhibiting intestinal development, and aggravating HFD-induced hepatic steatosis in adulthood (5, 9).

Gut microbiome refers to the complex community of microorganisms living in the digestive tract of human and animals, its number is about 10 times than our body cells (10). The balance between host and gut microbiome is essential to maintain a healthy gut barrier and optimal immune homeostasis, which helps to prevent the occurrence of diseases (11, 12). Gut microbiome contribute to the metabolic health of the human host, when aberrant, it will cause the pathogenesis of various common metabolic disorders including obesity, type 2 diabetes, non-alcoholic liver disease, cardio-metabolic diseases and malnutrition (13). Related research used fecal samples from Sprague Dawley rats that received artificial sweetener sucralose (1.1%) for 12 weeks, the results show that sucralose administration reduced the total number of anaerobic bacteria, aerobic bacteria, bifidobacteria, Lactobacillus, Bacteroides and Clostridium (14). Uebanso research showed that the abundance of Clostridium flora in the high-dose sucralose group decreased significantly, and the concentrations of butyric acid and bile acid increased in a dose-dependent manner with the intake of sucralose (15). So, sucralose administration significantly altered mice gut microbiome, and reduced the abundance of beneficial bacteria.

Although many studies have deeply explored the impact of sucralose on gut microbiome, most studies were close to the concentration of ADI (5 mg/kg BW/day) (16, 17). In this study, we found low concentration sucralose also significantly altered gut microbiome by setting four concentration gradients, and it might involve in the development of diabetes. It provides a research basis for the adverse effect mechanism of sucralose on human health, and provides guidance and theoretical support for the practical application of artificial sweeteners.

MATERIALS AND METHODS

Animals and Sampling

Forty specific pathogen-free (SPF) C57BL/6J male mice weaned at the age of 28 days were purchased from SLAC Laboratory Animal Co., Ltd (Shanghai, China). The mice were raised in cages at 25 ± 2°C for 12 h light/dark cycles with free access to water and mouse chow. After acclimatization for 1 week, the mice were weighed and randomly divided into 5 groups and treated for 16 weeks as follows: Control group mice were given distilled water (C, $n = 8$), Trichlorogalactosucrose (TGS) 1–4 groups mice were given a sucralose solution of 0.0003 g/mL (T1, $n = 8$), 0.003 mg/mL (T2, $n = 8$), 0.03 mg/mL (T3, $n = 8$), 0.3 mg/mL (T4, $n = 8$) per day. FDA defined ADI for sucralose in humans were 5 mg per kg (body weight) (18), 0.3 mg/ml is equal to a mouse with an average body weight of 0.02 kg, according to the following calculation:

$$\frac{\text{ADI } 5\text{mg/kg/day} \times \text{ average mouse weight } 0.02\text{Kg}}{\text{Average daily liquid intake } 3\text{ml}} \approx 0.3\ mg/mL$$

At the end of 16-week study, all mice were weighed individually and euthanized. The liver of each mouse was isolated and weighed. Segments of jejunum, ileum and colon were collected and fixed in 4% paraformaldehyde for H&E-stained. The contents of jejunum, ileum, cecum and colon were collected and stored at −20°C until DNA isolation and 16S rRNA gene sequencing. More detailed bioinformatics methods can be found in a previous study (19).

Histological Staining

The jejunum, ileum, and colon tissue segments (1 cm) were collected for histological staining from 3 mice per group, the tissues were rinsed with PBS, immediately fixed in 4% paraformaldehyde, and then cut into sections (4–5 mm), the H&E staining were used to stain the tissue sections according the methods described by previous study (20).

Histopathological scores were calculated according to the methods described by Ma (21): Epithelial surface loss, crypt destruction, and immune cell infiltration (0: no change, 1: localized and mild, 2: localized and moderate, 3: localized and severe, 4: extensive and moderate, 5: extensive and severe).

DNA Extraction and PCR Amplification

Microbial genomic DNA was extrtacted from each intestinal content according to the manufacturer's instructions (QIAamp DNA Stool Mini Kit QIAGEN, CA). The V4-V5 region of the bacteria 16S ribosomal RNA gene was amplified by PCR (95°C for 2 min, followed by 25 cycles at 95°C for 30 s, 55°C for 30 s, and 72°C for 30 s and a final extension at 72°C for 5 min) using primers 515 F 5′-barcode- GTGCCAGCMGCCGCGG)-3′ and 907 R 5′-CCGTCAATTCMTTTRAGTTT-3′, where the barcode is an eight-base sequence unique to each sample. The PCR reactions were performed in triplicate using 20 μL mixture which contained 4 μL of 5 × FastPfu Buffer, 2 μL of 2.5 mM dNTPs, 0.8 μL of forward primer (5 μM), 0.8 μL of reverse primer (5 μM), 0.4 μL of FastPfu Polymerase, 0.2 μL of BSA and 10 ng of template DNA, then add ddH_2O to 20 μL. Amplicons were extracted from 2% agarose gels and purified using the AxyPrep DNA Gel Extraction Kit (Axygen Biosciences, Union City, CA, U.S.) according to the manufacturer's instructions and quantified using QuantiFluor™-ST (Promega, U.S.).

Library Construction and Sequencing

Purified PCR products were quantified by Qubit®3.0 (Life Invitrogen) and every 24 amplicons whose barcodes were different were mixed equally. The pooled DNA product was

used to construct Illumina Pair-End library following Illumina's genomic DNA library preparation procedure. Then the amplicon library was paired-end sequenced (2 × 250) on an Illumina Novaseq platform [Mingke Biotechnology (Hangzhou) Co., Ltd] according to the standard protocols. The original image data files obtained by high-throughput sequencing were converted into Sequenced Reads by Base Calling analysis, the results were stored in FASTQ (referred to as fq) format file, which contains sequence information of reads and their corresponding sequencing quality information.

Statistical Analysis

All statistical analyses were performed by SPSS 23.0 (IBM, New York, NY, United States) using One way ANOVA (22). Data are presented as the mean ± SEM. Results were considered significant when $P < 0.05$.

RESULTS

Sucralose Administration Did Not Change the Phenotype of Mice

In order to confirm the effect of zero-calorie sucralose on body nutritional absorption, Mice was given with T1-4 (0.0003, 0.003, 0.03, and 0.3 mg/mL) of sucralose in drinking water, respectively. The results showed mice body weight and liver weight were not significant differences between Control group and T1–T4 groups (**Figures 1A,B**). To observe the effect of sucralose on intestines of mice. We stained mice intestinal tissue segments of each group. Compared with the Control group, the intestinal barrier and goblet cells of T1-4 groups were significantly damaged, and there was distinct lymphocyte aggregation in ileum and colon of T1 group and ileum of T4 group (**Figure 1C**). According to the scores of H&E staining, T1 and T4 group presented with severe acute colitis, crypt destruction, disappearance of superficial epithelial cells and goblet cells, and the increased infiltration of inflammatory cell (**Figure 1D**).

Sucralose Administration Altered Mice Gut Microbiome

To validate that sucralose administration will change the structure of gut microbiome in mice, the jejunal, ileal, cecal, colonic contents were collected for 16S rRNA gene sequencing. The alpha-diversity indicated that the number of features and Shannon index had an upward trend from the Control group to T1 and T2 groups, and there was a downward trend from T2 group to T3 and T4 group in mice jejunum (**Figures 2A,B**), ileum (**Figures 2C,D**), cecum (**Figures 2E,F**) and colon (**Figures 2G,H**). The beta-diversity showed significant changes in mice gut microbiome community membership and structure from Control group to T1-4 groups. Especially in T1 group (**Figures 3A–D**), its clustering is far away from all other groups in jejunum (**Figure 3A**) ileum (**Figure 3B**) cecum (**Figure 3C**) and colon (**Figure 3D**). In mice jejunum, ileum and cecum, T3 and T4 groups were closer to control group. In colon, T4 group was as far away from the control group as T1 group.

The Mice Gut Core Microbiome

To identify the core microbiome in mice gut, Top 51 bacterial features of mice gut core microbiome was obtained by referring the research of Li (23). Most of these features are associated with the phylum Firmicutes ($n = 26$), Bacteroidetes ($n = 14$). At the family level, the top three families were Erysipelotrichaceae ($n = 10$), Lactobacillaceae ($n = 6$) Staphylococcaceae ($n = 4$). The top feature was Allobaculums ($n = 4$) (F2, F20, F49, F66) at genus level. These features sequence and taxonomy are shown in **Table 1**. Phylogenetic tree analysis indicated the Firmicutes had the highest level of abundance in the phylum, the next was Proteobacteria based on the top 129 genus level (**Figure 4**).

We next confirmed the shifts of mice microbiome in different gut segments, top 30 most abundant bacterial features were shown on the bar chart (**Figure 5**). Among top 5 taxa, in jejunum and cecum, compared with Control group, Firmicutes-Allobaculums (F2) had an upward trend in T1 and T4 group, and it significantly rose in ileum and cecum ($P < 0.05$). In the colon, the T4 group had a significant increase in Firmicutes-Allobaculums (F49 and F66) compared with the Control group. Firmicutes-Staphylococcus (F5) increased significantly in T1 group compared with Control group in four different gut segments ($P < 0.05$) (**Figure 5**).

Bacterial Taxa Differentially Represented in Mice Gut Microbiome

Mice gut bacterial features were analyzed by using LEfSe (24), the abundance of these significantly different features were shown on the heat map. In jejunum (**Figure 6A**), Bacteroidetes-Tenacibaculum (F123) and Proteobacteria-Ruegeria (F116) had a significantly increase in T1 group compared with other groups (Control, T2, T3, T4). In ileum (**Figure 6C**), Firmicutes-Allobaculum (F2) in T1 and T4 group were significantly higher than other group (Control, T2, T3), Firmicutes-Staphylococcus (F5, F37, F10) and Actinobacteria-Corynebacterium 1 (F41) had a significantly increase in T1 group compared with other groups (Control, T2, T3, T4). In cecum (**Figure 6B**), Firmicutes-Lachnoclostridium (F134) and Firmicutes-Lachnospiraceae UCG-006(F156) in Control group were significantly higher than T1 and T4 group. In colon (**Figure 6D**), after removing these features which were uncultured or no rank in genus level, we found the Firmicutes-Allobaculum (F20) in T1 group and Firmicutes-Allobaculum (F66, F49) in T4 group increased significantly than other groups (Control, T2, T3).

DISCUSSION

Sweetness, whether provided by sugar or artificial sweeteners, enhances human appetite and reduce stress, so it is the preference of most people (25, 26). Besides, sucralose is one of the most consumed NNS in the world, since entering the food and beverage market (27), Recent research had shown that sucralose was used instead of sugar to reduce calorie and blood sugar intake (28). However, its effect on human health has been always controversial in recent years. Thus, in the present study,

TABLE 1 | The mice core gut microbiome.

Feature#	Feature ID	Phylum	Order	Family	Genus	Species
F1	6b16e3df5b1a43f80f1abba36a2f4fa4	Firmicutes	Erysipelotrichales	Erysipelotrichaceae		
F2	c7a8646670d35169426746bafae12863	Firmicutes	Erysipelotrichales	Erysipelotrichaceae	Allobaculums	
F4	e91c5ab4a5ff57293c61ab5f8af8f857	Bacteroidetes	Bacteroidales	S24-7		
F5	2baa2ccaf423b8f4b575c26dd5528527	Firmicutes	Bacillales	Staphylococcaceae	Staphylococcus	
F9	0e01940bde40f2c0199e553a5a89621f	Firmicutes	Erysipelotrichales	Erysipelotrichaceae	Turicibacter	
F10	db763fd81e8bbffe8d937b0b8e34ef3c	Firmicutes	Bacillales	Staphylococcaceae	Staphylococcus	
F3	74fe5a07ff7883bf6065905ae09dab02	Firmicutes	Erysipelotrichales	Erysipelotrichaceae	Faecalibaculum	
F12	daa7e3c372cba75996978c9413cb8023	Bacteroidetes	Bacteroidales	Porphyromonadaceae	Parabacteroides	
F6	bad7a42c2b923635697a99bfd9cfb4d4	Firmicutes	Lactobacillales	Lactobacillaceae	Lactobacillus	
F20	dee4854053933a4ec92f2ab0408b6617	Firmicutes	Erysipelotrichales	Erysipelotrichaceae	Allobaculum	
F16	46f1c0f94998484d634272566ab9045e	Bacteroidetes	Bacteroidales	Rikenellaceae	Alistipes; s	
F34	35af66e08002462940c4550f2caaae05	Proteobacteria	Rhodobacterales	Rhodobacteraceae	Donghicola	
F28	6e1541c94d068be4013d732546963c3b	Bacteroidetes	Bacteroidales	S24-7		
F42	98db5cc259f3b66be220f159b72736e0	Proteobacteria	Burkholderiales	Comamonadaceae	Delftia	
F49	2b380f7d47d59b2b9775fbb9c4d27b2e	Firmicutes	Erysipelotrichales	Erysipelotrichaceae	Allobaculum	
F52	8731e41abac7051ee170aea30cff35cd	Firmicutes	Clostridiales	Lachnospiraceae	Lachnoclostridium	
F45	1e7e2fecb3499fe7acf1ec450f55ae46	Firmicutes	Lactobacillales	Streptococcaceae	Streptococcus	
F50	ed18d5fd0e2193181 4692926017a6c25	Firmicutes	Clostridiale	Lachnospiraceae	NK4A136	
F39	1ec4262624d166b77c644117324ece51	Bacteroidetes	Bacteroidales	Porphyromonadaceae	Odoribacter	
F13	b27d135cb75eb333fb6d6e29f9496218	Firmicutes	Erysipelotrichales	Erysipelotrichaceae		
F41	bb96c3f96496dd3436c48cc3fe9b869b	Actinobacteria	Corynebacteriales	Corynebacteriaceae	Corynebacterium1	
F66	d99862e3d320187d202bf5427e084262	Firmicutes;	Erysipelotrichales	Erysipelotrichaceae	Allobaculum	
F46	963f23135f931531c59451f0fbb6e12c	Bacteroidetes	Bacteroidales	Prevotellaceae	UCG-001	
F36	88eacccbc95ec6f6264d25d8143274ec	Bacteroidetes	Bacteroidales	Porphyromonadaceae	Odoribacter	
F68	1bbcf22e72576560caa74a36d1034535	Bacteroidetes	Flavobacteriales	Flavobacteriaceae	Mesoflavibacter	
F60	a2c80a0fefad24ad09383620125620ac	Firmicutes	Clostridiales	Clostridiaceae 1	sensu stricto 1	
F11	b415fc5a8da6294f0a2be791c1763b46	Bacteroidetes	Bacteroidales	Bacteroidaceae	Bacteroides	
F77	49fe5c8102e07ba0b1060fe687e1ba41	Bacteroidetes	Flavobacteriales	Flavobacteriaceae	Mesoflavibacter	
F58	86823ff40593228f03d64f36dfcd0c7c	Firmicutes	Clostridiales	Ruminococcaceae	Ruminiclostridium 9	
F89	65e916ef00eacbed2d5068c2d14835b3	Firmicutes	Bacillales	Staphylococcaceae	Jeotgalicoccus	Halotolerans
F84	0a506ad68d12793df4055a2b76ebe412	Proteobacteria	Pseudomonadales	Pseudomonadaceae	Pseudomonas	
F17	3aa637bd332ff9fce9373b81613ec1e3	Proteobacteria	Burkholderiales	Alcaligenaceae	Parasutterella	
F95	4326af51eda901052e87d2bd8df04fee	Bacteroidetes	Flavobacteriales	Flavobacteriaceae	Mesoflavibacter	
F79	23e7dba569ab918cf641dc7c6a19cdca	Proteobacteria	Rhizobiales	Phyllobacteriaceae	Phyllobacterium	
F19	5358db5bc5ebe904ec7caf97db19ca41	Firmicutes	Erysipelotrichales	Erysipelotrichaceae	Faecalibaculum	
F73	18868dd1c73f1dc845edd0783806a273	Actinobacteria	Coriobacteriales	Coriobacteriaceae	Enterorhabdus	
F44	8094bb6c6dd711371552ae749d34bd2e	Bacteria	Bacteroidales	Rikenellaceae	RC9 gut	
F56	2e2b432ddf60afdd484cd4abd0a34fdb	Deferribacteres	Deferribacterales	Deferribacteraceae	Mucispirillum	
F100	a4177cc2db325e8adfae6d8003be7467	Firmicutes	Clostridiales	Lachnospiraceae	NK4A136	
F116	cdcab14f1a38a841458a3b63cdb952a2	Proteobacteria	Rhodobacterales	Rhodobacteraceae	Ruegeria	
F78	1fb77a25c3217ae147accb95cd6e3db9	Firmicutes	Clostridiales	Lachnospiraceae		
F108	d5ca97f9398c389f305fd8e5a89a3d8b	Firmicutes	Clostridiales	Lachnospiraceae	Marvinbryantia	
F123	e3940000c0af54fe0debb7325bb78c42	Bacteroidetes	Flavobacteriales	Flavobacteriaceae	Tenacibaculum	Litoreum
F144	630af886c8a8b7bbef2df85247c40bb7	Firmicutes	Clostridiales	Ruminococcaceae	Ruminiclostridium	
F133	884647b522ef48acb57a64e71987a20f	Proteobacteria	Pseudomonadales	Moraxellaceae	Enhydrobacter	
F148	e4f8ba7abc5dc204a7d9e55e7db910b6	Firmicutes	Bacillales	Planococcaceae	Sporosarcina	
F112	342bdcf4e03a5fa45327aa587fe1b2ce	Firmicutes	Clostridiales	Peptococcaceae		
F149	c1e75978abce59bd25cbfe9ac36067f2	Bacteroidetes;	Flavobacteriales	Flavobacteriaceae	Winogradskyella	
F132	2e9c75913d6338775f03b74a35fc8ece	Firmicutes	Clostridiales	Ruminococcaceae	Ruminiclostridium	
F137	8c7c75dfb1b25dbf2e80105777369689	Proteobacteria	Burkholderiales	Burkholderiaceae	Pandoraea	Oxalativorans
F167	c851e3a644c834c9a924fa361638b492	Firmicutes	Erysipelotrichales	Erysipelotrichaceae		

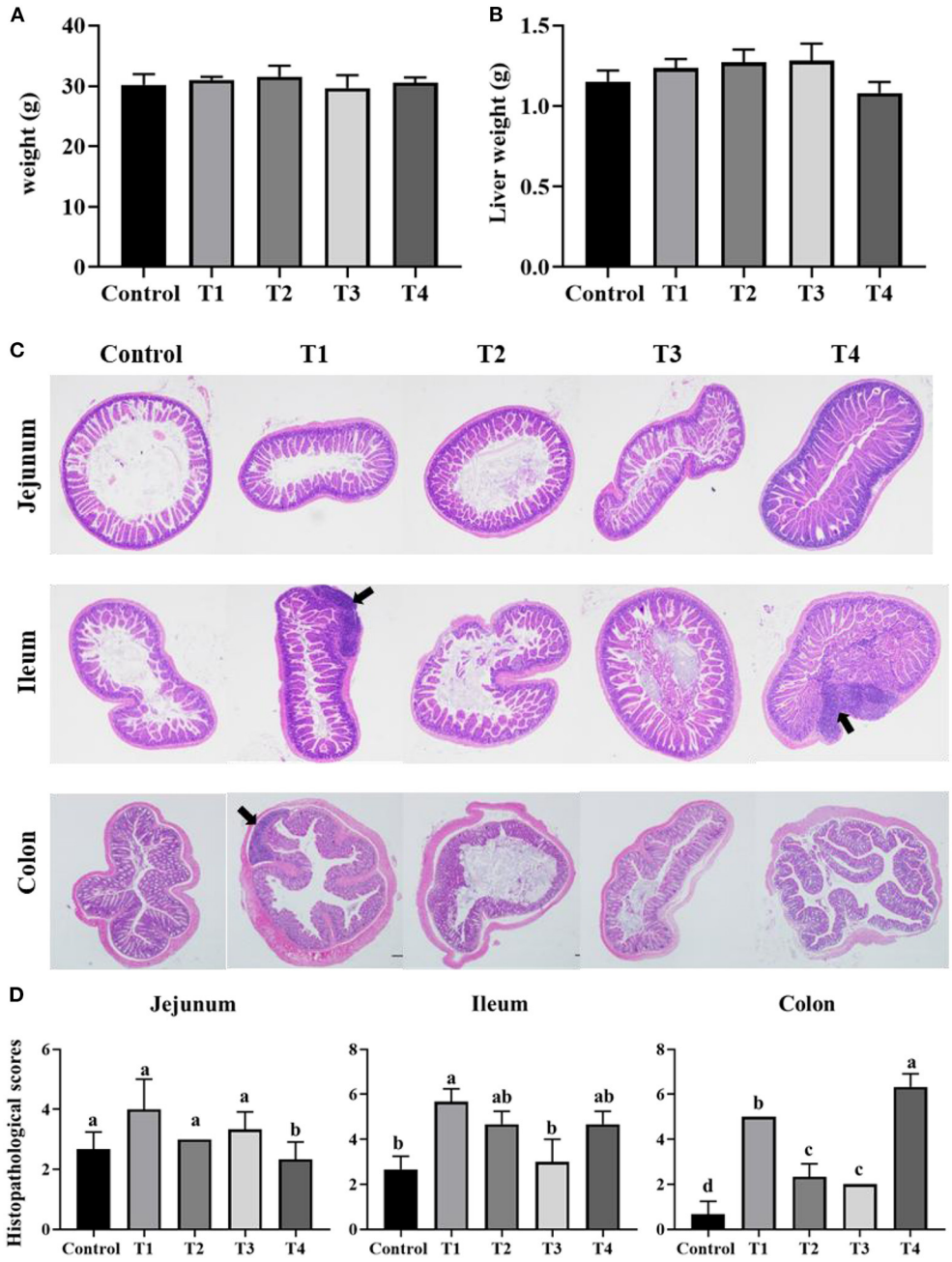

FIGURE 1 | Bar chart showing the mice body weight **(A)** and liver weight **(B)**. Representative H&E-stained sections from jejunum, ileum, cecum and colon **(C)**, the arrowhead points in the direction where lymphocyte aggregation. Histopathological scores of the H&E staining **(D)**. Data was expressed as mean ± SEM ($n = 8$) and analyzed by one-way ANOVA analysis. The different superscript letters on the histogram represent a significant difference **(D)** ($P < 0.01$).

we examined the effects of sucralose (0.0003, 0.003, 0.03, and 0.3 mg/mL) on mice weight. Finally, we found that sucralose administration did not change the phenotype of mice, including the body weight and liver weight. Resent research showing the body weight remained constant by short-term sucralose consumption in human (16). Azad searched Medline, Embase and Cochrane Library for randomized controlled trials that evaluated interventions for NNS, NNS administration had no significant effect on BMI in 1,003 participants (29). This all consistent with our study, and confirms that sucralose as a zero-calorie sweetener does not provide energy to the body.

The intestinal barrier is composed of physical barrier (intestinal epithelium and mucus elements) (30), immunologic (immune cells) (31), and microbial community (32).

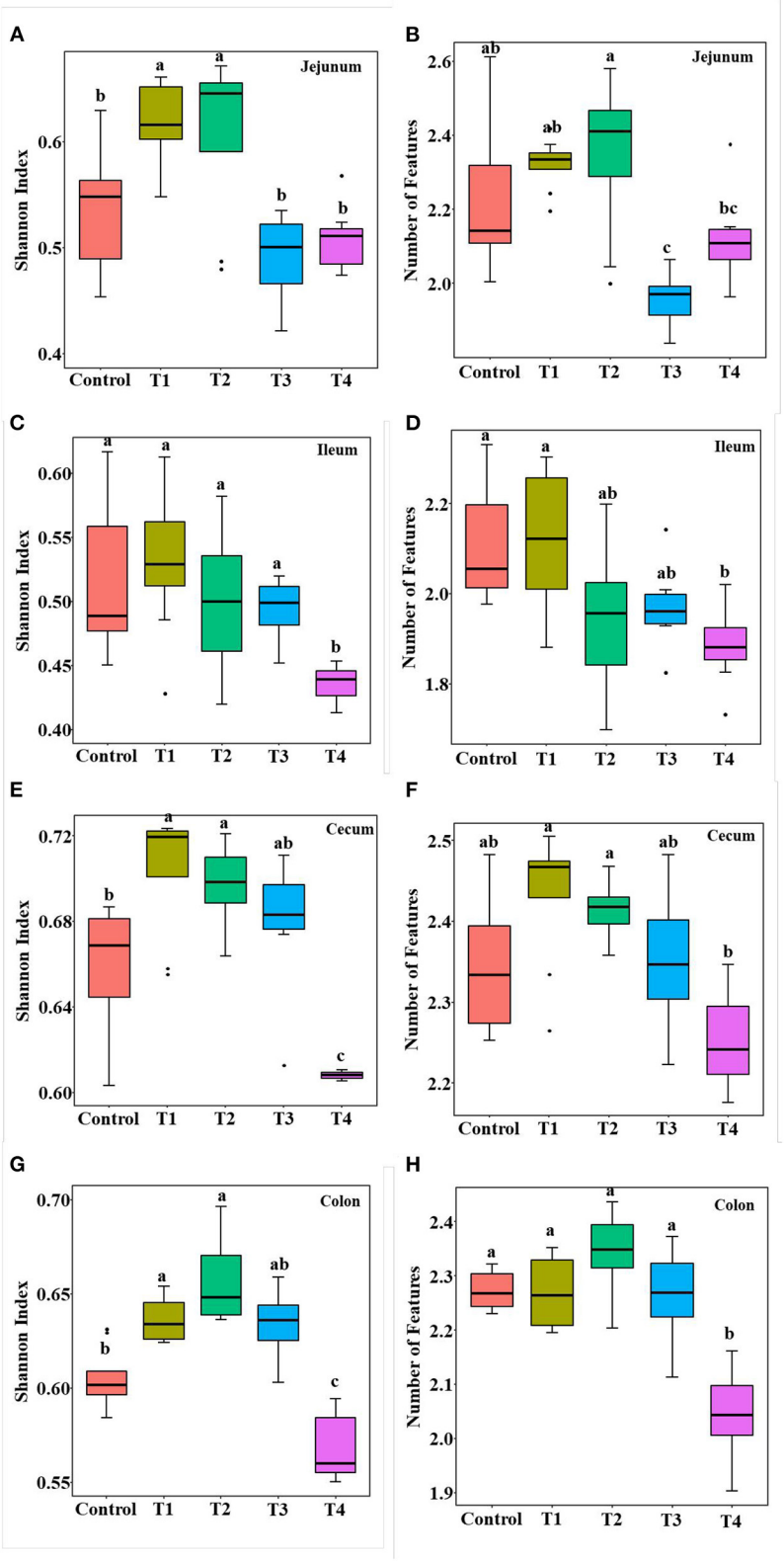

FIGURE 2 | Alpha diversity including Shannon index **(A,C,E,G)** and the number of features **(B,D,F,H)** in control group, Trichlorogalactosucrose (TGS) 1–4 (T1, T2, T3, T4) groups in jejunum **(A,B)**, ileum **(C,D)**, cecum **(E,F)**, colon **(G,H)**. Data was processed through log10, and expressed as mean ± SEM ($n = 8$) and analyzed by one-way ANOVA analysis. The different superscript letters on the boxplot represent a significant difference ($P < 0.01$).

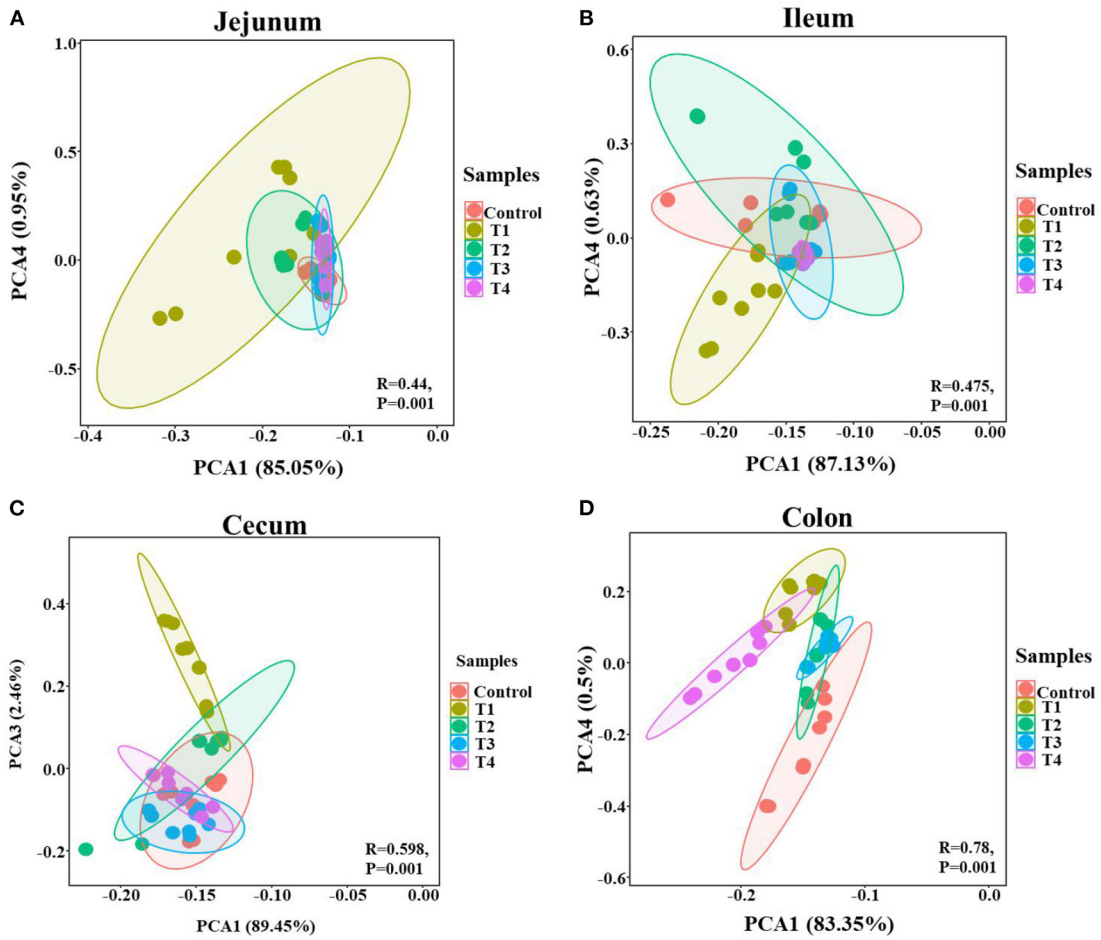

FIGURE 3 | PCA of the mice gut microbial community composition of the Control and T1-4 group based on the Bray-Curtis distances showed distinct clusters, *P*-value and *R*-value were calculated by ANOSIM. The jejunum **(A)**, ileum **(B)**, cecum **(C),** and colon **(D)** microbial community structure between the Control group and T1–4 groups were differentiated by colors (red, brown, green, blue, purple, respectively).

Intestinal barrier regulates the two-way flow of water, ions and macromolecules between the lumen and the host (33). Epithelial barrier dysfunction has been reported in a variety of intestinal diseases, including inflammatory bowel disease (IBD) and ulcerative colitis (34). With the administration of sucralose, T1-4groups intestinal epithelial barrier was destroyed, as evidenced by the lymphocyte aggregation, especially in T1 and T4 groups. Resent study indicated that high concentrations of sucralose [10 mmol, the public may consume generous sweetener in the diet to achieve up to 10 mmol exposure to sweeteners (35)] induced apoptosis and cell death of intestinal epithelial cells, low concentrations of sucralose (0.1 mmol) down-regulated cell surface claudin 3 (36). Dai et al. (5) research showed that maternal sucralose administration significantly inhibited intestinal development and destroyed the intestinal barrier function in 3-week-old offspring. MUC2 is one of the important products of goblet cells and is closely related to the formation of the mucus layer. Research showed that compared with the control group, the production of MUC2 was significantly decreased in the sucralose group (5). After 6 months of sucralose administration, the genes related to LPS synthesis increased significantly (37). The relative mRNA expression levels of proinflammatory factors, including IL-1β, IFN-γ, and TNF-α were significantly higher in sucralose group than those in control group in colon (5). In our study, sucralose administration induced lymphocyte aggregation, which may lead to the increase of inflammatory factors. These revealed that sucralose administration might disrupt intestinal barrier function, the sucralose concentration and the effect on intestinal barrier of these studies all consistent with T4 group in our study, more interestingly, we also found the intestinal barrier was significantly damaged in group T1.

Gut microbiome is also an important part of the intestinal barrier (38), it is a complex and dynamic system, intestinal imbalanced states or even unhealthy stable states will develop, or potentially lead to diseases, including IBD, Nonalcoholic fatty

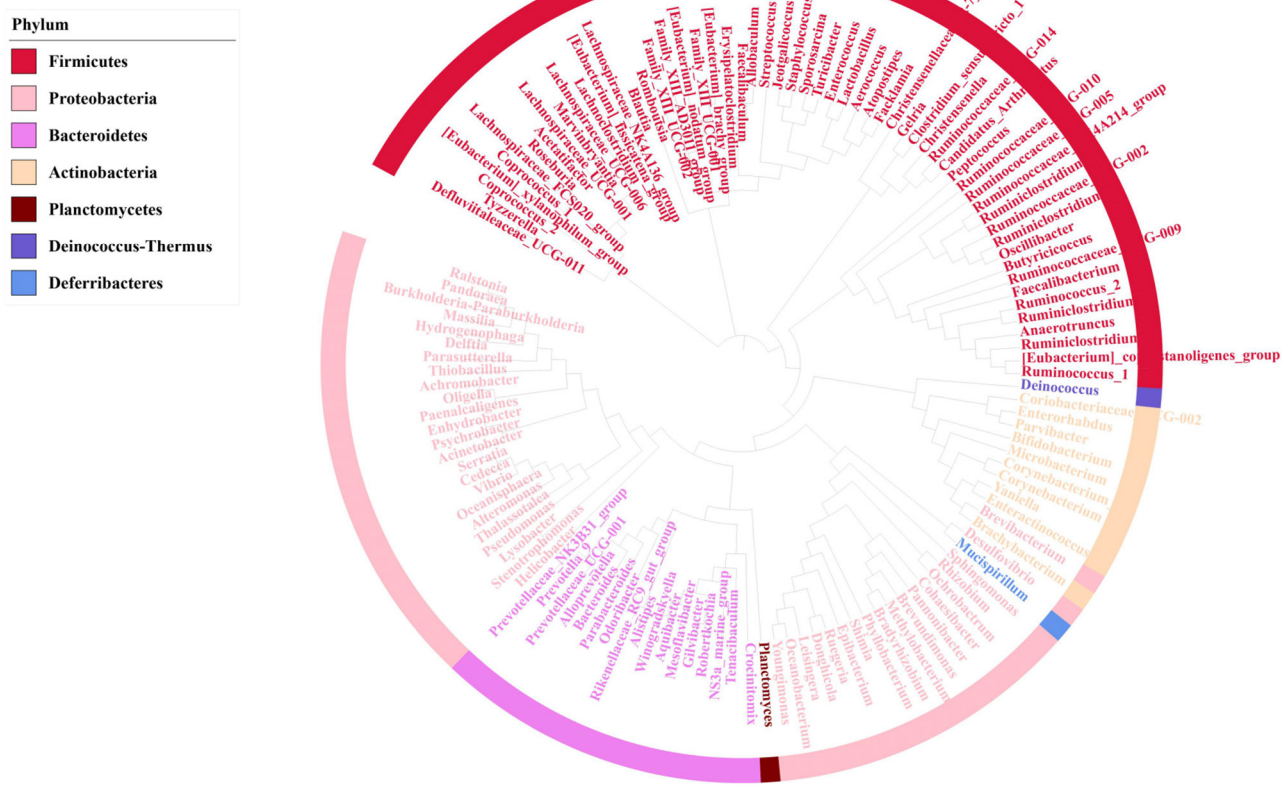

FIGURE 4 | Phylogenetic tree analysis showing top 129 bacterial taxa based on 16S rRNA gene V4-V5 hypervariable regions, after removing 21 features which were uncultured or no rank in genus level. The innermost clades and labels were colored by genus.

liver disease (NALFD) and Irritable Bowel Syndrome (IBS) (39, 40). In this study, we demonstrate low dose of sucralose alter gut microbiome in mice by using 16S rRNA gene sequencing, T1-4 groups mice accessed 0.0003 g/mL, 0.003 mg/mL, 0.03 mg/mL, 0.3 mg/mL sucralose for 16 weeks, 0.1 mg/ml of sucralose solution was FDA acceptable daily intake (18). The results showed the number of features and Shannon index had an upward trend in T1 group and a downward trend in T4 group compared with Control group, Beta-diversity indicated T1 group was distinct from other groups, especially Control group. Sánchez-Tapia research found 1.5% (1.5 mg/mL) concentration of sucralose led to the lowest α-diversity in rats gut microbiota, its PCoA analysis revealed that gut microbiota was differentially shifted by sucralose (41). Many previous studies had shown that ADI (0.1 mg/ml) of sucralose significantly altered mice gut microbiome (37, 42). These results were consistent with T4 group in our study, however, the new finding in our research was T1 (0.0003 mg/mL) group, like T4 (0.3 mg/mL), also altered mice gut microbiome.

Core microbiome is essential to understand its function in the gut, it has been well- researched in different species (43, 44). Generally, a core microbiome indicates common bacterial present in all or most (e.g., >90%) of the communities in the host (45). In this study, a total of 51 core microbiome members of mice were identified in five groups. Most of these features are associated with the phylum Firmicutes ($n = 26$), Bacteroidetes ($n = 14$). Research have shown 2.5% sucralose treatment group increased the Firmicutes in phylum level (46). In our study, we found the top feature was Allobaculums ($n = 4$) (F2, F20, F49, F66) at genus level. Besides, Allobaculums of T1 and T4 group were significantly higher in mice jejunum, ileum and colon. Many research had shown Allobaculums significantly increased in diabetes model group compared with normal group (47, 48). However, whether sucralose administration will induce diabetes by altering gut microbiota, it requires further research.

Sucralose intake associated bacterial features were identified by using LEfSe, an algorithm that not only analyze statistical significance but also biological consistency. The results showing, in jejunum, Bacteroidetes-Tenacibaculum (F123) and Proteobacteria-Ruegeria (F116) significantly increased in T1 group compared with Control group. Tenacibaculum is a genus of gram negative, filamentous bacteria, related to the disease (tenacibaculosis) existing in aquaculture farms all over the world (49). Rubio-Portillo research identified Ruegeria OUT was associated with tissue necrosis in their hosts (50). In ileum, Firmicutes-Staphylococcus (F5, F37, F10)

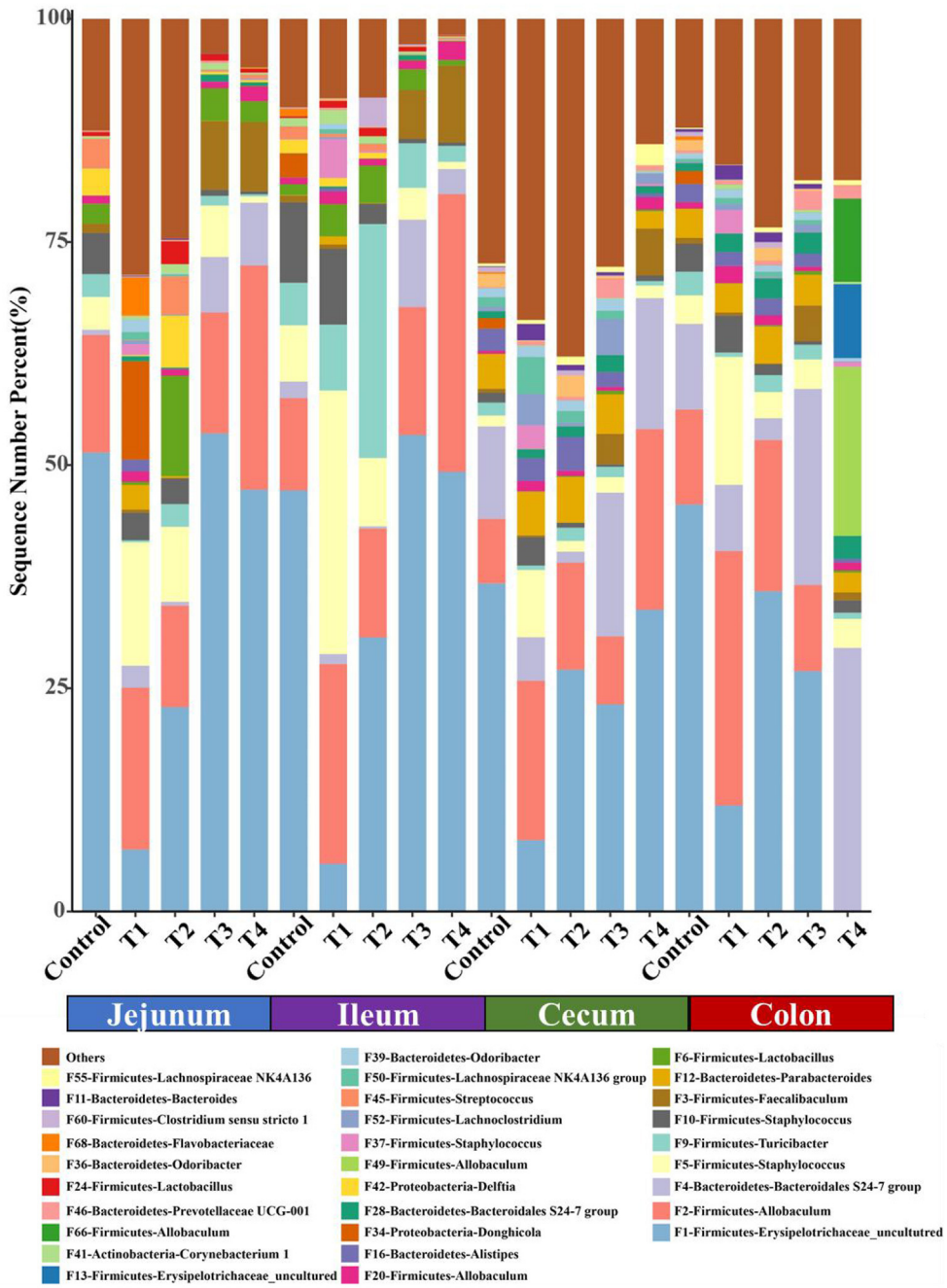

FIGURE 5 | The top 30 features in Control group and T1–4 groups of jejunum, ileum, cecum and colon microbiome in mice. Each color indicates the relative abundance of a bacterial taxon on the bar chart.

and Actinobacteria-Corynebacterium 1 (F41) significantly increased in T1 group compared with Control groups. The representative species of Staphylococcus are Staphylococcus aureus, it is a pathogen that usually colonizes the human anterior nostrils. This pathogen is one of main causes of life-threatening bloodstream infections, as sepsis and endocarditis (51). In cecum, Firmicutes-Lachnoclostridium (F134) and Firmicutes-Lachnospiraceae UCG-006 (F156) significantly decreased in T4 group than Control group. Lachnoclostridium was significantly up-regulated after treatment of obesity and inflammatory bowel disease (IBD) (52, 53). Lachnospiraceae is the major producers of short-chain fatty acids (SCFA), and is significantly related with enhanced gut barrier function (54, 55). In colon, Firmicutes-Allobaculum (F20) in T1 group

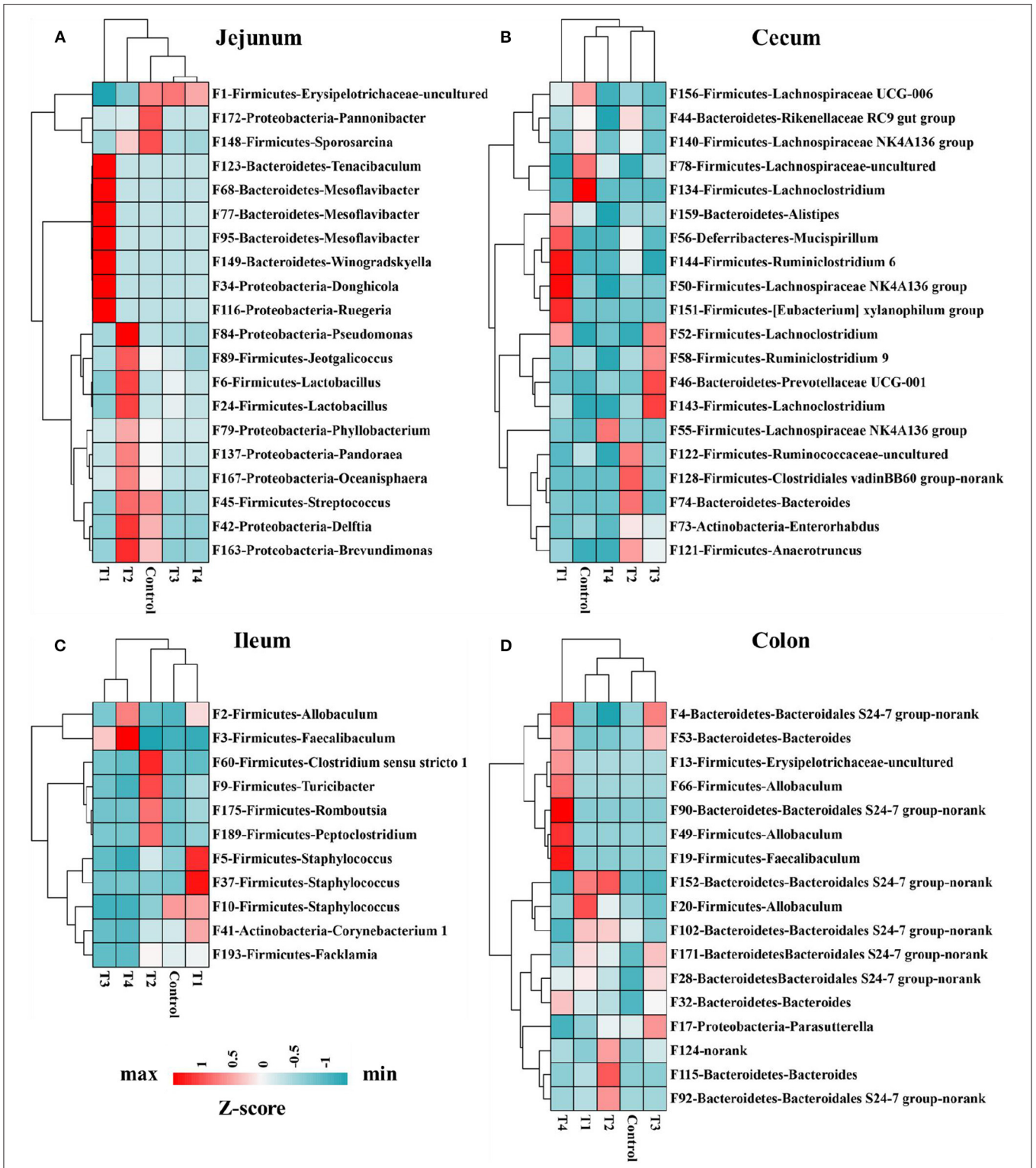

FIGURE 6 | Heat map indicated 68 bacterial taxa were identified by LEfSe (LDA > 3) in mice jejunum ($n = 20$) **(A)**, ileum ($n = 11$) **(C)**, cecum ($n = 20$) **(B),** and colon ($n = 17$) **(D)** microbiome. The top 1,000 features were used for LEfSe analysis. Heat map shows the average relative abundances on a Z-score.

and Firmicutes-Allobaculum (F66, F49) in T4 group increased significantly than other groups (Control, T2, T3). Allobaculum is not only positive related to diabetes (47, 48), but also related to ileal RORγT and IL-17 levels (56), induced susceptibility to autoimmune encephalitis (57), increased the expansion of inflammatory T helper 17 cells in gut (58). So, low dose

of sucralose (T1, 0.0003 g/mL) consumption significantly altered mice gut microbiome, it might contribute to the increased expression of pro-inflammatory, these changes same as most previous study had indicated sucralose intake at human ADI (T4, 0.03 mg/mL) altered the gut microbiome in mice (5, 18, 41, 46).

CONCLUSION

Overall, our study demonstrated sucralose administration did not change mice body weight, but low dose of sucralose (0.0003 mg/mL) significantly altered mice gut microbiome, including the increases of Tenacibaculum, Ruegeria, Staphylococcus and Allobaculum in genus level in mice jejunum, ileum and colon. The decrease of Lachnoclostridium and Lachnospiraceae in cecum of T4 group mice. Although the sucralose of ADI (0.3 mg/mL) level also altered the gut microbiome in mice, the human daily intake of sucralose is usually lower than this concentration. We should focus on the low dose of sucralose administration in human. Finally, our research is limited to the effect of low-dose sucralose on the gut microbiome of mice, and the relevance to human metabolic diseases warrant further investigation.

DATA AVAILABILITY STATEMENT

The datasets presented in this study can be found in online repositories. The names of the repository/repositories and accession number(s) can be found below: https://www.ncbi.nlm.nih.gov/, PRJNA787401.

ETHICS STATEMENT

The animal study was reviewed and approved by the Institutional Animal Care and Use Committee of Zhejiang Academy of Agricultural Sciences.

AUTHOR CONTRIBUTIONS

ZZ, YX, YR, and JL designed the experiment. ZZ, LM, HP, and XW conducted the animal experiments. ZZ, YX, LM, YR, and JL wrote and revised the manuscript. ZZ, YX, LM, YR, and JL did experimental analysis, collected, and analyzed the data. All authors reviewed the manuscript and contributed to the article and approved the submitted version.

FUNDING

This work was financially supported by the State Key Laboratory for Managing Biotic and Chemical Threats to the Quality and Safety of Agroproducts, Grant/Award Number: 2010DS700124-ZZ2017, the Open Project of Hubei Key Laboratory of Animal Nutrition and Feed Science (No. 201806), and the National Natural Science Foundation of China (31972999).

REFERENCES

1. Carocho M, Morales P, Ferreira I. Sweeteners as food additives in the XXI century: a review of what is known, and what is to come. *Food Chem Toxicol.* (2017) 107:302–17. doi: 10.1016/j.fct.2017.06.046
2. Magnuson BA, Carakostas MC, Moore NH, Poulos SP, Renwick AG. Biological fate of low-calorie sweeteners. *Nutr Rev.* (2016) 74:670–89. doi: 10.1093/nutrit/nuw032
3. AlDeeb OA, Mahgoub H, Foda NH. Sucralose. *Profiles Drug Subst Excip Relat Methodol.* (2013) 38:423–62. doi: 10.1016/B978-0-12-407691-4.00010-1
4. Martyn D, Darch M, Roberts A, Lee HY, Yaqiong Tian T, Kaburagi N, et al. Low-/no-calorie sweeteners: a review of global intakes. *Nutrients.* (2018) 10:357. doi: 10.3390/nu10030357
5. Dai X, Guo Z, Chen D, Li L, Song X, Liu T, et al. Maternal sucralose intake alters gut microbiota of offspring and exacerbates hepatic steatosis in adulthood. *Gut Microbes.* (2020) 11:1043–63. doi: 10.1080/19490976.2020.1738187
6. Olivier-Van Stichelen S, Rother KI, Hanover JA. Maternal exposure to non-nutritive sweeteners impacts progeny's metabolism and microbiome. *Front Microbiol.* (2019) 10:1360. doi: 10.3389/fmicb.2019.01360
7. Roberts A, Renwick AG, Sims J, Snodin DJ. Sucralose metabolism and pharmacokinetics in man. *Food Chem Toxicol.* (2000) 38:S31–41. doi: 10.1016/S0278-6915(00)00026-0
8. Sylvetsky AC, Welsh JA, Brown RJ, Vos MB. Low-calorie sweetener consumption is increasing in the United States. *Am J Clin Nutr.* (2012) 96:640–6. doi: 10.3945/ajcn.112.034751
9. Uebanso T, Ohnishi A, Kitayama R, Yoshimoto A, Nakahashi M, Shimohata T, et al. Effects of low-dose non-caloric sweetener consumption on gut microbiota in mice. *Nutrients.* (2017) 9:560. doi: 10.3390/nu9060560
10. Savage DC. Microbial ecology of the gastrointestinal tract. *Annu Rev Microbiol.* (1977) 31:107–33. doi: 10.1146/annurev.mi.31.100177.000543
11. Gomaa EZ. Human gut microbiota/microbiome in health and diseases: a review. *Antonie Van Leeuwenhoek.* (2020) 113:2019–40. doi: 10.1007/s10482-020-01474-7
12. Fassarella M, Blaak EE, Penders J, Nauta A, Smidt H, Zoetendal EG. Gut microbiome stability and resilience: elucidating the response to perturbations in order to modulate gut health. *Gut.* (2021) 70:595–605. doi: 10.1136/gutjnl-2020-321747
13. Fan Y, Pedersen O. Gut microbiota in human metabolic health and disease. *Nat Rev Microbiol.* (2021) 19:55–71. doi: 10.1038/s41579-020-0433-9
14. Abou-Donia MB, El-Masry EM, Abdel-Rahman AA, McLendon RE, Schiffman SS. Splenda alters gut microflora and increases intestinal p-glycoprotein and cytochrome p-450 in male rats. *J Toxicol Environ Health A.* (2008) 71:1415–29. doi: 10.1080/15287390802328630
15. Uebanso T, Kano S, Yoshimoto A, Naito C, Shimohata T, Mawatari K, et al. Effects of consuming xylitol on gut microbiota and lipid metabolism in mice. *Nutrients.* (2017) 9:756. doi: 10.3390/nu9070756
16. Thomson P, Santibañez R, Aguirre C, Galgani JE, Garrido D. Short-term impact of sucralose consumption on the metabolic response and gut microbiome of healthy adults. *Br J Nutr.* (2019) 122:856–62. doi: 10.1017/S0007114519001570
17. Ahmad SY, Friel J, Mackay D. The effects of non-nutritive artificial sweeteners, aspartame and sucralose, on the gut microbiome in healthy adults: secondary outcomes of a randomized double-blinded crossover clinical trial. *Nutrients.* (2020) 12:3408. doi: 10.3390/nu12113408
18. Suez J, Korem T, Zeevi D, Zilberman-Schapira G, Thaiss CA, Maza O, et al. Artificial sweeteners induce glucose intolerance by altering the gut microbiota. *Nature.* (2014) 514:181–6. doi: 10.1038/nature13793
19. Zheng Z, Lyu W, Ren Y, Li X, Zhao S, Yang H, et al. Allobaculum Involves in the modulation of intestinal ANGPTLT4 expression in mice treated by high-fat diet. *Front Nutr.* (2021) 8:690138. doi: 10.3389/fnut.2021.690138

20. Yang H, Xiang Y, Robinson K, Wang J, Zhang G, Zhao J, et al. Gut microbiota is a major contributor to adiposity in pigs. *Front Microbiol.* (2018) 9:3045. doi: 10.3389/fmicb.2018.03045
21. Ma L, Ni L, Yang T, Mao P, Huang X, Luo Y, et al. Preventive and therapeutic spermidine treatment attenuates acute colitis in mice. *J Agric Food Chem.* (2021) 69:1864–76. doi: 10.1021/acs.jafc.0c07095
22. Xiao Y, Wu C, Li K, Gui G, Zhang G, Yang H. Association of growth rate with hormone levels and myogenic gene expression profile in broilers. *J Anim Sci Biotechnol.* (2017) 8:43. doi: 10.1186/s40104-017-0170-8
23. Li Y, Wang X, Wang XQ, Wang J, Zhao J. Life-long dynamics of the swine gut microbiome and their implications in probiotics development and food safety. *Gut Microbes.* (2020) 11:1824–32. doi: 10.1080/19490976.2020.1773748
24. Segata N, Izard J, Waldron L, Gevers D, Miropolsky L, Garrett WS, et al. Metagenomic biomarker discovery and explanation. *Genome Biol.* (2011) 12:R60. doi: 10.1186/gb-2011-12-6-r60
25. Jacques A, Chaaya N, Beecher K, Ali SA, Belmer A, Bartlett S. The impact of sugar consumption on stress driven, emotional and addictive behaviors. *Neurosci Biobehav Rev.* (2019) 103:178–99. doi: 10.1016/j.neubiorev.2019.05.021
26. O'Connor D, Pang M, Castelnuovo G, Finlayson G, Blaak E, Gibbons C, et al. A rational review on the effects of sweeteners and sweetness enhancers on appetite, food reward and metabolic/adiposity outcomes in adults. *Food Funct.* (2021) 12:442–65. doi: 10.1039/D0FO02424D
27. Schiffman SS, Rother KI. Sucralose, a synthetic organochlorine sweetener: overview of biological issues. *J Toxicol Environ Health B Crit Rev.* (2013) 16:399–451. doi: 10.1080/10937404.2013.842523
28. Nadolsky KZ, COUNTERPOINT. Artificial sweeteners for obesity-better than sugary alternatives potentially a solution. *Endocr Pract.* (2021) 27:1056–61. doi: 10.1016/j.eprac.2021.06.013
29. Azad MB, Abou-Setta AM, Chauhan BF, Rabbani R, Lys J, Copstein L, et al. Nonnutritive sweeteners and cardiometabolic health: a systematic review and meta-analysis of randomized controlled trials and prospective cohort studies. *Cmaj.* (2017) 189:E929–39. doi: 10.1503/cmaj.161390
30. Luissint AC, Parkos CA, Nusrat A. Inflammation and the intestinal barrier: leukocyte-epithelial cell interactions, cell junction remodeling, and mucosal repair. *Gastroenterology.* (2016) 151:616–32. doi: 10.1053/j.gastro.2016.07.008
31. Mowat AM, Agace WW. Regional specialization within the intestinal immune system. *Nat Rev Immunol.* (2014) 14:667–85. doi: 10.1038/nri3738
32. Chopyk DM, Grakoui A. Contribution of the intestinal microbiome and gut barrier to hepatic disorders. *Gastroenterology.* (2020) 159:849–63. doi: 10.1053/j.gastro.2020.04.077
33. Odenwald MA, Turner JR. The intestinal epithelial barrier: a therapeutic target? *Nat Rev Gastroenterol Hepatol.* (2017) 14:9–21. doi: 10.1038/nrgastro.2016.169
34. Torres J, Petralia F, Sato T, Wang P, Telesco SE, Choung RS, et al. Serum biomarkers identify patients who will develop inflammatory bowel diseases up to 5 years before diagnosis. *Gastroenterology.* (2020) 159:96–104. doi: 10.1053/j.gastro.2020.03.007
35. Gardner C, Wylie-Rosett J, Gidding SS, Steffen LM, Johnson RK, Reader D, et al. Nonnutritive sweeteners: current use and health perspectives: a scientific statement from the american heart association and the american diabetes association. *Diabetes Care.* (2012) 35:1798–808. doi: 10.2337/dc12-9002
36. Shil A, Olusanya O, Ghufoor Z, Forson B, Marks J, Chichger H. Artificial sweeteners disrupt tight junctions and barrier function in the intestinal epithelium through activation of the sweet taste receptor, T1R3. *Nutrients.* (2020) 12:1862. doi: 10.3390/nu12061862
37. Bian X, Chi L, Gao B, Tu P, Ru H, Lu K. Gut microbiome response to sucralose and its potential role in inducing liver inflammation in mice. *Front Physiol.* (2017) 8:487. doi: 10.3389/fphys.2017.00487
38. Allam-Ndoul B, Castonguay-Paradis S, Veilleux A. Gut microbiota and intestinal trans-epithelial permeability. *Int J Mol Sci.* (2020) 21:6402. doi: 10.3390/ijms21176402
39. Sharpton SR, Schnabl B, Knight R, Loomba R. Current concepts, opportunities, and challenges of gut microbiome-based personalized medicine in nonalcoholic fatty liver disease. *Cell Metab.* (2021) 33:21–32. doi: 10.1016/j.cmet.2020.11.010
40. Dixit K, Chaudhari D, Dhotre D, Shouche Y, Saroj S. Restoration of dysbiotic human gut microbiome for homeostasis. *Life Sci.* (2021) 278:119622. doi: 10.1016/j.lfs.2021.119622
41. Sánchez-Tapia M, Miller AW, Granados-Portillo O, Tovar AR, Torres N. The development of metabolic endotoxemia is dependent on the type of sweetener and the presence of saturated fat in the diet. *Gut Microbes.* (2020) 12:1801301. doi: 10.1080/19490976.2020.1801301
42. Ruiz-Ojeda FJ, Plaza-Díaz J, Sáez-Lara MJ, Gil A. Effects of sweeteners on the gut microbiota: a review of experimental studies and clinical trials. *Adv Nutr.* (2019) 10:S31–48. doi: 10.1093/advances/nmy037
43. Wang X, Tsai T, Deng F, Wei X, Chai J, Knapp J, et al. Longitudinal investigation of the swine gut microbiome from birth to market reveals stage and growth performance associated bacteria. *Microbiome.* (2019) 7:109. doi: 10.1186/s40168-019-0721-7
44. Lundberg DS, Lebeis SL, Paredes SH, Yourstone S, Gehring J, Malfatti S, et al. Defining the core *Arabidopsis thaliana* root microbiome. *Nature.* (2012) 488:86–90. doi: 10.1038/nature11237
45. Hamady M, Knight R. Microbial community profiling for human microbiome projects: tools, techniques, and challenges. *Genome Res.* (2009) 19:1141–52. doi: 10.1101/gr.085464.108
46. Wang QP, Browman D, Herzog H, Neely GG. Non-nutritive sweeteners possess a bacteriostatic effect and alter gut microbiota in mice. *PLoS ONE.* (2018) 13:e0199080. doi: 10.1371/journal.pone.0199080
47. Jia L, Li D, Feng N, Shamoon M, Sun Z, Ding L, et al. Anti-diabetic Effects of Clostridium butyricum CGMCC0313.1 through promoting the growth of gut butyrate-producing bacteria in type 2 diabetic mice. *Sci Rep.* (2017) 7:7046. doi: 10.1038/s41598-017-07335-0
48. Shen D, Lu Y, Tian S, Ma S, Sun J, Hu Q, et al. Effects of L-arabinose by hypoglycemic and modulating gut microbiome in a high-fat diet- and streptozotocin-induced mouse model of type 2 diabetes mellitus. *J Food Biochem.* (2021) 45:e13991. doi: 10.1111/jfbc.13991
49. Nowlan JP, Lumsden JS, Russell S. Advancements in characterizing tenacibaculum infections in Canada. *Pathogens.* (2020) 9:1029. doi: 10.3390/pathogens9121029
50. Rubio-Portillo E, Ramos-Espla AA, Anton J. Shifts in marine invertebrate bacterial assemblages associated with tissue necrosis during a heatwave. *Coral Reefs.* (2021) 40:395–404. doi: 10.1007/s00338-021-02075-0
51. Kwiecinski JM, Horswill AR. Staphylococcus aureus bloodstream infections: pathogenesis and regulatory mechanisms. *Curr Opin Microbiol.* (2020) 53:51–60. doi: 10.1016/j.mib.2020.02.005
52. Wang P, Li D, Ke W, Liang D, Hu X, Chen F. Resveratrol-induced gut microbiota reduces obesity in high-fat diet-fed mice. *Int J Obes (Lond).* (2020) 44:213–25. doi: 10.1038/s41366-019-0332-1
53. Zhang W, Zou G, Li B, Du X, Sun Z, Sun Y, et al. Fecal microbiota transplantation (FMT) alleviates experimental colitis in mice by gut microbiota regulation. *J Microbiol Biotechnol.* (2020) 30:1132–41. doi: 10.4014/jmb.2002.02044
54. Ma L, Ni Y, Wang Z, Tu W, Ni L, Zhuge F, et al. Spermidine improves gut barrier integrity and gut microbiota function in diet-induced obese mice. *Gut Microbes.* (2020) 12:1–19. doi: 10.1080/19490976.2020.1832857
55. Vacca M, Celano G, Calabrese FM, Portincasa P, Gobbetti M, De Angelis M. The controversial role of human gut lachnospiraceae. *Microorganisms.* (2020) 8:573. doi: 10.3390/microorganisms8040573
56. Cox LM, Yamanishi S, Sohn J, Alekseyenko AV, Leung JM, Cho I, et al. Altering the intestinal microbiota during a critical developmental window has lasting metabolic consequences. *Cell.* (2014) 158:705–21. doi: 10.1016/j.cell.2014.05.052
57. Miyauchi E, Kim SW, Suda W, Kawasumi M, Onawa S, Taguchi-Atarashi N, et al. Gut microorganisms act together to exacerbate inflammation in spinal cords. *Nature.* (2020) 585:102–6. doi: 10.1038/s41586-020-2634-9
58. van Muijlwijk GH, van Mierlo G, Jansen P, Vermeulen M, Bleumink-Pluym NMC, Palm NW, et al. Identification of Allobaculum mucolyticum

as a novel human intestinal mucin degrader. *Gut Microbes.* (2021) 13:1966278. doi: 10.1080/19490976.2021.1966278

Conflict of Interest: The authors declare that the research was conducted in the absence of any commercial or financial relationships that could be construed as a potential conflict of interest.

Publisher's Note: All claims expressed in this article are solely those of the authors and do not necessarily represent those of their affiliated organizations, or those of the publisher, the editors and the reviewers. Any product that may be evaluated in this article, or claim that may be made by its manufacturer, is not guaranteed or endorsed by the publisher.

frontiers in Nutrition

ORIGINAL RESEARCH
published: 29 March 2022
doi: 10.3389/fnut.2022.821404

Nanoparticles Isolated From Porcine Bone Soup Ameliorated Dextran Sulfate Sodium-Induced Colitis and Regulated Gut Microbiota in Mice

Huiqin Wang[1], Jin Huang[1], Yanan Ding[1], Jianwu Zhou[1], Guanzhen Gao[1], Huan Han[1], Jingru Zhou[1], Lijing Ke[1], Pingfan Rao[1], Tianbao Chen[2] and Longxin Zhang[3]*

[1] Food Nutrition Science Centre, School of Food Science and Biotechnology, Zhejiang Gongshang University, Hangzhou, China, [2] School of Pharmacy, Queen's University Belfast, Belfast, United Kingdom, [3] Fujian Provincial Maternity and Children's Hospital, Affiliated Hospital of Fujian Medical University, Fuzhou, China

Daily foods contain a great number of self-assembled nanoparticles (NPs) which were incidentally produced during food processing. These food incidental NPs can directly access the human gastrointestinal tract in high frequency and large quantities. Limited reports were focused on whether and how these food incidental NPs affected the gastrointestinal tissues and gut microbiota. In the present study, bone soup and its NPs both significantly ameliorated colitis symptoms in dextran sulfate sodium (DSS)-induced mice and inhibited the release of pro-inflammatory cytokines. They also restored intestinal microbiota dysbiosis by improving the diversity and richness of intestinal microbiota and regulating community composition, such as a remarkable increase in *Muribaculaceae*, *Alistipes*, and *Alloprevotella*, and a decrease in *Helicobacter*. Moreover, the correlation analysis showed that pro-inflammatory cytokines were negatively correlated with *Muribaculaceae*, *Alloprevotella*, and *Alistipes*, but positively correlated with *Helicobacter*. These findings suggest that the food incidental NPs can influence human health through regulating the inflammation of the gastrointestinal tissues and the gut microbiota.

Keywords: bone soup, nanoparticles, ulcerative colitis, gut microbiota, inflammation, dextran sulfate sodium

OPEN ACCESS

Edited by:
Xin Wang,
Zhejiang Academy of Agricultural Sciences, China

Reviewed by:
Shusong Wu,
Hunan Agricultural University, China
Zhengpeng Li,
Chinese PLA General Hospital, China

****Correspondence:***
Guanzhen Gao
gaoguanzhen@zjgsu.edu.cn

Specialty section:
This article was submitted to Nutrition and Microbes, a section of the journal Frontiers in Nutrition

Received: *24 November 2021*
Accepted: *25 February 2022*
Published: *29 March 2022*

Citation:
Wang H, Huang J, Ding Y, Zhou J, Gao G, Han H, Zhou J, Ke L, Rao P, Chen T and Zhang L (2022) Nanoparticles Isolated From Porcine Bone Soup Ameliorated Dextran Sulfate Sodium-Induced Colitis and Regulated Gut Microbiota in Mice. Front. Nutr. 9:821404. doi: 10.3389/fnut.2022.821404

INTRODUCTION

In the past decades, nanoparticles (NPs) have been increasingly used in food processing and food packaging for improving the quality of food, extending the shelf-life, enhancing the uptake, absorption, and bioavailability of food nutrients, etc (1, 2). These engineered NPs could have direct access to the human gastrointestinal tract (GIT) along with the food (3) and subsequently affect the gut microbiota and the GIT itself, such as GIT inflammation and redox homeostasis (4).

Abbreviations: NPs, nanoparticles; GIT, gastrointestinal tract; DSS, dextran sulfate sodium; DHA, docosahexaenoic acid; EPA, eicosatetraenoic acid; IBD, inflammatory bowel disease; BS, bone soup; BSNPs, bone soup nanoparticles; SASP, sulfasalazine; 16S rRNA, 16S ribosomal RNA; DAI, disease activity index; GAPDH, glyceraldehyde 3-phosphate dehydrogenase; IL-6, interleukin 6; IL-1β, interleukin 1 beta; TNF-α, tumor necrosis factor alpha; PCoA, principal coordinates analysis; NMDS, non-metric multidimensional scaling; LEfSe, linear discriminant analysis effect size; OTUs, operational taxonomic units; LDA, linear discriminant analysis; NF-κB, nuclear factor kappa B.

Several studies revealed that these NPs, such as TiO_2 (5), SiO_2 (6), CuO (7), Ag (8), could induce intestinal inflammation and disruption of gut microbiota. On the contrary, some engineered NPs, e.g., Ce oxide (9), ZnO (10), and Ag (11) exerted an anti-inflammatory activity. The underlying mechanisms of the "nanoparticle-GIT" interaction were not fully understood, thus warranting further studies.

Apart from the engineered NPs in the food system, daily foods contained abundant amounts of incidental NPs, too, which were the assemblies of polar or non-polar food components derived by physical and chemical forces during the food processing (heating, cooling, and emulsification, etc.) (12). For instance, the proteoglycan–lipid NPs with an average diameter of 50–67 nm were generated during the heating processing of Freshwater Clams (*Corbicula fluminea* Muller) soup (12). Numerous spherical NPs were found in green tea infusions (13). A large number of self-assembly micro/nanoparticles containing docosahexaenoic acid (DHA) and eicosatetraenoic acid (EPA) have been observed in bigeye tuna (*Thunnus obesus*) head soup (14). Moreover, porcine bone soup, as a traditional nourishing food for preventing immune malfunction and inflammatory bowel disease (IBD) (15, 16), has been demonstrated to contain amounts of nanoscale colloidal particles with an average size of ca. 200 nm, and the formation of these incidental NPs has been investigated (17, 18). These food incidental NPs not only played a crucial role in the stability and texture characterization of food, but also made great contributions to the physiological effects of food due to the unique physicochemical properties at nanoscale. Similar to the engineered NPs, these food incidental NPs may directly encounter cells in human GIT and alter the intestinal microenvironment. To date, however, little has been known on these incidental food NPs and their biological impacts on the gut.

As we previously reported, the spherical NPs mainly consisted of lipids and proteins with an average size of ca. 200 nm and ζ-potential of ca. −15 mV derived from porcine bone soup were isolated and directly interacted with macrophages with preventing cells from peroxyl radical-induced membrane hyperpolarization, mitochondrial malfunction, and phagocytosis suppression (18). Moreover, these NPs derived from the porcine bone soup attenuated oxidative stress-induced intestinal barrier injury in the Caco-2 cell monolayer model (17). In this study, we set off to evaluate the alleviative effects of NPs derived from porcine bone soup on dextran sulfate sodium (DSS) induced colitis in mice, by modulating intestinal inflammation and gut microbiota.

MATERIALS AND METHODS

Preparation of Nanoparticles Derived From Porcine Bone Soup

Fresh porcine bones (Landrace pigs, *Sus scrofa*) were obtained from the fresh local market. The bone soup was prepared, and the NPs were isolated according to our previous reports (17–19). Briefly, 1 kg of fresh porcine bones was cooked with deionized water (1:3, w/v) for 3 h in a boiling water bath after removing the blood residues. Filtered through four layers of cotton gauze to remove the solid residues and the soup was centrifuged at 400 *g* for 10 min. The supernatant of bone soup was collected and named as BS. Then BS was applied to a pre-equilibrated size-exclusive chromatographic column. The fractions with strong light scattering intensity were collected and dialyzed against water, and the obtained NPs samples were freeze-dried and designated as BSNPs. Before the animal experiment, BSNPs were dissolved with deionized water to the same derived count rate as that of BS.

Animal Experiments

The 5-week-old specific pathogen-free (SPF) female BALB/c mice were supplied by Zhejiang Center of Laboratory Animals (Hangzhou, China). The mice were housed under the standard conditions (21 ± 1°C, 55.5 ± 5% relative humidity) with a controlled light–dark cycle of 12/12 h. The mice were fed on standard chow and distilled water *ad libitum*. After 1 week of adaptive feeding, the mice were randomly divided into five groups with six mice each. Acute colitis in BALB/c mice was established according to the previous study (20). The groups were as follows: (1) Control group, mice were fed with standard chow and distilled water *ad libitum*, daily administered normal saline (50 ml/kg/day) by oral gavage for 7 days. (2) DSS group, provided free access to 5% DSS (36–50 kDa; MP Biomedicals, Irvine, CA, United States) in distilled water and daily administered normal saline (50 ml/kg/day) by oral gavage for 7 days. (3) Sulfasalazine (SASP) group, provided free access to 5% DSS in distilled water and daily administered SASP (250 mg/kg, Shanghai Zhongxi Sanwei Pharmaceutical Co., Ltd., Shanghai, China) by oral gavage for 7 days. (4) The BS group provided free access to 5% DSS in distilled water and administered BS at 50 ml/kg/day by oral gavage for 7 days. (5) BSNPs group provided free access to 5% DSS in distilled water and administered BSNPs at 50 ml/kg/day by oral gavage for 7 days. On the 8th day, mice were sacrificed by cervical dislocation. The fecal samples were collected for 16S ribosomal RNA (16S rRNA) analysis. The colon samples were excised quickly and rinsed with ice-cold 0.9% NaCl. Their length and weight were subsequently measured. At last, colons were divided into three parts for histopathological analysis and real-time polymerase chain reaction (PCR).

All animal experiments were conducted according to the NIH Guidance for the care and use of laboratory animals and approved by the Animal Care and Welfare Committee of Zhejiang Center of Laboratory Animals, China.

Disease Activity Index

The severity of colitis was evaluated daily according to the DAI scoring system as described previously (21), such as body weight loss, stool consistency, and gross rectal bleeding.

Histological Analysis

For histological evaluation, hematoxylin and eosin (H&E) stained colon tissues were performed, and histological changes were evaluated by two independent investigators in a blinded manner according to a scoring system as described previously (22). The sum of each score reflected the colonic histological damage.

TABLE 1 | GenBank accession numbers, sequences of forward and reverse primers, and fragment sizes used for real-time PCR.

Target	GenBank number	Primer sequence	Size, bp
TNF-α	NM_013693.3	F:5′ TTGTCTACTCCCAGGTTCTCT3′ R: 5′ GAGGTTGACTTTCTCCTGGTATG3′	107
IL-6	NM_031168.2	F:5′ CTTCCATCCAGTTGCCTTCT3′ R:5′ CTCCGACTTGTGAAGTGGTATAG3′	134
IL-1β	NM_008361.4	F:5′ CCACCTCAATGGACAGAATATCA3′ R:5′ CCCAAGGCCACAGGTATTT3′	96
GAPDH	NM_001289726.1	F:5′ AACAGCAACTCCCACTCTTC3′ R:5′ CCTGTTGCTGTAGCCGTATT3′	111

RNA Extract and Real-Time PCR

The mRNA expression of inflammatory cytokines, such as interleukin 6 (IL-6), interleukin 1 beta (IL-1β), and tumor necrosis factor-alpha (TNF-α), were determined in ileum mucosa by real-time PCR. Total RNA was extracted from the colon tissue using with miRNeasy Mini Kit (QIAGEN, 217004, Hilden, North Rhine-Westphalia, Germany), its concentration and purity were measured using a NanoDrop 2000 spectrophotometer (Thermo Fisher Scientific, Waltham, MA, United States). cDNA was synthesized using RevertAid First Strand cDNA Synthesis Kit (Thermo Fisher Scientific, K1622, Waltham, MA, United States). The real-time PCR was conducted using Platinum SYBR Green qPCR SuperMix-UDG with ROX (Invitrogen, 11744-500, Carlsbad, CA, United States); the reaction solution contained 10 μl of 2 × SYBR Green, 1 μl of each primer (10 μM), 1 μl of reverse transcription product, and 8 μl of RNase/DNase-free water (total volume 20 μl). Glyceraldehyde 3-phosphate dehydrogenase (GAPDH) was used as an internal reference gene to normalize target gene transcript levels and the primers sequences of target genes (Sangon Biotech (Shanghai) Co., Shanghai, China) are presented in **Table 1**. The reaction conditions were as follows: 2 min at 95°C, 40 cycles for 15 s at 95°C, 30 s at 60°C, 30 s at 72°C. All the results were normalized to the internal reference gene: GAPDH. The relative expression of mRNA level was calculated with the $2^{-\Delta\Delta Ct}$ method.

16S rRNA Analysis

The gut microbiota composition of mice feces was determined by 16S rRNA gene amplification. Briefly, MagPure Stool DNA KF Kit B (Magen Biotechnology Co., Guangzhou, China) was used to extract genomic DNA from feces. DNA concentration and integrity were measured by a NanoDrop 2000 spectrophotometer (Thermo Fisher Scientific, Waltham, MA, United States) and agarose gel electrophoresis, respectively. The 16S rRNA gene V3–V4 region was amplified from the genomic DNA in a 25 μl reaction using the universal bacterial primers: (343F, 5′- TACGGRAGGCAGCAG-3′, and 798R, 5′-AGGGTATCTAATCCT-3′). The PCR products were purified with Agencourt AMPure XP beads (Beckman Coulter Co., Brea, CA, United States) and quantified by using a Qubit dsDNA assay kit (Thermo Fisher Scientific, Waltham, MA, United States). Sequencing was performed on an Illumina NovaSeq 6000 with two paired-end read cycles of 250 bases each (Illumina Inc., San Diego, CA, United States; OE Biotech Co., Ltd., Shanghai, China).

The Trimmomatic software was used to analyze the raw data. After trimming, operational taxonomic units (OTUs) were generated by using VSEARCH 2.7.1 with a 97% similarity cutoff. The representative read of each OTU was selected by using the Quantitative Insights into Microbial Ecology (QIIME) package. All representative reads were annotated and blasted against the Silva database (Version 132) using the RDP classifier (confidence threshold was 70%). The microbial richness and diversity in fecal content samples were estimated using the alpha diversity that includes Chao1 index, Observed species index, Simpson index, and Shannon index. The UniFrac distance matrix performed by QIIME software was used for the unweighted UniFrac Principal coordinates analysis (PCoA), Non-metric multidimensional scaling (NMDS) analysis, and phylogenetic tree construction. Linear discriminant analysis effect size (LEfSe) based linear discriminant analysis (LDA) and cladogram were generated to assess differentially abundant microbial taxa. The 16S rRNA gene amplicon sequencing and analysis were conducted by OE Biotech Co., Ltd. (Shanghai, China).

Statistical Analysis

Data were expressed as mean ± standard error of the mean (SEM) and performed with GraphPad Prism 7.0 (GraphPad Software, Inc., San Diego, CA, United States). The significant differences were analyzed using one-way analysis of variance (ANOVA) followed by Tukey's multiple comparisons in multiple groups. Correlations were analyzed by using Spearman's correlation analysis. The value of $p < 0.05$ was considered to be statistically significant.

RESULTS

Bone Soup Nanoparticles Alleviated the Symptoms of Dextran Sulfate Sodium-Induced Colitis in Mice

The influences of the BS or its BSNPs on the symptoms of DSS-induced colitis were investigated. As shown in **Figures 1A–E**, the DSS-treated group showed a significant reduction in bodyweight, increase in DAI score, reduction of colon length, and increment of colon weight/length ratio compared with the healthy control group ($p < 0.05$). The BS or BSNPs treatment, similar to that

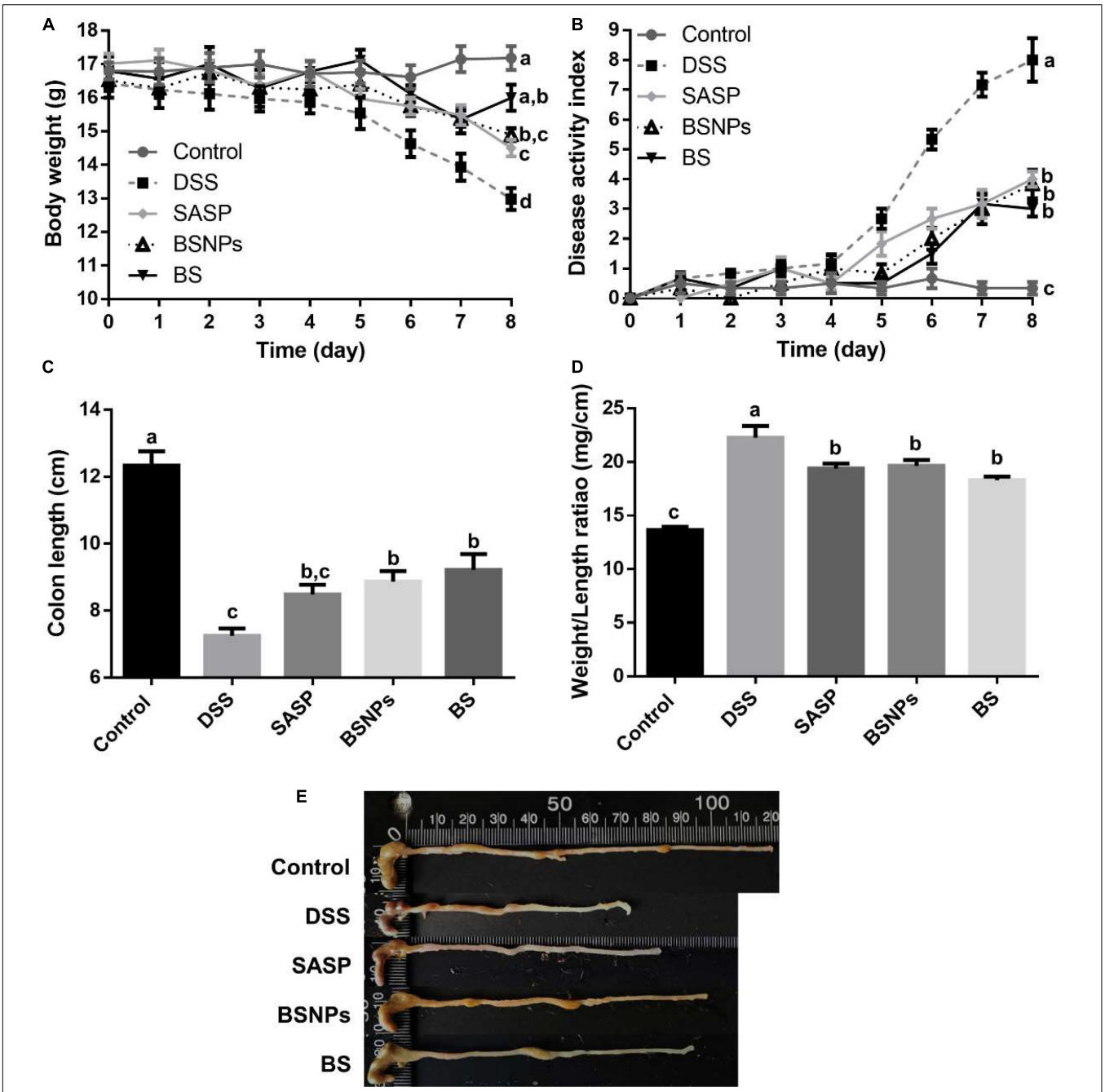

FIGURE 1 | Effect of BS or BSNPs treatment on clinical symptoms of dextran sulfate sodium (DSS)-induced colitis. **(A)** Bodyweight measurement. **(B)** Disease activity index. **(C)** Colon length of mice. **(D)** Colon weight/length ratio. **(E)** Representative images of the colon from a different group. Values were expressed as the mean ± SEM ($n = 6$). Means without a common letter are significantly different at $p < 0.05$ using one-way ANOVA followed by Tukey's test for *post hoc* analysis.

of SASP, significantly alleviated the bodyweight loss, the DAI score, and increment in the colon length. A significant reduction of colon weight/length ratio was observed in the BS/BSNPs-treated mice compared with the DSS group ($p < 0.05$). Moreover, no significant difference was observed between BS and BSNPs treatment, implying that the alleviative effects of BS in DSS-induced colitis might be mainly attributed to its NP components.

Bone Soup Nanoparticles Attenuated the Inflammation of Colonic Mucosa

The histological changes of colonic mucosa were consistent with the general symptoms described above, determined with H&E staining. As shown in **Figures 2A,B**, the DSS treatment induced inflammatory cell infiltration and significantly elevated histological score ($p < 0.05$). The treatment of BS or BSNPs

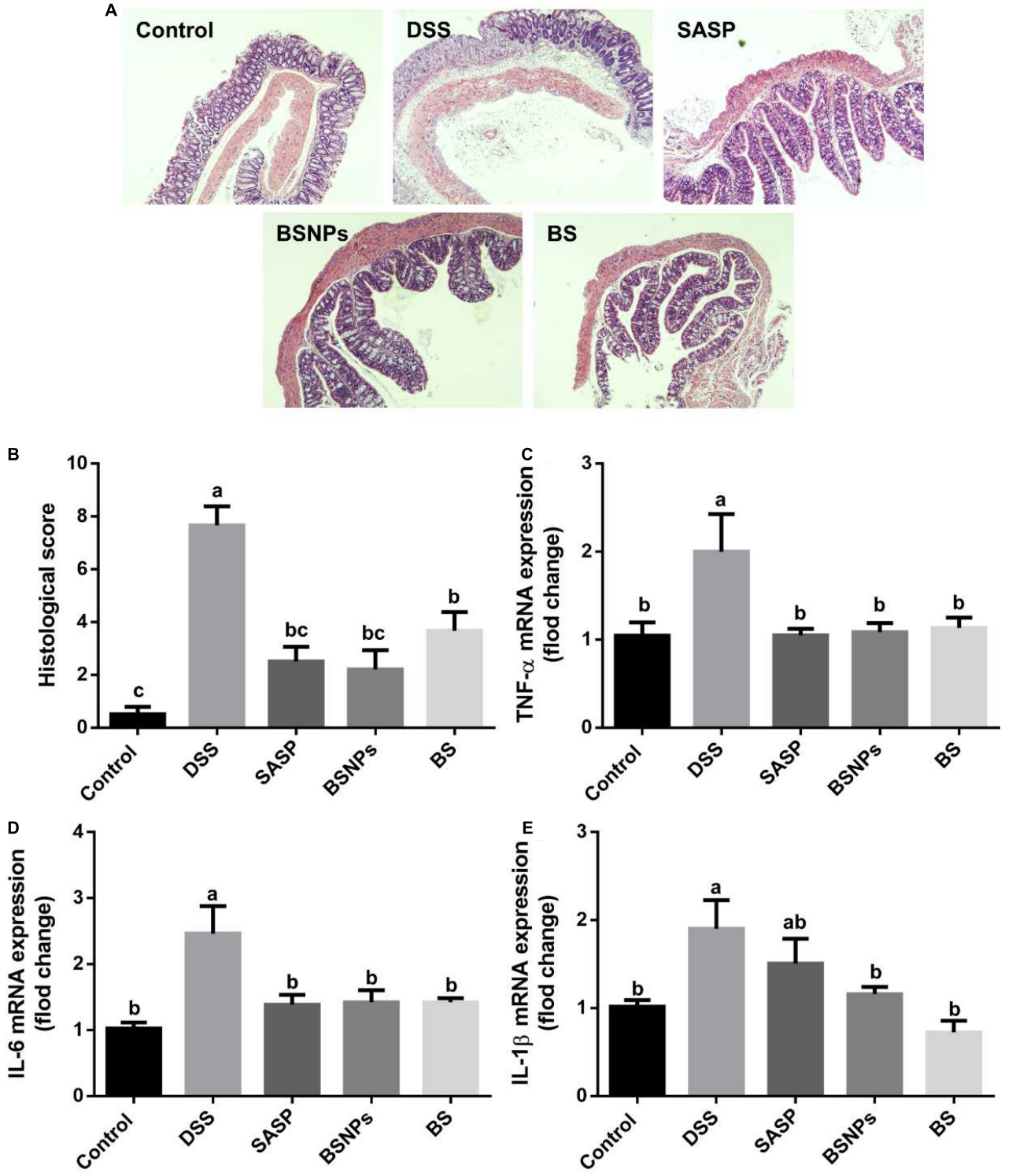

FIGURE 2 | Effect of BS, BSNPs, and SASP treatment on histopathological alteration and inflammatory cytokines in the colonic mucosa of DSS-induced colitis. **(A)** Representative images of colonic segments. **(B)** Histological scores. **(C)** TNF-α expression. **(D)** Interleukin 6 (IL-6) expression. **(E)** Interleukin 1 β (IL-1β) expression. Values are expressed as the mean ± SEM ($n = 6$). Means without a common letter are significantly different at $p < 0.05$ using one-way ANOVA followed by Tukey's test for *post hoc* analysis.

significantly inhibited the cell infiltration and histological score ($p < 0.05$).

In line with the histological changes, the pro-inflammatory cytokines (e.g., TNF-α, IL-6, and IL-1β) were boosted by DSS but downregulated by BS or BSNPs to an extent similar to that of SASP (**Figures 2C–E**), judging by quantitative real-time PCR determination of mRNA abundance of cytokines. The BS and BSNPs exhibited the same level of inhibition on colonic inflammation, elucidating the NPs are the principal active components of the bone soup in treating DSS-induced colitis.

Bone Soup Nanoparticles Restored Gut Microbial Diversity

The alpha diversity and beta diversity analysis of the gut microbial community in each group were assessed using a set of statistical analysis indexes. The gut microbial community richness index was calculated with Chao1 and Observed species index, while Shannon index and Simpson index were used to estimate the microbial diversity. As shown in **Figures 3A–D**, the Chao1 index, Observed species index, Shannon index, and Simpson index of the DSS group were found to be significantly lower than the normal mice, suggesting DSS reduced the microbial richness and diversity, disrupted the microbiota structure. The administration of either BS or BSNPs restored the microbial richness and diversity, in similar effectiveness with SASP. No significant difference was observed between the BS and BSNPs groups.

Besides, the PCoA of the microbial community showed that the microbial evolution of DSS-treated mice was vastly different from the normal mice, while the BS and BSNPs-treated mice were rather similar to the normal mice (**Figure 3E**). It is in line with the NMDS analysis (**Figure 3F**). In addition, the unweighted pair-group technique with arithmetic mean (UPGMA) was employed to construct a circular hierarchical clustering tree (**Figure 3G**), which indicated that the administration of BS, BSNPs, and SASP caused much fewer changes in microbial communities than that of DSS.

Modulation of Gut Microbiota by Bone Soup Nanoparticles

The gut microbiota community structure distribution and relative abundance of taxa were analyzed. At the phylum level, the gut microbiota composition in each group was shown in **Figure 4A**. Compared to the normal mice, mice in the DSS group exhibited the higher relative abundances of *Campilobacterota* (33.43 vs. 1.26%) and lower relative abundances of *Bacteroidetes* (25.53 vs. 63.95%). The DSS induced an elevated *Firmicutes/Bacteroidetes* (F/B) ratio, too ($p < 0.05$, **Figure 4C**). The administration of BSNPs or BS significantly reversed these microbiota composition changes at the phylum level and resorted the F/B ratio to a normal level.

Consistently, the BSNPs or BS administration also restored the microflora balance at the genus level (**Figure 4B**), characterized by significantly increased *Muribaculaceae* (**Figure 4D**), *Alistipes* (**Figure 4H**), and *Alloprevotella* (**Figure 4G**), markedly decreased *Helicobacter* and *Lachnospiraceae_NK4A136_group* (**Figures 4E,F**) ($p < 0.05$). Furthermore, a heatmap based on the relative abundance of the top 15 abundant genera of bacteria, a phylogenetic tree, and a heatmap showing relative abundances of OTUs together with a corresponding phylogenetic tree were performed (**Figures 4I,J**). These results confirmed that BS or

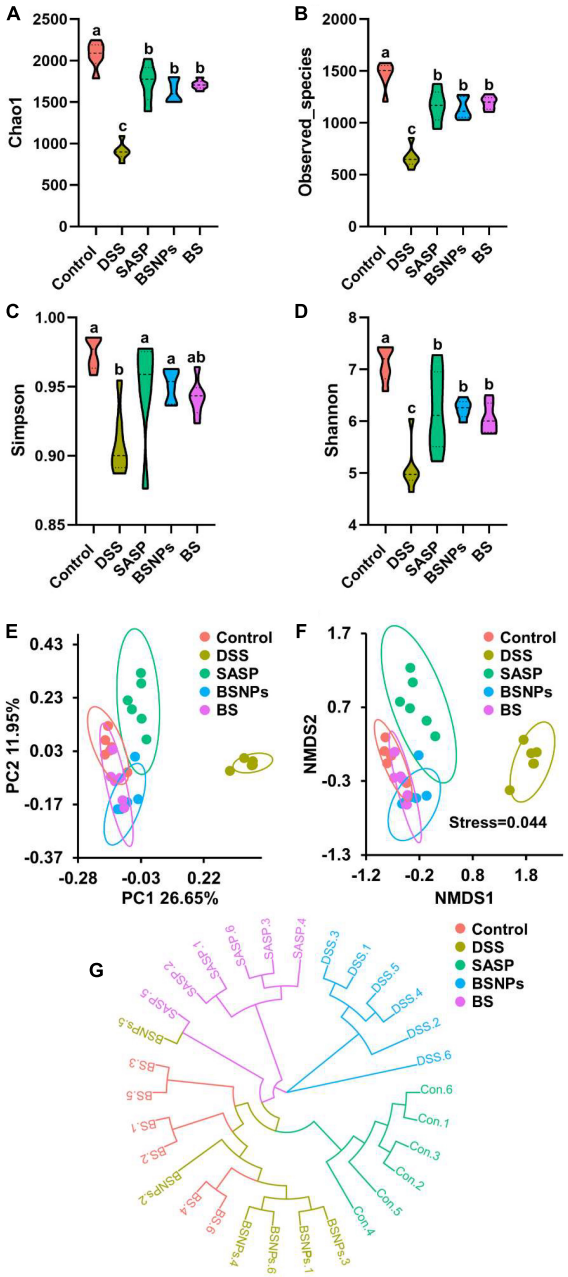

FIGURE 3 | Analysis of the alpha diversity and beta diversity of the differential microbial community among the control group, DSS group, SASP, BS, and BSNPs-treated group. Violin plots showing Chao1 index **(A)**, Observed_species index **(B)**, Simpson index **(C)**, Shannon index **(D)**. **(E)** UniFrac distance of unweighted PCoA analysis, **(F)** UniFrac distance of unweighted NMDS analysis, **(G)** the unweighted pair-group technique with arithmetic mean (UPGMA) analysis the differences between samples. Means without a common letter are significantly different at $p < 0.05$ using one-way ANOVA followed by Tukey's test for *post hoc* analysis.

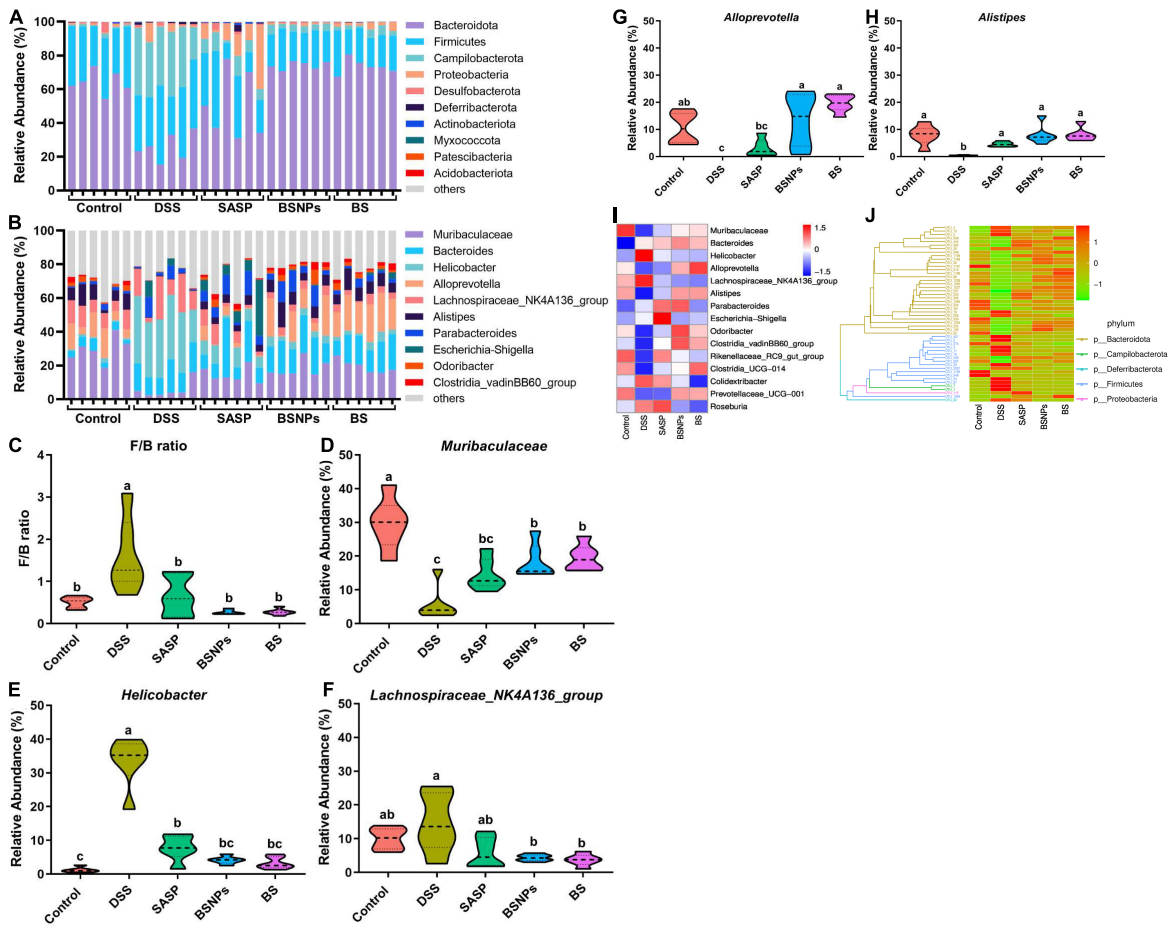

FIGURE 4 | Analysis of the microbial community structure of each group. **(A)** Relative abundance of each sample at the phylum level. **(B)** Relative abundance of each sample at the genus level. Violin plots showing *Firmicutes* to *Bacteroidetes* ratio (F/B ratio) **(C)** of each group, and relative abundance of *Muribaculaceae* **(D)**, *Helicobacter* **(E)**, *Lachnospiraceae_NK4A136_group* **(F)**, *Alloprevotella* **(G)**, and *Alistipes* **(H)** at the genus levels. **(I)** Heatmap illustrating the relative abundance of the 15 most abundant bacterial genus. **(J)** Phylogenetic tree and heatmap showing relative abundances of operational taxonomic units (OTUs) together with a corresponding phylogenetic tree. The clustering branch represents different bacterial phyla. The abundance graph was shown on the right, which corresponds to the abundance of left OTUs in each sample. Means without a common letter are significantly different at $p < 0.05$ using one-way ANOVA followed by Tukey's test for *post hoc* analysis.

BSNPs treatment could counteract the DSS-induced changes in the gut microbiota.

The LEfSe was performed to compare the difference in the abundance of gut microbiota compositions among different groups of mice (**Figures 5A,B**). From the phylum level to the genus level, there were 43 significant taxa in all groups. At the genus levels, *Lachnospiraceae_NK4A136_group* and *Helicobacter* were enriched in the DSS-treated mice, while 11 other taxa, such as *Muribaculaceae*, *Alloprevotella*, *Alistipes*, *Odoribacter*, *Clostridia_vadinBB60_group*, and *Rikenellaceae_RC9_gut_group*, were enriched in normal mice and SASP/BS/BSNPs-treated mice.

Correlations Between the Expressions of Pro-inflammatory Cytokines With Microbiota

The possible correlations between gut microbiota and pro-inflammatory cytokines were examined with Spearman's correlation analyses (23). As shown in **Figure 6**, six bacteria were negatively correlated with pro-inflammatory cytokines ($p < 0.05$), such as *Muribaculaceae*, *Alloprevotella*, *Alistipes*, *Odoribacter*, *Clostridia_vadinBB60_group*, and *Rikenellaceae_RC9_gut_group*. Notably, these six bacteria were separately enriched in BSNPs, BS, and control group (**Figure 5A**), and *Muribaculaceae*, *Alloprevotella*, and *Alistipes* were significantly lower in the DSS group than other groups (**Figures 4D,G,H**). Furthermore, *Helicobacter and Colidextribacter* were significantly positively correlated with the pro-inflammatory cytokines ($p < 0.05$). Intriguingly, *Helicobacter* was enriched in DSS treatment (**Figure 5A**), and the treatment of BS, BSNPs, or SASP can significantly decrease the abundances of *Helicobacter* (**Figure 4E**). These results revealed that the anti-inflammatory effects of BSNPs and BS on DSS-induced colitis might be correlated to the increased abundance in *Muribaculaceae*, *Alloprevotella*, and

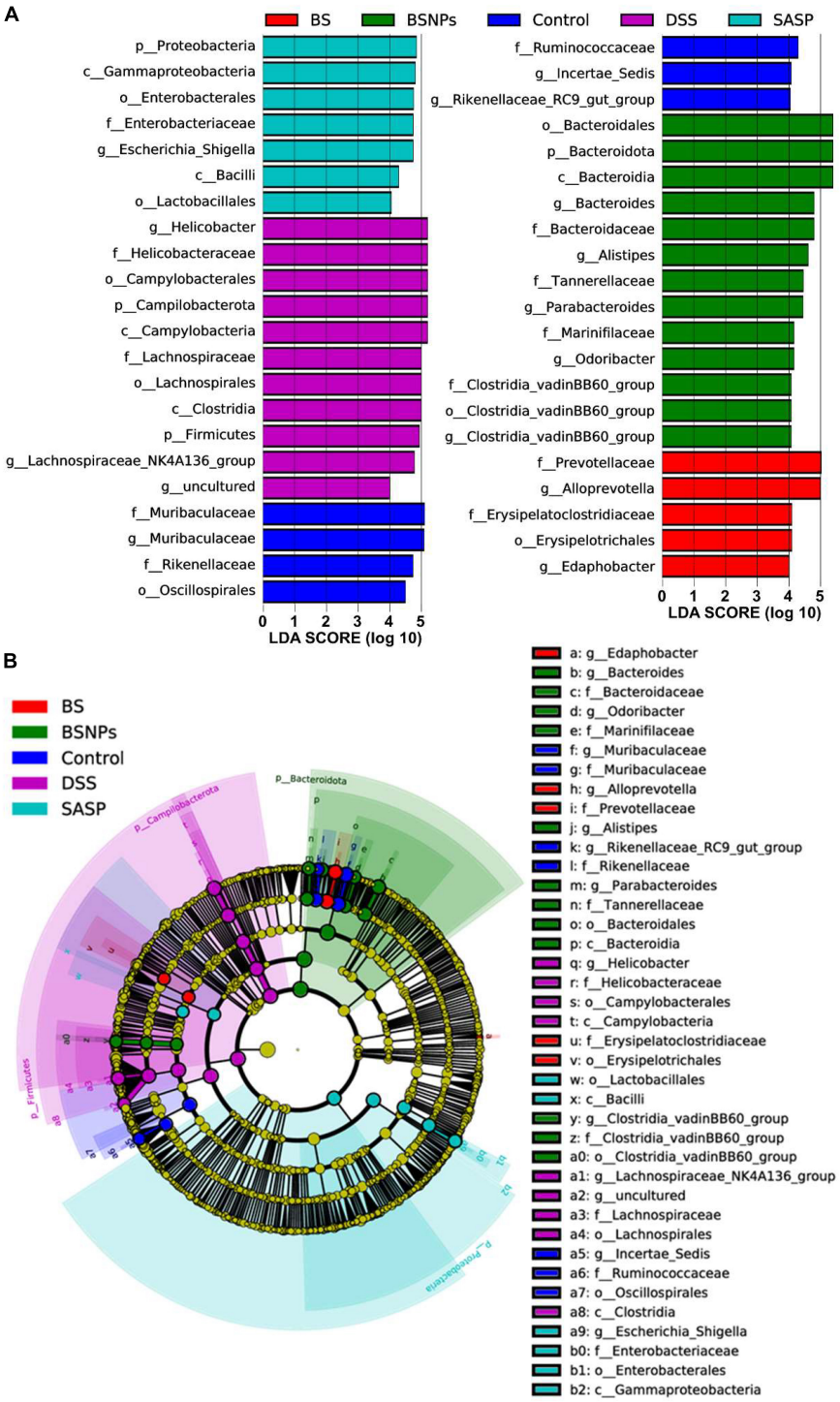

FIGURE 5 | Linear discriminant analysis (LDA) and effect size (LEfSe) analysis of bacterial among the different groups. **(A)** LDA indicates the most differential abundant bacterial taxa in specific samples. **(B)** Cladogram illustrating highly abundant taxa across various treatments.

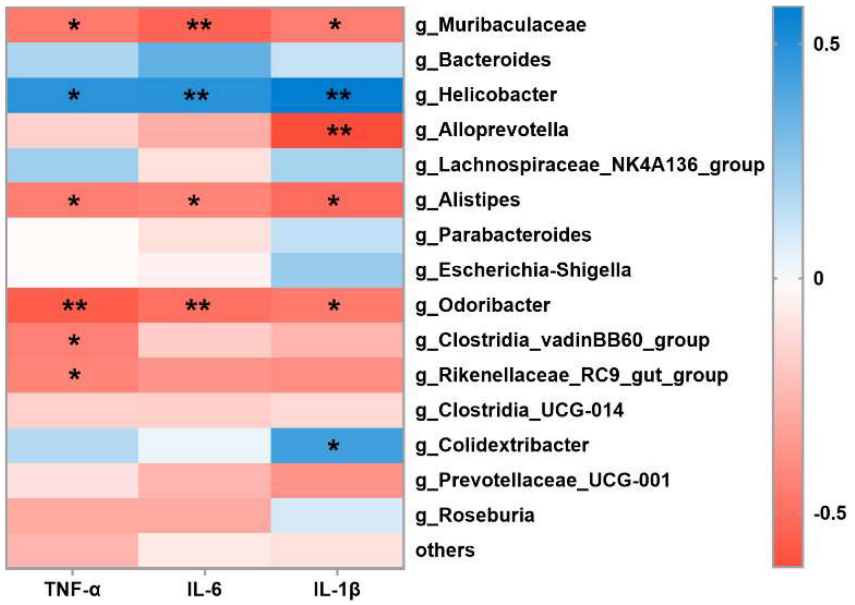

FIGURE 6 | Interrelationship between gut microbiota and pro-inflammatory cytokines. Heatmap of Spearman's correlation between gut bacteria (at the genus level) and pro-inflammatory cytokines. Significant difference determined at $^{*}p < 0.05$, $^{**}p < 0.01$.

Alistipes, and the decreased abundance in *Helicobacter* in the microbiota of mice.

DISCUSSION

The present study demonstrated that BS and BSNPs (the NPs isolated from bone soups) alleviated the pathological symptoms and inflammatory cytokines of DSS-induced colitis in mice. There was no significant difference between BS and BSNPs treatment, implying that BSNPs may exert protective effects against DSS-induced bowel disease in mice. BSNPs are mainly consisted of lipids and proteins, including collagen (18). It has been reported that the hybrid NPs of lipid–protein were resistant to hydrolysis of enzymes in saliva, stomach, and intestinal fluids and protected its inherent bioactive components from degradation (24, 25). The lipid–protein complex of BSNPs might make the particles resistant to gastrointestinal digestion, as was found in grapefruit-derived NPs (25). In our previous study, BSNPs have been demonstrated impressively high stability under harsh conditions of 4°C for 5 days (18). This indicated that BSNPs might as intact NP form to exert the anti-inflammatory effect in the gut.

Some inorganic NPs [such as Ce oxide (9), ZnO (10), and Ag (11)] could exhibit the therapeutic effects in the experimental colitis model *via* the anti-oxidative mechanism. Other NPs fabricated with natural biopolymers, such as chitosan and silk fibroin, acted as nanoscale drug delivery systems to alleviate ulcerative colitis (4, 26–28). The alleviative effects of BSNPs on intestinal inflammation might be attributed to its antioxidant activity and its constitutive collagen (17–19).

The cellular protective effects of BSNPs have been demonstrated in previous studies (17–19). According to the *in vitro* study, the BSNPs could be engulfed by oral and peritoneal macrophages, possess intracellular antioxidant activities, and suppress the membrane hyperpolarization induced by peroxyl radical on macrophage (18, 19). Such suppression could facilitate the anti-inflammatory effects (29). The healthier macrophages would promote the gut homeostasis and recovery of IBD (30). In addition, the disruption of the intestinal barrier is associated with disease of the GIT. Emerging evidence showed inadequate epithelial permeability resulted in IBD, IBS, UC, etc (31, 32). BSNPs could restore the intestinal barrier function of Caco-2 cells (17), which may also contribute to its alleviating effects on colitis.

Ulcerative colitis is accompanied by the dysbiosis of gut microbiota. Our results also revealed that BS or BSNPs could restore gut microbiota dysbiosis induced by the DSS. BS or BSNPs treatment increased the richness or diversity of gut microbial communities, which is badly damaged in IBD patients and DSS-induced colitis mice (33). The BS or BSNPs treatment markedly increased the abundance of *Muribaculaceae, Alistipes,* and *Alloprevotella,* while decreasing that of *Helicobacter*. The decrease of *Muribaculaceae* has been identified as the key to the development of colitis (34). *Alistipes* was reported to have protective effects against some diseases, including colitis (35). *Alloprevotella* was demonstrated to be lower in mice with DSS-induced colitis (36). *Helicobacter* was pathogens implicated in the formation of peptic ulcers and IBD (37). Moreover, the BS or BSNPs treatment decreased the F/B ratio. The ratio would be increased in colitis and other inflammatory diseases. A lower F/B ratio is connected to recovery or the health status (38, 39). Notably, our study demonstrated that *Muribaculaceae*, *Alloprevotella,* and *Alistipes*

were negatively correlated with TNF-α, IL-6, and IL-1β. Some previous studies have shown that *Muribaculaceae*, *Alloprevotella,* and *Alistipes* were negatively correlated with inflammation, cause they promoted SCFA production and improved the intestinal tissue's tolerance to the immune stimulations (34, 36, 40). In contrast, *Helicobacter* was positively correlated with three pro-inflammatory cytokines. Consistently, other reports have also described that *Helicobacter* genus could stimulate the immune response and cause the production of pro-inflammatory cytokines *via* activating proinflammatory nuclear factor kappa B (NF-κB) pathway (36, 41). These findings suggested that the protective effects of BSNPs on colitis might be attributed to its regulatory effects of gut microbiota correlated with immune responses and inflammation.

It has been reported that nanosized-food additives can bind to bacteria to form the NP-bacteria complex primarily *via* van der Waals attraction (42). This complex can induce the degradation of bacterial cell wall components, the alteration of metabolic pathways, oxidation of cellular components, and DNA damage, leading to the influence on the microbiome (43). In addition, naturally occurring NPs from beer could also bind to bacteria to form NP–bacteria complexation and then affect the microbiome (42).

However, it remains unknown whether the BSNPs could have the chance and ability to bind to the microorganisms in the alimentary tract and form a hybrid complex. The BSNPs may have been partially or completely digested before they reach the colon. The constitutive lipid and protein of BSNPs may also contribute to the bioactivities. The underlying mechanism of the interaction between NPs, their digestion products, and microbiota has not been fully understood and warrants further investigation.

CONCLUSION

Altogether, our study demonstrated that the isolated NPs from bone soup showed a preventing effect against DSS-induced colitis. The treatment of BSNPs alleviated the severity of colitis with reduction of the release of inflammatory cytokines, restored gut microbiota dysbiosis by redirecting the bacterial shift to a normal state with increasing the richness or diversity of gut microbial communities and regulating community composition, such as a remarkable increase in *Muribaculaceae*, *Alistipes*, and *Alloprevotella*, and a decrease in *Helicobacter*. It indicated that the food-derived NPs could influence human health by regulating the inflammation of the gastrointestinal tissues and the gut microbiota.

DATA AVAILABILITY STATEMENT

The datasets presented in this study can be found in online repositories. The names of the repository/repositories and accession number(s) can be found below: https://www.ncbi.nlm.nih.gov/search/all/?term=PRJNA779815, Sequence Read Archive (SRA) database (PRJNA779815).

ETHICS STATEMENT

The animal study was reviewed and approved by the Animal Care and Welfare Committee of Zhejiang Center of Laboratory Animals, China.

AUTHOR CONTRIBUTIONS

HW contributed to conceptualization, data curation, methodology, validation, formal analysis, and writing the original draft. JH and HH contributed to formal analysis, data curation, and methodology. YD and JRZ contributed to methodology, formal analysis, and investigation. JWZ contributed to formal analysis, supervision, and writing, reviewing, and editing the manuscript. GG contributed to conceptualization, methodology, supervision, investigation, validation, funding acquisition, project administration, and writing, reviewing, and editing the manuscript. LK contributed to formal analysis, project administration, and writing, reviewing, and editing the manuscript. PR contributed to conceptualization and writing, reviewing, and editing the manuscript. TC reviewed and edited the manuscript. LZ contributed to writing, reviewing, and editing the manuscript. All authors contributed to the article and approved the submitted version.

FUNDING

This work was supported by the National Key R&D Program of China (2016YFD0400202) and Fundamental Special Funds for the Provincial Universities of Zhejiang (Grant No. JDK21005).

REFERENCES

1. Nile SH, Baskar V, Selvaraj D, Nile A, Xiao J, Kai G. *Nanotechnologies in Food Science: Applications, Recent Trends, and Future Perspectives*. Singapore: Springer (2020). doi: 10.1007/s40820-020-0383-9
2. Singh T, Shukla S, Kumar P, Wahla V, Bajpai VK. Application of nanotechnology in food science: perception and overview. *Front Microbiol.* (2017) 8:1501. doi: 10.3389/fmicb.2017.01501
3. Ghebretatios M, Schaly S, Prakash S. Nanoparticles in the food industry and their impact on human gut microbiome and diseases. *Int J Mol Sci.* (2021) 22:1942. doi: 10.3390/ijms22041942
4. Bouwmeester H, van der Zande M, Jepson MA. Effects of food-borne nanomaterials on gastrointestinal tissues and microbiota. *Wiley Interdiscip Rev Nanomed Nanobiotechnol.* (2018) 10:e1481. doi: 10.1002/wnan.1481
5. Mu W, Wang Y, Huang C, Fu Y, Li J, Wang H, et al. Effect of long-term intake of dietary titanium dioxide nanoparticles on intestine inflammation in mice. *J Agric Food Chem.* (2019) 67:9382–9. doi: 10.1021/acs.jafc.9b02391
6. Ogawa T, Okumura R, Nagano K, Minemura T, Izumi M, Motooka D, et al. Oral intake of silica nanoparticles exacerbates intestinal inflammation. *Biochem Biophys Res Commun.* (2021) 534:540–6. doi: 10.1016/j.bbrc.2020.11.047

7. Ude VC, Brown DM, Stone V, Johnston HJ. Time dependent impact of copper oxide nanomaterials on the expression of genes associated with oxidative stress, metal binding, inflammation and mucus secretion in single and co-culture intestinal in vitro models. *Toxicol Vitro.* (2021) 74:105161. doi: 10.1016/j.tiv.2021.105161
8. Williams K, Milner J, Boudreau MD, Gokulan K, Cerniglia CE, Khare S. Effects of subchronic exposure of silver nanoparticles on intestinal microbiota and gut-associated immune responses in the ileum of Sprague-Dawley rats. *Nanotoxicology.* (2015) 9:279–89. doi: 10.3109/17435390.2014.921346
9. Asgharzadeh F, Hashemzadeh A, Rahmani F, Yaghoubi A, Nazari SE, Avan A, et al. Cerium oxide nanoparticles acts as a novel therapeutic agent for ulcerative colitis through anti-oxidative mechanism. *Life Sci.* (2021) 278:119500. doi: 10.1016/j.lfs.2021.119500
10. Li J, Chen H, Wang B, Cai C, Yang X, Chai Z, et al. ZnO nanoparticles act as supportive therapy in DSS-induced ulcerative colitis in mice by maintaining gut homeostasis and activating Nrf2 signaling. *Sci Rep.* (2017) 7:43126. doi: 10.1038/srep43126
11. Siczek K, Zatorski H, Chmielowiec-Korzeniowska A, Pulit-Prociak J, Śmiech M, Kordek R, et al. Synthesis and evaluation of anti-inflammatory properties of silver nanoparticle suspensions in experimental colitis in mice. *Chem Biol Drug Des.* (2017) 89:538–47. doi: 10.1111/cbdd.12876
12. Gao G, Wang H, Zhou J, Rao P, Ke L, Lin JJ, et al. Isolation and characterization of bioactive proteoglycan-lipid nanoparticles from freshwater clam (*Corbicula fluminea* Muller) soup. *J Agric Food Chem.* (2021) 69:1610–8. doi: 10.1021/acs.jafc.0c02402
13. Lin X, Gao X, Chen Z, Zhang Y, Luo W, Li X, et al. Spontaneously assembled nano-aggregates in clear green tea infusions from *Camellia ptilophylla* and *Camellia sinensis*. *J Agric Food Chem.* (2017) 65:3757–66. doi: 10.1021/acs.jafc.7b00068
14. Zhang J, Lin L, Tao N, Zhu Z, Wang X, Wang M. Effect of big eye tuna (*Thunnus obesus*) head soup with different colloidal particle size on TG and TC deposition in FFA-exposed HepG2 cells. *Food Sci Nutr.* (2021) 9:1143–51. doi: 10.1002/fsn3.2092
15. Siebecker A. Traditional bone broth in modern health and disease. *Townsend Lett.* (2005) 259/260:74–81.
16. Morell SF, Daniel KT. *Nourishing Broth: An Old-Fashioned Remedy for the Modern World*. New York, NY: Hachette Book Group Special Markets Department (2014).
17. Gao G, Zhou J, Jin Y, Wang H, Ding Y, Zhou J, et al. Nanoparticles derived from porcine bone soup attenuate oxidative stress-induced intestinal barrier injury in Caco-2 cell monolayer model. *J Funct Foods.* (2021) 83:104573. doi: 10.1016/j.jff.2021.104573
18. Wang H, Gao G, Ke L, Zhou J, Rao P, Jin Y, et al. Isolation of colloidal particles from porcine bone soup and their interaction with murine peritoneal macrophage. *J Funct Foods.* (2019) 54:403–11. doi: 10.1016/j.jff.2019.01.021
19. Ke L, Wang H, Gao G, Rao P, He L, Zhou J. Direct interaction of food derived colloidal micro/nano-particles with oral macrophages. *Npj Sci Food.* (2017) 1:3. doi: 10.1038/s41538-017-0003-3
20. Cançado GGL, Fiuza JA, De Paiva NCN, Lemos LDCD, Ricci ND, Gazzinelli-Guimarães PH, et al. Hookworm products ameliorate dextran sodium sulfate-induced colitis in BALB/c mice. *Inflamm Bowel Dis.* (2011) 17:2275–86. doi: 10.1002/ibd.21629
21. Hidalgo-Cantabrana C, Algieri F, Rodriguez-Nogales A, Vezza T, Martínez-Camblor P, Margolles A, et al. Effect of a ropy exopolysaccharide-producing *Bifidobacterium animalis* subsp. lactis strain orally administered on DSS-induced colitis mice model. *Front Microbiol.* (2016) 7:868. doi: 10.3389/fmicb.2016.00868
22. Tong LC, Wang Y, Wang ZB, Liu WY, Sun S, Li L, et al. Propionate ameliorates dextran sodium sulfate-induced colitis by improving intestinal barrier function and reducing inflammation and oxidative stress. *Front Pharmacol.* (2016) 7:253. doi: 10.3389/fphar.2016.00253
23. Hu R, Wu S, Li B, Tan J, Yan J, Wang Y, et al. Dietary ferulic acid and vanillic acid on inflammation, gut barrier function and growth performance in lipopolysaccharide-challenged piglets. *Anim Nutr.* (2022) 8:144–52. doi: 10.1016/j.aninu.2021.06.009
24. Yang C, Merlin D. Can naturally occurring nanoparticle-based targeted drug delivery effectively treat inflammatory bowel disease? *Expert Opin Drug Deliv.* (2020) 17:1–4. doi: 10.1080/17425247.2020.1698543
25. Wang B, Zhuang X, Deng ZB, Jiang H, Mu J, Wang Q, et al. Targeted drug delivery to intestinal macrophages by bioactive nanovesicles released from grapefruit. *Mol Ther.* (2014) 22:522–34. doi: 10.1038/mt.2013.190
26. Gou S, Huang Y, Sung J, Xiao B, Merlin D. Silk fibroin-based nanotherapeutics: application in the treatment of colonic diseases. *Nanomedicine.* (2019) 14:2373–8. doi: 10.2217/nnm-2019-0058
27. Gou S, Huang Y, Wan Y, Ma Y, Zhou X, Tong X, et al. Multi-bioresponsive silk fibroin-based nanoparticles with on-demand cytoplasmic drug release capacity for CD44-targeted alleviation of ulcerative colitis. *Biomaterials.* (2019) 212:39–54. doi: 10.1016/j.biomaterials.2019.05.012
28. Iglesias N, Galbis E, Díaz-Blanco MJ, Lucas R, Benito E, De-Paz MV. Nanostructured chitosan-based biomaterials for sustained and colon-specific resveratrol release. *Int J Mol Sci.* (2019) 20:398. doi: 10.3390/ijms20020398
29. Li C, Levin M, Kaplan DL. Bioelectric modulation of macrophage polarization. *Sci Rep.* (2016) 6:21044. doi: 10.1038/srep21044
30. Na YR, Stakenborg M, Seok SH, Matteoli G. Macrophages in intestinal inflammation and resolution: a potential therapeutic target in IBD. *Nat Rev Gastroenterol Hepatol.* (2019) 16:531–43. doi: 10.1038/s41575-019-0172-4
31. Antoni L, Nuding S, Wehkamp J, Stange EF. Intestinal barrier in inflammatory bowel disease. *World J Gastroenterol.* (2014) 20:1165–79. doi: 10.3748/wjg.v20.i5.1165
32. Camilleri M, Madsen K, Spiller R, Van Meerveld BG, Verne GN. Intestinal barrier function in health and gastrointestinal disease. *Neurogastroenterol Motil.* (2012) 24:503–12. doi: 10.1111/j.1365-2982.2012.01921.x
33. Manichanh C, Borruel N, Casellas F, Guarner F. The gut microbiota in IBD. *Nat Rev Gastroenterol Hepatol.* (2012) 9:599–608. doi: 10.1038/nrgastro.2012.152
34. Shang L, Liu H, Yu H, Chen M, Yang T, Zeng X, et al. Core altered microorganisms in colitis mouse model: a comprehensive time-point and fecal microbiota transplantation analysis. *Antibiotics.* (2021) 10:643. doi: 10.3390/antibiotics10060643
35. Parker BJ, Wearsch PA, Veloo ACM, Rodriguez-Palacios A. The genus *Alistipes*: gut bacteria with emerging implications to inflammation, cancer, and mental health. *Front Immunol.* (2020) 11:906. doi: 10.3389/fimmu.2020.00906
36. Li AL, Ni WW, Zhang QM, Li Y, Zhang X, Wu HY, et al. Effect of cinnamon essential oil on gut microbiota in the mouse model of dextran sodium sulfate-induced colitis. *Microbiol Immunol.* (2020) 64:23–32. doi: 10.1111/1348-0421.12749
37. Kaur CP, Vadivelu J, Chandramathi S. Impact of *Klebsiella pneumoniae* in lower gastrointestinal tract diseases. *J Dig Dis.* (2018) 19:262–71. doi: 10.1111/1751-2980.12595
38. Grigor'eva IN. Gallstone disease, obesity and the firmicutes/bacteroidetes ratio as a possible biomarker of gut dysbiosis. *J Pers Med.* (2021) 11:13. doi: 10.3390/jpm11010013
39. Tong L, Zhang X, Hao H, Liu Q, Zhou Z, Liang X, et al. *Lactobacillus rhamnosus* gg derived extracellular vesicles modulate gut microbiota and attenuate inflammatory in dss-induced colitis mice. *Nutrients.* (2021) 13:3319. doi: 10.3390/nu13103319
40. Wu M, Li P, An Y, Ren J, Yan D, Cui J, et al. Phloretin ameliorates dextran sulfate sodium-induced ulcerative colitis in mice by regulating the gut microbiota. *Pharmacol Res.* (2019) 150:104489. doi: 10.1016/j.phrs.2019.104489
41. Hu Y, Liu JP, Zhu Y, Lu NH. The importance of toll-like receptors in NF-κB signaling pathway activation by *Helicobacter pylori* infection and the regulators of this response. *Helicobacter.* (2016) 21:428–40. doi: 10.1111/hel.12292
42. Siemer S, Hahlbrock A, Vallet C, McClements DJ, Balszuweit J, Voskuhl J, et al. Nanosized food additives impact beneficial and pathogenic bacteria in the human gut: a simulated gastrointestinal study. *Npj Sci Food.* (2018) 2:22. doi: 10.1038/s41538-018-0030-8
43. Gangadoo S, Nguyen H, Rajapaksha P, Zreiqat H, Latham K, Cozzolino D, et al. Inorganic nanoparticles as food additives and their influence on the human gut microbiota. *Environ Sci Nano.* (2021) 8:1500–18. doi: 10.1039/d1en00025j

Conflict of Interest: The authors declare that the research was conducted in the absence of any commercial or financial relationships that could be construed as a potential conflict of interest.

Publisher's Note: All claims expressed in this article are solely those of the authors and do not necessarily represent those of their affiliated organizations, or those of the publisher, the editors and the reviewers. Any product that may be evaluated in this article, or claim that may be made by its manufacturer, is not guaranteed or endorsed by the publisher.

Advantages of publishing in Frontiers

OPEN ACCESS
Articles are free to read for greatest visibility and readership

FAST PUBLICATION
Around 90 days from submission to decision

HIGH QUALITY PEER-REVIEW
Rigorous, collaborative, and constructive peer-review

TRANSPARENT PEER-REVIEW
Editors and reviewers acknowledged by name on published articles

Frontiers
Avenue du Tribunal-Fédéral 34
1005 Lausanne | Switzerland

Visit us: www.frontiersin.org
Contact us: frontiersin.org/about/contact

REPRODUCIBILITY OF RESEARCH
Support open data and methods to enhance research reproducibility

DIGITAL PUBLISHING
Articles designed for optimal readership across devices

FOLLOW US
@frontiersin

IMPACT METRICS
Advanced article metrics track visibility across digital media

EXTENSIVE PROMOTION
Marketing and promotion of impactful research

LOOP RESEARCH NETWORK
Our network increases your article's readership